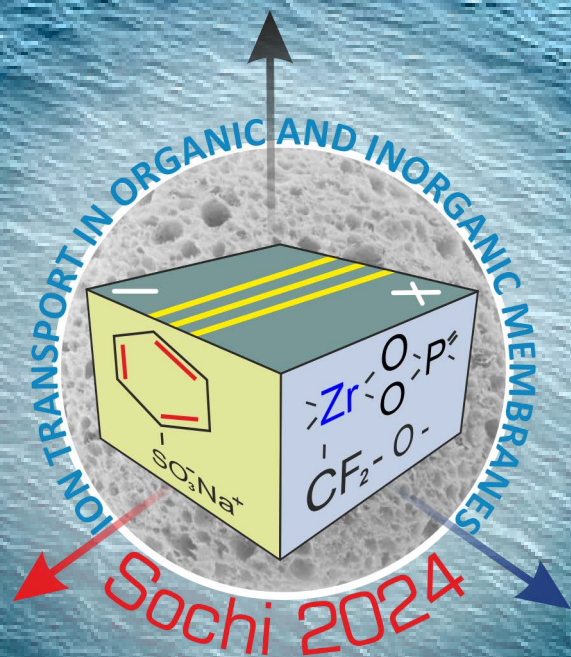


ISBN 978-5-6049504-4-9

ION TRANSPORT IN ORGANIC AND INORGANIC MEMBRANES

(I.T.I.M. 2024)

CONFERENCE PROCEEDING



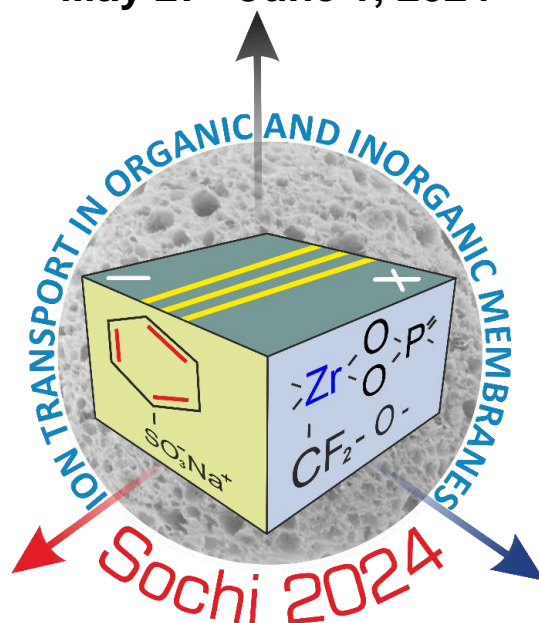
RUSSIAN ACADEMY OF SCIENCES
RUSSIAN MEMBRANE SOCIETY
MINISTRY OF SCIENCE AND HIGHER EDUCATION OF THE RUSSIAN
FEDERATION
RAS SCIENTIFIC COUNCIL ON PHYSICAL CHEMISTRY
RUSSIAN MEMBRANE NETWORK
KUBAN STATE UNIVERSITY
KURNAKOV INSTITUTE OF GENERAL AND INORGANIC CHEMISTRY RAS
JSC TVEL ROSATOM

INTERNATIONAL CONFERENCE

Ion transport in organic and inorganic membranes-2024

PROGRAMME

May 27 –June 1, 2024



SCIENTIFIC/ORGANIZING COMMITTEE

Chairman
Co-chairmen

YAROSLAVTSEV A.B. (*Russia*)
ZABOLOTSKY V.I. (*Russia*)
NIKONENKO V.V. (*Russia*)

Scientific secretary

KONONENKO N.A. (*Russia*)
SHKIRSKAYA S.A. (*Russia*)

BAZINET L. (*Canada*)

RYZHKOV I.I. (*Russia*)

BIESHEUVEL M. (*The Netherlands*)

SHELDESHOV N.V. (*Russia*)

BILDYUKEVICH A.V. (*Belarus*)

SMIRNOVA N.V. (*Russia*)

DAMMAK L. (*France*)

STAROV V.M. (*UK*)

FALINA I.V. (*Russia*)

VASIL'EVA V.I. (*Russia*)

FILIPPOV A.N. (*Russia*)

VOLFKOVICH Yu.M. (*Russia*)

KHOHLOV A.R. (*Russia*)

VOLKOV V.V. (*Russia*)

NEMUDRY A. (*Russia*)

VOROTYNTSEV M.A. (*Russia*)

NOVAK L. (*Czech Republic*)

WANG Y. (*China*)

OZERIN A.N. (*Russia*)

WU L. (*China*)

PISMENSKAYA N.D. (*Russia*)

XU T. (*China*)

RUBINSTEIN I. (*Israel*)

ZALTZMAN B. (*Israel*)

Local organizing committee (*Krasnodar, Russia*)

ACHOH A.R.

LOZA S.A.

BROVKINA M.A.

MAREEV S.A.

BUTYLSKII D.Yu.

MELNIKOV S.S.

ETEREVSKOVA S.I.

NOSOVA E.N.

GIL V.V.

PONOMAR M.A.

KOZMAI A.E.

POROZHNYI M.V.

KUTENKO N.A.

RULEVA V.D.

LOZA N.V.

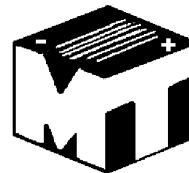
TITSKAYA E.V.

MINISTRY OF SCIENCE
AND HIGHER EDUCATION
OF THE RUSSIAN
FEDERATION



TVEL
ROSATOM

«MEMBRANE
TECHNOLOGY»
INNOVATION ENTERPRISE



Preface

The last few years have seemed to test our strength. The recent coronavirus pandemic disrupted all our plans, postponed the dates of our conferences and significantly changed our lives. Part of conference activities moved to an online format. The change in the international situation has complicated the interaction of Russian scientists with foreign colleagues and has significantly reduced the number of available international conferences. But we want to believe that we have successfully passed these tests. Our 48 conference is again taking place not only at the end of May, but also exactly a year after the previous one. And our foreign colleagues are again taking part in it, and the on-line format makes it possible for a large number of wonderful scientists to join us. But it's even more pleasing that many of them expressed a desire to come again to the Kuban region that has become our second native land. It is worth noting that science changes along with our lives. An analysis of the conference program shows that it reflects all the main modern vectors of development of membrane science and membrane technology.



The tasks are dictated by the pressing problems of humanity and the logic of the development of science itself. The most important challenge is reducing human impact on the environment, primarily in terms of achieving carbon neutrality and comprehensive wastewater recycling. Membrane technologies are entering deeper and deeper into these areas, helping to solve the problem in different directions.

An increasing number of reports are devoted to the problems of alternative energy: the development of renewable energy sources, as well as energy storage devices, such as metal-ion batteries and flow batteries. New approaches have emerged related to the production of hydrogen from biomass and its products, the development of microbial fuel cells, and the production of energy using reverse electrodialysis. It is pleasant to note that new membranes and membrane technologies are among the most demanded innovations in these areas. Water electrolysis with ion-exchange membranes is considered as the main method for producing “green” hydrogen.

Another important direction is the use of wastewater as a source of mining. Zero Liquid Discharge (ZLD) systems have been developed and used for quite some time. The application of membrane processes in these systems makes it possible to obtain pure water and a very concentrated salt solution from wastewater (e.g. mine water); the latter can be processed by conventional crystallization and evaporation processes to get dry salt. However, new achievements in membrane design, primarily, the development of monovalent-ion-selective (ion-exchange) membranes and their use in Selective Electrodialysis (or Selectrodialysis, SED) open up the possibility to produce not a mixture of dry salt, as in conventional ZLD systems, but individual dry salts, which can replace the salts extracted by traditional methods. Much attention is being given to the development of this method for extracting phosphates and other nutrients from wastewater as a way to produce fertilizers. Note that monovalent-ion-selective membranes belong to the class of multilayer membranes. The variety of possible applications of such membranes, including bipolar membranes, always attracts the attention of researchers and engineers. At the same time, it is worth noting that the use of wastewater for hydrogen production and direct

energy generation using bio- and electromembrane technologies are also in focus of attention of researchers.

Of considerable interest are works on the development of electro-baromembrane methods for ion separation, when two driving forces, a potential difference and a pressure difference, are simultaneously applied to a membrane (for example, a track-etched membrane). Ions are separated due to the difference in the ion electromigration velocity and ion convection velocity. The occurrence of two driving forces significantly increases the number of degrees of freedom for solving separation problems.

All of the above topics are touched upon in one way or another in the oral and poster presentations of the participants of the current conference. However, classical fundamental questions are not left aside either: how do ions and water molecules move in membranes and near-membrane solution? What are the mechanisms of concentration polarization and how to govern this phenomenon? Is it possible to control electroconvection and prevent some catastrophe at the micrometer level? Is it possible to change the charge on the pore walls by changing the potential difference across the membrane?

We believe that the conference will provide a number of useful answers and raise exciting questions that will stimulate the further development of membrane science and technology for the benefit of all inhabitants of our planet.



Organizing Committee

Contents

1.	Aslan Achoh, Stanislav Melnikov, Denis Bondarev, Victor Zabolotsky Electrical properties and selectivity of homogeneous bilayer membranes in ternary solutions of strong electrolytes (<i>Krasnodar, Russia</i>)	14
2.	Aslan Achoh, Stanislav Melnikov, Denis Bondarev, Mikhail Sharafan Electrochemical stability of the anion exchange membrane MA-41 modified by poly-N,N-diallylmorpholine bromide in overlimiting current modes (<i>Krasnodar, Russia</i>)	17
3.	Jahan Arif Ahmadova Sea water desalting system based on hybridization of nanofiltration and reverse osmosis methods (<i>Baku, Azerbaijan</i>)	20
4.	Elmara Akberova, Vera Vasil'eva Surface and cross-section morphology of heterogeneous Ralex membranes with different fractions of sulfonated cation exchange resin (<i>Voronezh, Russia</i>)	23
5.	Anastasia Alekseenko, Kirill Paperzh, Angelina Pavlets, Elizaveta Moguchikh, Julia Bayan, Ekaterina Kozhokar, Yana Astrovukh, Julia Pankova, Vladimir Guterman Development of highly efficient electrocatalysts for proton exchange membrane fuel cells: a compromise between activity and stability (<i>Rostov-on-Don, Russia</i>)	26
6.	Danil Alekseenko, Vladimir Guterman, Anastasia Alekseenko, Sergey Belenov Production of commercial electrocatalysts for low temperature fuel cells (<i>Rostov-on-Don, Russia</i>)	29
7.	Maxim Alekseev, Ilya Moroz, Georgy Ganchenko, Semyon Mareev, Evgeny Demekhin Numerical and experimental research of analyte concentration near ion-selective particle (<i>Moscow, Krasnodar, Russia</i>)	32
8.	Georgiy Andreev, Polina Pushankina, Sergey Ivanin, Marina Papezhuk, Aleksandr Simonov, Nikita Prokhorov, Stepan Dzhimak, Iliya Petriev Investigation of the dependence of the electrocatalytic activity of copper nanoparticles on morphology and shaping (<i>Krasnodar, Russia</i>)	35
9.	Tatyana Anokhina, Tatyana Ershova, Olga Shchegolikhina, Anton Anisimov, Aziz Muzafarov The effect of the molecular weight of ladder-like polyphenylsilsesquioxane (L-PPSQ) on membrane formation (<i>Moscow, Russia</i>)	37
10.	Marina Arapova, Elena Shubnikova, Olga Bragina, Sergey Bychkov, Alexander Nemudry Effect of surface modification on the oxygen permeability of doped strontium ferrites-based hollow fiber membranes (<i>Novosibirsk, Russia</i>)	40
11.	Kayo Santana Barros, Valentín Pérez-Herranz, Svetlozar Velizarov Electrodialytic and chronopotentiometric study on the separation of volatile fatty acids (<i>Caparica, Portugal; València, Spain</i>)	41
12.	Sergey Belenov, Alina Nevelskaya, Angelina Pavlets, Vladislav Menshikov, Elizaveta Moguchikh, Anastasia Alekseenko Influence of the heat treatment on structural and functional characteristics of the PtCu/C electrocatalysts on various carbon supports (<i>Rostov-on-Don, Russia</i>)	42
13.	Maarten Biesheuvel, Ilya Ryzhkov Resolving some controversies in water and ion transport in polymer membranes for water desalination: how do ions and water molecules move and partition? (<i>Leeuwarden, The Netherlands; Krasnoyarsk, Russia</i>)	45
14.	Denis Bondarev, Anastasia Samoilenko, Stanislav Melnikov Efficiency analysis of novel and conventional anion exchange membranes during electrodialysis of diluted sodium chloride solution (<i>Krasnodar, Russia</i>)	46
15.	Ilya Borisov, Dmitriy Matveev, Vladimir Vasilevskii, Andrey Didenko, Svetlana Khashirova, Vladimir Volkov, Alexey Volkov, Stepan Bazhenov,	49

- Tatyana Anokhina** From polymers to hollow fiber membranes and membrane modules (*Moscow, Russia*)
16. **Olga Bragina, Alexey Novikov, Elena Shubnikova, Marina Arapova, Alexander Nemudry** Study of oxygen permeability and catalytic performance of microtubular membranes based on strontium ferrite doped by tungsten (*Novosibirsk, Russia*) 52
17. **Olga Bragina, Elena Shubnikova, Marina Arapova, Alexander Nemudry** Surface modification of ceramic membrane based on strontium ferrite for coupling catalytic CO₂ conversion with partial oxidation of methane (*Novosibirsk, Russia*) 54
18. **Alexey Budnikov, Vasiliy Troitskiy, Dmitrii Butylskii** Lithium recovery from lithium-cobalt-nickel-containing solution using nanoporous membrane (*Krasnodar, Novochoerkassk, Russia*) 55
19. **Dmitrii Butylskii, Vasiliy Troitskiy, Roman Salichov, Nina Smirnova, Victor Nikonenko** Selective separation of lithium, potassium and sodium using membrane-based technologies (*Krasnodar, Novochoerkassk, Russia*) 57
20. **Olga Cherendina, Elena Shubnikova, Olga Bragina, Maria Khohlova, Alexander Nemudry** Ethylene production in catalytic membrane reactors based on perovskite-fluorite dual-phase materials (*Novosibirsk, Russia*) 59
21. **Natalya Chubyr, Anna Kovalenko, Makhamet Urtenov, Zulfa Laipanova** Asymptotic analysis of stationary transport of salt ions in the section of the desalting channel taken into account of the dissociation/recombination reaction of water molecules (*Krasnodar, Karachaevsk, Russia*) 60
22. **Aydın Cihanoğlu** Layer-by-layer assembly of polyelectrolytes on a poly(epichlorohydrin) based anion exchange membrane to enhance energy harvesting by reverse electrodialysis (*İzmir, Türkiye*) 63
23. **Andrea Culcasi, Antonia Filingeri, Julio Lopez, Marc Fernandez de Labastida, Alessandro Tamburini, José Luis Cortina, Giorgio Micale, Andrea Cipollina** Advancing in trace element recovery from brines: insights into differential ion transport through electrodialysis with bipolar membranes (*Palermo, Italy; Barcelona, Spain*) 64
24. **Ksenia Demidenko, Ekaterina Titskaya, Sergey Timofeev, Irina Falina** Influence of modification with zirconium phosphate on conductivity of MF-4SC perfluorinated membrane (*Krasnodar, Saint-Petersburg, Russia*) 67
25. **Mariia Dmitrenko, Anna Kuzminova, Roman Dubovenko, Artem Selyutin, Anastasia Penkova** Development and study of chitosan membranes modified with metal organic frameworks for enhanced water treatment (*Saint-Petersburg, Russia*) 69
26. **Roman Dubovenko, Ksenia Sushkova, Anna Mikulan, Danila Myznikov, Anna Kuzminova, Mariia Dmitrenko, Anastasia Penkova** Development and study of ultrafiltration membranes based on nitrocellulose (*Saint-Petersburg, Russia*) 70
27. **Margarita Elshina, Eugenia Falina, Aelita Pasechnik, Valeriia Plekunova, Ksenia Demidenko, Julia Loza, Nikita Kovalchuk, Sergey Loza** Hybrid membrane setup for utilization acid-containing waste from metallurgical industries (*Krasnodar, Novochoerkassk, Russia*) 71
28. **Anastasia Esina, Natalia Kononenko, Svetlana Shkirskaia** Electrotransport of water through the heterogeneous anion exchange membranes (*Krasnodar, Russia*) 73
29. **Irina Falina, Natalia Loza, Natalia Kononenko** Electrotransport characteristics of polyaniline-modified cations-exchange membranes in solutions of sulfuric acid and nickel and chromium sulfates (*Krasnodar, Russia*) 75

30. **Ilya Faykov, Mikhail Goikhman, Galina Polotskaya, Alexandra Pulyalina** 76
Membranes based on metal-polymer complex for pervaporation of organic-organic mixtures (*Saint-Petersburg, Russia*)
31. **Antonia Filingeri, Marc Philibert, Emmanuelle Filloux, Anne Brehant, Alessandro Tamburini, Andrea Cipollina, Giorgio Micale** 78
Transport of ions in assisted-reverse electrodialysis for surface water reverse osmosis permeate remineralization (*Palermo, Italy; Le Pecq, France*)
32. **Anatoly Filippov, Ludmila Ermakova, Tamara Philippova** 80
Hydrodynamic permeability of charged porous glass-like membranes (*Moscow, Saint-Petersburg, Russia*)
33. **Mario Fouad, Ivan Kovalev, Rostislav Guskov, Mikhail Popov, Alexander Nemudry** 83
Oxygen exchange in mixed ionic electronic conductivity perovskite-like oxide: lanthanum strontium ferrite doped tantalum (*Novosibirsk, Russia*)
34. **Elizaveta Frants, Artem Krylov, Evgeny Demekhin** 84
Flow of ions near a dielectric surface during nonlinear electrophoresis (*Krasnodar, Moscow, Russia*)
35. **Georgy Ganchenko, Vladimir Shelistov, Maxim Alekseev, Vladislav Popov, Evgeny Demekhin** 87
Electrophoresis of complex microparticles (*Moscow, Krasnodar, Russia*)
36. **Violetta Gil, Mikhail Porozhnyy, Dmitry Lopatin, Igor Voroshilov, Anton Kozmai** 89
Effect of polysulfone membrane structure on its transport characteristics during urea dialysis (*Krasnodar, Dinskaya, Russia*)
37. **Andrey Gorobchenko, Semyon Mareev, Victor Nikonenko** 92
Investigation of non-stationary processes of phosphoric acid salt anions transfer through anion-exchange membrane during electrodialysis (*Krasnodar, Russia*)
38. **Evgenia Grushevenko, Denis Kalmykov, Julia Matveeva, Stepan Bazhenov** 95
Electromembrane regeneration of alkanolamine absorbents: problems and solutions (*Moscow, Russia*)
39. **Evgenia Grushevenko, Tatiana Rokhmanka, George Golubev, Ilya Borisov** 97
Polyorganosiloxane-based membrane for ABE-fermentation broth separation: effect of fluoroalkylacrylate substituent (*Moscow, Russia*)
40. **Vera Guliaeva, Andrey Kislyi, Ilya Moroz, Yuri Prokhorov, Victoria Plis, Anastasiia Klevtsova, Elizaveta Evdochenko** 100
Influence of electrode particle size on the efficiency of anodic oxidation of oxalic acid in aqueous solution (*Krasnodar, Russia*)
41. **Rostislav Guskov, Michail Popov, Ivan Kovalev, Alexander Nemudry** 102
Modified strontium cobaltites as electrode materials for membrane technologies: structure and functional properties (*Novosibirsk, Russia*)
42. **Vladimir Guterman, Kirill Paperzh, Maria Danilenko, Elvira Zaitseva** 104
New approach to control the microstructure of platinum-carbon electrocatalysts during their liquid-phase synthesis (*Rostov-on-Don, Russia*)
43. **Denis Kalmykov, Sergey Shirokikh, Stepan Bazhenov** 106
Scale up estimates of an oxygen-removing membrane contactor for demo post combustion plant (*Moscow, Russia*)
44. **Tatyana Karpenko, Vladislava Shramenko, Ilia Averianov, Nikolay Sheldeshov** 109
Investigation of influence of organic acid salts nature on current-voltage characteristics of ion-exchange membranes (*Krasnodar, Russia*)
45. **Ruslan Kayumov, Anna Lochina, Alexander Lapshin, Lyubov Shmygleva** 112
Sodium-conducting polymer electrolytes based on commercially available analogues of nafion and carbonates (*Chernogolovka, Dolgoprudny, Russia*)
46. **Catherine Kazakovtseva, Anna Kovalenko, Marina Patykovskaya, Makhamet Urtenov** 114
Stationary electroconvection in galvanostatic mode when following the generalized Ohm's law (*Krasnodar, Russia*)

47. **Daria Khanukaeva, Petr Aleksandrov, Anatoly Filippov** Nonstationary effects at separation of solutions (*Moscow, Ulyanovsk, Russia*) 116
48. **Ivan Kharchenko, Natalia Fadeeva, Irina Volkova, Evgeny Elsuf'iev, Elena Fomenko, Galina Akimochkina, Ilya Ryzhkov** Electro / baromembrane separation of ionic dyes using electrically conductive ceramic membranes (*Krasnoyarsk, Russia*) 119
49. **Andrey Kislyi, Vera Guliaeva, Ilya Moroz, Yuri Prokhorov, Victoria Plis** Removal of micro- and nanoplastics from wastewater using the anodic oxidation process (*Krasnodar, Russia*) 122
50. **Andrey Kislyi, Anton Kozmai, Semyon Mareev, Victor Nikonenko** Mathematical modeling of the transport characteristics of ion exchange membranes with low water content (*Krasnodar, Russia*) 124
51. **Anastasiia Klevtsova, Evgeniia Pasechnaya, Maria Ponomar, Anastasiia Korshunova, Daria Chuprynina, Natalia Pismenskaya** The influence of the chemical nature of ion-exchange membranes on their fouling during electro dialysis tartrate stabilization of wine (*Krasnodar, Russia*) 127
52. **Pavel Kolinko, Sergey Saltykov, Vitaly Busko, Vasily Alimov, Evgenii Peredistov, Andrei Busnyuk, Alexander Livshits** Permeability of hydrogen through palladium and vanadium-based alloys (*Saint-Petersburg, Russia*) 130
53. **Natalia Kononenko, Irina Falina, Ekaterina Meshcheryakova, Ksenia Demidenko, Sergey Timofeev** Transport of ions through the modified MF-4SK membranes for hydrogen-air fuel cell (*Krasnodar, Saint-Petersburg, Russia*) 133
54. **Alexander Korzhov, Sergey Loza, Mikhail Sharafan** Polymer bipolar membranes: manufacturing and application (*Krasnodar, Russia*) 135
55. **Elizaveta Korzhova, Jonathan Brant, Dmitrii Lopatin** Preparation and characterization of hydrophobic poly(vinylidene fluoride-tetrafluoroethylene) nanofiber membranes by electrospinning for direct contact membrane distillation (*Krasnodar, Russia; Laramie, USA*) 138
56. **Nikita Kovalchuk, Nazar Romanyuk, Sergey Loza, Nina Smirnova** Investigation of competitive transfer of singly and doubly charged cations during limited electro dialysis concentration (*Novochoerkassk, Krasnodar, Russia*) 140
57. **Anna Kovalenko, Victor Nikonenko, Makhmet Urtenov, Aleksander Pismenskiy** Influence of spacers on salt ion transport in electromembrane systems considering the main coupled effects (*Krasnodar, Russia*) 142
58. **Ivan Kovalev, Rostislav Guskov, Mikhail Popov, Stanislav Chizhik, Alexander Nemudry** Oxygen exchange kinetics on lanthanum strontium cobalt ferrite doped with tungsten (*Novosibirsk, Russia*) 145
59. **Oleg Kozaderov, Olga Kozaderova, Sabukhi Niftaliev, Kseniya Kim** Degradation of ion exchange membranes during electro dialysis (*Voronezh, Russia*) 146
60. **Olga Kozaderova, Oleg Kozaderov** Regularities of lactic acid mass transfer in ion-exchange membrane systems (*Voronezh, Russia*) 149
61. **Olga Kudrinskaya, Olga Astashkina** Carbon sorbents modified with fullerenes (*Saint-Petersburg, Russia*) 152
62. **Vaibhav Kulshrestha** Polyelectrolyte membranes for strategic devising of electrochemical energy systems (*Bhavnagar, India*) 154
63. **Natalia Kutenko, Natalia Loza** Electrotransport properties of bilayer membrane based on heterogeneous cation exchange membrane and homogeneous layer with polyaniline (*Krasnodar, Russia*) 155
64. **Anna Kuzminova, Anna Karyakina, Anastasia Stepanova, Mariia Dmitrenko, Roman Dubovenko, Anastasia Penkova** Development and 157

- investigation of novel membranes based on poly(ester-block-amide) modified by holmium-based metal-organic frameworks (*Saint-Petersburg, Russia*)
65. **Konstantin Lebedev, Victor Zabolotsky, Vera Vasil'eva, Aslan Achoh, Polina Vasilenko** Mathematical modeling influence of the resin particle size in the cation-exchange membrane on the space charge distribution in the membrane system (*Krasnodar, Voironzh, Russia*) 159
 66. **Xingya Li** Angstrom-scale confined ion separation membranes (*Hefei, P. R. China*) 162
 67. **Anna Lochina, Ruslan Kayumov, Grigoriy Nechaev, Lyubov Shmygleva** Positive electrode for sodium-ion batteries based on manganese and cobalt layered oxide (*Chernogolovka, Dolgoprudny, Russia*) 163
 68. **Dmitrii Lopatin, Elizaveta Korzhova, Oleg Baranov, Igor Voroshilov** Development and production of membranes at the Krasnodar compressor plant (*Dinskaya, Russia*) 164
 69. **Julia Loza, Natalia Loza, Irina Falina** Evolution of properties of MF-4SK perfluorinated membranes during their modification with zirconium phosphate (*Krasnodar, Russia*) 167
 70. **Natalia Loza, Irina Falina, Marina Brovkina, Sergey Timofeev, Natalia Kononenko** Effect of thickness on diffusion permeability and conductivity of perfluorinated cation-exchange membranes (*Krasnodar, Saint-Petersburg, Russia*) 169
 71. **Sergey Loza, Nikita Kovalchuk, Nazar Romanyuk, Victor Zabolotsky** Selective electro dialysis concentration of solutions containing singly and doubly charged cations (*Krasnodar, Russia*) 171
 72. **Artyom Lunin, Fedor Andreyanov, Maxim Bermeshev** Vinyl-addition poli(ionic liquid)s based on 5-hexyl-norbornene and 5-(4-bromobutyl)-norbornene (*Moscow, Russia*) 173
 73. **Kirill Lyapishev, Alina Ivanchenko, Natalia Kononenko, Irina Falina** Gas permeability of modified MF-4SK perfluorinated membrane when operating in a fuel cell (*Krasnodar, Russia*) 174
 74. **Anna Lysova, Andrey Yaroslavtsev** Hybrid membranes polybenzimidazole/silica with silane crosslinking (*Moscow, Russia*) 177
 75. **Anna Lysova, Andrey Manin, Daniel Golubenko, Andrey Yaroslavtsev** Metal-polymer membranes based on cardo poly(benzimidazole) for electromembrane applications (*Moscow, Russia*) 179
 76. **Anna Maksimova, Ilya Ryzhkov** Modelling of concentration polarization in a tangential filtration cell with radial solution flow (*Krasnoyarsk, Russia*) 181
 77. **Andrey Manin, Andrey Yaroslavtsev** Modification of ion exchange membranes with cerium and zirconium phosphate particles to enhance the transport of single-charged ions (*Moscow, Russia*) 184
 78. **Semyon Mareev, Mikhail Petryakov, Andrey Gorobchenko, Artem Mareev, Ilya Moroz, Victor Nikonenko** Theoretical study of liquid flow in an electro dialyzer chamber with a spacer (*Krasnodar, Russia*) 187
 79. **Dmitry Matveev, Tatyana Anokhina, Vladimir Volkov, Ilya Borisov, Stepan Bazhenov** Polyimide membranes for the hydrogen concentration from gas mixtures (*Moscow, Russia*) 189
 80. **Dmitry Matveev, Ilya Borisov, Evgenia Grushevenko Vladimir Vasilevskii, Tatyana Anokhina, Vladimir Volkov** Porous polysulfone hollow fiber supports with low mass transfer resistance for the production of gas separation composite membranes (*Moscow, Russia*) 191

81. **Stanislav Melnikov, Victor Zabolotsky** Ion transport in electromembrane system with bilayer ion-exchange membrane with oppositely charged layers (*Krasnodar, Russia*) 194
82. **Stanislav Melnikov, Svetlana Eterevszkova, Victor Zabolotsky** Research of the process of limited electro dialysis concentration of salts, acids and alkali (*Krasnodar, Russia*) 197
83. **Ekaterina Meshcheryakova, Irina Falina, Natalia Kononenko, Sergey Timofeev** diffusion properties of the MF-4SK perfluorinated membranes with varying contents of inert fluoropolymer and hydrated zirconium phosphate (*Krasnodar, Saint-Petersburg, Russia*) 199
84. **Olga Mikhailovskaya, Ksenia Sushkova, Anna Kuzminova, Roman Dubovenko, Anastasia Penkova, Mariia Dmitrenko** Membranes based on polyelectrolyte complex of sodium alginate/polyethylenimine modified with graphene oxide (*Saint-Petersburg, Russia*) 201
85. **Elizaveta Moguchikh, Angelina Pavlets, Margarita Kozlova, Anastasia Solovyova, Anastasia Alekseenko** Study of the influence of the structure of iridium-containing electrocatalysts on the catalytic activity of the oxygen evolution reaction (*Rostov-on-Don, Moscow, Russia*) 203
86. **Ilya Moroz, Mikhail Petryakov, Valentina Ruleva, Maria Ponomar, Victor Nikonenko** Electro dialysis of moderately concentrated solutions using a specially designed cell chambers (*Krasnodar, Russia*) 205
87. **Sofia Morozova, Sergey Golubkov, Tatiana Statsenko, Vladimir Likhomanov, Grigorii Don, Evgenii Sanginov, Andrei Belmesov, Aleksey Kashin, Aleksey Levchenko** The effect of the conditions for obtaining membranes from perfluorinated ionomers on their proton conductivity, hydrogen permeability and electrochemical parameters of fuel cells based on them (*Dolgoprudny, Moscow, Chernogolovka, Russia*) 207
88. **Roman Nazarov, Anna Kovalenko, Victor Nikonenko, Makhamet Urtenov** Theoretical study of the effect of changes in the dissociation/recombination rate constant in the diffusion layer of a cation exchange membrane on salt ion transport (*Krasnodar, Russia*) 208
89. **Alexandra Nebesskaya, Yuliia Shvorobei, Alexey Yushkin, Evgeniia Grushevenko, Tatyana Anokhina, Alexey Volkov** Alginate-based composite membranes for antibiotics removal (*Moscow, Russia*) 210
90. **Alexandra Nebesskaya, Alexey Balynin, Vladimir Volkov, Alexey Yushkin** Application of PAN membranes for oil deasphalting (*Moscow, Russia*) 213
91. **Alexandra Nebesskaya, Alexey Yushkin, Alexander Markelov, Tatiana Anokhina, Vladimir Volkov** Membrane regeneration of used engine oil (*Moscow, Russia*) 215
92. **Alexander Nemudry** Oxidative conversion of light alkanes in a catalytic membrane reactor (*Novosibirsk, Russia*) 217
93. **Victor Nikonenko, Mikhail Sharafan, Natalia Pismenskaya** Coupled effects of concentration polarization in systems with ion-exchange membranes (*Krasnodar, Russia*) 219
94. **Elena Nosova, Stanislav Melnikov, Victor Zabolotsky** Alkali production by bipolar membrane electro dialysis from carbonate containing salt (*Krasnodar, Russia*) 221
95. **Ilya Pankov, Arshak Tsaturyan** Features of studying catalytic materials and thin films using transmission electron microscopy (*Rostov-on-Don, Russia*) 224
96. **Kirill Paperzh, Julia Pankova, Anastasia Alekseenko, Vladimir Guterman** Optimization of methods for synthesis of Pt-based electrocatalysts to increase their functional characteristics (*Rostov-on-Don, Russia*) 227

97. **Angelina Pavlets, Yana Astravukh, Anastasia Alekseenko, Ilya Pankov, Eugeny Gerasimov, Vladimir Guterman** Deciphering nanostructural evolution of Pt-based electrocatalyst via identical location transmission electron microscopy (*Rostov-on-Don, Novosibirsk, Russia*) 230
98. **Iliya Petriev, Polina Pushankina, Georgiy Andreev, Sergey Ivanin, Marina Papezhuk, Alexandr Simonov, Nikita Prokhorov** Methods for the creation of membrane alloys for the production of high-purity hydrogen (*Krasnodar, Russia*) 233
99. **Natalia Pismenskaya, Evgeniia Pasechnaya, Anastasiia Klevtsova, Anastasiia Korshunova, Daria Chuprynina** The influence of pulsed electric fields on the tartrate stabilization efficiency of wine materials by electro dialysis (*Krasnodar, Russia*) 235
100. **Victoria Plis, Andrey Kislyi, Ilya Moroz, Vera Guliaeva, Yuri Prokhorov, Anastasiia Klevtsova** Mineralization of photopolymer-based microplastics on a granular anode made of sub-stoichiometric titanium oxide (*Krasnodar, Russia*) 237
101. **Maria Ponomar, Elizaveta Korzhova, Dmitry Lopatin, Veronika Sarapulova, Lasaad Dammak, Igor Voroshilov** Characterization of pore-filling cation - exchange membrane in sodium chloride solution (*Krasnodar, Dinskaya, Russia; Thiais, France*) 239
102. **Roman Ponomarev, Maxim Alekseev, Georgiy Ganchenko, Irina Morshneva, Evgeny Demekhin** Modeling of analyte behavior and preconcentration in ternary electrolyte systems (*Moscow, Rostov-on-Don, Krasnodar, Russia*) 242
103. **Mikhail Porozhnyy, Veronika Sarapulova, Maria Ponomar, Victor Nikonenko** Asymmetry in diffusion permeability of commercial ion-exchange membranes as a result of discrepancy in surface roughness of different sides (*Krasnodar, Russia*) 244
104. **Yuri Prokhorov, Andrey Kislyi, Ilya Moroz, Vera Guliaeva, Victoria Plis, Anastasiia Klevtsova, Semyon Mareev** Theoretical and experimental study of anodic oxidation of organic pollutants on particle sub-stoichiometric titanium oxide anode in a flat electrolysis chamber (*Krasnodar, Russia*) 247
105. **Polina Pushankina, Georgiy Andreev, Sergey Ivanin, Marina Papezhuk, Aleksandr Simonov, Nikita Prokhorov, Stepan Dzhimak, Iliya Petriev** Synthesis and investigation of nanoparticles with non-classical habit as a highly active catalyst for hydrogen processes (*Krasnodar, Russia*) 249
106. **Anastasia Pyrkova, Irina Stenina, Andrey Yaroslavtsev** PVDF-based membranes as electrolytes for solid-state lithium metal batteries (*Moscow, Russia*) 252
107. **Alisa Raeva, Dmitry Matveev, Tatyana Anokhina, Azamat Zhansitov, Svetlana Khashirova, Ilya Borisov** Highly permeable membranes based on new polyphenylene sulfone and its copolymers for ultrafiltration of aqueous media (*Nalchik, Moscow, Russia*) 254
108. **Alisa Raeva, Ilya Borisov, Andrey Didenko, Tatyana Anokhina, Alexander Malakhov** Transport properties of membranes based on copolyurethanimides in the process of organic solvent nanofiltration (*Moscow, Saint-Petersburg, Russia*) 257
109. **Tatyana Rokhmanka, Evgenia Grushevenko, Stepan Sokolov, Julia Matveeva, Ilya Borisov** Dependence of structure and gas transport properties of polydecylmethylsiloxane on the type of crosslinking agent (*Moscow, Russia*) 259
110. **Nazar Romanyuk, Nikita Kovalchuk, Sergey Loza, Victor Zabolotsky** Transfer of a mixed solution of strong and weak electrolytes through ion exchange membranes (*Krasnodar, Russia*) 262
111. **Nazar Romanyuk, Aslan Achoh, Denis Bondarev, Anatoliy Minenko, Alexander Korzhov, Mikhail Sharafan** Transport and structural characteristics of ion exchange membranes in sodium chloride solution (*Krasnodar, Russia*) 265

112. **Isaak Rubinstein, Boris Zaltzman** Electroconvection in electrodeposition: electrokinetic mechanisms of wave-length selection and prevention of the short-wave catastrophe (*Be'er Sheva, Israel*) 267
113. **Valentina Ruleva, Andrey Gorobchenko, Maria Ponomar, Svetlana Shkirskaya, Natalia Kononenko, Victor Nikonenko** Simplified characterization of ion-exchange membranes for modeling the efficiency of electro dialysis of moderately concentrated solutions (*Krasnodar, Russia*) 268
114. **Ilya Ryzhkov, Ivan Kharchenko, Mikhail Simunin, Ivan Nemtsev, Denis Lebedev, Nikita Vaulin** Ionic conductivity enhancement in nanoporous membranes with electrically conductive surface (*Krasnoyarsk, Saint-Petersburg, Russia*) 271
115. **Ekaterina Safronova, Andrey Yaroslavtsev** Dispersion-cast perfluorosulfonic acid membranes of various chemical structure (*Moscow, Russia*) 274
116. **Nikolay Sheldeshov, Nikita Kovalev, Ilya Averianov, Tatyana Karpenko, Victor Zabolotsky** Rate constants of water dissociation in heterogeneous membrane containing catalytic additive particles (*Krasnodar, Russia*) 277
117. **Konstantin Shestakov, Dmitry Lazarev, Sergey Lazarev, Maxim Gessen** Digital technology applications for the membrane processes design (*Tambov, Russia*) 280
118. **Svetlana Shkirskaya, Natalia Kononenko, Diana Zotova** Water transport in modified perfluorinated membranes (*Krasnodar, Russia*) 283
119. **Lyubov Shmygleva, Ruslan Kayumov, Anna Lochina, Alexander Lapshin** Features of structure and ionic conductivity of Li⁺-membranes with Nafion structure plasticized with carbonates (*Chernogolovka, Dolgoprudny, Russia*) 285
120. **Lyubov Shmygleva, Ruslan Kayumov, Anna Lochina, Alexander Lapshin** Possibility of inion polymer membrane using in metal-ion batteries (*Chernogolovka, Dolgoprudny, Russia*) 286
121. **Vladislava Shramenko, Tatyana Karpenko, Nikolay Sheldeshov** Diffusion characteristics of ion-exchange membranes in organic acids salts solutions (*Krasnodar, Russia*) 288
122. **Elena Shubnikova, Olga Cherendina, Maria Khohlova, Olga Bragina, Alexander Nemudry** Hollow fiber membranes based on niobium doped LSF for oxygen separation (*Novosibirsk, Russia*) 291
123. **Zdenek Slouka, Jakub Strnad, Václav Lázníčka** Transport phenomena at heterogenous ion-exchange membranes (*Prague, Pilsen, Czech Republic*) 292
124. **Nina Smirnova, Tatyana Molodtsova, Anna Ulyankina, Daria Chernysheva** Pulse alternating current electrosynthesis as an effective way to multifunctional materials for hydrogen energy (*Novocherkassk, Russia*) 293
125. **Kseniia Solonchenko, Olesya Yurchenko, Natalia Pismenskaya** Electrochemical characteristics of anion-exchange membranes in solutions of tartaric and citric acid salts (*Krasnodar, Russia*) 296
126. **Anastasia Stepanova, Anna Kuzminova, Mariia Dmitrenko, Roman Dubovenko, Anastasia Penkova** Novel poly(ester-block-amide) membranes for removing of heavy metal ions by nanofiltration (*Saint-Petersburg, Russia*) 298
127. **Nastasia Stretton, Ekaterina Safronova, Andrey Yaroslavtsev** Hybrid recast membranes based on Aquivion® polymer and inorganic nanoparticles (*Moscow, Russia*) 300
128. **Andrey Terentyev, Daria Afanaseva, Kseniia Plinier, Aleksandr Dyachkov** Analysis of physico-chemical methods used in the development of novel types of membranes (*Russia, Moscow*) 302
129. **Denis Terin, Marina Kardash, Timur Turaev, Ivan Turin, Ilya Sinev** Low-temperature ion-plasma pre-treatment of fiber systems and its effect on the 303

- structure and properties of mosaic composite heterogeneous membranes Polykon
(*Saratov, Russia*)
130. **Ekaterina Tikhonova, Natalia Kononenko, Svetlana Shkirsraya, Ilya Strilets, Marina Kardash** Porous structure of anion exchange fibrous Polykon membranes on lavsane textile base (*Krasnodar, Saratov, Russia*) 306
131. **Vasiliy Troitskiy, Alexey Budnikov, Dmitrii Butylskii** Recycling lithium from spent lithium-ion batteries leaching solution using electrobaromembrane method (*Krasnodar, Russia*) 308
132. **Alexander Troshkin, Daria Khanukaeva, Petr Aleksandrov, Anatoly Filippov** Modeling of stationary thermopervaporation of a two-component mixture (*Moscow, Ulyanovsk, Russia*) 310
133. **Timur Turaev, Marina Kardash, Denis Terin** Structure and properties of the modified “Polykon” mosaic membranes (*Saratov, Russia*) 313
134. **Aminat Uzdenova** Mathematical modeling of overlimiting mass transfer in a three-layer electromembrane system in galvanodynamic mode (*Karachaevsk, Russia*) 316
135. **Vera Vasil’eva, Elmara Akberova, Svetlana Dobryden, Yana Beshpalova** Antibate influence of the fraction and sizes of ion exchange resin particles on the properties of the heterogeneous membrane MK-40 (*Voronezh, Russia*) 318
136. **Yulia Vilacheva, Alexander Lysenko** Production of gas diffusion layers using fluoroplastics (*Saint-Petersburg, Russia*) 321
137. **Yury Volkovich** Aluminum-ion batteries (*Moscow, Russia*) 323
138. **Vitaly Volkov, Irina Avilova** Cupper (II) ion exchange mechanism in amino phosphonic polyampholites studied by EPR (*Chernogolovka, Russia*) 324
139. **Daria Voropaeva, Ekaterina Safronova, Svetlana Novikova, Andrey Yaroslavtsev** Perfluorosulfonic acid membranes Aquivion® as gel-polymer electrolytes for lithium metal batteries (*Moscow, Russia*) 327
140. **Tongwen Xu** Next Generation ion exchange membranes (*Hefei, P. R. China*) 330
141. **Andrey Yaroslavtsev** Prospects and challenges of hydrogen energy (*Moscow, Russia*) 332
142. **Ala Yaskevich, Tatiana Plisko, Victor Kasperchik, Katsiaryna Burts, Maryia Makarava, Maria Krasnova, Alexandr Bilyukevich** Removal of sulfonamide antibiotics from water with using of biochars and nanofiltration (*Minsk, Belarus*) 334
143. **Polina Yurova, Irina Stenina, Andrey Yaroslavtsev** Grafted membranes based on fluorinated films and polyaniline for ion separation (*Moscow, Russia*) 337
144. **Victor Zabolotsky, Stanislav Melnikov, Sergey Loza, Nikolay Sheldeshov, Aslan Achoh, Nikita Kovalev, Denis Bondarev** Multilayer ion exchange membranes and electromembrane processes for environmentally friendly closed cycle technologies (*Krasnodar, Russia*) 338
145. **Changyong Zhang** The application of capacitive deionization for water treatment and resource recovery (*Hefei, P. R. China*) 339
146. **Ekaterina Zolotukhina, Alexei Vinyukov, Andrey Starikov, Ekaterina Gerasimova, Sofia Kleinikova, Konstantin Gor’kov, Vsevolod Pavlov** Impact of structure of redox polymer on electrochemical properties of glucose biosensors (*Chernogolovka, Moscow, Russia*) 340
147. **Ekaterina Zolotukhina, Alisa Freiman, Ekaterina Gerasimova, Polina Afanasieva** Towards redox mediator nature and composition of active layer in stability of glucose test-strips during storage (*Chernogolovka, Moscow, Russia*) 342

ELECTRICAL PROPERTIES AND SELECTIVITY OF HOMOGENEOUS BILAYER MEMBRANES IN TERNARY SOLUTIONS OF STRONG ELECTROLYTES

Aslan Achoh, Stanislav Melnikov, Denis Bondarev, Victor Zabolotsky

Kuban State University, Krasnodar, Russia, E-mail: achoh-aslan@mail.ru

Introduction

Research in the field of membrane materials science and membrane technologies is actively developing, as evidenced by a large number of domestic and foreign publications. One of the main tasks in the development of electromembrane technologies is the creation of membranes with high specific selectivity to one or more ions contained in multiionic solutions. Of particular interest is the direction associated with the creation and research of ion-exchange membranes with specific selective permeability (bilayer, multilayer, composite, etc.) membranes and the assessment of the effect of modification on their electric transport characteristics [1-2].

The purpose of this work is to study the electrochemical characteristics of surface-modified homogeneous cation exchange membranes MF-4SK in mixed solutions of $\text{CaCl}_2 + \text{NaCl}$.

Experiments

The objects of the study were experimental homogeneous membranes with a thin selective layer of N,N-diallyl-N,N-dimethylammonium chloride and ethyl methacrylate copolymer [3] on the surface of a membrane substrate made of sulfonated polytetrafluoroethylene (MF-4SK) manufactured by Plastpolymer. Modified membranes were obtained by laying a thin layer of DMDAAC liquid membrane on the surface of the substrate membrane. MF-4SK membranes and a DMDAAC-based modifying layer were also obtained from 10% solutions prepared with isopropyl alcohol. The modified MF-4SK membranes with a film thickness of 6 microns and 24 microns were subsequently designated MK-1 and MK-2, respectively. The transport and electrochemical properties of the DMDAAC modifying film obtained by watering on inorganic glass were independently studied, hereinafter referred to as MA-1. When conducting studies of the developed membranes, individual and mixed solutions of calcium and sodium chlorides were used as working solutions.

Table 1 shows the physicochemical and transport parameters of MF-4SK and MA-1 membrane films found experimentally.

Table 1: Physico-chemical and transport parameters of membrane films MF-4SK and MA-1

Parameters	MF-4SK/MA-1 ($\text{CaCl}_2 + \text{NaCl}$)			
	MF-4SK		MA-1	
	Ca^{2+}	Na^+	Ca^{2+}	Na^+
Hygrometric content, $\text{H}_2\text{O}/g_{\text{sw}}$, %	17,4±2	15,6±2	30,5±2	28,9±2
Electrical conductivity, mSm/cm	1,27±0.1	1,86±0.1	1,98±0.1	1,96±0.1
Diffusion coefficients, $\text{m}^2/\text{s} \cdot 10^{-11}$	1,41	3,93	0,24	0,65
Ion exchange constant	1,56		–	
Non-exchange sorption constant	–		0,73	
Donnan's constant		–	0,23	
The thickness of the diffusion layer, mmol-eq/cm ³	0,82±0.05		0,97±0.05	
he thickness of the diffusion layer, μm	53,3±1			
The thickness of the substrate membrane and the modifying layer, μm	210		6 ¹	
			24 ²	

¹ – modified membrane MK-1

² – modified membrane MK-2

The voltage-voltage characteristics of homogeneous ion-exchange membranes in a rotating membrane disk installation in mixed solutions of sodium chloride and calcium chloride were investigated. Figure 1a shows the general CVC of the studied bilayer homogeneous MF-4SK membranes with a thin ion exchange layer DMDAAC (MK-1 and MK-2 membranes) from different RMD rotation speeds.

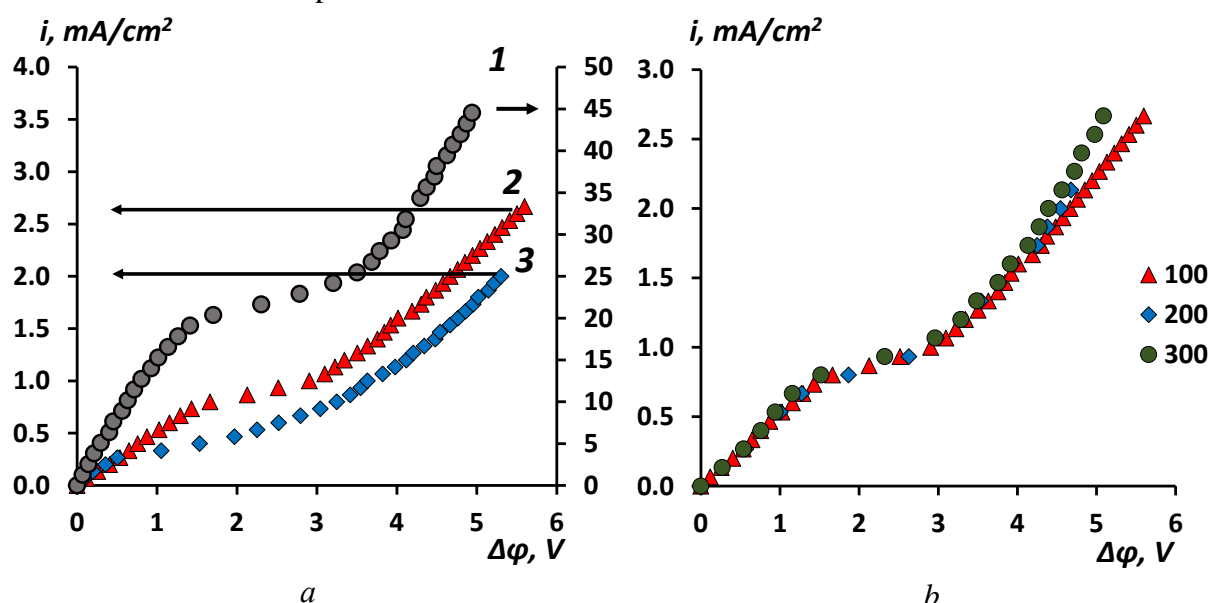
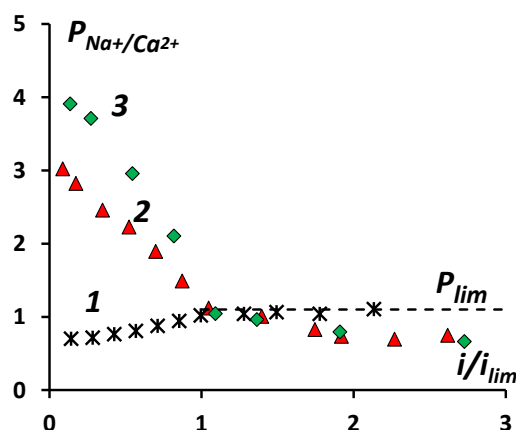


Figure 1. The general CVC of bilayer homogeneous membranes in a solution of 0.015 mol-eq/l NaCl and 0.015 mol-eq/l CaCl₂ at a rotation speed of the membrane disk of 100 rpm (a) and at different speeds of rotation of the membrane disk of the MK-1 membrane (b): 1 – homogeneous membrane MF-4SK; 2 – bilayer membrane MK-1 with a modifying film thickness of 6 μm ; 3 – bilayer membrane MK-2 with a modifying film thickness of 24 μm

As can be seen from Figure 1, the application of a thin anion exchange layer DMDAAC with a thickness of 6 microns to a homogeneous membrane leads to a decrease in the value of the limiting current density from 21 mA/cm² to 0.55 mA/cm². Increasing the anion exchange layer to 24 microns reduces the limiting current density to values < 0.25 mA/cm². This character of the CVC dependence indicates the formation of an intradiffusion limiting current at the boundary of the modifying layer/membrane-substrate. The conducted studies at different speeds of rotation of the membrane disk show that the limiting current density does not depend on the thickness of the diffusion layer for modified homogeneous MF-4SK membranes (Fig. 1b).

Figure 2 shows the specific selectivity from the dimensionless current of superficially modified MF-4SK membranes in a mixed solution of 0.015 mol-eq/l NaCl and 0.015 mol-eq/l CaCl₂ at a rotation speed of the membrane disk of 100 rpm.

As can be seen from Figure 2, the MA-1 membrane forming the selective layer has a higher specific permeability to sodium ions compared to calcium ions. High specific selectivity of two-layer membranes with different charges of polymer matrices of the modifying layer and the substrate membrane can be achieved with a small thickness of the modifying layer. Thus, the application of a 6 μm anion exchange layer of DMDAAC copolymer leads to a more than 3-fold increase in the specific permeability of a single-charge sodium ion relative to calcium ions.



1– homogeneous MF-4SK membrane, 2– MF-4SK membrane with a DMDAAC layer of 6 μm , 3– MF-4SK membrane with a DMDAAC layer of 24 μm

Figure 2. Dependence of the coefficient of specific selectivity of $P_{\text{Na}^+/\text{Ca}^{2+}}$ on the dimensionless density of electric current in a mixed solution of 0.015 mol-eq/l NaCl and 0.015 mol-eq/l CaCl_2 at a rotation speed of the membrane disk of 100 rpm

Applying a thicker modifying layer leads to an increase in specific permeability, but it also leads to a significant decrease in the limiting current density. The dependence of the value of the limiting current density and specific selective permeability on the thickness of the modifying layer is shown in Table 2.

Table 2. Dependence of the value of the limiting current density and specific selective permeability on the thickness of the modifying layer of the studied bilayer membranes.

Membrane	Thickness of the modifying layer, μm	The value of the limiting current, I mA/cm^2	Values of membrane specific selectivity coefficients
MF-4SK	0	17,8	0,77
MK-1	6	0,82	3,41
MK-2	24	0,26	4,78

Thus, the application of a thin anion exchange layer of DMDAAC and methyl methacrylate makes it possible to obtain bilayer charge-selective membranes with increased selectivity to single-charge metal cations. The bilayer membranes developed at this stage of the project can later be used for the selective extraction and concentration of single-charge ions in multiionic solutions of strong electrolytes.

Acknowledgement. This study was supported by the Russian Science Foundation, research project no. 22-13-00439, <https://rscf.ru/project/22-13-00439/>

References

1. Golubenko D.V., Yaroslavtsev A.B. // J. Membr. Sci. 2020. V. 612. P. 118408. <https://doi.org/10.1016/j.memsci.2020.118408>
2. Achoh A.R.; Zabolotsky V.I.; Lebedev K.A.; Sharafan, M.V; Yaroslavtsev A.B.// Membranes and membrane technologies. 2021. V. 3. P. 52-71. doi.org/10.1134/S2517751621010029
3. Bondarev D., Melnikov S., Zabolotsky V. New homogeneous and bilayer anion-exchange membranes based on N,N-diallyl-N,N-dimethylammonium chloride and ethyl methacrylate copolymer // J. Membr. Sci. 2023. V. 675. P. 121510. <https://doi.org/10.1016/j.memsci.2023.121510>

ELECTROCHEMICAL STABILITY OF THE ANION EXCHANGE MEMBRANE MA-41 MODIFIED BY POLY-N,N-DIALLYLMORPHOLINE BROMIDE IN OVERLIMITING CURRENT MODES

Aslan Achoh, Stanislav Melnikov, Denis Bondarev, Mikhail Sharafan

Kuban State University, Krasnodar, Russia, E-mail: achoh-aslan@mail.ru

Introduction

The course of the water dissociation reaction under high-intensity current conditions is one of the undesirable processes in electromembrane systems in the processes of classical electro dialysis. Under such conditions, commercial anion-exchange membranes based on benzyltrimethylammonium can undergo thermal alkaline hydrolysis, followed by degradation of anion-exchange functional groups [1]. An increase in the rate of water dissociation reaction is observed both in the case of chemical decomposition of ion exchange groups and in the destruction of the anion exchange membrane. The conversion of quaternary ammonium bases into tertiary amines in the surface layer of the anion exchange membrane further increases the rate of water dissociation reaction [2].

Experiments

The objects of the study were heterogeneous anion-exchange membranes MA-41 (Shchekinoazot LLC, Russia), and MA-41 membranes modified with poly-N,N-diallylmorpholinium bromide. The membranes were modified in an organic medium (a mixture of N-methylpyrrolidone and concentrated formic acid in a volume ratio of 1:1) according to the methodology described in [3]. The modified membranes were designated as MA-41M.

The electrochemical stability of the MA-41 and MA-41m membranes was studied in a four-chamber electro dialysis chamber with Luggin capillaries and electroplated platinum wires (Figure 1). Electrochemical impedance spectra and volt-ampere characteristics were obtained using an AUTOLAB 100N galvanostat potentiostat. The linear flow rate of the solutions was 0.15 cm/s (9 ml/min) both in desalination chambers and in concentration chambers. In the electrode chambers, the flow rate was set at 0.3 km/s (18 ml/min). The experiments were carried out using 0.02 M NaCl solution in desalination and concentration chambers and 0.05 m Na₂SO₄ solution in electrode chambers.

The current-voltage characteristics of MA-41 and MA-41M membranes are shown in the Figure 2.

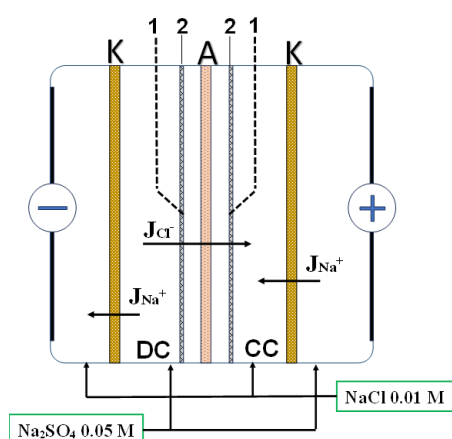


Figure 1. Electrochemical cell circuit: 1 – Luggin capillaries; 2 – platinum electrodes; K – auxiliary cation exchange membranes MK-40; A – anion exchange membrane MA-41 or MA-41M, DC – desalination channel, CC – concentration channel.

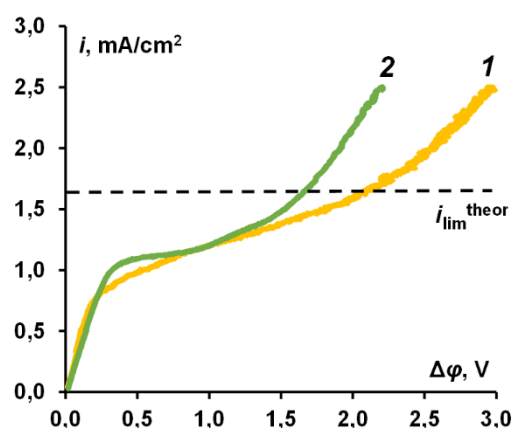


Figure 2. The general CVC of the membranes are: membrane 1 – MA-41; membrane 2 – MA-41 M; the dotted line indicates the theoretical maximum current density calculated by the Leveque equation

The results obtained show that the use of the modifier leads to an increase in the limiting current density in the electromembrane system. The maximum current density for the intact membrane MA-41 is 0.8 mA/cm², while for the membrane MA-41M it is 1.1 mA/cm². In both cases, the obtained values of the limiting current density are significantly lower than the calculated theoretical value, which is 1.6 mA/cm².

A significant discrepancy between the experimental and theoretical limiting current densities for the MA-41 membrane is explained by the heterogeneity of the membrane surface, where non-conductive sections of polyethylene reduce the area of the active surface. The fact that the current limit value for the modified membrane is also significantly lower than the theoretical value indicates that poly-N,N-diallylmorpholine does not form a continuous film on the surface of the substrate membrane. Thus, modification of the MA-41 membrane does not lead to homogenization of the membrane surface. It is possible that the modifier is fixed on the surface of the ion exchanger particles, which protrude from the surface of the modified membrane.

The intensity of water dissociation reaction at the membrane/solution interface can be estimated by observing the transfer of OH⁻ ions through the membrane. In [3], the transport numbers of hydroxide ions through both the original and modified membranes were determined under various current modes. The results indicated that the modified membrane exhibited low catalytic activity in the water dissociation reaction.

By comparing the intensity of water dissociation at the inter-face of the modified membrane/solution before and after resource tests, the stability of the modified membrane can be assessed. The electrochemical impedance method as the most effective and informative approach for evaluating the quality and properties of membranes. Different parts of the electrochemical impedance spectrum correspond to different physical and chemical processes occurring in the electromembrane system when it is exposed to a weak alternating current.

At current densities below the limiting current, several semicircles in different frequency ranges are observed in the electrochemical impedance spectrum (Figure 3, curve 1). The Warburg impedance is due to the change in electrolyte concentration in an electrically neutral solution under the action of varying current and potential difference.

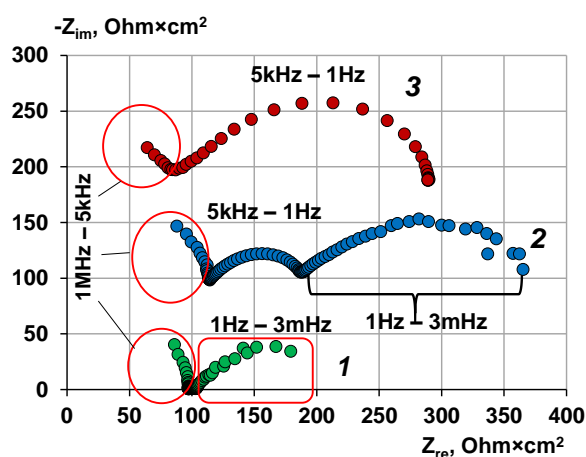


Figure 3. The spectra of the electrochemical impedance of the MA-41M membrane are presented in Nyquist coordinates at different polarizing current densities: 1 – low current mode ($i = 0.9i_{lim}$); 2 – limit current mode ($i = 1.0i_{lim}$); 3 – high current mode ($i = 4.0i_{lim}$), the numbers indicate the frequency ranges.

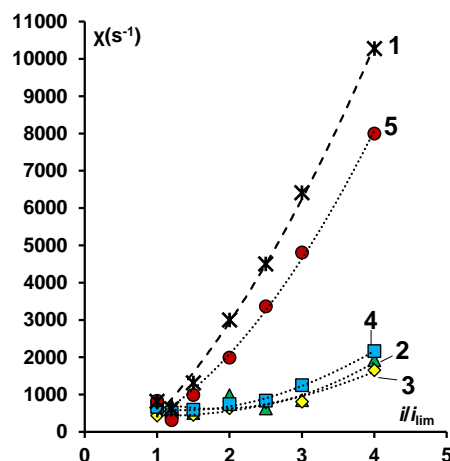


Figure 4. Dependence of water dissociation reaction rate constant on dimensionless current density and time of resource tests: 1 – original MA-41 membrane; 2 – modified MA-41M membrane; 3 – MA-41M after 10 h of testing; 4 – MA-41M after 25 h of testing; 5 – MA-41 after 50 h of testing.

In the case of the limiting current density (Figure 3, curve 2) a new semicircle appears in the mid-frequency region (5 kHz – 1 Hz). The emergence of processes in this frequency range for systems with ion-exchange membranes is attributed to the process of the water dissociation

reaction with the participation of ionogenic groups of the membrane, that is described by the Gerischer impedance. An increase in the current density leads to a decrease in the concentration of all ions present at the membrane/solution boundary, which also leads to an increase in the potential drop. However, the concentration recovery in the boundary layer is not only due to diffusion but also due to chemical reaction. Since the chemical reaction proceeds at a high rate, the characteristic frequencies of the Gerischer impedance are higher than those of the Warburg impedance.

When the electromembrane system is in an over-limiting current mode, the Warburg impedance disappears in the low-frequency region (below 1 Hz) and the complete dominance of the Gerischer impedance is observed (Figure 3, curve 3).

The values of the water dissociation reaction rate constant are shown in Figure 4. From Figure 8, it is evident that with an increase in current density ($i_{lim} \rightarrow 4i_{lim}$), there is an increase in the water dissociation reaction rate constant for all studied membranes. The intensity of the water dissociation reaction is influenced not only by the catalytic activity of functional groups but also by the strength of the electric field. The later is determined by the potential difference across the membrane/solution interface and exponentially increases with increase of polarizing current density. As a consequence, the water dissociation reaction rate constant increases, leading to an increase in the intensity of the water dissociation reaction at the membrane/solution interface for both the MA-41 and MA-41M membranes.

However, on the pristine MA-41 membrane, water dissociation occurs more intensely, as indicated by the steeper dependence of the water dissociation reaction rate constant on the dimensionless current density (Figure 4, curves 1 and 2). The water dissociation reaction rate constant on the modified membrane at $i = 4i_{lim}$ is 1650 s^{-1} , while on the MA-41 membrane under the same conditions it is 10275 s^{-1} . The higher intensity of the water dissociation reaction on the initial membrane can be attributed to the presence of catalytically active secondary and tertiary amino groups in the surface layer of the anion-exchange membrane.

The data shown in the Figure 8 confirms the low intensity of the water dissociation reaction at the MA-41M /solution interface, which persists during the initial 25 h of the resource tests. However, it was observed that after 50 h of highintensity electro dialysis, the intensity of the water dissociation reaction at the MA-41M /solution interface increases almost to the level exhibited by the pristine MA-41 membrane.

The deterioration of electrochemical characteristics of the modified membrane can occur due to the following processes: 1) the destruction of quaternary ammonium groups of the polymer modifier (poly-N,N-diallylmorpholine), leading to the formation of secondary and tertiary amines that accelerate the water dissociation process; 2) the desorption of poly-N,N-diallylmorpholine from the surface of the modified membrane, resulting in the restoration of the surface layer to its initial state.

Acknowledgement. This research was funded by the Ministry of Science and Higher Education of the Russian Federation, project number FZEN-2023-0006.

References

1. *Bauer B, Strathmann H, Effenberger F.* Anion-exchange membranes with improved alkaline stability // *Desalination.* 1990. V. 79. P.125–144. doi:10.1016/0011-9164(90)85002-R
2. *Zabolotskiy VI, But AY, Vasil'eva VI, Akberova EM, Melnikov SS.* Ion transport and electrochemical stability of strongly basic anion-exchange membranes under high current electro dialysis conditions // *J. Membr. Sci.* 2017. V. 526. P. 60–72. doi:10.1016/j.memsci.2016.12.028
3. *Bondarev D., Melnikov S., Zabolotsky V.* New homogeneous and bilayer anion-exchange membranes based on N,N-diallyl-N,N-dimethylammonium chloride and ethyl methacrylate copolymer // *J. Membr. Sci.* 2023. V. 675. P. 121510. <https://doi.org/10.1016/j.memsci.2023.121510>

SEA WATER DESALTING SYSTEM BASED ON HYBRIDIZATION OF NANOFILTRATION AND REVERSE OSMOSIS METHODS

Jahan Arif Ahmadova

Azerbaijan State Oil and Industry University, Baku, Azerbaijan

E-mail: ahmedova_cahan1975@mail.ru

Introduction

Fresh water scarcity has become a serious problem in many regions of the world. This problem is mainly aggravated with population growth and industrial development. Measures are being taken to solve this problem. Desalination of this water is considered as a radical way to solve this problem in regions with large reserves of mineralized water (sea, ocean, etc.).

One of the pressing problems of our time is the desalination of salt waters of the seas and oceans, which account for 97,5% of the Earth's waters. Among the desalting methods developed for this purpose, the most widely used are membrane methods, in particular the reverse osmosis (RO) method, which, globally, accounts for up to 65% of purified water [1]. The essence of the method is that sea water under pressure passes through a semi-permeable membrane, the pores of which allow predominantly water molecules to pass through and retain the vast majority of impurities. An important condition for increasing the efficiency of the RO method is to prevent the formation of various deposits on the membrane surface, mainly CaCO_3 and CaSO_4 , which are formed from supersaturated concentrates. According to the literature, one of the ways to achieve this condition is preliminary nanofiltration (NF) purification of seawater mainly from divalent ions: Ca^{2+} , Mg^{2+} and SO_4^{2-} [2]. In relation to these ions the selectivity of nanomembranes is quite high (74,2÷98,6%). Therefore, in the process of nanofiltration water is softened, desulfatized and partially desalinated. NF membranes are more permeable and less selective than RO membranes and are less prone to fouling. The choice of desalination technology depends on the quality of source water, availability of energy sources, plant capacity and several other factors. The present work is devoted to the study of seawater desalination system based on hybridization (combination) of NF and RO methods.

Research methodology

The studies were carried out using the example of Caspian Sea water with the following indicators, mg/dm^3 : $\text{Ca}^{2+}=321$, $\text{Mg}^{2+}=730$, $\text{Na}^+=3175$, $\text{Cl}^-=5034$, $\text{SO}_4^{2-}=3264$, $\text{HCO}_3^-=244$, TDS (Total Dissolved Solids)=12768; $\text{pH}=8,2$.

The specialized computer program IMSDesign Hydranautics was used [3]. Hybrid systems using two brands of membranes at the RO stage were studied: recommended for desalting waters with a salt content of 10÷15 g/dm^3 (CPA5MAX) and ocean waters with a salt content of 35 g/dm^3 (SWC4-LD). Provision was made for recycling the RO stage concentrate into the NF feed water (Fig.1).

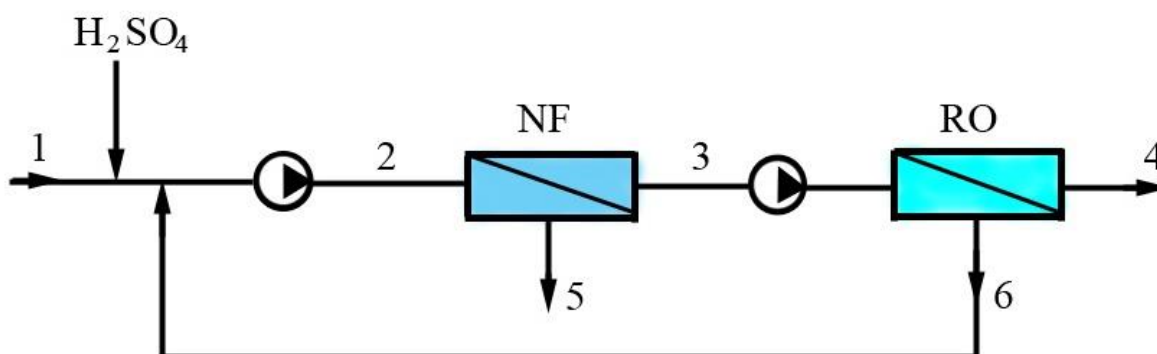


Figure.1. Schematic diagram of seawater desalting

According to the operating principle of the proposed scheme (Fig.1), clarified water from the Caspian Sea (1) is supplied to the hybrid NF+RO desalination system. The source water, after

sulfuric acid introduction, is mixed with RO concentrate (6). The resulting mixture (2) is pumped to the NF module. The NF concentrate (5) is discharged back to the sea, and the permeate (softened water) (3) is fed as feed water by a high-pressure pump to the RO module, where it is divided into two streams: permeate (desalinated water) (4) and concentrate (6).

The studies were carried out on the example of a system with a capacity of 35 m³/h for desalting water (permeate). To prevent the formation of CaCO₃ and CaSO₄ deposits at the NF stage, it was necessary to acidify the source water and introduce anti-scale agents into it. The supersaturation of the RO concentrate, changes in ion concentrations, salt content (TDS) of permeate and concentrate, and other indicators at each stage of processing were assessed. The permeate conversion values were assumed to be 80% at the NF stage and 70% at the RO stage. Thus, a study was carried out on two systems differing in the brands of membranes used at the RO stage: NF1-RO1 and NF2-RO2. In the first case, a membrane of the CPA5MAX brand was used, in the second case - SWC4-LD. At the NF stage, the same membrane was used - ESNA-LF2-LD.

Research results and discussion

Figure 2 shows data on the TDS values of the flows of the systems under study. It follows from the graph that due to the use of the same membrane, for both systems the TDS of NF permeate is on average 6300 mg/dm³, and the TDS of concentrate is on average 48300 mg/dm³. That is, the TDS of sea water is reduced by 2 times. The use of the more selective SWC4-LD membrane in the RO stage is reflected in the process performance. Thus, deep desalting with a permeate TDS of about 17 mg/dm³ is predicted when using the specified membrane (SWC4-LD). And in the case of the CPA5MAX membrane, the expected TDS value is 110 mg/dm³. At the same time, the TDS of the concentrates differs by only 0,5%

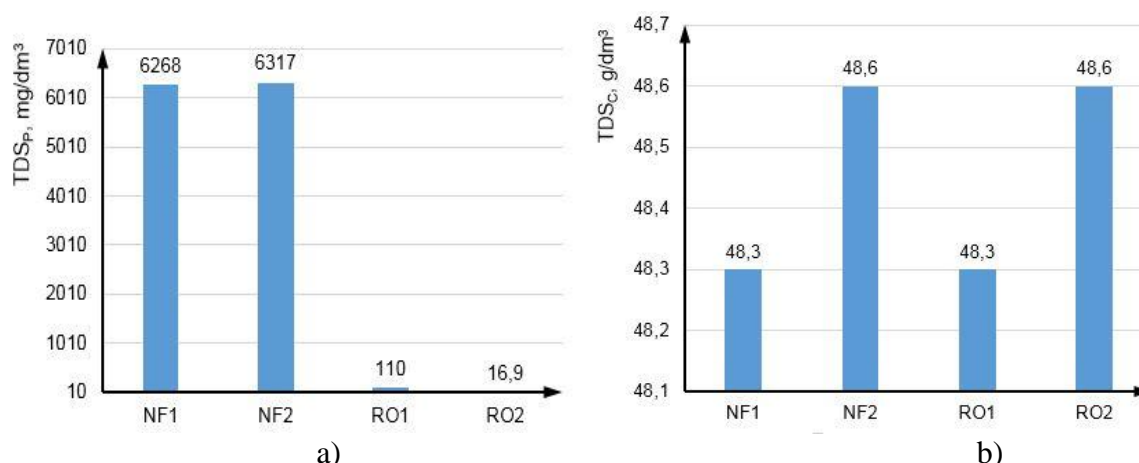


Figure 2. TDS values for permeates and concentrates. a) NF1-RO1; b) NF2-RO2

The use of a SWC4-LD membrane at the RO stage is also preferable in terms of reducing the boron concentration from 3,5 mg/dm³, characteristic of Caspian water, to the values standardized for drinking water: ≤0,5 mg/dm³. This circumstance and a number of key technological indicators are reflected in the table 1 below.

As follows from the table relatively low selectivity characteristic for membrane CPA5MAX contributes to boron reduction only up to 1,5 mg/dm³, which exceeds the standard value. In the NF concentrate the supersaturation of CaSO₄ exceeds 200%, therefore, in accordance with the programme recommendations, dosing of antiscaling agent into the source water is envisaged.

Table 1. Main technological indicators of the NF-RO hybrid desalting system

No	Indicators	Dimension	NF1-RO1	NF2-RO2
1	Bor	mg/dm ³	2,7±1,5	3,0±0,4
2	Supersaturation in CaSO ₄	%	212±6	211±6
3	Permeate hardness	m-eq/dm ³	9,9±0,0035	9,92±0,00027
4	Electricity consumption	kW·h/m ³	2,79	3,64
5	Permeate pH	-	5,8±5,1	5,8±4,2
6	Dose of sulfuric acid	mg/dm ³	131,7	131,7

Taking into account the uniqueness of the Caspian Sea, for ecological reasons, we recommend using so-called "green" antiscalants, the development of which has recently received much attention [4].

Low concentration of Ca and SO₄ ions in NF permeate (RO feed water) provides reliable protection of RO membranes from calcium sulphate precipitation – supersaturation concentrate is only 6%. The use of sulfuric acid with a dose of about 130 mg/dm³ ensures a value of the Langelier index close to zero, which eliminates the precipitation of CaCO₃ on the membranes. The achieved low values of permeate hardness (0,3÷3,5 μg-eq/dm³) make it possible to use it in many industries, including thermal power engineering, semiconductor production, chemical industry, etc.

References

1. *Sergio G. Salinas-Rodriguez et al.* Seawater Reverse Osmosis Desalination. // Assessment and Pre-treatment of Fouling and Scaling. IWA PUBLISHING, London, 2021, 301 p.
2. *Dong Zou et al.* Development of lower cost seawater desalination process using NF technologies – A review. // Journal of Desalination 376, 2015, P.109–116.
3. <https://membranes.com/solutions/software-imsdesign/>
4. *Konstantin Popov et al.* A Comparative Performance Evaluation of Some Novel (Green) and Traditional Antiscalants in Calcium Sulfate Scaling. // Advances in Materials Science and Engineering. 2016, P.1-10.

SURFACE AND CROSS-SECTION MORPHOLOGY OF HETEROGENEOUS RALEX MEMBRANES WITH DIFFERENT FRACTIONS OF SULFONATED CATION EXCHANGE RESIN

Elmara Akberova, Vera Vasil'eva

Voronezh State University, Voronezh, Russia, *E-mail: viv155@mail.ru*

Introduction

Theoretical and experimental works [1-3] show the possibility of intensifying mass transfer in an electromembrane system by improving the surface morphology of ion exchange membranes by their modification. The use of membranes with optimized surface morphology in the process of electrodialysis for the demineralization of natural waters and technological solutions creates the prerequisites for a significant increase in the efficiency of these processes in limiting and overlimiting current modes. The purpose of the work was to study the effect of changing the content of ion exchange resin in experimental heterogeneous Ralex membranes (MEGA a.s., Czech Republic) on their structural and physicochemical properties.

Experiments

The objects of the study were experimental samples of heterogeneous Ralex membranes ("MEGA" a.s., Czech Republic), differing in the ratio of sulfonated cation-exchanger and inert binder. During the manufacture of membranes, the fraction of ion-exchanger varied from 45 to 70 wt. %. All samples of the studied membranes were subjected to salt pretreatment by keeping them in sodium chloride solutions of different concentrations.

The physicochemical properties of the studied membrane samples were determined according to standard methods for testing ion exchange membranes. Scanning electron microscopy (SEM) was used to visualize and quantify the structural characteristics of the membrane surface and cross-section. A JSM-6380 LV microscope (JEOL, Japan) with an INCA 250 microanalysis system was used. The quantitative estimation of fraction and size of ion-exchangers (*S*) and macropores (*P*) was carried out with the help of the authors' software by using the digital processing of SEM images [4]. Equipping a scanning electron microscope with an energy-dispersive analyzer of elemental composition made it possible to study the nature of the distribution of elements on the surface and in the section of experimental membranes using electron probe X-ray microanalysis. The studies were carried out on air-dry membrane samples.

Results and Discussion

Information on the chemical composition of the membrane surface and cross-section, obtained by mapping the elemental composition, is presented in Fig. 1. Color coding for the X-ray images made it possible to combine data from several elements in one image. In the resulting images, areas colored red and green indicate the presence of sulfur and oxygen, respectively. They correspond to sections of the ion-exchanger containing fixed sulfogroups. The inert regions of polyethylene, which predominantly contain carbon atoms, are blue. It was revealed that with an increase in the content of cation exchange resin in the membranes on the surface and in the section of the samples, an increase in the content of sulfur and oxygen was observed by more than 2 times.

Ion-exchangers on the surface and in the section of all studied Ralex membranes have different shapes and are located randomly. An analysis of the radial distribution of ion exchange areas shows that their sizes both on the surface and in the cross-section of membrane samples, regardless of the content of ion-exchange resin, are 1-36 μm . In this case, the maximum on the distribution curve of all studied Ralex CM membranes is in the region of 1-2 μm . The value of the average radius of ion-exchanger particles when changing the ratio of the ion exchange and inert phases remains constant and amounts to $2.20 \pm 0.07 \mu\text{m}$ for the surface and $2.68 \pm 0.04 \mu\text{m}$ for the membrane cross-section.

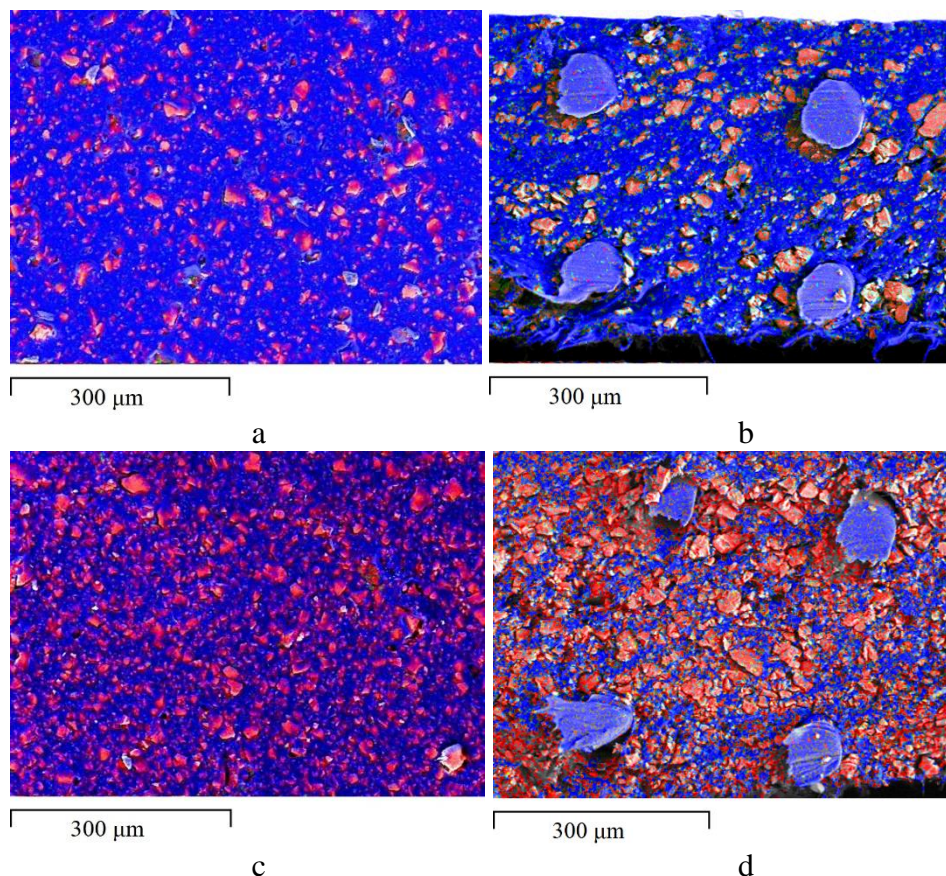


Figure 1. Composite X-ray maps of the distribution of sulfur and carbon elements on the surface (a, c) and in the section (b, d) of the Ralex SM Pes membrane with an ion exchange resin content of 45 (a, b) and 70 (c, d) wt % at a magnification of 200. S element corresponds to red color, C element to blue color.

Information about an increase in the content of ion-exchanger in membranes is consistent with the results of studies of surface and cross-section morphology. It has been established that with an increase in the content of cation exchange resin in the membrane composition from 45 to 70 wt % there is an increase in the proportion of the cation-exchanger by 80% and 40% on the surface and in the membrane section, respectively (Fig. 2a). In this case, the proportion of macropores increases by 1.7 and 2.0 times on the surface and in the cross section, respectively (Fig. 2b).

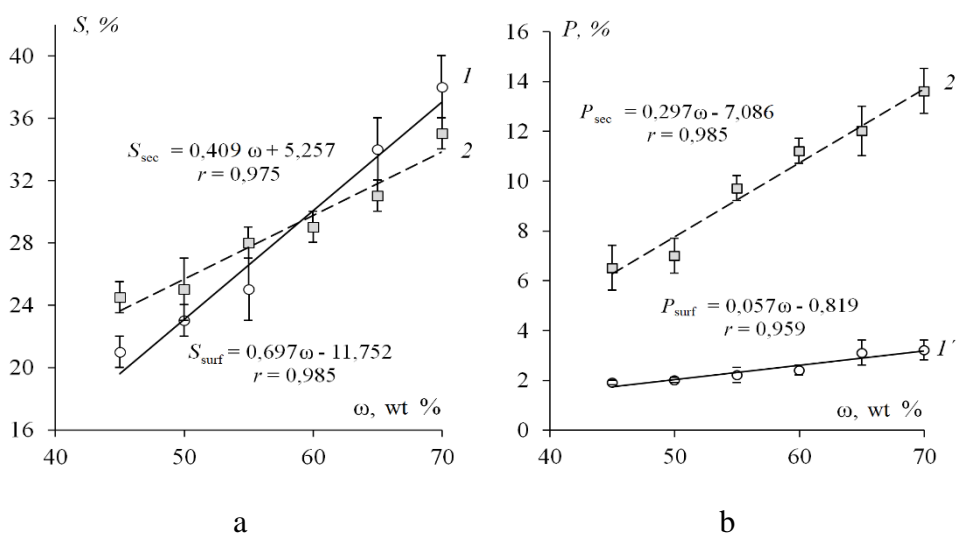


Figure 2. Dependence of the proportion of ion-exchanger (a) and macropores (b) on the surface (1, 1') and in the cross-section (2, 2') of swollen samples of experimental membranes on the content of ion exchange resin ω ; r is correlation coefficient.

When changing the ratio of the conductive phase and the inert binder, the values of the average radius of macropores on the surface and in the section of the samples were constant and, respectively, amounted to $1.9 \pm 0.1 \mu\text{m}$ and $2.2 \pm 0.2 \mu\text{m}$.

With an increase in the proportion of the conductive phase, the average value of the length of non-conductive areas between the particles of the ion exchange resin decreases almost by half and amounts to 4.9 and 2.5 μm for membranes with a minimum (45 wt %) and maximum (70 wt %) ion-exchanger content, respectively. Thus, the surface structure of the membranes becomes electrically more homogeneous with increasing ion exchange resin content.

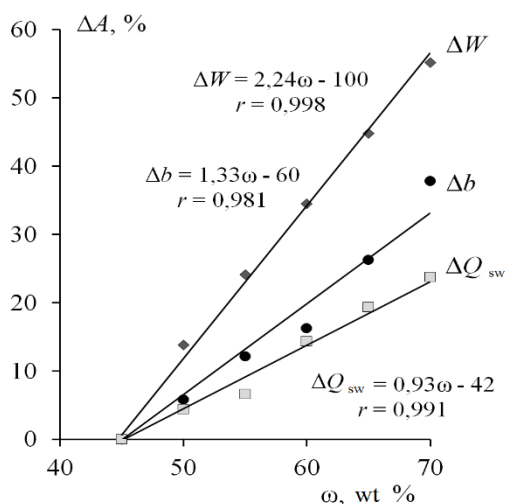


Figure 3. Dependences of relative changes in total exchange capacity (Q_{sw}), moisture content (W) and thickness (b) on the content of cation exchange resin in experimental Ralex membranes; r is correlation coefficient.

A comparative analysis of the properties of experimental cation exchange membranes with different mass fractions of ion exchange resin revealed the influence of changes in the structural characteristics of the samples on their physicochemical properties. It has been established that with an increase in the content of ion exchange resin from 45 to 70 wt %, the total exchange capacity of membranes increases by 24% (Fig. 3), while its value for the membrane with the maximum content of ion-exchanger is $2.24 \pm 0.05 \text{ mmol/g}_{sw}$. An increase in the proportion of the conductive phase is accompanied by an increase in moisture content and membrane thickness by 55 and 38%, respectively.

The maximum increase in the moisture content of membrane samples, revealed by a comparative analysis of relative changes in physicochemical characteristics, is due to a significant increase in porosity in the membrane cross-section compared to other structural characteristics (Fig. 2b) with an increase in the proportion of ion exchange particles in the composition.

Acknowledgements. The research results were partially obtained using the equipment of the Centre for Collective Use of Scientific Equipment of Voronezh State University. URL: <https://ckp.vsu.ru>

References

1. Zabolotsky V.I., Novak L., Kovalenko A.V., Nikonenko V.V., Urtenov M.H., Lebedev K.A., But A.Yu. // Petroleum Chemistry. 2017. 57. P. 779-789.
2. Nebavskaya K.A., Butylskii D.Yu., Moroz I.A., Nebavsky A.V., Pismenskaya N.D., Nikonenko V.V. // Petroleum Chemistry. 2018. Vol. 58. P. 780-789.
3. Vasil'eva V.I., Akberova E.M., Zabolotsky V.I., Novak L., Kostylev D.V. // Petroleum Chemistry. 2018. Vol. 58. P. 1133-1143.
4. Akberova E. M., Vasil'eva V. I. // Electrochemistry Communications. 2020. 111. Art. No 106659.

DEVELOPMENT OF HIGHLY EFFICIENT ELECTROCATALYSTS FOR PROTON EXCHANGE MEMBRANE FUEL CELLS: A COMPROMISE BETWEEN ACTIVITY AND STABILITY

Anastasia Alekseenko, Kirill Paperzh, Angelina Pavlets, Elizaveta Moguchikh, Julia Bayan, Ekaterina Kozhokar, Yana Astravukh, Julia Pankova, Vladimir Guterman
Southern Federal University, Rostov-on-Don, Russia, E-mail: an-an-alekseenko@yandex.ru

Introduction

Low-temperature fuel cells with a proton exchange membrane (PEMFC) are an important part of the intensively developing hydrogen power engineering [1-3]. Electrocatalysts are the key component of such electrochemical devices [1-2]. In almost all commercial PEMFC platinum or Pt-M nanoparticles, anchored on micro/nanoparticles of carbon supports, are used as catalysts for accelerating current-forming reactions (oxygen electroreduction, hydrogen electrooxidation). A number of requirements are put forward for electrocatalysts for PEMFC, the main of which are increased activity in current-generating reactions and long-term operation. The oxygen electrode is of particular importance for ensuring the efficient operation of PEMFC, since the oxygen reduction reaction (ORR) is accompanied by strong polarization. In addition, the processes of degradation of platinum and the catalyst as a whole are most pronounced at the cathode.

A significant increase in the activity of cathode electrocatalysts in ORR is associated with the need to move to more complex bimetallic systems. It is possible to increase the corrosion-morphological resistance of an electrocatalyst through the development of new carbon and composite supports. The production of electrocatalysts combining increased activity and durability is still an urgent task in hydrogen energy.

Review

There are several approaches to increasing the activity and durability of electrocatalysts related to the control of their structural and morphological characteristics. Obtaining electrocatalysts with increased uniformity of the spatial distribution of nanoparticles on the surface of the carbon support and their narrow size dispersion is one of the approaches to obtain highly efficient materials (Fig. 1). The use of platinum NPs as stabilizing agents in the process of liquid-phase synthesis of NPs makes it possible to slow down their growth and exclude aggregation. An important feature of this approach is the use of stabilizing agents that do not subsequently pollute the electrocatalyst [3]. The active surface area of electrocatalysts, with a uniform distribution of nanoparticles and a narrow size distribution, is characterized by high values (more than $80 \text{ m}^2/\text{g}(\text{Pt})$ at a load of 20% Pt) [3].

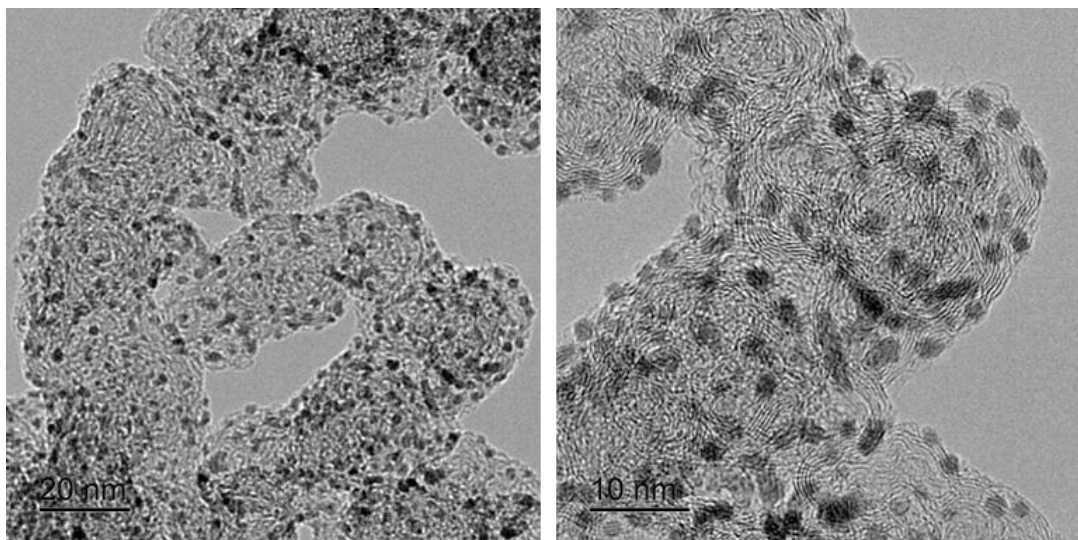


Figure 1. TEM-images of Pt/C samples with 20% Pt content.

One way to influence the morphological characteristics of electrocatalysts is to use a modified carbon support. Our recent studies demonstrate the possibility of increasing the functional characteristics of Pt/C based on a nitrogen-doped carbon support [4]. It is believed that additional active centers for the electroreduction of oxygen (surface fragments containing “pyrrole” and “pyridine” nitrogen atoms) have a positive effect on the activity of catalysts [5].

The electrocatalyst obtained on the basis of an N-doped carbon support Pt is characterized by the uniform distribution of nanoparticles (Fig. 2). In photographs of the Pt/C-N material obtained using HAADF-STEM, not only platinum nanoparticles are visible, but also individual Pt atoms and their accumulations in the form of clusters of several atoms are clearly visible. Pt atoms/clusters appear as bright white spots against the background of low-contrast (gray) substrate material.

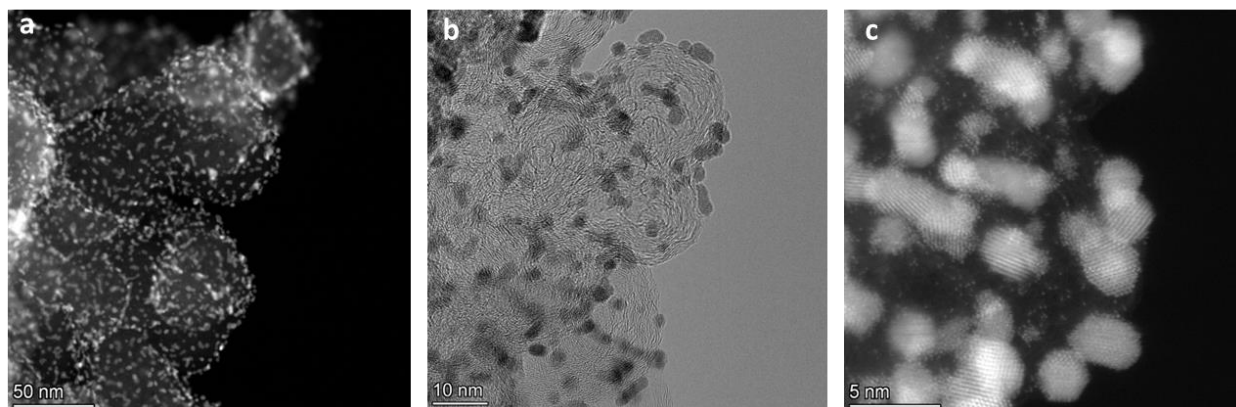


Figure 2. STEM-images (a), TEM-images (b) and HAADF-STEM images of Pt/C-N samples with 40% Pt content on N-doped carbon support.

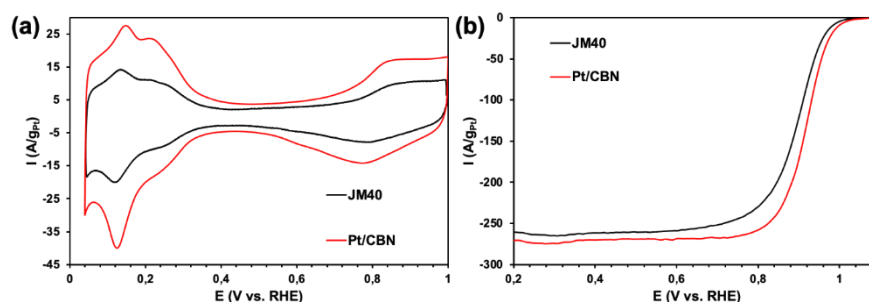


Figure 3. Cyclic voltammograms (a) of materials Pt/C-N (red) and HiSPECS4000 (Johnson MATthey) (black). Electrolyte HClO_4 , saturated with Ar, 20 mV/s. Linear voltammograms of ORR (b) materials Pt/C-N (red) and HiSPECS4000 (black). Electrolyte HClO_4 , saturated with O_2 , 20 mV/s. The RDE rotation speed is 1600 rpm.

The resulting Pt/CN-N catalyst is characterized by a higher ESA value and activity in the oxygen reduction reaction (ORR) compared to a commercial analogue (Fig. 3a, b). The ESA value of the Pt/C-N sample ($107 \text{ m}^2/\text{g}$) is $50 \text{ m}^2/\text{g}$ higher than that of the commercial HiSPEC4000 ($57 \text{ m}^2/\text{g}$).

The preparation of catalysts based on platinum doped with some d-metals (Ni, Co, Cu) is one of the current ways to increase activity in ORR [6, 7]. The atoms of the alloying component are able to increase the activity of NPs due to a number of effects: the formation of a new electronic structure of the metal; a decrease in the interatomic distance in a metal lattice, which facilitates the adsorption of oxygen molecules; surface development; forming a thin shell of platinum on the surface of the alloy particles; increasing the resistance of platinum to oxidation. The compositionally inhomogeneous architecture of such two-component Pt-M nanoparticles (“Pt-shell – M-core”), along with the size and shape of nanoparticles, can significantly affect not only the activity, but also the durability of catalysts (Fig. 4). The PtCu/C-N electrocatalyst we obtained, characterized by increased activity in the ORR, combines bimetallic nanoparticles with a special microstructure and an N-doped carbon support.

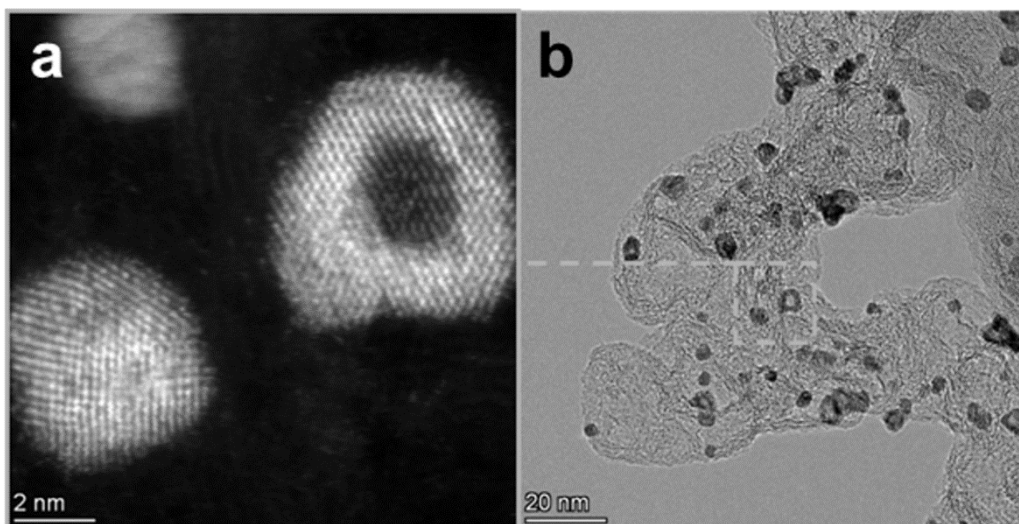


Figure 4 HAADF-STEM (a) and TEM (b) images of the PtCu/C-N catalysts in the as-prepared state.

The use of the approaches described above to control the structural and morphological parameters of electrocatalysts makes it possible to significantly improve their functional characteristics. An urgent applied problem implemented in our study is the use of easily scalable methods for the synthesis of materials with a reduced content of platinum, which at the same time allow achieving the indicated morphological characteristics.

Acknowledgement. This research was financially supported by the Ministry of Science and Higher Education of the Russian Federation (State assignment in the field of scientific activity №FENW-2023-0016), implemented at the Southern Federal University.

References

1. *Filippov S.P., Yaroslavtsev A.B.*, Hydrogen energy: development prospects and materials // *Russ. Chem. Rev.* 2021. V. 10. P. 627–643.
2. *Moriau L., Hrnji A., Pavli A., Kamsek A., Gatalo M., Hodnik N.* Resolving the nanoparticles' structure-property relationships at the atomic level: a study of Pt-based electrocatalysts // *iScience.* 2021. V. 24. P. 102102.
3. *Paperzh K., Alekseenko A., Volochaev V., Pankov I., Safronenko O., Guterman V.* Stability and activity of platinum nanoparticles in the oxygen electroreduction reaction: is size or uniformity of primary importance? // *Beilstein J. Nanotechnol.* 2021. V. 12. P. 593-606.
4. *Moguchikh E.A., Paperzh K.O., Alekseenko A.A., Gribov E.N., Tabachkova N.Yu., Maltseva N.V., Tkachev A.G., Neskromnaya E.A., Melezhik A.V., Butova V.V., Safronenko O.I., Guterman V.E.* Platinum Nanoparticles Supported on Nitrogen-Doped Carbons as Electrocatalysts for Oxygen Reduction Reaction // *J. Applied Electrochem.* 2022. V. 52. P. 231–246.
5. *Zhou, Y., Neyerlin, K., Olson, T. S., Pylypenko, S., Bult, J., Dinh, H. N., ... O'Hayre, R.* Enhancement of Pt and Pt-alloy fuel cell catalyst activity and durability via nitrogen-modified carbon supports // *Energy & Environmental Science.* 2010. V. 3. P. 1437.
6. *Pavlets A., Alekseenko A., Tabachkova N., Safronenko O., Nikulin A., Alekseenko D., Guterman V.* A novel strategy for the synthesis of Pt–Cu uneven nanoparticles as an efficient electrocatalyst toward oxygen reduction // *Int. J. Hydrogen Energy.* 2021. V. 27. P. 5355-5368.
7. *Kirakosyan S., Alekseenko A., Guterman V., Gerasimova E., Nikulin A.* De-Alloyed PtCu/C Catalysts of Oxygen Electroreduction // *Russ. J. Electrochem.* 2019. V. 55. P. 1258–1268.

PRODUCTION OF COMMERCIAL ELECTROCATALYSTS FOR LOW TEMPERATURE FUEL CELLS

Danil Alekseenko, Vladimir Guterman, Anastasia Alekseenko, Sergey Belenov
Southern Federal University, Rostov-on-Don, Russia, E-mail: alekseenko-da@yandex.ru

Introduction

A critical component of proton exchange membrane fuel cells are porous catalytic layers in which electrochemical reactions occur that produce electricity and water from hydrogen and oxygen. Carbon-supported platinum (Pt/C) catalysts are widely used in anode and cathode of low temperature fuel cells. The actual problem of such catalysts - reducing the content of precious platinum while maintaining high activity and stability, is solved both by selecting the optimal carbon carrier and by controlling the size, shape, size and spatial distribution of platinum nanoparticles. In this paper, we present the results of joint studies of Pt/C electrocatalysts obtained at R&D LLC PROMETHEY (Russia) and studied at the Laboratory of Nanostructured Materials for Electrochemical Energy of the Southern Federal University.

Review

Nanostructured Pt/C-electrocatalysts of the PM series were obtained by liquid-phase synthesis methods according to the original technology of Prometheus R&D, which is in the know-how mode. As a carbon support in the preparation of catalysts containing 5–70 wt % Pt, carbon black Vulcan XC72 (Cabot Co.) was used, for the catalyst with a platinum load more than 60 wt % – KetjenblackEC 300J.

All produced catalysts are characterized by small nanoparticle sizes and uniform distribution of nanoparticles over the surface of the carbon support [1].

Figure 1a shows a TEM photograph of fragments of the PM20, PM40 and PM60 electrocatalysts surface, indicating a small size of Pt NPs. The photographs of all the samples show the presence of a small number of aggregates about 4–5.5 nm in size (Fig. 1d, f). Among the electrocatalysts under study, the largest nanoparticles are characterized by samples with a high metal loading: PM60 (60 wt % Pt) and PM70 (70 wt % Pt) (Table 1).

Table 1. Structural and functional characteristics of the production of PM_X series catalysts and commercial catalysts

Products	Pt loading, % mass.	Average size of Pt (TEM), nm	ESA, m ² /g(Pt)
PM5	5	2.0 ± 0.2	105 ± 10
PM10	10	2.5 ± 0.2	100 ± 10
PM20	20	2.5 ± 0.2	80 ± 8
PM30	30	2.8 ± 0.3	75 ± 7
PM40	40	3.2 ± 0.3	70 ± 7
PM60	60	3.5 ± 0.3	60 ± 6
PM70	70	5.0 ± 0.5	50 ± 5

High ESA values are due not so much to the small size of platinum nanoparticles as to the uniformity of their spatial distribution (weak aggregation) and high accessibility with respect to the electrolyte and reagent (Fig. 1, Table 1). We believe that the positive structural features of the PM series catalysts are due to the use of colloidal chemistry methods in the technology of their synthesis, developed at Prometheus R&D LLC.

The following presents the results of measuring the PM40 sample as part of a membrane-electrode assembly in comparison with commercial imported analogues (Fig. 2).

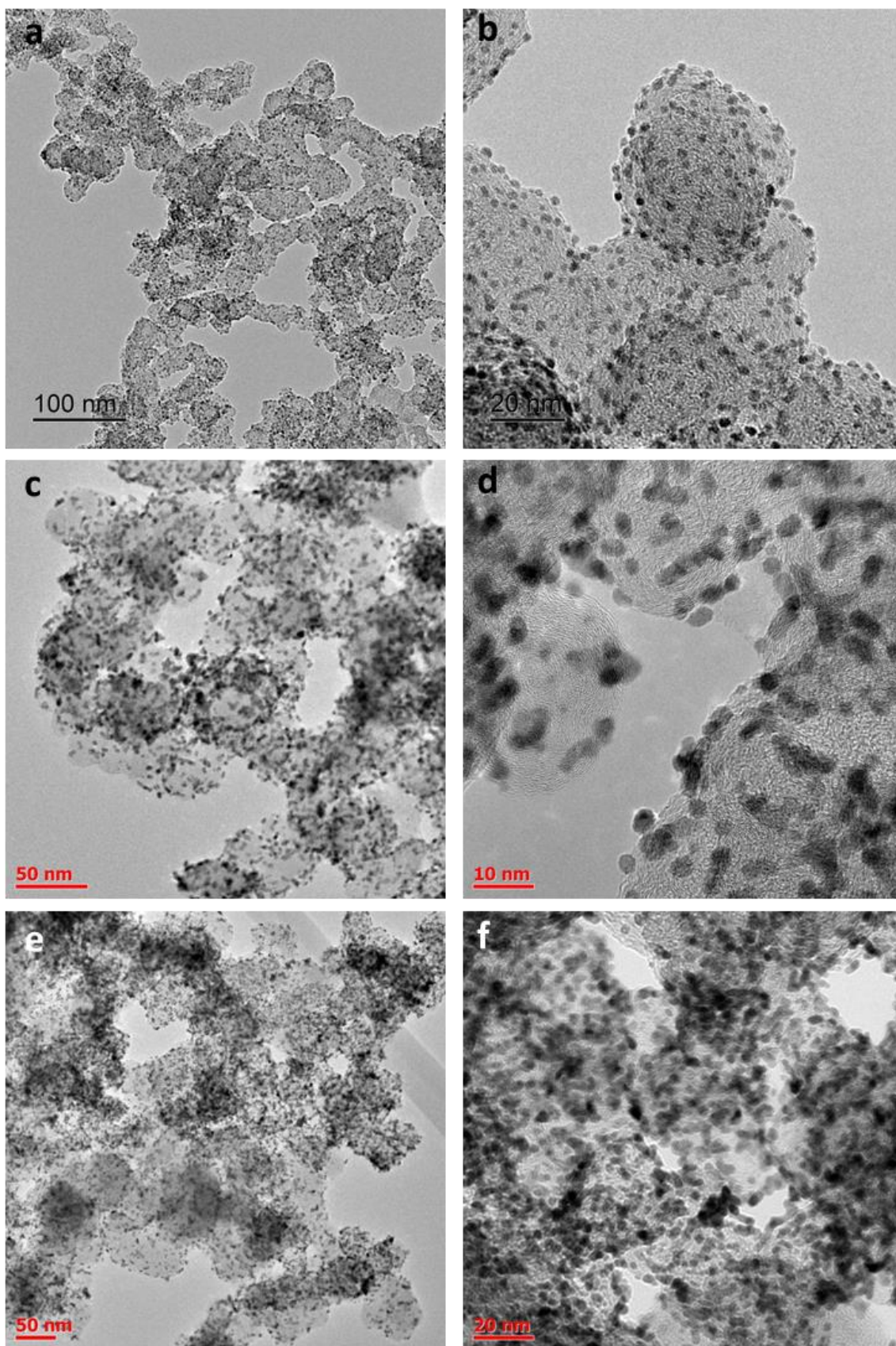


Figure 1 Micrographs of Pt/C samples with different Pt content: PM20 (a, b); PM40 (c, d); PM60 (e, f).

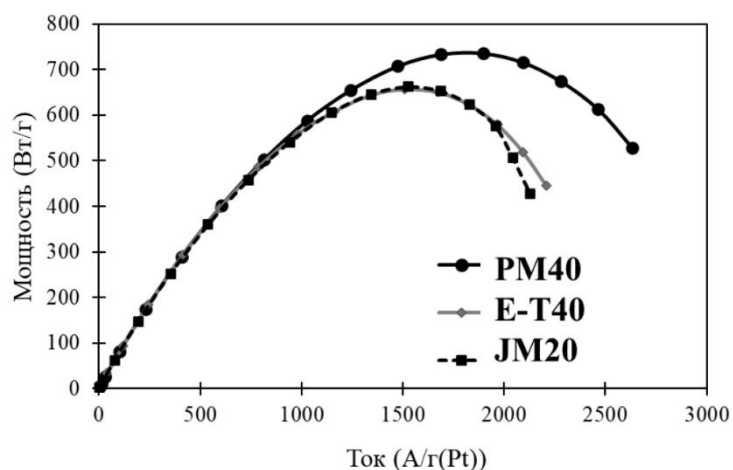


Figure 2 Power specific characteristics of MEAs with Pt/C catalysts [1].
 Commercial Pt/C electrocatalysts JM20 (HiSPEC3000, Johnson Matthey, 20 wt % Pt) and ET40 (E-tek, 40 wt % Pt)

The maximum specific power obtained in the MEA using the PM40 catalyst was 736 W/g(Pt), which exceeds the power values for ET40 and JM20 (657 and 662 W/g(Pt), respectively). Thus, based on the results of a study of the characteristics of the MEA under operating conditions at 25C and 100% gas humidity, an increase in functional characteristics when using the PM40 catalyst was demonstrated by more than 10%, compared to imported analogues [1].

References

1. Nefedkin S.I., Guterman V.E., Alekseenko A.A., Belenov S.V., Ivanenko A.V. Russian Technologies and Nanostructural Materials in High Specific-Power Systems Based on Hydrogen–Air Fuel Cells with an Open Cathode// Nanotechnologies in Russia. 15. 2020. V. 15. P. 370-378.

NUMERICAL AND EXPERIMENTAL RESEARCH OF ANALYTE CONCENTRATION NEAR ION-SELECTIVE PARTICLE

^{1,2}Maxim Alekseev, ²Ilya Moroz, ¹Georgy Ganchenko, ²Semyon Mareev, ^{1,3}Evgeny Demekhin

¹Laboratory of Micro- and Nanoscale Electro- and Hydrodynamics, Financial University under the Government of the Russian Federation, 53 Leningradsky Prospect str., Moscow 125167, Russia, *E-mail: gsganchenko@fa.ru*

²Kuban State University, 149 Stavropolskaya str., Krasnodar 350040, Russia

³Laboratory of General Aeromechanics, Institute of Mechanics, Moscow State University, 1 Michurinsky Prospect, Moscow 119192, Russia

Introduction

The concentration phenomenon occurring in a buffer solution near ion-selective surfaces have one of the most promising properties for biomedical applications. Among such phenomenon is superconcentration which become popular since it was discovered by Han [1] in his experiments. Superconcentration allows to preconcentrate molecules up to million times of their initial concentration and the efficiency of such preconcentration is only limited to by the electrokinetic instability of this electrolyte. This feature can be crucial for developing new medical diagnostic systems and lab-on-chip devices because of its ability to preconcentrate proteins, DNA and other biomolecules initial concentration of which can be so small traditional methods of medical diagnostics could not be used or large amounts of blood would be required. However particular conditions for this phenomenon are still rather unclear because of its complexity in both analytical [2] and numerical ways, thus additional research is required.

Our team considers a cell which utilizes spherical particle composed of ion-exchange resin in a spherical chamber instead of traditional flat ion-selective membranes [3]. Qualitatively two schemes of pre-concentration can be distinguished. The first concept based on using a complex planar system of channels, flat membranes and electrodes. Our concept is the second concept which uses device design based on a simpler spherical geometry, in this case tangential fluxes, which are usually non-existent near flat membranes, cause concentration phenomenon. Even though it would interesting to evaluate and compare efficiency of this 2 concepts in the future, it is beyond the scope of our current research. Numerical research was conducted, and its results were compared with the experimental data which closely simulate mathematical model.

Experiments

The design of the experimental cell differs in certain aspects from the numerical model. A cylindrical chamber has been used instead of a spherical one to simplify the task. The ion-selective microgranule has been mounted at a thin wire inserted through a special hole at the center of the chamber. A thin layer of cyanocrylate adhesive was used for attaching ion-selective particle to the kernel to anchor it. The influence of the kernel on the concentrations is minimal due to insignificant size of kernel and adhesive layer compared to particle. We have also used OPMN-P membranes (ZAO STC "Vladipor", Vladimir, Russia) to prevent the bubbles appearing on electrodes from entering the cylindrical chamber. Detachable reservoirs have been used in addition to electrode chambers. It has been made possible to pump the electrolyte individually through each section and rinse the electrode chambers from by-products that inevitably form on electrodes during experiment. The lower part of the experimental cell has been constructed through photopolymer printing on a 3D printer AnyCubic Photon (Shenzhen Anycubic Technology Co., Ltd., Shenzhen, China). The upper part was a 0.9 mm PMMA cover with high transparency to enable visualization.

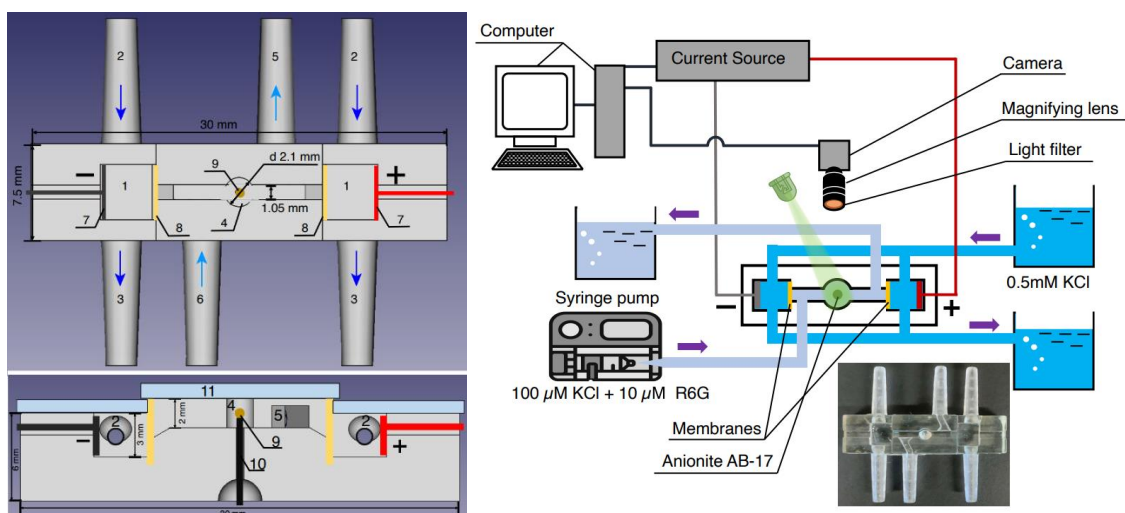


Figure 1. Schematics of experimental cell and experimental set-up respectively

The fluorescent agent Rhodamine-6G (reagent grade, LenReaktiv, Saint-Peterburg, Russia) has been used as an analyte, which was diluted in a buffer solution of potassium chloride (analytical grade, LenReaktiv, Saint-Peterburg, Russia). In our model, potassium chloride corresponds to the salt dissociating into cations (K^+) and anions (Cl^-), and cations of Rhodamine-6G correspond to the macromolecule/third species of ions in the solution. The concentration of Rhodamine-6G ($10 \mu M$) in the cylindrical chamber was significantly lower than that of potassium chloride ($100 \mu M$). The concentration of the salt in the electrode chambers has been kept higher than in the cylindrical chamber in order to reduce the resistance of the system. The accuracy of the preparation of solutions was achieved by weighing salts on laboratory scales with the accuracy of 10^{-4} g. The driving force for moving the liquid through the chamber has been created by the syringe pump Instilar Dixion 1428. The electrolyte flowrate varied from 0.04 mL/min to 0.16 mL/min in the cylindrical chamber; it was raised to 5 mL/min in the electrode chambers.

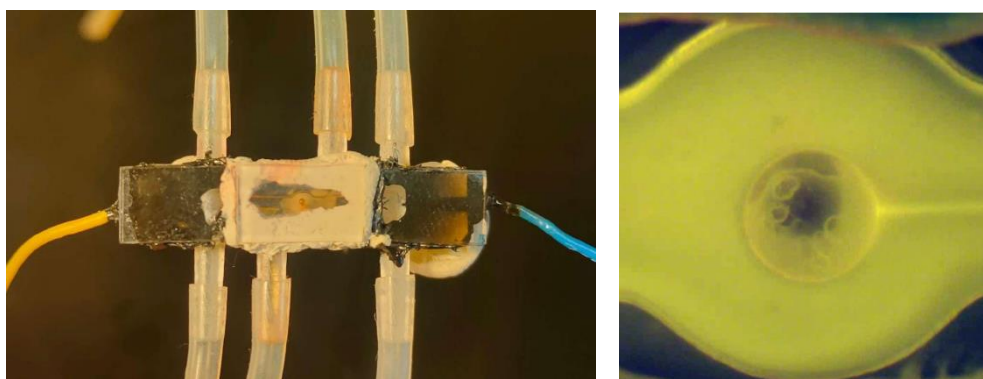


Figure 2. Assembled experimental cell and visualization of dye concentration inside it

The anion-selective particle was Anionite AV-17 with $762 \pm 5 \mu m$ diameter. A potential drop has been created by the Keithley 2400 SourceMeter current source. The Rhodamine molecules were excited by an LED light source with an emitted wavelength of 490 nm and re-emitted light in the wavelength range of $530\text{--}570 \text{ nm}$. The visualization of dye behavior was achieved using an optical microscope consisting of the camera TOUPCAM U3CMOS1800KPA with 20 frames-per-second framerate and a magnifying lens. Color post-processing was carried out using the RisingView software.

Results and Discussion

The comparison between results of numerical simulation and the experimental investigation of the analyte behavior was conducted and visible qualitative similarity is present. However direct numerical comparison poses many difficulties in terms of evaluating local salt concentration and charge in experimental device. During numerical simulation two distinct in their origin regimes of concentration were found.

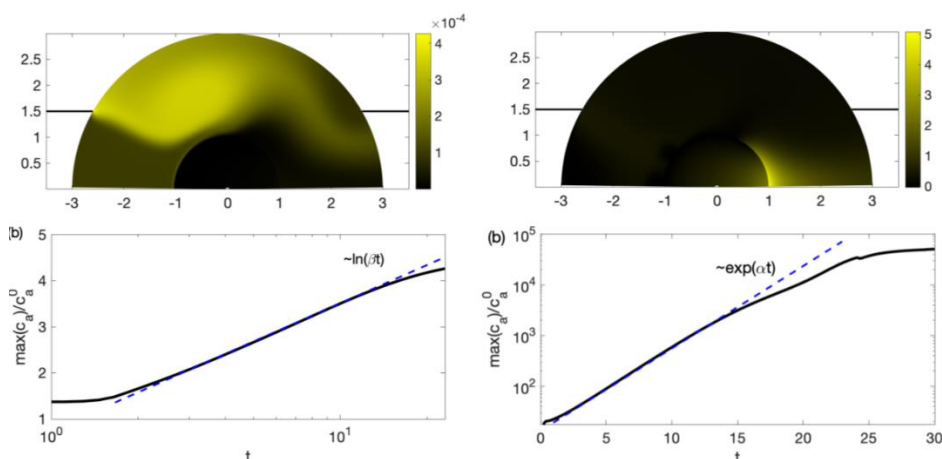


Figure 3. Concentration profiles for two regimes of slow and fast concentration with their respective concentration growth over time.

First regime for certainty we call slow concentration regime, its zone of concentration lies in the front of the particle where macromolecules are trapped within formed Dukhin vortex. The evolution in time of the maximum concentration has logarithmic law and it caps only at several (up to 4) times higher than initial concentration. The concentration region of second, fast concentration regime, now takes place behind the particle, in the region of salt jet, but the maximum concentration growth in time is exponential, moreover concentration can cap at thousands and even millions times of initial concentration. In our numerical study we have acquired a map of this regimes depending on diffusivity and valency of analyte.

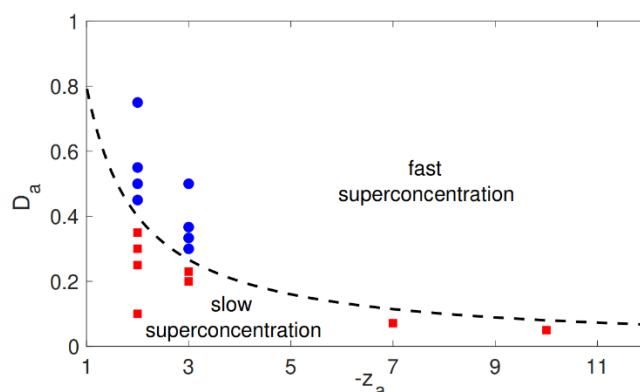


Figure 4. A diagram illustrating map of regimes, red squares are slow concentration regime, blue circles are the fast concentration regime.

The results provide clearer view on superconcentration phenomenon and allows to further improve microdevices based on its effect.

Acknowledgement. This work was supported by the Russian Science Foundation, project number 22-79-10085.

References

1. Lee J.H., Chung S., Kim S.J., Han J. Poly(dimethylsiloxane)-based protein preconcentration using a nanogap generated by Junction Gap breakdown // *Anal. Chem.* 79, 6868 (2007). <https://doi.org/10.1021/ac071162h>.
2. Demekhin E.A., Ponomarev R.R., Alekseev M.S., Morshneva I.V., Ganchenko G.S. Electrokinetic instability of a highly charged and weakly diffusing analyte in a buffer electrolyte near an ion-selective surface // *Eur. Phys. J. Spec. Top.* (2024). <https://doi.org/10.1140/epjs/s11734-024-01154-x>
3. Ganchenko G. S., Alekseev M. S., Moroz I. A., Mareev S. A., Shelistov V. S., Demekhin E. A. Electrokinetic and electroconvective effects in ternary electrolyte near ion-selective microsphere // *Membranes* 13, 503 (2023). <https://doi.org/10.3390/membranes13050503>

INVESTIGATION OF THE DEPENDENCE OF THE ELECTROCATALYTIC ACTIVITY OF COPPER NANOPARTICLES ON MORPHOLOGY AND SHAPING

Georgiy Andreev, Polina Pushankina, Sergey Ivanin, Marina Papezhuk, Aleksandr Simonov, Nikita Prokhorov, Stepan Dzhimak, Iliya Petriev

Kuban State University, Krasnodar, Russia, E-mail: petriev_iliya@mail.ru

Introduction

Nanomaterials based on inexpensive non-platinum metals attract special attention because of their potential as an alternative to expensive noble metal-based catalysts used in many commercial processes [1]. In this context, copper nanoparticles are particularly attractive due to the widespread distribution of copper in nature and low cost, as well as practical and simple methods for producing nanomaterials based on this metal [2-3]. In this regard, an urgent scientific task was the synthesis of copper-based nanocatalysts and the study of the dependence of their electrocatalytic activity on the morphology and formation of nanoparticles.

Experiments

Catalysts consisting of copper nanoparticles were synthesized by electrolytic deposition from a copper plating solution ($\text{CuSO}_4 \times 5\text{H}_2\text{O}$) on the surface of copper films. To vary the shape and structure of the particles, potassium bromide (KBr) was added to the working solution in concentrations from 0 to 2.0 g/l, and the current density during deposition varied in the range from 3 to 15 A/m^2 .

Results and Discussion

During the work, four types of catalysts with different surface morphology were obtained. The samples of the first series – the classic copper layer – were obtained using the classical method and did not have a special surface geometry. The samples of the second series had a large number of large pyramidal particles. Nanoparticles with a lamellar triangular shape and disclosure defects were observed in the samples of the third series. The nanocatalysts of the fourth series consisted of particles of regular cubic shape. Micrographs of synthesized catalysts are shown in Figure 1. The obtained samples were used as working electrodes in subsequent catalytic studies.

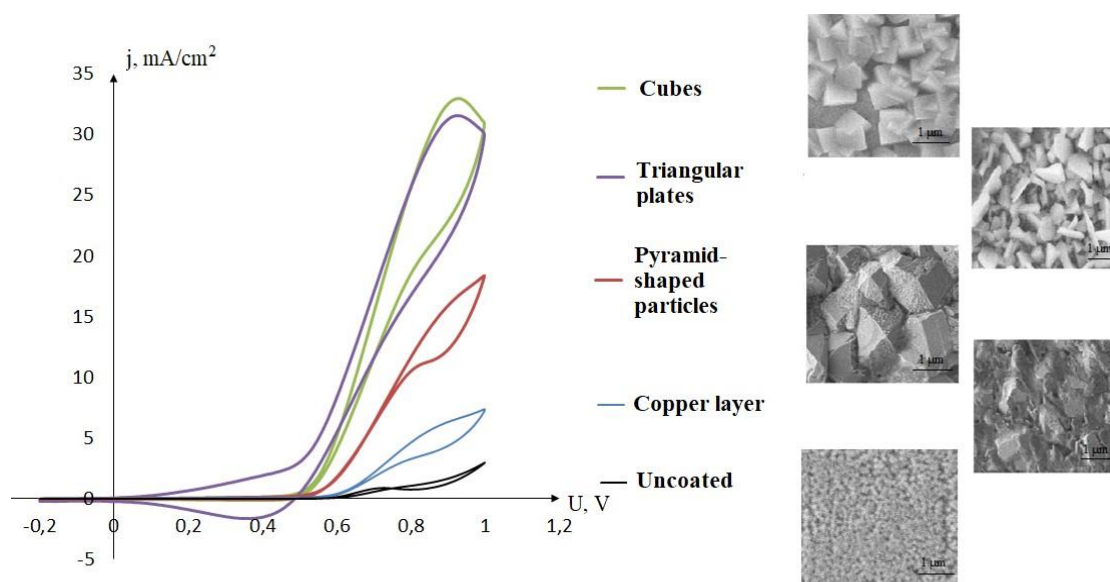


Figure 1. Cyclic voltammograms and micrographs of copper electrodes with four types of catalysts and a smooth unmodified electrode.

The electrocatalytic characteristics of the developed copper nanocatalysts were investigated by cyclic voltammetry in the reaction of alkaline oxidation of alcohols using a three-electrode cell. Samples of copper films with deposited copper nanoparticles of various shapes were used as

working electrodes. An Ag/AgCl electrode was used as a reference. A copper electrode is used as an antielectrode in all measurements. Cyclic voltammograms were taken in the operating potential range from -0.2 V to +1 V at a scanning speed of 10-15 mV/s in an alkaline ethanol solution. According to the data presented in Figure 1, the maximum peak current density was demonstrated by a catalyst with a regular cubic particle shape – 33.01 mA/cm², which indicates its highest catalytic activity compared to other samples. A catalyst consisting of triangular plate-shaped nanoparticles and disclination defects, where the peak current density was 31.59 mA/cm², had a similar but slightly less high activity. The catalyst with pyramidal particles -18 had significantly lower activity and peak current density 39 mA/cm². The peak current density, in comparison with cubic particles, turned out to be almost 2 times lower. The classical copper layer had the lowest activity – 7.08 mA/cm². With respect to an unmodified smooth copper film, the increase in the activity of synthesized catalysts was subject to the following dependence: up to 8 times for cubic particles > up to 7.5 times for particles with a lamellar triangular shape > up to 4.5 times for pyramidal particles > up to 2 times for a classical copper layer. As a result of the work, the dependence of catalytic activity on the formation of copper nanoparticles was established, among which samples with cubic surface morphology had the highest activity. The revealed patterns will allow us to competently vary the synthesis conditions to obtain highly efficient copper-based nanocatalysts with specified characteristics. Their use will significantly reduce the cost in comparison with platinum catalysts, thereby reducing the cost of many industrial processes.

Acknowledgement. This research was financially supported with the financial support of the state assignment of Kuban State University No. FZEN-2023-0006

References

1. *Gawande, M. B. Cu and Cu-Based Nanoparticles: Synthesis and Applications in Catalysis / Dr. M. B. Gawande, A. Goswami, F.-X. Felpin [et al.] // Chemical Reviews. 2016. V. 116. P. 3722-3811.*
2. *Xu, C. Development of stable water-resistant Cu-based catalyst for methanol synthesis / C. Xu, Z. Yan, J. Yu [et al.] // Applied Catalysis A: General. 2021. V. 623. № 118299. P. 1-8.*
3. *Jiang, C.-J. CO₂ electrocatalytic reduction on Cu nanoparticles loaded on nitrogen-doped carbon / C.-J. Jiang, Y. Hou, H. Liu [et al.] // Journal of Electroanalytical Chemistry. 2022. V. 915. № 116353. P. 1-5.*

THE EFFECT OF THE MOLECULAR WEIGHT OF LADDER-LIKE POLYPHENYLSILSESQUIOXANE (L-PPSQ) ON MEMBRANE FORMATION

¹Tatyana Anokhina, ^{1,2}Tatyana Ershova, ^{1,2}Olga Shchegolikhina, ²Anton Anisimov, ²Aziz Muzafarov

¹A.V. Topchiev Institute of Petrochemical Synthesis Russian Academy of Sciences, Moscow, Russia, E-mail: tsanokhina@ips.ac.ru

²A.N.Nesmeyanov Institute of Organoelement Compounds of Russian Academy of Sciences, Moscow, Russia, E-mail: anisimov.ineos@gmail.com

Introduction

The development of a low-carbon economy in the Russian Federation is of the utmost importance, as Russia is one of the world's five leading emitters of CO₂. Therefore, reducing CO₂ emissions to increase economic competitiveness and ensuring its significant contribution to the global climate agenda is a pressing issue [1].

Membrane technologies can significantly reduce costs associated with separation processes due to their compact size, modular design, improved separation efficiency, and reduced energy consumption when compared to traditional methods. In selecting membrane materials and developing membranes based on these materials, high permeability, selectivity, and stability at elevated temperatures are critical factors.

Polymer membranes based on glassy polymers currently dominate the market because of their relatively low cost, as well as the ease of production and scalability of the membrane production. Despite the potential of using membrane polymers at elevated temperatures, only poly(tetrafluoroethylene) (PTFE) and polysulfone are mechanically and hydrolytically stable against high-temperature, wet gases. However, the creation of membranes for the separation of gases and organic solvents using PTFE is not currently possible. Moreover, the operating temperatures of polysulfones do not exceed approximately 170 to 180°C.

A special place in the world of polymers is occupied by ladder-like poly(phenylsilsesquioxane)s (L-PPSQ), glassy polymers with a high thermal stability, with a decomposition temperature of 495°C even in the presence of water vapor. A recently developed original method for the synthesis of L-PPSQ made it possible to produce a polymer with high molecular weight, 1,000,000 g/mol, resulting in good mechanical properties, such as tensile strength of 39 MPa and an elongation at break of 9% [2]. The high thermal stability of L-PPSQ, with $T(\text{glass}) > T(\text{decomposition}) > 490$ °C, even in the presence of water vapor, and its high mechanical characteristics, make this polymer a unique material among existing membrane polymers.

Therefore, in this study, the possibility of producing membranes from L-PPSQ with three different molecular weights (400, 600, and 1,000 kg/mol) was explored.

Experiments

1 g of *cis*-tetraphenylcyclotetrasiloxanetetraol was loaded into an autoclave, and after cooling with liquid nitrogen, ammonia was pumped into the reactor using a flow controller. The autoclave was then thermostated to the required temperature for 4 hours. After that, ammonia decompression was carried out. The remaining silanol groups on the resulting polymer were blocked using trimethylchlorosilane. The polymer was then re-precipitated using the THF/ethanol system.

The molecular weights of the polymers were determined using the GPC (gel permeation chromatography) method on a Shimadzu chromatograph, with a RID-20A refractometer used as a detector. PSS SDV 105Å analytical columns (300x8mm) and THF were used as the eluent.

The solubility of several polymers was investigated in a variety of solvents, including: N-methyl-2-pyrrolidone (NMP), dimethylformamide (DMFA), Dioxane, dioxan-4-one (Dioxalane), Cyclohexanone, Toluene, Chloroform, Benzene, Propylene carbonate, and dimethyl sulfoxide (DMSO). Polymer casting solutions were prepared in 10 mL vials using NMP or dioxalan as the solvent, with a polymer concentration ranging from 15 to 25% by weight. The viscosity of these solutions was measured using an Anton Paar rheometer at 23 °C. To study the kinetics of

precipitation when in contact with water, all solutions were subjected to the limited-layer method [3].

Flat membranes were produced from polymer solutions using a process that involved applying a thin layer of polymer to a glass surface using a squeegee knife and then depositing the layer in a solution of water. The membrane structure was investigated using scanning electron microscopy (SEM) using a Thermo Fisher Phenom XL G2 Desktop SEM facility (USA).

Results and Discussion

The solubility of all synthesized L-PPSQ samples in various solvents has been studied. The results are presented in Table 1.

Table 1: Solubility of L-PPSQ in Various Solvents Depending on Molecular Weight (MW)

Solvent	L-PPSQ -400 (MW=400 kg/mol)	L-PPSQ -600 (MW=600 kg/mol)	L-PPSQ -1000 (MW=1000 kg/mol)
NMP	+	+	-
DMFA	+	-	-
Dioxane	-	-	-
Dioxalane	+	-	-
Cyclohexanone	+	+	+
Benzene	+	+	+
Toluene	+	+	+
Chloroform	+	+	+
DMSO	-	-	-
Propylene carbonate	-	-	-

Table 1 shows that as the M_w of the polymer increases, the amount of solvent needed for it to dissolve decreases. Thus, L-PPSQ with a M_w of 400 kg/mol can be dissolved in 8 different organic solvents, including NMP, dimethylformamide (DMF), dioxane, cyclohexanone, benzene, toluene, and chloroform from 10 organic solvents selected for operation. Polymer with M_w 600 kg/mol is soluble only in one solvent MP, miscible with water, and 4 immiscible. Polymer with M_w 1000 kg/mol is soluble in organic solvents that do not mix with water. This limits the use of high molecular weight L-PPSQ for the production of membranes by the solution method

Thus, NMP and dioxolane were used for the preparation and study of casting polymer solutions in the case of L-PPSQ-400. In the case of L-PPSQ-600, only NMP was used. The obtained solutions with different concentrations of 15 to 25% by weight polymer were studied in terms of their dynamic viscosity (Fig. 1a) and deposition kinetics (Fig. 1b).

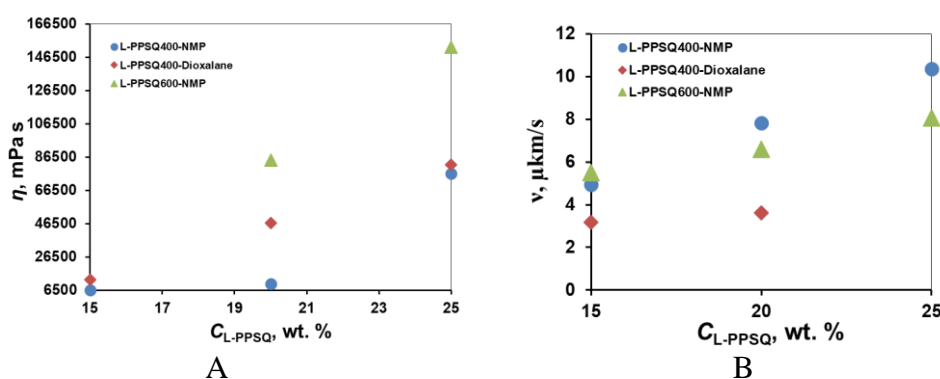


Figure 1. Dependence of A) viscosity B) on solvent and polymer concentration in solution

Figure 1a shows that the viscosity of the polymer solution increases with increasing concentration. In the case of L-PPSQ-600 at concentrations of 20 and 25 wt. % in NMP, the viscosity is significantly higher than for L-PPSQ-400 with the same concentration in NMP and dioxalane. When studying the kinetics of the precipitation of polymer solutions in contact with water, solutions of L-PPSQ-400 in dioxolane have a significantly lower precipitation rate. Flat

membranes were obtained from casting polymer solutions and investigated using the SEM method (Figure 2).

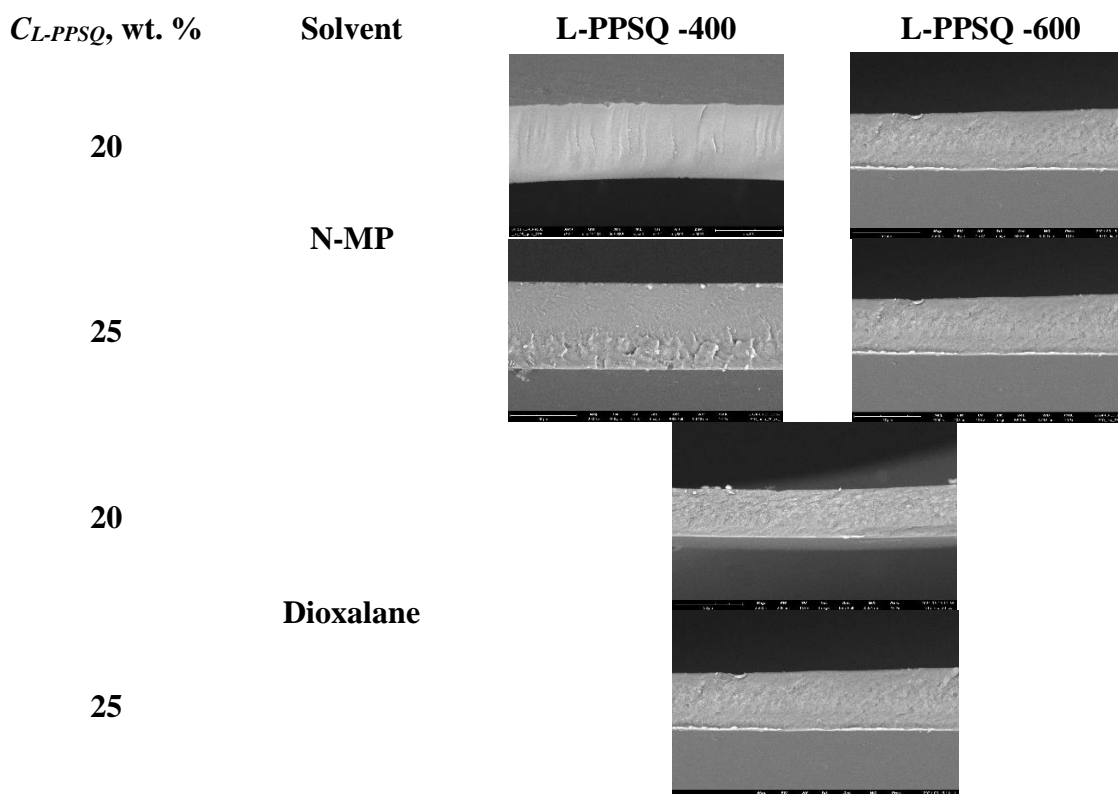


Figure 2. SEM photos of the obtained L-PPSQ membranes.

All membranes have a dense structure with no visible pores. This indicates further research in the field of developing formulations of solutions and a possible transition from two-component to three-component solutions to create a developed porous structure in the membrane.

Acknowledgement. The study was supported by a grant from the Russian Science Foundation No. 23-79-10256, <https://rscf.ru/en/project/23-79-10256/>

References

1. S. Bazhenov *et al.* Technical and economic prospects of CCUS projects in Russia // Sustainable Materials and Technologies. 2022. V. 33, P. 00452.
2. T.O. Ershova *et al.* A versatile equilibrium method for the synthesis of high-strength, ladder-like polyphenylsilsesquioxanes with finely tunable molecular parameters // Polymers. 2021. V.13. P.4452.
3. T.Anokhina *et al.* Phase Separation within a Thin Layer of Polymer Solution as Prompt Technique to Predict Membrane Morphology and Transport Properties // Polymers. 2020. V. 12 №12. P. 2785

EFFECT OF SURFACE MODIFICATION ON THE OXYGEN PERMEABILITY OF DOPED STRONTIUM FERRITES-BASED HOLLOW FIBER MEMBRANES

Marina Arapova, Elena Shubnikova, Olga Bragina, Sergey Bychkov, Alexander Nemudry

Institute of Solid State Chemistry and Mechanochemistry, Novosibirsk, Russia

E-mail: arapova@solid.nsc.ru

Introduction

Mixed ionic-electronic conducting (MIEC) membranes are extensively studied as an oxygen separation alternative to pressure swing adsorption and cryogenic distillation due to its numerous advantages. The main research efforts in this area are aimed at increasing oxygen fluxes through the membrane while maintaining the chemical and thermal stability of the material. To improve the performance of stable but insufficiently permeable materials, the membrane's surface can be modified with a catalyst that accelerates the surface oxygen exchange reaction, which often limits the entire transport process. In this work, the influence of silver modification on oxygen permeability of $\text{La}_{0.4}\text{Sr}_{0.6}\text{Fe}_{0.95}\text{W}_{0.05}\text{O}_{3-\delta}$ -based hollow fiber membrane was studied.

Experiments

The complex oxide $\text{La}_{0.4}\text{Sr}_{0.6}\text{Fe}_{0.95}\text{W}_{0.05}\text{O}_{3-\delta}$ (LSFW5) was synthesized by the ceramic method from metal oxides and strontium carbonate (chemically pure grade). Microtubular hollow fiber membranes were prepared using the phase inversion method described in [1]. The permeate surface was modified by Ag particles supported from AgNO_3 solution followed by drying and calcination in air at 900 °C for 1 h. The phase composition and crystal structure of the sample was studied using X-ray diffraction on a Bruker D8 Advance diffractometer. In situ high-temperature X-ray studies was performed using an HTK-1200N X-ray camera (Anton Paar, Austria). The effect of temperature, oxygen partial pressure and surface modification on the oxygen fluxes across LSF5 hollow fiber membranes were studied in oxygen permeability tests in a microtubular reactor followed by mathematical modelling.

Results and Discussion

Doped strontium ferrite $\text{La}_{0.4}\text{Sr}_{0.6}\text{Fe}_{0.95}\text{W}_{0.05}\text{O}_{3-\delta}$ crystallizes in the rhombohedral perovskite structure type $R\bar{3}c$, which transforms into a high-temperature cubic phase when heated above 500 °C, and maintains phase homogeneity up to 900 °C both in air and in vacuum, which makes it promising for use as a material for MIEC membrane. Oxygen permeability measuring was made on 4 cm length tubes with 2 mm outer radius and a gas-tight layer, surrounded by a developed system of radial elongated pores, formed after calcination in air at 1300 °C. The unmodified LSF5 membrane showed oxygen fluxes of 0.1-0.3 $\text{ml}\cdot\text{min}^{-1}\cdot\text{cm}^{-2}$ in the temperature range of 880-980 °C. Modification of the membrane inner surface with silver leads to a significant increase in the oxygen fluxes to 0.3-1.2 $\text{ml}\cdot\text{min}^{-1}\cdot\text{cm}^{-2}$, which can be assigned with the lowering of kinetic limitation on charge transfer from oxygen ions to iron cations with the participation of Ag particles. To accurately determine the kinetic parameters of the oxygen transport process (the effective activation energy and pre-exponential factor) in LSF5 hollow fiber membrane a previously developed mathematical model was used, which takes into account the geometric characteristics of tubular membranes [1]. The simulation results and experimental data comparison indicates that the oxygen fluxes through LSF5 hollow fiber membranes are limited by surface exchange reactions.

Acknowledgement. This research was performed within the framework of the state assignment of the ISSCM SB RAS, «Laboratory of Materials and Technologies of Hydrogen Energy» (project no. 075-03-2022-424/3).

References

1. Shubnikova E.V., Popov M.P., Bychkov S.F., Chizhik S.A., Nemudry A.P. The modeling of oxygen transport in MIEC oxide hollow fiber membranes // Chem. Eng. J. 2019. V. 72. P. 251–259.

ELECTRODIALYTIC AND CHRONOPOTENTIOMETRIC STUDY ON THE SEPARATION OF VOLATILE FATTY ACIDS

^{1,2} Kayo Santana Barros, ² Valentín Pérez-Herranz, ¹ Svetlozar Velizarov

¹LAQV / REQUIMTE, Department of Chemistry, NOVA School of Science and Technology, FCT NOVA, Universidade NOVA de Lisboa, 2829-516 Caparica, Portugal

E-mail: kayobarros.s@gmail.com

² IEC Group, ISIRYM, Universitat Politècnica de València – Spain. Address: Camí de Vera s/n, 46022, P.O. Box 22012, València E-46071, Spain

Introduction

Polyhydroxyalkanoates (PHAs) are biobased polymers that may partially substitute conventional plastics. In the PHAs production using open mixed microbial cultures, the carbon/nitrogen molar ratio must be controlled at certain stages [1]. Thus, researchers have evaluated the recovery of several volatile fatty acids (VFAs) present in fermentative solutions using membrane separation methods, such as electrodialysis (ED). In general, ED studies have been conducted with the aim of transferring all negatively charged VFAs from the fermentative to a receiver solution, although they affect the bioprocess differently [2]. Therefore, the aim of our study was to explore the degree of their separation by different types of commercial anion-exchange membranes.

Experiments

In the present work, the selective separation of four VFAs that have the same ionic charge but different molecular masses (acetic, propionic, butyric and valeric acids) was evaluated using ED with one anion-exchange membrane (Ralex AMH, Fumasep FAS PET-130, or PC200D) mounted between two Ralex CMH cation-exchange membranes. The process performance was tested under various underlimiting and overlimiting electric potentials. Before the ED experiments, polarization curves were obtained for each membrane by linear sweep voltammetry. A chronopotentiometric study was also conducted to elucidate the mass transfer mechanism(s) that govern ion transfer at each membrane/solution interface.

Results and Discussion

The linear sweep voltammetry and chronopotentiometric curves showed that when the membrane systems operate at overlimiting regimes, the Ralex membrane favors electroconvection, whereas both electroconvection and water dissociation occur intensely at the Fumasep and PC200D membranes. The different hydrophobicity degrees of the functional (quaternary and tertiary amines) groups most probably lead to the strong competition between these phenomena registered for PC200D.

The percent extraction of VFAs obtained with the Fumasep membrane under low and medium current values were higher than that with the Ralex membrane, while under high currents the percent extractions were similar, indicating that the effects of heterogeneity on the transfer of VFAs are suppressed by the occurrence of overlimiting phenomena. The membranes also showed distinct degrees of VFAs fractionation. With Fumasep, the fractionation degrees were slightly higher than with Ralex, while the fractionation degrees obtained with PC200D were significantly higher than those for the other membranes, which might be attributed to the presence of ternary amines at the former.

Acknowledgement. This work received financial support from FCT/MCTES (UIDP/50006/2020 DOI 10.54499/UIDP/50006/2020) through Portuguese national funds. Universitat Politècnica de València and Ministerio de Universidades de España (Plan de Recuperación, Transformación y Resiliencia – financed by European Union - Next GenerationEU) are acknowledged for the post-doctoral research grant attributed to K.S.B.

References

1. Silva, J.B., Pereira, J.R., Marreiros, B.C., Reis, M.A.M., Freitas, F. Microbial production of medium-chain length polyhydroxyalkanoates. *Process Biochemistry* 102 (2022) 393-407. doi: 10.1016/j.procbio.2021.01.020.
2. Brown, R.C., Tuffou, R., Nicolau, J.M., Dinsdale R., Guwy, A. Overcoming nutrient loss during volatile fatty acid recovery from fermentation media by addition of electrodialysis to a polytetrafluoroethylene membrane stack, *Bioresource Technology* 301 (2020) 122543. doi:10.1016/j.biortech.2019.122543.

INFLUENCE OF THE HEAT TREATMENT ON STRUCTURAL AND FUNCTIONAL CHARACTERISTICS OF THE PTCU/C ELECTROCATALYSTS ON VARIOUS CARBON SUPPORTS

Sergey Belenov, Alina Nevelskaya, Angelina Pavlets, Vladislav Menshikov, Elizaveta Moguchikh, Anastasia Alekseenko

Southern Federal University, Rostov-on-Don, Zorge st.,7, Russia, *E-mail: sbelenov@sfedu.ru*

Introduction

Low-temperature fuel cells (FCs) have become widespread in the contemporary world [1]. The key part of the associated FCs is platinum-based catalysts that imply mono-, bi- and trimetallic nanoparticles (NPs) deposited on a carbon support. Platinum being alloyed with different d-metals can significantly increase the activity and stability of the cathode catalysts used for the oxygen reduction reaction (ORR), this matter being dealt with in greater detail in [2]. Nevertheless, the alloying component subjected to the dissolution during the FC operation may significantly lose some of its specific characteristics. The fact of the bimetallic NPs being formed with a given architecture, core-shell [3] or gradient [4], when platinum is located on the surface and the alloying component is only located in the core, thus being protected from the selective dissolution by a platinum layer, enables us to solve the problem of synthesizing the catalysts with enhanced activity for use in FCs [5]

Experiments

To study the effect of the heat treatment on structural and functional characteristics of the bimetallic catalysts, the Pt(Cu)/C catalysts with gradient-obtained structured NPs were synthesized both on a standard Vulcan XC-72 carbon support and on a nitrogen-doped carbon support Ketjenblack EC600JD. The gradient-obtained structure shall refer to the structure of NPs, which is characterized by a gradual increase in the concentration of platinum and a decrease in the concentration of the alloying component in the direction from the core to the surface of NPs. For doping the Ketjenblack EC600JD support with nitrogen, its mixture with melamine (5 parts of melamine by weight per 1 part of the support) was heat-treated at 600 °C for 60 min in an inert atmosphere. The samples obtained on a standard Vulcan XC-72 support and a nitrogen-doped Ketjenblack EC600JD support were marked as Pt(Cu)/C and Pt(Cu)/CN, respectively. The synthesis of the Pt(Cu)/C catalysts with a gradient-obtained structure of bimetallic NPs was carried out by the method described in [6] in order that when they were completely reduced, the atomic ratio of Pt:Cu should amount to 1:1.

The heat treatment of the obtained samples was carried out using the PTK-1.2-40 oven (Teplopribor, Russia) in an argon atmosphere (99.998%) passed through a Drexel flask with an alkaline solution of pyrogallol A (analytical reagent grade) at 350 °C in accordance with the following scheme: rapid heating to a set temperature (~15 min), holding the set temperature for 60 min, slow natural cooling to room temperature for 240–300 min after turning off the heating. To refer to the heat-treated materials, the index 350 corresponding to the treatment temperature was added to the applicable designation.

Results and Discussion

According to the gravimetry data, all the PtCu/C catalysts obtained are characterized by a mass fraction of metals of about 30%. The mass fraction of platinum in the obtained catalysts ranges from 18 to 21 wt%. According to the X-ray fluorescence analysis results, the Pt:Cu ratio in the obtained catalysts ranges from 1:0.9 to 1:1.2 (Table 1), which is close to the atomic ratio per the loading of precursors – 1:1.

According to the XRD analysis, the presence of a carbon phase and a metal phase with a face-centered cubic (FCC) lattice has been observed in the PtCu/C catalysts studied (Fig. 1). It is worth noting that the reflection maxima of the metal phase in the X-ray diffraction patterns of the obtained PtCu/C catalysts are shifted towards larger angles of 2θ compared to the position of the

platinum reflection maximum, regardless of the type of a carbon support used, which indicates the entry of copper atoms into a solid solution with platinum.

Table 1. Structural characteristics of the bimetallic PtCu/C catalysts on a standard and nitrogen-doped carbon support.

Sample	ω (Pt), %	Composition		D_{ave} (cr), nm	D_{ave} (np), nm	a, Å	Degree of alloying, %
		XRF	XRD (Vegard's law)				
Pt(Cu)/C	18	PtCu _{1.2}	-	-	5.7 ± 0.2	-	-
Pt(Cu)/C_350		PtCu _{1.2}	PtCu _{0.9}	7.9 ± 0.3	7.4 ± 0.3	3.779	94
Pt(Cu)/C _N	21	PtCu _{1.0}	-	-	3.9 ± 0.2	-	-
Pt(Cu)/C _N _350		PtCu _{1.0}	PtCu _{0.9}	5.1 ± 0.3	5.5 ± 0.3	3.779	86

Using the TEM method, the micrographs of surface areas were obtained for the Pt(Cu)/C and Pt(Cu)/CN catalysts with a gradient-obtained NPs' structure on a standard and nitrogen-doped carbon support (Fig. 1). According to the TEM data, it has been shown that the material obtained on a standard Vulcan XC-72 support (Fig. 1a) is characterized by sufficiently large metallic NPs with an average size of 5.7 nm (Fig. 1e), which are non-uniformly distributed over the surface of the support (Fig. 1a, b). At the same time, as previously shown for the PtCu/C catalysts obtained by the multi-stage synthesis [6], some metallic NPs are characterized by a darker shell and a lighter core, which indicates a complex structure of the NPs and is confirmed by the results of high-resolution TEM (Fig. 1c, g) and STEM. Unfortunately, the elemental mapping and the line scanning of the elemental composition for the Pt(Cu)/CN material, although confirming the presence of bimetallic NPs, do not allow for the confirmation of a gradient-obtained NPs' structure.

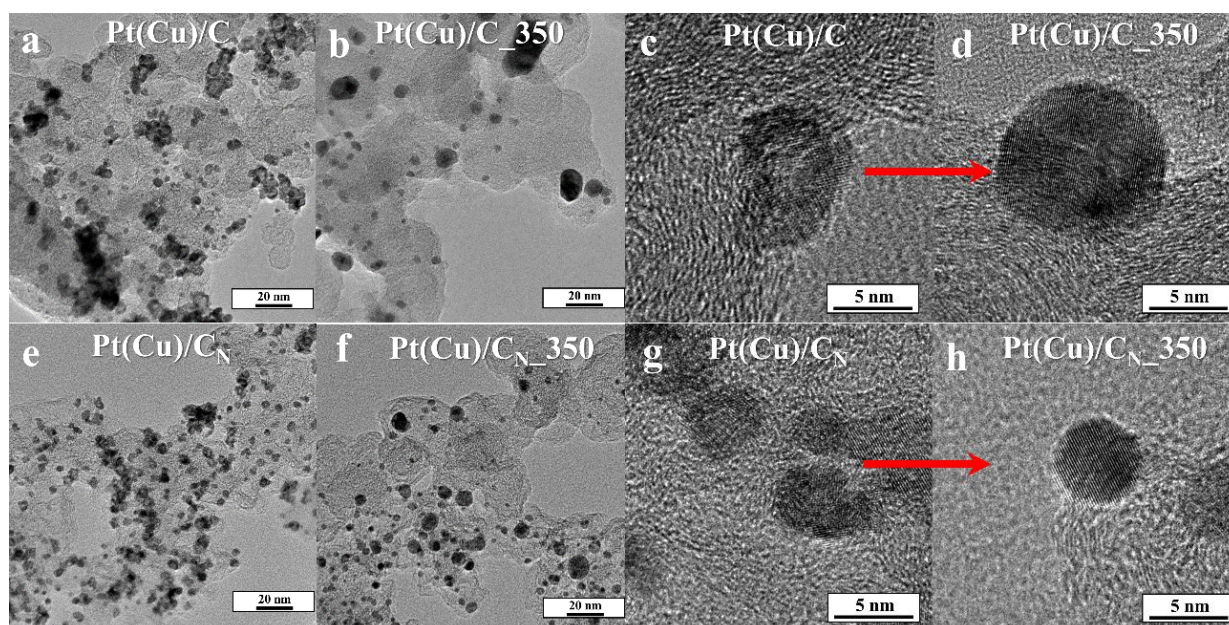


Figure 1. TEM micrographs for the Pt(Cu)/C (a–d) and Pt(Cu)/CN (e–h) catalysts before (a, c, e, g) and after (b, d, f, h) the heat treatment

It should be noted that the material obtained on the support doped with nitrogen is characterized by a significantly smaller average NPs' size of about 3.9 nm compared to the material on the Vulcan XC-72 support, whereas the NPs are uniformly distributed over the surface of the doped support (Fig. 1e). Similarly to the material on the doped support, the bimetallic NPs obtained on Vulcan XC-72 are characterized by a complex structure, whereas the formation of bimetallic NPs is confirmed by the elemental mapping and the line scanning of the elemental.

The study of the current–voltage characteristics of the most active catalysts Pt(Cu)/C_N and Pt(Cu)/C_N_350 as part of the membrane electrode assembly, at the platinum loading of 0.3 mg/cm²,

has shown an increase in the maximum specific power from 603 to 696 W/g (Pt) after the heat treatment, which exceeds characteristics of the commercial Pt/C analogs JM40 (648 W/g (Pt)) and JM20 (661 W/g (Pt)). Therefore, the Pt(Cu)/C_N_350 material exhibits the greatest catalytic activity due to the combination of the use of a nitrogen-doped carbon support and heat treatment.

Therefore, the heat treatment of the bimetallic catalysts obtained using a nitrogen-doped carbon support makes it possible to synthesize the catalyst whose functional characteristics exceed those of the commercial Pt/C analog and the equivalent materials presented in the literature data. The results obtained can be used in the development of new-generation electrocatalysts for low-temperature fuel cells.

According to the results of the study, it has been established that regardless of the type of a carbon support used, the heat treatment of the PtCu/C catalysts at 350 °C leads to the transformation of the structure of bimetallic NPs from a gradient-obtained one to a disordered solid solution and to an increase in the ORR activity up to 1.6 times due to changes in the chemical composition of the surface. The heat treatment of the PtCu/C catalyst on the carbon support doped with nitrogen at 350 °C has allowed obtaining the material with the specific ORR activity 6.4 times higher than that of the commercial Pt/C analog JM20 (Johnson Matthey). The application of the heat treatment for the PtCu/C catalyst has made it possible to increase the maximum power of the membrane electrode assembly by 15% up to 696 W/g (Pt), which exceeds characteristics of the equivalent MEAs that use commercial analogs. The results obtained can be used in the development of new-generation electrocatalysts for low-temperature fuel cells. These results have also confirmed the prospects of using the PtCu/C catalysts with a gradient-obtained structure on a nitrogen-doped carbon support after the heat treatment as a cathode catalyst in low-temperature fuel cells.

Acknowledgement. This research was financially supported by the Ministry of Science and Higher Education of the Russian Federation (State Assignment in the Field of Scientific Activity No. FENW-2023-0016).

References

1. *Cheryan M.* Ultrafiltration and microfiltration handbook, Technomic Publishing Inc., Lancaster PA., 1998. *Wang H., Wang R., Sui S., et al* Cathode Design for Proton Exchange Membrane Fuel Cells in Automotive Applications // *Automotive Innovation*. 2021. V.4. P.144–164.
2. *Wang X., Sokolowski J., Liu H., Wu G.* Pt alloy oxygen-reduction electrocatalysts: Synthesis, structure, and property // *Chinese Journal of Catalysis*. 2020. V. 41. P.739–755.
3. *Wang R., Wang H., Luo F., Liao S.* Core–Shell-Structured Low-Platinum Electrocatalysts for Fuel Cell Applications // *Electrochemical Energy Reviews*. 2018. V.1. p. 324–387.
4. *Lyu X., Jia Y., Mao X., et al* Gradient-Concentration Design of Stable Core–Shell Nanostructure for Acidic Oxygen Reduction Electrocatalysis // *Advanced Materials* 202032:2003493.
5. *Zhang X., Li H., Yang J., et al* Recent advances in Pt-based electrocatalysts for PEMFCs // *RSC Adv*. 2021. V. 11. P. 13316–13328.
6. *Alekseenko A., Guterman V., Belenov S., et al* Pt/C electrocatalysts based on the nanoparticles with the gradient structure // *Int J Hydrogen Energy*. 2018. V. 43. P.3676–3687.

RESOLVING SOME CONTROVERSIES IN WATER AND ION TRANSPORT IN POLYMER MEMBRANES FOR WATER DESALINATION: HOW DO IONS AND WATER MOLECULES MOVE AND PARTITION?

¹Maarten Biesheuvel, ²Ilya Ryzhkov

¹Wetsus, European Centre of Excellence for Sustainable Water Technology, The Netherlands,

E-mail: maarten.biesheuvel@wetsus.nl

²Institute of Computational Modelling SB RAS, Akademgorodok 50-44, Krasnoyarsk, Russia

The correct theory for ion and water absorption and transport in polymer membranes in water desalination is of great importance. Renewed attention is nowadays focused on the distinction in reverse osmosis between an approach where water is assumed to disperse as gaseous molecules in the membrane, which is the solution-diffusion model (SD model), and the opposite approach that considers the water as a continuum fluid filling pores in the membrane, with ions dissolved in that water. This is the solution-friction (SF) approach. This SF model is close to models known from nanofiltration (NF) such as Donnan Steric Pore Model (DSPM), but in that model the water transport is not related to pressure. So, the SF-model is an extension of DSP. We present an overview of the assumptions in the SD model and what evidence exists to show that these assumptions are not right.

For RO and NF we present a novel expression for salt transport and show how it extends earlier models where salt only diffuses through a neutral membrane, to the case when the membrane is charged. We apply this new expression to several datasets of commercial seawater RO membranes, and we propose an accurate method to compare the salt permeability of different membranes. In RO we also address the calculation of the CP layer and compare various literature approaches.

We also address electrodialysis, and discuss an improved expression for permselectivity, one that clearly shows how it depends on salt concentration and current density. Thus, it is a process parameter, not some membrane material property.

References

1. *Heiranian M., Fan H., Wang L., Lu X., Elimelech M.* Mechanisms and models for water transport in reverse osmosis membranes: history, critical assessment, and recent developments // *Chem. Soc. Rev.* 2023. V. 52. P. 8455--8480.
2. *Fan H. Heiranian M., Elimelech, M.* The solution-diffusion model for water transport in reverse osmosis: What went wrong? // *Desalination* 2024. V. 580 P. 117575.
3. *Biesheuvel P.M., Porada, S., Elimelech M., Dykstra, J.E.* Tutorial review of reverse osmosis and electrodialysis // *J. Membr. Sci.* 2021. V. 647. P. 120221.
4. *Biesheuvel, P.M., Rutten S.B., Ryzhkov I.I., Porada S., Elimelech M.* Theory for salt transport in charged reverse osmosis membranes: Novel analytical equations for desalination performance and experimental validation // *Desalination* 2023. V. 557, P. 116580.

EFFICIENCY ANALYSIS OF NOVEL AND CONVENTIONAL ANION EXCHANGE MEMBRANES DURING ELECTRODIALYSIS OF DILUTED SODIUM CHLORIDE SOLUTION

Denis Bondarev, Anastasia Samoilenko, Stanislav Melnikov

Kuban State University, Krasnodar, Russia, E-mail: melnikov.stanislav@gmail.com

Introduction

It has been established that the magnitude of the limiting current depends not only on the concentration of the external solution but is also determined by the membrane material itself. In a previous study [16], researchers developed a uniform anion-exchange membrane using a copolymer of N,N-dimethyl-N,N-diallylammonium chloride and ethyl methacrylate. Its electrochemical properties and stability were examined using a rotating membrane disk. The disk's design prevents the formation of a gradient in the diffusion layer thickness across the membrane surface, as well as the occurrence of thermal and gravitational convection. This setup allows for the separation of ion flow into components and the accurate assessment of each mechanism's contribution in underlimiting and overlimiting current modes.

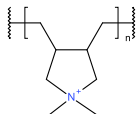
In practical electro dialysis modules, a variation in the diffusion layer thickness is observed as the solution flows along the membrane surface. This leads to an uneven distribution of current lines and, in some cases, the development of a local limiting state in specific membrane areas. When the limiting current on the membrane is exceeded, water dissociation and other concentration polarization effects occur. Under these circumstances, the magnitude of the limiting current, the impact of water dissociation, and electroconvection may significantly differ from the results obtained using the rotating disk membrane configuration. Therefore, it is recommended to investigate the new uniform anion-exchange membrane in the context of electro dialysis desalination processes.

The aim of this research is to analyze the electrochemical performance of the new uniform anion-exchange membrane composed of the copolymer of N,N-dimethyl-N,N-diallylammonium chloride and ethyl methacrylate and compare its properties with those of commercial anion-exchange membranes MA-41 and Neosepta AMX.

Experimental

For the study, two industrial anion-exchange membranes were selected: the heterogeneous MA-41 (Shchekinoazot, Russia) and the homogeneous AMX (Astom, Japan), as well as the experimental membrane MA-1. All membranes have the same ionogenic groups - quaternary ammonium bases, but with varying chemical compositions. The membranes also differ in their manufacturing methods, the presence and nature of the inert binder, and the reinforcing fabric, which lends mechanical strength to the material. The nature of the functional groups and the methods by which the studied membranes are manufactured are presented in Table 1.

Table1: Functional groups and thicknes of the studied membranes

Membrane	AMX	MA-1	MA-41
Inert binder	PVC	-	PE
Fabrication method	paste	casting	hot pressing
Reinforcing mesh	Teviron®	-	PA
Functional groups	$-\text{CH}_2-\text{N}^+(\text{CH}_3)_3;$		$-\text{CH}_2-\text{N}^+(\text{CH}_3)_3;$
Thickness, μm	180	150-200	540

The anion-exchange membrane MA-1 was produced by casting a 10% solution of the copolymer N,N-diallyl-N,N-dimethylammonium chloride and ethyl methacrylate in isopropyl alcohol onto a glass surface. The copolymer synthesis scheme and detailed synthesis methodology are described in paper [16].

The study of the electro dialysis desalination process of sodium chloride solution was conducted in a laboratory electro dialysis cell. The cell consisted of seven chambers: one desalination chamber, two concentration chambers, two buffer chambers, and two electrode chambers. The working dimensions of each chamber were: width – 2 cm, length – 2 cm, intermembrane distance (height) – 5 mm. The desalination chamber was formed by the MK-40 membrane and the studied anion-exchange membrane, while the other chambers of the cell used MK-40 and MA-41 membranes. A 0.02 M NaCl solution was used as the working solution in the desalination chamber, concentration chambers, and buffer chambers. For rinsing the electrode chambers, a 0.01 M Na₂SO₄ solution was used. The experiment was concluded when the concentration in the desalination chamber reached 0.01 M. Tests were conducted in a potentiostatic mode, maintaining a roughly constant potential drop across the studied membrane and adjacent solutions. For each of the studied membranes, three regimes were investigated at potential drops of 0.5, 1.0, and 2.0 V.

Results and Discussion

The current-voltage curves of the studied membranes in 0.01 M and 0.02 M sodium chloride solutions are shown in Figure 1.

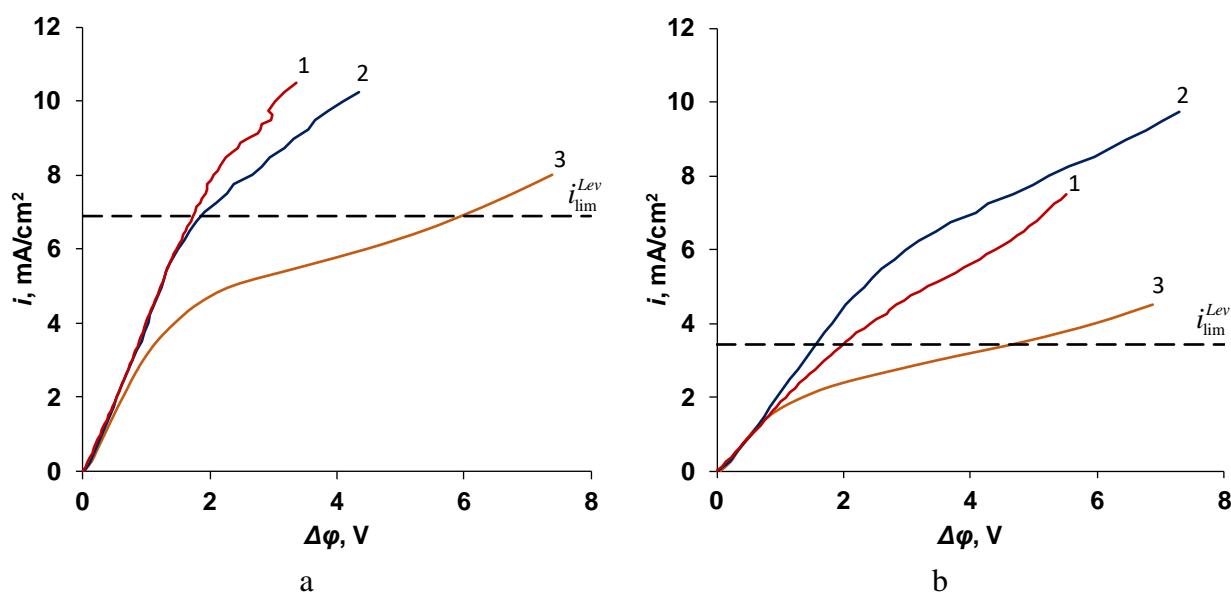


Figure 1. Current-voltage curves of the studied anion-exchange membranes in 0.02 M (a) and 0.01 M (b) sodium chloride solutions. 1 – AMX, 2 – MA-1, 3 – MA-41. The dashed line represents the theoretical limiting current value calculated using the Levich equation

Comparing the current-voltage curves with the theoretically calculated value of the limiting current reveals that for the heterogeneous MA-41 membrane, the limiting current is notably lower than the theoretical value in both 0.02 M and 0.01 M sodium chloride solutions. The limiting current value for the MA-1 membrane in the 0.02 M solution closely aligns with the theoretical prediction. In the electro dialysis cell, when transitioning to the 0.01 M solution, the limiting current on the MA-1 membrane remains almost unchanged compared to the value obtained for the 0.02 M solution, while the excess of the limiting current over the calculation according to the Levich equation amounts to 70%. For the AMX membrane in the 0.02 M solution, there is some exceedance of the theoretical limiting current density, which is also maintained when the solution is diluted to 0.01 M.

The kinetic curves illustrating the relationship between the electrolyte concentration and pH value in the desalination tract against the potential jump in the system for the studied membranes are depicted in Figure 2.

The time needed to desalinate a sodium chloride solution from 0.02 M to 0.01 M concentration decreases in the sequence of MA-41 > MA-1 > AMX. Increasing the potential drop generally results in a higher desalination rate for all three membranes studied. An exception is observed for the MA-41 membrane when transitioning from 1 V to 2 V.

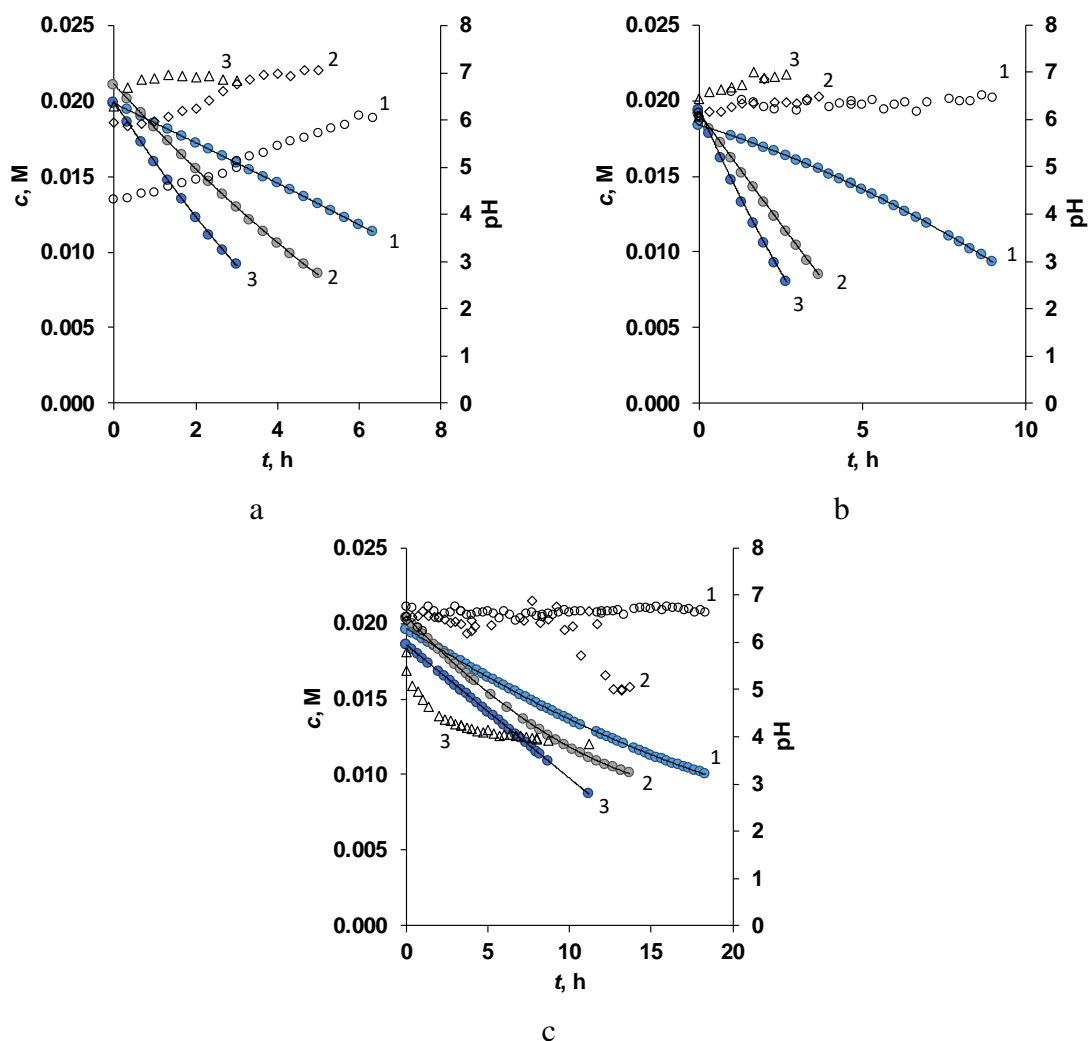


Figure 2. Kinetic dependencies of sodium chloride concentration and pH values in the desalination tract obtained at various potential jumps for systems with AMX (a), MA-1 (b), and MA-41 (c) membranes. Solid markers indicate electrolyte concentration, while hollow markers represent pH values in the desalination tract. Potential drop: 1 – 0.5 V, 2 – 1 V, 3 – 2 V

For commercial membranes, the desalination process involves transitioning into an overlimiting current mode. The AMX membrane experiences an increase in useful mass transfer due to electroconvection, while the MA-41 membrane experiences a decrease in salt ion flow due to the water dissociation reaction. In contrast, the MA-1 membrane transitions to an underlimiting current mode with a decrease in solution concentration, which may be associated with a significant contribution of equilibrium electroconvection to the ion transfer process in diluted solutions in electromembrane systems with this membrane. This difference in properties between the MA-1 and AMX membranes leads to higher mass transfer coefficients for the MA-1 membrane compared to the AMX membrane at potential drops of 1 and 2 V. The optimal operating mode for the MA-1 membrane is a potential jump of 1 V in the electromembrane system, where the specific energy consumption is 0.24 kWh/mol.

Acknowledgement. The study was supported by a grant from the Russian Science Foundation № 22-13-00439, <https://rscf.ru/project/22-13-00439/>.

References

1. Bondarev D., Melnikov S., Zabolotskiy V. New homogeneous and bilayer anion-exchange membranes based on N,N-diallyl-N,N-dimethylammonium chloride and ethylmethacrylate copolymer // J. Membr. Sci. 2023. V. 675. P. 121510.

FROM POLYMERS TO HOLLOW FIBER MEMBRANES AND MEMBRANE MODULES

Ilya Borisov, Dmitriy Matveev, Vladimir Vasilevskii, Andrey Didenko, Svetlana Khashirova, Vladimir Volkov, Alexey Volkov, Stepan Bazhenov, Tatyana Anokhina

A.V. Topchiev Institute of Petrochemical Synthesis Russian Academy of Sciences, Moscow, Russia
E-mail: tsanokhina@ips.ac.ru

Introduction

The global membrane market is over \$5 billion per year, with polymer membranes taking up the majority of it. Membranes are used to separate gases and liquids in medicine, food industry, biotechnology, pharmacology and water treatment. The industry's ever-growing demand for expanding membrane applications is inextricably linked to the development of a new generation of membranes that meet the ever-increasing requirements for their permeability, selectivity, chemical and thermal stability. This is accompanied by a relentless interest in this topic on the part of science. So, according to Scopus, over the past five years, according to the keywords, "polymer and membrane", about 30 thousand publications have been published. Every year the number of publications increases, which confirms the high scientific importance of this area of research.

The vast majority of membrane works are devoted to the study of the transport properties of new materials. Less well-represented are works studying the process of forming membranes with thin separation layers. This is especially true for the development of hollow fiber membranes. And in rare cases, the research is aimed at manufacturing and testing membrane modules.

The required morphology of the membranes, which determines their separation and performance characteristics, is formed at the stage of their preparation. However, the search for molding conditions is a laborious and time-consuming process that requires a large consumption of materials. The required morphology of the membranes, which determines their separation and performance characteristics, is formed at the stage of their preparation. However, the finding of spinning conditions is a laborious and time-consuming process that requires a large amount of materials. To reduce the time spent and the required reagents (polymer, solvent, precipitant and various additives), Laboratory of polymeric membranes of TIPS RAS has developed express methods for studying the kinetics of polymer solution deposition and forming of hollow fiber membrane samples under controlled conditions using a small amount of starting materials, allowing in a relatively short time (less than a year) to go from a membrane material to a hollow fiber membrane module.

Experiments

To study the kinetics of the deposition of polymers solutions, the "limited" layer technique was used [1]. It allows to simulate the process of forming a polymer membrane of a given thickness and visualize the process of pore formation. By gluing two cover glasses with double-sided tape, a rectangular channel with a depth (d) of 300 – 400 μm was formed, open to the atmosphere on one side. The channel was then filled with a polymers solution. The sample with a polymer solution was fixed on a slide. Using a Pasteur pipette, a precipitator (water) was added into the polymer solution from the side open to the atmosphere, and the process of phase separation of polymers solution was observed using a microscope and recorded on a video camera.

The kinetics of polymer deposition was evaluated using the deposition rate of a polymer solution in a layer of a given thickness. It was calculated as the ratio of the total thickness of the polymer layer (d , μm) to the time of its deposition (t , s).

A new technique has been developed for forming asymmetric hollow fiber filtration polymer membranes from solutions of small volume (5-10 ml) by dry-wet spinning. This technique is an express method for producing hollow fiber membranes, since it significantly reduces the molding time from ten hours to tens of minutes. In addition, this method is relevant for the case when there is a limited small amount of polymer, but it is necessary to quickly evaluate its membrane application. [2].

A compact research laboratory installation with a large number of degrees of freedom for varying the technological parameters of the process was used for forming asymmetric hollow fiber membranes [2]. The installation produced asymmetric hollow fiber membranes with an external and/or internal skin layer. In addition, the installation allows to vary the morphology of hollow fiber membranes by changing the pressure above the solution, the flow rate of the internal precipitant, the air gap width and the temperature of the precipitation baths.

Results and Discussion

The report on the cycle of work of the Polymer membrane laboratory will present the results of the research achieved using a number of experimental methods that made it possible to go from a membrane material to a semi-fiber membrane module.

A new method has been developed for studying the NIPS process (formation of an asymmetric porous polymer structure from a solution under the action of a non-solvent), which allows us to study the kinetics of deposition in a polymer solution film of a given thickness. In contrast to the "droplet" method used in the literature, the proposed method allows to estimate the time of formation of a polymer membrane in an express mode, adequately assess the morphology of the membrane without carrying out its formation stage and reduce the experimental time required to obtain membranes with the desired porous structure.

Express methods for forming hollow fiber membranes from small volumes of molding solution (less than 10 ml), which makes it possible to study the membrane properties of new, expensive and hard-to-reach polymers in a short time. Laboratory samples of hollow-fiber asymmetric and composite membranes based on laboratory and industrial samples of polymers, including polysulfone, polyphenylene sulfone, polyimides and polyurethanimides, were formed using express methods.

A compact research laboratory installation of dry-wet spinning with a high number of degrees of freedom for varying the technological parameters of the process has been created to develop experimental batches of hollow fiber membranes. Based on the data on the development of spinning solution compositions, methods of formation have been developed and samples of asymmetric hollow fiber gas separation membranes and ultrahigh permeable porous supports for hollow fiber composite membranes have been obtained.

Table 1: Polymers used in the work.

Polymer	Abbreviation	Process	Separation systems	Ref.
Polyimide	PI	Gas separation	He/CH ₄	
Polyamide acid	PAA	Nanofiltration	Aprotic solvents	[1]
Polyurethanimide	PUI	Nanofiltration	Aprotic solvents	[3]
Polydecylmethylsiloxane / Polysulfone		Gas separation	C ₂₊ /CH ₄	[4]
		Pervaporation	Oxygenates/water	[5]
Polyphenylene sulfone	PPSF	Ultrafiltration	Bacteria, viruses/water	[6]
Polysulfone	PSF	Gas separation	He/CH ₄ , H ₂ /CH ₄ , CO ₂ /CH ₄ , O ₂ /N ₂	[2]

Highly permeable porous support has been successfully used to create semi-fiber composite membranes with a thin selective layer of polydecylmethylsiloxane, promising for the separation of hydrocarbons C₂₊/CH₄. Based on asymmetric and composite gas separation membranes, hollow fiber membrane modules with a membrane surface area of up to 0.2 m² have been developed and studied for the tasks of separating hydrocarbons and recovering of helium from a mixture with methane.

Acknowledgement. This research was financially supported by the State Program of TIPS RAS.

References

1. *T.Anokhina, I.Borisov, A.Yushkin, G.Vaganov, A.Didenko, A.Volkov*. Phase Separation within a Thin Layer of Polymer Solution as Prompt Technique to Predict Membrane Morphology and Transport Properties // *Polym.* 2020.V. 12 №12. P. 2785
2. *D.N. Matveev, et.al.* // *Membranes and Membrane Technologies.* 2020. V. 2 №6 (2020) P. 351-356
3. *A.L.Didenko, A.G.Ivanov, V.E.Smirnova, G.V.Vaganov, T.S.Anokhina, I.L.Borisov, V.V.Volkov, A.V.Volkov, V.V.Kudryavtsev*. Selective Destruction of Soluble Polyurethaneimide as Novel Approach for Fabrication of Insoluble Polyimide Films // *Polymers.* 2022. V. 14 P.4130
4. *D.N.Matveev, I.L.Borisov, E.A.Grushevenko, V.P.Vasilevsky, T.S.Anokhina, V.V.Volkov*. Hollow fiber PSF fine porous supports with ultrahigh permeance for composite membrane fabrication: Novel inert bore liquid (IBL) spinning technique // *Separation and Purification Technology.* 2024. V. 330 Part B. P. 125363
5. *I.Borisov, I.Podtynnikov, E.Grushevenko, O.Scharova, T.Anokhina, S.Makaev, A.Volkov, V.Volkov*. High Selective Composite Polyalkylmethylsiloxane Membranes for Pervaporative Removal of MTBE from Water: Effect of Polymer Side-chain. // *Polymers.* 2020. V. 12 №6. P. 1213
6. *T.Anokhina, A.Raeva, S.Sokolov, A.Storchun, M.Filatova, A.Zhansitov, Z.Kurdanova, K.Shakhmurzova, S.Khashirova, I.Borisov*. Effect of Composition and Viscosity of Spinning Solution on Ultrafiltration Properties of Polyphenylene Sulfone Hollow-Fiber Membranes. *Membranes.* 2022. V. 12 №11 P. 1113

STUDY OF OXYGEN PERMEABILITY AND CATALYTIC PERFORMANCE OF MICROTUBULAR MEMBRANES BASED ON STRONTIUM FERRITE DOPED BY TUNGSTEN

¹Olga Bragina, ^{1,2}Alexey Novikov, ¹Elena Shubnikova, ¹Marina Arapova, ¹Alexander Nemudry

¹Institute of Solid State Chemistry and Mechanochemistry of the Siberian Branch of the RAS Novosibirsk, Russia, *E-mail: bragina@solid.nsc.ru*

²Novosibirsk state university, Novosibirsk, Russia, *E-mail: a.novikov9@g.nsu.ru*

Introduction

Non-stoichiometric oxides possessing mixed oxygen-electron conductivity are promising materials for catalytic membrane reactors (CMRs) used for the conversion of hydrocarbons, particularly methane and ethane. In the CMR, the oxidative dehydrogenation reactions of ethane can be coupled with the process of oxygen separation from air, water or CO₂ in one unit, which increases the energy efficiency of the process. At the same time, utilization of CO₂/H₂O with their transformation into valuable products (synthesis of gas, hydrogen) contributes to solving urgent environmental problems [1]. The aim of this work is to investigate the oxygen permeability of hollow-fiber membranes based on SrFe_{1-x}W_xO_{3-δ}, as well as the catalytic activity in the oxidative dehydrogenation of ethane.

Experiments

Non-stoichiometric oxides were synthesized by ceramic method from the corresponding metal oxides and carbonates. Hollow-fiber membranes were prepared by phase inversion method using N-methylpyrrolidone as solvent, polysulfone as polymer matrix and water as coagulant. The synthesized oxides with perovskite structure were investigated by X-ray diffraction, thermogravimetry, and scanning electron microscopy.

Results and Discussion

The membranes of SrFe_{0.85}W_{0.15}O_{3-δ} (SFW15) composition obtained by phase inversion method have a unique wall structure consisting of a 100-200 μm thick gas-tight layer located between the porous layers. Oxygen fluxes obtained through the microtubular SFW15 membrane in air/argon gradient reach values of 0.9 mL*min⁻¹*cm⁻² at T=980 °C. Studies of catalytic activity in reactions of oxidative dehydrogenation of ethane showed that ethane conversion increases with increasing temperature and reaches 98% at 880 °C. At the same time, the selectivity for ethylene decreases with increasing temperature, the optimum selectivity values of 43% are observed at 840 °C. The obtained results allow us to conclude that nonstoichiometric oxide of the composition SrFe_{0.85}W_{0.15}O_{3-δ} is a promising material for the creation of a catalytic membrane reactor used for ethylene production by oxidative dehydrogenation of ethane.

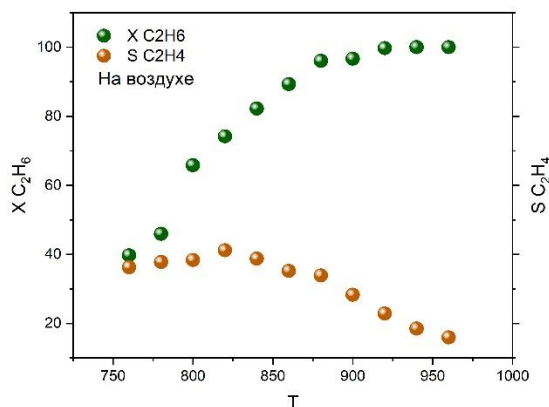


Figure 1. Dependence of ethane conversion and ethylene selectivity in oxidative dehydrogenation of ethane in air/ethane gradient

Acknowledgement. This research was financially supported by the Ministry of Science and Higher Education of the Russian Federation (The work was financially supported by RSF grant No. 23-43-00130)

References

1. *G. Chen, A. Feldhoff, A. Weidenkaff, C. Li, S. Liu, X. Zhu, J. Sunarso, K. Huang, X.Y. Wu, A.F. Ghoniem, W. Yang, J. Xue, H. Wang, Z. Shao, J.H. Duffy, K.S. Brinkman, X. Tan, Y. Zhang, H. Jiang, R. Costa, K.A. Friedrich, R. Kriegel.* Roadmap for Sustainable Mixed Ionic-Electronic Conducting Membranes // *Advanced Functional Materials.* – 2021. – V. 32. – Is. 6. – P. 2105702.

SURFACE MODIFICATION OF CERAMIC MEMBRANE BASED ON STRONTIUM FERRITE FOR COUPLING CATALYTIC CO₂ CONVERSION WITH PARTIAL OXIDATION OF METHANE

Olga Bragina, Elena Shubnikova, Marina Arapova, Alexander Nemudry

Institute of Solid State Chemistry and Mechanochemistry SB RAS, Novosibirsk, Russia

E-mail: bragina@solid.nsc.ru

Introduction

Currently, materials with mixed oxygen electronic conductivity have attracted great interest due to possibility of their use in catalytic membrane reactor, which allows to perform oxygen separation and partial oxidation of methane simultaneously. The materials for catalytic membrane reactor must possess both long-term stability under reducing atmosphere and acceptable oxygen fluxes. An effective way to improve functional properties of materials is substitution of A and B positions in perovskite ABO₃ structure. However, the stability enhancement obtained by doping is accompanied by a significant decrease in oxygen fluxes. The increase of oxygen fluxes can be achieved by optimization of the membrane thickness, membrane configuration, active surface area [1]. In this work we reported the results of surface modification of hollow fiber La_{0.4}Sr_{0.6}Fe_{0.95}Mo_{0.05}O_{3-δ} (LSFM5) membrane on oxygen fluxes and catalytic performance in partial oxidation of methane coupled with CO₂ splitting.

Experiments

Using the phase inversion method, hollow fiber LSF5 membranes with unique microstructure were prepared. The obtained membrane had oxygen fluxes in an air/argon gradient and T=960 °C at a level of 0.5 ml·min⁻¹·cm⁻². The further increase of oxygen fluxes through LSF5 membrane by a factor of 1.3 was achieved by different surface modification such as acid-etching and by surface decoration by porous layers. Conducted studies of hydrogen production by partial oxidation of the methane showed that Ni/LSFM5 catalytic membrane reactor provide 100% methane conversion with H₂ and CO selectivities above 90% and a H₂/CO ratio close to 2 starting already from 900 °C.

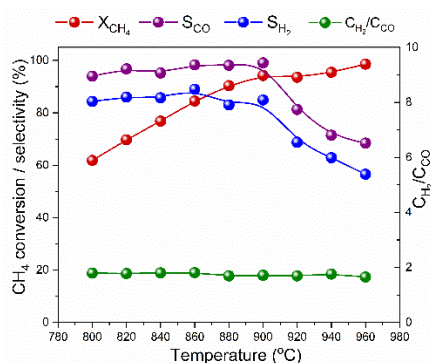


Figure 1. Temperature dependences of methane conversion, CO/H₂ selectivity and H₂/CO ratio in (CO₂+N₂)/diluted methane gradient obtained on LSF5 membranes decorated by nickel particles.

Acknowledgement. This research was funded within the state assignment to ISSCM SB RAS, «Laboratory of Materials and Technologies of Hydrogen Energy» (project no. 075-03-2022-424/3) and by the Russian Science Foundation (project no. 23-43-00130).

References

1. Chen G., Feldhoff A., Weidenkaff A., Li C., Liu S., Zhu X., Sunarso J., Huang K., Wu X.-Y., Ghoniem A.F, Yang W., Xue J., Wang H., Shao Z., Duffy J.H., Brinkman K.S., Tan X., Zhang Y., Jiang H., Costa R., Friedrich K.A., Kriegel R. Roadmap for sustainable mixed ionic-electronic conducting membranes // Adv. Funct. Mater. 2022. V. 22. P. 2105702.

LITHIUM RECOVERY FROM LITHIUM-COBALT-NICKEL-CONTAINING SOLUTION USING NANOPOROUS MEMBRANE

¹Alexey Budnikov, ^{1,2}Vasiliy Troitskiy, ¹Dmitrii Butylskii,

¹Kuban State University, Krasnodar, Russia, *E-mail: d_butylskii@bk.ru*

²Platov South-Russian State Polytechnic University (NPI), Novocherkassk, Russia

Introduction

Recycling lithium-ion batteries (LIBs) is an urgent issue in the world. Typically, hydrometallurgical approaches are used for their processing, including sulfonic acid leaching of valuable components and their sequential fractionation with reagents. The authors of some papers [1, 2] note that the extraction of lithium and no-less valuable cobalt from leachates of spent LIBs has clear advantages over their extraction from natural sources. The concentration of lithium and cobalt in leachates is usually quite high. The composition of leachates is more predictable and less varied. The leachates do not contain multiply charged ions such as Ca^{2+} and Mg^{2+} , which have low value and which make it difficult to extract lithium from natural solutions.

It is known from the literature that the processing of NMC-type batteries (the cathode is obtained from a mixture of lithium, nickel, manganese and cobalt) is more economically attractive than the recycling of cheaper LFP-type batteries (lithium iron phosphate cathode). This is due to the ability to extract valuable cobalt and nickel from leachates of NMC batteries in addition to lithium.

The membrane technologies can be used to recycle spent LIBs in addition to existing reagent-based methods. In recent years, the hybrid electrobaromembrane (EBM) method has been actively developed, which makes it possible to achieve high separation efficiency [3, 4]. Unlike electrodialysis, EBM separation uses non-selective porous membranes. Separated ions of the same charge sign move in an electric field through the pores of this membrane to the corresponding electrode, while a commensurate counter convective flow is created in the pores. The selectivity of separation is achieved due to the difference in the mobility of the competing ions.

The aim of our work is to apply EBM method to separate Li^+ , Co^{2+} and Ni^{2+} ions, contained in leachates of spent LIBs.

Experiments

A mixture of 0.05 M Li_2SO_4 , 0.025 M CoSO_4 and 0.025 M NiSO_4 (pH = 5.2) was used to determine the optimal separation parameters. In this work, a TEM #811 track-etched membrane with diameter of pores of 35 nm was used. It was produced from a polyethylene terephthalate (PET) film at the Joint Institute for Nuclear Research (Dubna, Russia). On the left- and right-hand sides the TEM is surrounded by auxiliary anion-exchange MA-41 heterogeneous membranes (JCC Shchekinoazot, Pervomayskiy, Russia) to form flow chambers.

The concentration of Li^+ -ions determine using a Dionex ICS-3000 ion-chromatograph with a conductometric detector (Dionex, Sunnyvale, CA, USA), and the concentration of cobalt and nickel was determined using direct spectrophotometric analysis with a UV-1800 TM ECOVIEW (Shanghai Mapada Instruments Co., Shanghai, China) instrument.

Results and Discussion

To evaluate the efficiency of separation of Li^+ , Co^{2+} and Ni^{2+} ions through the TEM #811 membrane, optimal parameters selected were used $\Delta p = 0.3$ bar; $i = 137.5$ A/m². Table 1 shows the results of the separation of $\text{Li}^+/\text{Co}^{2+}/\text{Ni}^{2+}$ -ions by the EBM method.

The flux of Ni^{2+} ions through the membrane is 0.04 mol/(m² × h). The difference between the fluxes of Co^{2+} and Ni^{2+} is explained by the fact that NiSO_4 dissociates in aqueous solutions better than CoSO_4 . The fraction of Ni^{2+} ions in the feed solution is approximately 0.61 (0.39 in the form of its sulfate), while that of Co^{2+} ions is 0.58 (pH = 5.2). The transport number (and hence the flux) of Ni^{2+} ions in pore solution is higher than the transport number of Co^{2+} ions ($t_{\text{Ni}^{2+}} = 0.07$

Table 1: Comparison of separation efficiency of Li⁺/Co²⁺/Ni²⁺-ions by EBM method at $\Delta p = 0.3$ bar

Current Density, i , A/m ²	Ions in the Feed Solution	$c_{M^{n+}}^0$, g/L	$j_{M^{n+}}$, mol/(m ² × h)	$S_{Li^+/M^{n+}}$
137.5	Li ⁺	0.69	0.33	—
	Co ²⁺	1.47	0.02	4
	Ni ²⁺	1.47	0.04	2
125	Li ⁺	0.69	0.30	—
	Co ²⁺	1.47	-0.02	n/a
	Ni ²⁺	1.47	-0.005	n/a

and $t_{Co^{2+}} = 0.06$). The z_2D_2/z_1D_1 [6] ratio for the Li⁺/Ni²⁺ pair is higher than for the Li⁺/Co²⁺ pair (0.76 and 0.71, respectively). This means that it is more difficult to separate Li⁺ and Ni²⁺ ions than Li⁺ and Co²⁺. To estimate competing ion fluxes, the change in concentration over time in the chambers of the EBM device is determined against the background of a high concentration of the analyte in the feed solution. Due to the fact that the fluxes of both Co²⁺ ions and Ni²⁺ ions were positive at 137.5 A/m² (controlled by migration), in order to increase the efficiency of lithium extraction, the current density was reduced to 125 A/m² at the same pressure value ($\Delta p = 0.3$ bar) (Table 1). This caused the fluxes of cobalt and nickel to become negative, which means that the dominant transport mechanism is convection. However, the lithium flux changed insignificantly, from 0.33 to 0.30 mol/(m² × h). This allowed lithium to be fractionated from the mixed solution. Taking into account that the fluxes of cobalt and nickel ions are negative, the separation coefficient is not available for calculation.

References

1. Decarolis A., Hong J. S., Taylor J. Fouling behavior of a pilot scale inside out hollow fiber UF membrane // J. Membr. Sci. 2001. V. 191. P. 165-178.
2. Butylskii, D.Y.; Dammak, L.; Larchet, C.; Pismenskaya, N.D.; Nikonenko, V.V. Selective recovery and re-utilization of lithium: Prospects for the use of membrane methods // Russ. Chem. Rev. 2023. V. 92. № 4. P. 1-30
3. Tabelin, C.B.; Dallas, J.; Casanova, S.; Pelech, T.; Bournival, G.; Saydam, S.; Canbulat, I. Towards a low-carbon society: A review of lithium resource availability, challenges and innovations in mining, extraction and recycling, and future perspectives // Miner. Eng. 2021. V. 163. P. 106743.
4. Butylskii, D.; Troitskiy, V.; Chuprynina, D.; Kharchenko, I.; Ryzhkov, I.; Apel, P.; Pismenskaya, N.; Nikonenko, V. Selective Separation of Singly Charged Chloride and Dihydrogen Phosphate Anions by Electrobaromembrane Method with Nanoporous Membranes // J. Membr. Sci.. 2023. V. 13. № 5. P. 455.
5. Forssell, P.; Kontturi, K. Experimental Verification of Separation of Ions Using Countercurrent Electrolysis in a Thin, Porous Membrane // Sep. Sci. Technol. 1983. V. 18. № 3. P. 205–214.
6. Butylskii, D., Troitskiy, V., Chuprynina, D., Dammak, L., Larchet, C., Nikonenko, V. Application of Hybrid Electrobaromembrane Process for Selective Recovery of Lithium from Cobalt-and Nickel-Containing Leaching Solutions // J. Membr. Sci. 2023. V. 13. №. 5. P. 509.

SELECTIVE SEPARATION OF LITHIUM, POTASSIUM AND SODIUM USING MEMBRANE-BASED TECHNOLOGIES

¹Dmitrii Butylskii, ^{1,2}Vasiliy Troitskiy, ¹Roman Salichov, ²Nina Smirnova, ¹Victor Nikonenko

¹Kuban State University, Krasnodar, Russia, *E-mail: d_butylskii@bk.ru*

²Platov South-Russian State Polytechnic University, Novocherkassk, Russia

Introduction

Separation of a mixture of singly charged ions is an important task in terms of practical applications. For example, valuable lithium salts are mainly (up to 99%) obtained from natural sources (brines, minerals, etc.). Natural brines and mineral leaching solutions are rich in coexisting single-charge K^+ and Na^+ ions. In industrial scale, to remove them, they resort to reagent-based processes of hydrometallurgical technology. Pressure-driven and electrically-driven membrane processes also can be involved in this technology for separation monovalent and multivalent ions [1]. However, these processes are not quite suitable for separation different monovalent ions. Various membrane design parameters, including geometry, surface charge, molecular structure, chemical affinity, nanochannel size, energy barrier, and driving force, can influence the lithium ion separation efficiency based on their separation mechanism [2]. Highly efficient lithium selective membranes have been recently developed with different materials, including metal-organic frameworks, graphene oxide, polyethylene terephthalate, vermiculate, etc. [1]. However, for such membranes a trade-off effect is true: with an increase in separation selectivity, the permeability of the membranes decreases.

Electrobaromembrane method (EBM) is a unique process under development, which can efficiently separate monovalent ions. The process is accomplished using a porous membrane under the simultaneous action of an electric field and a pressure field, which drive competing ions in opposite directions. The separation is achieved due to the difference in the mobility of the competing ions. In recent works on EBM devices, impressive results have been achieved in the separation of Li^+/K^+ ions, when using feed solutions imitating natural waters [3, 4]. It was shown that the ion separation coefficient for the Li^+/K^+ ions can be as high as 59 and even 150. For the Li^+/Na^+ pair, the selective permeability coefficient is somewhat lower and reaches 30.

Experiments

Solutions of the same composition and volume (2 L) containing separated Li^+ , K^+ and Na^+ ions were pumped on the left (stream I) and right-hand (stream II) sides of a track-etched membrane (TEM) with effective surface 30 cm^2 . The stream II was pumped under pressure of 0.2 bar. The TEM with a nominal pore diameter of 35 nm were produced at the Joint Institute for Nuclear Research (Dubna) from a polyethylene terephthalate. The samples of solutions were taken every 4 h during 40 h of experiment. Determination of the concentration of ions was carried out using a Dionex ICS-3000 ion-chromatograph with conductometric detector.

Results and Discussion

The transport of K^+ ions through TEM is driven predominantly by migration (positive). As for Na^+ , the number of moles of this ion increases in stream I at the beginning of the experiment, then starting from 10 h, the amount of this ion decreases in stream I (Fig. 1a). Therefore, we can conclude that up to 10 h, the transport of Na^+ is controlled by convection, as in the case of Li^+ ; however, at 10 h, the predominant driving force changes and the transport of Na^+ becomes controlled by migration. After 20 h from the beginning of the experiment, the fluxes become more or less stable and are evaluated as $j_{K^+} = 0.24\text{ mol}/(\text{m}^2 \times \text{h})$, $j_{Na^+} = 0.076\text{ mol}/(\text{m}^2 \times \text{h})$, $j_{Li^+} = -0.07\text{ mol}/(\text{m}^2 \times \text{h})$. Although the fluxes of separated ions were not high (Fig. 1c), the fact that lithium is directed in the opposite direction makes it possible to isolate it from a mixture with K^+ and Na^+ ions. Determination of the selectivity coefficient is not available. In fact, the ions move in different directions (Fig. 1b), but do not compete in the classical sense. However, it should be noted that the results previously obtained by our colleagues and us [1, 5] suggest that EBM

separation is significantly superior to ED in the efficiency of separation of singly charged ions (Fig. 1c,d).

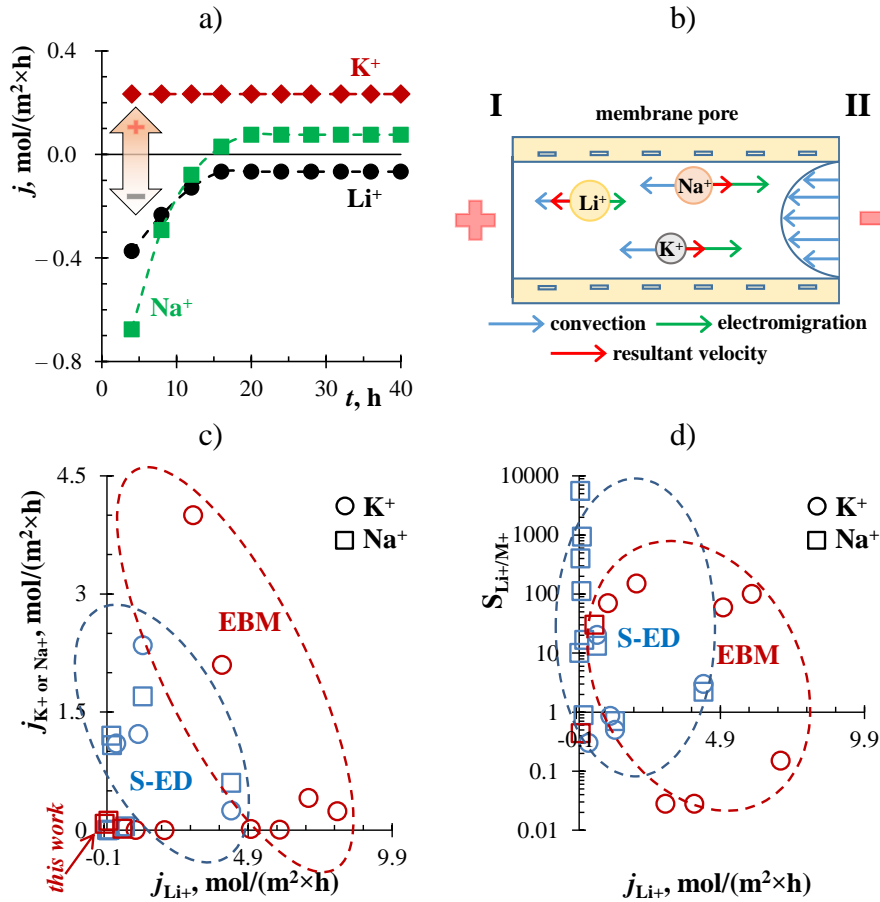


Figure 1. Time dependence of the flux densities of Li⁺, K⁺ and Na⁺ at a pressure difference of 0.2 bar and a current density of 117 A/m² (a), diagram of ion separation in a pore of the TEM-35 (b), achievements of selective electrodesionization and EBM separation in fluxes of Li⁺, K⁺ and Na⁺ (c) and separation coefficient (d).

References

1. Butylskii D., Dammak L., Larchet C., Pismenskaya N.D., Nikonenko V.V. Selective recovery and re-utilization of lithium: prospects for the use of membrane methods // Russ. Chem. Rev. 2023. 92
2. Farahbakhsh, J., Arshadi, F., Mofidi, Z., Mohseni-Dargah, M., K ok, C., Assefi, M., ... & Razmjou, A. Direct lithium extraction: A new paradigm for lithium production and resource utilization // Desalination. 2024. V. 575. 117249.
3. Butylskii, D.Y.; Pismenskaya, N.D.; Apel, P.Y.; Sabbatovskiy, K.G.; Nikonenko, V.V. Highly selective separation of singly charged cations by countercurrent electromigration with a track-etched membrane. J. Memb. Sci. 2021, 635, 119449.
4. Tang, C., Bondarenko, M.P., Yaroshchuk, A., Bruening, M.L. Highly selective ion separations based on counter-flow electromigration in nanoporous membranes. J. Memb. Sci. 2021, 638, 119684.
5. Butylskii, D.Y., Troitskiy, V.A., Chuprynina, D.A., Pismenskaya, N.D., Smirnova, N.V., Apel, P.Y., Dammak, L., Mareev S.A., Nikonenko, V.V.. Selective recovery of lithium ion from its mixed solution with potassium and sodium by electrobaromembrane method. Separation and Purification Technology. 2024. 126675.

ETHYLENE PRODUCTION IN CATALITIC MEMBRANE REACTORS BASED ON PEROVSKITE-FLUORITE DUAL-PHASE MATERIALS

Olga Cherendina, Elena Shubnikova, Olga Bragina, Maria Khohlova, Alexander Nemudry

Institute of Solid State Chemistry and Mechanochemistry, Kutateladze, 18, Novosibirsk, Russia
E-mail: o.cherendina@g.nsu.ru

Introduction

Ethylene is a commercially important product in the fields of automotive and petroleum refining, and the gas itself is one of the most commonly produced hydrocarbons on a global scale. A promising direction in the field of ethylene production is the use of a microtubular oxygen permeable membrane as a membrane reactor, which is presented by non-stoichiometric MIEC oxides with perovskite structure, possessing high mixed oxygen-electron conductivity [1].

Experiments

The composite SFM5-GDC was obtained by the Pechini method and validated by scanning electron microscopy and X-ray diffraction techniques. Oxygen permeability measurements were performed on microtubular membranes obtained from the SFM5-GDC composite by the phase inversion method. The high-temperature experiments on the catalytic activity of the membrane in the reaction of oxidative dehydrogenation of ethane was applied in the air and CO₂-containing atmosphere.

Results and Discussion

In this study, the dependences of oxygen fluxes on temperature and oxygen partial pressure of MT membranes of SFM5-GDC composition were obtained. The activation energy of the oxygen transport process was determined. The catalytic activity of MT membranes based on SFM5-GDC in the reaction of oxidative dehydrogenation of ethane was studied as a function of temperature. It is shown that at a temperature of 900 °C in the air/Ar gradient the selectivity for ethylene reaches a value of ~ 67% with ethane conversion of ~ 95%. When CO₂ is used as an oxygen source, ethylene selectivity reaches ~ 62% and ethane conversion ~ 99% at T=900 °C. Time dependences of ethane conversion and ethylene selectivity were obtained for SFM5-GDC-based microtubular membrane. It was shown that the material is stable under reducing conditions in air and CO₂-containing atmosphere.

Possibility of ethylene production by the oxidative dehydrogenation of ethane in the hollow fiber membrane reactor based on SFM5-GDC with the alternative current heating was demonstrated. It was shown that high selectivity of the ethylene can be achieved by the alternative current heating.

Acknowledgement. This work was financially supported by RSF grant No. 23-43-00130

References

1. Liang F. *et al.* Cobalt-free dual-phase oxygen transporting membrane reactor for the oxidative dehydrogenation of ethane //Separation and Purification Technology. – 2019. – T. 211. – C. 966-971.

ASYMPTOTIC ANALYSIS OF STATIONARY TRANSPORT OF SALT IONS IN THE SECTION OF THE DESALTING CHANNEL TAKEN INTO ACCOUNT OF THE DISSOCIATION/RECOMBINATION REACTION OF WATER MOLECULES

¹Natalya Chubyr, ¹Anna Kovalenko, ¹Makhamet Urtenov, ²Zulfa Laipanova

¹Kuban State University, Krasnodar, Russia, E-mail: chubyr-natalja@mail.ru

²Karachay-Cherkess State University named after U.D. Aliyeva, E-mail: laipanovazulfa@mail.ru

Introduction

Taking into account the global phenomenon of association/recombination of water molecules is important for understanding the processes of ion dispersion in electromembrane components, since the appearance of new charge carriers H^+ and OH^- can lead to a decrease or even absorption of the internal charge, which occurs based on other methods, for example, electroconvection [1,3,4]. This work investigates the effect of non-catalytic dissociation/recombination of water molecules on the transport of salt ions.

Materials and Methods

The stationary transport of salt ions in the cross section of the desalting channel is described by the following boundary value problem in dimensionless form [1]:

$$\begin{aligned}\frac{dC_i}{dx} &= z_i C_i \frac{d\varphi}{dx} - j_i, \quad i=1,..4 \\ \varepsilon \frac{dj_3}{dx} &= a(k_w - C_3 C_4) \\ \varepsilon \frac{dj_4}{dx} &= a(k_w - C_3 C_4) \\ \varepsilon \frac{d^2\varphi}{dx^2} &= -C_1 + C_2 - C_3 + C_4\end{aligned}$$

Boundary conditions:

$$\begin{aligned}\left(-C_1 \frac{d\varphi}{dx} - \frac{dC_1}{dx}\right)(0, \varepsilon) &= 0, \quad C_2(0, \varepsilon) = C_{2a}, \quad \left(-C_3 \frac{d\varphi}{dx} - \frac{dC_3}{dx}\right)(0, \varepsilon) = 0, \\ \frac{dC_4}{dx}(0, \varepsilon) &= 0, \quad \varphi(0, \varepsilon) = \varphi_0, \quad C_1(1, \varepsilon) = C_{1k}, \quad \left(C_2 \frac{d\varphi}{dx} - \frac{dC_2}{dx}\right)(1, \varepsilon) = 0, \\ \frac{dC_3}{dx}(1, \varepsilon) &= 0, \quad \left(C_4 \frac{d\varphi}{dx} - \frac{dC_4}{dx}\right)(1, \varepsilon) = 0, \quad \varphi(1, \varepsilon) = 0,\end{aligned}$$

where $\varepsilon > 0$, $k_w > 0$ – small parameters, $\varphi(x, \varepsilon)$ – potential, I_c – Faraday conduction current, caused by ion flow K^+ , Cl^- , H^+ , OH^- , $j_i(x, \varepsilon)$, $C_i(x, \varepsilon)$, D_i – flow, concentrations, diffusion coefficients of the i -th ion, k_w – equilibrium constant. In stationary case $j_1 = j_2 = 0$ [4]. Therefore, the current through salt ions is zero and, therefore, the total current is equal to the current through ions H^+ , OH^- : $I_c = j_3 - j_4$, that is, we have a limiting case.

It is proposed to use the method of merging asymptotic expansions for the asymptotic solution of the boundary value problem, namely, divide the initial segment $[0,1]$ into 7 segments, on each of which the solution is sought in its own way, since in this problem four boundary layers arise, two of which are located at ion exchange membranes are typical, and the other two boundary layers are internal boundary layers caused by the dissociation/recombination reaction:

- 1) external solution, - a solution to a degenerate problem in areas where the condition of electrical neutrality and equilibrium is satisfied ($\varepsilon = 0$),
- 2) solution in boundary layers near membranes,
- 3) solution in internal boundary layers,
- 4) merging of asymptotic expansions (determining integration constants and domain boundaries).

Results and Discussion

As a result of the asymptotic solution, formal asymptotic solutions were obtained for concentrations, fluxes and intensity at different intervals. As an example, Table 1 shows the results for threads.

Table 1: Asymptotic solution for flows at different intervals

	j_1	j_2	j_3	j_4
$[0; \delta_1)$	0	0	$I_c + \frac{ak_w}{\varepsilon}(x - \delta_1)$	$\frac{ak_w}{\varepsilon}(x - \delta_1)$
$(\delta_1; x_1 - \delta_2)$	0	0	I_c	0
$(x_1 - \delta_2; x_1 + \delta_3)$	0	0	$\frac{D_3}{D_3 + D_4} I_c +$ $\frac{D_4}{D_3 + D_4} I_c e^{-\sqrt{\frac{aC_3(x_1)(D_3+D_4)}{D_3D_4}} \frac{x-x_1}{\sqrt{\varepsilon}}}$	$-\frac{D_4}{D_3 + D_4} I_c +$ $\frac{D_4}{D_3 + D_4} I_c e^{-\sqrt{\frac{aC_3(x_1)(D_3+D_4)}{D_3D_4}} \frac{x-x_1}{\sqrt{\varepsilon}}}$
$(x_1 + \delta_3; x_2 - \delta_4)$	0	0	$\frac{D_3}{D_3 + D_4} I_c$	$-\frac{D_4}{D_3 + D_4} I_c$
$(x_2 - \delta_4; x_2 + \delta_5)$	0	0	$-\frac{D_4}{D_3 + D_4} I_c +$ $\frac{D_4}{D_3 + D_4} I_c e^{-\sqrt{\frac{aC_3(x_1)(D_3+D_4)}{D_3D_4}} \frac{x-x_2}{\sqrt{\varepsilon}}}$	$\frac{D_3}{D_3 + D_4} I_c +$ $\frac{D_4}{D_3 + D_4} I_c e^{-\sqrt{\frac{aC_3(x_1)(D_3+D_4)}{D_3D_4}} \frac{x-x_2}{\sqrt{\varepsilon}}}$
$(x_2 + \delta_5; 1 - \delta_6)$	0	0	0	$-I_c$
$(1 - \delta_6; 1)$	0	0	$\frac{ak_w}{\varepsilon}(x - 1 + \delta_6)$	$I_c + \frac{ak_w}{\varepsilon}(x - 1 + \delta_6)$

A comparison of the asymptotic and numerical solutions was carried out for all functions on each segment, which showed their agreement with an error of less than one percent.

Conclusion

In this work, an asymptotic solution to the problem of stationary transfer in the cross section of the desalting channel is constructed. It is shown that in this problem four boundary layers arise, two of which are located at ion-exchange membranes and are typical, and internal boundary layers arising due to the dissociation/recombination reaction. It is shown that outside the boundary layers, the conditions of local electrical neutrality and equilibrium are satisfied, which leads to a linear or constant distribution of concentrations. It has been shown that a region of depleted solution appears inside the desalting channel, where the concentrations of salt ions H^+ and OH^- are practically constant, and the concentrations of salt ions are significantly less than the concentrations of ions H^+ и OH^- . Comparison of the asymptotic solution with the numerical solution shows their agreement with good accuracy. The resulting asymptotic solution is valid in a wide range of changes in the initial concentration from 10^{-2} моль/м³ до 10^2 моль/м³, channel width H from 0.1 mm to 10 mm at which the parameters ε and k_w remain small.

The asymptotic solution of this problem allows us to construct, by analogy, asymptotic solutions for other singularly perturbed boundary value problems of membrane electrochemistry, thus this boundary value problem can be considered a reference one.

Acknowledgement. This study was supported by the Russian Science Foundation, research project no. 24-19-00648, <https://rscf.ru/project/24-19-00648> .

References

1. *Gudza V.A., Urtenov M.K., Chubyr N.O., Kirillova E.V.* Numerical and asymptotic study of non-stationary mass transport of binary salt ions in the diffusion layer near the cation exchange membrane at prelimiting currents / *Applied mathematics and information sciences*, 2021, p 411-422.
2. *Vasilyeva A.B., Butuzov V.F.* Asymptotic methods in the theory of singular perturbations. – M., 1990., 207c.
3. *Chubyr N.O., Kovalenko A.V., Urtenov M.Kh.* Numerical and asymptotic methods for analyzing 1:1 electrolyte transfer in membrane systems / *Krasnodar*, 2018, 106 c.
4. *Simons, R.* Water splitting in ion exchange membranes. *Electrochim. Acta* 1985, 30, 275–282.

LAYER-BY-LAYER ASSEMBLY OF POLYELECTROLYTES ON A POLY(EPOCHLOROHYDRIN) BASED ANION EXCHANGE MEMBRANE TO ENHANCE ENERGY HARVESTING BY REVERSE ELECTRODIALYSIS

^{1,2}Aydın Cihanoglu

¹Ege University, Department of Chemical Engineering, İzmir, Türkiye

²Ege University, Alağa Vocational School, Department of Refinery and Petrochemical Technology, İzmir, Türkiye, *E-mail: aydincihanoglu@gmail.com, aydin.cihanoglu@ege.edu.tr*

Introduction

Today, energy needs are mainly supplied by fossil fuels. This situation causes an increase in CO₂ footprint and global warming. Therefore, there is an urgent need to meet the energy demand from renewable energy sources. Reverse electrodialysis (RED), also known as blue energy, has gained interest in the scientific world and private companies over the last two decades [1]. This technology is ion exchange membranes (IEMs)-based technology, and two main restrictions decrease energy harvesting from the RED system. These are the organic fouling tendency and the uphill transport of multivalent ions across the membranes [2]. In this study, a poly(epichlorohydrin) (PECH)-based anion exchange membrane (AEM) synthesized was modified with polyelectrolytes via a layer-by-layer technique to eliminate the uphill transport and organic fouling behavior.

Experiments

The PECH-based AEM was synthesized by solvent evaporation technique [3]. Then, the surface of the synthesized membrane was modified with negatively charged poly(sodium-4-styrene sulfonate) (PSS) and positively charged poly(ethyleneimine) (PEI) polyelectrolytes via the layer-by-layer method under the current. The RED performance of the modified membranes was tested in the presence of Na₂SO₄ ions to check the uphill transport. Further, the modified membranes were fouled with organic foulant (a humic+fulvic acid mixture), and their RED performance was tested after fouling. Finally, the long-term RED performance of the synthesized, modified, and fouled membranes was tested using only monovalent ions (NaCl).

Results and Discussion

The fouling tendency of the PECH-based AEM decreased dramatically after modification with polyelectrolytes due to the creation of a more hydrophilic layer on the AEMs surface. This helped to improve the RED performance of the modified AEMs. The created polyelectrolyte multilayers on the AEMs surface increased the negative surface charge, resulting in the rejection of negatively charged divalent ions (SO₄²⁻) due to the electrostatic repulsion. Rejection of negatively charged divalent ions allowed for increased energy harvesting performance from the RED system by reducing uphill transport.

Acknowledgement. This research was financially supported by the Scientific and Technological Research Council of Türkiye (TÜBİTAK) with the National Postdoc Project (Project No: 118C549). The author acknowledges Prof. Dr. Nalan Kabay for her guidance and support and for providing access to all laboratory facilities. The author acknowledges Assoc. Prof. Dr. Enver Güler for his guidance. The author acknowledges Mitsubishi Chemical, Japan, especially Ando Kiyoto, for PAN polymer and Osaka Soda Co., Japan, for PECH polymer.

References

1. Tian H., Wang Y., Pei Y., Crittenden J. C. Unique applications and improvements of reverse electrodialysis: A review and outlook // *Appl. Energy* 2020. V. 262. P. 114482.
2. Vermaas D. A., Veerman J., Saakes M., Nijmeijer K. Influence of multivalent ions on renewable energy generation in reverse electrodialysis // *Energy Environ. Sci.* 2014. V. 7. P. 1434-1445.
3. Guler E., Zhang Y., Saakes M., Nijmeijer K. Tailor made anion exchange membranes for salinity gradient power generation using reverse electrodialysis // *ChemSusChem* 2012. V. 5. P. 2262-2270.

ADVANCING IN TRACE ELEMENT RECOVERY FROM BRINES: INSIGHTS INTO DIFFERENTIAL ION TRANSPORT THROUGH ELECTRODIALYSIS WITH BIPOLAR MEMBRANES

¹Andrea Culcasi, ¹Antonia Filingeri, ^{2,3}Julio Lopez, ^{2,3}Marc Fernandez de Labastida, ^{1,4}Alessandro Tamburini, ^{2,3}José Luis Cortina, ¹Giorgio Micale, ¹Andrea Cipollina

¹Dipartimento di Ingegneria, Università degli Studi di Palermo, Viale delle Scienze Ed. 6, 90128 Palermo, Italy

²Chemical Engineering Department, Escola d'Enginyeria de Barcelona Est (EEBE), Universitat Politècnica de Catalunya (UPC)-BarcelonaTECH, C/ Eduard Maristany 10-14, Campus Diagonal-Besòs, 08930 Barcelona, Spain

³Barcelona Research Center for Multiscale Science and Engineering, Campus Diagonal-Besòs, 08930 Barcelona, Spain

⁴ResourSEAs SrL, Viale delle Scienze, Ed.16, 90128 Palermo, Italy

E-mail: andrea.culcasi@unipa.it

Introduction

Currently, brines represent an interesting non-conventional source of Critical Raw Materials (CRMs) such as Mg, Li, B, Sr and other Trace Elements (TEs) such as Cs and Rb. As an example, brines from saltworks, which produce sea salt, are 20–40 times more concentrated than seawater in these elements [1], thus making them attractive for the recovery of such CRMs. In the framework of the SEArcularMINE project [2], a new treatment chain is proposed for the selective recovery of Mg, Li, B, Sr, and TEs using different technologies that require acidic and alkaline solutions as reagents to operate. In order to facilitate the process of moving from a linear economy to a fully circular approach, the in-situ generation of such reactants is essential. For this purpose, Electrodialysis with Bipolar Membranes (EDBM) represents a very promising solution, as it can produce the necessary reactants in-situ while also valorizing the remaining salt solution resulting from the recovery process.

The aim of this work is to investigate the “fate” of TEs conveyed by the feed stream in EDBM systems, by studying the migration across Ion Exchange Membranes (IEMs) of major and minor ions as well as of the TEs from the feed to the products solutions.

Experiments

A laboratory-scale EDBM unit was used to carry out the experimental campaign. The EDBM unit was a stack of 5 triplets with an active membrane area of 0.028 m². The experiments were conducted with i) NaCl solutions, ii) multi-ionic synthetic solutions and iii) real solutions from the Trapani saltworks, previously pre-treated to recover Mg in order to mimic the real operating condition of the EDBM unit within the SEArcularMINE treatment chain. Specifically, two different configurations were investigated by feeding the salty solutions into either the salt compartment or into both the salt and alkaline compartments. The latter operating configuration is of interest for ensuring a circular treatment chain, where the alkaline solution is re-used in the other process units, thereby reducing the water footprint and avoiding TEs dilution, as claimed in a recently filed patent [3]. A schematic representation of the two configurations is reported in Figure 1.

The EDBM experiments were carried out in a batch (closed-loop) configuration, where samples were collected every 30 minutes. The main process variables were recorded, and each sample underwent titration and chromatographic analyses to enable solution characterization. Minor and trace elements were determined via Inductively Coupled Plasma with Optical Emission Spectroscopy and Mass Spectroscopy.

The raw data obtained from the experiments were then used to calculate the main figures of merit of the EDBM unit, including the Specific Energy Consumption (SEC_{NaOH}) and Current Efficiency (CE). Furthermore, the migration of the major and minor ions and TEs across the IEMs was assessed through the calculation of the apparent transport numbers and the TEs fractions in the channels of the EDBM.

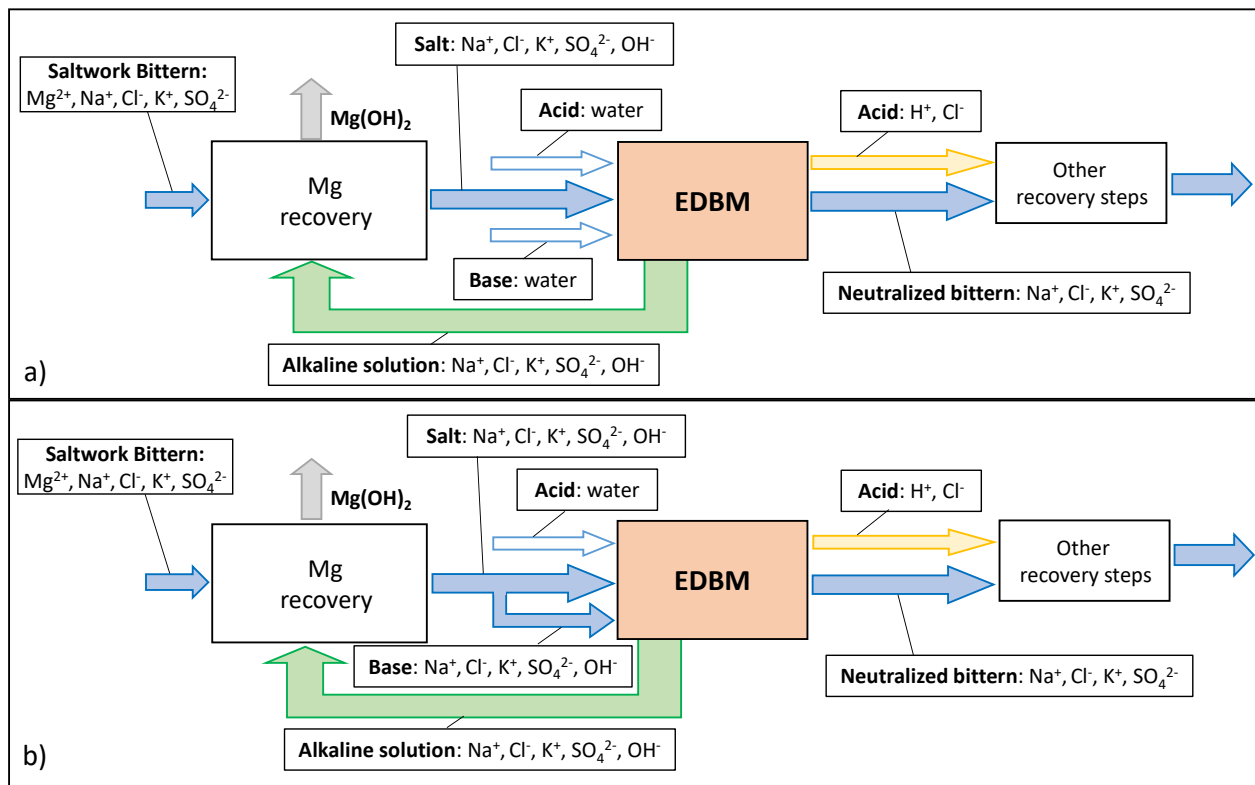


Figure 1. Treatment configurations tested in the experimental design, where the Mg-, Ca-free bittern solution was fed to (a) the salt compartment, and (b) the salt and base compartments.

Results and Discussion

The results highlighted that using the configuration with the real brine stream fed into both the base and salt compartments (case b in Figure 1) did not compromise the EDBM process. Indeed, a similar SEC value of ~ 1.1 kWh/kg NaOH and CE value of $\sim 76\%$ were achieved compared to the configuration where the brine was only fed into the salt compartment (case a in Figure 1). Notably, there was a significant reduction in water consumption of about 50% when using the case b design, thus increasing the sustainability of the process. Figure 2 shows the distribution of each TE across the four compartments at both the beginning and the end of the test for the two process configurations depicted in Figure 1. The minor ions present in the feed in the cationic form, such as Li, Rb, Sr and Cs, were found to be concentrating in the alkaline compartment due to the migrations of these cations from the salt to the base channels across the Cation Exchange Membrane (CEM). Conversely, these ions were predominantly excluded by the Anion Exchange Membrane (AEM) as their concentration in the acid solution was below 5%, thus meaning that ion diffusion was negligible.

Such findings highlight that EDBM can be operated in innovative configurations using circular approaches to valorize saline complex streams, producing acidic and alkaline solutions in-situ and facilitating the concentration of TEs prior to further selective separation steps in the treatment chain.

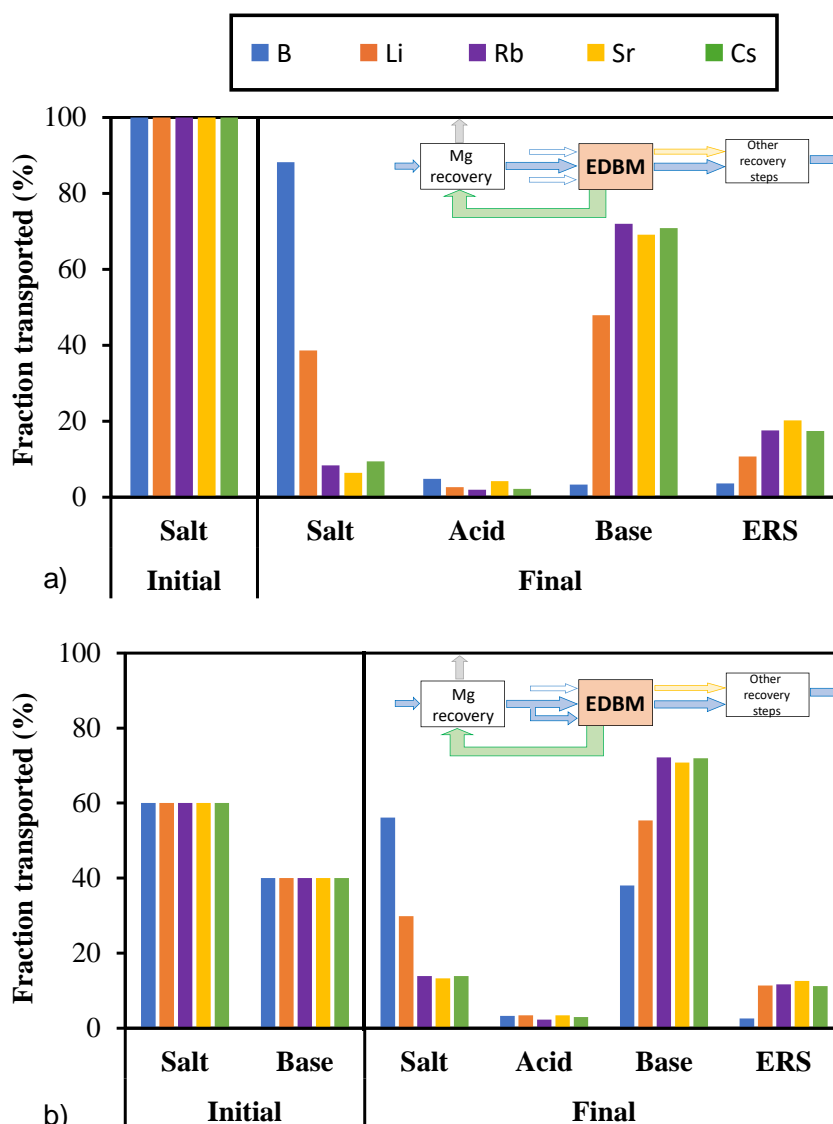


Figure 2. Distribution of each trace element across the four compartments for layout 1 (a) and 2 (b).

Acknowledgement. This work was supported by the EU within SEArcularMINE (Circular Processing of Seawater Brines from Saltworks for Recovery of Valuable Raw Materials) project – Horizon 2020 programme, Grant Agreement No. 869467. This output reflects only the author’s view. The European Health and Digital Executive Agency (HaDEA) and the European Commission cannot be held responsible for any use that may be made of the information contained therein. The work of J. López was supported within the scope of Margarita Salas fellowship, financed by the Ministerio de Universidades (Spain) and European Union – NextGenerationEU.

References

1. F. Vicari, S. Randazzo, J. López, M. Fernández de Labastida, V. Vallès, G. Micale, A. Tamburini, G. D’Alì Staiti, J.L. Cortina, A. Cipollina, Mining minerals and critical raw materials from bittern: Understanding metal ions fate in saltwork ponds, *Sci. Total Environ.* 847 (2022) 157544. <https://doi.org/10.1016/j.scitotenv.2022.157544>.
2. SEArcularMINE, (n.d.). <https://searcularmine.eu> (accessed March 1, 2022).
3. F. Vicari, J. López, C. Cassaro, G. Virruso, A. Culcasi, F. Vassallo, G. Battaglia, A. Filingeri, A. Tamburini, A. Cipollina, Procedimento Di Rimozione Di Cationi Divalenti E Carbonio Inorganico Da Acque Saline Per Il Recupero Di Elementi In Tracce E Relativo Impianto, Italian Patent Application IT102024000005104, 2024.

INFLUENCE OF MODIFICATION WITH ZIRCONIUM PHOSPHATE ON CONDUCTIVITY OF MF-4SC PERFLUORINATED MEMBRANE

¹Ksenia Demidenko, ¹Ekaterina Titskaya, ²Sergey Timofeev, ¹Irina Falina

¹Kuban State University, Krasnodar, Russia, E-mail: irina_falina@mail.ru

²JSC "Plastpolymer", Saint-Petersburg, Russia, E-mail: svtimof@mail.ru

Introduction

Perfluorinated membranes are mainly used as a proton conducting materials in proton exchange membrane fuel cells (FC). Despite their high chemical and thermal stability and high proton conductivity, these membranes have a number of disadvantages. The high cost and a strong decrease in conductivity while operating in low humidity conditions is one of the main disadvantages. In order to eliminate this problem, modification of such materials with various dopants is carried out. The aim of this work was to identify the effect of the content of zirconium hydrogen phosphate (ZrHP) in the membrane and the methods of its insertion on conductivity of membrane at different temperatures and in low humidity conditions.

Experimental

The objects of the study were membranes MF-4SK obtained by casting and extrusion methods. The casting samples were prepared from a mixture of solutions of $ZrOCl_2 \cdot 8H_2O$ and LF-4SK. The resulting polymer films were treated in phosphoric acid after drying. Then, the membranes were washed with water to remove the residues of reagent. To modify the extrusion samples, MF-4SK membranes were kept sequentially under heating for a predetermined period of time in solutions of zirconyl chloride and phosphoric acid. The amount of the inserted dopant depended on the time of immersion of the membrane in the precursor solution and was determined gravimetrically. Before the study, the membrane samples were washed with water to remove reagent residues, dried and pressed between sheets of carbon paper at 125 °C and 800 N/cm². The conductivity was measured for a membrane equilibrated with definite RH and temperature in a climatic chamber in cells with porous titanium electrodes using a four-electrode connection scheme.

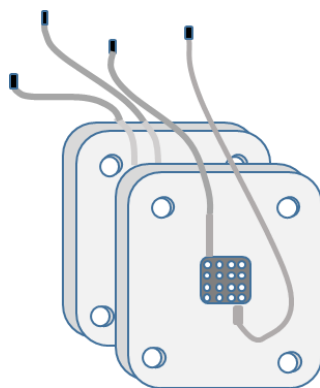


Figure 1. A scheme of a cell for measuring electrical conductivity of the membrane at different humidity and temperature.

Results and Discussion

The study of conductivity of samples at a relative humidity of 30% and various temperatures is shown in Figure 1. The conductivity of samples modified with ZrHP is greater, than the conductivity of the initial casting and extrusion membranes. The casting sample containing 6% ZrHP has the highest electrical conductivity. The extreme conductivity dependence on modifier content in casting membrane could be explained by the model of limited elasticity of the pore walls of perfluorosulfonic acid membranes [1]. According to standard contact porosimetry data the introduction of ZrHP into the membrane in an amount from 3 to 10 wt.% leads to a non-monotonic change in the structural characteristics. With an increase in the ZrHP content in the membrane, the total volume of cavities in the membrane filled with water decreases and reaches a minimum value

for a sample containing 8 wt.% ZrHP. This effect is associated with the displacement of free water from the cluster regions of the membrane by ZrHP nanoparticles.

For extrusion samples, the maximum dependence of electrical conductivity on the amount of dopant introduced is not observed. It may be due to the fact that this method of membrane modification does not allow obtaining samples with a pre-known amount of modifier. It was also found that with almost the same conductivity of the initial extrusion and casting membranes, the modified casting samples have better proton conductivity in comparison with the extrusion ones.

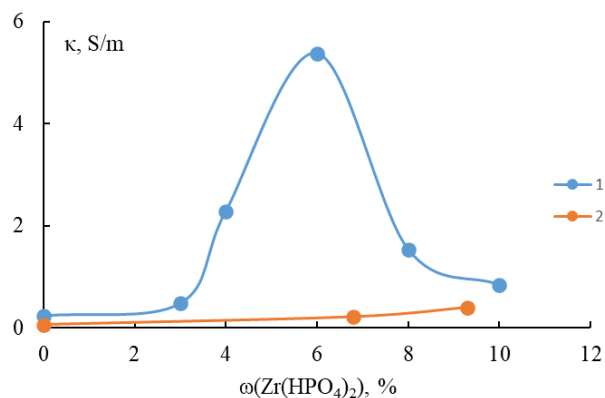


Figure 2. Dependence of conductivity of casting (curve 1) and extrusion (curve 2) samples on content of ZrHP (60 °C and RH = 30%).

The study of the temperature dependence of the conductivity of the initial and modified membranes in the temperature range 30-90 °C are performed. Processing of the obtained data in Arrhenius coordinates allowed to calculate the activation energies, which are shown in figure 3.

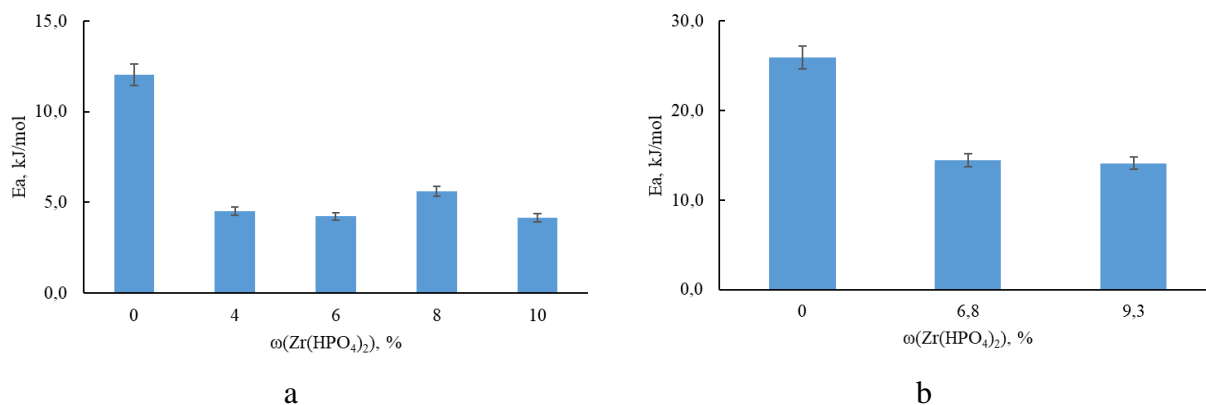


Figure 3. Dependence of activation energy on content of ZrHP for the samples obtained by casting (a) and extrusion (b) methods.

It can be seen, that there is a significant decrease in the activation energy of conductivity for the modified samples compared with the original membranes. At the same time, the amount of the introduced modifier does not influences on the activation energy value.

Acknowledgements. The work was supported by Russian Science Foundation and Kuban Science Foundation (project № 22-19-20101, <https://rscf.ru/project/22-19-20101/>).

References

1. Novikova, S.A.; Safronova, E.Y.; Lysova, A.A.; Yaroslavtsev, A.B. Influence of incorporated nanoparticles on the ionic conductivity of MF-4SC membrane. *Mendeleev Commun.* 2010, 20, 156–157.

DEVELOPMENT AND STUDY OF CHITOSAN MEMBRANES MODIFIED WITH METAL ORGANIC FRAMEWORKS FOR ENHANCED WATER TREATMENT

Mariia Dmitrenko, Anna Kuzminova, Roman Dubovenko, Artem Selyutin, Anastasia Penkova

St. Petersburg State University, 7/9 Universitetskaya nab., 199034 St. Petersburg, Russia
E-mail: m.dmitrienko@spbu.ru

Introduction

Wastewater from various industries poses a huge threat to the environment due to its toxicity. Pollution of industrial waters with low molecular substances and heavy metal ions is one of the main problems. Traditional methods for this separation task have disadvantages (low efficiency and the use of chemicals) compared to membrane technologies. Among them, nanofiltration and pervaporation are considered as promising, environmentally friendly and energy-efficient membrane separation processes for water treatment, including for the removal of heavy metal ions and impurities of low molecular substances, respectively. In this regard, novel inexpensive and environmentally friendly nanofiltration and pervaporation membranes from biopolymers (for example, chitosan) are required.

Experiments

The aim of this study was to develop novel membranes from chitosan (CS) for enhanced water treatment by nanofiltration and pervaporation. To increase the performance efficiency, synthesized metal organic frameworks (MOF) (namely, MIL-125, CuBTC, etc.) were used as membrane modifiers. MOF are promising candidates for creation of mixed matrix membranes (MMM) due to their large surface area, porosity, controlled surface functionality and pore sizes. The structure and properties of obtained composites and membranes from them were studied by spectroscopic (FTIR and NMR), microscopic methods (SEM and AFM), contact angle measurement, etc. Membranes were evaluated in the nanofiltration of model mixtures containing heavy metal ions and pervaporation of water-containing mixtures.

Results and Discussion

It was demonstrated that the modification of CS with synthesized MOF led to changes of membrane structure, morphology, physicochemical, and transport characteristics. Cross-sectional SEM micrographs of membranes based on CS, CS/CuBTC (10%) and CS/MIL-125 (10%) composites are presented in Figure 1. It was found that depending on the choice of MOF with different pore size, hydrophilic properties, and particle shapes, it was possible to vary CS membrane properties for a specific separation task (for nanofiltration and pervaporation). The creation of MMM from CS led to notable improvement of membrane performance due to significant changes in membrane inner and surface structure.

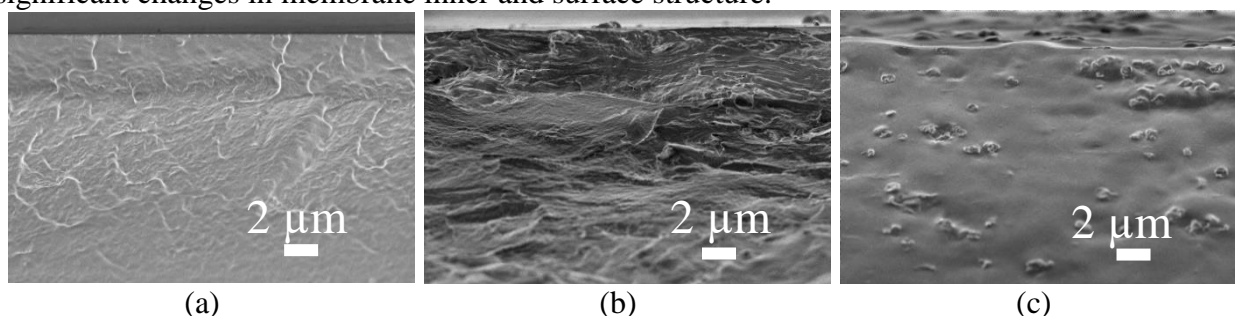


Figure 1. Cross-sectional SEM micrographs of membranes based on (a) CS, (b) CS/CuBTC (10%) and (c) CS/MIL-125 (10%) composites.

Acknowledgement. The authors acknowledge Saint-Petersburg State University for a research project 11602266. The experimental work of this study was facilitated by the equipment from the Resource Centre of Geomodel, Chemical Analysis and Materials Research Centre, Centre for X-ray Diffraction Methods, Magnetic Resonance Research Centre, Centre for Innovative Technologies of Composite Nanomaterials, Nanophotonics Centre, Cryogenic department, Thermogravimetric and Calorimetric Research Centre and the Interdisciplinary Resource Centre for Nanotechnology at the St. Petersburg State University.

DEVELOPMENT AND STUDY OF ULTRAFILTRATION MEMBRANES BASED ON NITROCELLULOSE

Roman Dubovenko, Ksenia Sushkova, Anna Mikulan, Danila Myznikov, Anna Kuzminova, Mariia Dmitrenko, Anastasia Penkova

Institute of Chemistry, St. Petersburg State University, St. Petersburg, Russia

E-mail: r.dubovenko@spbu.ru

Introduction

Research in the field of membrane technologies is of great significance and has vast potential for advancements in various industries and scientific disciplines. Membrane processes play a crucial role in diverse applications such as filtration, substance separation, water and gas purification, energy production, and medical practices. The focal points of research in this field include enhancing and optimizing membrane system performance, as well as developing novel, highly efficient membranes with superior selectivity and permeability. Therefore, undertaking studies in the realm of membrane technologies is a vital and indispensable step towards the progress and growth of modern industries.

As a prominent material for fabricating polymeric membranes, cellulose nitrate (CN) has gained popularity in immunological and biochemical analyses due to its strong protein adsorption capabilities. Consequently, during ultrafiltration, macromolecules can be effectively retained by the membrane through not only sieving mechanisms but also chemical interactions. Despite these attributes, the utilization of nitrocellulose membranes for ultrafiltration processes in protein separation has not received adequate attention.

Results and Discussion

In this study, the focus was on the development and investigation of nitrocellulose-based membranes. The transport characteristics were examined during the ultrafiltration separation of a solution containing bovine serum albumin. The influence of various modifying additives and the choice of solvent on the formation and performance of the membranes was explored. The structural and physicochemical properties of the membranes were assessed using porometry, scanning electron microscopy, and atomic force microscopy. Some examples of micrographs obtained during the study are presented in Figure 1. The hydrophilic-hydrophobic balance of the membrane surface was evaluated by measuring water contact angles using the bubble attachment method. In order to determine the molecular weight cut-off, experiments involving the separation of dextrans were conducted.

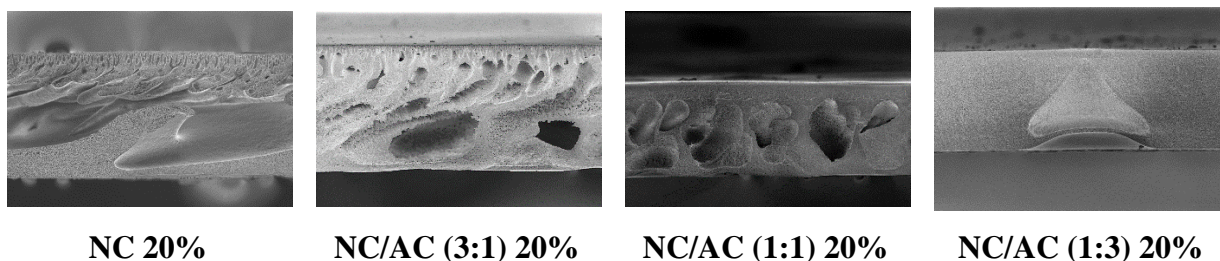


Figure 1. Cross-sectional SEM micrographs.

Acknowledgement. This work is supported by the Russian Science Foundation (grant № 20-79-10064, <https://rscf.ru/project/20-79-10064/>). The experimental work was facilitated by the equipment from the Resource Centers for Nanotechnology, Magnetic Resonance, Cryogenic Department, Thermogravimetric and Calorimetric Research Centre, Centre for Physical Methods of Surface Investigation, Centre for Innovative Technologies of Composite Nanomaterials, Computing Centre, Chemical Analysis and Materials Research Centre, and Centre “Nanofabrication of Photoactive Materials (Nanophotonics)” at the St. Petersburg State University.

HYBRID MEMBRANE SETUP FOR UTILIZATION ACID-CONTAINING WASTE FROM METALLURGICAL INDUSTRIES

¹Margarita Elshina, ¹Eugenia Falina, ¹Aelita Pasechnik, ¹Valeriia Plekunova, ¹Ksenia Demidenko, ¹Julia Loza, ^{1,2}Nikita Kovalchuk, ¹Sergey Loza

¹Kuban State University, Krasnodar, Russia, *E-mail: julialoza@list.ru*

²Platov South-Russian State Polytechnic University (NPI), Novocherkassk, Russia
E-mail: kovol13@yandex.ru

Introduction

Due to the increasing number of metallurgical companies and stricter environmental regulations, the issue of treating wastewater from such industries is becoming increasingly important. The composition of industrial wastewater is a complex, multicomponent mixture that varies depending on the type of product, technological process, and other production characteristics. For example, electroplating facilities produce effluents with low pH values and high concentrations of heavy metal ions.

To remove these pollutants, various treatment methods such as chemical precipitation, coagulation, sorption [1], ultrafiltration, and reverse osmosis are commonly used. One promising approach to solving the problem of metal ion extraction is diffusion dialysis. This method has several advantages over traditional methods, including the absence of the need for chemical reagents, ease of operation, and extremely low operating costs [2]. Additionally, diffusion dialysis has high selectivity, which means it can effectively remove specific metal ions while leaving other components intact.

At the same time, diffusion dialysis allows only to separate the components of the solution without the possibility of their reuse. To address this issue, we have proposed the use of an electro dialysis concentrator to process the solution obtained from dialysis.

Experiments

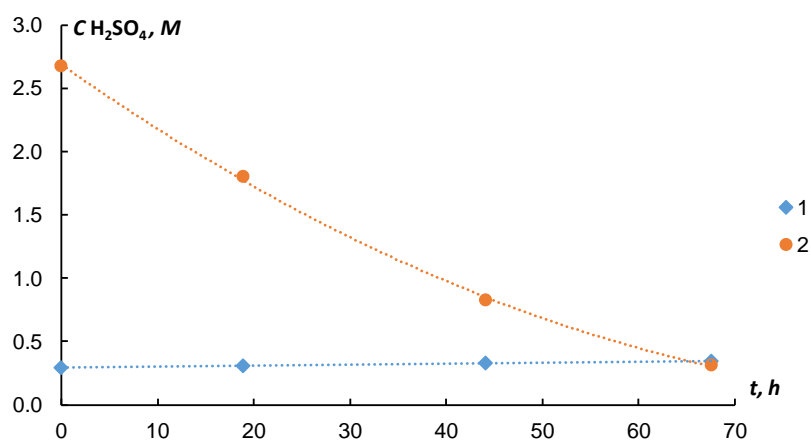
In the course of our work, we conducted dialysis separation and electro dialysis concentration experiments with different solutions. For the dialysis separation process, we used a real solution – the drain from the galvanic workshop at JSC Novgorod Metallurgical Plant, which had a concentration of 2.7 M H₂SO₄ and 0.3 M NiSO₄. For the electro dialysis concentration process, we used a model solution with a concentration of 0.05 M H₂SO₄. The objects of our study were domestic ion exchange membranes, such as MK-40, MA-41 and Chinese-made membranes Lancytom[®] CT-4 and AHT. We conducted these experiments independently in laboratory cells for dialysis separation and electro dialysis concentration. During the dialysis process, we monitored the following parameters: the volume of the initial solution, the concentration of sulfuric acid and nickel sulfate in the initial solution, and the pH of the buffer solution. During electro dialysis, we recorded parameters such as the current and voltage applied to the device, the acid concentration in the concentrating and desalinating chambers, the electrical conductivity and pH of the solutions in the desalinating chamber and the concentration chamber.

Results and Discussion

As a result of the work, we have obtained the following data. Figure 1 presents a graph illustrating the kinetic dependencies of changes in the concentrations of the components in the initial solution during the dialysis process.

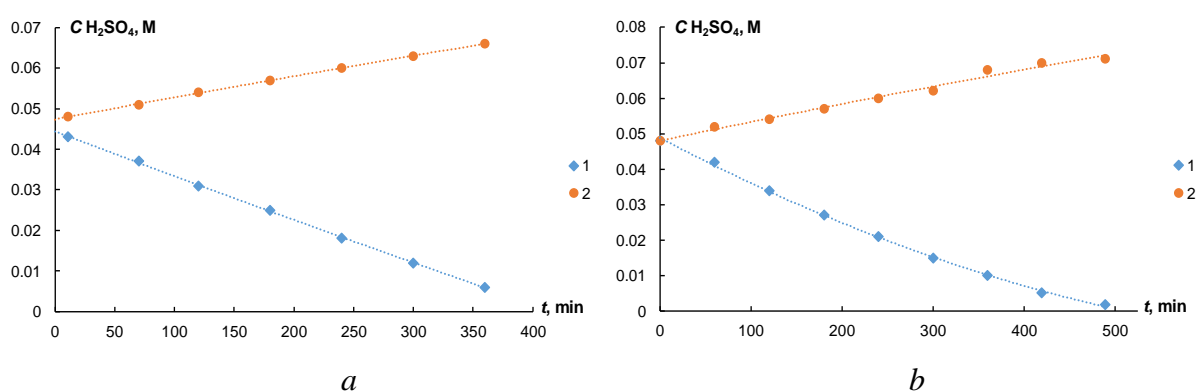
As you can see in the graph, during dialysis, the concentration of sulfuric acid decreases while the concentration of nickel sulfate remains relatively constant. This indicates that the process is effective.

Next, we performed electro dialysis on a model solution of sulfuric acid. We used two different membrane pairs: MK-40/MA-41 and Lancytom[®] CT-4/MA-41. The experimental results are shown in Figure 2.



1 – NiSO_4 ; 2 – H_2SO_4

Figure 1. Dependence of concentration of the initial solution during the experiment.



1 – desalination chamber; 2 – concentration chamber

Figure 2. Dependence of concentration of the components during the electro dialysis concentration experiments: a – Lancytom[®] CT-4/MA-41 membrane pair; b – MK-40/MA-41.

It can be seen from the presented data that the rates and degrees of concentration and desalination are practically the same for each membrane pair. In both cases, within the same time period (360 minutes), a sulfuric acid concentration of ~ 0.067 M is achieved in the concentration chamber and ~ 0.008 M in the desalination chamber.

Therefore, the effectiveness of a hybrid membrane system composed of two stages: dialysis desalination and electro dialysis concentration, has been demonstrated. The use of dialysis diffusion makes it possible to effectively remove acid from industrial wastewater without loss of nickel sulfate. The electro dialysis concentration step enables a sulfuric acid concentration of 0.067 M to be achieved, which is 1.3 times greater than the initial concentration.

Acknowledgement. The project was carried out within the framework of the "Sirius.Summer: Start Your Project"

References

1. Yu S., Tang H., Zhang D. [et al.] MXenes as emerging nanomaterials in water purification and environmental remediation // Sci. Tot. Env. 2022. V. 811 (10).
2. Gueccia R., Randazzo S., Chillura Martino D. [et al.] Experimental investigation and modeling of diffusion dialysis for HCl recovery from waste pickling solution // J. Env. Man. 2019. V. 235. P. 202-212.

ELECTROTRANSPORT OF WATER THROUGH THE HETEROGENEOUS ANION EXCHANGE MEMBRANES

Anastasia Esina, Natalia Kononenko, Svetlana Shkirskaya

Kuban State University, Krasnodar, Russia, E-mail: kononenk@chem.kubsu.ru

Introduction

The areas of application of electromembrane technologies are expanding. They are used for processing multicomponent solutions. This requires studying the transport characteristics of ion-exchange membranes in solutions of electrolytes of various nature [1]. The efficiency of electrodialysis concentration of electrolyte solutions depends on the electroosmotic permeability of both cation and anion exchange membranes. While the influence of the counter-ion type on the water transport through cation exchange membranes is quite well studied, the electroosmotic permeability of anion exchange membranes has been studied primarily in NaCl solutions [2]. The influence of the nature of the counterion on the dynamic hydration characteristics of anion exchange membranes has not yet been studied. The purpose of this work is to study the water transport in anion exchange membranes in NaCl and Na₂SO₄ solutions. The task included a also to study the the distribution of water in the hydrated fixed ion-counterion complex of anion exchange membranes.

Experiments

The objects of the study were commercial heterogeneous anion exchange membranes MA-40 and MA-41 produced in Russia. The electroosmotic permeability of these membranes was measured in NaCl solutions by the volumetric method, which allows the determination of water transport numbers only in solutions of chlorides due to the use of silver chloride electrodes. The electroosmotic permeability of membranes in Na₂SO₄ solutions was determined by the gravimetric method. It is based on measuring the amount of water transferred through a membrane when a certain amount of electricity passes. However, its use is associated with the need to take into account the chemical reactions occurring on the electrodes. The experimental conditions, such as current density, duration of the experiment, and concentration range of the electrolyte solution, are described in [3]. Additionally were measured the concentration dependences of the integral coefficient of diffusion permeability of anion-exchange membranes in NaCl and Na₂SO₄ solutions, as well as the water content.

Results and Discussion

The concentration dependences of the electroosmotic and diffusion permeability of anion-exchange membranes in NaCl and Na₂SO₄ solutions are presented in Fig. 1a, b. Both characteristics are higher in Na₂SO₄ than in NaCl solutions in the case of the MA-41 membrane. Thus, the nature of the counterion has a significant effect on the electroosmotic permeability of both cation [2] and anion exchange membranes.

The experimental data on equilibrium and dynamic hydrate characteristics were processed within the framework of the concept of the membrane as a two-phase system [3]. This made it possible to calculation the parameter A that gives information about the distribution of water in the hydrated fixed ion-counterion complex. It was established that the parameter $A \approx 1/5$ for the MA-41 membrane and $A \approx 1/2$ for the MA-40 membrane in a NaCl solution. It is known that in the heterogeneous cation exchange membrane MK-40 parameter $A \approx 1/2$. It means that the volume of water per 1 mole of fixed groups is 5 times less than the volume of water bound with 1 mol of Cl⁻ counterions in MA-41 membrane. The less symmetrical character of the water distribution in the MA-41 membrane compared to the MK-40 and MA-40 membranes is due to the fact that the quaternary ammonium cation, which is a fixed ion in the MA-41 membrane, is more hydrophobic than the sulfo group in the MK-40 membrane and secondary and tertiary amino groups in the MA-40 membrane.

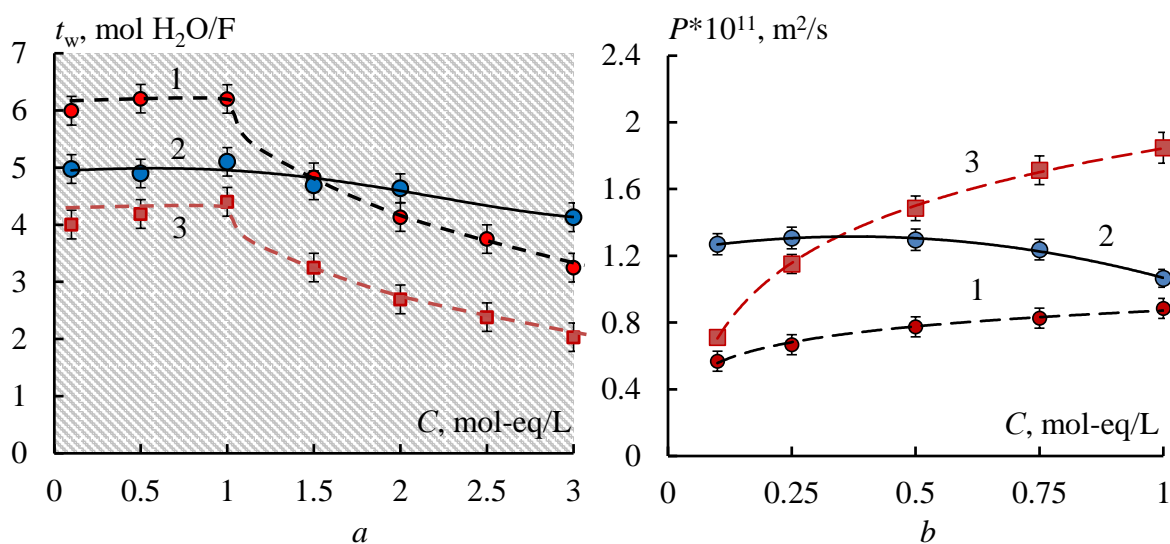


Figure 1. Concentration dependences of water transport numbers (a) and diffusion permeability (b): MA-41 membrane in NaCl (1) and Na₂SO₄ (2) solutions and MA-40 in NaCl (3) solutions

Conclusion

The study of the dynamic and equilibrium hydration characteristics of anion exchange membranes in NaCl and Na₂SO₄ solutions made it possible to establish the influence of the counter ion type on their electroosmotic permeability. The distribution of water in the hydrated fixed ion-counterion complex in the MA-41 anion exchange membrane is less symmetrical than in MA-40.

References

1. Strathmann H. Ion-Exchange Membrane Separation Processes, Elsevier, Paris, 2004.
2. Berezina N.P., Kononenko N.A., Dyomina O.A., Gnusin N.P. //Advances Colloid Interface Sci. 2008. V.139. P.3-28.
3. Nazyrova E.V., Kononenko N.A., Shkirskeya S.A., Demina O.A. // Membranes and Membrane Technologies. 2022. V. 4. No. 3. P. 145-152.

ELECTROTRANSPORT CHARACTERISTICS OF POLYANILINE-MODIFIED CATIONS-EXCHANGE MEMBRANES IN SOLUTIONS OF SULFURIC ACID AND NICKEL AND CHROMIUM SULFATES

Irina Falina, Natalia Loza, Natalia Kononenko

Kuban State University, Krasnodar, Russia, *E-mail: falina@chem.kubsu.ru*

Introduction

The electro dialysis is a promising method for recovering nickel from wastewaters because it is chemical-free. This can be achieved by applying so called monoselective membranes, which could be obtained by applying a thin layer that has the same charge sign as the counterions onto the surface of the membrane. Several studies demonstrated the efficiency of using composites based on an ion-exchange membrane and polyaniline (PANI) as a monoselective material. The goal of this work was to study the characteristics of cation exchange membranes modified by polyaniline immediately in the electro dialyzer in solutions of nickel and chromium sulfates and sulfuric acid in order to assess the prospects of their use in the electromembrane separation of multiply-charged ions.

Results and Discussion

The electrotransport and structural characteristics of MK-40 and MF-4SK cation-exchange membranes with sulfonic acid groups before and after their modification with PANI are studied. It is shown that the interaction of multiply charged counter-ions with several fixed ions decreases their mobility in the membrane but makes easier the transport of co-ions. As the charge of counterion increases, the conductivity of the membrane decreases and its diffusion permeability increases. Because of formation of PANI layer on the surface of the homogeneous membrane, the concentration dependence of its conductivity in solutions containing multiply charged cations is descending. Studying the structure of membrane MF-4SK in forms of different counter-ions by the standard contact porosimetry method shows that the transition from H^+ to Cr^{3+} form is accompanied by the 25 % decrease in the free water volume. However, after its modification with PANI, the membrane structure is stabilized and the substitution of the counterion Ni^{2+} for H^+ induces no substantial changes on the structural characteristics. It is found that modifying heterogeneous and homogeneous membranes with PANI has different effect on their current-voltage characteristics (CVC). For heterogeneous membranes, the earlier onset of the overlimiting state is observed, which is associated with the development of electroconvection due to the decrease in the electric heterogeneity of the surface. Modifying the homogeneous membrane induces substantial changes in the form of CVC leading to the appearance of asymmetry depending on the membrane orientation with respect to the counter-ion flow that points to the appearance of permselectivity with respect to singly charged ions as compared with multiply charged ions. It demonstrates the prospect of MF-4SK/PANI membrane for electro dialytic separation of singly and multiply-charged ions.

The competitive transport of sulfuric acid and nickel sulfate during electro dialysis separation and concentration is studied. It is shown that after modification the MF-4SK membrane by polyaniline the selective permeability coefficient $P(H_2SO_4/NiSO_4)$ increases from 0.7–1.7 up to 32.5–19.7 depending on the current density for electro dialysis separation. Using this membrane makes it possible to concentrate a solution containing 0.1 mol-equiv/L (4.9 g/L) H_2SO_4 and 0.1 mol-equiv/L (7.7 g/L) $NiSO_4$ with simultaneous separation to sulfuric acid with a concentration of about 2.4 mol-equiv/L (120 g/L) and a solution of nickel sulfate. Here, the concentration of nickel sulfate in the concentrate does not exceed 0.13 mol-equiv/L (10 g/L).

References

1. Falina I.V., Loza N. V., Kononenko N.A., Kutenko N.A. // Russian Journal of Electrochemistry, 2023, Vol. 59, No. 10, pp. 752–763.
2. Loza S.A., Romanyuk N.A., Falina I.V., Loza N.V. // Membranes and Membrane Technologies, 2023, Vol. 5, No. 4, pp. 236–256.

MEMBRANES BASED ON METAL-POLYMER COMPLEX FOR PERVAPORATION OF ORGANIC-ORGANIC MIXTURES

¹Ilya Faykov, ²Mikhail Goikhman, ²Galina Polotskaya, ¹Alexandra Pulyalina

¹Saint Petersburg State University, Institute of Chemistry, St. Petersburg, Russia

E-mail: st022544@student.spbu.ru

²Institute of Macromolecular Compounds, Russian Academy of Sciences, St. Petersburg, Russia

Introduction

Polymers having heteroaromatic structure are among the best representatives of membrane materials with excellent chemical resistance with respect to harsh organic media. Chemical structure of the monomer unit in polyheteroarylenes largely determines physico-chemical properties as well as transport parameters of the membranes obtained. Polymers containing organic ligands in the main chain or in side groups, such as 2,2'-biquinoline, 2,2'-dipyridyl, 2-pyridyl-quinoline which are capable of forming complexes with various transition metals, are of special interest. The formation of metal-polymer complexes allows to introduce inorganic compounds into polymers and modify the chain flexibility, macromolecular packing, and interchain interactions.

This work is aimed at the synthesis and investigation of novel copolyamide comprising 2-pyridyl-quinoline units as ligands (PA) and its complex with divalent copper salt (PA-Cu(II)). A comparative analysis of transport properties of the membranes based on these polymers was carried out by separating a mixture of methanol and toluene via pervaporation.

Experiments

Dense nonporous membranes based on PA and PA-Cu(II) were obtained by casting polymer solutions on a glass plate, followed by evaporation of the solvent. Films fixed on the glass plate were dried to a constant weight at 50°C in vacuum for 5 days.

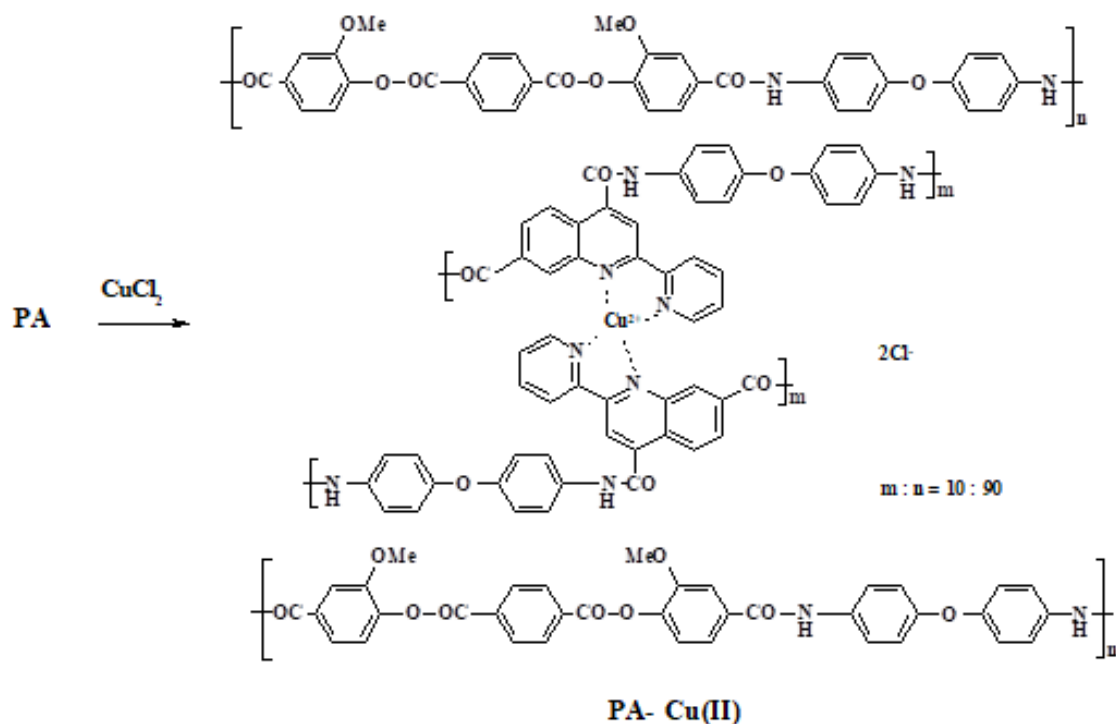


Figure 1. Scheme of PA-Cu(II) synthesis.

Morphology of the prepared membranes was characterized by scanning electron microscopy. Membrane surface was studied by atomic force microscopy. Sorption studies of the membrane samples were performed using pure liquid toluene and methanol. Transport properties were estimated in pervaporation of toluene/methanol mixtures in a wide range of concentrations, including an azeotropic point.

Results and Discussion

The results on the separation of toluene/methanol mixtures using the membranes based on PA and PA-Cu(II) demonstrate that these membranes are toluene-selective in the separation of said binary mixtures, despite the fact that the equilibrium sorption degree of methanol significantly exceeds the same of toluene for both the membranes. Quantum chemical calculations suggest that supramolecular association of PA and metal-polymer complex with methanol molecules via multiple hydrogen bonds leads to retention of the alcohol within the polymer matrix and to formation of special transport channels for toluene molecules via hydrophobic interactions. Further, it was established that the PA membrane exhibits a significantly higher separation factor than the PA-Cu(II) membrane, whilst the latter is characterized by an increased total flux as compared to PA.

Comparison of transport properties of novel membrane films with the literature data on pervaporation of the azeotropic toluene/methanol mixture has shown that the developed membranes have higher flux and selectivity than most of the known membranes.

Acknowledgement. This research was financially supported by the State Assignment Project “Novel membrane polymer materials with specified properties for energy-saving and environmentally friendly membrane technologies”.

TRANSPORT OF IONS IN ASSISTED-REVERSE ELECTRODIALYSIS FOR SURFACE WATER REVERSE OSMOSIS PERMEATE REMINERALIZATION

¹Antonia Filingeri, ²Marc Philibert, ²Emmanuelle Filloux, ²Anne Brehant, ¹Alessandro Tamburini, ¹Andrea Cipollina, ¹Giorgio Micale

¹Dipartimento di Ingegneria, Università degli Studi di Palermo, Viale delle Scienze Ed. 6, 90128 Palermo, Italy

²SUEZ - CIRSEE, 38, rue du Président-Wilson, 78230 Le Pecq, France

Email: antonia.filingeri@unipa.it

Introduction

Surface water potabilization through Low Pressure Reverse Osmosis has been widespread due to its ability to remove simultaneously micropollutants and ions [1]. However, the permeate produced by Reverse Osmosis (RO) is very poor in salts and requires remineralization steps to increase its hardness and alkalinity. As a new alternative to the common post-treatments based on the addition of external chemicals, Assisted-Reverse Electrodialysis (A-RED) has recently been proposed and proved for the recovery of minerals directly from the RO brine, via their selective transport into the permeate [2,3]. The aim of this work is to investigate the poorly-known aspects related to the differential transport of ions through A-RED membranes when using multi-ionic solutions.

Experiments

The experimental campaign was performed using a laboratory-scale A-RED unit, equipped with 5 cell pairs with an active membrane area of 0.028 m². Experiments were conducted with single-, two- and three-salts solutions including the presence of potassium, calcium, magnesium, sulphates and bicarbonates in addition to the common sodium and chlorides. Figure 1 shows the experimental setup.

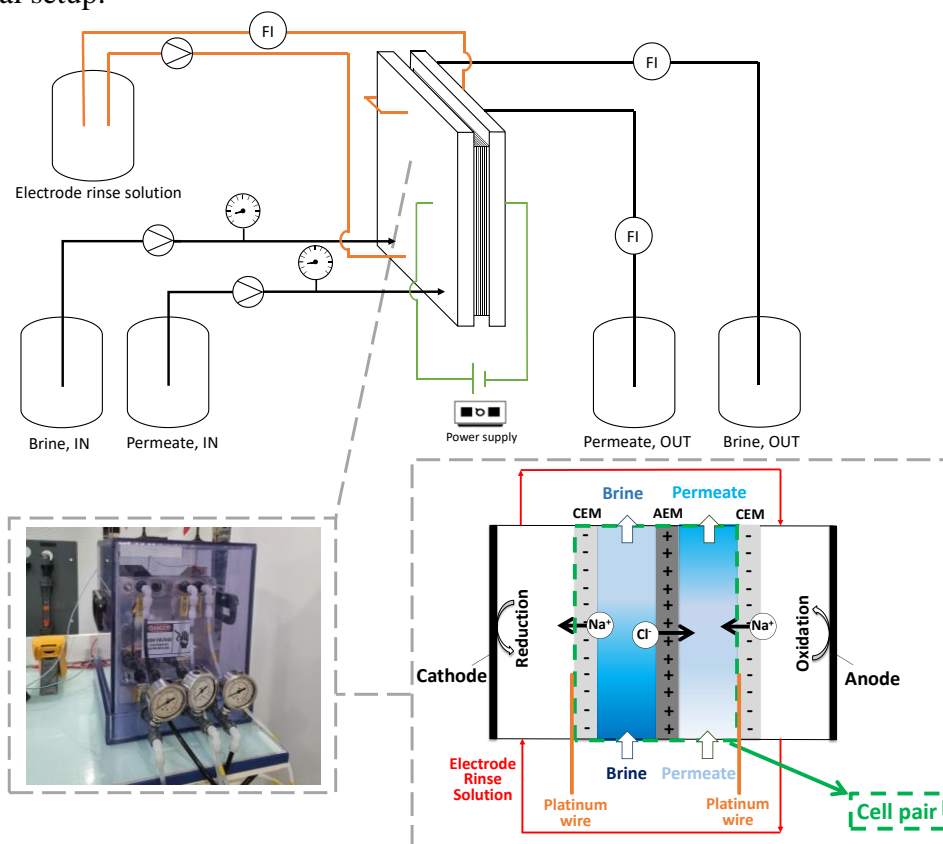


Figure 1. Schematic representation of A-RED setup with the main auxiliaries and picture of the stack.

The effect of inlet brine and permeate conductivities and ionic composition in the A-RED performance was studied. The different ions transport through the membranes was evaluated by using apparent transport numbers and membrane selectivities.

Results and Discussion

Results highlighted that the presence of calcium, sodium and chlorides guaranteed higher currents compared to magnesium, sulphates and bicarbonates which exhibited lower fluxes. Apparent transport numbers were independent on inlet permeate and brine conductivities as well as current density. Conversely, ion composition mainly affected both apparent transport number and membrane selectivities. An increasing trend of CEM selectivity was observed when the concentration of calcium, magnesium or potassium decreased compared to that of sodium (see Figure 2a), which positively affects the remineralization performance, guaranteeing efficient recovery of “water hardness”. Differently, AEM selectivity remained almost constant for both sulphates and bicarbonates in competition with chlorides (see Figure 2b), where the predominant presence of bicarbonates in typical surface water RO brines guarantees an excellent remineralization capacity also in terms of alkalinity recovery.

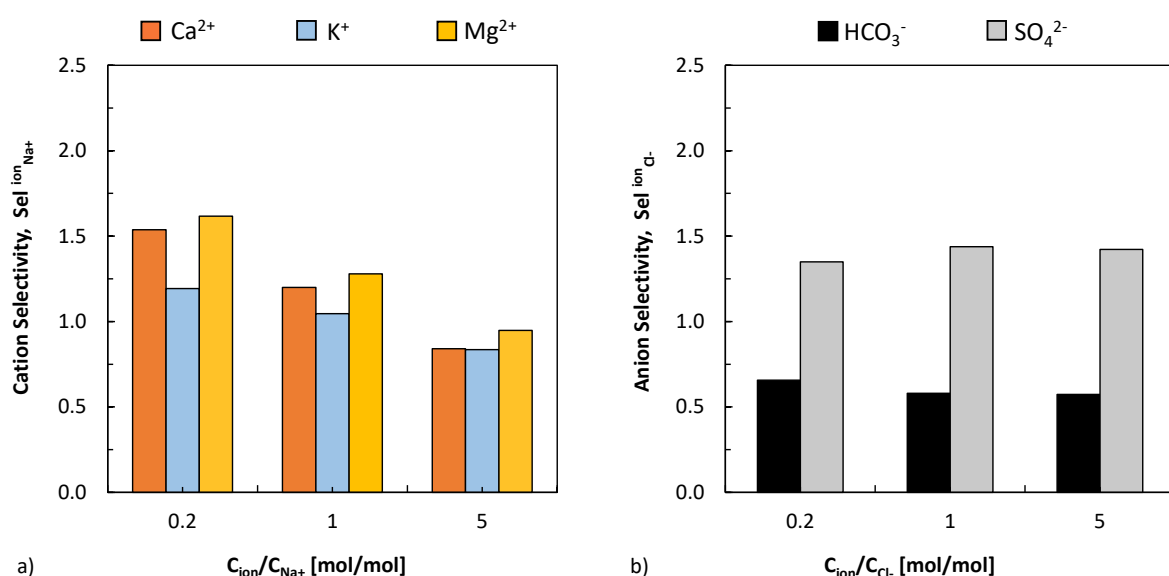


Figure 2. Apparent selectivities as function of the ion concentration ratios for competitive a) cations and b) anions for two-salts solutions. Sodium and chlorides were selected as reference ions among cations and anions, respectively. Inlet brine and permeate conductivities equal to 3.0 mS/cm and 0.07 mS/cm, respectively. Platinum wires voltage ~ 7.8 V.

These results provided valuable information on ion transport across ion-exchange membranes when different ions are in “competition” that can be useful for the widespread application of A-RED for surface RO permeate remineralization.

References

1. R. López-Roldán, S. Platikanov, J. Martín-Alonso, R. Tauler, S. González, J.L. Cortina, Integration of Ultraviolet-Visible spectral and physicochemical data in chemometrics analysis for improved discrimination of water sources and blends for application to the complex drinking water distribution network of Barcelona, J. Clean. Prod. 112 (2016) 4789–4798. <https://doi.org/10.1016/j.jclepro.2015.06.074>.
2. M. Philibert, E. Filloux, C. Garriou, D. Steinmann, A. Cipollina, Installation and process for providing mineralized drinking water, European Patent EP19306565, 2019.
3. M. Philibert, A. Filingeri, C. Nataello, N. Moe, E. Filloux, A. Cipollina, Surface water RO permeate remineralization through minerals recovery from brines, Desalination. 531 (2022) 115725. <https://doi.org/10.1016/j.desal.2022.115725>.

HYDRODYNAMIC PERMEABILITY OF CHARGED POROUS GLASS-LIKE MEMBRANES

¹Anatoly Filippov, ²Ludmila Ermakova, ¹Tamara Philippova

¹Gubkin University, Moscow, Russia, *E-mail: filippov.a@gubkin.ru*

²St. Petersburg State University, Russia, *E-mail: l.ermakova@spbu.ru*

Introduction

The previously developed cell model of an ion-exchange membrane [1] has been successfully applied to the description of the filtration process of sodium chloride aqueous solutions with different concentrations from 10^{-4} to 10^{-1} M on macroporous membranes prepared from sodium borosilicate glass. These membranes were obtained by additional alkaline treatment of microporous glasses with KOH solution [2, 3]. Additional alkaline treatment led to the removal of “secondary silica” from the pore space and partial dissolution of the silica membrane skeleton. Numerical values of the model parameters were determined for microporous glass-like membranes of the grades PG-26, PG-42, PG-66, PG-160 and a good correspondence between theoretical and experimental data was obtained.

Porous glass-like membranes hold a number of advantages over other porous materials: homogeneity of chemical composition; low level of impurities; thermal, chemical, and microbiological resistance; transparency in visible region of the spectrum; and adjustable structural characteristic. Porous glass-like membranes are also favorable materials for solving the problems of the membrane separation of mixtures. When using membranes in the baro-electromembrane separations of liquid mixtures, along with the adsorption and surface electrical properties, the structural characteristics of the pore space of the membrane are particularly important, which largely determine the membrane’s transport mechanisms upon application of external forces like gradients of pressure, electric and chemical potentials. It is well known that the size of the globules and the packing density determine the pore sizes of porous glasses containing secondary silica. In this concern, the task of this work is to study and compare the structural parameters of porous glass-like membranes, made from sodium borosilicate glass, in the aqueous solution of NaCl electrolyte of different concentrations based on the cell model of a charged membrane in comparison with the capillary model.

So, the goal of the present study is to verify the cell model of a charged membrane based on experimental data on filtration of electrolyte solutions through porous glasses.

Statement of the problem

The process of filtration of an aqueous solution of 1:1 electrolyte through a negatively charged porous layer composed of identical porous balls of radius a with specific permeability k_D bearing a constant volumetric charge density $-\rho_V$ is considered. The layer is under the action of a constant pressure gradient in the absence of external gradients of electrical potential and concentration. It is assumed that the porous layer is ideally selective, that is, it practically does not pass co-ions (anions). In this case, the coefficient γ_m of equilibrium distribution of a pair of ions in the pores of the layer is infinitely large. Then the formula for the kinetic coefficient L_{11} [1], representing the hydrodynamic permeability of the layer, is significantly simplified:

$$L_{11} = \frac{1}{45(1-m_0)} \frac{a^2}{\mu^0} \left[\frac{5(6+s^2(1-2(s/\tanh s-1)^{-1}))m_0^2}{s^2} + 3(1-m_0)^2 - 18\sqrt{1-m_0} + \frac{45}{s^2 \left(1 + A \frac{\bar{\rho}}{\rho_0}\right)} \right], \quad A = \frac{\left(\frac{\bar{\rho}}{C_0} - 1\right)}{\frac{\bar{\rho}}{C_0} \frac{D_{m+}}{D_+} + \left(\frac{3}{m_0} - 1\right)}, \quad (1)$$

where $\bar{\rho} = \frac{\rho_V}{F_0}$, $s = \frac{a}{\sqrt{k_D}}$, $\bar{\rho}_0 = \frac{\mu^0 D_+}{k_D RT}$ – characteristic exchange capacity of the granule (grain),

m_0 – macroscopic porosity of the layer, C_0 – concentration of electrolyte, μ^0 – dynamic viscosity of electrolyte, D_+ and D_{m+} – the diffusion coefficients of cations in a bulk solution and in a porous layer, respectively, R is the universal gas constant, T is the absolute temperature. In equation (1), the last term in square brackets stands for the effect of the charge of granules on the permeability of the layer, and the first four terms determine the hydrodynamic permeability of the layer in pure water. Moreover, the second of these four terms gives the contribution of filtration directly through porous particles, and the other three – the contribution of filtration between them. Since parameter A decreases with increasing electrolyte concentration and tends to a constant negative value (the denominator of the corresponding fraction remains positive), L_{11} increases with increasing concentration and also approaches an asymptotic value greater than the value of L_{11} when filtering pure water.

Experiments, calculations, and discussion

Filtration coefficients were measured for macroporous glass-like membranes PG-26, PG-42, PG-66, PG-160 at external pressures of 0.1–2 atm and four concentrations of 10^{-4} , 10^{-3} , 10^{-2} and 10^{-1} M of aqueous sodium chloride solution. Figure 1 shows the chip of macroporous glass-like membrane using scanning electron microscopy. The values of the average pore radius of glass-like membranes were previously determined based on the capillary model [2] and represent numbers (in nanometers) in the label of membranes used. For example, PG-66 stands for a glass-like membrane with an average pore radius of 66 nm. However, looking at Fig. 1, it can be assumed that the cell model [1] will better describe the structural and transport properties of such glass-like membranes than the capillary model.

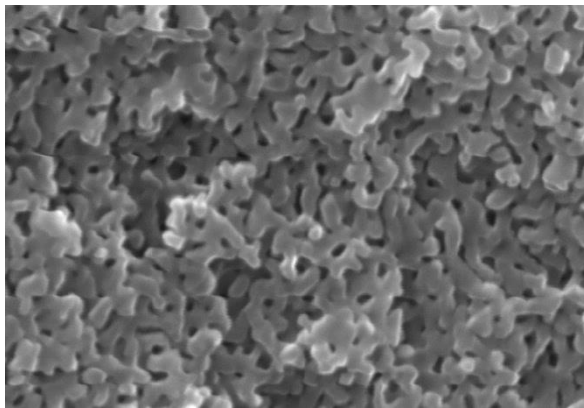


Figure 1. The chip image of macroporous sodium borosilicate monolithic glass-like membrane PG-26.

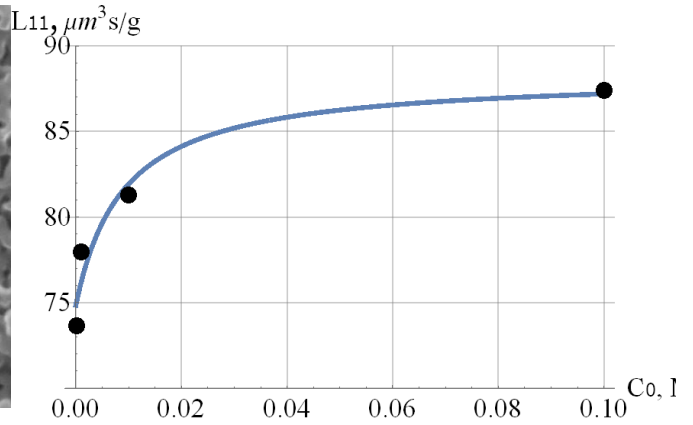


Figure 2. Concentration dependence of hydrodynamic permeability L_{11} (PG-42); points – experimental, line – theoretical.

For this purpose, the available experimental data on filtration coefficients were analyzed using Equation (1). The model parameters found by the least squares method are presented in the Table 1. Note that the values of macroporosity m_0 were determined in independent experiments.

Table 1: The Model Parameters of Glass-like Membranes

The grade of glass	a, nm	$\rho/\rho_0, mmol/dm^3$	$s=a/\sqrt{k_D}$	$k_D, nm^2/R_B, nm$	$D_{m+}, \mu m^2/s$	$m_0, \%$
PG-26	27	35.6/118.4	12.5	4.7/2.2	309	56
PG-42	45	39.2/78.5	16.9	7.1/2.7	413	60
PG-66	110	21.2/30.8	25.9	18.0/4.3	385	52
PG-160	245	17.2/27.3	54.4	20.3/4.5	577	58

Table 1 shows that for the first two membranes, the average particle radius a surprisingly coincided with the average pore radius calculated using the capillary model, while for the other

two membranes it is about one and a half times higher. Thus, there is a direct correlation between these characteristics of porous glasses. The volume charge density $\bar{\rho}$ decreases with increasing particle radius and is about 100-300 times lower than that of the well-known Russian ion-exchange membranes MK-40, MA-41 and MF-4SK. The characteristic parameter $\bar{\rho}_0$, as can be seen, also decreases with increasing particle radius a and this means that the specific permeability k_D of the granule and the Brinkman radius R_B (the size of the filtration zone in the surface layer of the granule) increases. Nevertheless, the ratio of the Brinkman radius to the granule radius decreases with the growth of the latter. As for the values of the diffusion coefficient D_{m+} of sodium cation in a porous granule, it is within physically acceptable limits: 2.3-4.4 times lower than in a bulk solution ($D_+=1350 \mu\text{m}^2/\text{s}$).

Figure 2 shows the results of comparing the experimental and theoretical values of the hydrodynamic permeability L_{11} of the glass-like membrane PG-42 depending on the concentration of NaCl. The theoretical curve is constructed according to Equation (1) with the parameters presented in Table 1. There is a very good agreement between theory and experiment, which is maintained for the remaining grades of porous glasses.

Thus, the presence of a volume charge of porous glass granules makes it possible to increase the coefficient of hydrodynamic permeability L_{11} of membranes by 3-25% with an increase in electrolyte concentration by 3 orders of magnitude – from 10^{-4} to 10^{-1} M. Moreover, with an increase in the size of silica granules, this growth decreases in relative units. Note that here we did not take into account the opposite electroosmotic flow of the solvent. In the latter case, the coefficient of hydrodynamic permeability should be calculated using a different formula:

$$\tilde{L}_{11} = L_{11} - \frac{L_{12}L_{21}}{L_{22}}, \quad (2)$$

where kinetic coefficients L_{12} , L_{21} and L_{22} are calculated in [4, 5]. This will result in a slight correction of the model parameters listed in Table 1.

Acknowledgement. The work is supported by RSF (grant No. 23–19–00520, <https://rscf.ru/project/23-19-00520/>).

References

1. *Filippov A.N.* A Cell Model of an Ion-Exchange Membrane. Hydrodynamic Permeability // *Colloid J.* 2018. V. 80. P. 716-727.
2. *Ermakova L.E., Sidorova M., Jura N., Savina I.* Adsorption and electrokinetic characteristics of micro- and macroporous glasses in 1:1 electrolytes // *J. Membr. Sci.* 1997. V. 131. P. 125-141.
3. *Ermakova L.E., Antropova T.V., Volkova A.V., Kuznetsova A.S., Grinkevich E.A. and Anfimova I.N.* Structural Parameters of Membranes from Porous Glass in Aqueous Solutions of Electrolytes, Containing Singly-Charged (Na^+ , K^+) and Triple-Charged (Fe^{3+}) Cations // *Glass Physics and Chemistry.* 2018. V. 44. P. 269-278.
4. *Filippov A.N.* A Cell Model of an Ion-Exchange Membrane. Electrical Conductivity and Electroosmotic Permeability // *Colloid J.* 2018. V. 80. P. 728–738.
5. *Filippov A.N.* Dissymmetry of kinetic coefficients in the cell model of a charged porous layer (membrane). PERM HYDRODYNAMIC SCIENTIFIC READINGS. Collection of articles based on the materials of VIII All-Russian Conference. Perm, October 5-7, 2022. P. 26-33 (in Russian).

OXYGEN EXCHANGE IN MIXED IONIC ELECTRONIC CONDUCTIVITY PEROVSKITE-LIKE OXIDE: LANTHANUM STRONTIUM FERRITE DOPED TANTALUM

^{1,2}Mario Fouad, ²Ivan Kovalev, ²Rostislav Guskov, ²Mikhail Popov, ²Alexander Nemudry

¹Novosibirsk State University, Novosibirsk, Russia

²Institute of Solid State Chemistry and Mechanochemistry SB RAS, Novosibirsk, Russia

E-mail: fouad@solid.nsc.ru

Introduction

Researchers are focusing on developing environmentally friendly, sustainable fuels to combat global warming and reduce greenhouse gas emissions. Fuel cells are a promising energy source with high efficiency, sustainability, and flexibility [1, 2]. Clean energy requires cathode materials with high mixed ionic electronic conductivity (MIEC). Lanthanum strontium ferrite oxides ($\text{La}_{1-x}\text{Sr}_x\text{FeO}_{3-\delta}$) are mixed ionic electronic conductors used as cathode materials in solid oxide fuel cells [3]. However, their performance is insufficient compared to SOFC demands. Improved methods include composite cathodes, metal ion doping, and surface modification [4].

In this study, a doping approach was used to synthesize tantalum-doped lanthanum strontium ferrite perovskite ($\text{La}_{0.6}\text{Sr}_{0.4}\text{Fe}_{1-x}\text{Ta}_x\text{O}_{3-\delta}$). Tantalum may effectively stabilize the perovskite lattice.

Experiments

The powders of $\text{La}_{0.6}\text{Sr}_{0.4}\text{Fe}_{1-x}\text{Ta}_x\text{O}_{3-\delta}$ ($x = 0.015, 0.035, 0.05, 0.1$) was synthesized by a solid-state reaction. The characteristics and microstructural were studied by XRD and SEM respectively. Equilibrium properties and kinetic properties of $\text{La}_{0.6}\text{Sr}_{0.4}\text{Fe}_{0.965}\text{Ta}_{0.035}\text{O}_{3-\delta}$ were studied by oxygen partial pressure relaxation [5] and a quasi-equilibrium oxygen release [6].

Results and Discussion

Equilibrium isothermal diagram “ $\lg p\text{O}_2 - 3-\delta - T$ ” of LSFT0.035 was constructed. The equilibrium exchange rate R_0 and chemical diffusion coefficient in oxide D_{chem} were determined.

It was shown that the linear free-energy relationship is of the Brønsted–Evans–Polanyi type.

Acknowledgement. This work was supported by the Russian Science Foundation (project No. 21-79-30051).

References

1. Liu W., Cui Y., Du X., Zhang Z., Chao Z., Deng Y. High efficiency hydrogen evolution from native biomass electrolysis // *Energy Environ. Sci.* 2016. V. 9. P. 467-472.
2. Choudhury A., Chandra H., Arora A. Application of solid oxide fuel cell technology for power generation — A review // *Renew. Sustain. Energy Rev.* 2013. V. 20 P. 430-442.
3. Kindermann L., Das D., Nickel H., Hilpert K. Chemical compatibility of the LaFeO_3 base perovskites $(\text{La}_{0.6}\text{Sr}_{0.4})_z\text{Fe}_{0.8}\text{M}_{0.2}\text{O}_{3-\delta}$ ($z = 1, 0.9$; $M = \text{Cr, Mn, Co, Ni}$) with yttria stabilized zirconia // *Solid State Ion.* 1996. V. 89. P. 215-220.
4. Desta H. G. et al. Enhanced performance of $\text{La}_{0.8}\text{Sr}_{0.2}\text{FeO}_{3-\delta}\text{-Gd}_{0.2}\text{Ce}_{0.8}\text{O}_{2-\delta}$ cathode for solid oxide fuel cells by surface modification with BaCO_3 nanoparticles // *Micromachines* 2022. V. 13. P. 884.
5. Starkov I., Bychkov S., Matvienko A., Nemudry A. Oxygen release technique as a method for the determination of “ $\delta\text{-}p\text{O}_2\text{-}T$ ” diagrams for MIEC oxides // *Phys. Chem. Chem. Phys.* 2014. V. 16. P. 5527-5535.
6. Bychkov S. F., Gainutdinov I. I., Chizhik S. A., Nemudry A. P. Novel oxygen partial pressure relaxation technique for study of oxygen exchange in nonstoichiometric oxides. The model of relaxation kinetics // *Solid State Ion.* 2018. V. 320 P. 297-304.

FLOW OF IONS NEAR A DIELECTRIC SURFACE DURING NONLINEAR ELECTROPHORESIS

¹Elizaveta Frants, ²Artem Krylov, ^{1,3}Evgeny Demekhin

¹ Laboratory of Micro- and Nanoscale Electro- and Hydrodynamics, Financial University under the Government of the Russian Federation, Krasnodar, Russia, *E-mail:* eafnants@fa.ru

² Department of Computer Technologies and Applied Mathematics, Kuban State University, Krasnodar, Russia, *E-mail:* artem.krilof2002@mail.ru

³ Research Institute of Mechanics, Lomonosov Moscow State University, Moscow, Russia, *E-mail:* eademehin@fa.ru

Introduction

In the recent work [1] it was found that the electric field intensity and the surface charge density on the particle have the most significant impact on the emergence of non-linear effects associated with dielectric particle. When there is a high degree of non-linearity, a structure of thin boundary layers nested within one another (see Fig. 1 (right)) forms around the particle's surface. In particular, the formation of a space charge region (SCR) around a non-conducting surface was discovered. It was previously believed that SCR only forms around surfaces with ion-exchange properties.

The problem of ionic fluxes

The work [2] discusses electrophoresis at large zeta potential values. The authors present a general analysis of electrokinetic transport near a strongly charged dielectric particle in the thin double layer limit. They do not limit themselves to only a weak electric field. The authors use effective boundary conditions for moderately charged surfaces. They developed a microscale model, which, however, does not work for highly charged surfaces, as tangential ion flows arise, which in turn lead to significant ion flows normal to the surface. For a highly charged surface, the authors conduct an asymptotic analysis for three layers (see Fig. 1 (left)). In addition to the well-known Debye layer and the electroneutral region, they consider the so-called "Dukhin sublayer" of thickness $O(\nu^2)$, which is part of the Debye layer of thickness $O(\nu)$ and directly adjoins the charged surface. In this layer, significant flows of charged fluid tangential to the surface are observed, causing what is known as surface conductivity. Surface conductivity can be characterized by the dimensionless Dukhin number.

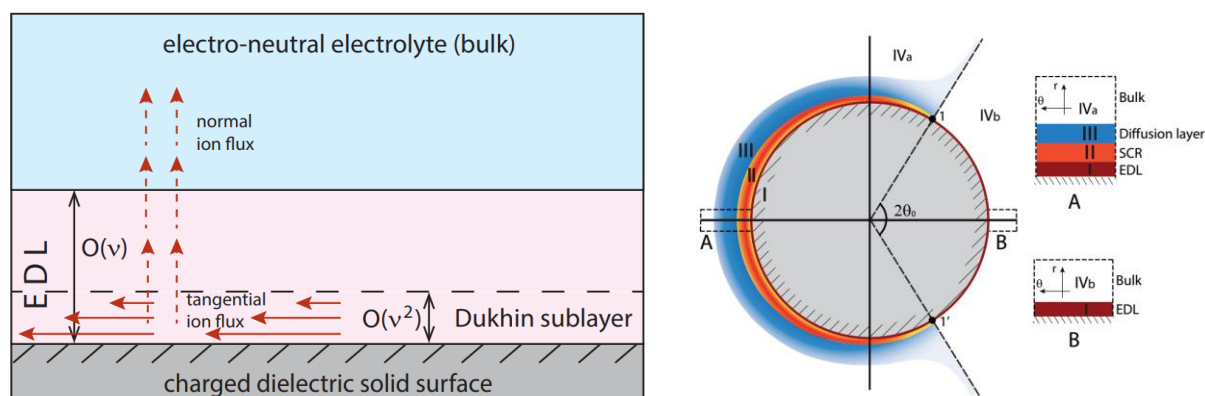


Figure 1. (left) Representation of layers structure used in asymptotic analysis [2] for highly charged surface, (right) Structure of thin boundary layers nested within each other in nonlinear electrophoresis mode.

Results and Discussion

The results of the numerical modeling had been verified against theoretical outcomes for weak electric fields (Smoluchowski's theory) and experimental data for high-intensity electric fields and/or high surface charge densities [3] and [4]. The comparison had shown excellent consistency for weak electric fields and reasonable consistency for moderate and strong electric fields.

Figures 2 and 3 show the total normal fluxes (including flows caused by convection, diffusion, and electromigration) of positive and negative ions for angles of 45 and 135 degrees (the upstream fluid flow region and the opposite region, respectively). Both ion streams change signs when passing through 90 degrees, thereby altering their direction. It is also noted that the magnitude of the cation flow is four times greater than the anion flow.

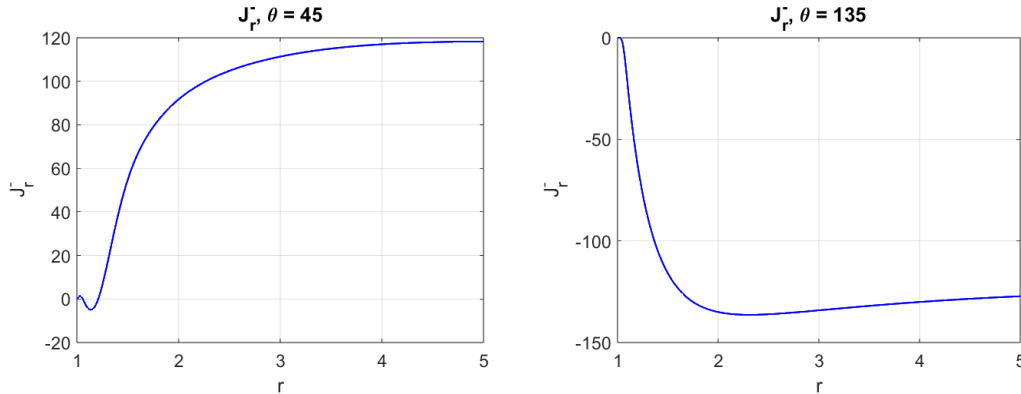


Figure 2. The full normal flux of anions for angles of 45 and 135 degrees as a function of distance from the particle surface. Parameters: $v = 0.0086$, $\sigma = -15$, $\kappa = 0.26$, $\delta = 0.05$, $E = 250$.

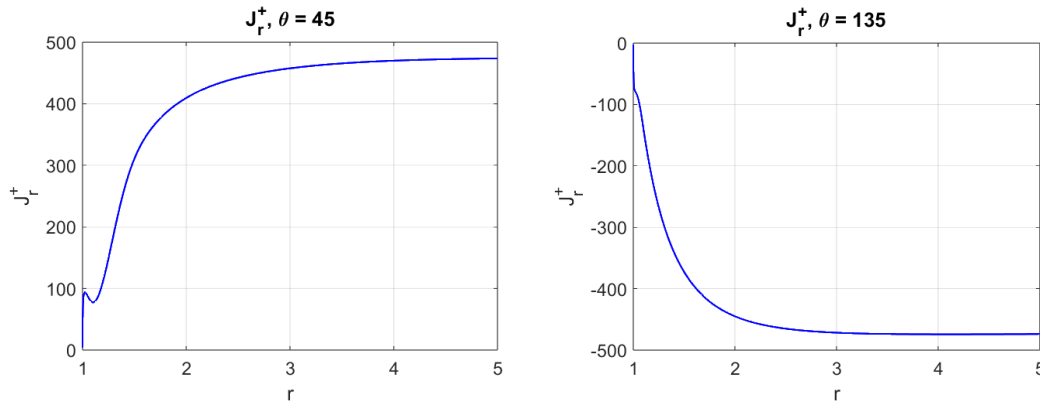


Figure 3. The full normal flux of cations for angles of 45 and 135 degrees as a function of distance from the particle surface. Parameters: $v = 0.0086$, $\sigma = -15$, $\kappa = 0.26$, $\delta = 0.05$, $E = 250$.

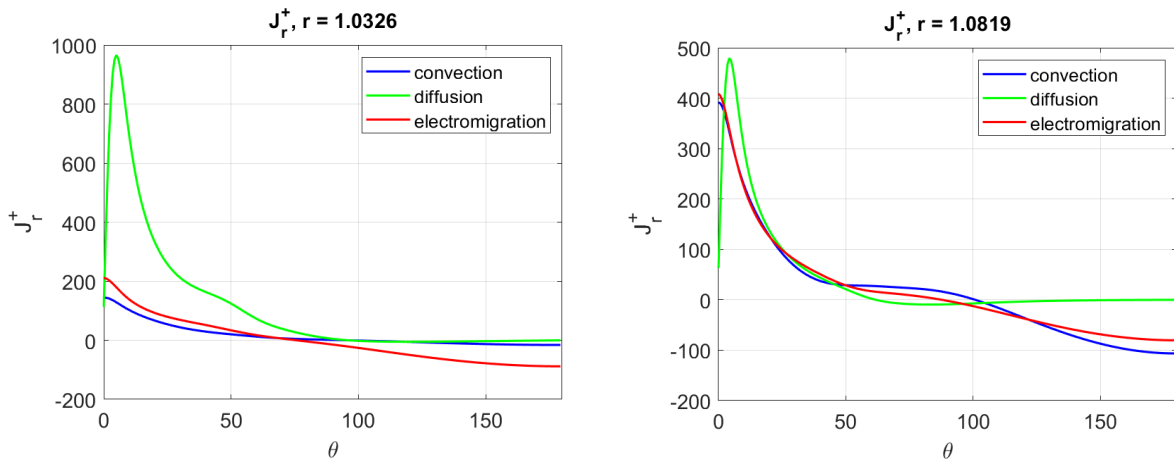


Figure 4. Components of normal flux of cations near the surface of dielectric particle ($r = 1$ corresponds to particle surface) for different distances from the particles as functions of angle. Parameters: $v = 0.0086$, $\sigma = -15$, $\kappa = 0.26$, $\delta = 0.05$, $E = 250$.

Figure 4 shows three components of the normal cation flow at different distances from the particle but near its surface. From these graphs, it can be seen that in the immediate vicinity of the surface, the flow of ions caused by diffusion predominates, which is almost five times greater than the flow of ions caused by convection and electromigration. However, as the distance from the

particle's surface increases, the situation changes and all three components of the flow become almost equal to each other.

Acknowledgement. This work was supported by the Russian Science Foundation, project No 22-79-00082.

Conclusion

The analysis of anion and cation flows, both normal and tangential, can lead to an understanding of the processes occurring near the dielectric surface in a strong electric field. This will also help explain how, in this case, a space charge region is formed, caused by the imbalance of ions in the area (accumulation of ions of one sign).

References

1. *Frants E.A., Amiroudine S., Demekhin E.A.* DNS of Nonlinear Electrophoresis // Microgravity Science and Technology (2024). DOI: 10.1007/s12217-024-10108-w (in press).
2. *Schnitzer O., Yariv E.* Macroscale description of electrokinetic flows at large zeta-potentials: Nonlinear surface conduction. *Physical Review E*, 86(2):021503, 2012.
3. *Tottori S., Misiunas K., Keyser U.F., Bonthuis D.J.* Nonlinear Electrophoresis of Highly Charged Nonpolarizable Particles // *Physical Review Letters* 123, 014502 (2019).
4. *Bentor J., Dort H., Chitrao R.A., Zhang Y., Xuan X.* Nonlinear electrophoresis of dielectric particles in Newtonian fluids. *Electrophoresis*.

ELECTROPHORESIS OF COMPLEX MICROPARTICLES

¹Georgy Ganchenko, ¹Vladimir Shelistov, ^{1,2}Maxim Alekseev, ¹Vladislav Popov, ^{1,3}Evgeny Demekhin

¹Laboratory of micro- and nanoscale electro- and hydrodynamics, Financial University, Moscow, Russia, E-mail: GSGanchenko@fa.ru

²Kuban State University, Krasnodar, Russia

³Laboratory of General Aeromechanics, Institute of Mechanics, Moscow State University, Moscow, Russia

Introduction

Currently, the importance of medical research into viruses is clear. However, bacterial studies are less popular, as there is a perception that the discovery of antibiotics has completely solved the issue of bacterial infections. Nevertheless, recent research indicates that bacteria are developing resistance to antibiotics, which could become a significant concern in the future. Antibiotics are no longer a preventative measure, and it is essential to accurately identify the specific type of bacteria causing an infection to initiate appropriate treatment.

To this end, new methods for bacterial analysis have been developed, including single-cell analysis, which involves isolating individual bacterial cells from bodily fluids for chemical and genetic analysis. One of the most commonly used methods for controlling microscopic particles in liquids is dielectric and electrokinetic phenomena [1]. This involves using an external electrical field to manipulate particles. This technique has long been used and has been the subject of numerous experimental studies. However, recent studies [2-4], including experiments, have demonstrated that the conventional linear approach fails in strong electric fields and for complex particles, such as ions. These situations require a more sophisticated theoretical analysis.

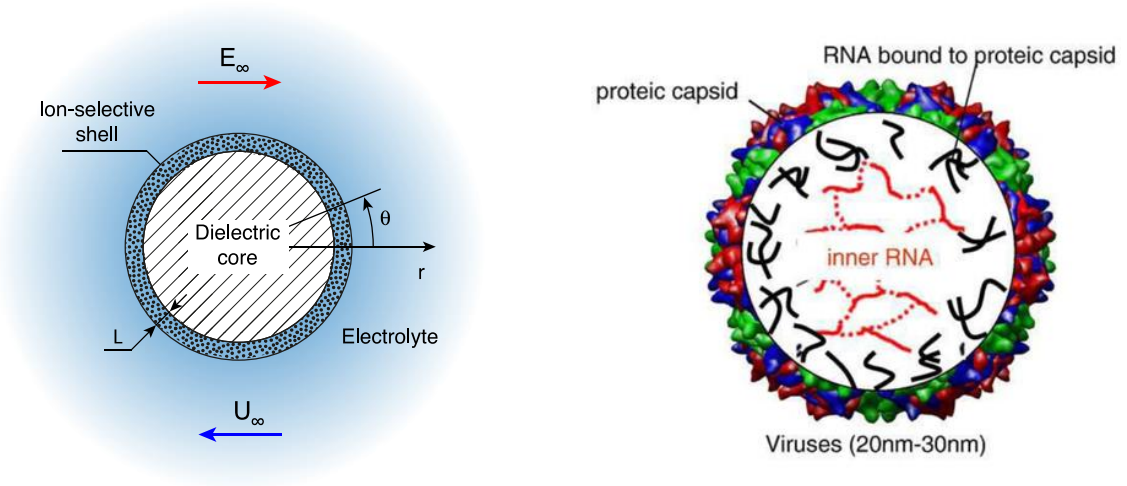
Results and Discussion

The report will present the results of numerical modeling of the electrophoresis of a spherical microparticle consisting of a dielectric solid core and a thin ion-selective shell (figure). This model simulates the mechanical and electrokinetic properties of some bacteria and viruses quite well [5]. Even with a sufficiently thin ion-selective shell, the phenomenon of concentration polarization can be observed. The velocity of electrophoresis for composite particles is much less than that of a fully charged dielectric particle, making composite particle electrophoresis more robust than fully ion-selective electrophoresis. For the steady-state regime, the rate of electrophoresis of a composite particle is nearly independent of the charge on the cores.

An oscillatory regime of electrophoresis was observed, which, at moderate values of the electric field, reaches a steady-state through oscillations. The amplitude of the oscillation before reaching the stationary solution depends on the surface charge density of the dielectric core. This regime could be used to develop a method for studying the properties of composite particles under an external electric field without destroying them. Currently, such studies present certain difficulties, as the shell of composite particles completely isolates the core from electrokinetic effects in the electrolyte. However, this technology could also find application in medicine, as the composite particle model could be considered an approximation of biological cells and viruses.

The amplitude of oscillations in the electrophoretic velocity depends on the charge of the particle, and this dependence increases with the strength of the applied electric field. However, at high field strengths, a regime of large fluctuations in velocity arises, where the amplitude of the oscillations becomes so large that the particles can change direction of motion. In this regime, the dependence of amplitude on charge is negligible. There is an optimal external electric field strength where the dependence of velocity amplitude on charge becomes most noticeable. The presented results could be useful not only in modifying existing methods for controlling viruses and bacteria, but could also form the basis for creating new technologies to analyze the properties of these particles by measuring their electrophoretic characteristics.

Acknowledgement. The work was supported by the Russian Science Foundation, project 22-79-10085.



Schematic representation of the model formulation (left) and the scheme of the virus (right)
<http://viprdb.scripps.edu>.

References

1. *Ganchenko G. S. et al.* Extreme nonequilibrium electrophoresis of an ion-selective microgranule // *Phys Rev Fluids*. 2019. V. 4(4). P. 043703.
2. *Tottori S. et al.* Nonlinear Electrophoresis of Highly Charged Nonpolarizable Particles // *Phys Rev Lett*. 2019. V. 123(1). P. 014502.
3. *Schnitzer O., Yariv E.* Dielectric-solid polarization at strong fields: Breakdown of Smoluchowski's electrophoresis formula // *Phys Fluids*. 2012. V. 24(8). P. 082005–13.
4. *Ganchenko G. S. et al.* Instabilities, bifurcations, and transition to chaos in electrophoresis of charge-selective microparticle // *Phys Fluids*. 2020. V. 32(5). P. 054103.
5. *Lesniewska N., Beaussart A., Duval J. F. L.* Electrostatics of soft (bio)interfaces: Corrections of mean-field Poisson-Boltzmann theory for ion size, dielectric decrement and ion-ion correlations // *J. Colloid Interface Sci*. 2023. V. 642. P. 154–168.

EFFECT OF POLYSULFONE MEMBRANE STRUCTURE ON ITS TRANSPORT CHARACTERISTICS DURING UREA DIALYSIS

¹Violetta Gil, ¹Mikhail Porozhnyy, ²Dmitry Lopatin, ³Igor Voroshilov, ¹Anton Kozmai

¹Kuban State University, Krasnodar, Russia, *E-mail: kozmay@yandex.ru*

²LLC "New Service Company", village of Dinskaya, Russia, *E-mail: dimitrylsm@gmail.com*

³LLC "Krasnodar Compressor Plant", village of Dinskaya, Russia, *E-mail: gendir@kkzav.ru*

Introduction

In this work, experimental membranes based on polysulfone were obtained and their characterization was carried out. The influence of the pore-forming agent (polyethylene glycol and polyvinylpyrrolidone) on the structure and transport properties of the obtained membranes was compared. A non-steady state one-dimensional mathematical model of urea dialysis is proposed. A special feature of the model is the accounting the membrane microheterogeneous structure which determines the physicochemical characteristics of the membrane.

Experiments

For the manufacture of membranes, polysulfone (PSF) PSF-150-V-VD was used, dissolved in N-methylpyrrolidone (N-MP). Pore-forming agents capable of dissolving in water were added to the polymer solution: polyethylene glycol (PEG, grade PEG-2000) or polyvinylpyrrolidone (PVP, grade K30). To obtain polymer films of a given thickness, the prepared solution was applied to a glass substrate using the Doctor Blade method [1]. The substrate with the applied composition was placed in a container with distilled water to carry out interfacial inversion. The membrane thus obtained was placed in a container with boiling distilled water for 30 minutes to remove residual solvent and dried in air for 24 hours.

Electric conductivity [2] and diffusion permeability [3] in a NaCl solution (0.1 – 0.75 M) were obtained for the three membrane samples: mb 1 (made of a PSF solution without the addition of pore-forming agents), mb 2 (containing 30% PEG by weight of PSF) and mb 3 (containing 10% PVP by weight of PSF).

Theoretical

A parameter characterizing the membrane structure is the volume fraction of the pores available transport (f_p). To determine f_p a microheterogeneous model [4] (MHM) was applied. When applied to an non-charged membrane, the structure of which is formed by an inert polymer and solution-filled pores, the basic equations of the MHM can be transformed to determine the transport characteristics of the membrane, such as electrical conductivity (κ^{mb}) (equation (1)) and diffusion permeability (P^{mb}) (equation (2)):

$$\kappa^{mb} = F^2 f_p^{1/\alpha} (L_{Na} + L_{Cl}) \quad (1)$$

$$P^{mb} = RT f_p^{1/\alpha} (L_{Na} + L_{Cl}) / c \quad (2)$$

$$L_i = D_i c / (RT) \quad (3)$$

where L_i and D_i are the transport coefficient and diffusion coefficient of ion i ($i = Na^+, Cl^-$) in solution, respectively; c is the solution concentration; α is the structural parameter characterizing the relative arrangement of the phases that make up the membrane ($-1 \leq \alpha < 0 \cup 0 < \alpha \leq 1$, where $= 1$ corresponds to a parallel arrangement, and $= -1$ corresponds to a serial arrangement); R is the universal gas constant; T is the absolute temperature.

To describe the process of urea dialysis, a non-steady state one-dimensional model was developed, in which the diffusion transport of urea in the membrane and diffusion boundary layers is described by the Fick equation and the material balance equation.

Results and discussion

The results of application of equations (1) – (3) to describe the concentration dependences of κ^{mb} and P^{mb} of the three studied membrane samples are shown in Fig. 1

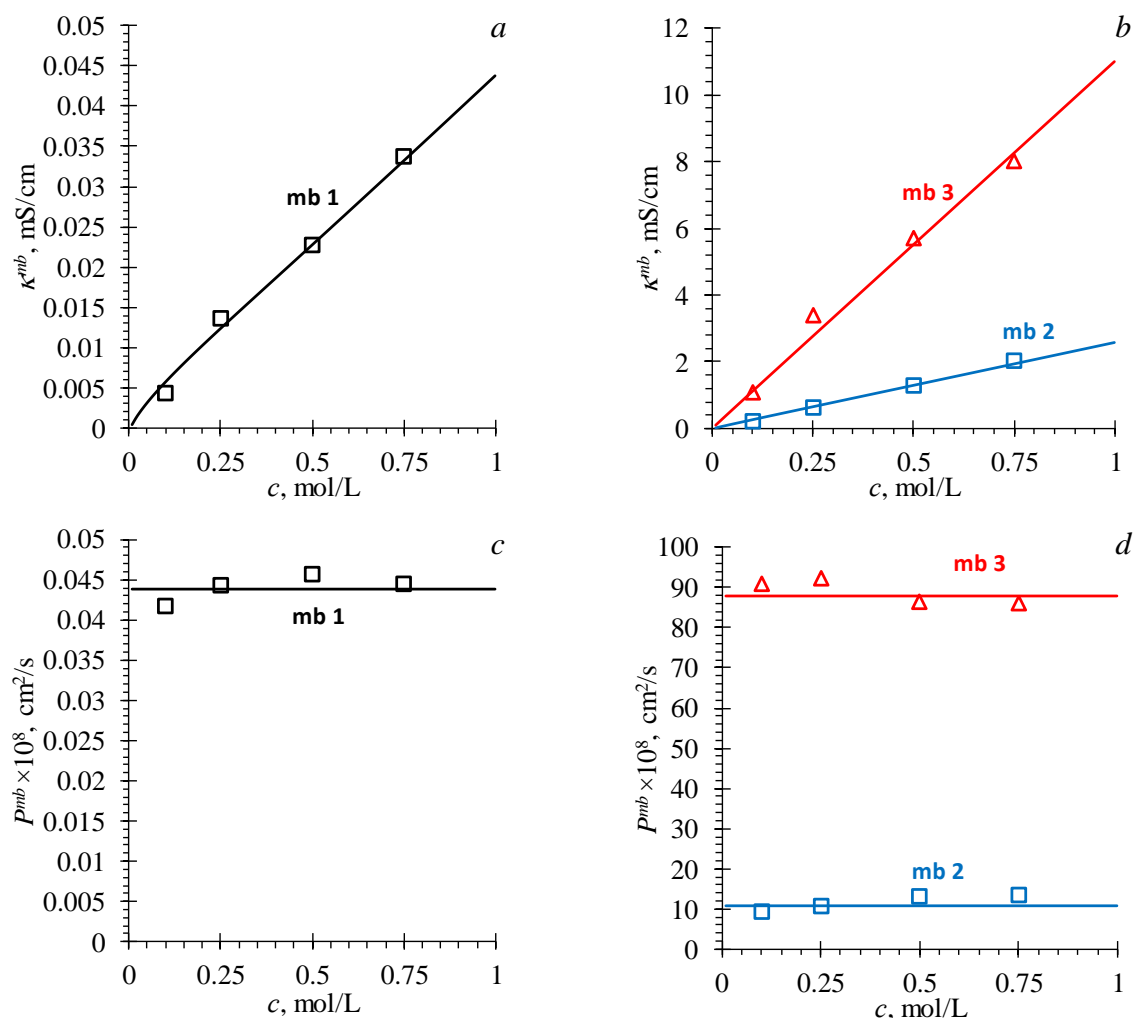


Figure 1. Concentration Dependences of Electrical Conductivity (a, b) and Diffusion Permeability Coefficient (c, d) of the Studied Samples (Indicated Near the Corresponding Curves). Markers Indicate Experimental Data, Lines Indicate the Results of Calculations Using the MHM.

Structural parameters of membranes found from the best fit between calculated and experimental data in Fig.1 are presented in Table 1.

Table 1. Structural parameters of samples found using a microheterogeneous model

Sample	f_p	α
mb 1	0.11	0.210
mb 2	0.34	0.250
mb 3	0.40	0.315

As can be seen from Table 1, mb 1, obtained without the use of a pore former, is characterized by the smallest volume fraction of pores $f_p = 0.11$. While for other studied membranes, it takes greater values. Further, only mb 2 and mb 3 will be considered.

The diffusion coefficient of urea in the studied membranes was found as a fitting parameter when modeling the urea dialysis process by comparing the calculated and experimental values of urea concentration in the dialysate chamber of the dialysis cell using independently determined structural parameters of the membranes. As can be seen from Fig. 2, simulated and experimental

data on the concentration of urea in the dialysate chamber in the case of mb 2 and mb 3 demonstrate good agreement. The model parameters are presented in Table 2.

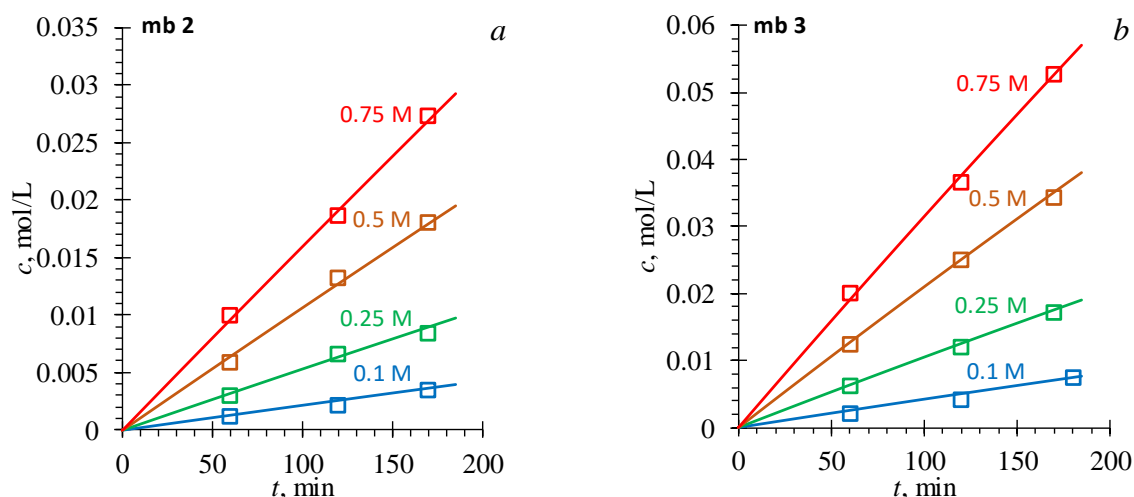


Figure 2. Time Dependences of Urea Concentration in the Dialysate Chamber at Various Values of Urea Concentration in the Diluate Chamber (Indicated Near the Corresponding Curves) for mb 2 (a) and mb 3 (b). Markers Indicate Experimental Data, Lines Indicate the Results of Simulations.

Table 2. Parameters of the model of urea dialysis in a laboratory dialysis cell

Sample	δ , microns	ξ	$D_{Ur}^{mb} \times 10^6$, cm ² /c
mb 2	230	0.125	1.72
mb 3		0.260	3.60

In Table 2, δ is the diffusion boundary layer thickness, ξ is the tortuosity coefficient of conducting pathways in the membrane, D_{Ur}^{mb} is the urea effective diffusion coefficient in the membrane.

The results of modeling the urea dialysis process, as well as the results of characterization of the studied membranes, show that the use of PVP as a pore-forming agent in the manufacture of membranes allows the formation of a more developed pore system in the membrane compared to the case of using PEG. The resulting membrane structure ensures its relatively high diffusion permeability with respect to urea due not only to the significant volume fraction of the pores in the membrane (f_p), but also to the mutual orientation of these pores along the transport axis (greater α).

Acknowledgement. The research is carried out with the financial support of the Kuban Science Foundation, LLC “New Service Company” in the framework of the scientific project Num. MFI-P-20.1/48.

References

1. Patil, G.C. Doctor Blade: A Promising Technique for Thin Film Coating. In: Sankapal B.R., Ennaoui A., Gupta R.B., Lokhande C.D. (eds) Simple Chemical Methods for Thin Film Deposition. Singapore: Springer, 2023.
2. Karpenko L.V., Demina O.A., Dvorkina G.A., Parshikov S.B., Larchet C., Auclair B., Berezina N.P. // *Russ. J. Electrochem.* 2001. V. 37. № 3. P. 287–293.
3. Pismenskaya, N.D., Nevakshenova, E.E., Nikonenko, V.V. // *Pet. Chem.* 2018. V. 58. P. 465–473.
4. Zabolotsky, V.I., Nikonenko, V.V. // *J. Membr. Sci.* 1993. V. 79. P. 181–198.

INVESTIGATION OF NON-STATIONARY PROCESSES OF PHOSPHORIC ACID SALT ANIONS TRANSFER THROUGH ANION-EXCHANGE MEMBRANE DURING ELECTRODIALYSIS

Andrey Gorobchenko, Semyon Mareev, Victor Nikonenko

Membrane Institute, Kuban State University, Krasnodar, Russia, *E-mail: gorobchenkoandrey@mail.ru*

Introduction

Phosphates in increasing amounts enter the environment, causing eutrophication of water bodies and, therefore, a rapid deterioration in the quality of life of people. The reason is the widespread use of phosphorus fertilizers. In addition, phosphates are contained in human waste, as well as waste from industrial poultry and livestock farming. University of Technology Sydney researchers D. Cordell and S. White estimate that about 98 % of phosphorus consumed ends up as waste [1]. At the same time, modern estimates indicate a critical reduction in phosphate rock reserves, predicting a phosphorus crisis within the next 260 years [2]. With an ever-increasing world population, reducing the amount of fertilizer used and/or the volume of industrial livestock farming is unacceptable, as this will lead to global food shortages. Phosphorus recovery from discharged wastewater will not only solve the problem of pollution of natural and artificial water bodies with phosphates, but will also provide secondary raw materials for the production of new fertilizers. One of the most attractive technologies for solving such a complex problem is electrodialysis (ED). This technology allows not only to selectively recover phosphates from dilute multicomponent solutions, but also to concentrate them in subsequent stages to commercially attractive concentrations.

However, phosphates, like other ampholytes, can enter proton-transfer reactions with water, which significantly complicates the mechanism of their transfer through ion-exchange membranes. To date, the mechanisms of stationary transport of ampholytes (including phosphates) have been well studied. The results of a large number of theoretical and experimental studies have made it possible to establish that proton-transfer reactions between phosphates and water at stationary ED of phosphate-containing solutions lead to the several effects. They are: intensive generation of H^+ and OH^- ions both in underlimiting and overlimiting current regimes; high energy consumption and low current efficiencies of pentavalent phosphorus recovery compared to the case of ED of strong electrolyte solutions; abnormal rapid degradation of anion-exchange membranes. There are also experimental studies showing that carrying out ED in a non-stationary mode (ED at pulsed electric field or batch ED with rapid desalting of small solution volumes) can reduce energy consumption, as well as increase the service life of anion-exchange membranes, current efficiency and the degree of phosphorus recovery. However, the available experimental data do not explain the reason for achieving such advantages compared to stationary ED. In addition, still no mathematical models would allow us to establish the mechanisms of non-stationary transport of phosphates in electromembrane systems. In this regard, this work is devoted to the theoretical and experimental study of the patterns/mechanisms of non-stationary transfer of phosphoric acid anions through an anion-exchange membrane in an applied electric field to improve the ED phosphorus recovery from phosphate-containing solutions.

Results and Discussion

A one-dimensional non-stationary mathematical model of the transfer of polybasic acid salt ions through an ion-exchange membrane in an applied electric field has been developed [3]. Using this model, the experimental non-stationary total and partial current-voltage curves (CVCs) of Neosepta AMX anion-exchange membrane (Astom, Japan) in phosphoric acid salt solution are quantitatively described (Figure 1).

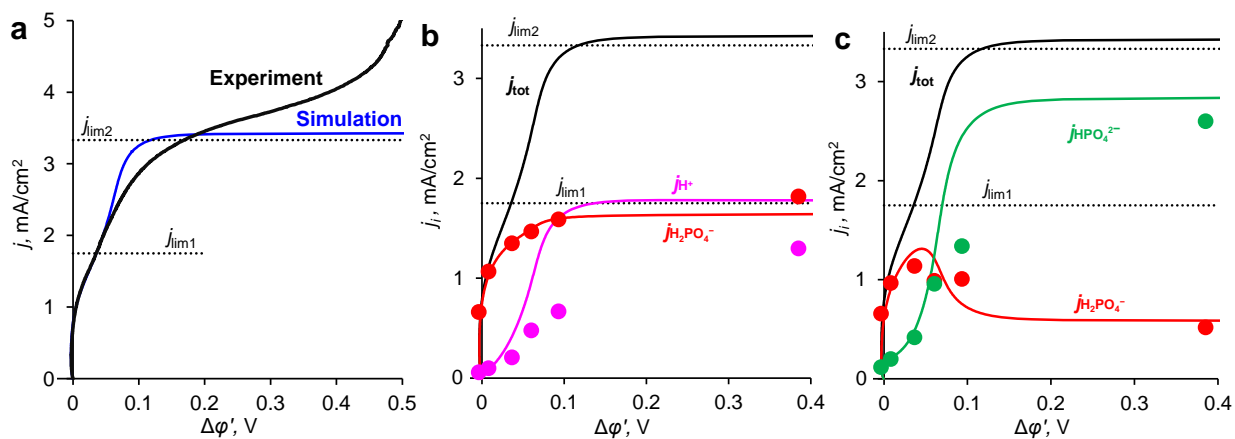


Figure 1. Simulated and Experimental Total (a) and Partial (b,c) CVCs of an AMX Membrane in a 0.02 M KH_2PO_4 Solution (pH 4.7) at Current Density Sweep Rate of $2.3 \times 10^{-3} \text{ mA}/(\text{cm}^2 \cdot \text{s})$. Dotted Horizontal Lines Show the Values of the First ($j_{\text{lim}1}$) and Second ($j_{\text{lim}2}$) Limiting Current Densities. In Figures b and c, the Solid Lines Correspond to the Simulation Results, and the Markers Correspond to the Experimental Data; j_i is the Partial Current Density (Current Density Carried by Ion i).

The dissociation reactions of phosphoric acid anions when they enter the anion-exchange membrane cause the appearance of two limiting currents in the current-voltage curves (Figure 1), the values of which significantly depend on the current density sweep rate (Figure 2a) and the values of the dissociation rate constants (Figure 2b).

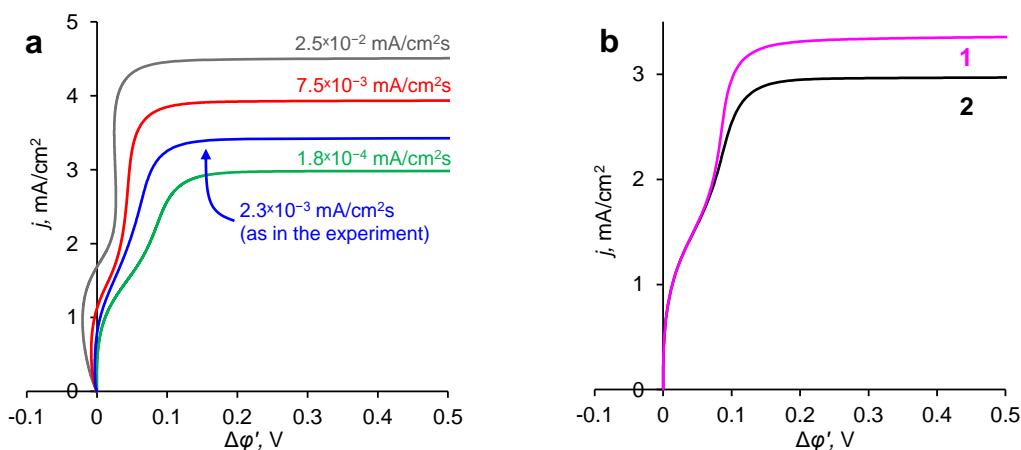


Figure 2. CVCs of an AMX Membrane in a 0.02 M KH_2PO_4 Solution (pH 4.7), Simulated (a) at Different Current Density Sweep Rates (Shown in the Figure) and at Fixed Chemical Reactions Rate Constants Taken from the Literature; (b) at Infinitely Large (1) and Finite (Taken from the Literature) (2) Rate Chemical Reactions Constants and at a Fixed Infinitely Small Current Density Sweep Rate (Stationary CVCs).

The reasons for the long time it takes for an electromembrane system with a phosphate-containing solution to reach a stationary state are proton transfer reactions and ion diffusion that slowly occur in the membrane pore solution and at the membrane-solution interfaces. The dissociation of phosphoric acid anions when they enter the anion-exchange membrane increases the charge of the transferred phosphate anion, which leads to a decrease in the amount of transferred phosphorus for the same amount of transferred electrical charge. As a result, the current efficiency of pentavalent phosphorus, η_P , decreases over time (Figure 3).

Recombination reactions of phosphoric acid anions occurring at the anion-exchange membrane/enriched solution interface lead to a local increase in pH and can cause membrane scaling during ED of multicomponent phosphate-containing solutions (Figure 4).

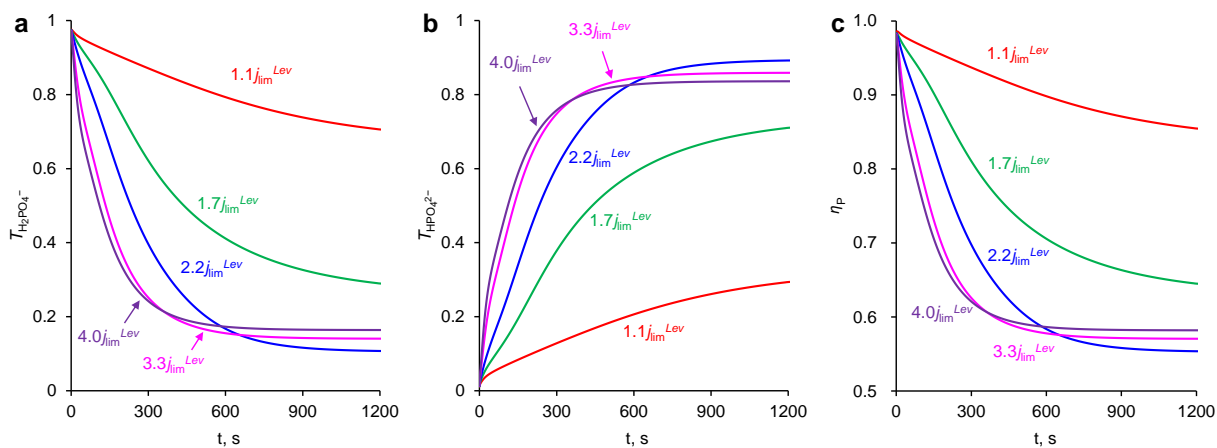


Figure 3. Time Dependences of the Effective Transport Numbers of H_2PO_4^- (a) and HPO_4^{2-} (b) Anions and Corresponding Current Efficiencies of Phosphorus Recovery (c). All Values are Calculated in the Enriched Solution at a Distance of $0.2 \mu\text{m}$ from the Membrane. Simulation is Carried out for the AMX / $0.02 \text{ M KH}_2\text{PO}_4$ (pH 4.7) System at Different Current Densities Normalized to the Limiting Current Density, $j_{\text{lim}}^{\text{Lev}}$ (Indicated Near the Curves).

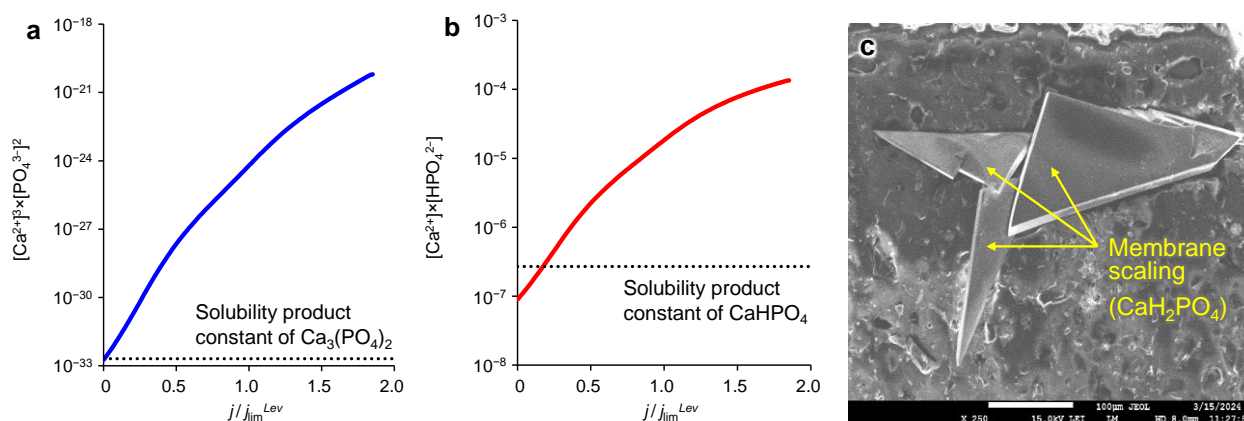


Figure 4. Simulated Dependences of the Product of the Concentration of Ions Forming $\text{Ca}_3(\text{PO}_4)_2$ (a) and CaHPO_4 (b) Compounds on the Electric Current Density; Ion Concentrations are Taken in the Enriched Solution at the Distance of $1 \mu\text{m}$ from the AEM Surface; the Horizontal Dotted Line Shows the Value of the Solubility Product Constant of the Corresponding Compound; Figure (c) is a SEM Image of MA-41P Anion-Exchange Membrane Surface (which was Facing the Concentration Compartment) after 10 Hours of ED at a Current Density of $1.5j_{\text{lim}}^{\text{Lev}}$. The Experiment and Simulation are Carried out for an ED System with an MA-41 Membrane and Feed Solutions of $0.045 \text{ M KH}_2\text{PO}_4$ (pH 4.5) in the Diluate Stream and of $0.045 \text{ M KH}_2\text{PO}_4 + 0.001 \text{ M CaCl}_2$ in the Concentrate Stream.

Acknowledgment. The study is realized with the financial support of the Russian Science Foundation, project № 24-19-00451.

References

1. Cordell D., White S. Life's Bottleneck: Sustaining the World's Phosphorus for a Food Secure Future // *Annu. Rev. Environ. Resour.* 2014. V. 39. P. 161–188.
2. He Y., Osabutey A., Gao T., Haleem N., Yang X., Liang P. Emerging electro-driven technologies for phosphorus enrichment and recovery from wastewater: A review // *Water Res.* 2023. V. 246. 120699.
3. Gorobchenko A. D., Mareev S. A., Rybalkina O. A., Tsygurina K. A., Nikonenko V. V., Pismenskaya N. D. How do proton-transfer reactions affect current-voltage characteristics of anion-exchange membranes in salt solutions of a polybasic acid? Modeling and experiment // *J. Memb. Sci.* 2023. V. 683. 121786.

ELECTROMEMBRANE REGENERATION OF ALKANOLAMINE ABSORBENTS: PROBLEMS AND SOLUTIONS

Evgenia Grushevenko, Denis Kalmykov, Julia Matveeva, Stepan Bazhenov

A.V.Topchiev Institute of Petrochemical Synthesis RAS, Moscow, Russia

E-mail: evgrushevenko@jps.ac.ru

Introduction

Industrial separation of acidic gases is mainly accomplished through absorption with aqueous solutions of alkanolamines, such as monoethanolamine (MEA), diethanolamine (DEA), and methyldiethanolamine (MDEA). However, despite their high efficiency and reliability, amine purification plants face a challenge with the degradation of the absorption solutions over time, particularly during periodic desorption operations. Due to heating to temperatures between 110 and 130°C and the presence of oxygen, alkanolamine molecules undergo thermal-oxidative degradation. The products of this degradation include both amine condensation products and thermally stable ionic compounds, commonly referred to as heat stable salts or HSS. These compounds can promote corrosion and negatively affect the performance of the absorbent by decreasing its sorption capacity. In light of the need to fully replace imports, the traditional method of solving the problem of amine degradation, which involves partially or completely replacing the absorbent, becomes economically unfeasible. Therefore, it is important to extend the life of the existing absorbent without having to dispose of it.

One of the methods to effectively removal HSS from absorption solutions is electro dialysis, which is a membrane process that uses a directed electric field to extract HSS anions from the absorption solution and transfer them into a concentrate. The HSS counter ion, depending on the organization of the process and the configuration of the electro dialyzer, can be an amine, an alkali that has been pre-added, or a proton that is formed due to water dissociation.

Despite the fact that electro dialysis can demonstrate almost quantitative regeneration of alkanolamines in model solutions, in real-world systems there may be suspended particles, corrosion products, heavy metal compounds, resinous compounds, and dissolved petroleum products. This can lead to a decrease in current output during electro dialysis and associated problems such as an increase in specific energy consumption, transfer of amines to the concentrate, and other issues. This is mainly due to the formation of a non-ionic sediment on the surface of the ion-exchange membrane in the desalting chamber. In this case, the transfer of the amine to the concentrate increases through a diffusion process in the form of a neutral molecule. This work is devoted to finding a solution to the problem of clogging of ion exchange membranes with nonionic impurities. This work is dedicated to finding a solution to the problem of fouling ion exchange membranes with nonionic impurities.

Experiments

To analyze the effect of monoethanolamine degradation products on the transport properties of MA-41 and MK-40 ion-exchange membranes (Shchekinoazot, Russia), a carbonized MEA solution was aged under conditions close to the actual desorption process. For this purpose, 1 l of 30% wt. MEA solution with a degree of carbonization of 0.4 mol CO₂/mol MEA and thermostated at 120°C for 316 hours. The degree of degradation of the solution was assessed spectrophotometrically.

Ion-exchange membranes were kept in distilled water for 24 hours. Then, the membranes were placed in a degraded MEA solution (336 hours) and kept in continuous contact with it for 6 months (4392 hours). The choice of a solution corresponding to 336 h of degradation is determined by the degree of its degradation (the presence of a significant amount of sediment, the presence of metals in the solution, as well as MEA compaction products). Such a solution makes it possible to most clearly demonstrate the effect of soluble degradation products on the transfer of ions through membranes during electro dialysis purification. To assess the electrokinetic activity of MEA degradation products, a comparison was made of the electro dialysis treatment of a model 30% wt. carbonized aqueous MEA solution with a residual carbon dioxide content of 0.2 mol CO₂/mol

MEA using fresh MK-40 and MA-41 membranes and the same membranes after 6 months of contact with a pre-degraded MEA solution.

Results and Discussion

To study the electrokinetic activity of degradation products, this work was divided into two parts: 1) obtaining a degraded amine solution; 2) comparison of the efficiency of electro dialysis treatment of a carbonized amine solution before and after contact of ion-exchange membranes with a degraded solution. The article also considers the approach of regeneration of ion-exchange membranes from degradation products [1].

After exposure of ion-exchange membranes in a model absorption solution of MEA, the depth of desalination decreases by 34%, while the magnitude of the current flowing through the apparatus decreases by 25%. A single regeneration with an alkaline solution (5 g/l NaOH) made it possible to reduce this gap to 14.8. However, no noticeable change in current strength was observed. An increase in the number of regeneration cycles up to 4 made it possible to reduce the decrease in the CO₂ extraction depth to 10%. It should be noted that the current after 4-fold alkaline regeneration reaches 1.5 A, however, the transfer of carbonate ions remains higher than in the case of clogged membranes. This is also confirmed by the dependence of the current output on the time of electro dialysis. The dependence of the flow rate after 1 regeneration cycle is higher in the case of clogged membranes. Four successive regeneration cycles make it possible to multiply the current output at the initial stage of electro dialysis. However, by the end of the hourly cycle, the current efficiency decreases, but remains higher than in the case of a single regeneration. Comparison of the depth of CO₂ removal, as well as the integral current efficiency during the electro dialysis of the model MEA solution on the initial, clogged, and regenerated membranes, is presented in Table 1.

Table 1. Comparison of CO₂ removal depth and integral current efficiency during electro dialysis of a model MEA absorbent.

Membranes	Removal depth, %	Relative removal depth, %	Integral current efficiency
Initial	25.5	100	0.25
After 6 month expose	16.8	66	0.10
After 1 cycle of alkaline regeneration	19.0	75	0.18
After 4 cycles of alkaline regeneration	23.0	90	0.24

When analyzing the performance of ion-exchange membranes per hour of electro dialysis, it becomes obvious that the regeneration performed makes it possible to increase the their efficiency. It should be noted that alkaline regeneration made it possible to achieve a high degree of restoration of the ion-exchange properties of membranes (relative extraction depth 90%, current efficient 96%). This allows us to state that the clogging of ion-exchange membranes occurs mainly by products of thermal degradation of MEA.

Acknowledgement. This work was supported by the State Program of TIPS RAS (*FFZN-2022-0004 Carbon dioxide capture and utilization № 1022090100031-1-1.4.3.*).

References

1. *E.G.Novitsky, E.A.Grushevenko, I.L.Borisov, T.S.Anokhina, S.D.Bazhenov.* Monoethanolamine (MEA) Degradation: Influence on the Electro dialysis Treatment of MEA-Absorbent // Membranes. 2023. V. 13. Art. 491.
2. *Davis J., Rochelle, G.* Thermal Degradation of Monoethanolamine at Stripper Conditions // Energy Procedia. 2009. V. 1. P. 327–333.

POLYORGANOSILOXANE-BASED MEMBRANE FOR ABE-FERMENTATION BROTH SEPARATION: EFFECT OF FLUOROALKYLACRYLATE SUBSTITUENT

Evgenia Grushevenko, Tatiana Rokhmanka, George Golubev, Ilya Borisov

A.V.Topchiev Institute of Petrochemical Synthesis RAS, Moscow, Russia

E-mail: evgrushevenko@ips.ac.ru

Introduction

The current trend towards reducing the carbon footprint and switching to “green” energy leads to an increasing role of biofuels in the fuel basket [1]. Acetone-butanol-ethanol (ABE) fermentation using *Clostridium* bacteria is the main technology for the production of biobutanol. It is known that in the case of classical ABE fermentation, the biobutanol concentration in the broth is limited by inhibition of the microorganisms activity to a value close to 2% wt., which is extremely low for distillation separation from the mixture [2]. In order to overcome this limitation, approaches have been proposed for the continuous biobutanol separation from the fermentation mixture, including hydrophobic pervaporation. Pervaporation has a noticeable advantage from an energy point of view: the energy consumption for the pervaporation release of biobutanol is only 9 MJ/kg compared to 24 MJ/kg for distillation [3]. In addition, it does not require regeneration of the carrier phase, the consumption of additional reagents and does not have harmful effects on microorganisms. The ability to carry out the separation process at low (30-50°C) operating temperatures makes pervaporation especially attractive for operation in combination with a bioreactor without compromising the activity of microorganisms [4]. Most commercial membranes for hydrophobic pervaporation are silicone rubber based composite membranes (mainly polydimethylsiloxane (PDMS)) due to its high performance and low cost [5]. However, the PDMS-based membranes selectivity towards butanol is not sufficient to achieve its high concentrations in the permeate. Accordingly, the task of developing sorption-selective pervaporation membranes based on polysiloxanes, superior in separation ability to n-butanol PDMS, is relevant. Another problem of pervaporation separation of fermentation mixtures is the problem of the formation of deposits on the membrane surface. The introduction of fluorine-containing fragments into PDMS significantly reduces membranes fouling based on such a polymer by components of the fermentation mixture and increases the stability of the transport properties of the membrane during the pervaporation release of butanol from the ABE-fermentation mixture [6].

In this work, the effect of introducing fluoroacrylate side substituents into polyalkylmethylsiloxane was studied for the first time. Composite membranes based on a copolymer of polydecylmethylsiloxane (C10) and polyalkyl-n-fluoroacrylate siloxanes were created and characterized. The influence of the ratio of decyl groups, which is characterized by high hydrophobicity and selectivity towards n-butanol, and has been studied n-fluoroalkyl acrylate groups on the sorption, surface and pervaporation properties of the membrane [7].

Experiments

Composite membranes were obtained by applying a selective layer of C10, polyalkyl-n-fluoroacrylate siloxanes or copolymers onto a porous microfiltration support MFFK-1 (Vladipor). The synthesis of polymers of the selective layer was carried out similarly to the method presented in the work [8]. According to the hydrosilylation reaction, a side agent (1-decene, trifluoroethyl acrylate (F3), pentafluoropropylacrylate (F5), hexafluoroisopropylacrylate (F6) or a mixture of 1-decene and fluoroalkyl acrylate in ratios from 0:100 to 100:0) was introduced into polymethylhydrosiloxane (PMHS). Vinyl-terminated PDMS ($M_n=25000$ g/mol) was used as a cross-linking agent. The structure of the resulting polymers was confirmed by IR and 1H NMR spectroscopy and elemental analysis. The surface properties of the selective layer of composite membranes were investigated by determining the contact angle and interpreted based on IR and elemental analysis data. The effect of the ratio of side substituents on the volumetric sorption of ethanol, acetone and n-butanol was assessed by measuring the change in the mass of polymer films

before and after long-term exposure to individual liquids. The transport and separation properties of the membranes were investigated by pervaporation separation of a model ABE-fermentation mixture containing 0.76 wt% acetone, 1.6 wt% BuOH, and 0.3 wt% EtOH in water at 30, 40, and 50 °C. The separation process was performed in a vacuum pervaporation setup describe elsewhere [8].

Results and Discussion

¹H NMR spectroscopy data clearly confirm the introduction of fluoroalkyl acrylate substituents at the C=C bond in PMHS. It is worth noting that the degree of conversion of fluoroalkyl acrylate compounds is higher than that of 1-decene due to their greater nucleophilicity. The presence of fluorine substituents in polysiloxane is also confirmed by IR spectroscopy data. It was found that with an increase in the proportion of fluoroalkyl acrylate in the reaction mixture and, accordingly, a decrease in the proportion of 1-decene, it leads to a disproportionate decrease in -CH₂- groups on the surface of the film. However, when studying the polymer film through transmission, this effect is not observed. Apparently, this is due to the orientation of alkyl substituents deep into the film, while fluoroalkyl acrylate substituents, on the contrary, come to the surface. This, in turn, determines both the greater hydrophobicity of the membrane surface and the reduced surface energy. This trend is confirmed by the data of elemental analysis of the membrane surface and the volume of the polymer: a relative decrease in the proportion of carbon on the membrane surface is observed compared to the concentration of C atoms in the volume (Fig. 1).

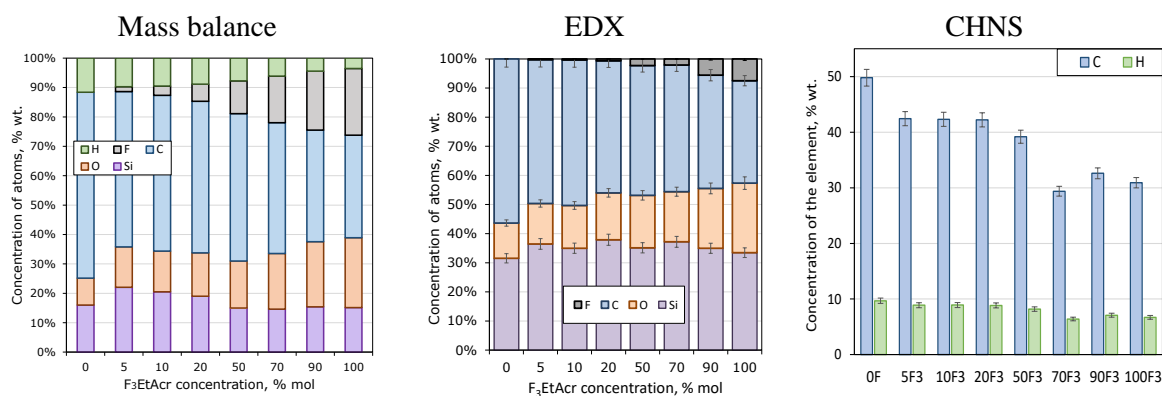


Figure 1. Elemental analysis of samples on the surface (EDX) and in bulk (Mass balance, CHNS) with different contents of trifluoroethyl acrylate groups (0-100).

Analysis of sorption data demonstrates that for all studied polymers there is a maximum sorption of n-butanol at a ratio of fluoroalkyl acrylate substituent to 1-decene of 50:50, and maximum sorption of ethanol and acetone at a ratio of 70:30 (Fig. 2). Thus, the most attractive samples from the point of view of sorption affinity for n-butanol are 50F3, 50F5 and 50F6. On their basis, pervaporation membranes were obtained, which were studied during the separation of a model ABE mixture in the vacuum pervaporation mode.

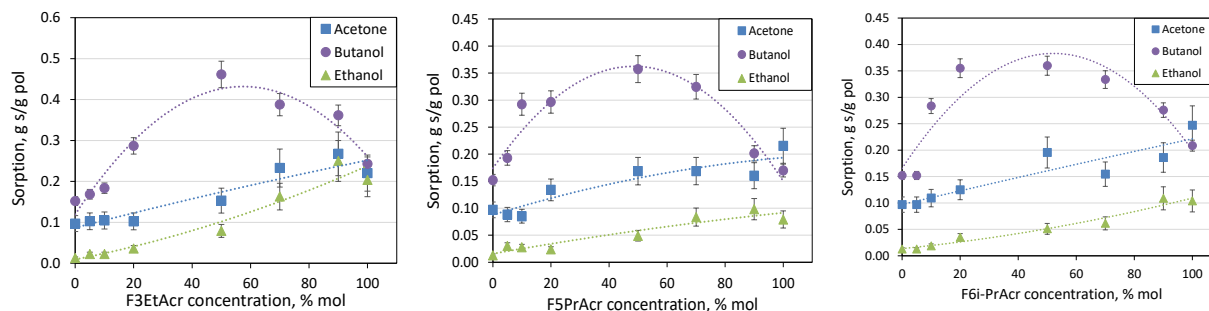


Figure 2. Sorption of acetone, butanol and ethanol by samples with varying contents of F₃-Acr, F₅PrAc and F₆i-PrAc.

A comparison of the pervaporation properties of membranes based on copolymers of polydecylmethylsiloxane and polyfluoroalkyl acrylate methylsiloxanes (50F3, 50F5 and 50F6)

and membranes made of polydecylmethylsiloxane (OF), made on porous MFFK-1 support, is presented in Fig. 3.

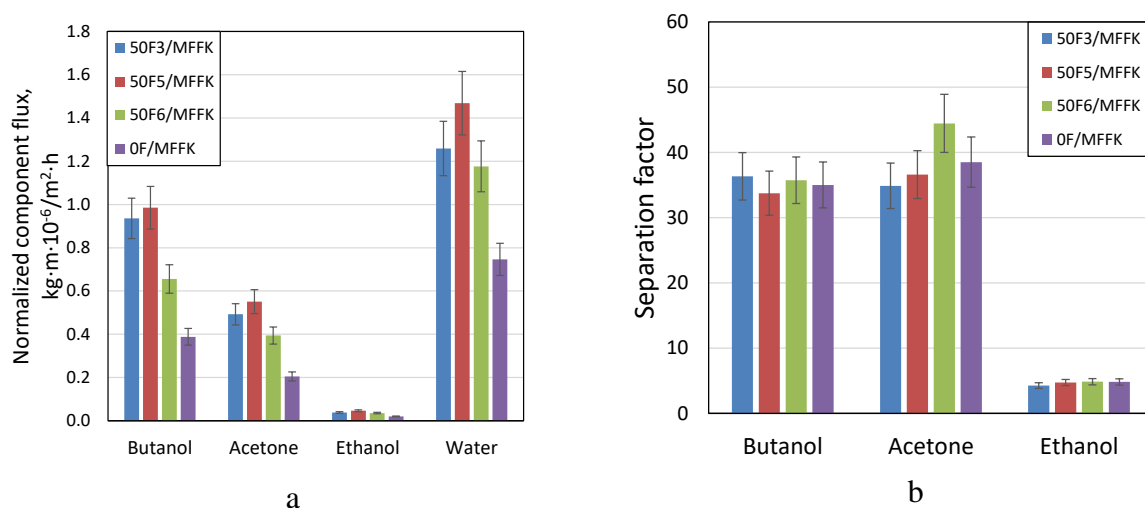


Figure 3. Normalized flux (a) and separation factors (b) of composite membranes 50F3/MFFK, 50F5/MFFK, 50F6/MFFK and OF/MFFK during pervaporation separation of a model ABE-mixture.

The introduction of fluoroalkyl acrylate substituents into polysiloxane leads to an increase in flux through membranes. It is worth noting that, in comparison with the original sample OF, samples 50F3/MFFK, 50F5/MFFK, 50F6/MFFK are characterized by larger flux values and comparable values of separation factors. Taking into account the discovered greater resistance of these samples to clogging, it can be argued that they are more effective in the process of pervaporation separation of n-butanol from the fermentation mixture.

Acknowledgement. This research was financially supported by the Russian Science Foundation grant № 22-79-10332, <https://rscf.ru/project/22-79-10332/>.

References

1. Mridha B., Ramana G.V., Pareek S., Sarkar B. An efficient sustainable smart approach to biofuel production with emphasizing the environmental and energy aspects // *Fuel*. 2023. V. 336. P. 126896.
2. Lin Z., Cong W., Zhang J. Biobutanol Production from Acetone–Butanol–Ethanol Fermentation: Developments and Prospects // *Fermentation*. 2023. V. 9. №. 9. P. 847.
3. Oudshoorn A., van der Wielen L.A.M., Straathof A.J.J. Assessment of options for selective 1-butanol recovery from aqueous solution // *Ind.Eng.Chem.Res.* 2009. V. 48. P. 7325-7336.
4. Shin C., Baer Z.C., Chen X.C., Ozcam A.E., Clark D.S., Balsara N.P. Block copolymer pervaporation membrane for in situ product removal during acetone–butanol–ethanol fermentation // *J.Membr.Sci.* 2015. V. 484. P. 57-63.
5. Wu H., Qin P., Van der Bruggen B. Polydimethylsiloxane based membranes for biofuels pervaporation // *Sep.Purif.Technol.* 2022. V. 298. P. 121612.
6. Zhu H., Li X., Pan Y., Liu G., Wu H., Jiang M., Jin W. Fluorinated PDMS Membrane with Anti-biofouling Property for in-situ Biobutanol Recovery from Fermentation-Pervaporation Coupled Process // *J. Membr. Sci.* 2020. V. 609. P. 118225.
7. Grushevenko E. A., Podtynnikov I. A., Borisov I. L. High-selectivity pervaporation membranes for 1-butanol removal from wastewater // *Rus. J. Appl.Chem.* 2019. V. 92. P. 1593-1601.
8. Grushevenko E.A., Rokhmanka T.N., Balynin A.V., Golubev G.S., Borisov I.L. Trifluoroethyl Acrylate-Substituted Polymethylsiloxane—a Promising Membrane Material for Separating an ABE Fermentation Mixture // *Membr.Membr.Technol.* 2023 V. 5. P. 394-404.

INFLUENCE OF ELECTRODE PARTICLE SIZE ON THE EFFICIENCY OF ANODIC OXIDATION OF OXALIC ACID IN AQUEOUS SOLUTION

Vera Guliaeva, Andrey Kislyi, Ilya Moroz, Yuri Prokhorov, Victoria Plis, Anastasiia Klevtsova, Elizaveta Evdochenko

Kuban State University, Krasnodar, Russia, *E-mail: vera_gulyaeva_2002@mail.ru*

Introduction

Currently, electrochemical advanced oxidation processes (EAOPs) are widely used during the treatment of natural and wastewaters containing various organic pollutants. EAOPs have high oxidation efficiency and ease of automation and versatility. Among EAOPs, anodic oxidation is the most efficient method, which provides mineralization of organics dissolved in water by generating highly active hydroxyl radicals or by direct electron transfer from the organic compound to the electrode surface [1].

The most promising materials for anodic oxidation process are porous ceramics, such as sub-stoichiometric titanium oxide (Ti_4O_7). This material has a large electrochemically active surface area, which increases the rate of oxidation process due to rapid delivery of organic substances to the reactive zone enclosed to the electrode surface [2]. In addition, Ti_4O_7 has high electrical conductivity, chemical stability, high oxygen evolution potential, and relatively low production cost. More affordable particle electrodes may be a simple alternative to porous electrodes [3].

In this study, the effect of electrode particle size on the anodic oxidation efficiency of organic pollutants on a particle anode was evaluated.

Experiments

The experimental setup consists of an electrochemical flow cell and a hydraulic system providing a continuous supply of solution at a constant rate. The constant current is maintained by means of a current source, the potential drop between the cathode and anode is recorded by a voltmeter. The electrochemical cell is a rectangular flow electrolysis chamber with a plate stainless steel cathode and a particle anode made of porous Ti_4O_7 . The electrodes are divided by a mesh separator made of inert material (polypropylene). The sealed case of the cell is made of polytetrafluoroethylene, which ensures the tightness of the system.

To study the effect of electrode particle size on the anodic oxidation efficiency, two fractions of particles with an average size of 0.5 and 1.5 mm were obtained, respectively. For each fraction, the electrochemically active surface area was evaluated and experiments on kinetics of oxidation of oxalic acid were performed. The concentration of oxalic acid in aqueous solution after treatment is measured by the ion chromatography method.

Results and Discussion

The kinetics of anodic oxidation of oxalic acid at an electrical current of 100 mA is shown in Figure 1a. According to the experimental data, it can be concluded that the oxidation rate of organic molecules increases significantly when the anode particle size decreases. After one hour of anodic oxidation process using fine backfill (small electrode particles), the oxalic acid concentration became less than 100 mg/L, while with coarse backfill (large electrode particles) the concentration is an order of magnitude higher. By the end of the experiment, the organic content decreases to zero value in both cases, indicating the overall efficiency of the particle anode.

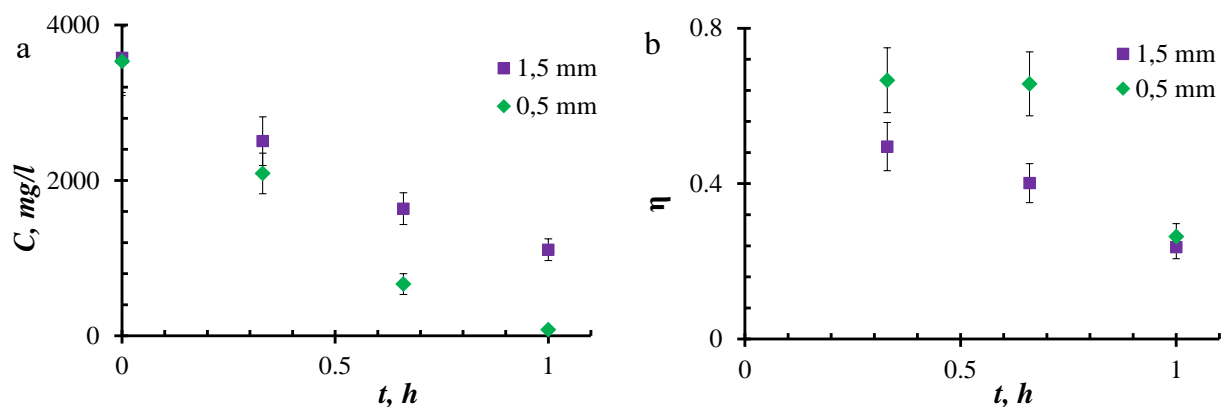


Figure 1. Dependence of the Concentration of Oxalic Acid (C , mg/L) (a) and the Current Efficiency (η , %) (b) on the Time of Experiment at a Current of 100 mA with Big (1.5 mm) and Small (0.5 mm) Particles.

The current efficiency of anodic oxidation using small particles reaches almost 0.7 and in the case of large ones only 0.5 (Figure 1b). This data consistent with the measured electrochemically active surface area: in the case of electrode with 0.5 mm particles it is 84500 m^{-1} and in the case of 1.5 mm only 60500 m^{-1} . However, a possible reason for the increase in efficiency could be the intensification of mass transfer near the electrode surface.

Acknowledgments. The study is realized with the financial support of the Russian Science Foundation, project № 22-79-10177.

References

1. Sirés I., Brillas E., Oturan M. A., Rodrigo M. A., Panizza M. Electrochemical advanced oxidation processes: Today and tomorrow. A review // *Environ. Sci. Pollut. Res.* 2014. V. 21. P.8336-8367.
2. Trellu C., Coetsier C., Rouch J. C., Esmilaire R., Rivallin M., Cretin M., Causserand C. Mineralization of organic pollutants by anodic oxidation using reactive electrochemical membrane synthesized from carbothermal reduction of TiO_2 // *Water Res.* 2018. V.131 P. 310–319.
3. GracePavithra K., Senthil Kumar P., Jaikumar V., SundarRajan P. S. A review on three-dimensional electrochemical systems: analysis of influencing parameters and cleaner approach mechanism for wastewater // *Rev. Environ. Sci. Biotechnol.* 2020. V. 19. P. 873–896.

MODIFIED STRONTIUM COBALTITES AS ELECTRODE MATERIALS FOR MEMBRANE TECHNOLOGIES: STRUCTURE AND FUNCTIONAL PROPERTIES

Rostislav Guskov, Michail Popov, Ivan Kovalev, Alexander Nemudry

Institute of Solid State Chemistry and Mechanochemistry of the Siberian Branch of the Russian Academy of Science, Novosibirsk, Russia, *E-mail: rostislav.guskov@yandex.ru*

Introduction

Over the past decades, the study of oxygen exchange reactions in perovskite oxides with mixed ion-electron conductivity with the general formula $ABO_{3-\delta}$ has attracted much of attention of scientists from all over the world.¹ After the discovery of an abnormally high oxygen conductivity in $SrCo_{0.8}Fe_{0.2}O_{3-\delta}$ in 1985,² an active search for various dopants capable of improving the properties of such oxides began. The first attempts to replace cations in the *A* and *B* sublattices resulted only in the stabilization of the phase composition by «blocking» structural transitions, and the transport characteristics were significantly reduced.³ A positive effect of doping is observed, for example, in the case of doping with high-valent cations, where effects are observed in the values of oxygen conductivity/permeability, resistance to CO_2 , the formation of domain and nanostructured systems with facilitated oxygen diffusion along the phase boundaries etc.

In order to establish the regularity of doping effect on the kinetic and equilibrium characteristics of the oxide in oxygen exchange, a deep understanding of the mechanism of oxygen exchange itself is necessary. Close attention should be paid to the fact that the studied substances are capable of significant stoichiometry deviations, which should have an effect on certain features characterizing the relationship between their equilibrium and kinetic parameters.

Thus, this study, which is one of a series of studies on the fundamental functional and applied characteristics of standard compositions of perovskite oxides, is aimed at studying the dependences of kinetic and equilibrium parameters on the nonstoichiometry δ and temperature *T*, and checking the presence of LFER according Brønsted-Evans-Polanyi principle. In addition, testing the original oxygen partial pressure relaxation⁴ and quasi equilibrium oxygen release techniques,⁵ in order to develop a research methodology, obtain reference points for further development of methods and improvement of fundamental models was included. For these purposes, strontium cobaltites doped with tantalum and molybdenum were chosen

Experiments

SCT and SCM compound were synthesized using ceramic method. The obtained compounds were qualified by X-ray spectroscopy. Samples for OPPR method were pressed into pellets of specified shape and studied using scanning electron microscopy. After OPPR experiments pellets were grounded into powder of a narrow particle size range (64 – 160 μ) for QEOR. The data obtained was processed using original fundamental model developed earlier.

Results and Discussion

The oxygen partial pressure dependencies on time and non-stoichiometry were obtained for two compounds. The curves presented on figure 1 show the results of fitting experimental OPPR data with TIS (tank in series) macrokinetics model. For each composition, measurements were carried out at the same temperature ranges, as well as at the same relaxation steps of oxygen partial pressure. The gas flow rates were selected based on the oxygen exchange rate, which is estimated at the stage of the experiment by the magnitude of the relaxation amplitude of oxygen desorption/adsorption.

The isothermal dependencies of $3-\delta$ non-stoichiometry on oxygen partial pressure are shown on figure 2. Thermoprogrammed oxygen desorption (TPD- O_2) data are also shown to confirm the validity of data obtained.

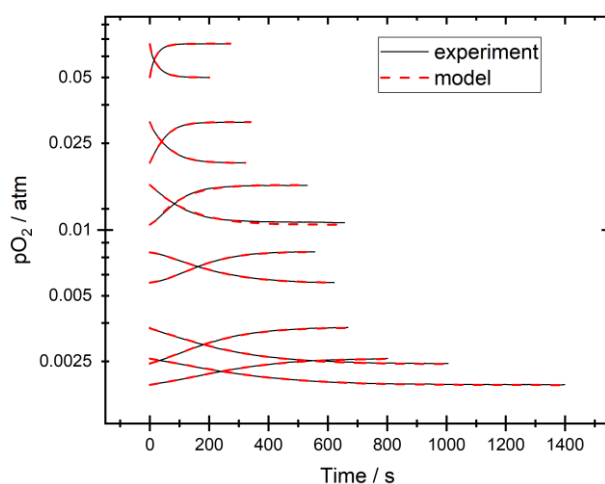


Figure 1. Experimental data obtained with OPPR method fitted with fundamental theoretical model ($T = 850\text{ }^{\circ}\text{C}$, $J = 50\text{-}100\text{ ml/min}$) on SCT10 compound

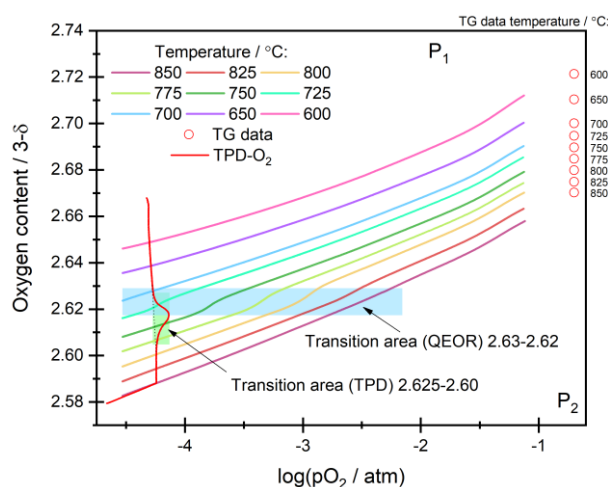


Figure 2. Experimental dependencies of $3-\delta$ on oxygen partial pressure obtained with QEOR and TPD- O_2 methods and thermogravimetric data of SCT10 compound

Acknowledgements. The reported study was funded by Russian Science Foundation (Project № 21-79-30051).

References

1. Den Otter, M. W.; Boukamp, B. A.; Bouwmeester, H. J. M. Theory of Oxygen Isotope Exchange. *Solid State Ion.* 2001, 139 (1–2), 89–94.
2. Teraoka, Y.; Zhang, H.-M.; Furukawa, S.; Yamazoe, N. Oxygen permeation through perovskite-type oxides. *Chem. Lett.* 1985, 14 (11), 1743–1746.
3. Tikhonovich, V. N.; Zharkovskaya, O. M.; Naumovich, E. N.; Bashmakov, I. A.; Kharton, V. V.; Vecher, A. A. Oxygen Nonstoichiometry of $\text{Sr}(\text{Co},\text{Fe})\text{O}_{3-\delta}$ -Based Perovskites: I. Coulometric Titration of $\text{SrCo}_{0.85}\text{Fe}_{0.10}\text{Cr}_{0.05}\text{O}_{3-\delta}$ by the Two-Electrode Technique. *Solid State Ion.* 2003, 160 (3–4), 259–270.
4. Bychkov, S. F.; Gainutdinov, I. I.; Chizhik, S. A.; Nemudry, A. P. Novel Oxygen Partial Pressure Relaxation Technique for Study of Oxygen Exchange in Nonstoichiometric Oxides. The Model of Relaxation Kinetics. *Solid State Ion.* 2018, 320, 297–304.
5. Starkov, I.; Bychkov, S.; Matvienko, A.; Nemudry, A. Oxygen Release Technique as a Method for the Determination of “ δ - PO_2 -T” Diagrams for MIEC Oxides. *Phys. Chem. Chem. Phys.* 2014, 16 (12), 5527–5535.

NEW APPROACH TO CONTROL THE MICROSTRUCTURE OF PLATINUM-CARBON ELECTROCATALYSTS DURING THEIR LIQUID-PHASE SYNTHESIS

^{1,2}Vladimir Guterman, ^{1,2}Kirill Paperzh, ¹Maria Danilenko, ¹Elvira Zaitseva

¹Chemistry Department, Southern Federal University, Rostov-on-Don, Russia, *E-mail: guter@sfedu.ru*

²Prometheus R&D LLC, Rostov-on-Don, Russia, *E-mail: Prometheus.rd.ltd@gmail.com*

Introduction

Platinum-containing electrocatalysts are a key component of the catalytic layers of proton conducting membrane fuel cells (PEM FCs). The operating conditions of PEM FC and the catalyst characteristics they determine can vary significantly. This makes it necessary to control the composition and microstructure of catalysts and requires the development of production technologies that can be easily customized to produce products with specified microstructure and properties.

Experiments

The synthesis of platinum-containing catalysts was carried out in the liquid phase, changing the nature of the reducing agent, the composition of the solution, pH, atmosphere & temperature. H_2PtCl_6 was used as a platinum precursor. Continuous measurement of the intensity of the three colored components of the solution during the synthesis process was carried out using a digital micro camera. An indicator electrode was used to measure the redox potential of the reaction medium. Standard methods were used to study the composition, structural characteristics, and electrochemical behavior of the catalysts.

Results and Discussion

When carrying out liquid-phase synthesis of platinum-containing catalysts, the composition of the reaction medium and synthesis conditions significantly affects the shape of Pt or PtM nanoparticles, their size, and size distribution. Unfortunately, the use of known methods for studying the composition of the reaction medium and monitoring the kinetics of transformation under technological conditions is difficult due to the high concentration of reagents, gas purging and mixing of the reaction medium during the synthesis process. Simultaneous study of the dynamics of color changes and redox potential of the reaction medium provided information on the influence of temperature, pH, atmospheric composition and two-component solvent on the kinetics of the multi-stage transformation $\text{Pt(IV)} \rightarrow \text{Pt}_x(0)$ in relation to various synthesis methods [1-3]. Particular attention was paid to studying the duration of the nucleation/growth stages of platinum-containing NPs. As an example, the Fig. 1 shows characteristic dependences demonstrating the change in the intensity of the three components of the solution color and the redox potential of the medium during the synthesis of Pt/C.

The study of the obtained Pt/C materials by XRD and TEM methods, measurement of their electrochemically active surface area and activity in the oxygen electroreduction reaction (ORR), made it possible to find correlations between the kinetics of transformation, the role of the “influencing factor” and the parameters characterizing the microstructure and electrochemical behavior of platinum-carbon catalysts.

It has been established that the implementation of synthesis under conditions of rapid nucleation and subsequent growth of metal nanoparticles promotes their mono-size distribution, which leads to the production of Pt/C catalysts with high functional characteristics. For example, the electrochemically active surface area of a Pt/C catalyst obtained by reducing Pt(IV) with formic acid, determined from the results of cyclic voltammetry (Fig. 2), increases from 40 to 95 $\text{m}^2/\text{g(Pt)}$ as a result of a targeted change in synthesis conditions.

It has been shown that changes in the composition of the atmosphere in which liquid-phase synthesis is carried out have a significant effect on both the kinetics of the $\text{Pt(IV)} \rightarrow \text{Pt(0)}_x$ transformation, the size and shape of platinum nanoparticles.

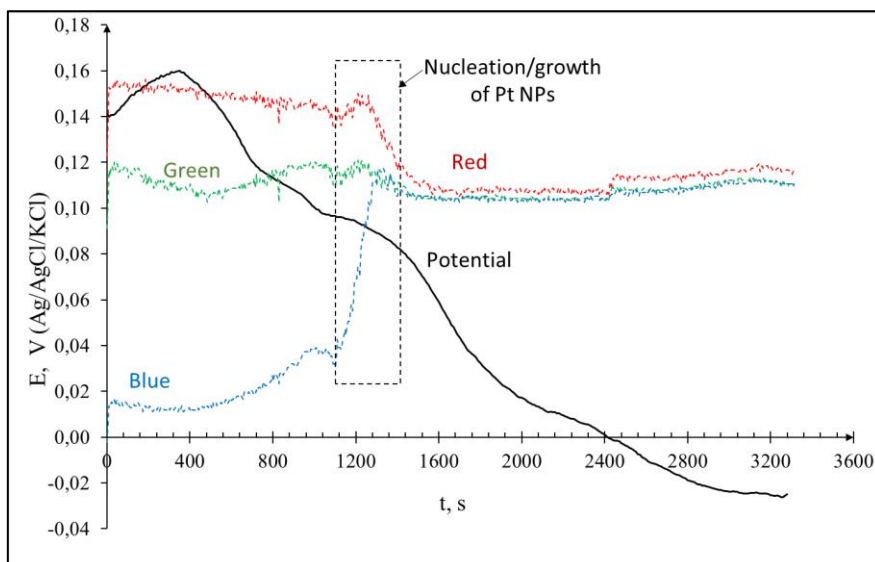


Figure 1. Changes in the redox potential and three components of the color of the reaction medium during the liquid-phase synthesis of platinum nanoparticles.

The use of developed methods for controlling the kinetics of multi-stage transformation made it possible to obtain Pt/C catalysts that combine high ECA, ORR activity and stability, which is largely associated with the optimal microstructure (morphology) of these materials.

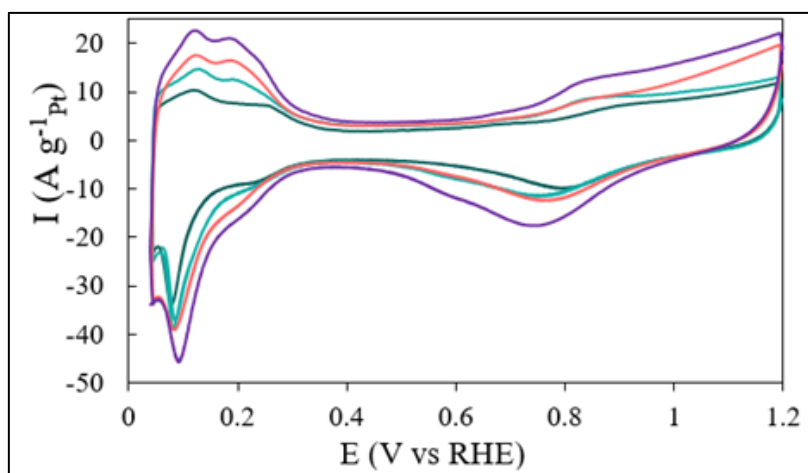


Figure 2. Cyclic voltammograms of standardized Pt/C catalysts obtained by colloidal syntheses with formic acid at different conditions. The potential sweep rate is 20 mV s^{-1} . 0.1 M HClO_4 .

Acknowledgement. This work was supported by the Ministry of Science and Higher Education of the Russian Federation within the framework of the State Assignment in the field of scientific activity no. FENW-2023-0016.

References

1. Danilenko M.V., Guterman V.E., Vetrova E.V., Metelitsa A.V., Paperzh K.O., Pankov I.V. and Safronenko O.I. Nucleation/growth of the platinum nanoparticles under the liquid phase synthesis // *Colloids and Surfaces A: Physicochem. and Engineering Aspects*. 2021. V.630. No 127125.
2. Danilenko, M.V., Guterman, V.E., Paperzh, K.O., Alekseenko, A.A., Pankov, I.V., CO Effect on the Dynamics of Platinum Nucleation/Growth under the Liquid-Phase Synthesis of Pt/C Electrocatalysts // *J. Electrochem. Soc.* 2022. V. 169(9). No 092501.
3. Danilenko, M.V., Guterman, V.E., Novomlinskiy, I.N., Pankov I.V. The effect of a gas atmosphere on the formation of colloidal platinum nanoparticles in liquid phase synthesis // *Colloid and Polymer Sci.* 2023. V. 301. P. 433–443.

SCALE UP ESTIMATES OF AN OXYGEN-REMOVING MEMBRANE CONTACTOR FOR DEMO POST COMBUSTION PLANT

Denis Kalmykov, Sergey Shirokikh, Stepan Bazhenov

TIPS RAS, Moscow, Russia, E-mail: denis.kalmykov@ips.ac.ru, shirokikh@ips.ac.ru, sbazhenov@ips.ac.ru

Introduction

A wide range of studies demonstrate the harm from CO₂ emissions into the atmosphere [1]. The need to reduce them is expressed in the policies of majority of states [2]. The CO₂ capture with alkanolamine-based absorption is the most mature technology that can be readily implemented for different industrial and energy plants on the immediate horizon [3]. The main technique for amine solvent regeneration continues to be high-temperature CO₂ stripping. A significant disadvantage of this technique is the gradual solvent degradation in the presence of dissolved oxygen [4], accelerating at elevated temperatures (100-130 °C). Oxidative amine degradation leads to the formation of heat stable salts (HSS). The presence of HSS intensify the corrosion process [5], decrease the solvent sorption capacity, changes the solvent viscosity leading to foaming, which together increase the solvent circulation rate and energy costs [6]. Oxygen removal can be delivered in a compact, modular and mobile form using hollow fiber membrane contactors due to their high specific surface area (interfacial area per unit volume), modular design, ease of installation and operation, independent adjustment of phase flows [7]. Despite the wide applications of membrane contactors, the O₂ removal from amine CO₂ capture solvents to prevent their oxidative degradation is rather unexplored field [8; 9].

Recently, our team carried out the studies on the materials selection to develop composite membranes for this target. Firstly, it was shown that the majority of widely used commercial materials and porous membranes are poorly suited for membrane contactor system due to chemical or morphological alterations after contact with amine solvents [10]. Secondly, we developed a promising polymeric material of a thin protective layer [11]: a blend of ultra-permeable poly[1-(trimethylsilyl)-1-propyne] (PTMSP) with addition of polyvinyltrimethylsilane (PVTMS) as an aging-preventing agent was developed. Thirdly, we studied the effect of the PVTMS additives to PTMSP matrix in the protective layer on the O₂ removal efficiency from MEA solvent in contactors with polysulfone hollow fibers and tubular ceramic supports [12]. However, these works mainly focused on materials selection issue and the initial pre-demonstration of O₂ removal with fabricated membranes without deep study of the deoxygenation process.

In this paper, the overall mass-transfer coefficients and mass-transfer resistances of membranes and solvent boundary layers are estimated for the first time and the membrane scale up to size the developed composite membrane for a hypothetical post-combustion CO₂ capture plant with a solvent flow rate of 120 m³/h is presented for various amine temperatures.

Experiments

A 30% aqueous solution of monoethanolamine was used as a model for the alkanolamine-based absorbent. Composite membranes on the PSF hollow fiber supports were fabricated by deposition of the PTMSP/PVTMS solution in n-hexane on the outer surface of the hollow fiber support. The hollow fiber membrane contactor was prepared as follows: composite membranes were placed in a module body made of pneumatic push-in fittings and polyethylene tubes. Membranes fixing and sealing were done using universal epoxy glue. The parameters of the hollow fiber module are presented in Table 1.

Table 1: Parameters Of Membrane Contactors

Membrane inner diameter, mm	1.06
Membrane external diameter, mm	1.64
Module operating length, mm	100
Module shell diameter, mm	8.5
Number of membranes in the module, pcs	5
Surface area of membranes, m ²	3.8·10 ⁻³
Packing density, m ² /m ³	664

The O₂ mass transfer data was estimated from deoxygenation of the MEA solution as a reference solvent. The transmembrane O₂ flux J (m³/s) was calculated as follows:

$$J = \frac{(V_0 - V_t)}{t} \quad (1)$$

where V_0 and V_t are the O₂ volumes in the liquid phase at the process beginning and at time t , respectively, m³; t – time of the deoxygenation experiment, s.

The overall O₂ mass transfer coefficient K_{ov} was calculated as follows:

$$K_{ov} = \frac{J}{\Delta C_{ln} \cdot S} \quad (2)$$

where J is the transmembrane O₂ flux, m³/s, S is the membrane surface area, m², ΔC_{ln} is the average logarithmic difference in the O₂ volume fractions at the initial time and after deoxygenation process, m³/m³. O₂ mass transfer resistance was calculated as $1/K_{ov}$.

As a parameter for assessing the practical efficiency of the membrane deoxygenation, one can use the estimated membrane area required to remove of O₂ from certain flowrate of O₂-rich solvent. In this work, for such estimation, data on the post-combustion large demonstration plant (Technology Centre Mongstad, Norway) was used with the following parameters: solvent flowrate – 120 m³/h, flue gas flowrate – 60,000 standard m³/h. The membrane area (A_m in m²) required for oxygen removal efficiency η can be calculated as follows [9]:

$$A_m = \frac{\eta \cdot X_{in} \cdot Q}{K_{ov} \cdot \Delta C_{ln}(\eta)} \quad (3)$$

where η is the degree of dissolved O₂ removal, X_{in} volume fraction of oxygen in the O₂-rich solvent, m³/m³, Q is the solvent flowrate, m³/s, K_{ov} is the overall mass transfer coefficient, m/s, $\Delta C_{ln}(\eta)$ is the average logarithmic change of volumetric O₂ fraction depending on the degree of dissolved O₂ removal during the deoxygenation process, m³/m³.

Results and Discussion

The deoxygenation tests were conducted on the MEA solvent at linear velocities of the liquid phase of 0.5, 2.8 and 5.5 cm/s. Based on this data obtained on the deoxygenation of the MEA solvent with contactor, the main parameters of O₂ mass transfer were calculated and presented in Table 2.

Table 2: Oxygen Mass Transfer Parameters

Amine linear velocity, cm/s	0.5	2.8	5.5
Transmembrane oxygen flux $J \cdot 10^{-7}$, m ³ /h	6.7	9.2	11.7
Mass transfer coefficient $K_{ov} \cdot 10^{-5}$, m/s	1.40	2.14	2.97
Mass transfer resistance $1/K_{ov} \cdot 10^4$, s/m	7.11	4.67	3.36

The area of the membranes in gas-liquid contactor sized to remove dissolved O₂ with required degree η from 30% aqueous MEA solution was estimated using Formula (5). The temperature of the incoming amine stream was 60 °C. Fig. 1 shows the calculated areas required to remove oxygen at a given temperatures (n.b. areas are given in hundreds of square meters).

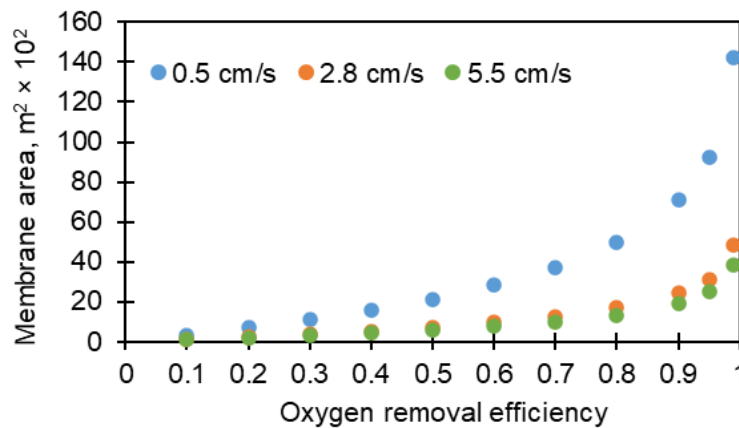


Figure 1. Membrane areas needed for different oxygen removal efficiencies from post-combustion CO₂ capture plant with a solvent flowrate of 120 m³/h.

Assuming 90% dissolved O₂ removal degree with its content of ~4.1 ppm in the incoming solvent stream at 60°C, the membrane sizes of 7108 m² for 0.5 sm/s, 2412 m² for 2.8 sm/s and 1911 m² for 5.5 sm/s are obtained. Porous membrane supports of the calculated scale are readily commercially available.

Acknowledgement. This work was carried out in A.V. Topchiev Institute of Petrochemical Synthesis (Russian Academy of Sciences) and was funded by Russian Science Foundation, grant number 21-79-10400.

References

1. *Jacobson T.A., Kler J.S., Hernke M.T., Braun R.K., Meyer K.C., Funk W.E.* Direct human health risks of increased atmospheric carbon dioxide//*Nature Sustainability*, 2019, Vol. 2, No. 8, P. 691-701.
2. *Li B., Haneklaus N.* Reducing CO₂ emissions in G7 countries: The role of clean energy consumption, trade openness and urbanization//*Energy Reports*, 2022, Vol. 8, Reducing CO₂ emissions in G7 countries, P. 704-713.
3. *Bazhenov S., Chuboksarov V., Maximov A., Zhdaneev O.* Technical and economic prospects of CCUS projects in Russia//*Sustainable Materials and Technologies*, 2022, Vol. 33, P. e00452.
4. *Bazhenov S.D., Novitskii E.G., Vasilevskii V.P., Grushevenko E.A., Bienko A.A., Volkov A.V.* Heat-Stable Salts and Methods for Their Removal from Alkanolamine Carbon Dioxide Absorbents (Review)//*Russian Journal of Applied Chemistry*, 2019, Vol. 92, No. 8, P. 1045-1063.
5. *Choi Y.-S., Duan D., Nešić S., Vitse F., Bedell S.A., Worley C.* Effect of Oxygen and Heat Stable Salts on the Corrosion of Carbon Steel in MDEA-Based CO₂ Capture Process//*CORROSION*, 2010, Vol. 66, No. 12, P. 125004-125004-10.
6. *ElMoudir W., Supap T., Saiwan C., Idem R., Tontiwachwuthikul P.* Part 6: Solvent recycling and reclaiming issues//*Carbon Management*, 2012, Vol. 3, Part 6, No. 5, P. 485-509.
7. *Zhao S., Feron P.H.M., Deng L., Favre E., Chabanon E., Yan S., Hou J., Chen V., Qi H.* Status and progress of membrane contactors in post-combustion carbon capture: A state-of-the-art review of new developments//*Journal of Membrane Science*, 2016, Vol. 511, Status and progress of membrane contactors in post-combustion carbon capture, P. 180-206.
8. *Monteiro J., Figueiredo R.V., Bakker D., Stellwag I., Huijzinga A., Abu Zahra M., van Os P., Goetheer E.* De-oxygenation as countermeasure for the reduction of oxidative degradation of CO₂ capture solvents//14th Greenhouse Gas Control Technologies Conference Melbourne. – 2018. – P. 21-26.
9. *Figueiredo R.V., Srivastava T., Skaar T., Warning N., Gravesteijn P., van Os P., Ansaloni L., Deng L., Knuutila H., Monteiro J.* Impact of dissolved oxygen removal on solvent degradation for post-combustion CO₂ capture//*International Journal of Greenhouse Gas Control*, 2021, Vol. 112, P. 103493.
10. *Kalmykov D., Shirokikh S., Grushevenko E.A., Legkov S.A., Bondarenko G.N., Anokhina T.S., Molchanov S., Bazhenov S.D.* Stability of Porous Polymeric Membranes in Amine Solvents for Membrane Contactor Applications//*Membranes*, 2023, Vol. 13, No. 6, P. 544.
11. *Kalmykov D., Balynin A., Yushkin A., Grushevenko E., Sokolov S., Malakhov A., Volkov A., Bazhenov S.* Membranes Based on PTMSP/PVTMS Blends for Membrane Contactor Applications//*Membranes*, 2022, Vol. 12, No. 11, P. 1160.
12. *Kalmykov D.O., Shirokikh S.A., Matveev D.N., Anokhina T.S., Bazhenov S.D.* Deoxygenation of CO₂ Absorbent Based on Monoethanolamine in Gas–Liquid Membrane Contactors Using Composite Membranes//*Membranes and Membrane Technologies*, 2023, Vol. 5, No. 5, P. 333-343.

INVESTIGATION OF INFLUENCE OF ORGANIC ACID SALTS NATURE ON CURRENT-VOLTAGE CHARACTERISTICS OF ION-EXCHANGE MEMBRANES

Tatyana Karpenko, Vladislava Shramenko, Iliia Averianov, Nikolay Sheldeshov
Kuban State University, Krasnodar, Russia, E-mail: tany1328@mail.ru

Introduction

In recent years, cation- and anion-exchange membranes have been increasingly used in membrane technologies for the production of organic acids [1,2]. In fermentation solutions, these acids mainly exist in the form of neutral salts. Before producing organic acids by electro dialysis with bipolar membranes, their neutral salts are concentrated by traditional electro dialysis. In this case, acid anions are transferred from the fermentation solution to the concentrated solution through anion exchange membranes. In other cases, anion exchange membranes are used at the stage of producing organic acids from their salts without prior salt concentration to isolate organic acid anions from mixtures with mineral salts [3] or to separate organic acids from their mixtures [4].

To improve the processes of producing and separating organic acids from solutions, it is necessary to understand the processes occurring at anion exchange membranes in contact with solutions of organic acid salts under conditions of electric current flowing through the membrane system. A simple method for detecting additional processes occurring in the membrane system is the cyclic voltamperometry method. The purpose of this work was to study the effect of sodium salts of acetic, malonic and citric acids on the current-voltage characteristics of anion exchange membranes.

Experiments

Heterogeneous Ralex AMH (Mega, Czech Republic), homogeneous Lancytom® AHT (LANRAN, China) and two-layer Ralex AMH/MF-4SK membrane were used as the anion exchange membranes under study. To determine the value of the limiting electrodiffusion current in systems with anion exchange membranes, as well as to identify part of current-voltage characteristics (CVC) that are not typical for classical CVC and which indicate the development of new processes in the membrane system, the cyclic current-voltage characteristics of membrane systems were measured. Measurements were carried out in solutions of neutral and acidic sodium salts of acetic, malonic and citric acids. In addition, CVC measurements were carried out in "acetic – malonic acid" and "acetic – citric acid" solutions at different pH values of the solutions. The choice of solution compositions was carried out on the basis of the distribution curves of various forms of acetic and malonic acids (Fig. 1a) and acetic and citric acids (Fig. 1b) depending on the pH of the solution.

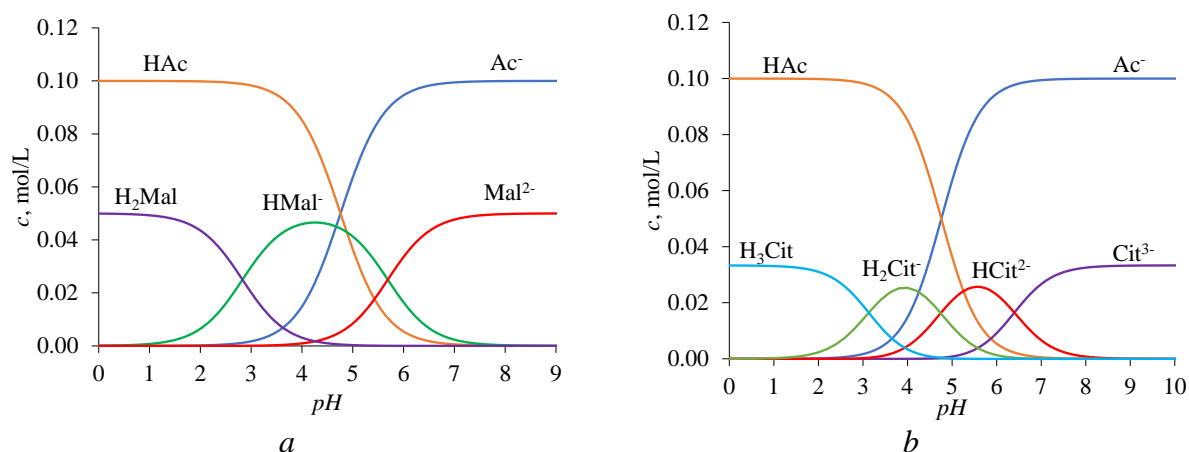


Figure 1. Concentration dependences of various forms of acetic and malonic acids (a) and acetic and citric acids (b) on the pH of solutions.

Results and Discussion

The current-voltage characteristics of the heterogeneous Ralex AMH anion exchange membrane in solutions of neutral salts of acetic, malonic and citric acids have a traditional form with a well-defined part of the limiting current (Fig. 2).

The current-voltage characteristics of the homogeneous Lancyotom® AHT anion exchange membrane have a traditional form only in solutions of neutral salts of acetic and citric acids (Fig. 3a,c). In a solution of sodium malonate (neutral salt) CVC at under-limiting current is not linear (Fig. 3b). Both membranes have the same nonlinear CVC at under-limiting current in solutions of acidic salts of malonic and citric acids (Fig. 2b,c and 3b,c). These features can be explained by the protonation-deprotonation reactions in solution involving anions of acid salts [5] and ionogenic groups of membranes.

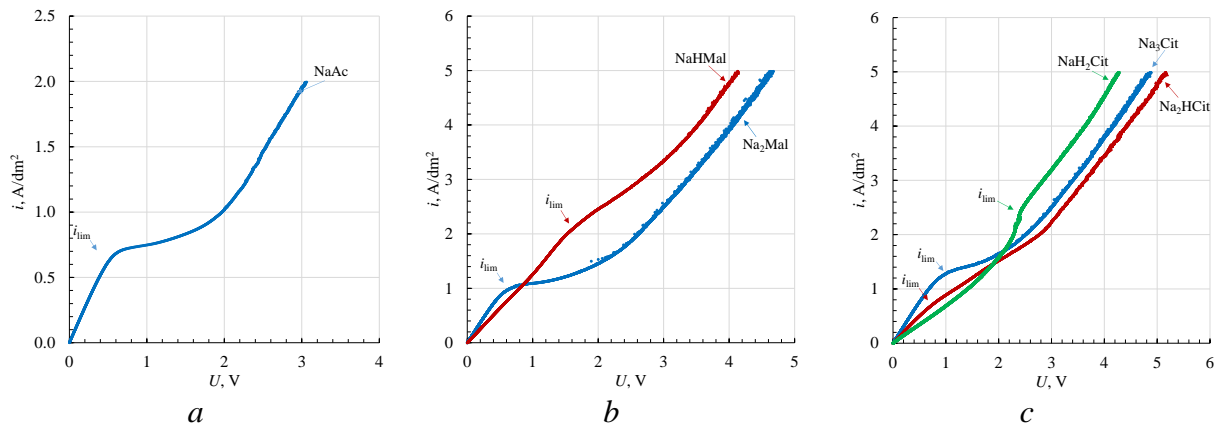


Figure 2. Current-voltage characteristics of heterogeneous Ralex AMH anion exchange membrane in 0.1 mol-eq/L solutions of acetic (a), malonic (b) and citric acid (c) salts.

The cyclic current-voltage characteristics of the Ralex AMH anion exchange membrane in solutions of "acetic – malonic acid" (Fig. 4a) and "acetic – citric acid" mixtures (Fig. 4b) at all pH values of the solutions have nonlinear parts at currents less than the limiting one, as in the case of pure acidic salts of malonic and citric acids.

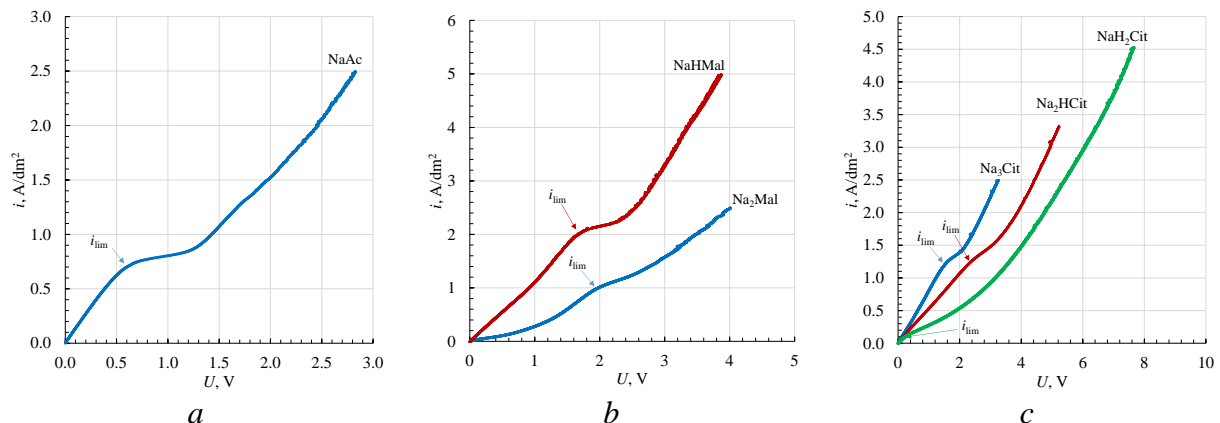


Figure 3. Current-voltage characteristics of homogeneous Lancyotom® AHT anion exchange membrane in 0.1 mol-eq/L solutions of acetic (a), malonic (b) and citric acid (c) salts.

Probably, an increase in the slope of the curves with an increase in the current density at under-limiting current can be caused by deprotonation of molecules and single-charge anions of malonic acid and acetic acid molecules (Fig. 4a) or single-charge and double-charge anions of citric acid and acetic acid molecules (Fig. 4b) at the "anion exchange membrane – solution" interface, which leads to the transition anion exchange membrane in the form of anions with a higher charge. This, in turn, leads to an increase in its electrical conductivity.

The application of a thin MF-4SK film to the surface of a heterogeneous Ralex AMH anion exchange membrane leads to a noticeable decrease in the limiting current (Fig. 5).

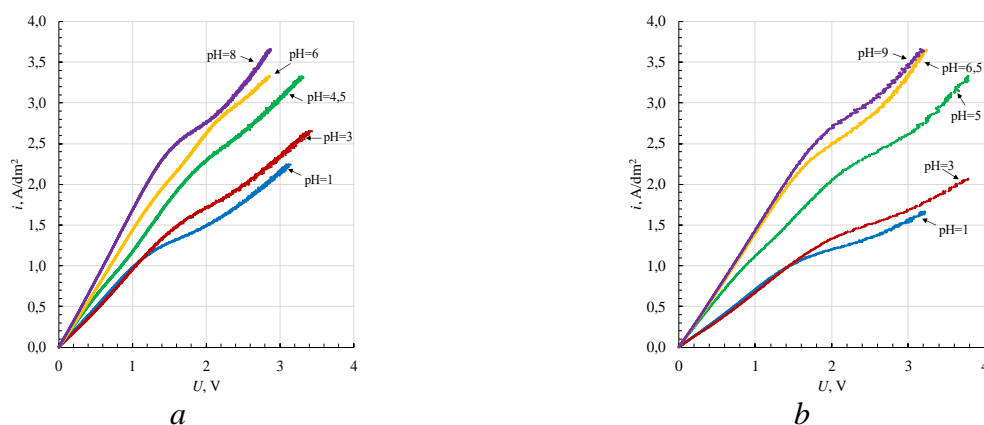


Figure 4. CVC of the Ralex AMH anion-exchange membrane in "acetic – malonic acid" system (a) and in "acetic – citric acid" system (b) at different values of pH.

This change may be caused by a faster decrease in the concentration of electrolytes at the «MF-4SK | Ralex AMH» interface with an increase in electric current density than at the «diffusion layer in solution | Ralex AMH» interface under the same conditions.

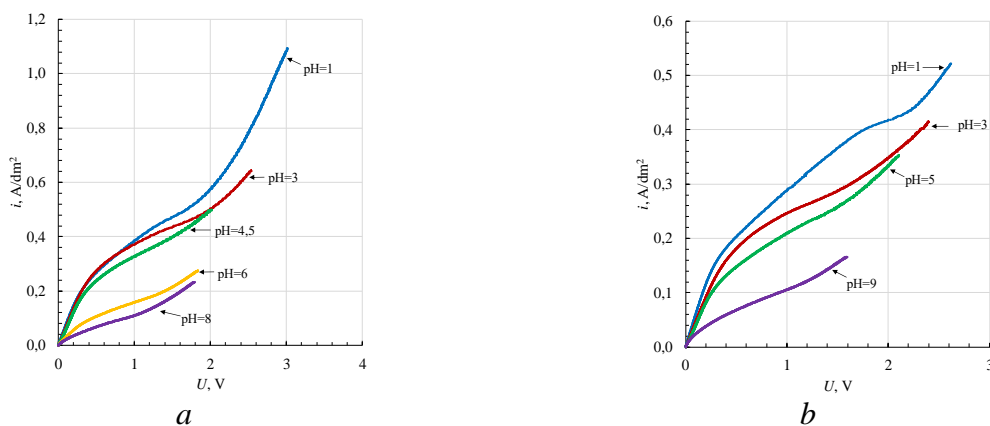


Figure 5. CVC of the Ralex AMH/MF-4SK double-layer membrane in "acetic – malonic acid" system (a) and in "acetic – citric acid" system (b) at different values of pH.

In this case, the processes of protonation – deprotonation of various forms of salts and molecules of organic acids can occur not only at the «membrane – solution» interface, but also at the interface between the MF-4SK cation exchange film and the Ralex AMH membrane when an electric current flows through two-layer Ralex AMH/MF-4SK membrane.

Acknowledgement. This research was financially supported by the RSF according to the research project № 23-23-00660, <https://rscf.ru/en/project/23-23-00660/>.

References

1. Jiang C., Wang Y., Xu T. Membranes for the recovery of organic acids from fermentation broths. In: *Membrane Technologies for Biorefining*. Woodhead Publishing. 2016. P. 135-161.
2. Ran J., Wu L., He Y., et al. Ion exchange membranes: New developments and applications // *J. Membr. Sci.* 2017. V. 522. P. 267-291.
3. Melnikov S.S., Nosova E.N., Melnikova E.D., et al. Reactive separation of inorganic and organic ions in electrodialysis with bilayer membranes // *Sep. Purif. Technol.* 2021. V. 268. 118561.
4. Chandra A., Tadimeti J.G.D., Bhuvanesh E., et al. Switching selectivity of carboxylic acids and associated physico-chemical changes with pH during electrodialysis of ternary mixtures // *Sep. Purif. Technol.* 2018. V. 193. P. 327–344.
5. Pismenskaya N.D., Rybalkina O.A., Kozmai A.E., et al. Generation of H⁺ and OH⁻ ions in anion-exchange membrane/ampholyte-containing solution systems: A study using electrochemical impedance spectroscopy // *J. Membr. Sci.* 2020. V. 601. 117920.

SODIUM-CONDUCTING POLYMER ELECTROLYTES BASED ON COMMERCIALY AVAILABLE ANALOGUES OF NAFION AND CARBONATES

¹Ruslan Kayumov, ^{1,2}Anna Lochina, ¹Alexander Lapshin, ¹Lyubov Shmygleva

¹Federal Research Center of Problems of Chemical Physics and Medicinal Chemistry RAS, Chernogolovka, Russia, *E-mail: kayumov@icp.ac.ru*

² Moscow Institute of Physics and Technology, Dolgoprudny, Russia

Introduction

Lithium-ion batteries (LIBs) have taken a strong place in everyday life. But despite this, great interest is directed towards the creation of post-lithium current sources, in particular sodium-ion batteries (SIBs). Replacing lithium with sodium reduces production costs, improves sustainability, increases safety and reduces the environmental impact of SIBs. Basically, now electrolytes of commercial LIBs and SIBs consist of the metal salts, which are sources of charge transfer, dissolved in liquid aprotic solvents. Cyclic and linear carbonates and their mixtures, as well as ethers are mainly used as the solvents due to their high ionic conductivity, optimal dipole moment, viscosity and dielectric constant [1]. Due to fire and explosion hazards, a transition from liquid to solid polymer electrolytes is necessary. One of the optimal and best in many respects, such as electrical transport and physicochemical properties, are Nafion-like membranes.

A product from DuPont, produced under the Nafion® brand turned out to be the most in demand as a polymer membrane for PEM fuel cells, as well as batteries. The production of ionomers with a similar chemical structure was later developed by other companies: Asahi Glass Company (Flemion®), Asahi Kasei (Aciplex®), FuMA-Tech (Fumion®), Thinkre Membrane Materials (NEPEM®), CTPEM (China), GP-IEM (Liaoning Grepalofu NewEnergy Co., Ltd., Panjin, China). Such membranes are usually called Nafion-like. They have high ionic conductivity, chemical and thermal stability. Currently the original Nafion membranes are not commercially available. Therefore, the aim of the work was to establish the general laws of the formation of the physicochemical and transport properties of polymer electrolytes based on the sodium forms of the commercial analogs of Nafion (GP-IEM and CTPEM membrane) plasticized by such aprotic solvents as ethylene carbonate (EC) and propylene carbonate (PC).

Experiments

Polymer membranes in the acidic form with a thickness of 15–125 µm were purified according to a known method; to remove water, the membrane was first dried at 100 °C in a vacuum oven for 3 hours. To obtain sodium form according to the standard procedure the membranes were aging in 1 M water-ethanol (1:1 by volume) NaOH solution at 80–100 °C for 2 hours, followed by thorough washing with distilled water. The samples were first dried at 60 °C in drying oven Binder (Germany) for one hour, and then in dried in a glass vacuum oven Buchi (Switzerland) at temperature of 100 °C a pressure of 10 mbar for 3 hours.

A dry membrane sample was placed in an excess volume of the solvent (EC or PC) over activated 3 Å molecular sieves at room temperature. All experiments with aprotic solvents were carried out in a dry box. The physico-chemical properties of the obtained samples were studied by the methods of gravimetry, synchronous thermal analysis, small-angle X-ray scattering, IR and impedance spectroscopy.

Results and Discussion

According to IR spectroscopy data, the molecular structure and thermal stability of studied polymer membranes also completely coincides with the structure of Nafion [2]. Swelling of the studied membranes in EC leads to excessive swelling degree (Table 1), which is much higher than for Na-Nafion. On the other side, the polymers, plasticizing with PC does not differ from Na-Nafion.

Table 1. Thickness change (Δd), swelling degree (W), temperature of thermal degradation (T_{deg}) for the sodium form of the studied membranes

Sample	$\Delta d, \mu\text{m}$	$W, \text{wt}\%$	$W_{\text{TGA}}, \text{wt}\%$	$T_{deg}, ^\circ\text{C}$
Na-G102/EC	47	154	121	488
Na-G105/EC	34	131	130	489
Na-G102/PC	4	25	27	492
Na-G105/PC	17	22	26	492
Na-CT1/PC	25	39	37	485
Na-CT3/PC	-20	29	28	491

Supramolecular pacing of the samples also similar to Nafion, but CTPEM membranes show the lowest crystallinity. According to impedance spectroscopy the ion conductivity of studied membranes, plasticized with EC inferior the same electrolyte based on Nafion, despite higher swelling degree. The report will present the detailed results and summarized analyses, obtained during this work.

Acknowledgement. The reported study was supported by a grant of Russian Science Foundation No. 24-29-00484, <https://rscf.ru/en/project/24-29-00484/>.

References

1. Roscher D., Kim Y., Stepien D., Zarrabeitia M., Passerini S. Solvent-free ternary polymer electrolytes with high ionic conductivity for stable sodium-based batteries at room temperature // *Batter. Supercaps.* 2023. V. 6. P. 1–10.
2. Kayumov R.R., Radaeva A.P., Nechaev G.V., Lochina A.A., Lapshin A.N., Bakirov A.V., Glukhov A.A., Shmygleva L.V. Polymer electrolyte based on Nafion plasticized with carbonates and their ternary mixtures for sodium-ion batteries // *Solid State Ionics* 2023. V. 399. P. 116294.

STATIONARY ELECTROCONVECTION IN GALVANOSTATIC MODE WHEN FOLLOWING THE GENERALIZED OHM'S LAW

Catherine Kazakovtseva, Anna Kovalenko, Marina Patykovskaya, Makhamet Urtenov
Kuban State University, Krasnodar, Russia, E-mail: morskaia83@mail.ru

Introduction

In membrane systems, the phenomenon of electroconvection is of particular interest: in the field of electrodialysis, it significantly increases the useful mass transfer in the processes of desalting dilute solutions [2]; in the field of microfluidics, it is the dominant mechanism in applications such as electrokinetic pumps, fast electrophoresis, etc. [2].

In [1], the simplest model of the transport of salt ions in membrane systems is proposed in the generalized Ohm's law approximation for a symmetrical 1:1 electrolyte taking into account electroconvection, for example, an aqueous solution of KCl, which in some cases allows an analytical solution.

Mathematical modeling and numerical research

The mathematical model in dimensionless form is given in [1]. Let us consider a desalting channel formed by anion-exchange ($x=0$) and cation-exchange membranes ($x=1$), where it corresponds to the entrance to the channel where the KCl solution is supplied, and to the exit $y=L$ (length of the desalting channel L). At the entrance to the region, the ion concentration and potential distribution are assumed to be known, and the velocity is given by the Poiseuille parabola.

The work carried out a numerical analysis of a 2D transport model of a symmetric binary electrolyte in the Ohm's law approximation taking into account electroconvection using a combination of the finite element method with the time-based method.

The boundary value problem of the model has the form:

$$\frac{1}{Pe} \Delta \tilde{S} - \text{div}(\tilde{S}\vec{V}) = 0, \quad \frac{\varepsilon}{2} \|\vec{E}\|^2 \vec{E} + \tilde{S}\vec{E} - \vec{\Phi} = 0, \quad \Delta \eta = - \left(\nabla(\tilde{S} + \frac{\varepsilon}{2} \|\vec{E}\|^2), \vec{E} \right)_1,$$
$$\frac{\partial \vec{V}}{\partial t} + (\vec{V}\nabla)V = -\nabla P + \frac{1}{Re} \Delta \vec{V} + K_{ei} \varepsilon \vec{E} \text{div} \vec{E}, \quad \text{div} \vec{V} = 0, \quad \Phi_1 = -\frac{\partial \eta}{\partial y}, \quad \Phi_2 = \frac{\partial \eta}{\partial x}.$$

Where Φ_1, Φ_2 are the components of the total current, which are the sum of the Faraday current and the displacement current [1], \tilde{S} is the generalized concentration (indicator function), \vec{E} is the electric field strength, η is the current function for the current density, Pe – Peclet number, $\varepsilon > 0$ is a small parameter, Re is the Reynolds number.

Border conditions

$$\left. \frac{\partial \eta}{\partial x} \right|_{x=0} = 0, \quad \left. \frac{\partial \eta}{\partial x} \right|_{x=1} = 0, \quad \eta|_{y=0} = 0, \quad \eta|_{y=L} = -i_{av} L = -2i_{av},$$
$$\tilde{S}|_{x=0} = \tilde{S}|_{x=1} = I_{np} - i_{av} = 1 - i_{av}, \quad \tilde{S}|_{y=0} = 4(x-x^2) + 1 - i_{av}, \quad \left. \frac{\partial \tilde{S}}{\partial y} \right|_{y=L} = 0.$$

These conditions mean that the current does not flow along the membrane, they give the condition at the entrance to the channel, the condition at the exit from the channel, here is the average current passing through the channel, for the speed the sticking condition on the AEM and KEM is used, the Poiseuille parabola is specified at the input, and at the output there is a condition of absence of normal voltages.

Main results

The work established the basic laws of electroconvection under conditions of fulfillment of the generalized Ohm's law, namely:

1) the existence of a stationary solution is shown numerically at currents less than the limiting current and slightly greater than the limiting current.

2) at currents less than the limit, no electroconvective vortices are formed, although the solution streamlines are bent and the flow at currents close to the limit differs from the Poiseuille flow.

3) at currents greater than the limiting one, but close to it, with values of the order parameter ε of 0.001, two electroconvective vortices are formed at the beginning of the channel; at currents significantly exceeding the limiting current, for example, one and a half limiting current, the flow structure strongly depends on the small parameter ε .

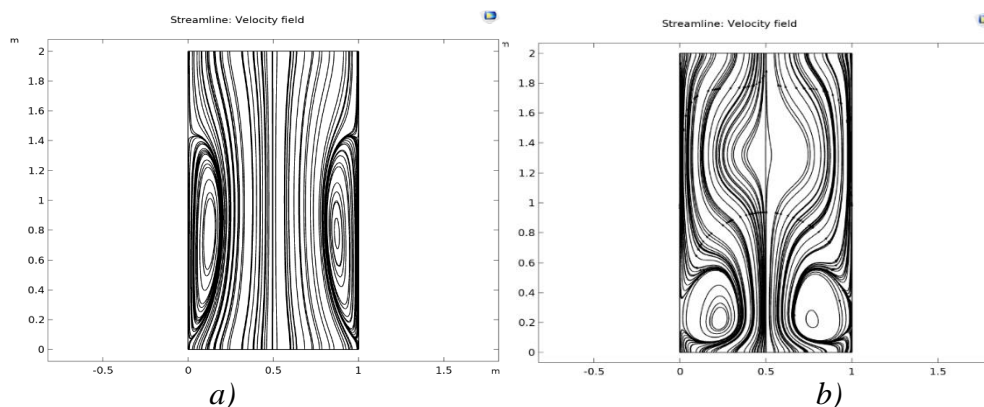


Figure 1. Electroconvective vortices $\varepsilon = 0.002$, $Pe = 7.5$, at various values: a) $-i_{av} = 1.1$,
b) $-i_{av} = 1.5$

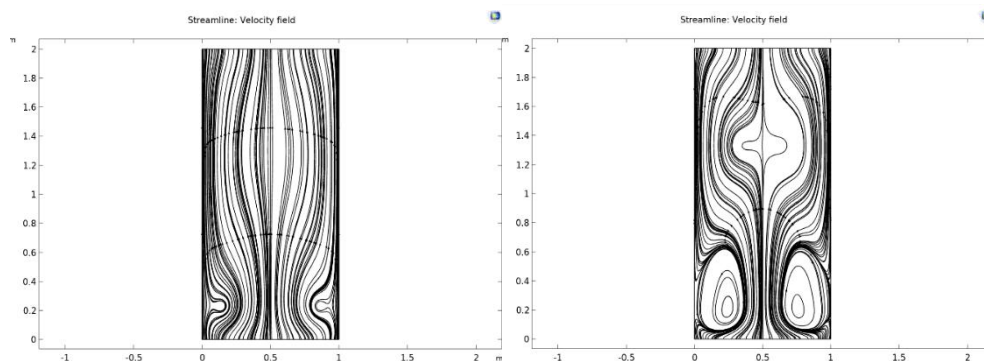


Figure 2. Electroconvective vortices $i_{av} = 1.5$, $Pe = 7.5$, at various values: a) $-\varepsilon = 0.005$,
b) $-\varepsilon = 0.015$

Properties 1)-3) correspond to similar properties of electroconvection studied in [1] using the basic model of electroconvection, which is a boundary value problem for the coupled system of Nernst-Planck-Poisson and Navier-Stokes equations. At the same time, the proposed model of electroconvection with a generalized Ohm's law is much simpler than the basic model. In some cases, the boundary value problem allows an analytical solution, which is convenient for a comprehensive study and analysis of electroconvection and its influence on the transport of salt ions.

Acknowledgement. This study was supported by the Russian Science Foundation, research project no. 24-19-00648, <https://rscf.ru/project/24-19-00648>.

References

1. Urtenov M.K., Uzdénova A.M., Kovalenko A.V., Nikonenko V.V., Pismenskaya N.D., Vasil'eva V.I., Sistat P., Pourcelly G. Basic mathematical model of overlimiting transfer enhanced by electroconvection flow-through electro dialysis membrane cells // Journal of Membrane Science. 2013. V. 447. P. 190-202.
2. Kwak R., Guan G., Peng W.K., Han J. Microscale electro dialysis: concentration profiling and vortex visualization // Desalination. 2012. V. 308. P. 138-146.

NONSTATIONARY EFFECTS AT SEPARATION OF SOLUTIONS

¹Daria Khanukaeva, ²Petr Aleksandrov, ¹Anatoly Filippov

¹Gubkin University, Moscow, Russia, E-mail: khanuk@yandex.ru

²"Kurs-Simbirsk" JSC, Ulyanovsk, Russia, E-mail: darkpriest@mail.ru

Introduction

Any membrane process starts with the transient period, which is principally non-stationary. Usually, it takes not so much time to achieve the steady state mode of the process, but the very start stage may play a crucial role in the further membrane stability and operation. In the experimental work [1], it was demonstrated that the time of the dialysis stationary mode establishment may reach 14 hours for some matters. A numerical non-stationary model of dialysis in circulation regime was developed in [2] and subsequent works of this group. They verified the model on their experimental data, nevertheless, the general principles and the laws of the dialysis on-set mode are not demonstrated yet.

The goal of the present study is to investigate the nonstationary mode of some membrane separation processes, to reveal its specifics and to formalize it. Also, we are aimed to the representation of the conclusions in as simple form as possible to make them useful for engineers and experimentalists.

Statement of the problem

We consider three classical problems: A) a diffusion in a closed membrane cell; B) a diffusion in a flow cell with the tangential flow of the feeding solution and the permeate; C) a convective diffusion in a flow cell as in case B. The variation of the dissolved matter (DM) concentration $c(x,t)$ is described by Fick's law with the additional convective terms in case C, the diffusion coefficients being different for the solution regions (D_0) and the membrane (D_M). The thickness of the membrane is h , the width of the cell cameras are l . The uniform initial concentration of the DM c^0 is set in the region of feeding solution ($-l < x < 0$), while the membrane ($0 < x < h$) and permeate camera ($h < x < h+l$) are assumed to be free of DM. The boundary conditions at the left and right walls of the closed membrane cell (problem A) represent zero fluxes. The boundary conditions for the flow cells (problems B and C) can be taken as given values of the DM and set at the boundaries of diffusion layers. We also denote their positions as $-l$ and $h+l$ for the sake of notation uniqueness. In the framework of homogeneous thin-porous membrane model offered in [3] the concentration of the DM undergoes a jump on both membrane surfaces, while the fluxes remain continuous. The described initial-boundary value problem can be formalized as follows:

Problem A	Problem B	Problem C
$\frac{\partial c_1}{\partial t} = D_0 \frac{\partial^2 c_1}{\partial x^2}, \quad -l < x < 0,$ $\frac{\partial c_2}{\partial t} = D_M \frac{\partial^2 c_2}{\partial x^2}, \quad 0 < x < h,$ $\frac{\partial c_3}{\partial t} = D_0 \frac{\partial^2 c_3}{\partial x^2}, \quad h < x < h+l,$		$\frac{\partial c_1}{\partial t} = -v \frac{\partial c_1}{\partial x} + D_0 \frac{\partial^2 c_1}{\partial x^2}, \quad -l < x < 0,$ $\frac{\partial c_2}{\partial t} = -av \frac{\partial c_2}{\partial x} + D_M \frac{\partial^2 c_2}{\partial x^2}, \quad 0 < x < h,$ $\frac{\partial c_3}{\partial t} = -v \frac{\partial c_3}{\partial x} + D_0 \frac{\partial^2 c_3}{\partial x^2}, \quad h < x < h+l,$
$c_1(x,0) = c^0, \quad c_2(x,0) = 0, \quad c_3(x,0) = 0,$		
$\frac{\partial c_1(-l,t)}{\partial x} = 0, \quad \frac{\partial c_3(h+l,t)}{\partial x} = 0,$	$c_1(-\delta,t) = c^0,$ $c_3(h+\delta,t) = 0,$	$c_1(-\delta,t) = c^0,$ $c_3(h+\delta,t) = c^0(1-\phi),$
$-D_0 \frac{\partial c_1(0,t)}{\partial x} = -D_M \frac{\partial c_2(0,t)}{\partial x},$ $c_1(0,t) = \gamma c_2(0,t),$		$-D_0 \frac{\partial c_3(h,t)}{\partial x} = -D_M \frac{\partial c_2(h,t)}{\partial x},$ $c_3(h,t) = \gamma c_2(h,t).$

Here we introduced the distribution coefficient γ related to the value of the potential barrier which is overcome by particles at the membrane surfaces. Besides, the values v, av in the setting of

Problem C denote the velocity of the convection in the diffusion layers and in the membrane, correspondingly, coefficient ϕ is the retention coefficient.

Solution and discussion

Three formulated initial-boundary-value problems were solved using the Laplace Transform. The solution in the transform domain was found analytically in [3]. We use the algorithm of fast and precise Inverse Laplace Transform developed in [4]. It relies on the properties of Fast Fourier Transform and includes an additional procedure for improving calculation accuracy. In addition, we modified the algorithm to supply it with extra stability.

It is worth mentioning that Problem A has a model character. The corresponding stationary solution is the equilibrium distribution of the DM with constant values of concentrations. Having the solution of the nonstationary problem we can follow how the concentration profile approaches its limiting position and evaluate the time required for the profile to achieve it. In Fig.1, one of such series of profiles are demonstrated. One can see, that for the chosen set of parameters the profile modifies noticeably and quickly achieves its stationary position, denoted by red.

We define the process as achieved its steady state if the difference between the calculated DM concentration and its stationary value at the right boundary of the calculation domain is less than 1 percent. There are three non-dimensional parameters that influence the time T for the steady state establishment: the ratio of the diffusion coefficients, D_0/D_M , the distribution coefficient, γ , the relative width of the membrane cell chambers, l/h . In Fig.2, the dependence of time T on l/h is presented. It is obviously non-linear, and we managed to find its character along with the dependencies of T on D_0/D_M and γ in the following non-dimensional form:

$$T(D_0/D_M, \gamma, l/h) = 0.075(D_0/D_M + 0.6)(\gamma + 0.3)(L^2 + 26.4L). \quad (A)$$

To proceed to the dimensional values, one needs to multiply the obtained non-dimensional magnitude by h^2/D_0 . For example, for $h \sim 100$ mcm, $D_0 \sim 10^{-9}$ m²/s, $T(10,10,10) \sim 500$ min.

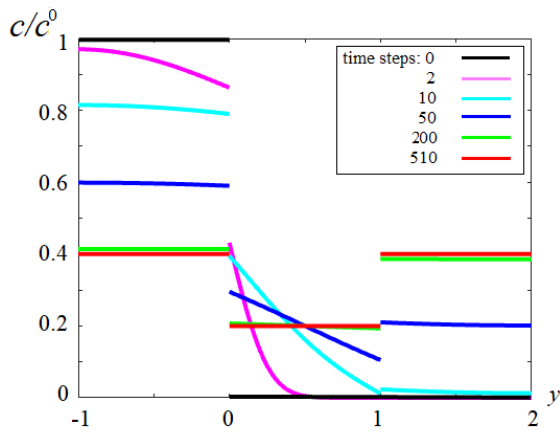


Figure 1. Concentration profiles (problem A) for $D_0/D_M=10$, $\gamma=2$, $l/h=1$.

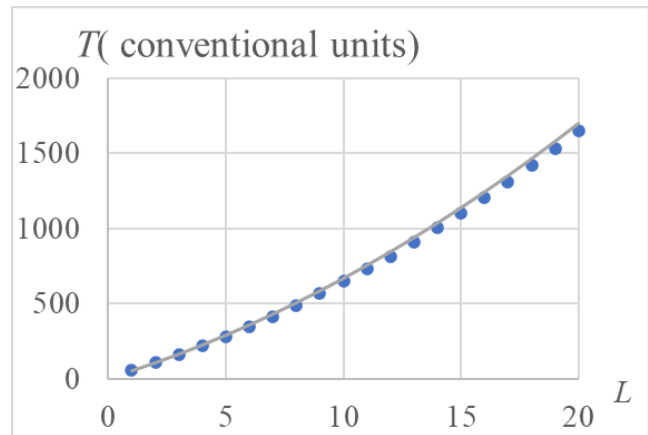


Figure 2. Dependences $T(l/h)$ (problem A); points – numerical, line – approximating.

We fulfilled analogous analysis of the solutions for problem B and C. The obtained dependence for problem B looks as follows

$$T(D_0/D_M, \gamma, l/h) = 0.007(D_0/D_M + 14.5)(1/\gamma + 1.9)(L^2 + 17.5L). \quad (B)$$

In dimensional values defined above, $T(10,10,10) \sim 20$ min according to formula (B).

An unexpected difference of formula (B) from formula (A) is in the dependence on parameter γ . The higher the jump the longer the stationary state is established in the closed membrane cell (problem A). Therefore, the dependence of $T(\gamma)$ is direct in formula (A). In formula (B) this dependence is inverted. The reason may lay in the specifics of flow membrane cell operation. The steady state in this case is the concentration drop from one to another given and invariable values of DM concentration at the boundaries of diffusion layers. The higher the jump, the sooner the drop is established.

The approximation of time T for the steady state establishment in the flow cell with convection (problem C) looks like

$$T(\gamma, L, \alpha, Pe) = 0.055(\gamma + 4)(L^{1/2})(1/\alpha + \sqrt{2})(Pe + 1)^{1.2}. \quad (C)$$

It should be noted that Peclet number $Pe = vh/D_0$ is introduced in expression (C), while parameters D_0/D_M and ϕ are absent there. The dependence of T on D_0/D_M and ϕ in case (C) turned out to be so weak that we excluded it. The estimate of T in dimensional units defined above $T(10,10,1,2) \sim 3$ min.

In Fig.3, the evolution of concentration profiles in the diffusion layers and the membrane is represented. The stationary distribution is shown in red. Fig.4 demonstrates the dependence of time T on the Peclet number, which turned out to be one of the most influencing parameters.

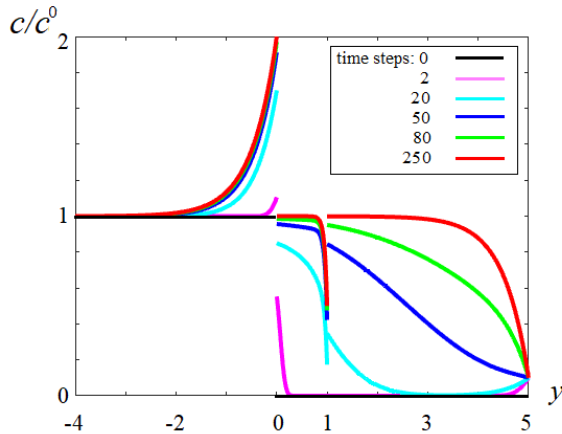


Figure 3. Concentration profiles (problem C) for $D_0/D_M=10$, $\gamma=2$, $l/h=4$, $Pe=2$, $\phi=0.9$.

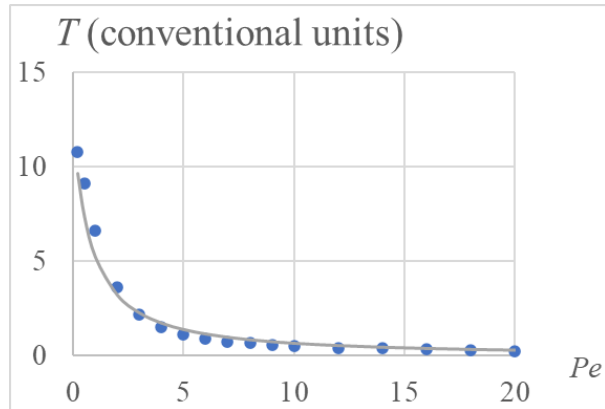


Figure 4. Dependences $T(Pe)$ (problem C); points – numerical, line – approximating.

The solutions of non-stationary problems found in all three cases allowed to make estimates of time T required for the process establishment. The influence of each parameter on time T was analyzed and analytically formalized in the form of explicit expressions. It was demonstrated that the diffusion coefficient ratio and the distribution coefficient to a lesser degree influence the speed of the process establishment than the relative width of the diffusion layer or the flow regime (Peclet number) for the case of convective diffusion. Besides, it was shown that the time of the process establishment is much less than the time of the very process in each of the considered problem.

Acknowledgement. The work is supported by RSF (grant No. 23-19-00520, <https://rscf.ru/project/23-19-00520/>).

References

1. Vasil'eva V.I., Vorob'eva E.A. Dynamics of the Separation of Amino Acid and Mineral Salt in the Stationary Dialysis of Solutions with an MK-40 Profiled Sulfo Group Cation Exchange Membrane // Russian J. Phys. Chem. A. 2012. V. 86. No. 11. P. 1726–1731.
2. Kozmai A., Chérif M., Dammak L., Bdiri M., Larchet C., Nikonenko V. Modelling non-stationary ion transfer in neutralization dialysis // J. Membr. Sci. 2017. V. 540. P. 60-70.
3. Martynov G.A., Starov V.M., Churaev N.V. Theory of membrane separation of Solutions. 1. Formulation of the Problem and a Solution to Transfer Equations // Kolloidn. Zhurn. 1980. V. 42. No. 3. P. 489–499.
4. Brancik L. Programs for fast numerical inversion of Laplace transforms in MATLAB language environment // Proceedings of the 7th Conference MATLAB. Czech Republic, Prague, 1999. V. 99. P. 27–39.

ELECTRO / BAROMEMBRANE SEPARATION OF IONIC DYES USING ELECTRICALLY CONDUCTIVE CERAMIC MEMBRANES

^{1,2}Ivan Kharchenko, ^{1,3}Natalia Fadeeva, ¹Irina Volkova, ^{1,4}Evgeny Elzufiev, ³Elena Fomenko, ³Galina Akimochkina, ^{1,4}Ilya Ryzhkov

¹ Institute of Computational Modeling, Federal Research Center KSC SB RAS, Krasnoyarsk, Russia

² Kirensky Institute of Physics, Federal Research Center KSC SB RAS, Krasnoyarsk, Russia

³ Institute of Chemistry and Chemical Technology, Federal Research Center KSC SB RAS, Krasnoyarsk, Russia

⁴ Siberian Federal University, Krasnoyarsk, Russia

E-mail: harchenko@icm.krasn.ru

Introduction

Membrane technologies for separating liquid and gas mixtures are widely used in chemical, fuel and energy, medical and food industries. The current trends in the development of filtration membranes are improving rejection and selectivity, enhancing permeability, reducing fouling as well as increasing chemical stability and service life. One of the promising solutions is the development of membranes with an electrically conductive surface [1]. Such membranes open up the possibility of controlled transport of charged components under the influence of electric field.

Currently, the attention of many researchers is focused on synthesis, characterization, and applications of ceramic membranes. Such membranes have a number of advantages in comparison with polymeric ones: greater mechanical strength, chemical and thermal stability, and the ability to regenerate. Therefore, the development of new types of ceramic ultra- and nano-filtration membranes with controlled selectivity is of undoubted relevance and will contribute to improving the effectiveness of separation and purification techniques in various industries.

This work deals with the preparation of ceramic membranes with electrically conductive selective layer and application of these membranes for separation of ionic dyes from aqueous solutions.

Experimental

A narrow fraction of dispersed microspheres ($\sim 10 \mu\text{m}$) obtained by the method of aerodynamic separation from fly ash was used as a raw material for obtaining ceramic substrates. Substrates with a diameter of 25 mm and a height of 3 mm were prepared by cold pressing at a pressure of 40 MPa followed by annealing in a muffle furnace at 1100 °C. Then, a selective layer about 30 μm in thickness was formed on the substrates by vacuum filtration using alumina nanofibers with the diameter of 10–15 nm. The electrical conductivity of the selective layer was achieved by depositing carbon layers on the nanofibers by chemical vapor deposition in a flow tube reactor at a temperature of 900 C using ethanol as a precursor.

Filtration experiments were carried out in a laboratory setup, consisting of a 400 ml filtration cell (Fig. 1), a compressor, a pressure regulator, a scale and a magnetic stirrer. The test solution was poured into a cell located on a magnetic stirrer. Compressed air was supplied to the upper part of the cell through a pressure regulator, which sets the required pressure in the cell. In the filtration cell, the membrane served as the working electrode, and the titanium porous plate served as the counter electrode. The effective membrane area was 3.8 cm². The electric field between the two electrodes was created using a P-20X potentiostat in potentiostatic mode. The time dependence of the permeate flow was recorded using a balance connected to a computer. Special software was developed to automatically record data at a given time interval and process it.

The rejection properties of membranes with a selective layer of carbon-coated nanofibers were studied by filtration of aqueous solutions of Victoria Blue B (506 Da) dye (20 mg/l) at the pressure of 5 bars applying the potential of +800 mV and –800 mV to the membrane surface. During the experiment, up to 5 permeate samples with a volume of 10 to 20 ml were collected.

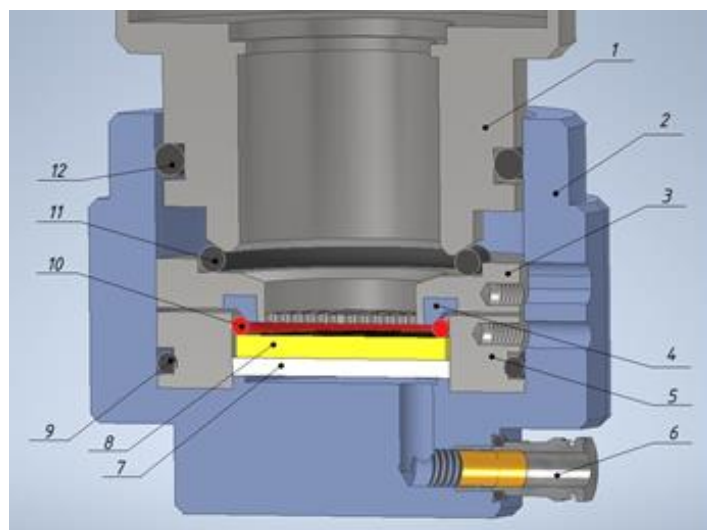


Figure 1. CAD model of the bottom part of a dead-end filtration cell: 1 – cell body; 2 – bottom of the cell; 3 – counter electrode; 4 – insulator; 5 – electrode; 6 – output push-in fitting; 7 – 2mm fluoroplastic insert; 8 – ceramic membrane 25x2.5mm; 9, 10, 12 – sealing ring; 10 – conductive ring.

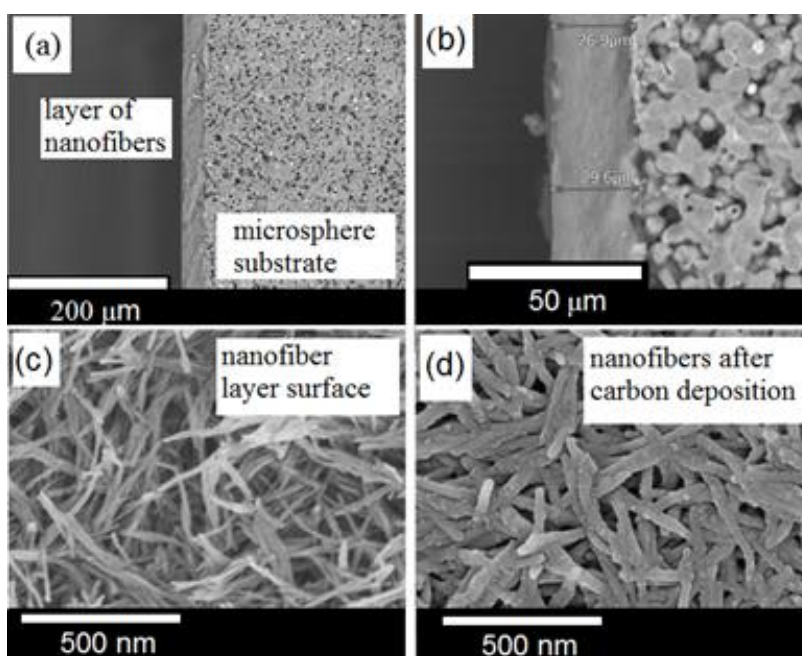


Figure 2. SEM images of a two-layer membrane (a substrate prepared from fly ash fraction and a selective layer of alumina nanofibers) (a, b); The surface of selective layer before (c) and after (d) deposition of a carbon.

The concentration of dyes in the initial solution and permeate samples was determined photometrically using a Genesys 10S-Vis spectrophotometer (Thermo Scientific, USA).

Results and Discussion

The SEM images of microsphere substrate with the selective layer are presented in Fig. 2 (a) and (b). The morphology of microspheres in the substrate after heat treatment is preserved and ensures the porosity of membrane. The formation of contacts between particles is also observed. The SEM images of selective layer surface before and after deposition of carbon are shown in Fig. 2 (c) and (d), respectively. From these images, it is clear that the selective layer consists of disordered alumina nanofibers with an electrically conductive carbon coating. The average pore size of the selective layer is about 33 nm and 26 nm before and after deposition of carbon, respectively.

The filtration experiments were performed with an aqueous solution of cationic dye Victoria Blue B (506 Da) at the transmembrane pressure of 5 bars. The rejection for five consecutive permeate samples is presented in Table 1 for different applied potentials. When the potential +800 mV was applied to the membrane, the permeate flow varied from 75 l/m² h to 30 l/m² h during 8 hours. The rejection initially was 100%, but decreased to 96.95 % and 83.58 % for permeate samples 4 and 5. When the potential of –800 mV was applied, the permeate flow varied from 75 l/m² h to 20 l/m² h during 8 hours, and the rejection was stable at 99.90–99.95%.

The analysis showed that during the filtration of Victoria Blue B, dye molecules adsorbed on the membrane and reduced its permeability. At positive potential, the adsorption of cationic dye was diminished, so the rejection decreased with time. The negative potential favoured the adsorption resulting in stable and high rejection.

Table 1. The results of filtration experiments depending on the applied potential to the membrane surface.

Applied potential	Rejection, %	
	+800 mV	–800 mV
Permeate 1	100	99.95
Permeate 2	100	99.90
Permeate 3	100	99.95
Permeate 4	96.95	99.95
Permeate 5	83.58	99.95

Conclusion

The application of voltage to conductive membrane surface can improve the rejection of ionic dyes depending on the sign of the applied voltage. Our results indicate that electro/baromembrane separation is promising for selective separation / purification of molecular mixtures.

Acknowledgement. The work is supported by the Russian Science Foundation, project 23-19-00269. Physico-chemical analysis of the materials was carried out at the Krasnoyarsk regional center for collective use of the Federal Research Center KSC SB RAS.

References

1. *I. Ryzhkov, M. A. Shchurkina, E. V. Mikhlina, M. M. Simunin, I. V. Nemtsev.* Switchable ionic selectivity of membranes with electrically conductive surface: Theory and experiment. *Electrochimica Acta*, 2021, Vol. 375, 137970.
2. *E. V. Fomenko, G. V. Akimochkina, A. G. Anshits, N. P. Fadeeva, I. A. Kharchenko, E. V. Elsufov, K. A. Shabanova, A. A. Maksimova, and I. I. Ryzhkov.* Ceramic substrates for filtration membranes based on dispersed fly ash microspheres. *Membranes and Membrane Technologies*, 2024, Vol. 6, No. 2, pp. 71–83.

REMOVAL OF MICRO- AND NANOPLASTICS FROM WASTEWATER USING THE ANODIC OXIDATION PROCESS

Andrey Kislyi, Vera Guliaeva, Ilya Moroz, Yuri Prokhorov, Victoria Plis

Kuban State University, Krasnodar, Russia, *E-mail: andrey.kislyi@mail.ru*

Introduction

In the early 2000s, for the first time, a new threat was recognized not only for the health of the human population but also for the fauna of the planet - nano- and microparticles of plastic. Its concentration is rapidly increasing in natural waters (lakes, seas, oceans). Entering living organisms, micro- and nanoplastics injure organ tissues and transfer toxic components formed during their decomposition or adsorbed from wastewater [1].

Some micro- and nanoplastic particles can be separated by baromembrane methods such as ultrafiltration or reverse osmoses. However, the problem is not completely solved since particles of plastic are not dissimilated but accumulate and await final processing, or are again released into the environment with waste [2].

Thus, the conventional separation of plastics from wastewaters is not enough, a complete processing is required. Anodic oxidation is a promising method of removing biologically non-biodegradable organic substances, in which they are mineralized by the hydroxyl radicals and other reactive oxygen species to carbon dioxide, water, and other simple compounds [3].

Experiments

We prepared microplastics in the laboratory by dissolving 4.73 g of polyvinyl acetate in 1 L H₂O. This plastic dissolves well in water and is toxic. The average particle size was 21.44 μm. A SOPTOP CX40M microscope was used to characterize the particle sizes of microplastics. The solution of polyvinyl alcohol was prepared by dissolving a suspension under prolonged heating. The resulting solution is colorless, indicating the very small size of the dissolved particles.

At first step the working solution containing microplastics and 0.1 M Na₂SO₄ as background electrolyte was pumped into the system and circulated for 30 min without applied electrical current (for polyvinyl acetate), then a sample was taken. It allows to estimate the sorption of microparticles on the electrode surface. After that 0.5 A current was applied for 3 h and another sample was taken in the end of experiment. The total volume of solution in the experimental setup was 250 mL.

During the experiment, the concentration of polyvinyl alcohol was determined from the value of chemical oxygen demand (COD) by the dichromate COD test (ISO 15705:2002 Water quality - Determination of the chemical oxygen demand index (ST-COD) - Small-scale sealed-tube method).

The concentration of polyvinyl acetate was determined by the turbidity of the solution. For this purpose, the turbidity of polyvinyl acetate suspension at different concentrations was measured and a linear dependence of optical density on concentration was obtained.

Results and Discussion

Initial experiments on oxidation of prepared solutions of microplastics were carried out. It was found that the optical density of the PVA suspension drops immediately after we start pumping the microplastics suspension through the cell. The optical density of the initial polyvinyl acetate solution was 0.038. After pumping for 30 minutes, it decreased to 0.028. Probably, the plastic particles are well adsorbed on the developed surface of the anode, and large particles get stuck in the pores. After 3 hours of experiment with 0.5 A current, the optical density remained almost unchanged (0.030). During the experiment, active foaming was observed, which is due to the gas bubbles entering the water, which entrapped the plastic particles. For polyvinyl alcohol, the step with solution pumping without current was not performed because it is soluble. Samples were taken before and after the current was switched on. The COD of the solution decreased from 469 to 320 mgO/L in 3 hours of the experiment.

Based on the above, we can conclude that electrocoagulation or electroflotation are more promising for the purification of microplastics from wastewater and AO will be more effective at the last stages of purification.

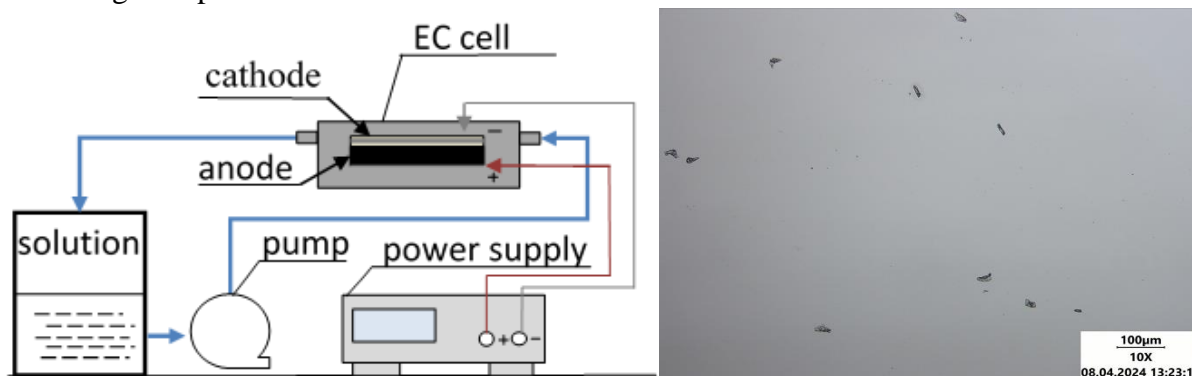


Figure 1. Schematic Representation of the Experimental Setup (a) and Optical Image of a Suspension of Microplastic PVA (b).

Acknowledgments. The study is realized with the financial support of the Russian Science Foundation, project № 22-79-10177.

References

1. Ghosh S., Sinha J. K., Ghosh S., Vashisth K., Han S., Bhaskar R. Microplastics as an Emerging Threat to the Global Environment and Human Health // *Sustain.* 2023. V.15. No. 10821.
2. Parashar S., Hait S. Recent advances on microplastics pollution and removal from wastewater systems: A critical review // *J. Environ. Manage.* 2023. V. 340. No. 118014.
3. Kiendrebeogo M., Karimi Estahbanati M. R., Khosravanipour Mostafazadeh A., Drogui P., Tyagi R. D. Treatment of microplastics in water by anodic oxidation: A case study for polystyrene // *Environ. Pollut.* 2021. V.269. No. 116168.

MATHEMATICAL MODELING OF THE TRANSPORT CHARACTERISTICS OF ION EXCHANGE MEMBRANES WITH LOW WATER CONTENT

Andrey Kislyi, Anton Kozmai, Semyon Mareev, Victor Nikonenko
Kuban State University, Krasnodar, Russia, E-mail: andrey.kislyi@mail.ru

Introduction

Ion exchange membranes (IEMs) are essential for efficient and safe production and storage of energy. Modern ion exchange membranes are subject to stringent requirements for commercial use. In particular, the IEMs must have high conductivity and ion transport numbers as well as low diffusion permeability. At the same time, membrane production should not be too expensive and harmful to the environment [1].

Among all possible analogs of Nafion®, partially fluorinated membranes based on the polyvinylidene fluoride (PVDF) copolymers attract special attention. Such membranes are relatively inexpensive, easy to manufacture, and are characterized by the flexibility in their properties. In addition, such membranes can be applicable not only to fuel cells. They can also be used in electrodialysis, electro deionization, membrane electrolysis, etc. [2].

To determine optimal synthesis conditions and obtain IEMs with optimal properties, in particular, for use in fuel cells, it is necessary to deeply understand the IEM structure-property relationship.

It was found that, in contrast to most charged membranes, the NaCl diffusion permeability of the membranes decreased with increasing NaCl concentration. This result was explained via a model that incorporates ideas from the microheterogeneous model, Gregor's swelling model, and percolation theory. In essence, this interesting diffusion permeability behavior was attributed to the osmotic deswelling of the membranes, which affected co-ion diffusion coefficients to a greater extent than counter-ion diffusion coefficients (the conductivity behavior is as expected).

A good quantitative agreement is achieved. The described model could be useful in understanding ion transport in IEMs with a low water content.

Model formulation

The model is based on the microheterogeneous model (MHM). Within this model, an ion exchange membrane is considered as a two-phase system consisting of a microporous gel phase and inclusions of equilibrium solution filling intergel spaces (Fig. 1). MHM allows to calculate ion transport numbers, conductivity and diffusion permeability of the membrane.

It is known that when the water content of membrane decreases, its electrical conductivity decreases. This phenomenon is explained from the point of view of the percolation theory. We use the percolation theory to relate the membrane water content to the values of ion diffusion coefficients in the gel phase. In turn, the water content at a given concentration of bathing solution can be calculated using the Gregor model.

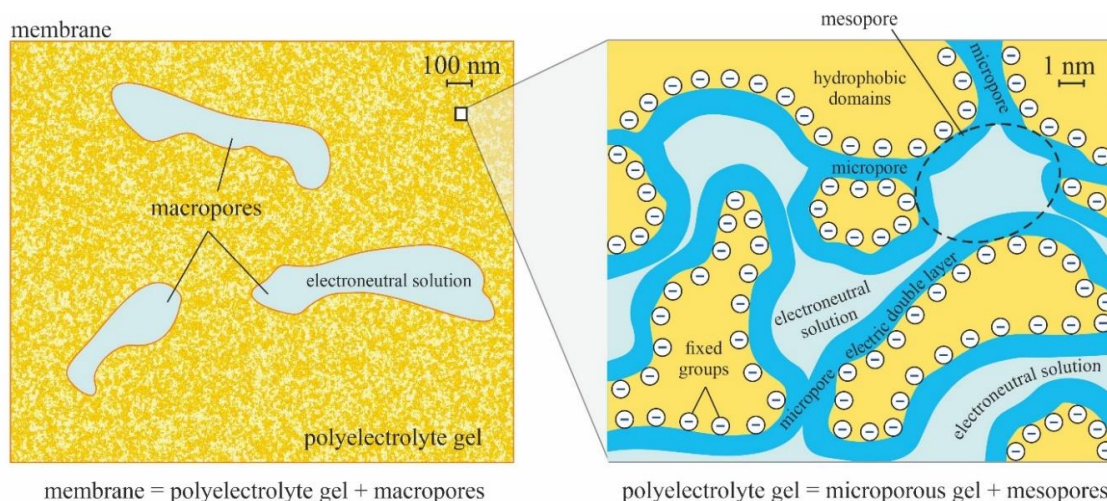


Figure 1. Schematic View of a Two-Phase Microheterogeneous Membrane.

Experiments

The studied membranes were synthesized on the basis of PVDF in two stages. First, unsaturated PVDF is obtained by its dehydrofluorination. Then simple radical polymerization is carried out. In this case 3-sulfopropyl methacrylate potassium salt acts as a copolymer. The obtained polymer is dissolved in DMAc solvent, poured off and the solvent is evaporated. A more detailed description is given in Ref. [3].

Some characteristics of the membranes under study are present in Table 1. It is important that the membranes under study have relatively large open pores extending from the membrane surface to a certain depth. Their formation probably occurred during the membrane manufacturing at the stage of casting [3] due to gas evolution upon evaporation of solvent. The presence of such macropores, non-selective for the counterion transport, determines some peculiarities in the behavior of the membranes, similar to the behavior of track-etched membranes. The pore density and range of pore diameters are given in Table 1.

Table 1: Some Characteristics of the PEM-RCF and PEM-RCF-2 Membranes

Membrane	Q^* , mmol g ⁻¹ wet	Water content, w , g _{H2O} g ⁻¹ _{wet} , %	Diameter of open extended pores, nm	Pore density, pores cm ⁻²	Surface pore fraction	Membrane thickness, d , μm
PEM-RCF	0.12 ± 0.02	26 ± 2	133 ± 10 (162 ± 14)	1.26 × 10 ⁹ (9.13 × 10 ⁸)	0.18 (0.19)	29 ± 2
PEM-RCF-2	0.08 ± 0.01	7 ± 2	121 ± 10 (98 ± 18)	5.73 × 10 ⁸ (9.94 × 10 ⁷)	0.07 (0.01)	86 ± 2

Results and Discussion

Figure 2 shows a good agreement between simulated curves and experimental data on the concentration dependencies of electric conductivity, diffusion permeability and Na⁺ transport numbers of PEM-RCF and PEM-RCF-2 membranes.

As can be seen from Fig. 2a, the concentration dependence of the conductivity of both membranes, κ^* , under study is close to linear. This is due to the presence of macropores and a relatively high f_2 value along with low conductivity of the microporous gel phase. The increase in electrical conductivity with an increase in the c value is due to an increase in the conductivity of the electroneutral solution in the intergel spaces of the membranes. This contribution is approximately proportional to c , while the contribution of the microporous gel phase to the membrane conductivity only slightly increases with increasing c .

The presence of macropores and a relatively high f_2 value for the PEM-RCF membrane determine, apparently, a relatively high diffusion permeability (Fig. 2b) and a low counterion transport number (Fig. 2c). The water content of this membrane is quite high. As a result, the P^* value decreases only slightly with increasing c (Fig. 2b). On the contrary, the closeness of the water content and its critical values in the case of PEM-RCF-2 membrane causes a sharp decrease in parameters D_-^s and α as c increases. A decrease in coion mobility and an increase in the proportion of series connections of the gel phase and intergel spaces leads to a sharp decrease of P^* with increasing c (Fig. 2b).

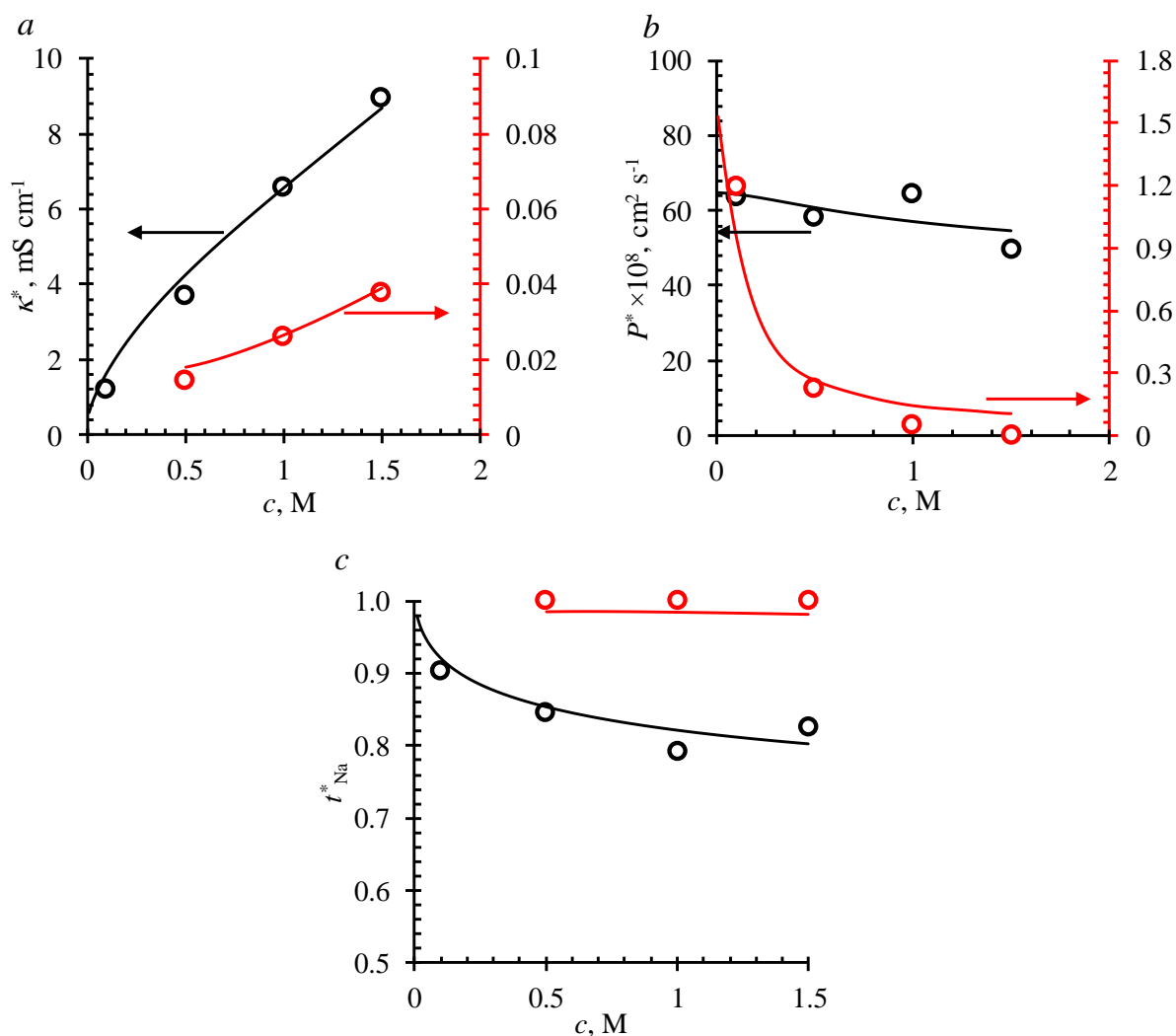


Figure 2. Simulated (Solid Curves) and Experimental (Markers) Concentration Dependencies of Electric Conductivity (a), Local Diffusion Permeability (b) and Na⁺ Transport Numbers for PEM-RCF (Black) and PEM-RCF-2 (Red) Membranes.

Acknowledgments. The research is carried out with the financial support of the Kuban Science Foundation, LLC “New Service Company”, in the framework of the science project Num. MFI-P-20.1/48.

References

1. Pan M., Pan C., Li C., Zhao J. A review of membranes in proton exchange membrane fuel cells: Transport phenomena, performance and durability // *Renew. Sustain. Energy Rev.* 2021. V.141. No. 110771.
2. Liu F., Hashim N. A., Liu Y., Abed M. R. M., Li K. Progress in the production and modification of PVDF membranes // *J. Memb. Sci.* 2011. V. 375. P. 1-27.
3. Ponomar M., Ruleva V., Sarapulova V., Pismenskaya N, Nikonenko V. Structural characterization and physicochemical properties of functionally porous proton-exchange membrane based on PVDF-SPA graft copolymers // *Int. J. Mol. Sci.* 2024. V. 25. I. 1. No. 598.

THE INFLUENCE OF THE CHEMICAL NATURE OF ION-EXCHANGE MEMBRANES ON THEIR FOULING DURING ELECTRODIALYSIS TARTRATE STABILIZATION OF WINE

Anastasiia Klevtsova, Evgeniia Pasechnaya, Maria Ponomar, Anastasiia Korshunova, Daria Chuprynina, Natalia Pismenskaya

Kuban State University, Krasnodar, Russia, E-mail: *nastyak1314@yandex.com*

Introduction

Electrodialysis (ED) is widely used method for wine stabilization in the world. In Russia also this trend is gaining popularity. It is still open topic how the chemical nature and structure of the ion exchange membrane affects fouling by wine components. We studied 4 pairs consisting of heterogeneous (MA-41//MK-40 and AMH-PES//CMH-PES) and homogeneous (CJMA-3//CJMC-3 and AMX-Sb//CMX-Sb) membranes, which were used in electrodialysis tartrate stabilization of wine.

Experiments

A model solution of wine material was made from dry red wine, to which tartaric acid and potassium chloride were added. Tartrate stabilization experiments were performed using a laboratory six-compartment electrodialysis cell, until the electrical conductivity in the desalted stream decreased by 20%. Before and after the studied membranes were subjected to a comprehensive analysis. The current-voltage curves in 0.02 NaCl solution and the values of electrical conductivity in 0.5 NaCl solution were obtained. In addition, the analysis of membrane surfaces and cross-sections were carried out using contact angle measurements, optic microscopy of the surface, as well as IR-spectroscopy of membranes.

Results and Discussion

The contact angle values (Table 1) demonstrate an increase in the hydrophilicity of the surfaces of all membranes after electrodialysis. This parameter remains unchanged only in the case of a CMX-Sb cation exchange membrane within the limits of measurement error. Apparently, the adsorption of highly hydrated polyphenols by the surfaces of most membranes is the main reason for the decrease in contact angles.

Table 1: Contact Angles of the Surface of the Studied Membranes

Membrane	Pristine	After ED	Membrane	Pristine	After ED
AEM			CEM		
AMX-Sb	68±7	50±3	CMX-Sb	41±3	46±3
CJMA-3	53±5	19±3	CJMC-3	52±4	36±3
AMH-PES	60±5	57±3	CMH-PES	65±4	40±4
MA-41	69±3	57±4	MK-40	70±1	51±2

Note, the foulants and the materials from which the membranes are made have a very similar chemical nature. Therefore, comparison of the IR spectra of the pristine and used membranes does not provide additional information about fouling (Fig. 1).

Figure 2 shows that after electrodialysis, the electrical conductivity of AMX-Sb and CJMA-3 membranes decreases more than 30%. It is noteworthy that other membranes do not undergo significant changes in this parameter. We hypothesize that homogeneous anion-exchange membranes contain a number of weakly basic fixed groups that form "bound species" with the anions of tartaric and other polybasic carboxylic acids.

Fouling of the surfaces of the cation- and anion-exchange membranes causes acidification of the solution in the desalting compartment and also causes an increase in potential drops in underlimiting (favorable for tartrate stabilization) current modes (Fig. 3).

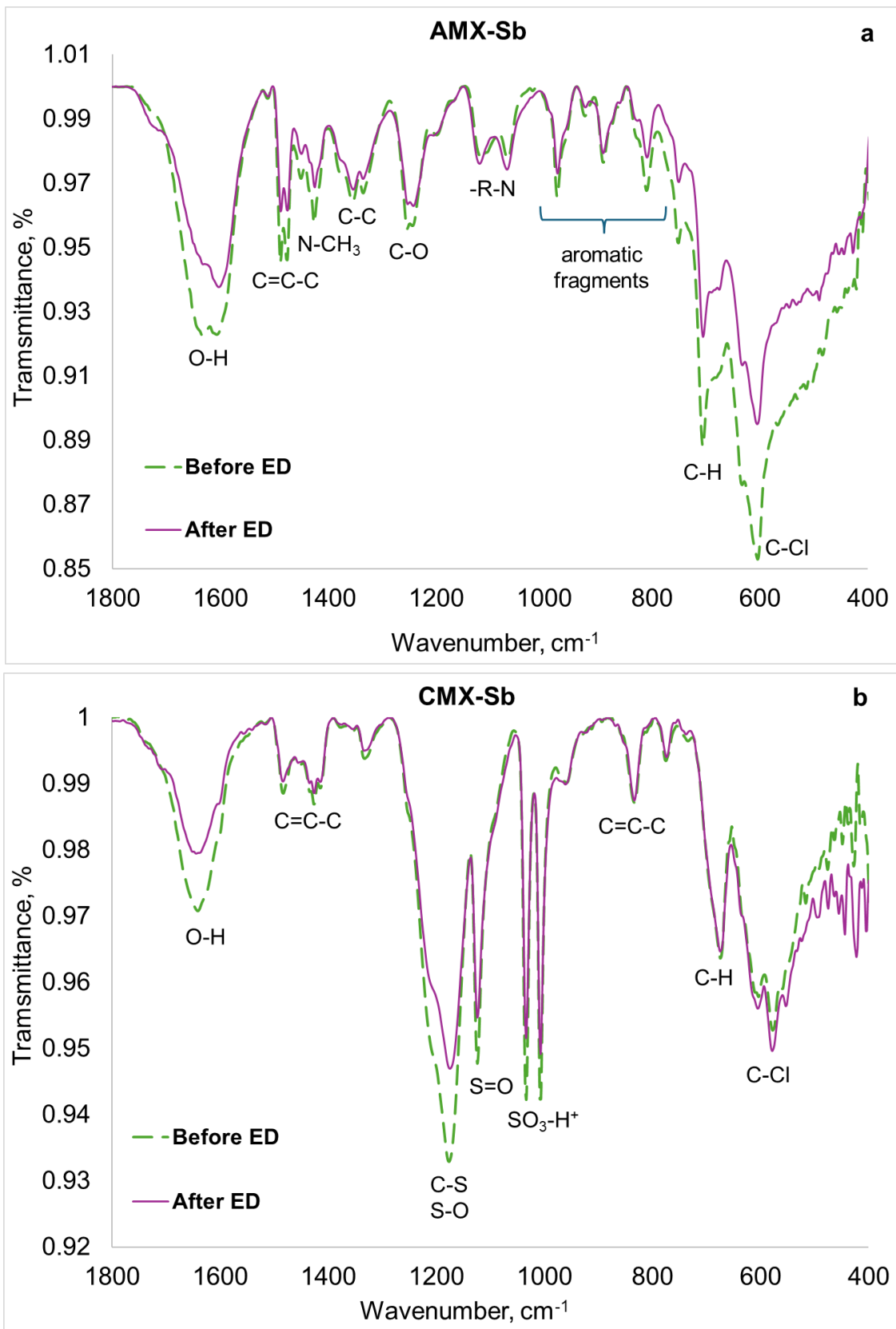


Figure 1. IR-spectra of AMX-Sb (a) and CMX-Sb (b) Membranes Before and After Electrodesialysis.

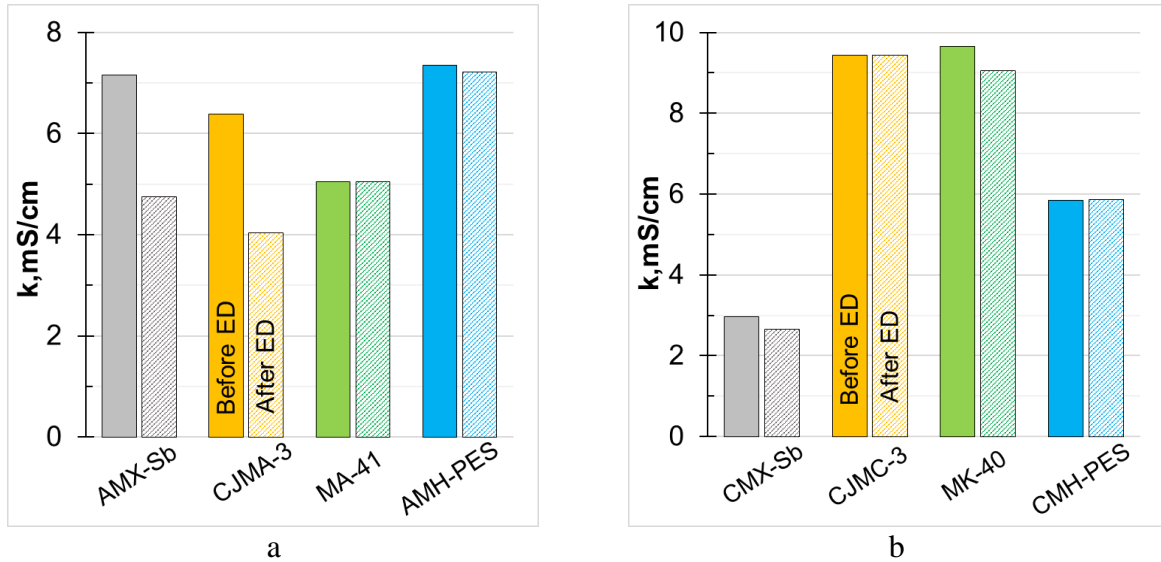


Figure 2. Conductivity of Anion- (a) and Cation-Exchange Membranes (b) in 0.5 M NaCl Solution before and after Electrodialysis.

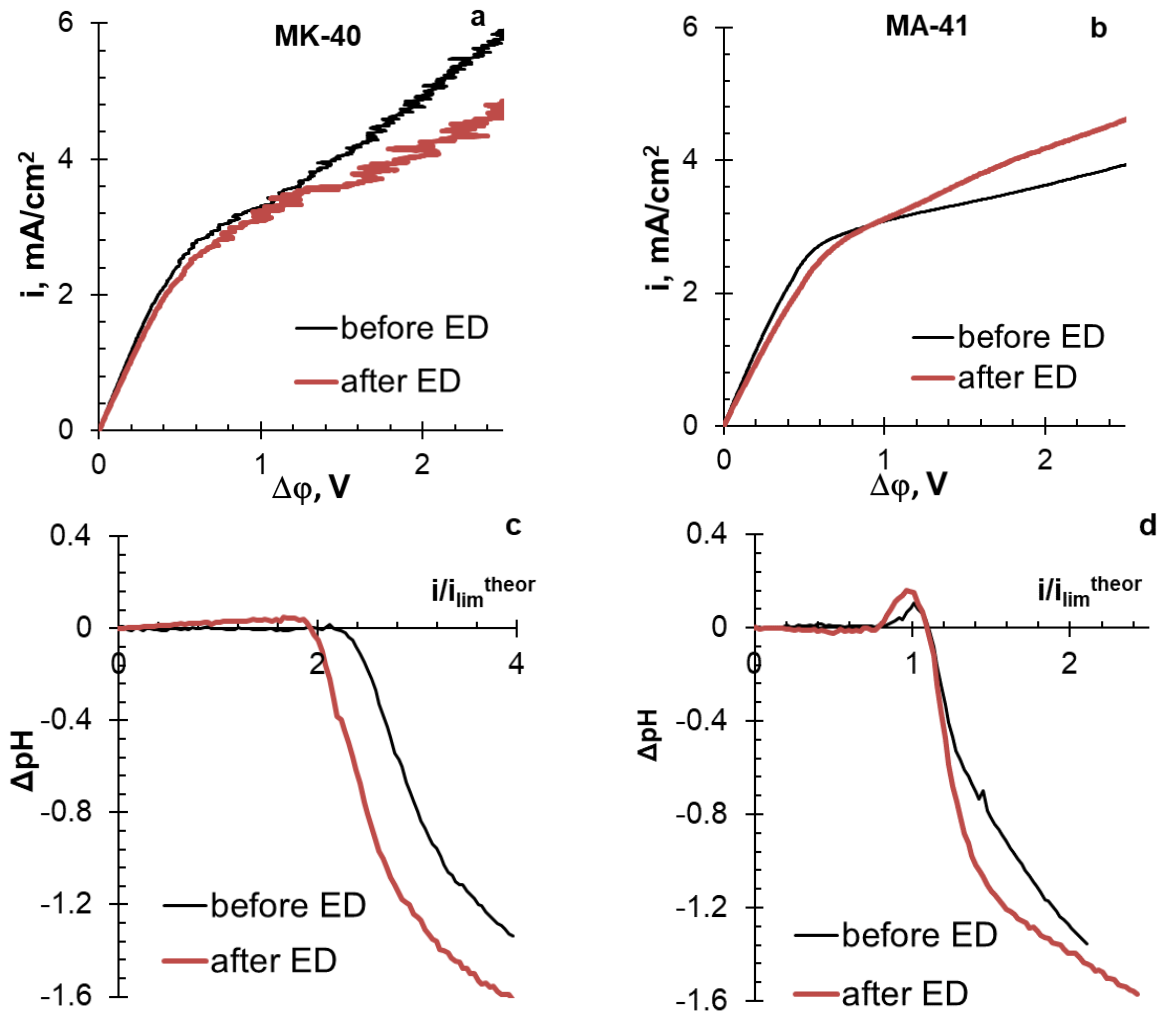


Figure 3. Current-Voltage Curves (a, b) and pH Difference at the Outlet and Inlet of the Desalting Compartment Depending on the Current Density Divided by the Theoretical Limiting Current (c, d). Data Obtained for Membranes MK-40 (a, c) and MA-41 (b, d).

Acknowledgement. The Kuban Science Foundation, project No. MFI-20.1/78, funded this study.

PERMEABILITY OF HYDROGEN THROUGH PALLADIUM AND VANADIUM-BASED ALLOYS

¹Pavel Kolinko, ¹Sergey Saltykov, ¹Vitaly Busko, ^{2,3}Vasily Alimov, ^{2,3}Evgenii Peredistov, ^{2,3}Andrei Busnyuk, ^{2,3}Alexander Livshits

¹PJSC "MMC "Norilsk Nickel", E-mail: kolinkopa@nornik.ru

²The Bonch-Bruевич Saint Petersburg State University of Telecommunications

³Mevodena Ltd.

Introduction

Ultrapure hydrogen is widely used in semiconductor production and microelectronics technologies, as well as in other applications. Hydrogen is increasingly required in the emerging hydrogen energy industry.

The simplest and most efficient way to obtain ultrapure hydrogen is its separation using metal membranes. Usually, membranes made of Pd alloys are used for this purpose, which are able to extract hydrogen from gas mixtures with 100 % selectivity. The problem is the extremely high price of such membranes at their relatively low performance. The lack of productive and affordable membranes hinders the development of many important areas that might be based on advanced membrane technologies.

In work over the past few decades, it has been found that, contrary to the accepted view of palladium's unique ability to permeate hydrogen, hydrogen transport through Group 5 metals (vanadium, niobium, and tantalum) is orders of magnitude faster. If the surface of membranes made of these metals is coated with a thin layer of palladium, it provides catalysis of dissociative-associative processes in the absorption-desorption of H₂ molecules. The Pd layer also provides corrosion protection. As a result, the specific performance of such membranes is more than an order of magnitude higher compared to membranes made of palladium and its alloys, with a lower price of the material.

Experiments

Metal membranes made of vanadium alloys have many times higher hydrogen productivity compared to membranes made of palladium and its alloys [1, 2]. In particular, V-Pd alloys were used to create high-performance tubular membranes capable of extracting ultrapure hydrogen from products of steam conversion of hydrocarbon fuels [3]. Such high membrane performance was achieved mainly due to two experimentally discovered effects: firstly, Pd as an alloying element significantly suppresses the solubility of H in V, thus solving the problem of mechanical stability in the operation of vanadium alloy membranes; secondly, the diffusion coefficient of H in V-Pd substitution alloys is commensurate with the diffusion coefficient of H in pure vanadium.

Figure 1 presents a schematic diagram of the membrane located in the membrane cell. The tubular membrane hermetically separates the inlet and outlet volumes.

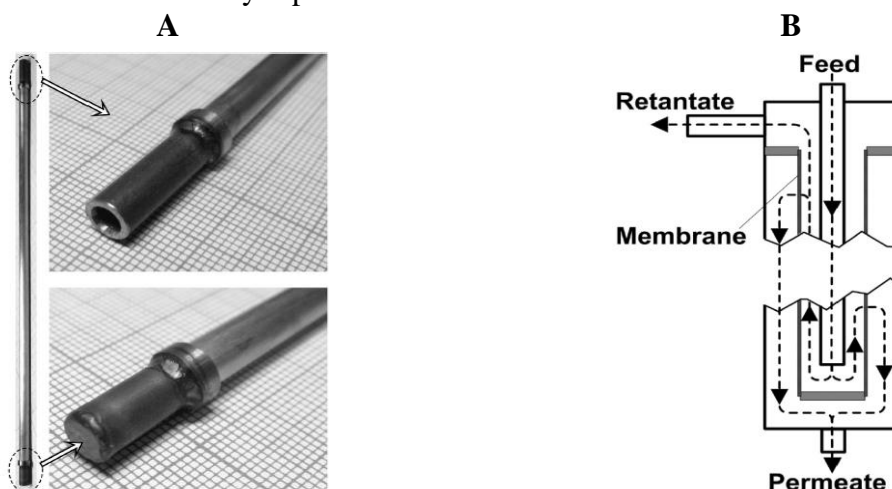


Figure 1. A - Photograph of tubular membrane made of V-Pd alloy; B - Schematic diagram of the membrane in the process cell

Results and Discussion

Tubular membranes made of V- κ Pd alloy were manufactured by Mevodena Ltd. The Pd content in the alloys varied from 5 to 7 at.%.

The hydrogen extraction from various gas mixtures under different conditions was investigated. The temperature, inlet pressure and gas mixture composition were subjected to variations.

Figure 2 and Table 1 present the processed experimental data on the dependence of the permeation flux value of hydrogen on the total pressure of the mixture at the inlet (black curve) and on the dependence of the fraction of hydrogen extracted from the mixture (the ratio of the output H₂ flux to the inlet flux), calculated from the experimental data.

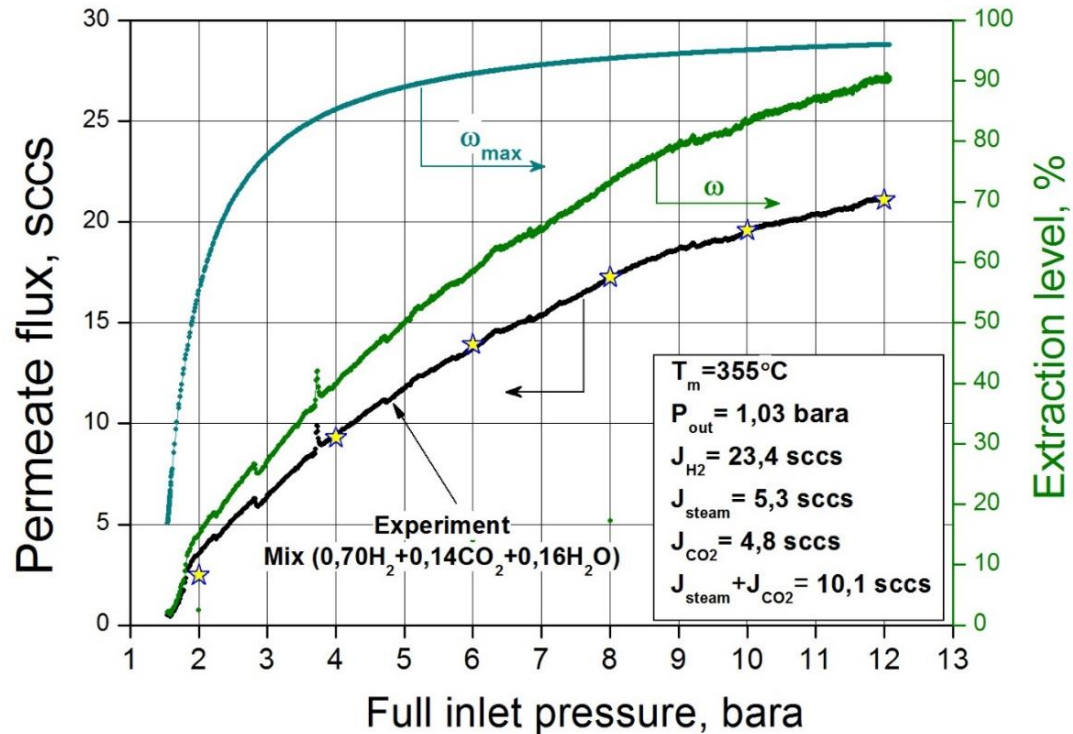


Figure 2. Black curve (left axis of ordinates) - dependence of H₂ permeation flux on the total inlet pressure. Green curve (right ordinate axis) - extraction ratio of hydrogen from the mixture (ratio of H₂ output flux to the input flux). Blue curve (right axis of ordinates) - maximum possible hydrogen extraction degree (calculated curve, the value does not depend on the membrane performance and is equal to the extraction degree at infinite membrane length). Asterisks - calculated value of H₂ permeate flux value, assuming the constant surface properties for absorption/desorption process

Table 1: Dependence of the H₂ output flux and the ratio of H₂ extraction from the gas mixture

Full inlet pressure, bar	H ₂ partial pressure at the membrane inlet, bar	Hydrogen output flux, cm ³ /c	Extraction level, %
2	1,4	3,5	15
3	2,1	6,3	27
4	2,8	9,4	40
5	3,5	11,7	50
6	4,2	13,7	59
7	4,9	15,4	66
8	5,6	17,2	73
9	6,3	18,7	79
10	7	19,5	83
11	7,7	20,4	87
12	8,4	21,1	90

As the result of the experiments carried out it was shown that:

- in the presence of vapor in the composition of the mixture component, CO₂ does not specifically affect the membrane surface, its catalytic activity and does not reduce membrane performance

- the maximum allowable flux of the mixture with 70% hydrogen content, at which 80% of hydrogen is extracted, is 42.6 cm³/s.

- membrane leak tightness is preserved, the upper estimate of gas admixture in the hydrogen output stream (caused by possible membrane leakage) is 10⁻⁸ %.

References

1. *Yukawa H., Nambu T., Matsumoto Y.* V-W alloy membranes for hydrogen purification // *J. Alloys Compd.* 2011 V. 509 P. 881–884.
2. *Alimov V. N., Busnyuk A. O., Notkin M. E., Livshits A. I.* Hydrogen transport through V-Pd alloy membranes: hydrogen solution, permeation and diffusion // *J. Membr. Sci.* 2015 V. 481 P. 54–62.
3. *Alimov V.N. Bobylev I.V., Busnyuk A.O., Kolgatin S.N., Kuzenov S.R., Peredistov E. Yu., Livshits A.I.* Extraction of ultrapure hydrogen with V-alloy membranes: From laboratory studies to practical applications // *Int. J. Hydr. Energy* 2018. V. 43. N 29. P. 13318–13327.

TRANSPORT OF IONS THROUGH THE MODIFIED MF-4SK MEMBRANES FOR HYDROGEN-AIR FUEL CELL

¹Natalia Kononenko, ¹Irina Falina, ¹Ekaterina Meshcheryakova, ¹Ksenia Demidenko, ²Sergey Timofeev

¹Kuban State University, Krasnodar, Russia, E-mail: kononenk@chem.kubsu.ru

²JSC «Plastpolymer», St. Petersburg, Russia, E-mail: svtimof@mail.ru

Introduction

Polymer proton-conducting membranes for hydrogen-air fuel cells (FC) are subject to a number of requirements: high proton conductivity under limited humidity and elevated temperature conditions; low gas permeability, since the flow of hydrogen through the membrane determines the concentration of hydroxyl radicals and the rate of chemical degradation of the membrane. An increase in proton conductivity is achieved, as a rule, by introducing hydrophilic inorganic components, but this leads to an increase in the permeability of the membrane due to an increase in its water content [1]. A compromise could be the introduction of both an inert polymer, which improves mechanical properties and inhibits membrane swelling [2], and a hydrophilic inorganic dopant, which provides high conductivity of the membrane under fuel cell operating conditions. The goal of this work is to evaluate the effect of the simultaneous presence of an inert polymer and an inorganic hydrophilic dopant on the equilibrium and transport characteristics of the perfluorinated MF-4SK membrane.

Inert fluorocarbon polymers

Fluorocarbon polymers with different mechanical properties, soluble in dimethylformamide, are used as an inert component to obtain modified membranes by casting from a polymer solution. The poly(vinylidene fluoride) (PVDF) and its copolymers with hexafluoropropylene (PVDF-HFP) and tetrafluoroethylene (PVDF-TFE) are among the fluorocarbon polymers. The amount of inert fluoropolymer in the membrane varies from 5 to 40% wt. It is established that with an increase in the content of the inert polymer, the exchange capacity and water content of the samples, as well as their electrical conductivity and diffusion permeability, naturally decrease. However, the pattern of the decrease in the equilibrium and transport properties of membranes is influenced by the mechanical characteristics of the fluorocarbon polymer, such as tensile strength and elongation. When a polymer with a low crystallite content (PVDF-HFP) is used, the membrane characteristics decrease monotonically. However, when adding even 5% of rigid polymers (PVDF, PVDF-TFE), the membrane characteristics change sharply. This is demonstrated in Fig. 1, which shows the change in the integral coefficient of diffusion permeability (P) of MF-4SK membranes with different contents of PVDF-HFP and PVDF-TFE.

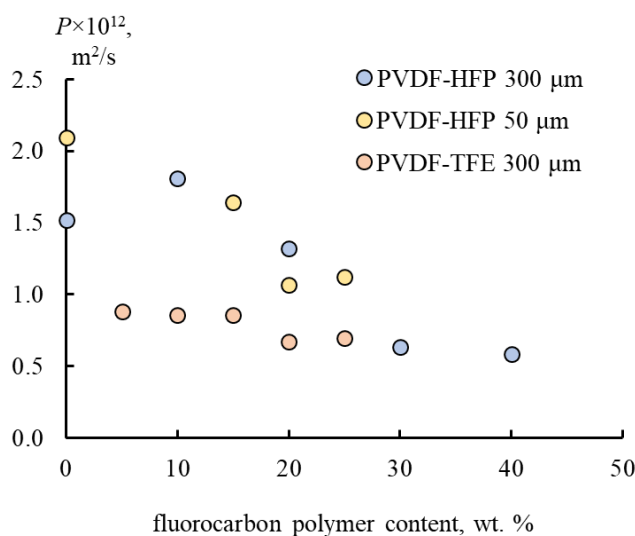


Figure 1. Influence of inert fluorocarbon polymers content on diffusion permeability of perfluorinated membranes in 0.1 NaCl solution.

Analysis of the mechanical characteristics of membranes shows that with the addition of rigid polymers (PVDF-TFE, PVDF), a monotonic increase in tensile strength is observed with increasing amount of inert polymer, while the introduction of PVDF-HFP has a plasticizing effect, significantly increasing the relative elongation at break. Thus, the introduction of PVDF-HFP allows for more “fine” regulation of the transport characteristics of membranes by changing its content.

Zirconium Hydrogen Phosphate

Zirconium hydrogen phosphate (ZrHP) is chosen as an inorganic hydrophilic dopant. Two methods for modifying ZrHP membranes are used in this work, depending on the method of membrane preparation. When using the in situ method, the synthesis of particles occurs inside the pores of the membrane. The membrane is kept in water-alcohol mixture to expand the structure and in $ZrOCl_2$ aqueous solution as a precursor, and then ZrHP is precipitated by treatment by phosphoric acid solution. When producing membranes by casting, the precursor is introduced into the polymer solution, and ZrHP is precipitated by treatment with phosphoric acid after casting the film. The amount of ZrHP in the MF-4SK membrane varies from 3 to 10 wt. %. Regardless of the modification conditions, the introduction of ZrHP leads to a non-monotonic change in the transport characteristics of membranes. The minimum values of diffusion permeability of the electrolyte solution and hydrogen permeability are observed at a dopant content of 6 %.

The conductivity of the membranes is studied at different temperatures and relative humidity $RH = 30\%$, which made it possible to identify the optimal content of the modifier and calculate the values of activation energy for the electrical conductivity of the membranes. It is found that the maximum value of conductivity is observed for membranes with 6 % wt. ZrHP, and the activation energy is practically independent of its content in the membranes.

Inert Fluorocarbon Polymer + Zirconium Hydrogen Phosphate

It is of interest to evaluate the effect of the simultaneous presence of a fluorocarbon polymer and ZrHP on the transport properties of the MF-4SK membrane. The amount of introduced modifiers is chosen based on the results described above and is 10-25 % for PVDF and 4-8 % for ZrHP. It is found that the simultaneous introduction of PVDF and ZrHP leads to a less significant increase in the water content and diffusion permeability of the samples compared to membranes containing only ZrHP. The presence of a sufficiently rigid polymer even in an amount of 10 % inhibits membrane swelling. Modifiers also have the opposite effect on the mechanical properties of membranes. The addition of an inert fluorocarbon polymer leads to an increase in strength and elongation of the samples, which prevails over the decrease in mechanical characteristics caused by the introduction of ZrHP. The conductivity of all studied samples in a 0.005 M HCl solution is in the range of 0.2 – 0.4 S/m. Investigation of the membranes conductivity in conditions of restricted humidity and elevated temperature would permit to obtain additional information about influence of both components on membrane transport properties.

Acknowledgement. The study was supported by the Russian Science Foundation and Kuban Science Foundation (project No. 22-19-20101), <https://rscf.ru/en/project/22-19-20101/>

References

1. *Shkirskaya S.A., Kononenko N.A., Timofeev S.V.* Structural and Electrotransport Properties of Perfluorinated Sulfocationic Membranes Modified by Silica and Zirconium Hydrophosphate // *Membranes*. 2022. Vol.12. 979.
2. *Falina I., Kononenko N., Timofeev S., Rybalko M., Demidenko K.* Nanocomposite Membranes Based on Fluoropolymers for Electrochemical Energy Sources // *Membranes*. 2022. V. 12, № 10. P. 935.
3. *Kononenko N. A., Shkirskaya S. A., Rybalko M. V., Zotova D. A.* The influence of inert fluoropolymer on equilibrium and dynamic hydration characteristics of MF-4SC membrane // *Colloid J.* 2023. V. 85, P. 908.

POLYMER BIPOLAR MEMBRANES: MANUFACTURING AND APPLICATION

Alexander Korzhov, Sergey Loza, Mikhail Sharafan

Kuban State University, Krasnodar, Russia, *E-mail: shtrih_000@mail.ru*

Introduction

Baro-electromembrane processes and technologies for the purification of aqueous solutions are widely used in various fields from the production of drinking water to the purification and disposal of industrial wastewater from enterprises: chemical, metallurgical, heat power engineering, water treatment and others [1-4].

The first bipolar ion exchange membranes were obtained and investigated in 1953. Only 20 years after that, works began to appear in which the mechanism of the dissociation reaction of water molecules was investigated. Bipolar membranes capable of generating hydrogen and hydroxyl ions from water have found their application in various industries. Further development of ideas about the mechanism of dissociation of water molecules became possible after the results of an experimental study by electrochemical impedance of the characteristics of the bipolar region of bipolar membranes, differing in the nature of ionogenic groups. Thus, in recent decades, as a result of Simons, Comb, and Timashev's research, the mechanism of the dissociation reaction of water molecules in bipolar membranes has been discovered.

Traditionally, BPM is obtained by pressing, rolling, extrusion or watering. The hot pressing method is one of the most common and simple enough for the manufacture of ion-exchange bipolar membranes from monopolar and thermoplastic cation-exchange and anion-exchange membranes. In this method, for the manufacture of bipolar membranes, cation exchange and anion exchange layers are combined with each other, then with the help of a press or wolves, the initial layers of the bipolar membrane heated to the required temperature are compressed during pressing or rolling. The advantage of this method is the possibility of using industrial cation exchange and anion exchange membranes as starting materials. Currently, only one type of BPM is produced in Russia – the MB-2 membrane by hot pressing on a hydraulic press at the Shchekinoazot Innovative Enterprise LLC. This membrane has unsatisfactory electrochemical characteristics, which narrows the scope of its application.

The object of the study is reagentless electromembrane processes of pH correction of solutions and processes of recovery of acids and alkalis from salt solutions by electro dialysis with bipolar membranes. The development of the scientific foundations of the technology for producing bipolar membranes from relatively cheap heterogeneous monopolar membranes will make it possible to obtain bipolar membranes competitive on the world market, the characteristics of which will ensure their wide application in electrochemical processes.

Using the obtained bipolar membranes, two pilot-industrial electromembrane complexes have been developed and tested, allowing the recovery of sulfuric acid and sodium alkali, and the processing of acidic vanadium-containing industrial effluents.

Experiments

A technology has been developed for the production of bipolar membranes with catalytic additives of the water dissociation reaction, having a size that allows the creation of pilot-industrial electro dialysts. The resulting membranes have a low overvoltage to the water dissociation reaction and good physical and mechanical properties.

The bipolar membrane was manufactured by hot pressing of heterogeneous membranes – cation exchange Ralex CMH and anion exchange Ralex AMH. Before pressing, a layer of finely ground water dissociation catalyst containing phosphoric acid groups was applied to the surface of the cation exchange membrane. Phosphoric acid groups, which are located in the bipolar region of the membrane, are catalysts for the dissociation reaction of water molecules and this leads to a decrease in the operating voltage on the bipolar membrane. The P-474 laboratory press was upgraded to produce semi-industrial scale bipolar membranes. Modernization made it possible to obtain enlarged bipolar membranes (Figure 1).



Figure 1 – Appearance of the bipolar membrane surface

The developed automated electromembrane complex for the recovery of sulfuric acid and sodium alkali from sodium sulfate, the appearance of which is shown in Figure 2.



Figure 2 – External view of the developed electromembrane complex in the business incubator of KubSU.

The computer control panel for the electrolyzer with bipolar membranes (EDBM) is shown in Figure 3.

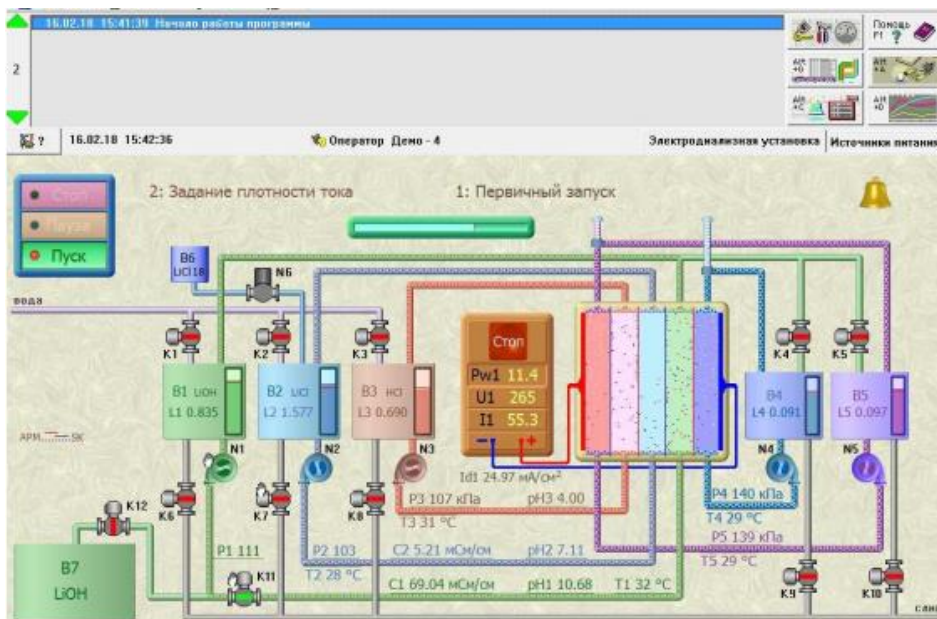


Figure 3 – External view of the control panel of the electromembrane complex.

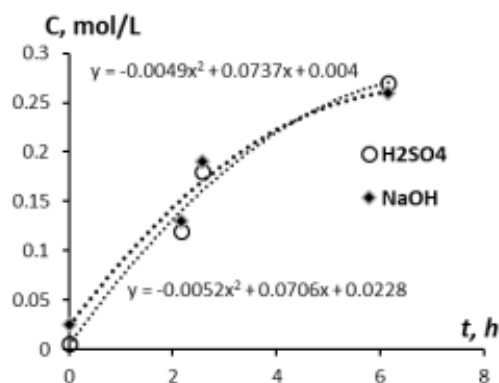


Figure 4 – Dependence of the concentration of sodium hydroxide and sulfuric acid in solutions circulating through the electrolysator-synthesizer (EDS) on time.

This graph shows the changes in the concentrations of these chemicals as they are converted from one to the other during the electrolysis reaction. Based on these results, we can conclude that the electrolysator process is effective in converting sodium sulfate into sulfuric acid and sodium hydroxide.

Results and Discussion

Analysis of the results of the study of industrial MB-3, an analogue of industrial MB-2, experimental-industrial bipolar membranes (containing catalytic additives), allow us to conclude that a bipolar membrane containing phosphoric acid polyelectrolyte as a catalyst for the dissociation reaction of water has a lower overvoltage in the bipolar region than an industrial bipolar membrane MB-3. An electromembrane complex with bipolar membranes has been developed and tested. The specific productivity for sulfuric acid was 2.0 mol/(m²·h), specific energy consumption was 5.5 kWh/kg of sulfuric acid.

Acknowledgments. This work was carried out under the government contract № FZEN-2023-0006 of the Ministry of Science and Higher Education of the Russian Federation.

References

1. V. I. Zabolotsky, A. N. Korzhov, A. Yu. But, S. S. Melnikov Reagent-Free Electromembrane Process for Decarbonization of Natural Water // Membranes and membrane technologies. – 2019 – Vol. 1. – Iss. 6. – P. 341-346.
2. S. A. Loza, N. A. Smyshlyaev, A. N. Korzhov, N. A. Romanyuk Electrolysis concentration of sulfuric acid // Chimica Techno Acta. – 2021. – V. 8(1). – 20218106.
3. D. V. Davidov, E. N. Nosova, S. A. Loza, A. R. Achoh, A. N. Korzhov, S. S. Melnikov Using a microheterogeneous model to assess the applicability of ion-exchange membranes in the process of reverse electrolysis // Chimica Techno Acta. – 2021. – V. 8(2). – № 20218205
4. S.A. Loza, N.V. Loza, A.N. Korzhov, N.A. Romanyuk, N.O. Kovalchuk, S. Melnikov Hybrid membrane technology for acid recovery from wastewater in coated steel wire production: pilot scale study // Membranes. – 2022. V. 12. – № 12. – P. 1196..

PREPARATION AND CHARACTERIZATION OF HYDROPHOBIC POLY(VINYLIDENE FLUORIDE-TETRAFLUOROETHYLENE) NANOFIBER MEMBRANES BY ELECTROSPINNING FOR DIRECT CONTACT MEMBRANE DISTILLATION

^{1,2}Elizaveta Korzhova, ²Jonathan Brant, ¹Dmitrii Lopatin

¹Krasnodar Compressor Plant, Krasnodar, Russia, *E-mail: korzhova_e@kkzav.ru*

²University of Wyoming, Laramie, USA

Introduction

Membrane distillation (MD) – is a thermally-driven desalination process that has been explored for treating high-salinity brines. MD is attractive for this application as it is not limited by the osmotic pressure of the saline feed as is reverse osmosis (RO). The driving force in MD for water transport is the vapor pressure gradient that exists between the saline feed and purified streams, which is generated by a temperature gradient between the two streams [1]. In this process, only water vapor passes through the microporous hydrophobic membrane. The membrane is important in this process because its MD characteristics, such as rejection (R) and water flux (J) determine its efficiency [2]. The purpose of this study is to fabricate electrospun poly(vinylidene fluoride-tetrafluoroethylene) (P(VDF-TFE)) nanofiber membranes and optimize their membrane performances by varying polymer solution for direct contact MD (DCMD).

Experiments

Membranes from solutions of P(VDF-TFE) polymer of different concentrations (5%, 6% and 7% w/w) in a solvent mixture of DMF:acetone (7:3) were prepared by electrospinning. All other spinning parameters were kept constant: voltage = 20 kV, spinning distance = 20 cm, flow rate = 1 ml/h. All samples were tested in a DCMD cell. The feed solution consisted of a 1 g/L sodium chloride solution made using doubly deionized water. Membrane performance was assessed in terms of salt rejection quantified using the electrical conductivities of the feed and purified water solutions.

$$R = \frac{C_{feed} - C_{cond}}{C_{feed}} \times 100\%$$

$$J = \frac{V}{S\Delta t}$$

Results and Discussion

Scanning electron microscope (SEM) images of the nano-fibrous membranes are presented in Figure 1. With increasing polymer concentration in solution, the diameter of the fibers increases, while the hydrophobicity of the membrane surface decreases. At the same time, all contact angle results show fairly high values: more than 150°.

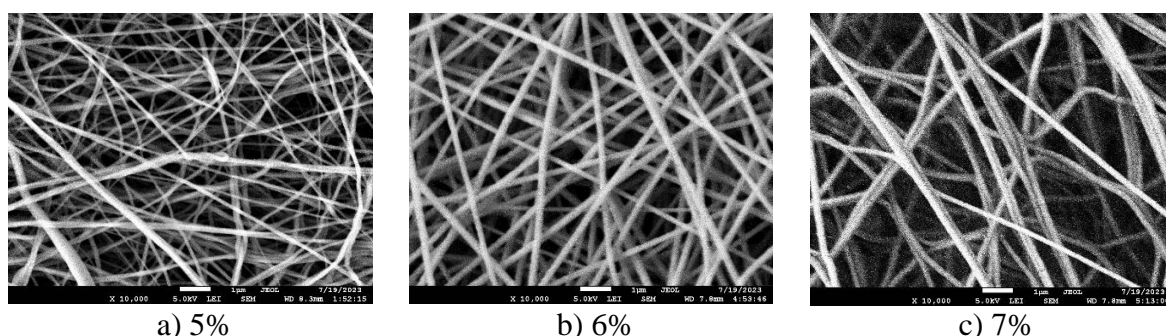


Figure 1. Images of electrospun membranes of different polymer concentration.

The PTFE commercial membrane has the lowest flux (9.6 LMH) then all nanofiber electrspon membranes. However, the electrospun membrane of 6% polymer solution has the highest flux (21.7 LMH). The nanofiber membranes show high salt rejection values: more than 99.9% after a 6 h continuous separation test, suggesting the great potential of P(VDF-TFE) nanofiber membranes in DCMD (Figure 2).

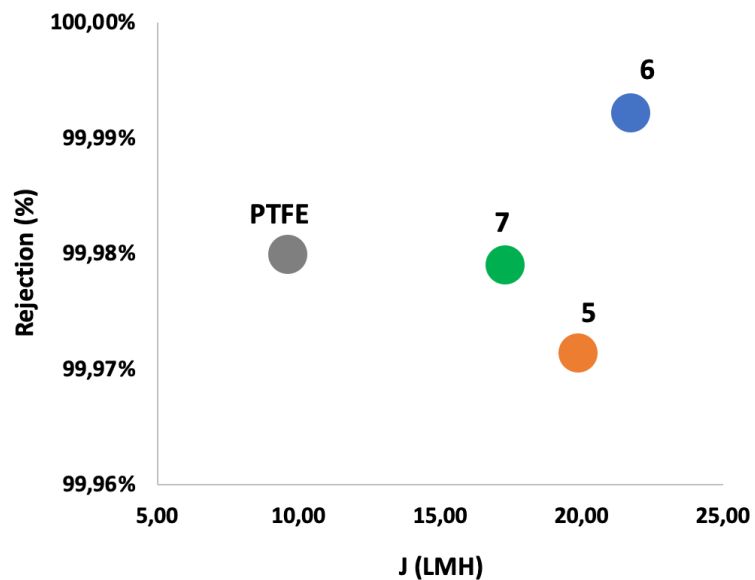


Figure 2. Rejection with flux of electrospun and commercial membranes.

Acknowledgement. This research was financially supported by the University of Wyoming's School of Energy Resources.

References

1. A. Alkudhiri, N. Darwish, N. Hilal. Membrane distillation: A comprehensive review // Desalination. 2012. V. 287, P. 2–18.
2. Y. Liao, R. Wang, M. Tian, C. Qiu, A. G. Fane. Fabrication of polyvinylidene fluoride (PVDF) nanofiber membranes by electro-spinning for direct contact membrane distillation // J. Membr. Sci. 2013. V. 425–426. P. 30–39.

INVESTIGATION OF COMPETITIVE TRANSFER OF SINGLY AND DOUBLY CHARGED CATIONS DURING LIMITED ELECTRODIALYSIS CONCENTRATION

¹Nikita Kovalchuk, ²Nazar Romanyuk, ²Sergey Loza, ¹Nina Smirnova

¹Platov South-Russian State Polytechnic University (NPI), Novocherkassk, Russia

²Kuban State University, Krasnodar, Russia, *E-mail: kovol13@yandex.ru*

Introduction

At the moment, the issue of treating complex industrial wastewater is a significant and urgent challenge. To address this, techniques such as chemical precipitation, coagulation, and filtration are employed [1]. However, these approaches primarily rely on the use of chemicals, which also results in the generation of waste products that are difficult to manage. This leads to additional expenses for the procurement of chemicals and does not completely resolve the pollution issue. Electrodialysis is a modern and advanced method of recycling multicomponent industrial solutions that relies on the selective ability of ion-exchange membranes [2-3]. These membranes allow certain ions to pass through, while blocking others. Depending on the types of ions that pass through, ion-exchange membranes can be categorized as cation-exchange or anion-exchange. By alternating cation and anion exchange membranes in an electrodialysis system, desalination and concentration chambers are created when an electrical current is applied. In the desalination chamber, the concentration of ions decreases, while in the concentration chamber it increases. To achieve higher concentrations in the concentration chamber, an electrodialysis machine with non-flowing concentration chambers is used. This configuration allows you to reach maximum concentrations, up to a saturated solution.

Experiments

During the course of the work, experiments were conducted on the limiting electrodialysis concentration of NaCl and CaCl₂ solutions, both individually and as an equimolar mixture. In all experiments, the solution concentration was 0.4 mol-eq/L for Cl⁻ ions. The current-voltage characteristics of the cation exchange membrane were measured. The objects of the study were domestic anion-exchange membranes MA-41 and cation-exchange membranes produced by casting from a solution of LF-4SK in isopropyl alcohol. All experiments were performed on a laboratory cell consisting of 5 anion exchange membranes and 4 cation exchange membranes. Capillaries were connected to one of the cation exchange membranes, allowing us to record the potential drop across the membrane during the concentration process. In the process of electrodialysis concentration, we monitored the following parameters: the current and voltage across the cell, the potential drop across the cation exchange membrane being studied, the electrical conductivity and pH values in the desalination chamber and electrode chamber, and the concentration and density of the solution in the concentration chamber.

Results and Discussion

Figure 1 shows graphs that show the dependence of the concentrations of components in the concentration chamber on the applied current during the processing of single-component solutions. As can be seen in the graph, there is a proportional increase in concentration in the first part, but then the increase slows down and reaches a plateau. Further increasing the current causes the flow of salt into the concentration chamber to increase. At the same time, the flow of solvent also increases, due to the osmotic flow of water from the desalination chamber to the concentration chamber, diluting the solution in the concentration chamber. When processing a solution with 0.4 mol-eq/L NaCl, we were able to achieve a final salt concentration of 3.9 mol-eq/L. When processing a CaCl₂ solution with the same concentration, the maximum concentration achieved was 4.0 mol-eq/L.

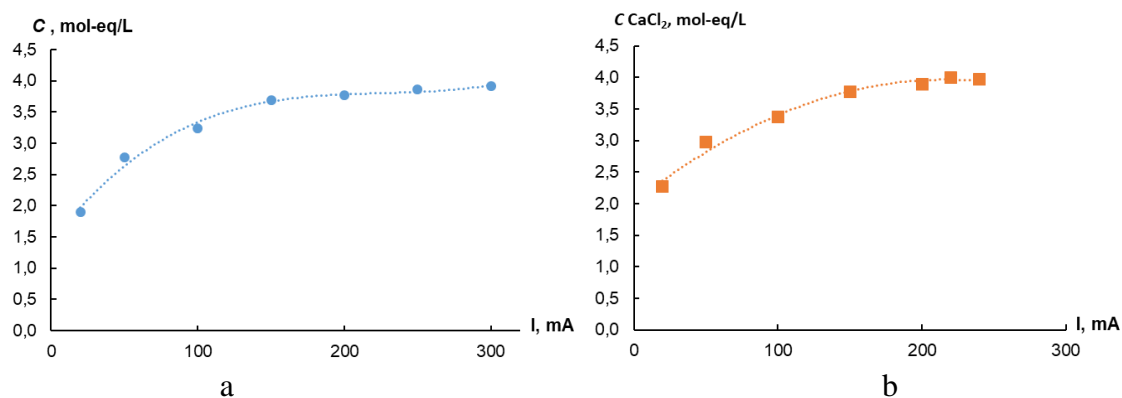


Figure 1. Dependence of concentration in the concentration chamber on the current for solutions: a – NaCl, b – CaCl₂.

Next, we conducted selective concentration of a mixture of equimolar NaCl and CaCl₂ at 0.4 mol-eq/L concentration. The results are shown in Figure 2.

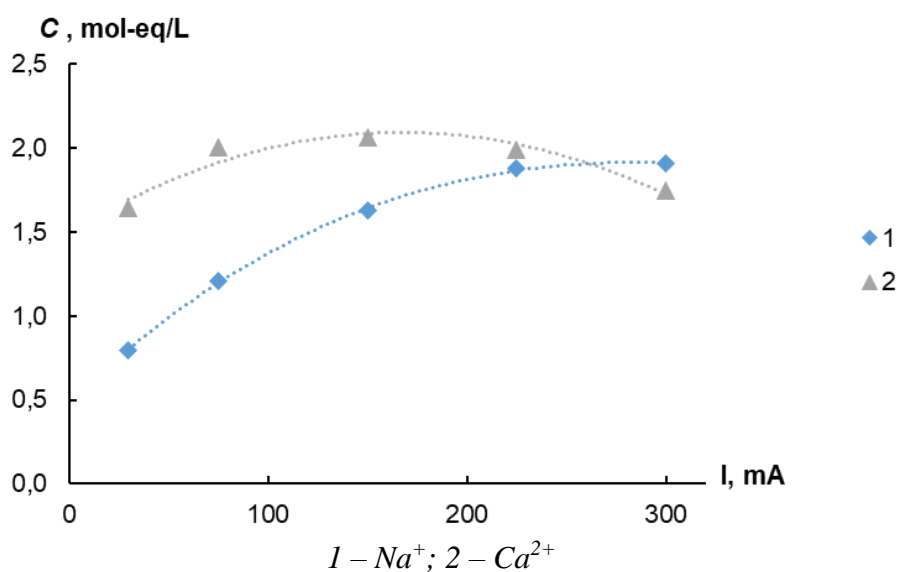


Figure 2. The dependence of the concentration in the concentration chamber on the current.

As can be seen from the data presented, with increasing current, the concentration of Na⁺ ions increases, while the concentration of Ca²⁺ ions exhibits an extreme behavior. As the current continues to increase, the difference between the two concentrations decreases and becomes practically equal. Therefore, it can be inferred that effective separation of the components at extreme concentrations is possible, although it may be more efficient at lower currents.

Acknowledgement. The research was funded by the Russian Science Foundation (project No. 22-13-00439), <https://rscf.ru/project/22-13-00439/>

References

1. Chen Q., Yao Y., Li X. [et al.] Comparison of heavy metal removals from aqueous solutions by chemical precipitation and characteristics of precipitates // J. Wat. Proc. Eng. 2018. V. 26. P. 289-300.
2. Juve J.-M. A., Christensen F. M. S., Wang Y., Wei Z. Electrodialysis for metal removal and recovery: a review // Chem. Eng. J. 2022. V. 435.
3. Gurreri L., Tamburini A., Cipollina A., Micale G. Electrodialysis applications in wastewater treatment for environmental protection and resources recovery: A systematic review on progress and perspectives // Membr. 2020. V. 10 (7).

INFLUENCE OF SPACERS ON SALT ION TRANSPORT IN ELECTROMEMBRANE SYSTEMS CONSIDERING THE MAIN COUPLED EFFECTS

Anna Kovalenko, Victor Nikonenko, Makhamet Urtenov, Aleksander Pismenskiy
Kuban State University, Krasnodar, Russia, *E-mail: savanna-05@mail.ru*

Introduction

Electrodialysis has gained global recognition as a water purification method with the potential to enhance the overall efficiency of the purification process. The efficiency of electrodialysis depends strongly on the hydrodynamics of the process, as the advent of new high performance membranes on the world market removes the kinetic limitations associated with membranes and shifts the stage that determines the economic efficiency of desalination towards the liquid phase. Studies in recent years show that there are two approaches that reduce the mass transfer limitations on the electrolyte solution side. The first is the use of spacers with which the flow of the solution can be controlled. We have investigated this approach in our study [1]. Secondly, the use of electroconvection under intense current modes. However, in this case, such destructive processes as the long-known dissociation reaction of water molecules and the recently discovered space charge breakdown [2] arise, which lead to the problem of a joint study of all these processes and their complex influence on salt ions. For the first time, the main regularities of salt ion transport in a desalting channel with spacers, electroconvection, and the dissociation/recombination reaction of water molecules [3] and the interaction of these phenomena are established in this work theoretically, using the method of mathematical modeling.

Materials and Methods

We consider a desalting channel formed by AEM and CEM through which a binary salt solution (e.g., KCl) flows with average velocity $V_0 = 0.1 \text{ mm} \cdot \text{s}^{-1}$. The concentration of the solution at the inlet is $C_0 = 0.01 \text{ mol} \cdot \text{m}^{-3}$, pH is 7. The potential difference between $x = 0$ and $x = H$, increases linearly with time: $\varphi(t, 0, y) = d \cdot t$, where $d = 10 \text{ mV/s}$ is the sweep speed of the potential drop. The intermembrane distance H is 0.5 mm; the channel length $L = 2 \text{ mm}$. The non-stationary transfer of salt ions for a 1:1 electrolyte, taking into account the space charge and the dissociation/recombination reaction, is described by 2D system of equations [1].

Mathematical model is a boundary value problem for a system of nonlinear partial differential equations of the second order. The numerical solution of such boundary value problems causes significant difficulties, since such problems are multidimensional and contain a large number of variables. In addition, when solving the problems, it is necessary to take into account the change of variables at different scales—from several nanometers in the volume of the electric double layer at the interfacial boundary to several centimeters along the length of the channel formed by two membranes.

The numerical solution is based on the finite element method and splitting the problem at each current time layer into hydrodynamic (Navier–Stokes equation) and electrochemical (Nernst–Planck–Poisson) problems following by successive alternating solutions to convergence with a given accuracy. We successfully applied this method to solve a number of electrochemical problems.

The theoretical study methodology consists of numerical investigation of different mathematical models. All these models consider diffusion, electromigration, convective transport, and electroconvection, and differ in that they take into account or do not take into account the influence of spacers and dissociation/recombination reactions of water molecules. Thus, to theoretically investigate the fundamental ion transport patterns of a binary 1:1 salt, we perform a comparative analysis of the different characteristics for four different cases: 1. Spacers are present and the dissociation/recombination reaction of water molecules is considered; 2. Spacers are absent and the dissociation/recombination reaction of water molecules is considered; 3. Spacers are present and the reaction of dissociation/recombination of water molecules is not considered; 4.

Spacers are absent and the reaction of dissociation/recombination of water molecules is not considered.

Results and Discussion

Let us consider the formation and development of electroconvection in the desalting channel of the electro dialyzer (Figure 1). Considering the dissociation/recombination reaction of water molecules significantly changes both the formation and development of electroconvection.

Initially the concentration of salt ions decreases faster under the action of dissociation/recombination reaction due to the effect of exaltation. Further, the curvature of the fluid flow stream lines increases, which increases the inflow of solution from the middle part of the channel in the direction of ion exchange membranes. As a result, a desalting region is formed in the middle part of the channel. At the same time, in the absence of dissociation/recombination reactions, electroconvective vortices appear, with the presence of the spacer system slow-ing down their development for a few seconds. However, with time, the spatial charges at the ion-exchange membranes begin to be suppressed by H^+ and OH^- ions arising from the dissociation reaction and having opposite signs to their respective spatial charges. Therefore, the electroconvective vortices decrease (Figure 1).

Thus, the dissociation/recombination reaction of water molecules leads to a faster desalting of the solution initially at first and thus an earlier onset of electroconvection. However, with time, electroconvection begins to be inhibited by new H^+ and OH^- charge carriers. In addition, the spacers provide better mixing of the solution and, consequently, the influence of the dissociation/recombination reaction of water molecules decreases, due to the lengthening of the first period.

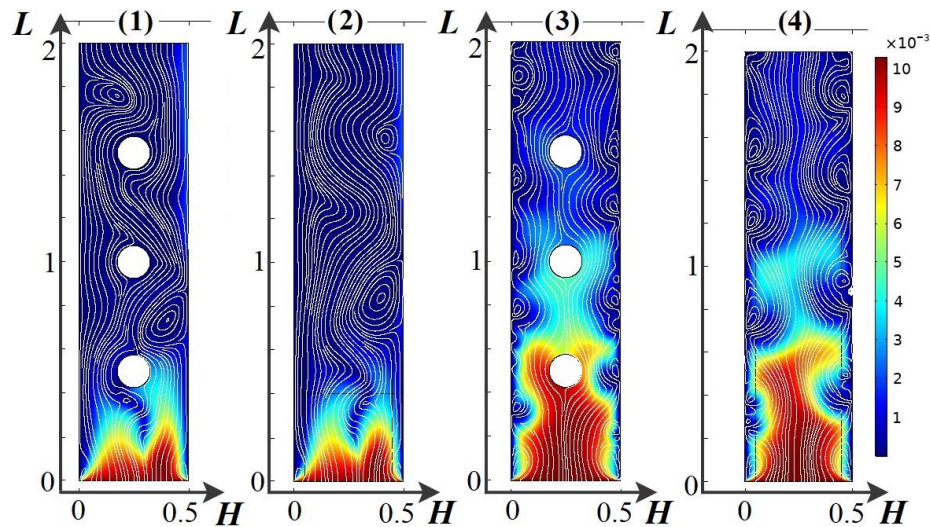


Figure 1. Cation concentration surfaces (color scale) and fluid stream lines (white) for four electro dialyzer desalting channels at $t = 150$ s, $d = 1.5$ V: (1) spacers are present and the dissociation/recombination reaction of water molecules is considered, (2) spacers are absent and the dissociation/recombination reaction of water molecules is considered, (3) spacers are present and the dissociation/recombination reaction of water molecules is not considered, (4) spacers are absent and the dissociation/recombination reaction of water molecules is not considered.

Figure 2 shows general cross-sectional views of the normalized spatial charge density ρ in the vicinity of the spacer without considering the spatial charge at ion exchange membranes, which shows the complex and non-stationary interaction of solution flow and spatial charge distribution.

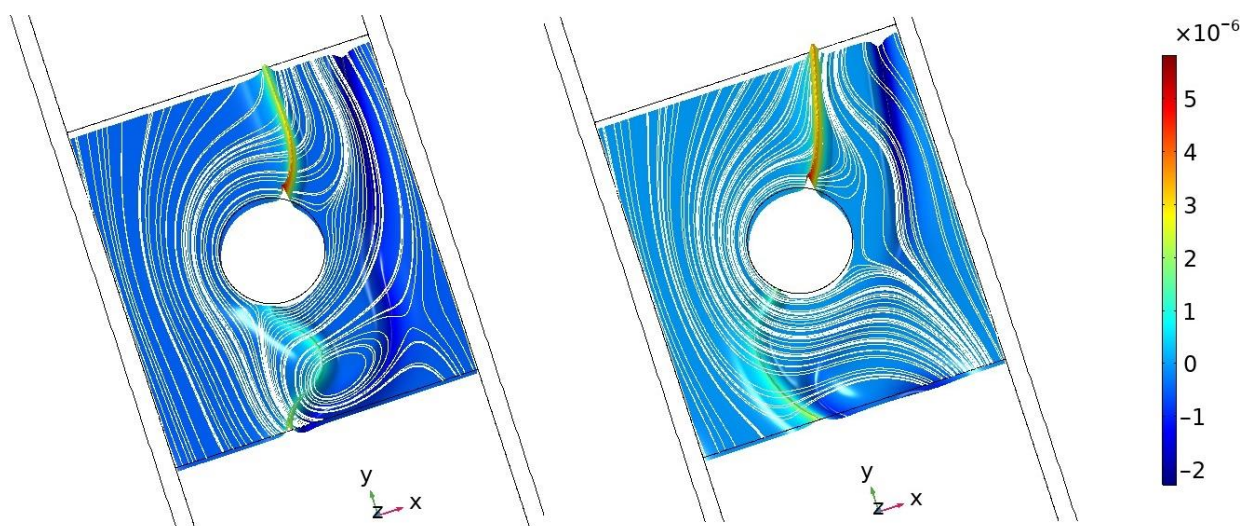


Figure 2. General view of the cross section of normalized space charge density without considering space charge at ion exchange membranes (highlighted) solution current lines (white lines) at times (a) 130 s and (b) 131 s.

Conclusion

A theoretical study of the influence of spacers on the transport of salt ions with regard to the dissociation/recombination reaction of water molecules and electroconvection has been carried out in this paper. A complex, nonlinear, contradictory, nonstationary interaction and the mutual influence of spacers, dissociation/recombination reaction, and electroconvection between each other are shown. The results show that spacers slightly suppress water splitting, namely, water splitting starts earlier in the absence of spacers. In addition, the electroconvection in the thin boundary layer is slightly reduced when spacers are used, which reduces the mixing of the solution and consequently the transport of salt ions. On the other hand, spacers promote convective transport of the electrolyte solution from the middle part of the channel with a high content of salt ions to the vicinity of the ion-exchange membranes, where the salt content is lower, and therefore increase the transport of salt ions.

Acknowledgement. This study was supported by the Russian Science Foundation, research project no. 24-19-00648, <https://rscf.ru/project/24-19-00648>.

References

1. Kovalenko A., Urtenov M., Chekanov V., Kandaurova N. Theoretical Analysis of the Influence of Spacers on Salt Ion Transport in Electromembrane Systems Considering the Main Coupled Effects. *Membranes* 2024, V. 14, P. 20.
2. Kovalenko A.V., Wessling M., Nikonenko V.V., Mareev S.A., Moroz I.A., Evdochenko E., Urtenov M.K. Space-Charge breakdown phenomenon and spatio-temporal ion concentration and fluid flow patterns in overlimiting current electro dialysis. *J. Membr. Sci.* 2021, V. 636, P. 119583.
3. Kovalenko A.V., Nikonenko V.V., Chubyr N.O., Urtenov M.K. Mathematical modeling of electro dialysis of a dilute solution with accounting for water dissociation-recombination reactions. *Desalination* 2023, V. 550, P. 116398.

OXYGEN EXCHANGE KINETICS ON LANTHANUM STRONTIUM COBALT FERRITE DOPED WITH TUNGSTEN

Ivan Kovalev, Rostislav Guskov, Mikhail Popov, Stanislav Chizhik, Alexander Nemudry
Institute of Solid State Chemistry and Mechanochemistry SB RAS, Novosibirsk, Russia
E-mail: kovalev.ivan.vyacheslavovich@gmail.com

Introduction

Nonstoichiometric perovskite-like $ABO_{3-\delta}$ oxides with mixed ionic and electronic conductivity (MIEC) have attracted the interest of researchers over the past three decades. MIEC oxides materials are being considered for use in a number of different chemical and energy technologies owing to high mixed ion-electron conductivity and catalytic activity. Research fields of MIEC oxides include oxygen and hydrogen production, carbon dioxide utilization, cathode development for solid oxide fuel cells, etc. [1-4]. Because MIEC oxides are able to exist in a wide range of oxygen stoichiometry, it becomes a challenging task to reliably determine their transport properties, as evidenced by a substantial contradiction in the literature for the same compositions. Thus, the purpose of the present work was to determine the kinetic parameters of the perovskite system as a function of temperature and oxygen content using the proposed approach [5-7].

Experiments

Equilibrium properties and kinetic properties of $La_{0.6}Sr_{0.4}Co_{0.2}Fe_{0.75}W_{0.05}O_{3-\delta}$ were studied by an original approach involving two methods: oxygen partial pressure relaxation and a quasi-equilibrium oxygen release.

Results and Discussion

The kinetic parameters (equilibrium exchange rate R_0 and chemical diffusion coefficient in oxide D_{chem}) of $La_{0.6}Sr_{0.4}Co_{0.2}Fe_{0.75}W_{0.05}O_{3-\delta}$ were found. Equilibrium isothermal diagram “lg $pO_2 - 3-\delta - T$ ” was constructed. It was shown that the linear free-energy relationship—between activation energy of the reaction rate constant and standard Gibbs energy of the reaction—is of the Brønsted–Evans–Polanyi type.

Acknowledgement. This work was supported by the Russian Science Foundation (project No. 21-79-30051).

References

1. Sunarso J. et al. Mixed ionic–electronic conducting (MIEC) ceramic-based membranes for oxygen separation // *J. Membr. Sci.* 2008. V. 320. P. 13-41.
2. Ten Elshof J. E., Van Hassel B. A., Bouwmeester H. J. M. Activation of methane using solid oxide membranes // *Catal. Today.* 1995. V. 25. P. 397.
3. Leo A., Liu Sh., Diniz da Costa J.C. Development of mixed conducting membranes for clean coal energy delivery // *Int. J. Greenh. Gas Con.* 2009. V. 3. P. 357.
4. Mahato N. et al. Progress in material selection for solid oxide fuel cell technology: A review // *Prog. Mater. Sci.* 2015. V. 72. P. 141.
5. Chizhik S. A. et al. Development of the Crank’s diffusion model for the case of material-gas feedback regime in gas flow reactors. Advanced methodology of oxygen partial pressure relaxation for the kinetics of oxygen exchange in nonstoichiometric oxides // *Chem. Eng. J.* 2021. V. 420. P. 127711.
6. Starkov I. A., Bychkov S. F., Chizhik S. A., Nemudry A. P. Oxygen release from grossly nonstoichiometric $SrCo_{0.8}Fe_{0.2}O_{3-\delta}$ perovskite in isostoichiometric mode // *Chem. Mater.* 2014. V. 26. P. 2113.
7. Chizhik S. A., Nemudry A. P. Nonstoichiometric oxides as a continuous homologous series: linear free-energy relationship in oxygen exchange. // *Phys. Chem. Chem. Phys.* 2018. V. 20. P.18447.

DEGRADATION OF ION EXCHANGE MEMBRANES DURING ELECTRODIALYSIS

¹Oleg Kozaderov, ^{1,2}Olga Kozaderova, ²Sabukhi Niftaliev, ²Kseniya Kim

¹Voronezh State University, Voronezh, Russia, *E-mail: ok@chem.vsu.ru*

²Voronezh State University of Engineering Technologies, Voronezh, Russia

E-mail: kozaderova-olga@mail.ru

Introduction

The operation of ion exchange membranes in an electrolysers takes place under conditions of direct current, elevated temperature, and the solution pH changes. This leads to variations in their structure and chemical composition, which affect the selectivity and transport characteristics of ion-exchange membranes. The service life of modern heterogeneous membranes is from two to five years. This is the main part of electrolysers. Their cost is 25-35% of the total capital costs, and replacement at the end of use is the second, after the cost of energy, item of operating costs. Knowledge about the degradation processes of ion-exchange membranes in an electrolysers, is necessary to extend their useful life, as well as to find ways to regenerate them.

Experiments

The objects of research are commercially available cation and anion exchange membranes Ralex CM(H)-Pes (Ralex CM) and Ralex AM(H)-Pes (Mega, Czech Republic), used in the electrolysis of wastewater formed during the production of nitrogen-containing mineral fertilizers. The composition of such wastewater is shown in Table 1. The membranes separated the desalination and concentration chambers, and were located in the middle of the electrolysers.

Table 1: Composition of wastewater formed during the production of nitrogen-containing mineral fertilizers

Cations	Concentration, mg/dm ³	Anions	Concentration, mg/dm ³
Ca ²⁺	0.9 – 6.7	Cl ⁻	1.3 – 16.9
Mg ²⁺	0.2 – 3.8	SO ₄ ²⁻	2.2 – 39.8
Na ⁺	0.10	F ⁻	3.2 – 92.3
K ⁺	0.15	NO ₃ ⁻	15.4 – 312.1
Fe ²⁽³⁾⁺	0.01 – 0.17	PO ₄ ³⁻	0.6 – 2.3
NH ₄ ⁺	15.9 – 258.5		

The electrical conductivity (by contact-difference method in 0.03-0.20 M NaCl solution), diffusion permeability, ion fluxes and current-voltage characteristics were determined for each new membrane and for the membrane used during electrolysis of an aqueous 0.012 M NH₄NO₃ solution (in the seven-chamber electrolysers with alternating cation and anion exchange membranes, with an active area of one membrane of 14 cm², and solution feed rate of 0.046 cm/s). In addition, structural changes of membranes using the scanning electron microscopy were considered.

Results and Discussion

Changes in some characteristics of ion exchange membranes are shown in Table 1. Index 0 refers to new conditioned samples, indices 1 and 6 – to ion exchange membranes after one and six years of operation in an industrial apparatus, respectively. It is possible to note a decrease in the exchange capacity of both anion and cation exchange membranes, which indicates the destruction of the ion exchanger. The destruction of functional groups and the crosslinking agent of ion-exchange particles in the composition of membranes may occur due to local changes in temperature and pH of the solution during electrolysis.

Table 2: Characteristics of ion exchange membranes

Membrane	Ralex CM (0)	Ralex CM (1)	Ralex CM (6)	Ralex AM (0)	Ralex AM (1)	Ralex AM (6)
Diffusion permeability (according to 0.5 M NH ₄ NO ₃), 10 ⁻¹² m ² /s	2.4 ± 0.2	2.5 ± 0.2	6.7 ± 0.5	1.1 ± 0.1	1.2 ± 0.1	6.5 ± 0.6
Exchange capacity (according to NaOH/HCl), mmol/g	2.2 ± 0.2	1.8 ± 0.1	1.8 ± 0.1	2.1 ± 0.2	1.9 ± 0.1	1.7 ± 0.1

The parameters a, b, c, d, e, f₁, f₂ and α of the extended three-wire model [1] for Ralex CM found from the concentration dependence of the specific electrical conductivity of the membrane are shown in Figure 1. With increasing operating time, minor changes in parameters b (the proportion of current flowing through the gel phase of the membrane) and a (through the mixed gel-solution channel), an increase in parameter c (inter-gel solution), d (the proportion of solution in the mixed channel "a"), f₂ (the volume fraction of the inter-gel phase) and α (a parameter reflecting the relative position of the phases in the material with respect to the direction of current), as well as a decrease in f₁ (the proportion of current transfer through the gel phase of the membrane) can be concluded. In general, similar dependencies were obtained for Ralex AM too.

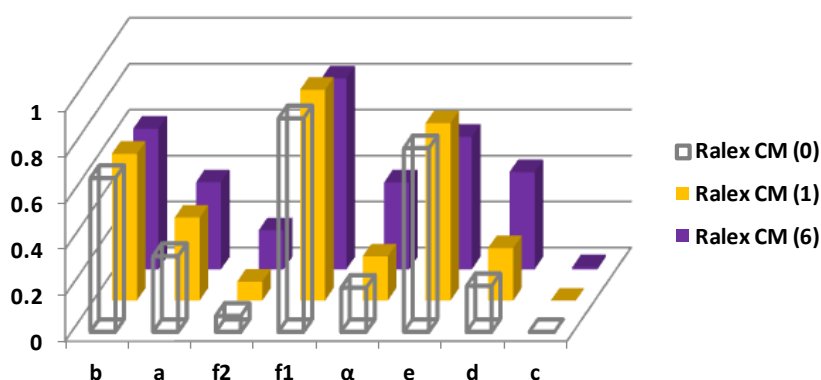
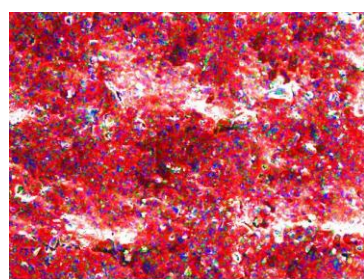
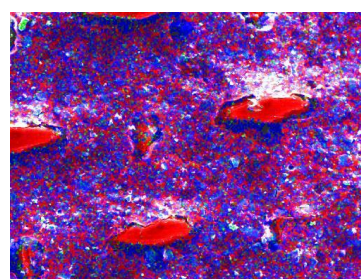


Figure 1. Parameters of the combined microheterogenic and three-wire conductivity model for the studied heterogeneous ion exchange membranes

Elemental analysis of the surface of Ralex CM membranes (Figure 2) showed an increase in sulfur content. The absence of calcium on the surface of the samples suggests that there is no formation of insoluble calcium sulfate on the membrane. Most likely, the increase in sulfur content is associated with the release of functional sulfonic acid groups of the cation exchanger to the surface as a result of surface abrasion and partial removal of the polyethylene layer.



C – red, S – blue, Na - green
RalexCM(0)



C – red, S – blue, Na - green
RalexCM(6)

Figure 2. Surface distribution map of C, S, Na elements for heterogeneous membranes

The fluxes of salt ions during electro dialysis for the Ralex CM(1) and Ralex AM(1) membranes do not differ from the fluxes of these ions through the new Ralex CM(0) and Ralex AM(0) membranes. For anion exchange membranes Ralex AM(6), it was found that the fluxes of nitrate

ions at a current density not exceeding the limiting value are noticeably lower than the fluxes of these ions through new Ralex AM(0) samples.

Figure 3 shows the volt-ampere characteristics of the Ralex CM(6)/Ralex AM(6) and Ralex CM(0)/Ralex AM(0) membranes in ammonium nitrate solution. A feature of Ralex AM(6) is an increase in both the length of the limiting current plateau and the tangent of its inclination to the potential axis. This characterizes the appearance of additional current carriers in the solution – H^+ and OH^- – ions formed as a result of heterolytic dissociation of water molecules and allows us to estimate the ability of the membrane system to develop electroconvection. The increase in the limiting current density may be a consequence of an increase in the proportion of the conductive surface of Ralex AM(6), as well as an increase in the reverse diffusion flux from the concentration chamber due to an increase in the diffusion permeability of the membrane and the proportion of the inter-gel phase in the sample composition. The increase in the length of the plateau on the volt-ampere characteristics is associated with an increase in the hydrophilicity of the surface. For Ralex CM(6) cation exchange membranes, an increase in the limiting current density is also found.

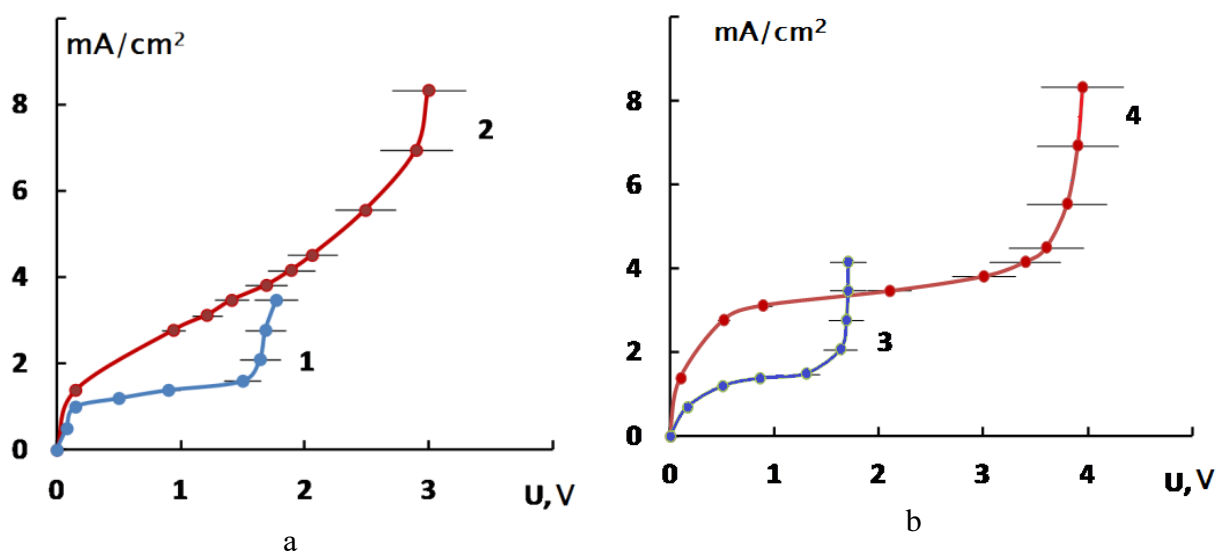


Figure 3. Volt-ampere characteristics of anion exchange membranes RalexAM (a) and cation exchange membranes RalexCM (b) during electro dialysis of 0.012 M NH_4NO_3 solution: 1- RalexAM(0); 2 - RalexAM(6); 3 - RalexCM(0); 4 - RalexCM(6)

With prolonged use of heterogeneous ion-exchange membranes in the electro dialysis treatment of waste from the production of mineral fertilizers, the increase is observed for their diffusion permeability, electrical conductivity (because of an increase in the contribution of the inter-gel solution to the membrane conductivity), as well as the proportion of the conductive surface.

References

1. Demina O.A., Kononenko N.A., Falina I.V. New approach to the characterization of ion-exchange membranes using a set of model parameters // Petroleum Chemistry. 2014. V. 54. P. 515-525.

REGULARITIES OF LACTIC ACID MASS TRANSFER IN ION-EXCHANGE MEMBRANE SYSTEMS

^{1,2}Olga Kozaderova, ²Oleg Kozaderov

¹ Voronezh State University of Engineering Technologies, Voronezh, Russia

E-mail: kozaderova-olga@mail.ru

² Voronezh State University, Voronezh, Russia, E-mail: ok@chem.vsu.ru

Introduction

Membrane technologies, including dialysis separation processes using ion-exchange membranes, can be used in the production of lactic acid from whey. To implement optimal technological conditions for the use of membrane processes for such systems, it is necessary to know not only the basic characteristics of ion-exchange membranes, such as sorption capacity, diffusion permeability, and their electrical conductivity in solutions of lactic acid and mineral salt, but also the regularities of lactic acid mass transfer in ion-exchange membrane systems, the determination of which is the purpose of this study.

Experiments

The sorption of lactic acid HLac by anion exchange membranes MA-41 (Shchekinoazot, Russia) and Ralex AM(H)-PP (Mega, Czech Republic) in Cl⁻ ionic form from solutions with a concentration of 0.03-0.15 mol/dm³ is considered. The main difference between these heterogeneous membranes is the higher dispersity of the ion-exchange component Ralex AM(H)-PP. The diffusion permeability of these membranes was found in solutions of lactic acid, sodium chloride, as well as in mixed solutions of lactic acid and sodium chloride, where organic acid and mineral salt are in an equimolar ratio (concentration range was 0.03-0.5 mol/dm³). The specific electrical conductivity of membranes in solutions of lactic acid and sodium chloride was measured. In solutions of the studied concentrations, lactic acid is initially found mainly in molecular form (the proportion of HLac in these solutions is 0.94-0.97).

Results and Discussion

Lactic acid sorption involves both ion exchange and non-exchange absorption. The non-exchange absorption of lactic acid by the MA-41 membrane is higher than by the Ralex AM(H)-PP membrane (Fig. 1). This may be due to both the growth of macropores on the sample surface and the greater unevenness of the fixed charge distribution over the membrane volume due to the lower degree of dispersity of the ion exchanger included in its composition. The values of total sorption are comparable for solutions of the same concentrations, both for MA-41 and Ralex AM(H)-PP.

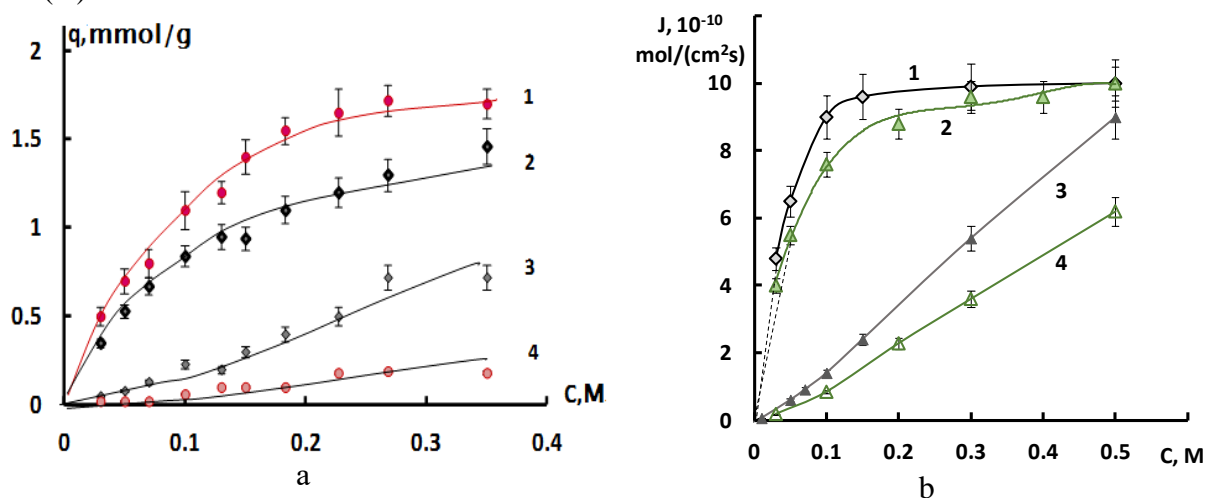


Figure 1. (a) - isotherms of exchange sorption of lactic acid (1, 2) and its non-exchange absorption (3, 4) from individual aqueous solutions by anion exchange membranes Ralex AM(H)-PP (1, 4) and MA-41 (2, 3) in Cl⁻ ionic form; (b) – diffusion fluxes of lactic acid (1, 2) and sodium chloride (3, 4) for Ralex AM(H)-PP (2, 4) and MA-41 (1, 3) membranes.

According to the data on the electrical conductivity of the samples in extremely dilute solutions, the diffusion coefficients of lactate anions in ion exchange membranes according to the Nernst-Einstein equation were calculated. At the same time, it was believed that the electrical conductivity of the samples is provided by two types of counterions, namely by chloride and lactate ions. At the same time, non-exchangeably sorbed lactic acid does not contribute to the overall electrical conductivity of the membrane. The obtained diffusion coefficients ($2.55 \cdot 10^{-7}$ and $2.34 \cdot 10^{-7}$ cm²/s for Ralex AM(H)-PP and MA-41, respectively) were used to simulate the diffusion transfer of lactic acid through an anion exchange membrane.

For lactic acid, diffusion fluxes through the anion exchange membrane have a higher value than for sodium chloride. Unlike NaCl, lactic acid exists mainly in molecular form in solutions of the studied concentrations, and the electrostatic repulsion of molecules from negatively charged fixed groups is almost not manifested. The diffusion transfer depends on the grinding degree of the ionite that is part of the membranes. In addition to the uniformity of the distribution of a more dispersed charged ionite in the membrane, we can talk about an increase in the area of the charged surface inside the membrane.

However, the mechanism of lactic acid transfer through the anion exchange membrane is more complex given the role of pH inside the anion exchange membrane. It was demonstrated [1, 2] that it is higher than the pH of the equilibrium solution because of the Donnan exclusion of H⁺-ions as co-ions from the anion exchanger. We simulated the lactic acid transfer as the dialysis of “lactic acid + NaCl” aqueous solution based on the membrane ion transport in the studied system. The transport of ions in the system was assumed to be performed by the diffusion mechanism. The problem was solved numerically by the finite element method using the COMSOL Multiphysics software package for a one-dimensional three-layer model, which simulated the membrane together with the adjacent interface diffusion layers (Figure 2).

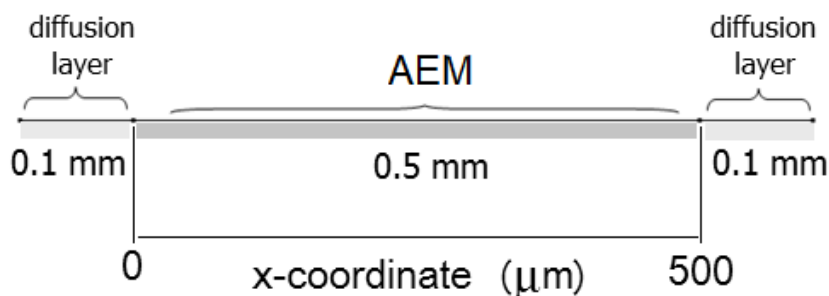


Figure 2. One-dimensional three-layer model scheme

The initial concentrations of Na⁺- and Cl⁻-ions were assumed to be equal to the volume concentration of the salt. The concentrations of the components on the outer borders of the studied three-layer model were assumed to be same in the volume of the intermembrane space. The ion exchange membrane was considered as a homogeneous phase. The reactions of water and lactic acid dissociation in external diffusion layers and in the membrane internal solution were also taken into account. The results are shown on Fig. 3.

In the solution on the receiving side of the membrane, lactic acid is in molecular form. However, its dissociation is observed in the membrane, and with a gradient distribution of Lac⁻-anion along the membrane thickness. This correlates with the change in pH inside the membrane: on the receiving side of the anion exchange membrane it has a lower value, whereas on the permeate side which is in contact with water it has a higher value.

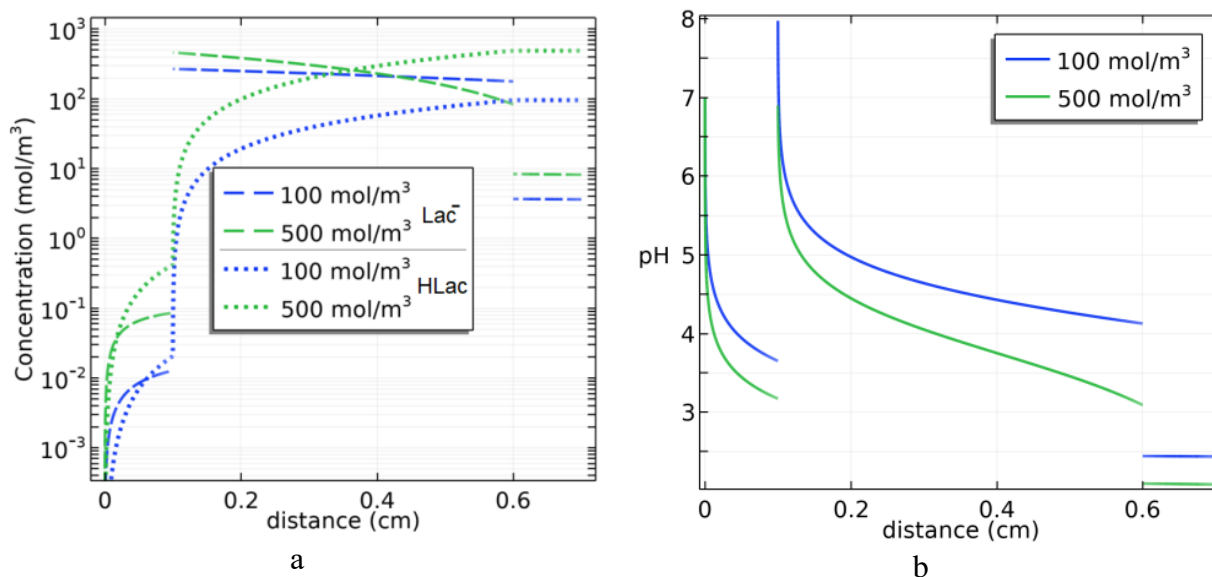


Figure 3. (a) – concentration profiles of lactate-anion (Lac^-) and lactic acid (HLac) and (b) – pH distribution of the solutions in the adjacent layers and in the membrane calculated at different origin HLac concentration in the solution.

References

1. Pismenskaya N., Laktionov E., Nikonenko V., El Attar A., Auclair B., Pourcelly G. Dependence of composition of anion-exchange membranes and their electrical conductivity on concentration of sodium salts of carbonic and phosphoric acids // J. Membr. Sci. 2001. V. 181. P. 185–197.
2. Franck-Lacaze L., Sizat P., Huguet P. Determination of the pKa of poly (4-vinylpyridine)-based weak anion exchange membranes for the investigation of the side proton leakage // J. Membr. Sci. 2009. V. 326. P. 650–658.

CARBON SORBENTS MODIFIED WITH FULLERENES

Olga Kudrinskaya, Olga Astashkina

St. Petersburg State University of Industrial Technologies and Design; St. Petersburg

E-mail: kudrinskaya.2002@mail.ru

Introduction

The widespread use of carbon materials is currently observed all over the world. Activated carbon materials are actively used as sorbents for the purification of polluted media, both liquid and gas, as well as for the concentration and isolation of noble substances. Relatively new little-studied carbon materials discovered in 1985 are fullerenes. Due to their unique structure and method of production, they have different properties. For example, modification of materials with fullerenes can lead to an improvement in physical and mechanical properties, as well as to an increase in sorption-active characteristics.

Experiments

In the course of this work, experiments were carried out on the modification of activated carbon fibers with fullerenes and the study of their sorption-active characteristics. Activated carbon fibers were obtained on the basis of hydrate cellulose fibers, and C60 fullerenes were selected from the entire line of fullerenes. Various technologies for modifying activated carbon fiber with fullerenes were studied. Based on the data from the source [1], a modification technology was applied using an aromatic compound (ort-, paraxylene) as a solvent for fullerenes and ultrasonic treatment of fullerenes followed by drying of samples for one hour at a temperature of 50°C and further, with an increase in temperature every hour by 10 ° C, the maximum drying temperature was 100 °C. The second variant of modification of the activated carbon fiber with fullerenes excluded aromatic solvents and ultrasonic treatment. Carbon tetrachloride was used as a solvent, drying was carried out according to the first option.

Results and Discussion

The sorption characteristics determined by GOST methods (by absorption of methylene blue dye, toluene, iodine) of the obtained materials were compared with the characteristics of the initial activated carbon fiber. It was shown that the maximum (before the onset of sorption equilibrium) adsorption capacity for methylene blue in non-modified sorbents was 523 mg/g, and after modification according to the first variant with a fullerene content of 0.005 wt.% decreased to 244 mg/g. The total volume of the sorption space determined by toluene also decreases from 0.61 to 0.55 cm³/g. Iodine adsorption drops from 110% to 32%. Such a decrease in the characteristics of the modified activated carbon fiber by fullerenes indicates a change in the porous structure of the sorbent. One of the reasons for the deterioration of sorption characteristics may be the fact that the solvent is not completely removed from the sorbent volume at the drying temperature, and an increase in drying temperatures above 100 ° C is impossible due to the fact that fullerenes C60 are resolved at this temperature.

When carrying out the modification according to the second option, it was shown that the adsorption capacity of methylene blue in the modified fiber (containing fullerenes 0.005 wt.%) was 477 mg/g, which is lower than the sorption capacity of the initial activated carbon fiber, but higher than that of the modified activated carbon fiber with fullerenes in the first variant. The total volume of the sorption space determined by toluene vapor is 0.38 cm³/g, which is significantly less than that of the starting material and the sample modified according to the first variant (which is the purpose of further research). The value of iodine adsorption was 77%. The data obtained indicate the advantage of the second modification option over the first.

In order to identify the effect of the fullerene content in the sorbent on sorption characteristics, the kinetics of adsorption of methylene blue was studied. The sorption process was carried out before the onset of sorption equilibrium under conditions similar to previous experiments. As can be seen from the presented data (Figure 1) at a concentration of fullerenes above 0.005 wt.%

sorption equilibrium occurs after 200 minutes and is 477 mg/g, and for a sorbent containing 0.001 wt.% fullerenes sorption capacity at the same time is 405 mg/g.

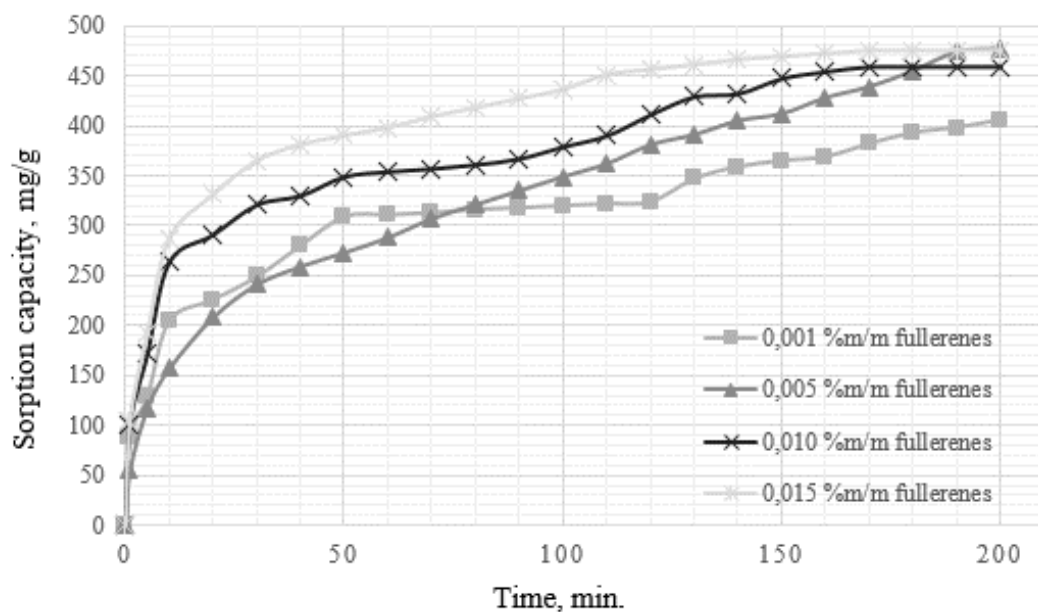


Figure 1. The kinetics of the sorption of methylene blue with modified activated carbon fiber (Sorption conditions: of $C_{initial}$ (methylene blue)=1500 mg/l, modulus 500, stirring, temperature 20 ± 5 ° C).

References

1. Pat. 2575712 Russian Federation, IPC B 01 J 20/20, B 01 J 20/30. Sorbent based on activated carbon containing fullerene and the method of its preparation / V.V. Samonin ; applicant and patent holder Federal State Budgetary Educational Institution of Higher Professional Education "St. Petersburg State Technological Institute (Technical University)". No. 2014145174/05 ; application No. 10.11.14 ; publ. 02/20/16, Issue No. 5.

POLYELECTROLYTE MEMBRANES FOR STRATEGIC DEVISING OF ELECTROCHEMICAL ENERGY SYSTEMS

Vaibhav Kulshrestha

Council of Scientific and Industrial Research-Central Salt and Marine Chemicals Research Institute (CSIR-CSMCRI), Bhavnagar, INDIA-364 002, *E-mail: vaibhavk@csmcri.res.in, vaibhavphy@gmail.com*

Rapid changes in global energy trends and sustainable energy policies has catalysed the demands for scientific and technological innovations to avail net-zero carbon footprint energy harvesting technologies. Ever since 1970s, the electrochemical energy devices (EEDs) seems to be reliable and most promising alternative to intermittent renewables. In EEDs like fuel cell, redox flow batteries and electrolyzers, the polyelectrolyte membranes (PEMs) plays a crucial role and allows selective passage of ions (preferably, H^+ and OH^-) to complete the electrochemical circuit and generation/store electricity. To introduce, the PEMs are advanced functional thin films bearing fixed charged groups viz positive ($-N^+R_4$) in anion conducting PEMs and, negative ($-SO_3^-$) in cation conducting PEMs which allows counter-ions to pass through it and exclude any co-ion migration.

In recent years, the challenges underlies developing strategic designing of stable and cost-effective membrane materials. Thus, the objective of this work focuses on the introduction of some efficient PEM designs for its strategic devising in electrochemical energy storage and conversion systems like vanadium redox flow batteries, alkaline organic redox flow batteries and fuel cells, respectively. It is expected that the polyelectrolyte membrane materials are potential alternative to elite fluorinated PEMs for respective energy applications.

Keywords: Advanced functional materials, polyelectrolyte membranes, stable hydrocarbon architectures, electrochemical energy, electrolyzers, fuel cells, batteries.

ELECTROTRANSPORT PROPERTIES OF BILAYER MEMBRANE BASED ON HETEROGENEOUS CATION EXCHANGE MEMBRANE AND HOMOGENEOUS LAYER WITH POLYANILINE

Natalia Kutenko, Natalia Loza

Kuban State University, Krasnodar, Russia, E-mail: natalakutenko818@gmail.com

Introduction

Electrodialysis allows for a number of important processes, such as separation and concentration of electrolyte solutions, extraction of precious and non-ferrous metal salts, conditioning of food raw materials and products, separation of organic acids from mixed solutions, removal and recovery of nutrients from wastewater. The main element of the electrodialyzer is ion exchange membranes. Available commercial membranes, despite their variety, cannot fully satisfy the needs of electrodialysis processes. Therefore, a large number of articles is dedicated to developing new types of ion exchange membranes or modifying the existing ones.

Experiments

The aim of the work is to change the microstructure of the surface of a heterogeneous cation exchange membrane by applying a thin film of a homogeneous cation exchange polymer to it, followed by the formation of a barrier layer of a modifier. A layer of a homogeneous cation-exchange film MF-4SK (MK40/MF-4SK) was preliminarily deposited on one of the surfaces of the MK-40 membrane. Then, polyaniline was synthesized in it as a result of the oxidative polymerization of aniline under the action of ammonium persulfate (MK-40/MF-4SK/PANI). Comprehensive characterization of the obtained materials, including the determination of specific conductivity, diffusion permeability, and CVCs in solutions of sodium chloride, calcium, and hydrochloric acid will allow us to evaluate the prospects for using the obtained materials in electrodialysis.

Results and Discussion

The deposition of an MF-4SK film on the surface of a heterogeneous MK-40 membrane does not significantly affect the electrotransport properties of the membrane. However, after its modification with polyaniline, a significant decrease in the diffusion permeability and conductivity of the samples is observed in comparison with the initial MK-40 membrane and MK-40/MF-4SK one in all the studied solutions.

Based on the obtained concentration dependences of the electrical conductivity of the initial and modified membranes in HCl, NaCl, and CaCl₂ solutions, the transport numbers of counterions in the membrane were estimated within the extended three-wire model (fig.1).

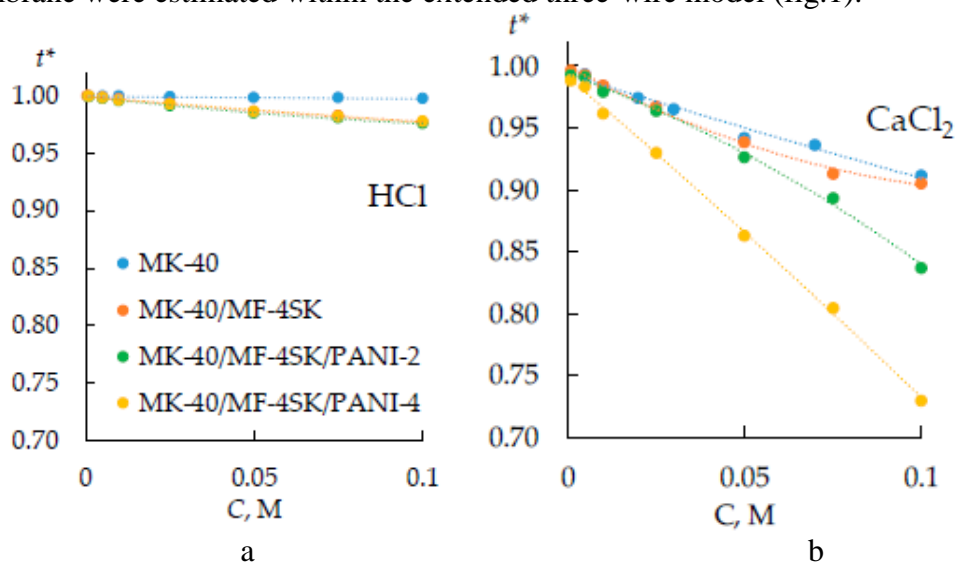


Figure 1. The transport numbers of counterions in the membranes in HCl (a) and CaCl₂ (b) solutions.

The modification of bilayer membranes with PANI leads to a slight decrease in their selectivity in a solution of NaCl and HCl. However, in the calcium chloride solution, there is a significant decrease in the transport numbers of counterions for the two samples.

An asymmetry of the CVC of bilayer membranes modified with PANI was found. It consists of an increase in the length of the limiting current plateau when the composite is oriented with the modified side to the counterion flux compared to the reverse orientation by 25–30%, regardless of the membrane modification time. For the composite with the longest PANI synthesis time (4 h), an insignificant decrease of about 8% in the limiting current density is observed when the modified side is oriented towards the counterion flux.

The change in the slope of the ohmic section ($\Delta i_{\text{ohm}}/\Delta E_{\text{ohm}}$) of the CVC is coherent with the data on the specific conductivity of membranes: for bilayer membranes, the lowest values of the specific conductivity of the electromembrane system are observed (fig.2). The traditional dependence of the limiting current density and the slope of the ohmic section on the nature of the electrolyte is also observed: the limiting current density and the slope of the ohmic section decrease in the series HCl > NaCl > CaCl₂.

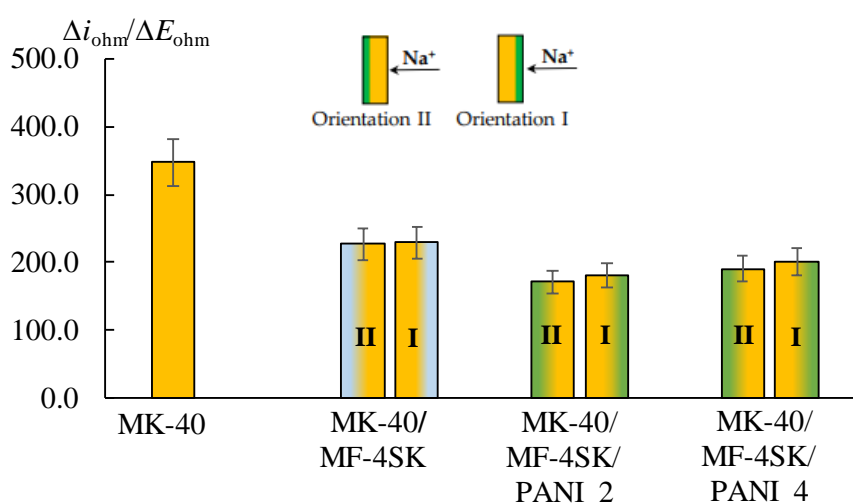


Figure 2. The slope of the ohmic section of the CVC of the initial and modified MK-40 membrane in solutions of 0.05 mol-eq/l NaCl.

A decrease in the diffusion permeability and specific conductivity of the membranes was found after their modification with PANI. This allows us to conclude that a PANI barrier layer is formed on the membrane surface. The selectivity of the heterogeneous cation-exchange membranes MK-40/MF-4SK/PANI significantly decreases in calcium chloride solution but hardly changes in hydrochloric acid and sodium chloride solutions, compared to the initial MK-40. This indicates the appearance of charge selectivity for modified membranes. However, the detected slight asymmetry in the shape and parameters of the CVC is insignificant and does not indicate the presence of the specific selectivity of the obtained bilayer membranes to singly charged cations.

References

1. Loza N., Falina I., Kutenko N. [et al.] Bilayer heterogeneous cation exchange membrane with polyaniline modified homogeneous layer: preparation and electrotransport properties // Membranes. 2023. V. 13. № 829.

DEVELOPMENT AND INVESTIGATION OF NOVEL MEMBRANES BASED ON POLY(ESTER-BLOCK-AMIDE) MODIFIED BY HOLMIUM-BASED METAL-ORGANIC FRAMEWORKS

Anna Kuzminova, Anna Karyakina, Anastasia Stepanova, Mariia Dmitrenko, Roman Dubovenko, Anastasia Penkova

St. Petersburg State University, 7/9 Universitetskaya nab., 199034 St. Petersburg, Russia

E-mail: a.kuzminova@spbu.ru

Introduction

Dense (nonporous) membranes are used for the separation of low molecular weight components in different membrane process, including nanofiltration (namely, for removal of metal ions and salt from water). Besides high selectivity, nanofiltration is an environmentally-friendly and low energy consuming process with inexpensive and compact equipment. However, for the effective separation the advanced membrane materials is needed to develop. One of the perspective way to get membranes with tailored properties is the creation of mixed matrix membranes (MMMs) by modifying a polymer with an inorganic and/or organic modifier. MMMs combine the simplicity of preparation of polymer membranes with the superior properties of modifier.

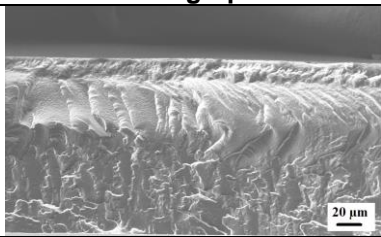
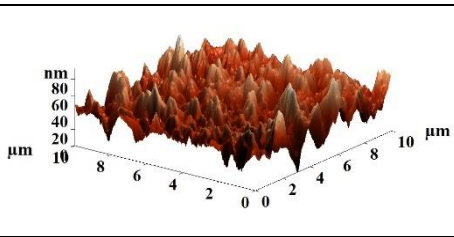
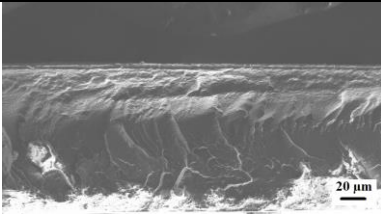
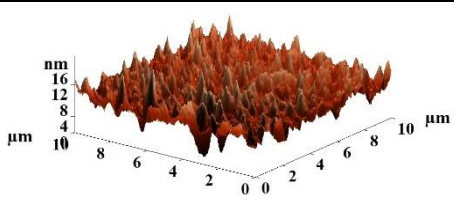
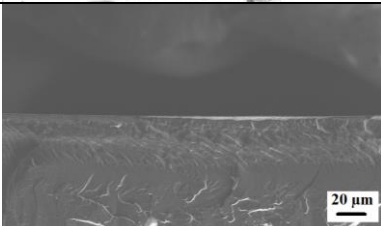
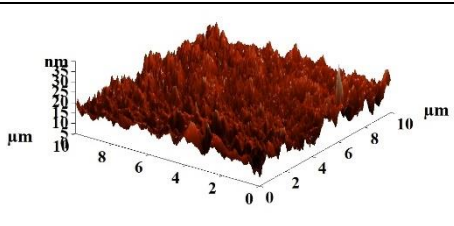
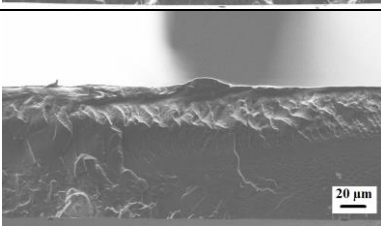
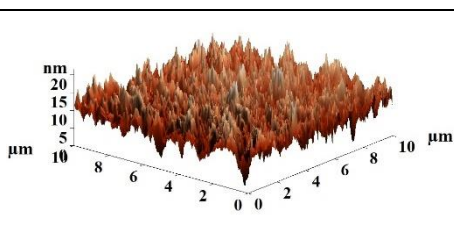
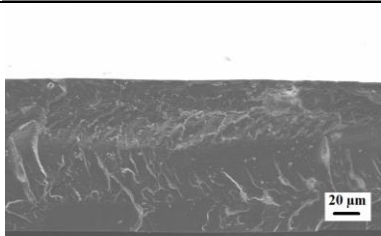
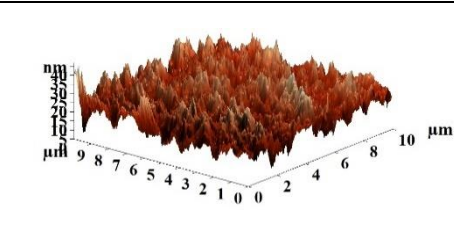
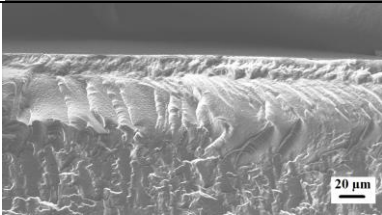
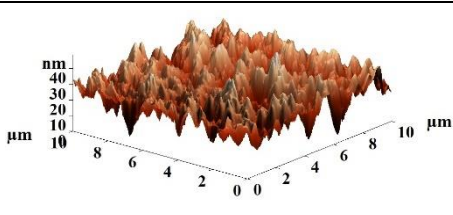
Experiments

In this study, the novel mixed matrix membranes based on poly(ester-block-amide) (PEBA, Pebax[®] 2533) modified with Ho-based metal-organic frameworks (Ho-MOFs) were developed. Ho-1,3,5-H₃btc, Ho-1,2,4-H₃btc, Ho-1,2-H₂bdc, Ho-1,3-H₂bdc, Ho-1,4-H₂bdc were used as Ho-MOFs. Dense (nonporous) membranes were formed by evaporation induced phase inversion method (EIPS). The developed membranes based on PEBA and PEBA/Ho-MOFs composite were studied by different physicochemical methods, such as Fourier-transform infrared spectroscopy (FTIR), scanning electron microscopy (SEM), atomic force microscopy (AFM), thermogravimetric analysis (TGA), swelling experiments and measurement of contact angles. The transport properties of the developed membranes were studied during the nanofiltration of water with heavy metal ions (Cd²⁺, Cu²⁺, Pb²⁺).

Results and Discussion

It was found that the introduction of Ho-MOFs into the PEBA matrix led to changes in the structural, physicochemical, and transport properties of membranes. The tailored membrane properties were achieved due to the unique physicochemical and structural properties of the Ho-MOFs modifiers such as particle shape and pore size, thermal and chemical stability, large specific surface area and its ability to change the surface roughness, hydrophilic-hydrophobic balance, and swelling characteristics of dense PEBA membranes. There was a slight change in the structure of the membranes (shown by FTIR and NMR), a change in the morphology of the cross-section and surface (confirmed by SEM and AFM, Table 1), as well as a change in the surface hydrophilic-hydrophobic balance (confirmed by contact angle measuring) and sorption characteristics (confirmed by swelling degree measuring) of membranes. The introduction of MOFs led to an increase in the permeability and rejection coefficients of heavy metal ions (Cd²⁺, Cu²⁺, Pb²⁺), which could be explained by the structure of modifiers, containing both hydrophilic and hydrophobic parts in the structure.

Table 1: Cross-section SEM Micrographs and AFM Images of Developed Membranes

Membrane	Cross-section SEM micrographs	AFM images
PEBA		
PEBA/Ho-1,3,5-H ₃ btc		
PEBA/Ho-1,2,4-H ₃ btc		
PEBA/Ho-1,2-H ₂ bdc		
PEBA/Ho-1,3-H ₂ bdc		
PEBA/Ho-1,4-H ₂ bdc		

Acknowledgements. This research was funded by the Russian Science Foundation, grant №23-29-00473, <https://rscf.ru/project/23-29-00473/>. The experimental work of this study was facilitated by the equipment from the Resource Centre of Geomodel, Chemical Analysis and Materials Research Centre, Centre for X-ray Diffraction Methods, Magnetic Resonance Research Centre, Centre for Innovative Technologies of Composite Nanomaterials, Nanophotonics Centre, Cryogenic department, Computing Centre, Thermogravimetric and Calorimetric Research Centre and the Interdisciplinary Resource Centre for Nanotechnology at the St. Petersburg State University.

MATHEMATICAL MODELING INFLUENCE OF THE RESIN PARTICLE SIZE IN THE CATION-EXCHANGE MEMBRANE ON THE SPACE CHARGE DISTRIBUTION IN THE MEMBRANE SYSTEM

¹Konstantin Lebedev, ¹Victor Zabolotsky, ²Vera Vasil'eva, ¹Aslan Achoh, ¹Polina Vasilenko

¹Kuban State University, Krasnodar, Russia, *E-mail: klebedev.ya@yandex.ru*

²Voronezh State University, Voironzh, Russia, *E-mail: viv@mail.ru*

Introduction

The aim of this work is theoretical and experimental study of the influence of cation-exchange resin particle size on the electrochemical and transport characteristics of heterogeneous membranes, as well as the mechanism of transmembrane transfer under different current regimes.

The theoretical evaluation of the influence of the size of resin particles in the membrane on the internal parameters of electromembrane systems MK-40/0.01M NaCl solution has shown that the crucial role in the development of electroconvection is played not by the field effect, but by the peculiarities of electrical heterogeneity of the membrane surface.

Experiments

The geometry of heterogeneities on the membrane surface is complex, and its mathematical description is difficult. One of the possible solutions to this problem can be modeling of the real surface of a heterogeneous membrane by a simpler surface having parameters equivalent to the surface of the real membrane. As an equivalent substitute, the geometry of the surface was used, in which the conductive regions of circular shape are equidistant from each other and staggered, and the rest of the surface is covered with a non-conductive material.

Numerical values of the distance between the conductive regions l are found from the known values of the radius of the resin particles \bar{R} and the fraction of non-conductive surface θ . The side of an equilateral triangle a must satisfy the equation $\frac{1}{2}\pi\bar{R}^2 / \frac{1}{2}a^2 \frac{\sqrt{3}}{2} = 1 - \theta$.

Equation shows that the ratio of the area of half a circle to the area of an equilateral triangle with side a is equal to the fraction of conductive regions. From (14) we obtain the value $a =$

$$\bar{R} \sqrt{\frac{2\pi}{\sqrt{3}(1-\theta)}}. \text{ The value for the distances between the neighboring circles is equal to } l = a - 2\bar{R} \text{ or}$$
$$l = \bar{R} \left(\sqrt{\frac{2\pi}{\sqrt{3}(1-\theta)}} - 2 \right) \quad (1)$$

Results and Discussion

The total and partial current-voltage characteristics of the membranes were studied by the RMD method [1]. The scheme of the RMD setup is shown in Figure 1. Based on the obtained experimental total current-voltage curves and the Hittorf ion transport numbers, partial CVCs of hydrogen cations Figure 2 we have calculated the spatial charge with mathematical model Figures 3,4.

To solve the nonlinear boundary value problem [2], a solution method was developed [2-4]. With increasing size of cation-exchange resin particles in the studied membranes, a decrease in the maximum value of the spatial charge density in the diffusion layer of the solution was revealed with a simultaneous increase in the absolute value of the SCR thickness. However, taking into account the difference in the values of the solution diffusion layer thickness δ in the studied systems, the dimensionless thickness of the SCR in the solution at the membrane boundary at the current $4i_{lim}$ decreases from 0.092δ to 0.085δ when the resin particle size increases from $<20 \mu\text{m}$ to $56\text{-}71 \mu\text{m}$.

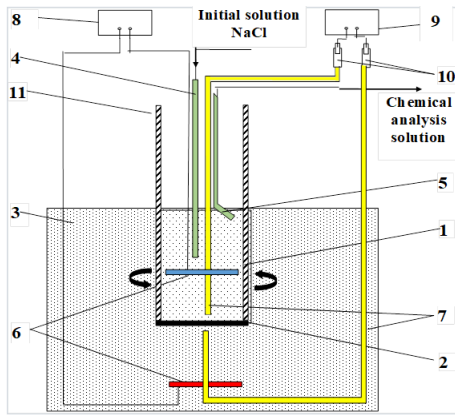


Figure 1 Scheme of the setup with a rotating membrane disc. 1 - upper half-cell (anode chamber); 2 - membrane under study; 3 - lower half-cell (cathode chamber); 4 - capillary for the solution inlet; 5 - capillary for the solution outlet; 6 - Pt electrodes; 7 - Luggin-Haber capillaries; 8 - galvanostat; 9 - millivoltmeter; 10 - reference electrodes Ag/AgCl; 11 - pulley (Zabolotskii et al., 2006b).

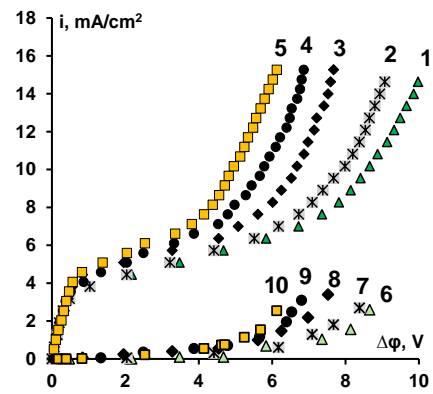


Figure 2: Total (1-5) and partial CVCs of H^+ ions (6-10) of cation-exchange membranes with different resin particle sizes obtained in 0.01 M NaCl solution at an RMD rotation speed of 100 rpm. Resin particle sizes, μm : 1, 6 – 56-71; 2, 7 – 40-56; 3, 8 – 32-40; 4, 9 – 20-32; 5, 10 – <20.

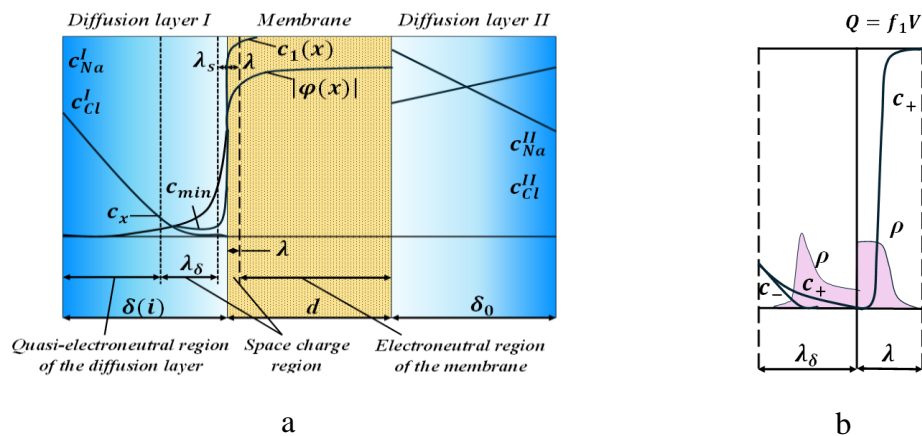


Figure 3 Scheme of distribution of concentrations of counterions c_+ , co-ions c_- , electric potential drop φ (a) and volumetric spatial charge density ρ (b) in the region of diffusion layer and cation-exchange membrane under overlimiting current regime ($i \geq i_{lim}$). δ and d are thicknesses of the diffusion layer and the membrane; λ_s, λ are space charge regions in the diffusion layer and in the membrane; λ_s is thickness of the dense part of the SCR in the diffusion layer.

The mathematical program calculates the spatial charge, which is the cause of the observed phenomena: electroconvection and dissociation of water molecules. The spatial charge in the diffusion layer is the cause of electroconvection, and the spatial charge in the membrane is the cause of the decomposition of water molecules into catalytically active ionogenic groups. The charges in the diffusion layer and in the membrane are equal in absolute magnitude, but different in sign $|q_1| = |q_2|$, $q_1/F = \int_0^\delta (\sum_{i=1}^4 c_i) dx$, $q_2/F = \int_0^d (\sum_{i=1}^4 c_i - Q) dx$ ensuring the electroneutrality of the system as a whole. However, the relative charge changes with a change in particle size are significantly different $|\Delta q_1|/c_0/F \gg |\Delta q_2|/Q/F$, which is clearly seen from Fig. 4, in which the difference between curves 1 and 2 is noticeable in the diffusion layer, whereas in the membrane they practically do not differ. This leads to the fact that the spatial charge affects the electrical convection, and the effect on the dissociation of water is weak, in addition, with a decrease in particle size, the total surface of the catalytically active groups decreases, which

follows from formula (1). This leads to a slight decrease in the rate of dissociation of water molecules.

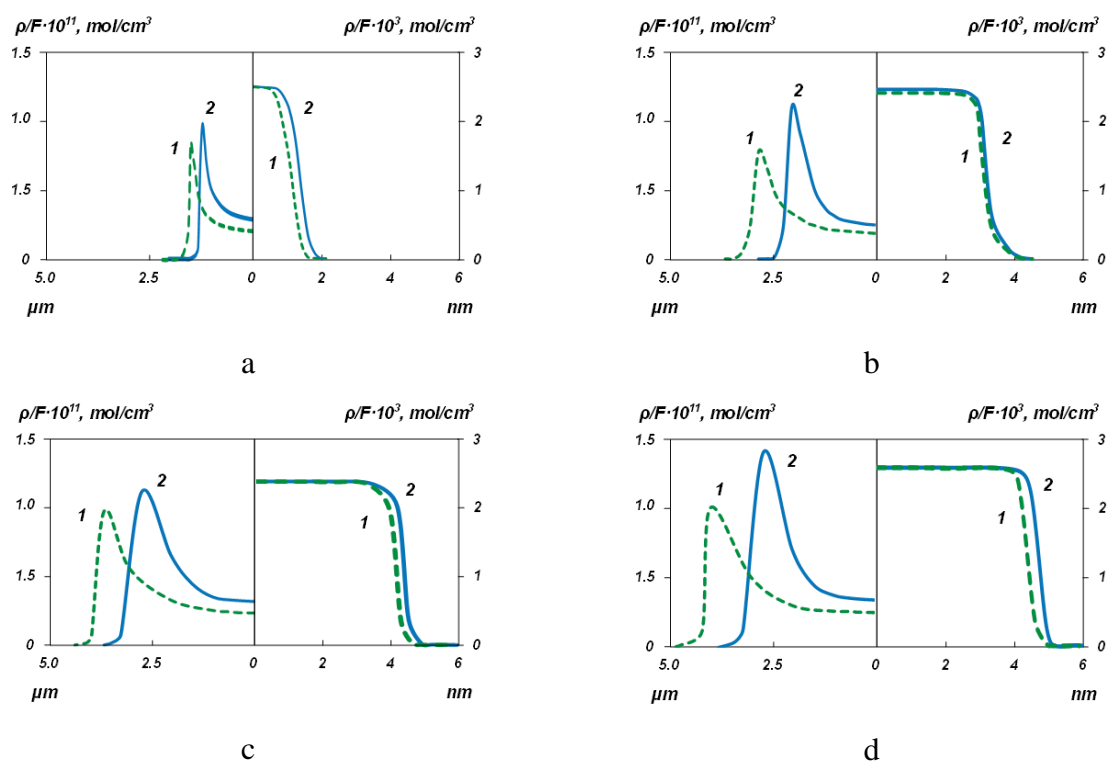


Figure 4. Distribution of volumetric spatial electric charge density (ρ/F in concentration units) in the solution diffusion layer (μm) and membrane (nm) at current density $1.5i_{lim}$ (a), $2i_{lim}$ (b), $3i_{lim}$ (c) and $4i_{lim}$ (d) and the membrane disc rotation speed of 100 rpm for MK-40 cation-exchange membranes with different resin particle sizes: 1 – 56-71 μm ; 2 – $<20 \mu\text{m}$.

Theoretical and experimental studies of the mechanism of transport of electrolyte ions and water splitting products through sulfonated cation-exchange heterogeneous membranes with particle size of resin KU-2-8 from $<20 \mu\text{m}$ to 56-71 μm have been carried out. It is shown that as the size of the resin particles decreases, the contribution of electroconvection to the total mass transfer increases, whereas the contribution of electrodiffusion and water splitting reaction products decreases.

Acknowledgement. The study was supported by a grant from The Russian Science Foundation No. 21-19-00397, <https://rscf.ru/en/project/21-19-00397/>

References

1. Sharafan, M., Zabolotsky, V., Study of electric mass transfer peculiarities in electromembrane systems by the rotating membrane disk method // Desalination. 2014. V.343. P.194–197. <https://doi.org/10.1016/j.desal.2013.12.023>
2. Zabolotskii, V.I., Lebedev, K.A., Lovtsov, E.G. Mathematical model for the overlimiting state of an ion-exchange membrane system // Russ. J. Electrochem. 2006. V.42, P.836–846, <https://doi.org/10.1134/S1023193506080052>.
3. Vasilenko, P.A., Suleymanov, S.S., Lebedev, K.A. Regularized Newton method with step selection for solving a system of nonlinear algebraic equations // Science Prospects. 2023. № 8. P.90-98. [in Russian]
4. Vasilenko, P.A., Lebedev, K.A. A shooting method with continuation in parameters for solving two-point boundary value problems // Science Prospects. 2023. №12. P.84-90. [in Russian]

ANGSTROM-SCALE CONFINED ION SEPARATION MEMBRANES

Xingya Li

Department of Applied Chemistry, School of Chemistry and Materials Science, University of Science and Technology of China, Hefei, 230026, P. R. China, E-mail: xingyali@ustc.edu.cn

Precise and efficient ion separation, one of the most difficult and challenging tasks to be tackled in chemical separations, has a major national demand in the fields including lithium extraction from salt lakes, sea water refining, and water purification. Microporous framework materials such as metal-organic frameworks (MOFs), porous organic cages (POCs) and covalent-organic frameworks (COFs), have permanent porosity, angstrom-sized pores and various functional sites. Our research¹⁻⁶ has demonstrated that MOFs, POCs and COFs with tailorable angstrom (\AA) scale channels can be used as a platform for constructing fast and selective ion transport channels, indicating microporous frameworks have great potentials for developing angstrom-porous ion channels and membranes (Figure 1). These findings also provide some strategies to further improve the permeability and selectivity of current membranes for energy-efficient separations and high-efficiency energy conversion⁷.

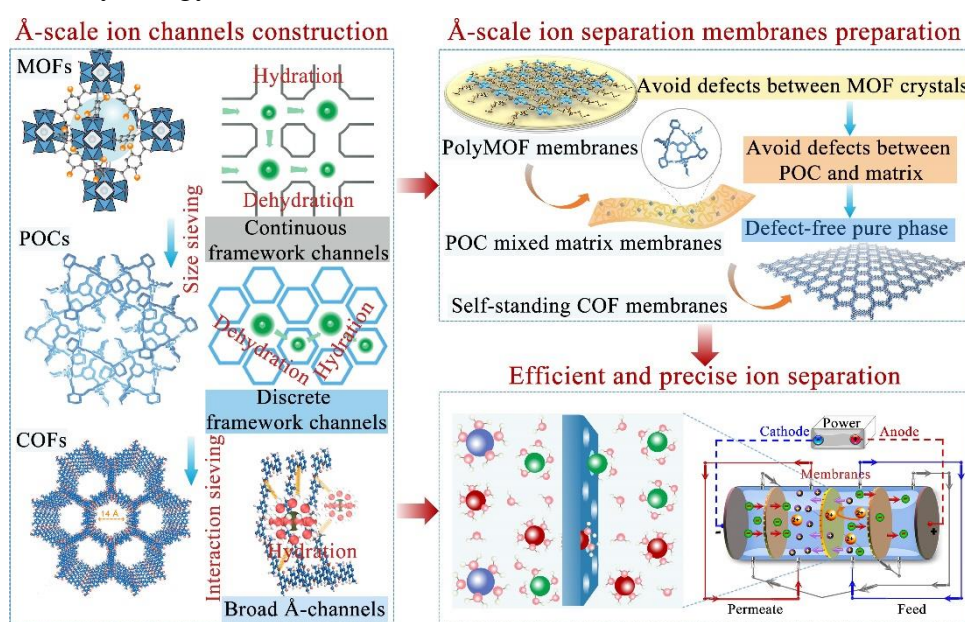


Figure 1. Angstrom-scale confined membranes for precise and efficient ion separations.

Acknowledgement. This research was financially supported by the National Key R&D Program Young Scientists Project, National Natural Science Foundation of China, and USTC Research Funds of the Double First-Class Initiative.

References

1. X.Y. Li, H.C. Zhang *, J. Z. Liu *, H.T. Wang *, et al. Nat. Commun. 2019, 10, 2490.
2. X.Y. Li, H. Yu, H.C. Zhang *, H-A. Wu *, H.T. Wang *, et al. Adv. Mater. 2020, 32, 2001777.
3. X.Y. Li, H.C. Zhang *, H.T. Wang *, et al. J. Am. Chem. Soc. 2020, 142, 21, 9827-9833.
4. F.M. Sheng, B. Wu, X.Y. Li *, L. Ge *, T.W. Xu *, et al. Adv. Mater. 2021, 33, 2104404.
5. T.T. Xu, B. Wu, X.Y. Li *, L. Ge *, T.W. Xu *, et al. J. Am. Chem. Soc. 2022, 144, 23, 10220-10229.
6. X.Y. Li, G.P. Jiang *, H.C. Zhang *, Nat. Commun., 2023, 14, 286.
7. H.C. Zhang *, X.Y. Li *, et al. Chem. Soc. Rev. 2022, 51, 2224-2254.

POSITIVE ELECTRODE FOR SODIUM-ION BATTERIES BASED ON MANGANESE AND COBALT LAYERED OXIDE

^{1,2}Anna Lochina, ¹Ruslan Kayumov, ¹Grigoriy Nechaev, ¹Lyubov Shmygleva

¹Federal Research Center of Problems of Chemical Physics and Medicinal Chemistry RAS, Chernogolovka, Russia

²Moscow Institute of Physics and Technology, Dolgoprudny, Russia, E-mail: krupina.aa@phystech.edu

Introduction

One of the main issues of modern power industry is the development of post-lithium power sources such as sodium-ion batteries (SIBs) with improved electrochemical characteristics. For this reason the search and investigation of novel electrode materials are needed. For example, manganese and cobalt based layered oxides are promising materials with high specific capacity and rate capability. In this work $P2\text{-Na}_{0.68}\text{Mn}_{0.45}\text{Co}_{0.55}\text{O}_2$ was synthesized and characterized, its ionic and electronic conductivity were determined as well as percolation thresholds of mixtures with carbon additives were found. The aim of the research was to find the best carbon additive and composition with the active material to obtain the best electrochemical properties.

Experiments

$P2\text{-Na}_{0.68}\text{Mn}_{0.45}\text{Co}_{0.55}\text{O}_2$ was synthesized from Mn and Co nitrates using self-combustion method and annealed at 500 °C for 6 h and then at 950 °C for 15 h in air. The structure of the as-prepared samples was characterized by X-Ray Diffraction (XRD), the morphology was determined by Scanning Electron Microscopy (SEM) and elemental composition by Atomic Absorption Spectroscopy. Mixtures with three different carbon additives were investigated: Acetylene Black (ACB), Vulcan XC-72 (VUL) and Carbon Nanotubes (CNT). The electronic conductivity and impedance of the mixtures were investigated in two-electrode cells. After optimum compositions were found, electrodes were made with PVDF binder. Sodium half-cells were assembled with the 1M NaClO_4/PC electrolyte. The electrochemical properties of the cells were characterized by Cyclic Voltammograms (CVs) and Charge-Discharge Curves.

Results and Discussion

XRD analysis revealed pure P2-phase structure of the synthesized material with good crystallinity, while SEM photographs showed uniform disc-like micron-sized particles (Fig. 1 (left)). The intrinsic electronic conductivity of the material is $(5.8 \pm 0.5) \cdot 10^{-8}$ S/cm and of the carbon additives ~ 20 S/cm. The percolation thresholds were 4, 2 and 1 vol. % for ACB, VUL and CNT, respectively. The dependence of the conductivity on carbon additive fraction is shown on Fig. 1 (right). The sodium half-cells with positive electrode based on mixture with ACB showed 110 mAh/g discharge capacity being cycled with 0.05C current. Having a good specific capacity and cyclability, the studied materials proved their performance in SIBs.

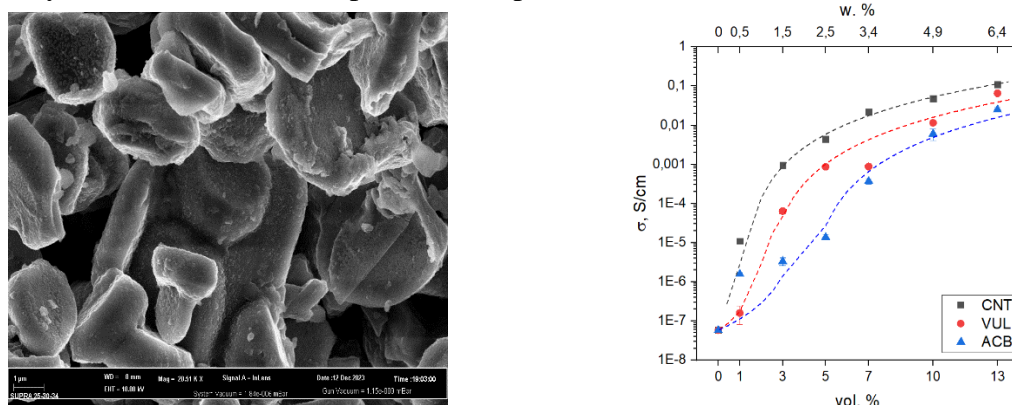


Figure 1. SEM photograph of the as-prepared $P2\text{-Na}_{0.68}\text{Mn}_{0.45}\text{Co}_{0.55}\text{O}_2$ (left); Dependence of the conductivity on carbon additive fraction (right)

Acknowledgment. The reported study was supported by a grant of Russian Science Foundation No. 24-29-00484, <https://rscf.ru/en/project/24-29-00484/>.

DEVELOPMENT AND PRODUCTION OF MEMBRANES AT THE KRASNODAR COMPRESSOR PLANT

Dmitrii Lopatin, Elizaveta Korzhova, Oleg Baranov, Igor Voroshilov

LLC "Krasnodar Compressor Plant", Dinskaya, Russia; *E-mail: Lopatin_d@kkzav.ru*

Introduction

Starting from 2019, the Krasnodar compressor plant has been developing not only compressor, but also a membrane and gas separation equipment, which includes hollow fiber membranes for gas separation and hemodialysis, proton exchange membranes for electrolysis, desalination unit with membrane distillation.

Hollow fiber membranes

The membrane technology of the gas detention is relevant and in demand in the market for gas separation for more than 20 years. The main suppliers of membranes to the Russian market are foreign manufacturers such as Air Products (USA), Air Liquide (France). Membrane modules based on hollow fibers have the highest value of the surface area, and are most convenient for gas detection, but are quite difficult to manufacture. The team of the Krasnodar compressor plant (KKZ) has experience in operating membrane installations for nitrogen stations since 1999 - flat membranes, since 2002 – hollow fiber membrane modules.

On production and laboratory section of the KKZ, an laboratory hollow fiber spinning machine was developed in an initiative to study the technology of manufacturing hollow fibers from Russian polymers with gas separation properties. The fiber spinning machine was successfully tested and a trial batch of hollow fiber was made, Fig. 1, the mechanical parameters of hollow fibers are approaching those from Air Products. Membrane module was measured the characteristics: a) for the separation of nitrogen and oxygen, b) for dehumidification and purification of methane in natural gas. Hollow fibers for hemodialysis and the technology of filling dialysis cartridges have been developed, Fig. 2. The size of the pore is less than 1 μm .

Flat sheet membranes

Technology and installation for the manufacture of flat membranes based on polymer nano-rod using the electro-spinning method were developed. Spiral membranes with a dividing layer of cellulose acetate and a substrate of nano-rod nylon for signs for natural gas, and for the separation of methane and carbon dioxide, are investigated. Also, the manufacture of a filter for filtering droplets of oil, dust and soot in front of the membranes was mastered from the nanofibers, which increases the service life. Testing showed 99.5 % filtration for particles of 0.06 μm .

Membrane distillation

Desalination unit and membranes have been developed for desalination of sea water by membrane distillation, which allows the use of the energy of solar collectors and cooling diesel generators. The process is more energy-efficient compared to conventional distillation and membranes more durable compared to the reverse osmosis.

The technology for the production of membranes for membrane distillation was developed and patented [1,2] - membranes are hydrophobic, do not pass water, but pass air and water vapor. The size of the fibers is less than the sizes of the viruses and does not pass them.

The membrane essentially works as a valve for a water vapor. Normally, a part of the molecules breaks off the surface from the surface and condenses back. With membrane distillation, a molecule with low kinetic energy can condensate behind a thin membrane, but do not contain salts. It works as follows by sea water enters the filter, Fig 3, then from the filter it enters the cell where it heats up, the heated water is in contact with the membrane, where the upward steam rises and condenses on the metal plate having an environment cooled by the radiator and cooler. Next, the condensate is absorbed by vacuum pump and accumulated in a vessel with drain. Brine salt water through an electric valve passes from the other end of the cell, gives its warmth of incoming water and merges.

The energy consumption was 0.8-1 kWh of electric/mechanical energy + 12-20 kW hours of thermal energy per 1 cubic meter of desalinated water. For thermal energy, 15 degrees of temperature difference is enough.

The desalination of 5% (50,000 ppm) of the salinity of water from the shallow lagoon of the Gulf of Persian canals has been achieved to 1100 ppm, 0.1% desalinated water, which is included in the norms of GOST for drinking and agricultural water, the rejection of the membrane module amounted to 98%.

Proton exchange membranes for electrolysis

The development of proton exchange membranes and their manufacturing technologies from completely Russian materials, according to some characteristics, exceeding foreign counterparts [3,4].

Electrolyzers were also developed for hydrogen production. The company has a full cycle of the production of membranes and most components of the electrolyzer, thanks to this it achieves less cost, greater energy efficiency and more service life compared to analogues. Container electrolyzers can be autonomous without energy, for example, for the accumulation of energy from remote solar and wind farms.

Catalytic and electrode materials

Nano-fibers have a high specific area for catalysis and filtering. Materials were developed based on electrically conductive carbonic fibers for converting the synthesis of gas into methanol, and the use for electrolysis, fuel cells and anodes of lithium-ion accumulators are also researched.

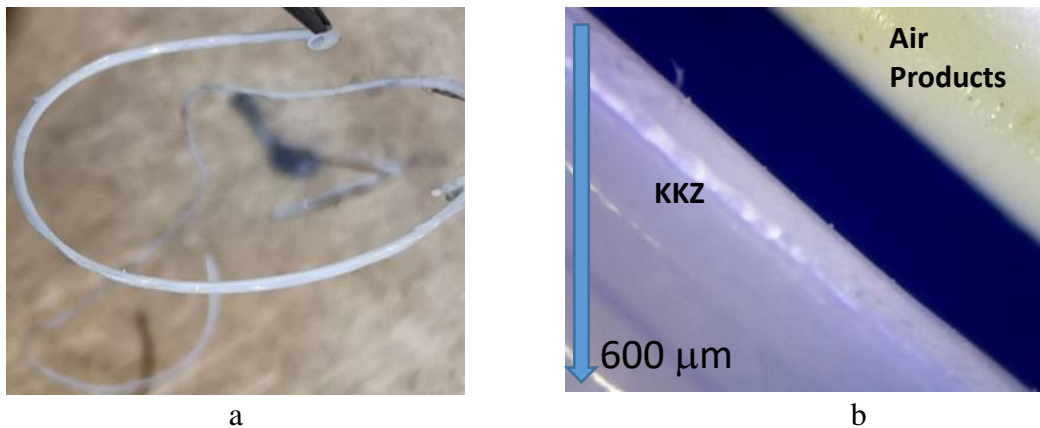


Figure 1. Hollow Fiber for Gas Separation (a), Comparison of the Surface of the KKZ Manufactured Gas Separation Hollow Fiber (b, Below on the Left) and Hollow Fiber Air Products (b, From Top Right), Frame Size 800x600 μm.

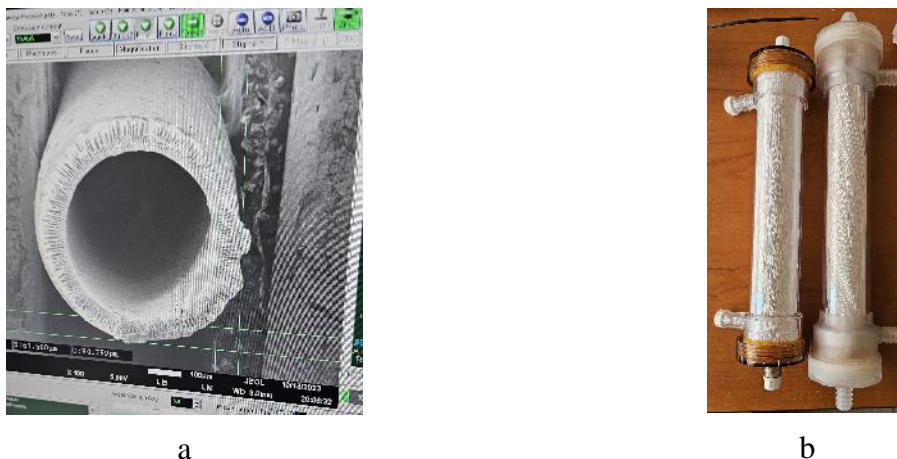


Figure 2. SEM of Hollow Fiber for Hemodialysis, Made by KKZ (left), Cartridge Samples (Right).

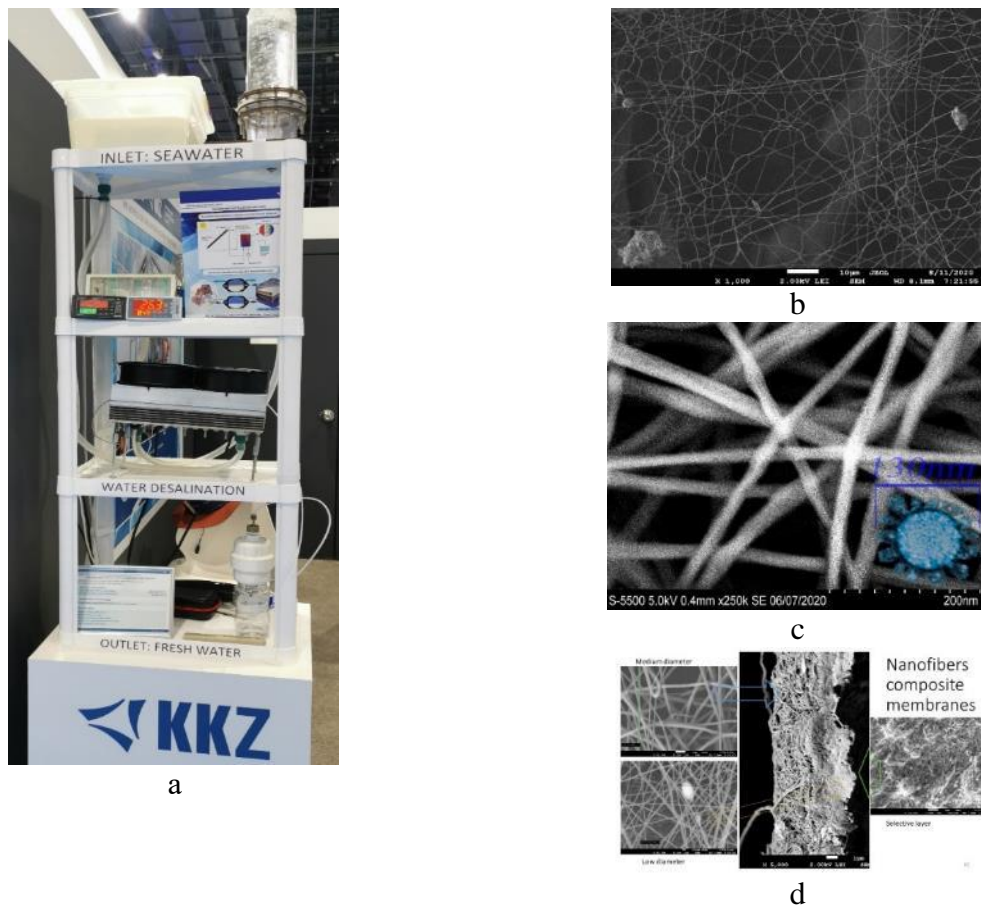


Figure 3. Membrane Distillation Unit (a) and SEM of the Nanofiber Membranes for Membrane Distillation, Surface (b-c), Cross Section (d)

References

1. Lopatin D.S., Baranov O.A., Korzhova E.S., Pismenskaya N.D., Nikonenko V.V. Modified anion exchange membrane and its manufacturing method – patent for invention RU 2676621C2 dated 04/07/2016, publ. 09.01.2019 Issue No. 1.
2. Lopatin D.S., Baranov O.A., Korzhova E.S., Pismenskaya N.D., Nikonenko V.V. Modified anion-exchange membrane and method for manufacturing said membrane, International patent application WO2017176163, publ. 12.10.2017.
3. Korzhova E., Pismenskaya N., Lopatin D., Baranov O., Nikonenko V., Dammak L. Effect of surface hydrophobization on chronopotentiometric behavior of an AMX anion-exchange membrane at overlimiting currents // J. Membr. Sci. 2016. V. 500. P. 161–170
4. Korzhova E., Lopatin D.S., Baranov O.A., Déon S., Koubaa Z., Fievet P. Modification of commercial UF membranes by electrospray deposition of polymers for tailoring physicochemical properties and enhancing filtration performances // J. Membr. Sci. 2020. V. 598. No. 117805.

EVOLUTION OF PROPERTIES OF MF-4SK PERFLUORINATED MEMBRANES DURING THEIR MODIFICATION WITH ZIRCONIUM PHOSPHATE

Julia Loza, Natalia Loza, Irina Falina

Kuban State University, Krasnodar, Russia, E-mail: julialoza@list.ru

Introduction

Perfluorinated membranes are the most important element of the membrane-electrode assembly (MEA). They combine high thermochemical resistance and optimal mechanical properties. However, their conductive properties under conditions of low humidity and high temperature are unsatisfactory. To improve the performance of a perfluoropolymer, it is modified with various organic and inorganic additives, in particular zirconium phosphate [1].

The goal of the work was to obtain composites based on zirconium phosphate and perfluorinated homogeneous membrane, study the physical-chemical and transport properties of the resulting material.

Experiments

The MF-4SK membrane produced by Plastpolymer JSC (St. Petersburg, Russia) in air-dry state was conditioned by oxidative-thermal preparation: it was successively boiled in 5% HNO₃, 10% H₂O₂ and deionized water for 3 hours in each. The resulting material in wet state, H⁺-form, has been marked as "MF-4SK" and is considered the initial membrane.

The modification procedure included three stages. Firstly, the initial membrane was exposed to water-ethanol mixture (1:1 vol.) at a temperature of 60±5 °C. An organic solvent, such as ethanol, has a wedging effect on the polymer chains of the membrane. Due to this effect, the membrane enters an expanded state [2]. Secondly, the membrane was held in ZrOCl₂ solution for 9 hours at a temperature of 70-85 °C, thus taking the zirconyl-ion form. Lastly, the membrane was exposed to H₃PO₄ solution for 8 hours at a temperature of 70±10 °C. During the last stage, X-ray amorphous zirconium hydrogen phosphate had been forming in the membrane matrix.

To evaluate the effect of each stage of modification, two separate samples were prepared. The first one was not exposed to ZrOCl₂ solution. It has been marked as "MF-4SK_a", where "a" stands for alcohol treatment. The second one went through the full modification procedure. It has been marked "MF-4SK/ZrHP". All three of the samples were studied. Their specific conductivity, diffusion permeability and CVCs in HCl solutions and physical-chemical properties were determined.

Results and Discussion

Figure 1 presents physical-chemical properties of studied membranes normalized to the properties of initial MF-4SK. Figure 2 shows the conductivity and diffusion permeability of the samples in 0.2 and 0.25 M HCl solution correspondingly. Water content, thickness, diffusion permeability and specific conductivity are significantly higher for MF-4SK_a than for MF-4SK due to higher swelling of the membrane in alcohol. After ZrHP intercalation water content, diffusion permeability and specific conductivity decrease while the membrane thickness does not change. The ion-exchange capacity for MF-4SK/ZrHP is almost two times higher than for the initial membrane, because the modifier itself contains protons. Minor differences in the CVCs of the samples might be explained by the surface peculiarities and structure differences.

According to microheterogeneous model [3], transport-structural parameters such as the volume fractions of the gel and intergel phases in membrane, mobility of counter-ions and transport numbers, are calculated. Structural changes in the membrane as a result of treatment with alcohol and deposition of the modifier were distinguished. The increase in mobility of counter- and co-ions caused by swelling of the polymer chains in alcohol is revealed.

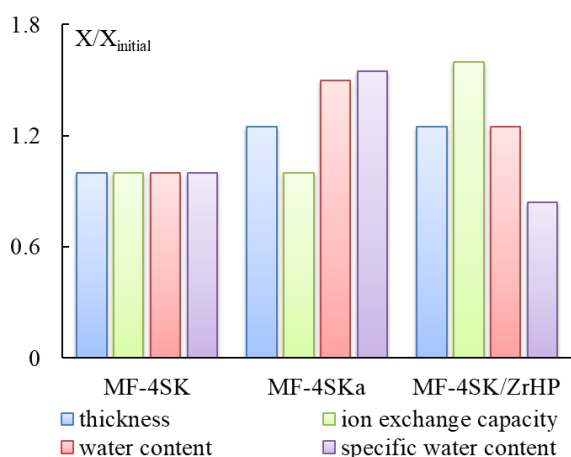


Figure 1. Physical-chemical properties of membranes in dimensionless coordinates.

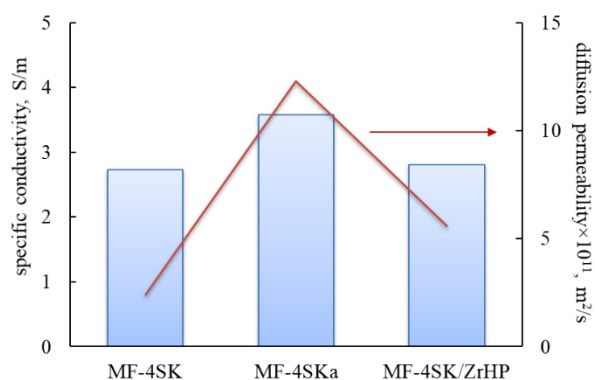


Figure 2. Transport properties of membranes in M HCl solution.

Thus, the key influence on the structural characteristics and transport properties of perfluorinated membranes when they are modified with ZrHP by the saturation-sedimentation method is exerted by the stage of heat treatment in a water-alcohol solution. The introduction of ZrHP mitigates this effect.

Acknowledgement. This work was supported by the Russian Science Foundation and Kuban Science Foundation (project No 22-19-20101), <https://rscf.ru/project/22-19-20101/>

References

1. Safronova, E.Y.; Lysova, A.A.; Voropaeva, D.Y.; Yaroslavtsev, A.B. Approaches to the Modification of Perfluorosulfonic Acid Membranes. *Membranes* 2023, 13, 721. <https://doi.org/10.3390/membranes13080721>.
2. Kononenko, N.A., Fomenko, M.A., Volkovich, Yu.M. // *Adv. Colloid Interface Sci.* 2015. Volume 222. P. 425-435.
3. Berezina, N.P., Kononenko, N.A., Dyomina, O.A., Gnusin, N.P. // *Adv. Colloid Interface Sci.* 2008. Volume 139. P. 3-28.

EFFECT OF THICKNESS ON DIFFUSION PERMEABILITY AND CONDUCTIVITY OF PERFLUORINATED CATION-EXCHANGE MEMBRANES

¹Natalia Loza, ¹Irina Falina, ¹Marina Brovkina, ²Sergey Timofeev, ¹Natalia Kononenko

¹Kuban State University, Krasnodar, Russia, E-mail: nata_loza@mail.ru

²JSC "Plastpolymer", St. Petersburg, Russia, E-mail: svtimof@mail.ru

Introduction

Perfluorinated membranes such as Nafion (DuPont, Wilmington, DE, USA), Flemion (Asahi Glass Co., Ltd., Japan), Aquivion (Solvay SA, Belgium), 3M (3M India Ltd., India), Fumion/Fumapem (FUMATECH BWT GmbH, Germany), and MF-4SK (JSC "Plastpolymer", Russia) widely used as a polymer electrolyte in the fuel cell because of their high conductivity, stability in redox environments and at elevated temperatures. Currently, the undisputed leader between these materials is the perfluorinated Nafion membrane. Nowadays the insufficient attention is paid to the patterns of the influence of membrane thickness on its transport characteristics, which is of fundamental importance [1]. The present work discusses the conductivity and diffusion permeability of perfluorinated sulfonic cation exchange membranes of various thicknesses in hydrochloric acid solutions.

Experiments

The objects of research are the experimental samples of perfluorinated MF-4CK membranes with sulfonic acid groups (JSC "Plastpolymer", St. Petersburg, Russia). The series of studied membranes includes samples of various thicknesses obtained via extrusion and casting. The perfluorinated Nafion NRE-212 membrane (Du Pont, Wilmington, DE, USA) is also studied. The main physical-chemical properties of membranes were presented in Table 1.

The conductivity of membranes was obtained from the active part of the membrane AC resistance measured by the mercury contact method. The diffusion permeability was measured for the membrane in freestanding state under the diffusion of hydrochloric acid solution with defined concentration through the membrane into distilled water [2].

Table 1. Physical-chemical properties of membranes

No	Membrane	l, μm	IEC, $\text{mmol/g}_{\text{dry}}$	W _{dry} , %	n_m , $\text{mol H}_2\text{O/mol SO}_3^-$
1	Nafion NRE-212	65 \pm 2	1.05 \pm 0.05	23 \pm 0.5	23
2	MF-4SK (extrusion)	60 \pm 2	0.93 \pm 0.05	20 \pm 0.5	20
3	MF-4SK (cast)	60 \pm 2	0.98 \pm 0.05	18 \pm 0.5	18
4	MF-4SK (extrusion)	90 \pm 2	0.93 \pm 0.05	13 \pm 0.5	13
5	MF-4SK (extrusion)	170 \pm 2	0.93 \pm 0.05	13 \pm 0.5	13
6	MF-4SK (extrusion)	240 \pm 2	0.91 \pm 0.05	14 \pm 0.5	14
7	MF-4SK (extrusion)	300 \pm 2	0.65 \pm 0.05	20 \pm 0.5	20

Results and Discussion

The diffusion permeability for studied membranes in 0.1 M hydrochloric acid solution are resented in Figure 1, a. The points for MF-4SK membranes form one group regardless on thickness and water content of membranes while Nafion membrane has higher value of diffusion permeability that is probably caused by its high water content.

An isoconductivity value of studied membranes was calculated based on the concentration dependents of membranes conductivity and microheterogeneous model. Isoconductivity value is the conductivity of a gel membrane pseudophase [2]. Obtained results presented in Figure 2, b. The points presented in Figure 1, b form two groups: samples 4-7 with thickness from 90 to 300 μm and close values of water content about 22 – 23 %; and samples 1-3 with thickness about 60-70 μm and higher water content in the range from 30 to 44 %. Among membranes with a thickness above 70 μm , the electrical conductivity decreases as their water content decreases. The sample 2 of extrusion membrane has higher conductivity compared to casting sample 3 and close value of diffusion permeability that makes it most promising for use in fuel cells.

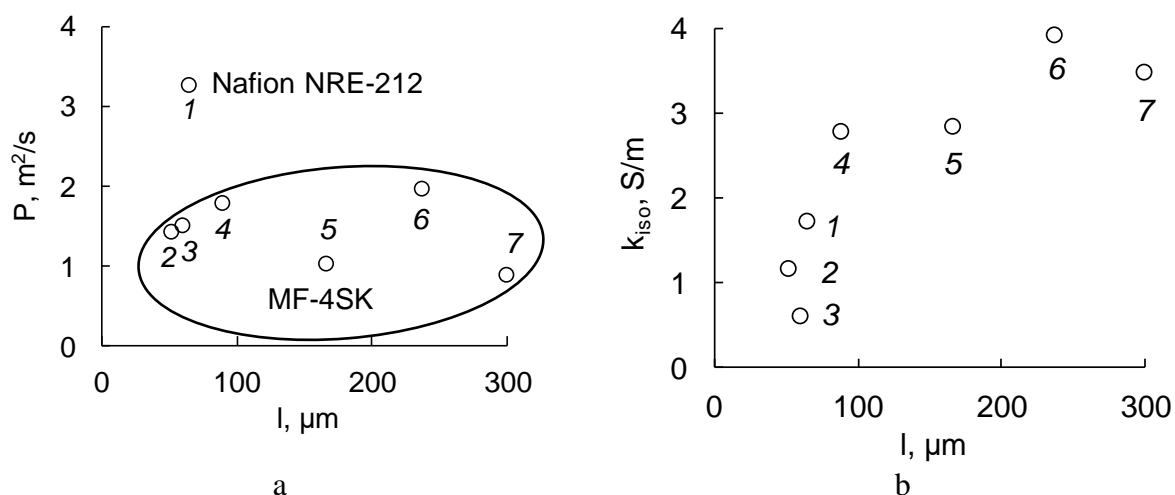


Figure 1. Diffusion permeability in 0.1 M HCl and isoconductivity of perfluorinated membranes. The numbers of points correspond to the sample number in Table 1.

Unusual effect is lower conductivity of Nafion NRE-212 membrane in comparison with MF-4SK membrane samples No 4 and 5 while Nafion has higher diffusion permeability and water content.

Acknowledgement. This work was supported by the Russian Science Foundation and Kuban Science Foundation (project No 22-19-20101), <https://rscf.ru/project/22-19-20101/>

References

1. Branco C.M., El-kharouf A., Du S. Materials for Polymer Electrolyte Membrane Fuel Cells (PEMFCs): Electrolyte Mem-brane, Gas Diffusion Layers and Bipolar Plates // Ref. Modul. Mater. Sci. Mater. Eng. 2017. V. 2. P. 378.
2. Berezina N.P., Kononenko N.A., Dyomina O.A., Gnusin, N.P. Characterization of ion-exchange membrane materials: Properties vs structure // Adv. Colloid Interface Sci. 200. V. 139. P. 3-28.
3. Loza N., Falina I., Kutenko N., et al. Electrotransport properties of perfluorinated cation-exchange membranes of various thickness // Membranes. 2023. V. 13. 829.

SELECTIVE ELECTRODIALYSIS CONCENTRATION OF SOLUTIONS CONTAINING SINGLY AND DOUBLY CHARGED CATIONS

¹Sergey Loza, ^{1,2}Nikita Kovalchuk, ¹Nazar Romanyuk, ¹Victor Zabolotsky

¹Kuban State University, Krasnodar, Russia, *E-mail: s_loza@mail.ru*

²Platov South-Russian State Polytechnic University (NPI), Novocherkassk, Russia

Introduction

Electrodialysis is often used in practice to concentrate electrolyte solutions. For example, currently more than 1 million tons of edible salt per year are extracted from seawater by electrodialysis with further evaporation [1]. Electrodialysis is also used to concentrate mine waters and increase the salt content of ultrafiltration and reverse osmosis concentrates [2, 3].

To concentrate solutions, electrodialyzers of two designs are used: with flow-through and non-flow-through concentration chambers. The first type of electrodialyzers has no different from the devices used for desalting. To increase the salt concentration, the process is carried out in several stages or the concentration chambers of the electrodialyzer are not flow-through. The concentrate is formed due to the transfer of ions and solvent through ion-exchange membranes [4]. Unlike conventional desalting in electrodialyzers with flow chambers, where the process of water transfer is not significant, in electrodialysis concentration this process determines the current output, productivity and maximum concentration of the resulting solution. Water transfer can be carried out by various mechanisms. When concentrating salts, water is transferred to the concentration chamber mainly by the electroosmotic mechanism in the hydration shells of ions. In the case of acid concentration, along with electroosmosis, the proportion of osmotic water transfer increases. The maximum concentration of acids in the process of electrodialysis concentration of acids is limited due to the leakage of protons through the anion exchange membrane from the concentration chamber to the desalting chamber, which significantly reduces the current efficiency. In practice, the task is often to separate or extract substances present in a multicomponent solution. The use of technologies based on electrodialysis can successfully solve this problem. Thus, electrodialysis with special membranes that have specific charge selectivity allows the separation of singly charged and multiply charged ions [5].

Experiments

In this work, to impart specific selectivity to the membranes, a selective anion exchange layer of N,N-dimethyl-N,N-diallylammonium chloride and ethyl methacrylate copolymer was deposited on the surface of the MF-4SK cation exchange membrane. Applying a thin homogeneous anion exchange layer to the surface of a cation exchange membrane leads to a significant decrease in the limiting current density, but the selectivity of the membrane to singly charged ions increases significantly. Selective concentration of salts of singly charged ions from mixed solutions will reduce the risk of sedimentation in concentration chambers. For example, when concentrating seawater, predominantly sodium chloride will be transferred through such a membrane, which will significantly reduce the risk of precipitation of poorly soluble calcium compounds in the concentration chamber.

The process of limited electrodialysis concentration of an equinormal mixture of sodium and calcium chlorides was studied using bilayer membranes MF-4SK with a thickness of 200 μm with a selective layer 5 μm thick on the surface facing the flow of counterions. In all experiments, the solution concentration was 0.4 mol-eq/L for Cl^- ions. MA-41 membranes were used as anion exchange membranes. The experiments were carried out in galvanostatic mode. The composition of the solution in the desalting chamber was maintained constant. During the experiment, using a measuring cylinder, the volume of the solution formed in the concentration chamber, the concentration of sodium and calcium chlorides in this solution, as well as the value of the voltage drop across the electrodialyzer were determined.

Additionally, the electrical conductivity of the membranes in a mercury contact cell and the diffusion permeability in sodium chloride solutions were measured.

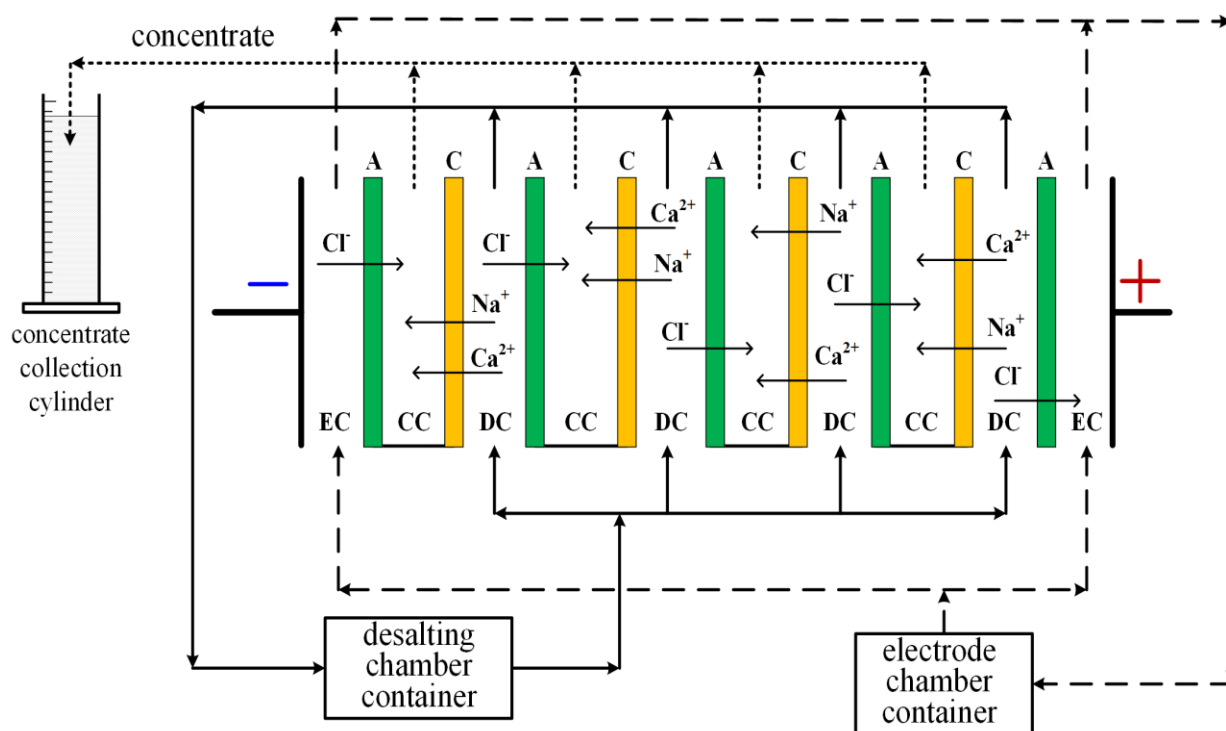


Figure 1. Hydraulic scheme of a laboratory setup for electro dialysis concentration.

Results and Discussion

The results of the experiments showed that the electrical conductivity of the modified membranes decreases by 15-30 % depending on the concentration of sodium chloride. In this case, diffusion permeability decreases by 5-10 times.

The permselectivity coefficient $P_{Na^+/Ca^{2+}}$ will increase from values of 0.5-1 to 1.6-2 when using model solutions of sodium and calcium chlorides, that is, the membrane after applying the modifier layer becomes selective to singly charged ions. Thus, the use of bilayer membranes will make it possible to selectively isolate salts of singly charged metal ions from multicomponent mixtures. Reducing the concentration of multiply charged ions in the concentration chamber of the electro dialyzer will significantly reduce the risk of sedimentation during electro dialysis concentration of industrial wastewater and natural waters.

Based on the research performed, processes for selective electro dialysis concentration of electrolytes from multiionic solutions can be developed using new bilayer and industrial ion-exchange membranes.

Acknowledgement. The research was funded by the Russian Science Foundation (project No. 22-13-00439), <https://rscf.ru/project/22-13-00439/>

References

1. Tanaka Y. A computer simulation of ion exchange membrane electro dialysis for concentration of seawater // *Membrane Water Treatment*, V. 1. No. 1. 2010. P. 13-37.
2. Reig M., Casas S., Aladjem C. [et al.] Concentration of NaCl from seawater reverse osmosis brines for the chlor-alkali industry by electro dialysis // *Desalination*. 2014. V. 342. P. 107-117.
3. Nayar K.G., Fernandes J., McGovern R.K. [et al.] Cost and energy requirements of hybrid RO and ED brine concentration systems for salt production // *Desalination*. 2019. V. 456. P. 97-120.
4. Gnusin N.P., Demina O.A. Modeling of transfer in electro dialysis systems // *Theoretical Foundations of Chemical Engineering*. – 2006. V. 40. № 1. P. 27-31.
5. Zabolotsky V.I., Achoh A.R., Lebedev K.A., Melnikov S.S. Permselectivity of bilayered ion-exchange membranes in ternary electrolyte // *Journal of Membrane Science*. 2020. V. 608. 118152.

VINYL-ADDITION POLY(IONIC LIQUID)S BASED ON 5-HEXYL-NORBORNENE AND 5-(4-BROMOBUTYL)-NORBORNENE.

^{1,2}Artyom Lunin, ¹Fedor Andreyanov, ¹Maxim Bermeshev

¹A.V.Topchiev Institute of Petrochemical Synthesis (TIPS RAS), Moscow, Russia

²National University of Oil and Gas «Gubkin University», Moscow, Russia

E-mail: lunin@ips.ac.ru

Introduction

Norbornenes derivatives are attractive monomers for their use as precursors for obtaining polymer ionic liquids because of the variety of polymerisation mechanisms of norbornenes and the high chemo- and thermostability of the resulting polymeric materials [1].

Vinyl-addition polynorbornenes exhibit high mechanical strength, high ionic conductivity, and chemical stability in various pH environments [2].

During the ionic conductivity study, it was found that the block copolymers can form ionic channels and have an increased ionic conductivity in contrast to the random copolymers, in which the ionic conductivity is markedly lower. However, in the case of polynorbornenes, random copolymers could also have high ionic conductivity close to the block copolymers. Moreover, the obtained polymers retained their mechanical properties after ageing in 1 M NaOH at 80 °C for 1000 h [3].

Results and Discussion

This work describes the optimization of the conditions for synthesising high-molecular-weight homo- and random copolymers based on 5-(4-bromobutyl)bicyclo[2.2.1]hept-2-ene (figure 1, R) with 5-hexylbicyclo[2.2.1]hept-2-ene (figure 1, R₁). As a result, vinyl-addition polymers obtained in the work have high molecular weights, improving the resulting membranes' mechanical properties. In addition, physicochemical properties of the obtained polymers, were studied with various methods such as DSC, TGA, WAXD and others.

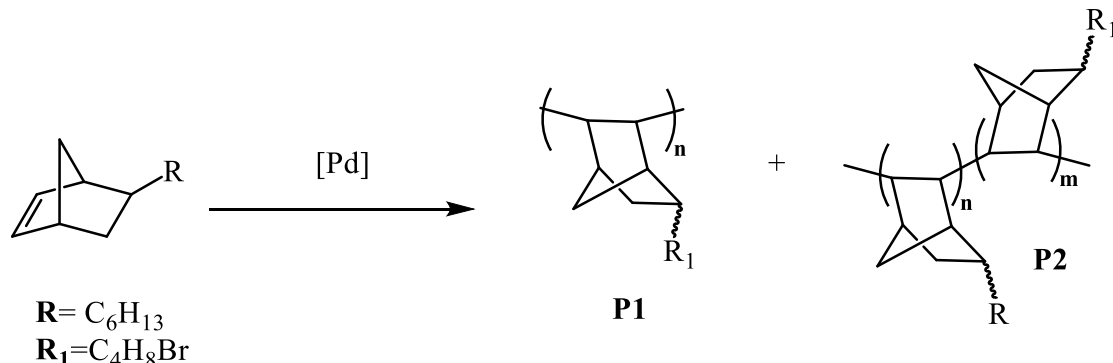


Figure 1. Vinyl-addition homo- and copolymerization of 5-(4-bromobutyl)-norbornene and 5-hexyl-norbornene.

Acknowledgment: 5-hexylbicyclo[2.2.1]hept-2-ene was received with the financial support of a grant from the President of the Russian Federation number MK-983.2022.1.3.

References

1. Finkelshtein E.S. et al.. Substituted polynorbornenes as promising materials for gas separation membranes // Russ. Chem. Rev. 2011. T. 80, № 4. C. 341–361.
2. Lehmann M. et al. Quaternized Polynorbornene Random Copolymers for Fuel Cell Devices // ACS Appl. Energy Mater. 2023. T. 6, № 3. C. 1822–1833.
3. Mandal M., Huang G., Kohl P.A. Highly Conductive Anion-Exchange Membranes Based on Cross-Linked Poly(norbornene): Vinyl Addition Polymerization // ACS Appl. Energy Mater. 2019. T. 2, № 4. C. 2447–2457

GAS PERMEABILITY OF MODIFIED MF-4SK PERFLUORINATED MEMBRANE WHEN OPERATING IN A FUEL CELL

Kirill Lyapishev, Alina Ivanchenko, Natalia Kononenko, Irina Falina
Kuban State University, Krasnodar, Russia, E-mail: k.m.lyapishev@gmail.com

Introduction

Fuel cells (FC) are promising energy sources. One of the most used are hydrogen-air FC with proton exchange perfluorinated membranes. The advantages of FC include environmental friendliness and high efficiency. The main disadvantage at the moment is the higher cost of energy production compared to classical energy generation methods. To overcome this drawback, it is important to improve the characteristics of FC and increase their efficiency [1]. One of the main factors reducing the efficiency of FC is the so-called hydrogen crossover, i.e. the diffusion of hydrogen through the membrane without its decomposition on the catalyst. The purpose of this work is to study the influence of various factors (membrane thickness, the amount of inert additives and modifier in the membrane) on the power characteristics and gas permeability of the membrane when operating in a hydrogen-air FC.

Experiments

To study the hydrogen crossover and the power characteristics of FC, a measurement setup was assembled that can operate both in the mode of supplying air to the anode side of the membrane-electrode assembly (MEA) (to measure power characteristics) and in the mode of supplying nitrogen (to measure the hydrogen crossover current), hydrogen was fed to catode side of the MEA. The membranes were tested in an MEA with a commercial catalyst E-TEK; a solution of perfluorosulfonic acid LF-4SK in isopropanol was used to prepare the catalytic ink.

The gas permeability of the membranes was assessed based on the hydrogen crossover current using cyclic voltammetry and potential step method (PSM) [2]. The hydrogen crossover current was determined as the arithmetic mean between the reverse and forward response current at a voltage of 400 mV on a cyclic voltammogram measured in the potential range from 0.1 to 1.2 V with a sweep rate of 0.01 V/s. For the PSM, the hydrogen crossover current was determined as the cutoff on the ordinate axis tangent to the limiting current plateau in the potential range 250-400 mV on a potentiostatic current-voltage curve measured in the potential range from 0.025 V to 0.4 V with a step of 0.025 V.

Results and Discussion

To assess the effect of membrane thickness on its gas permeability, a series of MF-4SK membranes: base with a thickness of 220, 45, 30 μm and modified with zirconium hydrogen phosphate (ZrHP) with a thickness of 30 μm , are selected. The hydrogen crossover current measured by the PSM increases from 0.14 mA/cm² for a membrane with a thickness of 220 μm to 0.73 mA/cm² for a membrane with a thickness of 30 μm , and for the modified membrane the hydrogen crossover current is 1.6 mA/cm² (Fig. 1).

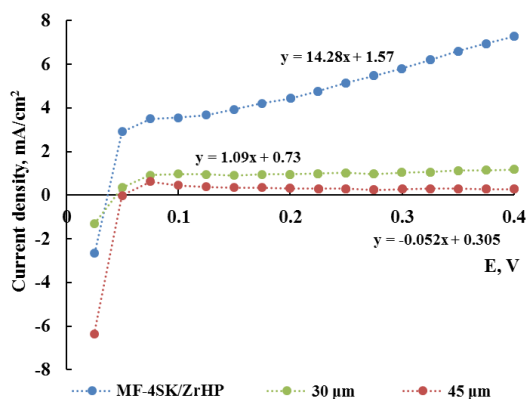


Figure 1. Hydrogen crossover current determined by PSM for membrane with a thickness 30 and 45 μm

Based on the results for membranes of various thickness, we can conclude that a decrease in membrane thickness leads to an increase in gas permeability, which seems absolutely natural. At the same time, the modification with ZrHP leads to an increase in gas permeability by approximately 2 times compared to a nonmodified membrane. At the same time the power densities of the modified and nonmodified samples have close values about 90 mW/cm^2 , and for the membrane with a thickness of $220 \mu\text{m}$ the power density is noticeably lower. Thus, reducing the thickness of the membrane leads to an improvement in power characteristics, but worsens its degradation stability.

To maintain performance characteristics, a promising direction is to introduce an inert fluoropolymer into the membrane composition. To evaluate the effect of the content of inert fluoropolymer, a number of experiments were carried out.

The object of study is a series of perfluorinated membranes MF-4SK with a thickness of about $300 \mu\text{m}$ containing an inert fluoropolymer F-26 (a copolymer of vinylidene fluoride with hexafluoropropylene) from 10 wt. % to 30 wt. %. It is established that the power density of MEA with a membrane containing 10% F-26 is approximately 15% higher compared to a membrane without additive (Fig. 2). However, the introduction of more than 20% F-26 into the membrane composition leads to a decrease in this characteristic, so that the power density of MEA with a membrane containing 30% F-26 is almost 40% lower than that of a MEA with a membrane without additive.

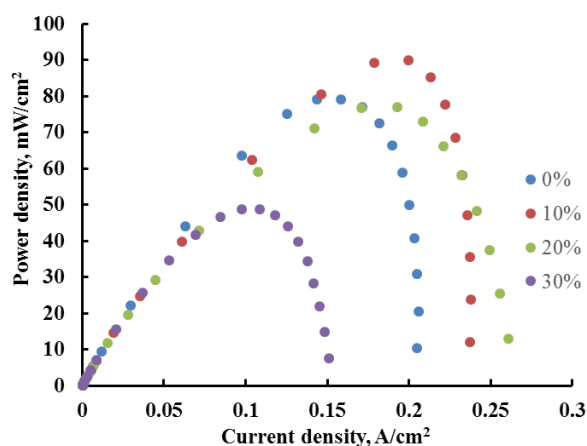


Figure 2. Power density of the MEA for membranes with different F-26 contents

The gas permeability of the membranes with inert polymer is very low due to their large thickness and decreases with increasing content of inert fluoropolymer in the MF-4SK membrane. For samples containing 20% and 30% of inert fluoropolymer, the hydrogen crossover current is below the detection limit of both cyclic voltammetry and PSM. Thus, the optimal amount of inert polymer F-26 in the perfluorinated membrane MF-4SK is 10%. This does not have a significant effect on the structure and electrotransport properties of the membrane, while elasticity of the membrane increases [3]. When it is used in a hydrogen-air FC, it reduces the hydrogen crossover current and increases the maximum power density by 15%.

To study the effect of ZrHP on the power characteristics of the FC and the gas permeability of the MF-4SK membrane, a series of membranes were selected in which the amount of ZrHP varied from 0 to 10 wt. %. The results of the hydrogen crossover current by the PSM (Fig. 3), the hydrogen flux density (Fig. 4) and the diffusion flux in 0.1 M HCl (Fig. 5) [4] are given below.

Modification with ZrHP showed an increase in the gas permeability of the membrane compared to the original membrane of the same thickness. However, ZrHP modification gives an increase in efficiency due to the higher conductivity of the membrane at low humidity, which prevails over the negative factor of increasing the gas permeability of the membrane. It was found that the optimal ZrHP content in the membrane is 6%, because it provides the increase in power density in 29% compared to the membrane without a modifier, and the hydrogen crossover current for this sample is minimal. The results obtained are in qualitative agreement with the change in the diffusion flux through these membranes in electrolyte solution.

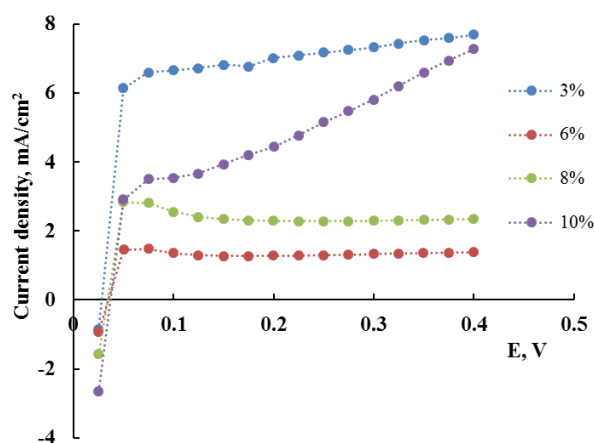


Figure 3. Hydrogen crossover current determined by PSM for membranes with different ZrHP contents

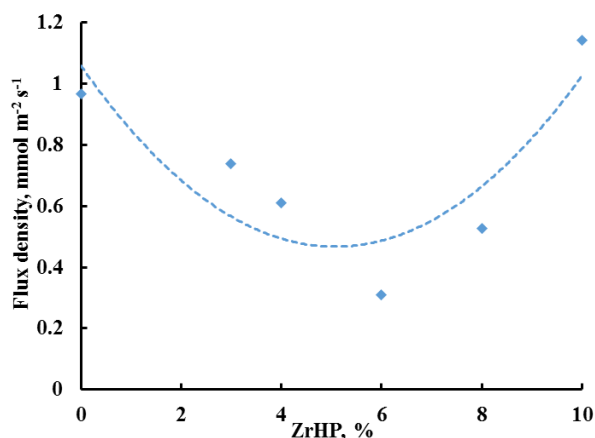


Figure 4. Flux density on the ZrHP content in the membrane

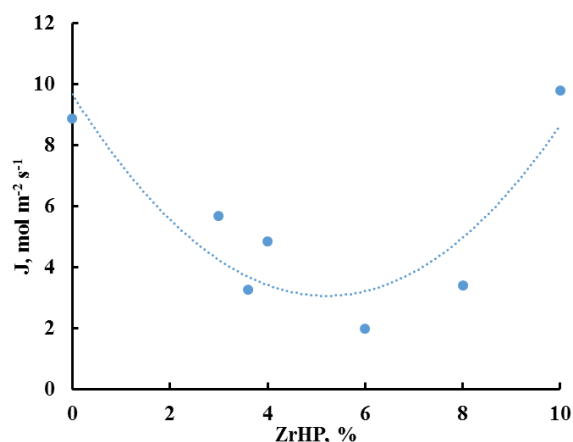


Figure 5. Diffusion flux in 0.1 M HCl solution on the ZrHP content in the membrane

Conclusion

Summing up the results of the study, we can conclude that reducing the thickness of the membrane leads to an increase in power characteristics and the gas permeability. To reduce the gas permeability of thin membranes, the inert fluoropolymers could be introduced into the membrane, in an amount of 10 wt. %. Modification with ZrHP improves the power characteristics of the MEA, with the optimal content being 6 wt. %.

Acknowledgements. This work was supported by the Russian Science Foundation and Kuban Science Foundation (project No 22-19-20101), <https://rscf.ru/project/22-19-20101/>.

References

1. Lyapishev K., Ostanin E., Ivanchenko A., Kononenko N. // *Electrochemistry-2023*. International Conference. Moscow, 2023. P. 397.
2. Li S., Wei X., Dai H., Yuan H., Ming P. // *iScience*. 2022. V. 25. P. 103576.
3. Falina I., Kononenko N., Timofeev S., Rybalko M., Demidenko K. // *Membranes*. 2022. 12. 935.
4. Titskaya E., Varich A., Timofeev S., Lyapishev K., Kononenko N. // *Ion transport in organic and inorganic membranes*. International Conference. Sochi, 2023. P. 293.

HYBRID MEMBRANES POLYBENZIMIDAZOLE/SILICA WITH SILANE CROSSLINKING

Anna Lysova, Andrey Yaroslavtsev

Kurnakov Institute of General and Inorganic Chemistry RAS, Moscow, Russia

E-mail: lysova@igic.ras.ru

Introduction

High temperature polymer electrolyte membrane fuel cells (HT_PEMFC), capable of operating at 120–200 C and low humidity, are among the many promising devices for producing environmentally clean energy [1]. Under these conditions, the catalytic activity of platinum, its tolerance to an increase in CO impurities and fuel cell management are simplified. One of the main types of membrane materials for their construction are polybenzimidazoles (PBI) doped with phosphoric acid (PA). These are of interest due to their high thermal stability, excellent mechanical properties and high proton conductivity at FC operating temperatures.

The PA doping level, temperature and relative humidity are important parameters affecting the proton conductivity of PBI membranes. At the same time, a high PA doping level leads to a deterioration in mechanical strength, dimensional stability and membrane selectivity (an increase in gas permeability). In addition, the conductivity decreases due to acid leaching during FC operation, which leads to an irreversible loss of battery power and the corrosion of components.

The membrane modification by inorganic oxides with high sorption activity promotes both stabilisation of the acid and an increase in the degree of doping, which is important for maintaining high conductivity values [2]. However, as the doping degree increases, the mechanical properties of the membranes and their dimensional stability inevitably deteriorate. Additionally, there is a possibility of migration of dopant particles outside the membrane during FC operation. Covalent crosslinking is a possible method of modification that can enhance mechanical properties and improve the morphological and oxidative stability of membranes [3]. Restricting the pore size of cross-linking bridges can lead to a more compact structure, resulting in reduced gas permeability and acid sorption.

In this work an approach to membrane modification is proposed that combines the introduction of silicon oxide, which has enhanced sorption capacity due to the surface modification with imidazolinpropyl groups, and covalent silanol crosslinking to maintain mechanical and dimensional stability. 3-(Bromopropyl)trimethoxysilane was chosen as the crosslinking agent, on base of previous work [4].

Experiments

Membrane modification was performed using an in situ method. On the first stage, 3-(Bromopropyl)trimethoxysilane was linked to the main PBI chains. On the second one, precursor for silica particle was added. After film formation the hydrolysis was performed with the formation of silane network. The samples are referred to as PBI/SiO₂-(silane)-x, where x is the silica content. The PBI-O-PhT membrane without silane-crosslinking was used as a comparison sample. To ensure conductive properties, all the obtained samples were kept for seven days at 25 C in phosphoric acid (conc. 75%). After that, the weight of the membranes increased 2.5–3 times.

The samples were investigated by different physico-chemical methods. Morphology, conductive properties, oxidative and thermal stability, gas permeability were characterized.

Results and Discussion

The silanol cross-linked samples exhibited higher stability when tested with Fenton's reagent and retained their morphological integrity even after 360 hours of testing. The study shows that covalent crosslinking improves the stability of dopant particles in the membrane matrix and prevents their leaching during acid treatment.

One of the most important properties affecting the capacity of fuel cells based on polyelectrolyte membranes is the proton conductivity. When silica is added, the conductivity increases. Its maximum increase is reached in the high temperature region (36 mS/cm for the reference sample,

52-58 mS/cm for the samples with SiO₂ at 160°C). For the cross-linked samples, the conductivity increases with increasing dopant content and is 33, 38, 43 and 55 mSm/cm at 160°C for samples with 0, 3, 5 and 10 wt% SiO₂, respectively. The silanol cross-linked sample without silica has a slightly lower conductivity compared to the original PBI. This is due to the fact that the structure of the polymer matrix becomes more rigid and the nitrogen atoms of the imidazole ring associated with the organic substituent of the silane are excluded from the proton transfer process. However, as the silica content increases, the membrane conductivity increases slightly, which, according to the theory of the limited elasticity of membrane pore walls, is determined by the simultaneous expansion of pores and connecting channels, which limit the conductivity. An additional factor may be the creation of additional proton transfer centres at the oxygen atoms of SiO₂.

Gas permeability also plays an important role in the application of membranes in FCs. It determines the fuel transfer through the membrane that is not accompanied by energy production. All the samples obtained are characterised by a lower hydrogen permeability compared to the initial PBI membrane, which makes their use in hydrogen energy technology even more attractive.

Acknowledgement. This research was funded by Russian Science Foundation, grant number 21-73-20229.

References

1. Kalathil A., Raghavan A., Kandasubramanian B. // *Polym. Plast. Technol. Mater.* 2019. V. 58. P. 465.
2. Özdemir Y., Üregen N., Devrim Y. // *Int. J. Hydrogen Energy.* 2017. V. 42. P. 2648.
3. Peng J., Fu X., Luo J., Liu Y., Wang L., Peng X. // *J. Membr. Sci.* 2022. V. 643. 120037.
4. Lysova A.A., Ponomarev I.I., Skupov K.M., Vtyurina E.S., Lysov K.A., Yaroslavtsev A.B. // *Membranes.* 2022. V. 12. 1078.

METAL-POLYMER MEMBRANES BASED ON CARDO POLY(BENZIMIDAZOLE) FOR ELECTROMEMBRANE APPLICATIONS

¹Anna Lysova, ^{1,2}Andrey Manin, ¹Daniel Golubenko, ^{1,2}Andrey Yaroslavtsev

¹Kurnakov Institute of General and Inorganic Chemistry of the Russian Academy of Sciences (IGIC RAS), Moscow, Russia, *E-mail: ailyina@yandex.ru*

²Faculty of Chemistry, HSE University, Moscow, Russia

Introduction

Membrane materials have enabled the rapid development of various high-tech processes and devices. The use of ion-exchange membranes in electro dialysis processes allows for deep purification of aqueous media, isolation of valuable components from wastewater [1], production of high-frequency hydrogen in membrane electrolyzers [2], and increased efficiency of fuel cell-based power units [3]. However, creating ion-exchange membranes for electromembrane applications is labour-intensive. Additionally, the resulting materials may not possess the necessary properties for operational and chemical stability.

Poly(benzimidazole)-based membranes, which are used in medium-temperature fuel cells, are among the most stable materials [4]. To confer conductive properties, these materials should be impregnated with concentrated phosphoric acid. However, the most effective method could be the introduction of charged functional groups into the structure of poly(benzimidazole). Therefore, the objective of this study was to create ion-exchange membranes doped with d-metal ions based on carded poly(benzimidazole).

Experiments

The starting material for this study was poly(benzimidazole) based on 3,3',4,4'-tetraaminodiphenyloxide and 3,3-bis(p-carboxyphenyl)phthalide, obtained through a polycondensation reaction. The metal ions selected for the study were Zn²⁺, Cu²⁺, and Cr³⁺. The studied membranes are labelled as *M-number*, where M corresponds to the metal ion in the structure of the cardo-PBI (Zn, Cu and Cr) and the number is the content of the metal ion. The metal thickness distribution of the obtained membranes was studied using scanning electron microscopy with EDX, and IR-spectra were recorded in the ATR mode. To investigate the transport properties of the membranes, we measured the ionic conductivity by impedance spectroscopy and the anion transfer number using a SmartStat PS-20 potentiostat-galvanostat.

Results and Discussion

Ion-exchange membranes are characterised by their conductivity. Non-functionalised membranes based on PBI-analogous polymers lack ionic conductivity. Therefore, the introduction of stable charged groups, such as metal ions, into their structure should result in the appearance of ionic conductivity. The conductivity of the resulting membranes was studied in nitrate form using the contact method. The initial membrane exhibited a conductivity lower than 5·10⁻⁸ S/cm. However, with the introduction of metals, conductivity increases and reaches the level of classical anion exchange membranes. The maximum conductivity value at 25°C was 0.73 mS/cm. Additionally, impedance hodographs of the studied membranes were analyzed, which is another important factor to consider. For both Zn-50 and Zn-100 membranes, the high-frequency half-circle (capacitive) and low-frequency half-circle (double electric layer at the membrane-electrode boundary) are not completely separated and instead smoothly transition into each other. The low-frequency half-circle slope angle of these membranes corresponds to 45 degrees, indicating the significant role of diffusion in the charge/discharge of the double electric layer at the membrane/electrode interface. This is associated with contact inhomogeneity due to changes in surface morphology or composition. For membranes containing copper and chromium ions, the impedance hodographs have a classical form. The data on the conductivity of the membranes obtained in nitrate form confirm the presence of charged groups in the polymer structure, with metal ions playing a role. Additionally, the obtained materials have high transfer

numbers of nitrate-ions, exceeding the corresponding values for commercial anion-exchange membranes.

Acknowledgement. This work was supported by the Russian Science Foundation Grant (23-43-00138).

References

1. *Golubenko D. V., Manin A. D., Wu L., Xu T., Yaroslavtsev A. B.* On the analysis of monovalent-ion selectivity of anion-exchange membranes // *Desalination*. 2024. V. 573. P. 117178.
2. *Stenina I. A., Yaroslavtsev A. B.* Modern Technologies of Hydrogen Production // *Processes*. 2022. V. 11. P. 56.
3. *Safronova E. Yu., Lysova A. A., Voropaeva D., Yaroslavtsev A. B.* Approaches to the Modification of Perfluorosulfonic Acid Membranes // *Membranes*. 2023. V. 13. P. 721.
4. *Lysova A.A., Ponomarev I.I., Skupov K.M., Vtyurina E.S., Lysov K.A., Yaroslavtsev A.B.* Effect of Organo-Silanes Structure on the Properties of Silane-Crosslinked Membranes Based on Cardo Polybenzimidazole PBI-O-PhT // *Membranes*. 2022. V. 12. P. 1078.

MODELLING OF CONCENTRATION POLARIZATION IN A TANGENTIAL FILTRATION CELL WITH RADIAL SOLUTION FLOW

¹Anna Maksimova, ^{1,2}Ilya Ryzhkov

¹Siberian Federal University, Krasnoyarsk, Russia, *E-mail: sokolova.ann2001@gmail.com*

²Institute of Computational Modeling SB RAS, Krasnoyarsk, Russia, *E-mail: away2004@inbox.ru*

Introduction

Baromembrane processes (microfiltration, ultrafiltration, nanofiltration and reverse osmosis) are widely used to separate, purify and concentrate solutions [1]. In these processes, a transmembrane pressure difference is applied, which causes solvent and solute to flow across the membrane. The dissolved substance is completely or partially rejected by the membrane resulting in a highly concentrated layer on its surface that resists mass transfer. This phenomenon is known as concentration polarization [2]. Polarization phenomena accompany many membrane separation processes. Since the reduction of transmembrane flow negatively affects technical and economic performance of the membrane, it is necessary to take measures to eliminate the causes associated with this phenomenon. To reduce concentration polarization, various measures can be applied: stirring the solution, regulating the flow rate along the membrane, or affecting the mass transfer coefficient by changing the module shape and size, e.g. reducing the length or increasing its hydrodynamic diameter [3]. Mathematical modelling is used to better understand and predict the effects of concentration polarization. Previous works considered one-dimensional (film) models and two-dimensional models of concentration polarization, which showed good agreement with experimental data [4].

The purpose of this work is to develop a mathematical model that describes the phenomenon of concentration polarization in a tangential filtration cell with a radial flow of solution. Figure 1a shows a cross-section of a filtration cell, for which we developed a mathematical model and carried out calculations. The feed flow is supplied to the center of the membrane perpendicular to its surface. Then the fluid moves in a radial direction from the center to the edges of the membrane, and is removed through a slot gap adjacent to the membrane edge. The membrane is characterized by liquid permeability and rejection of solute.

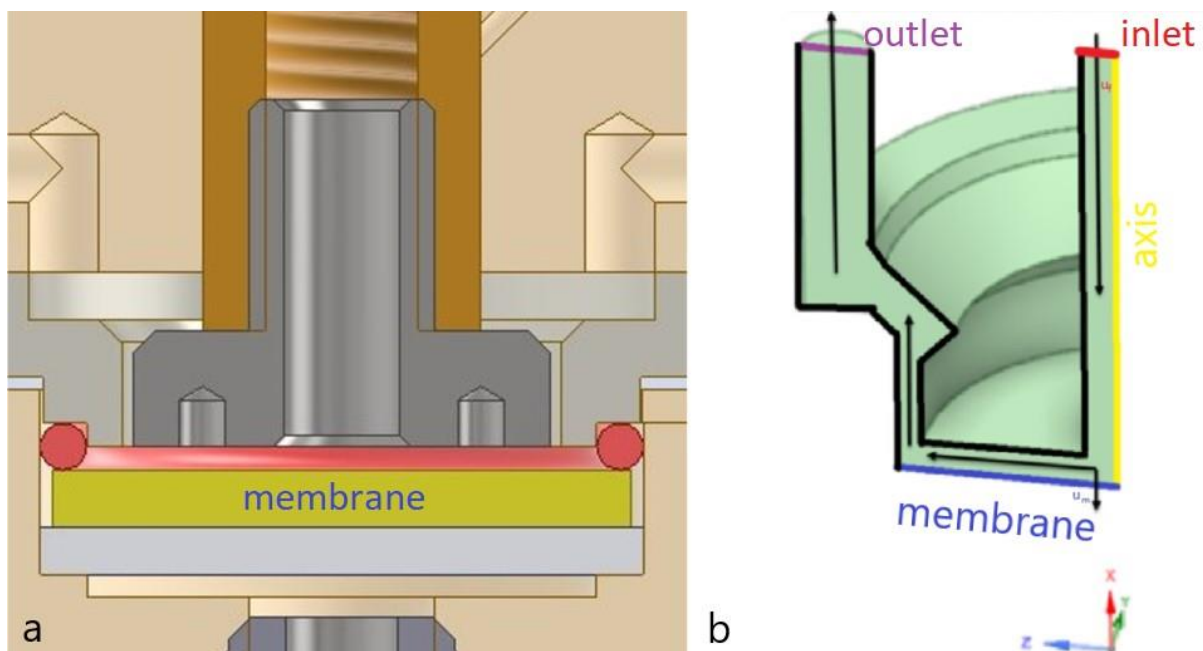


Figure 1 – Cross-sectional view of the filtration cell (a) and the geometry of computational domain (b).

Mathematical model

To simulate the flow in the filtration cell, an axisymmetric mathematical model is used. It is based on the Navier-Stokes equations, the continuity equation and the solute transport equation in

cylindrical coordinates (r, z) . Let us introduce the following notation: $\mathbf{V} = (V_r, V_z)$ is the velocity vector (mm/s), P is the pressure (Pa) and C is the concentration (mol/m³).

A constant volume flow of solution is supplied to the inlet perpendicular to the membrane surface V_f . The solution moves in radial direction from the center to the edges of the membrane and is removed through the slot gaps in the upper part (Figure 1b). At the inlet, the radial velocity component is set to zero and the solute concentration is specified

$$V_z = -V_f, V_r = 0, C = C_f.$$

The no-slip condition and the absence of mass flow of the dissolved component are set on the walls

$$\mathbf{V} = 0, \quad C\mathbf{V} \cdot \mathbf{n} - D \frac{\partial C}{\partial n} = 0,$$

where \mathbf{n} is the surface normal vector, D is the solute diffusion coefficient.

On the surface of the membrane, a constant volume flow of solution it is set to V_m , and the radial velocity component is assumed to be zero

$$V_z = -V_m, \quad V_r = 0.$$

Let us denote the permeate concentration by C_p , and the concentration on the membrane surface by C_m . Then the flux through the membrane is given by

$$J = -C_m V_m - D \frac{dC}{dz}.$$

We assume that $J = -C_p V_m$ resulting in the following boundary condition on the membrane surface

$$C_m R V_m + D \frac{\partial C}{\partial z} = 0, \quad R = 1 - \frac{C_p}{C_m},$$

where R is the rejection of solute. It is assumed that the velocity vector components and concentration do not change in the normal direction to the outlet

$$\frac{\partial V_r}{\partial n} = \frac{\partial V_z}{\partial n} = \frac{\partial C}{\partial n} = 0.$$

Calculations are performed for an aqueous solution of potassium chloride with a diffusion coefficient $1.996 \cdot 10^{-9}$ m²/s, kinematic viscosity $\nu = 1.005 \cdot 10^{-6}$ m²/s and density $\rho = 998.2$ kg/m³.

Results and discussion

Using the computational fluid dynamics package Ansys Fluent R21, we have calculated the dependences of average solute concentration \bar{C}_m on the membrane surface on the feed concentration, the feed flow rate, and the flow rate through the membrane.

Figure 2a shows the curves corresponding to solute rejection of 100%, 90% and 80%. Regardless of the percentage of rejection, in all three cases an increase in the feed flow rate reduces

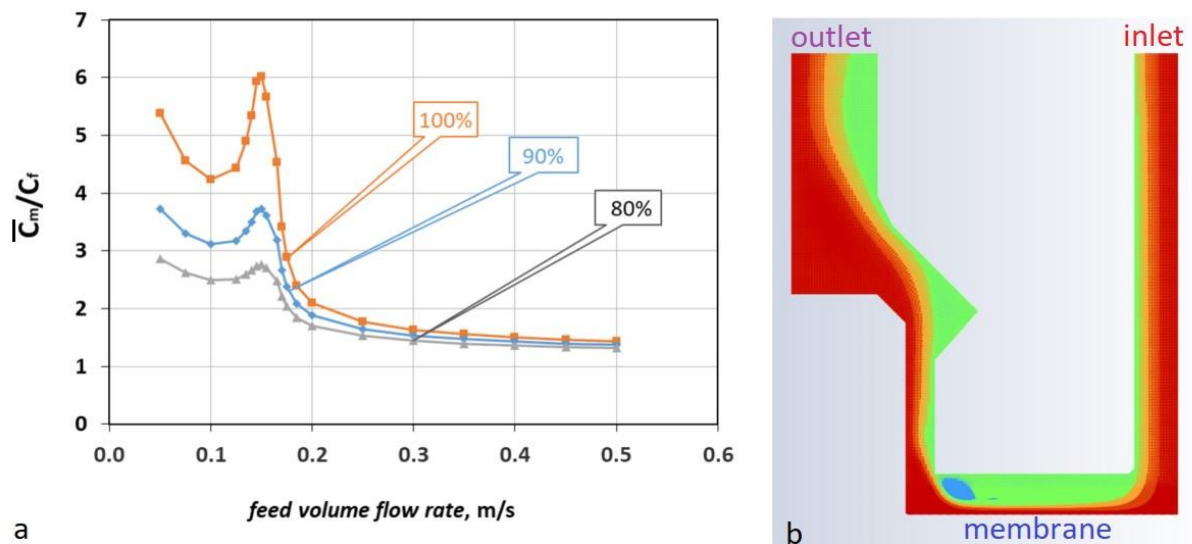


Figure 2 – Dependence of the ratio of average membrane concentration to the feed concentration on feed volume flow rate for a membrane flow rate of 0.0278 mm/s (a). Flow streamlines on the filtration cell (b).

the concentration at the membrane surface due to convective flow along its surface. It is found that the average concentration on the membrane surface increases with increasing solute rejection.

Note that due to the peculiar geometry of the filtration cell, flow separation from the membrane occurs at a distance of 7 mm from the center (Figure 2b, blue color) at feed volume flow rate in the range from 0.1 m/s to 0.2 m/s. It gives a noticeable increase of concentration at the membrane surface near the outlet (Figure 2a). The concentration reaches its maximum value when the feed volume flow rate is about 0.15 m/s. The calculations show that further optimization of the filtration cell design is necessary to eliminate areas with increased concentration on the membrane surface.

Acknowledgement. The work was supported by the Russian Science Foundation, project № 23-19-00269.

References

1. Mulder M. *Basic principles of membrane technology* / Kluwer Academic publishers, Dordrecht / Boston / London, 1999. 512 p.
2. Andrew L. Zydney. *Stagnant film model for concentration polarization in membrane systems* / *Journal of Membrane Science* 130 (1997). P. 275-281.
3. Miranda M., Campos B.L.M., *Concentration polarization in a membrane placed under an impinging jet confined by a conical wall — a numerical approach* / *Journal of Membrane Science* 182 (2001). P. 257–270.
4. Sablani S.S., Goosena M.F.A., Al-Belushi R., Wilf M. *Concentration polarization in ultrafiltration and reverse osmosis: a critical review* / *Desalination* 141 (2001). P. 269-289.

MODIFICATION OF ION-EXCHANGE MEMBRANES WITH CERIUM AND ZIRCONIUM PHOSPHATE PARTICLES TO ENHANCE THE TRANSPORT OF SINGLE-CHARGED IONS

^{1,2}Andrey Manin, ^{1,2}Andrey Yaroslavtsev

¹Kurnakov Institute of General and Inorganic Chemistry of the Russian Academy of Sciences (IGIC RAS), Moscow, Russia, *E-mail: manin1609@mail.ru*

²Faculty of Chemistry, HSE University, Moscow, Russia

Introduction

Ion-exchange membranes have a crucial role in water treatment processes, such as electrodialysis, by allowing for the selective separation of ions with different charge signs under a potential gradient. However, it is also essential to ensure selectivity of ion-exchange membranes for the transportation of ions with the same charge sign but different charge values [1,2]. The membrane materials currently used in the electrodialysis process are unfortunately more selective towards the transport of multi-charged ions. It is challenging to develop materials with a completely new mechanism of ion separation. Therefore, it is urgent to search for barrier-free methods to modify commercial materials to alter their transport selectivity. For instance, composite materials are noteworthy for their ability to combine the properties of the introduced filler (dopant) and the initial matrix in one object. Dopants such as cerium [3], zirconium, silicon, titanium [4] oxides and cerium oxide with functionalized surfaces [5] can be used. Additionally, hybrid membranes containing inorganic ion-exchangers as dopants, such as acidic zirconium phosphate or acidic cerium phosphate, are worth studying.

Modification of Ralex CM membrane with acidic zirconium phosphate increased the selectivity of sodium ion transport in sodium-calcium pairs. Symmetric surface modification also had a similar effect [6]. The study of these materials for the separation of lithium and magnesium ions is also of interest. In the case of anion-exchange membranes, an increase in selectivity for the transport of single-charged anions can be achieved by introducing acidic cerium phosphate, which has cation-exchange properties.

The aim of this work was to obtain and study the properties of hybrid ion-exchange membranes modified with inorganic particles of acidic cerium phosphate and zirconium phosphate and phosphonate.

Experiments

The investigated hybrid membranes were obtained by surface or bulk modification of commercial membranes Ralex® AM and CM, Neosepta AMX and FujiFilm® AEM. To modify the surface, the membranes were fixed in a two-section cell and treated alternately on one side with $(\text{NH}_4)_2[\text{Ce}(\text{NO}_3)_6]$ solutions (for anion-exchange membranes, AEMs), ZrOCl_2 or $\text{Ce}(\text{NO}_3)_3$ solution (for cation-exchange membranes, CEMs). Then, the same side of the membrane was treated with different phosphorus-containing precipitants ($\text{NH}_4\text{H}_2\text{PO}_4$, H_3PO_4 , $\text{Ph-P}(\text{O})(\text{OH})_2$). The CEMs were modified volumetrically by incubating a membrane sample in solutions of concentrated phosphoric acid, in which CeO_2 was pre-dissolved, or in ZrOCl_2 solution. Subsequently, the same membrane samples were placed in a solution of phosphorus-containing precipitant ($\text{NH}_4\text{H}_2\text{PO}_4$, H_3PO_4 , $\text{Ph-P}(\text{O})(\text{OH})_2$). The values of water-uptake ($W_{\text{H}_2\text{O}}$), ion exchange capacity (*IEC*), ionic conductivity (σ), potentiometric transfer numbers (t_i), and selectivity coefficients $P(A/B)$ for the transport of single-charged ions were investigated for all the obtained materials.

Results and Discussion

Ten hybrid commercial AEMs with a gradient distribution of cerium phosphate over the thickness were obtained by varying the time and number of treatment cycles, the concentration of $(\text{NH}_4)_2[\text{Ce}(\text{NO}_3)_6]$, and the nature of the phosphorus-containing precipitant. The content of cerium phosphate varied from 0.5 to 12 wt.% depending on the type of membrane. The study involved varying the type of dopant and its distribution in the polymer matrix, the number of cycles

of surface treatment with precursors, and the type of precipitant for hybrid cation-exchange membranes. This resulted in the production of four volumetrically modified membranes and six surface-modified membranes, containing between 1.2 and 27 wt.% of inorganic dopant, depending on the modification method used.

The study analysed the impact of modification on characteristics such as IEC and W_{H_2O} for the obtained materials. The introduction of acidic cerium phosphate into the membrane resulted in a decrease in IEC and W_{H_2O} for several hybrid AEMs. This was due to the formation of salt bridges between the negatively charged surface of the nanoparticles and the positively charged functional groups of the membrane. The effect was levelled out by increasing the concentration of $(NH_4)_2[Ce(NO_3)_6]$ due to the preferential formation of dopant on the surface. Introducing neutral cerium(III) phosphate into the CEM matrix resulted in a 27% decrease in IEC . However, bulk modification with acidic cerium phosphate had little effect on IEC and W_{H_2O} values. In the case of modifying CEM with zirconium phosphates and phosphonates, a decrease in IEC was observed, particularly for the bulk modified membranes. The introduction of zirconium phosphate led to an increase in W_{H_2O} for all modified membranes. However, for the membrane with volumetric distribution of zirconium phosphonate, the value of W_{H_2O} decreased by more than 20%.

The influence of modification on the transport properties of the studied membranes was considered. Specifically, the σ values in the forms of single- and double-charged ions and t_i were examined. The introduction of cerium phosphate particles into the system of pores and channels of AEMs resulted in a significant decrease in $\sigma(Cl)$. Conversely, the study of $\sigma(SO_4)$ showed a preference for increased values. For CEMs with neutral cerium(III) phosphate, there was a decrease in both $\sigma(Li)$ and $\sigma(Mg)$. In contrast, for membranes with acidic cerium phosphate, these values decreased insignificantly. When modifying CEMs with zirconium phosphates, the values of $\sigma(Li)$ and $\sigma(Mg)$ were lower compared to the original membrane. On the other hand, the values of $\sigma(Na)$ and $\sigma(Ca)$ increased for membranes whose dopant was precipitated with $NH_4H_2PO_4$ and H_3PO_4 , but decreased for all other samples. The hybrid membranes, however, were strongly dependent on the method of dopant production.

As part of the work, model experiments were conducted to study the values of $P(Cl/SO_4)$, $P(Na/Ca)$ and $P(Li/Mg)$. The introduction of cerium phosphate into the pore and channel system of AEMs resulted in a 55% increase in the rate of selective transport of chloride ions relative to sulfate. When investigating the effect of modification with cerium phosphate on the selectivity values of CEMs for transporting single charge ions, it was found that the maximum increase in $P(Li/Mg)$ was 12%. Modification of CEMs with zirconium phosphate allows for an even greater relative increase in selectivity coefficients. The maximum increase in the $P(Na/Ca)$ value was 168%, and the maximum increase in $P(Li/Mg)$ was 108%. The increase in selectivity coefficients in the lithium-magnesium pair is consistent with an increase in the conductivity ratio in these ionic forms. However, the increase in selectivity in the sodium-calcium pair cannot be explained in the same way.

Thus, the work developed methods for modifying commercial ion-exchange membranes with cerium phosphate or zirconium phosphate and phosphonate. The use of cerium phosphate in AEMs resulted in increased selectivity coefficients in both dilute and concentrated salt solutions. It has been demonstrated that modifying CEMs with zirconium phosphate or phosphonate membranes results in the greatest increase in selectivity coefficients.

Acknowledgement. This work was financially supported by Russian Science Foundation (grant No 23-43-00138)

References

1. Sun Y., Wang Q., Wang Y., Yun R., Xiang X., Recent advances in magnesium/lithium separation and lithium extraction technologies from salt lake brine // Sep. Purif. Technol. 2021. V. 256.

2. *Liao J., Chen Q., Pan N., Yu X., Gao X., Shen J., Gao C.*, Amphoteric blend ion-exchange membranes for separating monovalent and bivalent anions in electrodialysis, *Sep. Purif. Technol.* 2020. V. 242.
3. *Kurian M.*, Cerium oxide based materials for water treatment // *J. Environ. Chem. Eng.* 2020. V. 8.
4. *Golubenko D., Shaydullin R., Yaroslavtsev A.*, Improving the conductivity and permselectivity of ion-exchange membranes by introduction of inorganic oxide nanoparticles: impact of acid–base properties // *Colloid Polym. Sci.* 2019. V. 297. P. 741-748.
5. *Stenina I., Yurova P., Achoh A., Zabolotsky V., Wu L., Yaroslavtsev A.*, Improvement of Selectivity of RALEX-CM Membranes via Modification by Ceria with a Functionalized Surface // *Polymers.* 2023. V. 15. P. 647.
6. *Golubenko D., Karavanova Yu., Melnikov S., Achoh A., Pourcelly G., Yaroslavtsev A.*, An approach to increase the permselectivity and mono-valent ion selectivity of cation-exchange membranes by introduction of amorphous zirconium phosphate nanoparticles // *J. Membr. Sci.* 2018. V. 563. P. 777-784.

THEORETICAL STUDY OF LIQUID FLOW IN AN ELECTRODIALYZER CHAMBER WITH A SPACER

Semyon Mareev, Mikhail Petryakov, Andrey Gorobchenko, Artem Mareev, Ilya Moroz, Victor Nikonenko

Kuban State University, Krasnodar, Russia, *E-mail: mareev-semyon@bk.ru*

Introduction

Electrodialysis (ED) is one of the effective methods in wastewater treatment [1]. The limiting factor of ED is the concentration polarization, which depends on the diffusion layer thickness. A various spacers are actively used to reduce this factor [2]. Significant progress in the development of spacer has been achieved in the ultrafiltration and reverse osmosis processes. Along with experiments, mathematical modeling is carried out for the above processes. In this study, the spacer proposed in [2] theoretically was studied with the aim of it application in the ED process.

Experiment

One of the proposed spacers was adapted from [2]. It was created using a 3D modeling program FreeCAD and printed using a Phrozen Sonic Mighty 8K Resin 3D Printer (Fig. 1) for experimental studies, described in [3]. The spacer has the following characteristics: the diameter of longitudinal rods is 0.75 mm, located at a distance of 5 mm from each other in two directions at an angle of 45 and 135 degrees relative to the walls of the electro dialyzer chamber, cylinders perpendicular to the surface of the membranes with a diameter of 2 mm, ensuring fixation of the rods at a strictly specified distance from membranes.

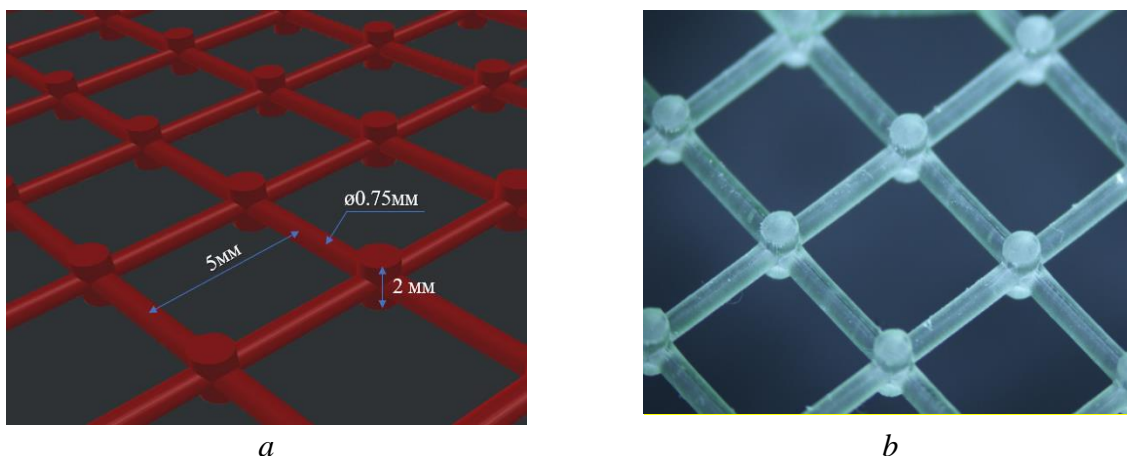


Figure 1. 3D Model (a) and 3D Printed Version (b) of Spacer.

Theory

A three-dimensional model of liquid flow in electro dialyzer was created. The model geometry accurately repeats the constructed geometry of the electro dialyzer chamber (Fig. 2). The stationary liquid flow is described by the Navier-Stokes equations for a solid ideal incompressible Newtonian fluid. The following boundary conditions were used: a plug-flow profile is set at the inlet, a constant pressure and zero back-flow are set at the outlet, and a no-slip condition is set at all other boundaries.

The calculations were carried out in COMSOL Multiphysics 5.5 software.

Results and Discussion

The theoretical distribution of liquid flow in the system under study was obtained using spacer and without using it (Fig. 3). This spacer made it possible to evenly distribute the liquid flow, significantly reduce the stagnant areas and increase the liquid flow directly near the surface of the membranes. It can be seen that despite the lateral location of the inlet and outlet of the electro dialyzer chamber, the efficiency of spacer is beyond doubt. Further theoretical studies will make it possible to determine the optimal arrangement of spacer rods across the chamber width.

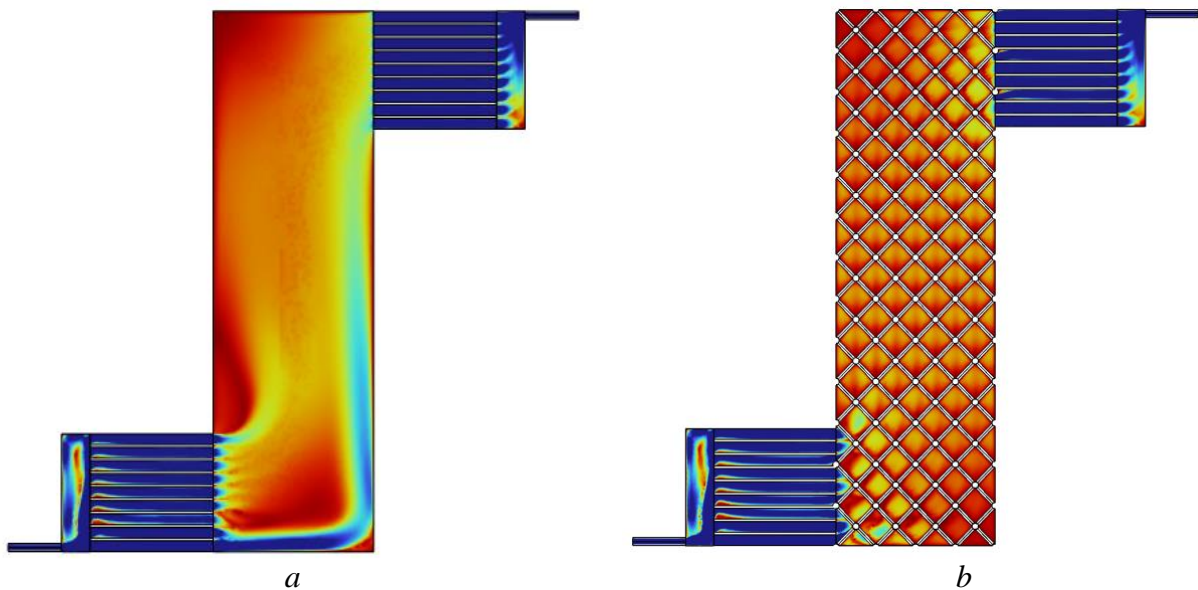


Figure 2. Theoretical Distribution of Liquid Flow in the Studied Electrodialyzer Chamber Without a Spacer (a) and With It (b). Red Color Corresponds to Low Flow Velocity, Blue – High Flow Velocity.

Acknowledgement. The study is realized with the financial support of the Russian Science Foundation, project № 22-79-10177.

References

1. Garcia-Vasquez W., Dammak L., Larchet C., Nikonenko V., Grande D. Effects of acid-base cleaning procedure on structure and properties of anion-exchange membranes used in electro dialysis // *J. Membr. Sci.* 2016. V. 507. P. 12–23.
2. Qamar A., Kerdi S., Ali S.M. Novel hole-pillar spacer design for improved hydrodynamics and biofouling mitigation in membrane filtration // *Sci. Rep.* 2021. V. 16. No. 6979.
3. Ruleva V. D., Ponomar M. A., Gorobchenko A. D., Moroz I. A., Shkirskaya S. A., Kononenko N. A., Wang Y., Jiang C., Xu T., Nikonenko V. V. Electro dialysis of moderately concentrated solutions: Experiment and modeling based on a simplified characterization of ion-exchange membranes // *Desalination.* 2024. V. 508. 117533.

POLYIMIDE MEMBRANES FOR THE HYDROGEN CONCENTRATION FROM GAS MIXTURES

Dmitry Matveev, Tatyana Anokhina, Vladimir Volkov, Ilya Borisov, Stepan Bazhenov

A.V. Topchiev Institute of Petrochemical Synthesis Russian Academy of Sciences, Moscow, Russia

E-mail: dmatveev@ips.ac.ru, tsanokhina@ips.ac.ru, vvolkov@ips.ac.ru, Boril@ips.ac.ru, sbazhenov@ips.ac.ru

Introduction

Ammonia is an important intermediate in various branches of the chemical industry, and as a result is produced in significant volumes (19.9 million tonnes in 2021). In order to improve efficiency, the process of producing ammonia from a mixture of hydrogen and nitrogen involves a step of recovering hydrogen from purge gases. In addition to its traditional applications (in the production of fertilizers, plastics, and other products), ammonia has been recently seen as a potential easily liquefiable carrier of hydrogen for transportation of hydrogen fuel to locations of consumption and the development of a hydrogen-based energy infrastructure. This development further increases the importance of research into hydrogen extraction techniques from gas mixtures that contain nitrogen and its derivatives.

Among the existing technologies for the separation of gas mixtures, membrane gas separation processes have a significant prospect for the separation and purification of hydrogen. Membrane devices are characterized by their modularity, compact design due to the high packing density of membranes in the device, ease of installation and maintenance, as well as scalability. Additionally, the performance of the membrane-based separation system is excellent. Polymer membranes based on polyimides have been successfully used for the separation and purification of hydrogen due to their thermal and chemical stability, satisfactory performance, and separation selectivity.

Therefore, the aim of this study was to investigate a polyimide film as a potential material for concentrating hydrogen from gas mixtures.

Experiments

The dense membranes were cast from solution in chloroform with polymer concentrations of 2 wt.% onto commercial cellophane. The cast film was then covered with a Petri dish and left for slow evaporation for several days, followed by drying until a constant sample weight was reached. This enabled membranes to be obtained with a thickness of 20–30 μm .

The resulting film was analysed for the permeability of individual gases using a Time Lag Machine. Gas permeability and diffusion coefficients of membrane materials for individual gases (N_2 , CO_2 , CH_4) were measured at 30 °C according to Daynes–Barrer standard technique using the precise unit “Helmholtz-Zentrum Geesthacht” mounted with a pressure sensor (“Baratron”), with an accuracy of 10^{-7} bar. Permeability was given in Barrer. Pure gas permeability coefficient P_i was determined by the variable pressure/constant volume method, the diffusivity D_i was measured according to the time-lag method, and the solubility coefficient S_i was estimated as.

Results and Discussion

The results of the measurements of the polyimide film for individual gases are provided in Table 1 below.

Table 1: Gas transport properties of polyimide film for individual gases.

Gas	Permeability coefficient, Barrer	Diffusion coefficient, cm^2/s	Solubility coefficient, $\text{cm}^3/(\text{cm}^3 \cdot \text{cm Hg})$
H_2	11.4	$2.2 \cdot 10^{-6}$	$5.2 \cdot 10^{-4}$
N_2	0.064	$1.4 \cdot 10^{-8}$	$4.6 \cdot 10^{-4}$
He	12.3	$4.9 \cdot 10^{-5}$	$2.5 \cdot 10^{-5}$
CH_4	0.076	$1.2 \cdot 10^{-9}$	$6.3 \cdot 10^{-3}$
CO_2	3.6	$5.8 \cdot 10^{-9}$	$6.1 \cdot 10^{-2}$

The table shows the gas transport properties of polyimide. It can be noted that the polymer has acceptable values of gas permeability coefficients for helium, hydrogen and carbon dioxide, as

well as a low gas permeability value for methane. As a result, the material is characterized by high selectivity for helium/methane, hydrogen/methane and carbon dioxide/methane (162, 150 and 47, respectively). Thus, the polymer is promising for membrane separation applications such as natural gas conditioning and hydrogen separation from process gas streams.

Acknowledgement. The study was supported by a grant from the Russian Science Foundation No. 24-49-02058, <https://rscf.ru/en/project/24-49-02058/>

POROUS POLYSULFONE HOLLOW FIBER SUPPORTS WITH LOW MASS TRANSFER RESISTANCE FOR THE PRODUCTION OF GAS SEPARATION COMPOSITE MEMBRANES

Dmitry Matveev, Ilya Borisov, Evgenia Grushevenko Vladimir Vasilevskii, Tatyana Anokhina, Vladimir Volkov

A.V. Topchiev Institute of petrochemical synthesis RAS, Moscow, Russia, *E-mail: dmatveev@ips.ac.ru, Boril@ips.ac.ru, evgrushevenko@ips.ac.ru, vasilevskii@ips.ac.ru, tsanokhina@ips.ac.ru, vvvolkov@ips.ac.ru*

Introduction

Membrane separation is a low-energy; environmentally friendly technology that effectively solves many issues of gas separation and purification, due to, among other factors, the ease of scale-up and operation. For real applications where cost and energy efficiency should be considered, an important factor, along with selectivity, is the performance of the membrane. Composite membranes with ultra-thin selective layers are a rapidly developing area of academic research and commercialization for new types of membranes [1]. The simplest version of a composite membrane is a structure composed of a layer of a selective, usually nonporous material, located on the surface of a porous support made from another material [1]. It is worth noting that hollow fiber composite membranes have several advantages compared to flat-sheet membranes. The most significant advantage is the high packing density of the hollow fibers in the module [2]. This significantly increases the efficiency of the device per unit volume. In early research on composite membranes, it was believed that the porous support performed only a mechanical role for a thin selective layer [3]. However, later research has shown that, at high flow rates, the porous support can significantly contribute to the overall resistance to gas transfer through the membrane [4]. Therefore, it is important to minimize the contribution of the porous support when development of highly permeable composite membranes.

Experiments

To create a hollow fiber membrane, a dope solution was prepared using polysulfone (PSF) as the membrane-forming polymer, N-methyl-2-pyrrolidone as the solvent, and polyethylene glycol with an average molecular weight of 400 g/mol (PEG-400) as pore-forming additive. PSF and PEG-400 were combined in a thermostated reactor and stirred at 150 rpm at a temperature of 50 °C. N-methyl-2-pyrrolidone was then added to the reactor, increasing the stirring speed to 500 rpm. The resulting dope solution was then filtered under a pressure of 0.18 to 0.2 MPa using a stainless steel filter with a mesh size of 4 to 5 µm. The filtered solution was degassed using a vacuum pump to remove any air bubbles.

Samples of hollow fiber membranes were prepared using a dry-wet phase inversion method in the "free spinning" mode. Different bore liquids (n-hexane, n-heptane, ethanol/hexane mixture (20/80 wt.%) were introduced into the liquid capillary of the dope solution, and the top side of the capillary was irrigated with distilled water. This is known as the "wet air gap" method. After spinning, the membranes were successively washed with tap water, ethanol for two hours, and n-hexane for two hours, followed by drying in air at room temperature.

To evaluate the gas transport properties of the produced hollow fiber membranes, the permeability of helium (He), nitrogen (N₂) and carbon dioxide (CO₂) was measured using the volumetric method. The membrane structure was investigated using scanning electron microscopy (SEM) using a Thermo Fisher Phenom XL G2 Desktop SEM facility (USA).

A thin polymer layer of polydecylmethylsiloxane (PDecMS) was applied onto the top surface of the hollow fiber supports. Composite PDecMS/PSF membranes were produced by the direct dip coating process [27]. The support was immersed in the PDecMS solution for several minutes, then removed and dried in an oven for 24 hours at 100°C, where the solvent evaporated and crosslinking occurred.

Results and Discussion

Three samples of hollow fiber porous supports were spun using n-hexane, n-heptane and an ethanol/hexane mixture (20/80 wt.%) as bore liquids, respectively. They are designated as S-hex, S-hep and S-e/h, respectively. The hollow fiber supports were studied by SEM. As an example, Figure 1a displays a photomicrograph of a cross-section of the S-hex support. In the first approximation, the support morphology can be described as consisting of the following layers of porous structures: a finely porous skin layer on the top surface, a transitional layer with a spongy structure, and, next, an internal drainage layer with characteristic finger-like macrovoids. Figures 1b-1d shows micrographs of the lumen side for all supports in more detail. As be seen in Figures 1b-1d, large pores are observed on the lumen side of PSF supports spun using C6–C7 alkanes. However, if a weak coagulant (ethanol/hexane mixture) is used, there are no micron-sized pores on the lumen side of the hollow fiber, which indicates a denser skin layer structure.

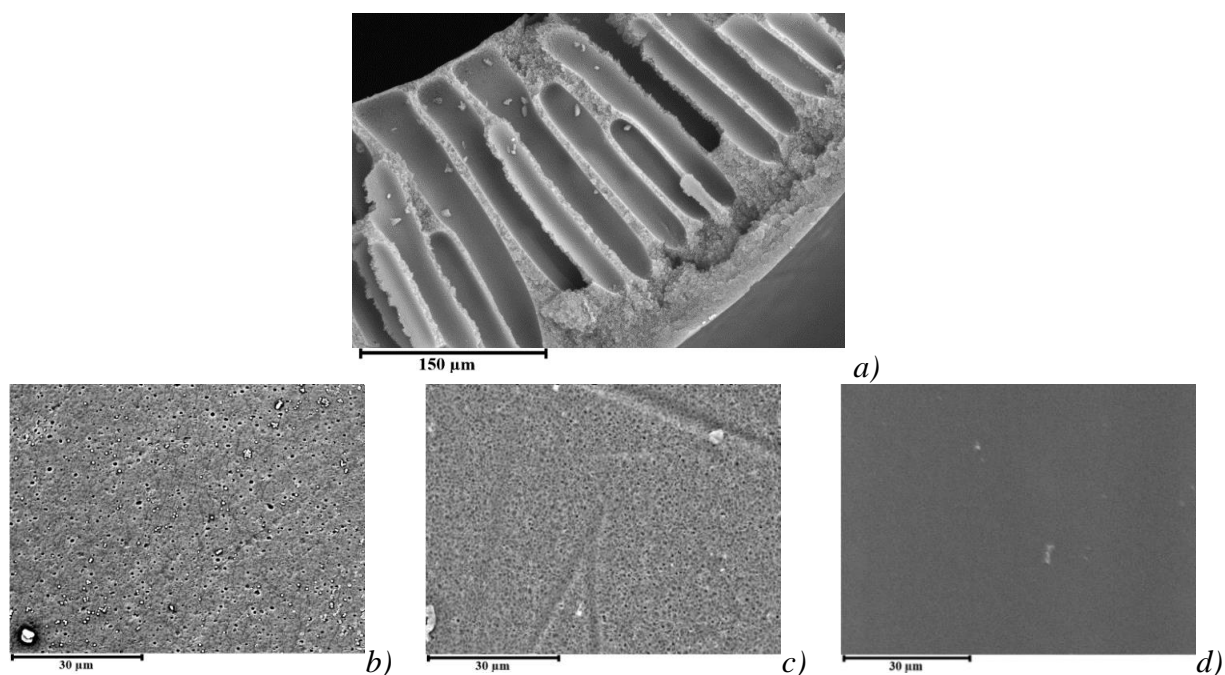


Figure 1. SEM images of a) the cross-section of the S-hex support; b) the lumen side of the S-hex; c) the lumen side of the S-hep and d) the lumen side of the S-e/h.

Table 1 presents the geometric dimensions of hollow fiber PSF supports: inner (ID) and outer (OD) diameters and wall thickness (L). The transport properties of the resulting hollow fiber PSF supports are shown in Table 1. It was found that when hexane and heptane are used as bore liquids, the permeance of the hollow fiber support membranes significantly increases. For example, in the case of CO₂, these values increase from 20400 to 36700 GPU for hexane and heptane, respectively. The ideal He/CO₂ selectivity is equal to 3 for S-hex and S-hep supports, which indicates that the Knudsen regime of gas flow through the porous structure of the membranes is realized. Of particular interest is the comparison of the gas permeances of S-hex and S-e/h hollow fiber supports with the same geometric dimensions (Table 1). It can be seen that the addition of as little as 20% of ethanol, which is a coagulant for PSF, to hexane reduces the CO₂ permeance by a factor of forty: 20400 and 550 GPU for S-hex and S-e/h, respectively. Thus, it can be concluded that the spinning of hollow fiber supports using alkanes (hexane or heptane) as “inert bore liquids” results in significantly more efficient PSF supports than by addition of a weak coagulant into the fiber. As it can be seen from Figures 1b and 1d, in the case of an ethanol/hexane (20/80 wt.%) mixture, a porous structure that is formed on the lumen side of the S-e/h support is denser than on the S-hex support. The presence of this additional skin layer significantly impairs the gas transport properties of the S-e/h support. It is worth adding that the transport properties of hollow fiber PSF supports developed in this work using hexane and heptane as the bore liquids are by an order of magnitude better than those of similar PSF supports described in the literature [5].

Table 1: Properties of the hollow fiber PSF supports.

Support	ID, mm	OD, mm	L, μm	Permeance, GPU			α (He/CO ₂)
				He	CO ₂	N ₂	
S-hex	1.1	1.7	300	61500	20400	25200	3.0
S-hep	1.5	1.9	200	110000	36700	44400	3.0
S-e/h	1.1	1.7	300	1700	550	670	3.1

Using S-hex and S-e/h supports, hollow fiber composite membranes with a selective layer of PDecMS with a thickness of 3 μm were obtained (PDecMS/S-hex and PDecMS/S-e/h, respectively) and the transport properties was investigated. For the first time, a modified resistance model has been proposed that takes into account the resistances of a selective polymer layer on the membrane surface (R_1), a layer of this polymer that has penetrated into the pores of the support and the surface layer of the support material (R_2) and transport pores of the support (R_3). At the same time, for the first time a more general approach is being considered, where the thickness of the selective polymer layer that has penetrated the pores of the support is not necessarily equal to the thickness of the porous support skin-layer itself. Using a modified resistance model, it has been demonstrated that the presence of macropores on the lumen side of a hollow fiber can reduce the contribution from the support resistance by up to 10%, while simultaneously increasing the contribution from the selective layer resistance to the overall resistance of the composite membrane by a factor of two (see Table 2).

Table 2: Resistance components for gas permeation in the PDecMS/PSF hollow fiber composite membrane.

Resistance Membrane	$R_1, \times 10^{10}$ s Pa/mol	$(R_2+R_3), \times 10^{10}$ s Pa/mol	$R, \times 10^{10}$ s Pa/mol	$R_1/R, \times 100\%$
N ₂				
PDecMS/S-hex	6.43	23.91	30.34	21.2
PDecMS/S-e/h	5.37	42.01	47.38	11.3
CO ₂				
PDecMS/S-hex	0.59	2.29	2.88	20.5
PDecMS/S-e/h	0.50	3.34	3.84	13.0

Acknowledgement. This research was financially supported by the State Program of TIPS RAS.

References

1. Baker R., Low B. Gas separation membrane materials: a perspective // *Macromolecules*. 2014. V. 47. № 20. P. 6999-7013.
2. Peng N., Widjojo N., Sukitpaneelit P., Teoh M., Lipscomb G., Chung T., Lai J. Evolution of polymeric hollow fibers as sustainable technologies: Past, present, and future // *Prog. Polym. Sci.* 2012. V. 37. № 10. P. 1401-1424.
3. Henis J., Tripodi M. A novel approach to gas separations using composite hollow fiber membranes // *Sep. Sci. Technol.* 1980. V. 5. № 4. P. 1059-1068.
4. Park H., Kamcev J., Robeson L., Elimelech M., Freeman B. Maximizing the right stuff: The trade-off between membrane permeability and selectivity // *Science*. 2017. V. 356. № 6343. P. eaab0530.
5. Matveev D., Borisov I., Grushevenko E., Vasilevsky V., Anokhina T., Volkov V. Hollow fiber PSF fine porous supports with ultrahigh permeance for composite membrane fabrication: Novel inert bore liquid (IBL) spinning technique // *Sep. Purif.* 2024. V. 330. P. 125363.

ION TRANSPORT IN ELECTROMEMBRANE SYSTEM WITH BILAYER ION-EXCHANGE MEMBRANE WITH OPPOSITELY CHARGED LAYERS

Stanislav Melnikov, Victor Zabolotsky

Kuban State University, Krasnodar, Russia, E-mail: melnikov.stanislav@gmail.com

Introduction

In the field of membrane electrochemistry, anisotropic ion-exchange membranes were initially discussed by Friette (as a bipolar membrane) [1] and Leitz (as cationic-anionic) [2]. Both studies outline an ion-exchange membrane comprising cation-exchange and anion-exchange layers; the distinction lies in Leitz's proposal of a membrane capable of desalting sodium chloride while simultaneously alkalizing or acidifying the solution.

Researchers in [3] referred to membranes capable of both desalting and adjusting the pH of a solution as "semi-bipolar." The drawbacks of these semi-bipolar membranes include a lack of mechanical stability. However, incorporating a modifying layer made of an ion-polymer film can yield mechanically stable "semi-bipolar" membranes.

Enhancing stability and specific ion selectivity involves depositing thin layers/films on the substrate membrane's surface. This specificity typically targets singly charged ions [4], focusing on the permselectivity coefficient. Some studies also highlight a reduction in the limiting current on the modified membrane compared to the original one [5].

When the charge of the modifying layer's matrix opposes the charge of the membrane-substrate matrix at their interface, a space charge region forms, with electric field strengths reaching around 109 V/m. Essentially, most ion-exchange membranes with similar surface modifications can be considered asymmetric bipolar membranes. Zabolotskiy et al. [6] demonstrated that asymmetric bipolar membranes can maintain high salt flux at low currents, functioning similarly to bipolar membranes at high current densities.

Unlike the production of acid and alkali, adjusting the pH of a solution does not necessitate the use of bipolar membranes with high selectivity. Additionally, it is feasible to integrate the desalination process with simultaneous pH adjustment, as suggested by Leitz. However, the salt ion flux through bipolar membranes is notably low. Nevertheless, asymmetric bipolar membranes are well-suited for this specific application.

In our prior studies, we have made progress in understanding the regulations governing ion transfer processes in bilayer membranes. In [7], we demonstrated the feasibility of creating inorganic catalysts for the water splitting reaction in an asymmetric bipolar membrane. In [6], we illustrated that the combination of Gerischer and finite Warburg elements in series could elucidate the impedance spectrum of an asymmetric bipolar membrane. In [8] we observed a transition in the nature of the limiting current in bilayer membranes from outerdiffusional to interdiffusional. In [9] a mathematical model was introduced for the numerical simulation of the current-voltage curve of the bilayer (bipolar) membrane.

In this study, we define asymmetric and conventional bipolar membranes and monovalent selective membranes as bilayer membranes. The term "bilayer membranes" emphasizes that their main function is not predetermined during synthesis but can change based on operational conditions. We aim to investigate the electrochemical processes with the use of bilayer membranes under different working conditions, considering factors such as current density, solution composition, and chemical nature of the layers.

Results and Discussion

Reactive separation of a mixture of strong and weak electrolytes

Effective removal of the strong electrolyte (chloride ion) from a mixture with the anion of a weak acid is possible when the water dissociation reaction on the bipolar membrane proceeds at a noticeable rate, while the rate of accumulation of molecular acid in the volume of the processed solution is still sufficiently low. Evaluation of ion transport numbers through the bipolar membrane shows that effective separation is possible within a fairly narrow range of ratios of salt ion (chloride ions) and hydrogen ions transport numbers (1.5-1.8), in a "mixed" mode of bipolar operation,

where salt ion transport and water dissociation proceed with sufficient efficiency. Under these conditions, the selectivity coefficient of the chloride/total acetate pair increases from 3.3 ± 0.2 (for the substrate membrane) to 61 ± 21 .

Electrodialysis desalination with simultaneous pH correction

A kinetic model of an electromembrane system has been developed to describe the ion transport process and pH changes over time. Analytical expressions have been derived for the concentration dependence of all solution components over time for certain specific cases. These analytical expressions can be used to calculate small electrolysers designed for pH adjustment of solutions. Solving the mathematical model yields a dataset showing the pH dependence of the solution in the acidic or alkaline chambers of the electrolysers as a function of current density and membrane channel length. By knowing the operational dimensions of one chamber of the electrolysers, the volumetric flow rate of the solution, and the linear flow rate of the solution through the electrolysers chamber, one can determine the number of elementary cells required to adjust the pH to the desired value.

Preparation of lithium hydroxide from lithium chloride in the presence of non-aqueous solvents (dimethylacetamide and isobutyl alcohol)

The study presents the test results of an electromembrane installation designed for the comprehensive processing of the process solution formed during the production of para-aramid fibers. The installation is divided into two main blocks and employs three different electrolysers: the first block is an electrolysers with bipolar membranes aimed at producing lithium hydroxide (EDS-m); the second block is a standard electrolysis module intended for the preliminary treatment of the process solution and concentration of lithium chloride (ED-m), while a dialyser with ion-exchange packing (EDN-16) is used for final purification and complete removal of ionic impurities from the solution. Optimal process parameters were identified, enabling the processing of 6.3 m³ of process solution per day.

The original process solution contains N,N-dimethylacetamide, isobutyl alcohol, lithium chloride, hydrochloric acid, iron ions, and water. The lithium hydroxide production process was tested using both an aqueous concentrate of lithium chloride obtained through ED-m (cycles 31-77) and a neutralized process solution containing up to 40% organic solvents (cycles 1-30). The composition of the solutions at the inlet and outlet of the main tracts of the installation is presented in a table.

Table 1: Mean chemical composition of the solutions

Component	H ₂ O, %	DMAA, %	IBA, %	LiCl, %	HCl, %	LiOH, %	pH
Unit inlet (cycles 1-30)	59.71	25.46	14.75	0.84	-	0.03	11.3
Unit inlet (cycles 31-77)	98.13	1.31	0.56	2.09	-	0.08	11.8
ED-m DC outlet	59.07	27.01	13.93	0.07	-	0.03	9.7
EDS-m alkali outlet	99.26	0.56	0.18	0.17	-	0.66	12.7
EDS-m acid outlet	99.41	0.5	0.09	-	0.89	-	0.8
EDN-16 DC outlet	57.46	27.32	15.22	-	-	-	7.6

Sodium naphthenate conversion

The study focused on processing sodium naphthenate to produce naphthenic acids and alkalis using bipolar electrolysers. A membrane stack arrangement was proposed, comprising a bipolar membrane and two cation exchange membranes. To enhance the process efficiency, it was recommended to add a strong electrolyte (like sodium sulfate) to the sodium naphthenate solution. The incorporation of sodium sulfate into the solution resulted in an increase in current yields for naphthenic acids from 0.23 to 0.4 and a decrease in specific energy consumption from 0.9 to 0.4 kWh/L.

Two-stage electrodialysis scheme for wastewater treatment.

In practical processes (including the ones described above), the current efficiencies for bipolar electrodialysis often drop to 0.3-0.5. The decline in current efficiency during bipolar electrodialysis is directly related to the non-selective transfer of salt ions into acid or alkaline solutions.

A potential solution to this issue is a two-stage technology for recovering concentrated acids and alkalis from salt solutions. In the first stage, salt recovery is performed, resulting in diluted solutions containing few salt impurities. In the second stage, these diluted solutions (either acid, alkali, or both) are concentrated in an electrodialyzer-concentrator with non-flow-through concentration chambers.

The results of the research on the two-stage scheme for obtaining sulfuric and nitric acids are presented in Table 2.

Table 2: Results for different acids production using one-stage and two-stage scheme

Acid	Stage	Acid concentration, M	Salt cations concentration in acid (Na ⁺ /NH ₄ ⁺), M	Current efficiency, η	Specific energy consumption, E, kWh/mole
H ₂ SO ₄	BPED using MB-3	0.41	0.024	0.66	0.73
	BPED using MB-2m	0.71	0.050	0.75	0.68
	Stage I (BPED using MB-3)	0.10	0.002	0.89	0.40
	Stage II (EDC)	1.16	0.005	0.26	0.43
HNO ₃	BPED using MB-3	0.38	0.087	0.49	1.26
	Stage I (BPED using MB-3)	0.10	0.005	0.91	0.40
	Stage II (EDC)	1.69	0.005	0.22	0.86

Acknowledgement. The study was supported by a grant from the Russian Science Foundation № 22-13-00439, <https://rscf.ru/project/22-13-00439/>

References

1. *Frilette V.J.* Preparation and Characterization of Bipolar Ion Exchange Membranes. // J. Phys. Chem. 1956. V. 60. P. 435–439.
2. *Leitz F.B.* Cationic-Anionic Ion-Exchange Membrane. U.S. Patent 3,562,139, 9 February 1971.
3. *Antonov Y.A., Ponomarev M.I., Volkov S.A., Grebenyuk V.D.* Production of alkali with simultaneous water desalination in electrodialyzer with semi- bipolar membranes. // Sov. J. Water Chem. Technol. 1983. № 5. P. 454–456.
4. *Luo T., Abdu S., Wessling M.* Selectivity of ion exchange membranes: A review. // J. Memb. Sci. 2018. Vol. 555. P. 429–454.
5. *White N., Misovich M., Yaroshchuk A., Bruening M.L.* Coating of Nafion membranes with polyelectrolyte multilayers to achieve high monovalent/divalent cation electrodialysis selectivities. // ACS Appl. Mater. Interfaces. 2015. № 7. P. 6620–6628.
6. *Zabolotskii V.I., Sheldeshov N.V., Melnikov S.S.* Effect of cation-exchange layer thickness on electrochemical and transport characteristics of bipolar membranes. // J. Appl. Electrochem. 2013. V. 43. P. 1117–1129.
7. *Melnikov S.S., Shapovalova O.V., Sheldeshov N.V., Zabolotskii V.I.* Effect of d-metal hydroxides on water dissociation in bipolar membranes. // Pet. Chem. 2011. V. 51. P. 577–584.
8. *Melnikov S., Bondarev D., Nosova E., Melnikova E., Zabolotskiy V.* Water splitting and transport of ions in electromembrane system with bilayer ion-exchange membrane // Membranes. 2020. V. 10. P. 346.
9. *Melnikov S.* Ion transport and process of water dissociation in electromembrane system with bipolar membrane. Modelling of symmetrical case // Membranes. 2023. V. 13. P. 47.

RESEARCH OF THE PROCESS OF LIMITED ELECTRODIALYSIS CONCENTRATION OF SALTS, ACIDS AND ALKALI

Stanislav Melnikov, Svetlana Eterevsikova, Victor Zabolotsky

Kuban State University, Krasnodar, Russia, E-mail: vizab@chem.kubsu.ru

The impact of electrolyte nature on the concentration process utilizing a Ralex CMH/Ralex AMH membrane pair has been investigated (fig. 1).

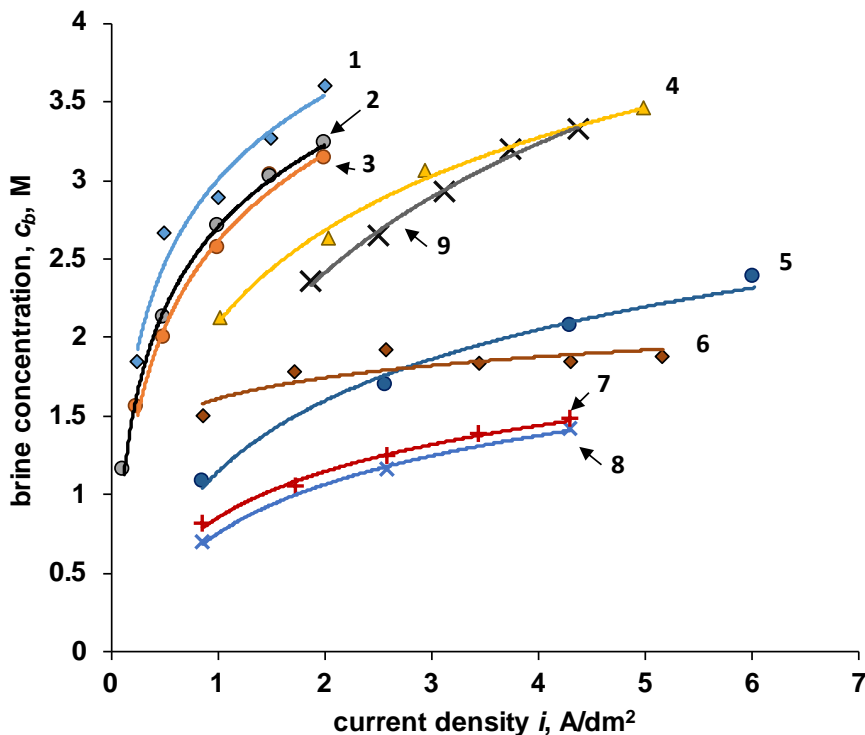


Figure 1. Brine concentration vs. current density. Solutions are:

1 – 0,1 M NaCl, 2 – 0,06 M NH₄NO₃, 3 – 0,3 M NH₄NO₃, 4 – 0,28 M LiCl, 5 – 0,3 M HNO₃, 6 – 0,15 M Na₂SO₄, 7 – 0,15 M H₂SO₄, 8 – 0,3 M H₂SO₄, 9 – 0,15 M NaOH

The data reveals that the maximum achievable concentrations for salt solutions surpass those of acid and alkali solutions. Through the lens of the limiting electro dialysis concentration model, transport coefficients for various membrane pairs have been determined (Table 1).

Table 1 – Calculated transport coefficients for membrane pair Ralex CMH/Ralex AMH for various solutions

Solution	η	β , molH ₂ O/mol-solute	P_s , 10 ⁻³ dm/h	P_w , 10 ⁻³ dm/h
NaCl 0,28 M	0,82	11,8±0,5	1,4	31
NH ₄ NO ₃ 0,06 M	0,68	10,0±0,6	1,7	49
NH ₄ NO ₃ 0,3 M	0,65	11,1±0,5	2,2	31
LiCl 0,28 M	0,76	16,6±1,1	1,6	270
Na ₂ SO ₄ 0,15 M	0,49	26,8±0,8	1,4	105
H ₂ SO ₄ 0,15 M	0,30	12,2±0,9	1,8	400
H ₂ SO ₄ 0,3 M	0,28	14,5±0,9	1,2	358
HNO ₃ 0,3 M	0,29	11,2±1,2	1,3	217
NaOH 0,15 M	0,60	5,5±0,8	0,6	325

It has been ascertained that for ammonium nitrate and sodium chloride, the primary reason for brine concentration decrease is the electroosmotic transfer of solvent within the hydration shells of ions, with osmotic transfer and electrolyte back diffusion exerting minimal influence. In the case of lithium chloride, at current densities up to 1 A/dm², osmotic solvent transfer to the concentration chamber predominates over the electroosmotic mechanism. However, at current densities exceeding 2 A/dm², electroosmotic water transfer emerges as the limiting mechanism.

In a sulfuric acid solution, osmotic water transfer remains significant across all current densities examined, alongside nonselective proton transfer through the anion-exchange membrane, contributing significantly to the electrolyte concentration decrease in the concentration chamber. For sodium hydroxide, the primary concentration-reducing mechanism is the osmotic water flow. These findings on the influence of electrolyte nature on transfer mechanisms can inform the design and operation of concentrator electrolysers and/or bipolar electrolysers.

The salt flux through the membrane pair is solely dictated by the electromigration current efficiency, while the brine concentration is restricted by the electrolyte hydration number. In the case of acids, solution concentration diminishes due to both electroosmotic and osmotic water flows into the concentration chamber, whereas for sodium hydroxide, the osmotic solvent flow holds the most sway. The diminished current efficiency observed during acid solution concentration stems from the non-selective proton transfer through the anion-exchange membrane from the concentration chamber to the desalination chamber. These conducted studies enable the selection of membranes and electrical modes that optimize the concentration of electrolytes in specific electrolysis processes.

Acknowledgement. This study was supported by the Russian Science Foundation, research project no. 22-13-00439, <https://rscf.ru/project/22-13-00439>

DIFFUSION PROPERTIES OF THE MF-4SK PERFLUORINATED MEMBRANES WITH VARYING CONTENTS OF INERT FLUOROPOLYMER AND HYDRATED ZIRCONIUM PHOSPHATE

¹Ekaterina Meshcheryakova, ¹Irina Falina, ¹Natalia Kononenko, ²Sergey Timofeev

¹Kuban State University, Krasnodar, Russia, E-mail: katerina6327095@gmail.com

²JSC «Plastpolymer», St. Petersburg, Russia, E-mail: svtimof@mail.ru

Introduction

There are several requirements for membranes used in a fuel cell, including mechanical strength, proton conductivity in limited humidity conditions, low gas permeability and resistance to degradation in an oxidizing conditions [1]. Introduction the inert fluoropolymer to the membrane composition permits to reduce the diffusion and gas permeability of the membrane. Intercalation of the zirconium hydrogen phosphate (ZrHP) improves the proton conductivity of the membrane in restricted humidity, but increases its permeability [2, 3]. It is possible to achieve a compromise of these characteristics by adding inert fluoropolymer and zirconium hydrogen phosphate in membranes structure simultaneously. The purpose of present study is to investigate the effect of adding the inert fluoropolymer and hydrated zirconium phosphate to the perfluorinated membrane structure on its diffusion properties.

Experiments

The objects of study were the series of experimental cation exchange perfluorinated MF-4SK membranes obtained by casting with content of inert F-2M fluoropolymer (polyvinylidene fluoride) from 15 to 25 % and zirconium hydrogen phosphate (ZrHP) from 4 to 8%. The two-compartment cell was used to determine diffusion permeability of membranes. The diffusion flux was determined under the transport of electrolyte through the membrane to chamber initially filled with water. The concentration growth was registered by conductometry.

Results and Discussion

Dependences of the membrane diffusion permeability in hydrochloric acid solution on inert fluoropolymer and ZrHP content are presented in Figures 1 and 2. It is shown that diffusion permeability coefficient value for the samples containing 4% and 6% of ZrHP decreases with introduction of F-2M fluoropolymer in membrane structure. However, varying the content of the inert fluoropolymer in the pure membranes from 15 to 25% does not lead to a significant change in diffusion permeability (Figure 1). The diffusion permeability of membranes containing 20% of F-2M fluoropolymer does not significantly change as the content of ZrHP changes from 0 to 6 wt. %, while the sample with 8 wt. % of ZrHP has 20 % higher diffusion permeability than other samples (Fig. 2).

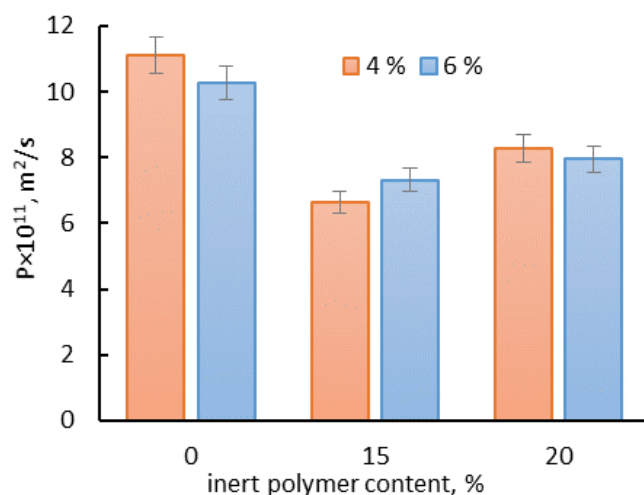


Figure 1. Dependence of the diffusion permeability of perfluorinated MF-4SK membranes with various concentration of ZrHP on the mass fraction of inert F-2M fluoropolymer in 0.5 M HCl.

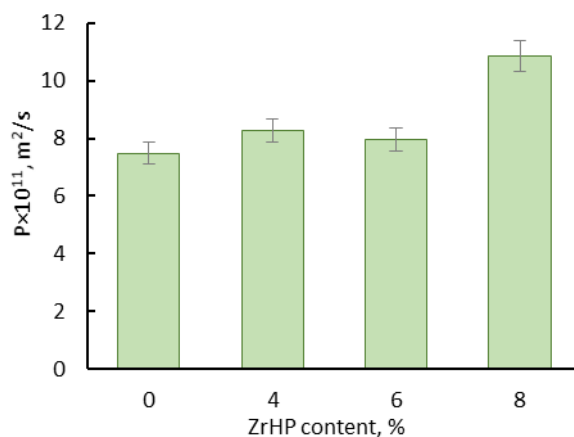


Figure 2. Dependence of the diffusion permeability of perfluorinated MF-4SK membranes with 20% of F-2M fluoropolymer on the mass fraction of ZrHP in 0.5 M hydrochloric acid solution.

A study of the concentration dependences of the specific conductivity of membranes in hydrochloric acid solutions with concentrations from 0.01 to 0.075 M shows that for all samples it amounts to 0.2 – 0.45 S/m.

Investigation of the membranes conductivity in conditions of restricted humidity and elevated temperature would permit to obtain additional information about influence of both components on membrane transport properties.

Acknowledgement. The study was supported by the Russian Science Foundation and Kuban Science Foundation (project No. 22-19-20101), <https://rscf.ru/en/project/22-19-20101/>

References

1. Falina I., Kononenko N., Timofeev S., Rybalko M., Demidenko K. Nanocomposite Membranes Based on Fluoropolymers for Electrochemical Energy Sources // *Membranes*. 2022. V. 12, № 10. P. 935.
2. Golubenko D.V., Shaydullin R.R., Yaroslavtsev A.B. Improving the conductivity and permselectivity of ion-exchange membranes by introduction of inorganic oxide nanoparticles: impact of acid–base properties // *Colloid and Polymer Science*. 2019. V. 297. P. 741–748.
3. Karimi M.B.; Mohammadi F.; Hooshyari K. Recent approaches to improve Nafion performance for fuel cell applications: A review. *Int. J. Hydrogen Energy* 2019. V. 44. P. 28919–28938.

MEMBRANES BASED ON POLYELECTROLYTE COMPLEX OF SODIUM ALGINATE/POLYETHYLENIMINE MODIFIED WITH GRAPHENE OXIDE

Olga Mikhailovskaya, Ksenia Sushkova, Anna Kuzminova, Roman Dubovenko, Anastasia Penkova, Mariia Dmitrenko

St. Petersburg State University, 7/9 Universitetskaya nab., St. Petersburg 199034, Russia,
E-mail: mihajlovskaya.olga.1@yandex.ru, <https://go.spbu.ru/rgpenkova>

Introduction

Nowadays, membrane technologies can be an alternative for traditional separation methods as they are related to sustainable processes. Pervaporation is the most perspective method for separation of liquid mixtures of compounds with low molecular weights, especially for bioalcohol dehydration. The use of bioalcohols as a sustainable energy source is gaining global interest. The rapid development of pervaporation requires novel materials with tailored properties and effective membranes based on them. Thereby, polyelectrolytes are received great attention as a promising membrane material for this. The creation of membranes based on polyelectrolyte complex (PEC) (formed from opposite charged polyelectrolytes) allow getting optimal membrane functionality and improved selective water permeation due to the “salting-out-effect” towards organic substances. Also, one of the promising areas is the modification of membranes with nanoparticles, namely, the creation of mixed matrix membranes.

Experiments

In this work, novel highly effective pervaporation membranes based on a polyelectrolyte complex (PEC) made from polyethylenimine (PEI) and sodium alginate (SA) modified with graphene oxide (GO) were developed for dehydration of bioalcohols. The effect of PEI/SA ratio and GO (1-5 wt.%) concentration in the PEC composition on membrane characteristics was investigated. To enhance the performance of dense membranes, supported membranes with a thin selective layer, obtained from PEC and PEC/GO composite, and deposited onto a porous substrate from polyacrylonitrile (PAN) were developed. To achieve stability of supported membranes in diluted solutions, chemical cross-linking with glutaraldehyde and H_2SO_4 as a catalyst was applied. Structure and physicochemical properties of composites and membranes from them were studied by microscopic and spectroscopic methods, measurements of water contact angles, thermogravimetric analysis. Transport properties of membranes were evaluated in pervaporation for dehydration of ethanol in a wide concentration range (4-90 wt.% water).

Results and Discussion

The development of the supported membrane allowed decreasing the thickness of the selective layer from 50 μm to 500 nm, while the cross-linking led to smoother structure of the inner morphology and surface of the selective layer (Figure 1).

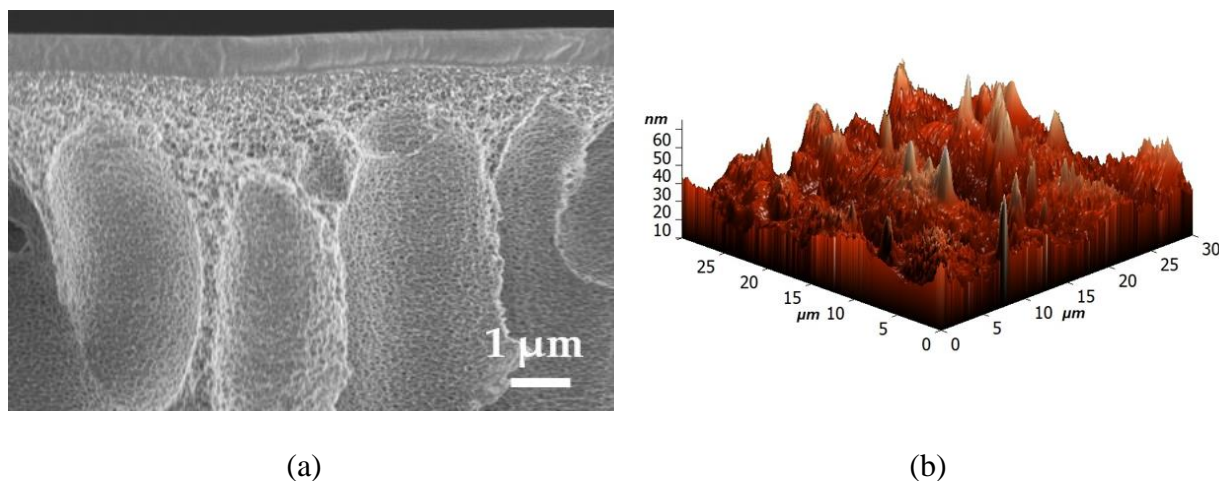


Figure 1. (a) The cross-sectional SEM micrographs and (b) surface AFM image of cross-linked supported membrane based on PEC (50/50 ratio of SA/PEI) modified with 2.5 wt.% GO.

The cross-linked supported membrane with the thin selective layer based on PEC (50/50 ratio of SA/PEI) modified with 2.5 wt.% GO deposited onto PAN substrate demonstrated 2 times increased permeation flux and higher selectivity compared to the pristine SA membrane.

Acknowledgements. This research was funded by Russian Science Foundation, grant number 23-73-01070, <https://rscf.ru/en/project/23-73-01070/>. The experimental work was facilitated by the equipment from the Resource Centers for Nanotechnology, Magnetic Resonance, Cryogenic Department, Thermogravimetric and Calorimetric Research Centre, Computing Centre, Chemical Analysis and Materials Research Centre, and Centre “Nanofabrication of Photoactive Materials (Nanophotonics)” at the St. Petersburg State University.

STUDY OF THE INFLUENCE OF THE STRUCTURE OF IRIIDIUM-CONTAINING ELECTROCATALYSTS ON THE CATALYTIC ACTIVITY OF THE OXYGEN EVOLUTION REACTION

¹Elizaveta Moguchikh, ¹Angelina Pavlets, ²Margarita Kozlova, ¹Anastasia Solovyova, ¹Anastasia Alekseenko

¹Southern Federal University, Rostov-on-Don, Russia, *E-mail: liza.moguchix@mail.ru*

²National Research University "Moscow Power Engineering Institute", Moscow, Russia

Introduction

Electrolysis of water is an electrochemical process that produces pure green hydrogen, which can later be used as fuel [1]. However, the slow kinetics of the anodic oxygen evolution reaction (AER) and the insufficient durability of the catalysts limit the conversion efficiency and large-scale application of electrolyzers [2]. Currently, much research is aimed at developing highly efficient, durable and economical electrocatalysts for OER. Under highly electro-oxidative conditions in an acidic environment, the precious metal Ir and its oxides are considered the most effective materials, possessing high catalytic activity in the OER and stability [3, 4].

Experiments

In this study, we investigated the influence of the composition and structure of iridium-containing electrocatalysts on their activity in the oxygen evolution reaction.

For the study, iridium catalysts were obtained using liquid-phase synthesis methods. Ethylene glycol and NaBH₄ were used as reducing agents. The structural characteristics of the obtained materials were studied using X-ray phase analysis. Catalysts obtained using ethylene glycol as a reducing agent have an Ir/IrO₂ and Ir/IrO_x structure (Tab. 1) and are characterized by a small crystallite size of up to 1.5 nm. The material obtained using NaBH₄ is iridium black (Tab. 1), with a crystallite size of up to 3 nm. The electrochemical characteristics of the resulting materials were assessed using a rotating disk electrode in a three-electrode cell.

Table 1: Functional characteristics of iridium containing catalysts

Material	Average crystallite size (XRD), nm	I.mA/cm ² (E=1.53V)	I.mA/cm ² (E=1.55V)	Overvoltage, mV	Tafel, mV/Dec
Ir/IrO _x	<1	12.3	29.0	324	44
Ir/IrO ₂	1.5	10.9	25.6	336	46
Ir	2.9	3.2	8.3	406	50
Com	3.0	1.7	3.5	412	54

Results and Discussion

The Ir/IrO_x and Ir materials show current density values at a potential of 1.53 and 1.55 V, as well as a lower overvoltage OER value, compared to commercial materials. A catalyst with an oxidized surface of nanoparticles exhibits activity 8.3 times higher than its commercial counterpart. The activity of materials in OER was assessed by linear voltammetry using polarization curves (Table 1). For comparison of activity, a commercial analogue of Com is shown in Figure 1d. To achieve 10 mA/cm² the commercial catalyst required an initial overvoltage of 412 mV. The overvoltage values of the materials under study change: Ir/IrO_x > Ir/IrO₂ >> Ir ≥ Com.

Materials with an oxidized surface of Ir/IrO₂ and Ir/IrO_x nanoparticles exhibit activity 8 times higher than the commercial analogue and show an overvoltage value of the OER significantly lower than for iridium black and the commercial analogue. Thus, the use of ethylene glycol as a reducing agent helps to obtain an iridium catalyst with a small crystallite size, having a non-binary structure, which is a mixture of iridium and iridium oxides and is characterized by high functional characteristics, significantly exceeding the commercial analogue.

Acknowledgement. The research was carried out with the support of the Ministry of Science and Higher Education of the Russian Federation within the framework of the state assignment in the field of scientific activity No. FENW-2023-0016

References

1. *Tan X., Shen J., Semagina N., Secanell M.* Decoupling structure-sensitive deactivation mechanisms of Ir/IrOx electrocatalysts toward oxygen evolution reaction // *Journal of Catalysis*. 2019. V. 371, P. 57–70
2. *Tahir M., Pan L., Idrees F., Zhang X., Wang L., Zou J.-J., Wang Z.L.*, Electrocatalytic oxygen evolution reaction for energy conversion and storage: A comprehensive review // *Nano Energy*. 2017. V. 37. P. 136–157
3. *Pushkarev A. S., Pushkareva I. V., Akelkina S.V., Kozlova M. V., Grigoriev S. A., Kuleshov N. V., Bessarabov D. G.* Electrocatalytic materials for solid polymer electrolyte water electrolyzer // *J. Phys.: Conf. Ser.* 2020. V. 1683. P. 052022
4. *Zlatař M., Escalera-López D., Rodríguez M. G., Hrbek T., Götz C., Joy R. M., Savan A., Tran H. P., Nong H.N., Strasser P., Cherevko S.* Standardizing OER Electrocatalyst Benchmarking in Aqueous Electrolytes: Comprehensive Guidelines for Accelerated Stress Tests and Backing Electrodes // *ACS Catal.* 2023. V. 13. P. 15375–15392.

ELECTRODIALYSIS OF MODERATELY CONCENTRATED SOLUTIONS USING A SPECIALLY DESIGNED CELL CHAMBERS

Ilya Moroz, Mikhail Petryakov, Valentina Ruleva, Maria Ponomar, Svetlana Shkirkaya, Natalia Kononenko, Victor Nikonenko

Kuban State University, Krasnodar, Russia, E-mail: ilya__moroz@mail.ru

Introduction

In recent years, Zero Liquid Discharge (ZLD) or Minimal Liquid Discharge has received an increasing amount of attention in the literature. ZLD systems use combined circuits including membrane methods. It is known from the literature that the use of internal collectors leads to a decrease in current efficiency due to current leakage through these collectors [1,2], also known as ionic shortest currents, possibly due to transport of ions through the multimembrane system past the membranes. With an increase in the concentration of the processed brine, when using membranes with large area resistance, in the case of relatively short channels and large manifolds, leakage currents increase. In addition, spacers significantly influence the efficiency of electro dialysis by reducing the concentration polarization phenomenon.

Development

A new electro dialyser chamber with external collectors was designed and printed on a Phrozen Sonic Mighty 8K Resin 3D Printer. The chambers were printed directly with spacers was adapted from the work [3].

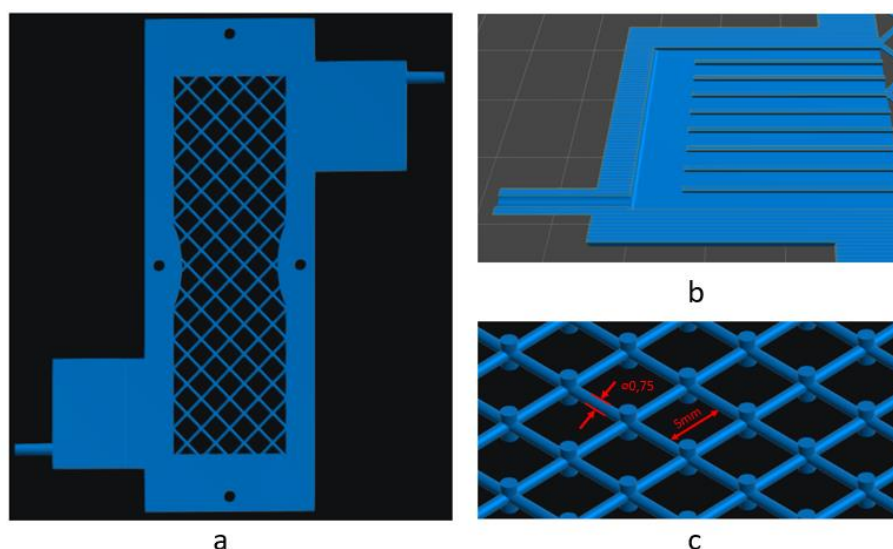


Figure 1. 3D Model of the Developed Chamber (a), Collector that is Located at the Inlet and Outlet of the Chamber (b) and the Spacer (c).

The working area of the chamber is 10 cm long and 3 cm wide, the intermembrane distance is 2 mm. A small wall refinement is also added in the center of the chamber to avoid leaks and membrane damage. The collector consists of a connector with nine channels each 2 mm wide, 23 mm long and 0.6 mm high. In spacer, all threads and cylinders across the solution flow are 0.75 mm.

Results and Discussion

For experiments, an electro dialysis cell with three desalination, three concentration and two buffer chambers were assembled. MA-41 and MK-40 membranes were used. Concentration and desalination were carried out using 0.1 M NaCl solution which was pumped in desalination, concentration and buffer chambers. 0.065 M Na₂SO₄ solution was pumped in the electrode chambers, at this concentration the electrical conductivity of the solution coincided with the other chambers.

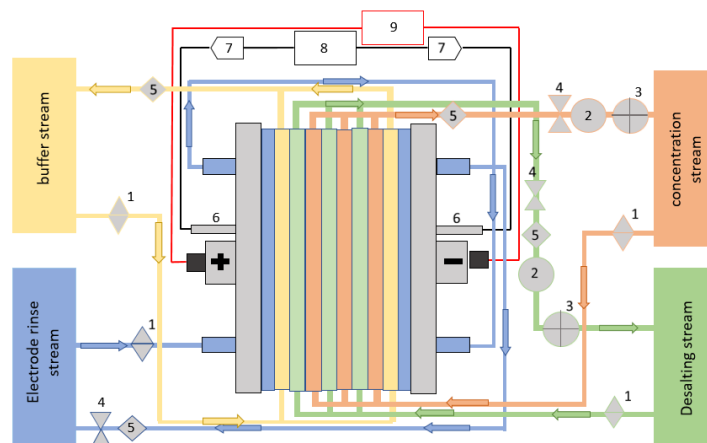


Figure 2. Schematic Representation of the System Used for Electrodialysis concentration of Solutions: 1 - Membrane Pump; 2 - pH Sensor; 3 - Conductometric Sensor; 4 - Solution Cooling System; 5 - Rotameter; 6 - Luggin Capillaries; 7 - Silver Chloride Electrodes; 8 - Voltmeter; 9 - Current Source.

During concentration, 100 ml of solution was pumped through the concentration chambers and 10 L was pumped through the desalination chambers. For desalination, 10 L of solution was pumped through the concentration chambers and 100 ml through the desalination chambers. In 3600 seconds, the solution was concentrated at a current of 0.75 A from 0.011 S to 0.055 S, in order to know if we do not reach the limit state, the pH was monitored in the cells. The distillation process was carried out at 11 V, and in 1800 seconds an electrical conductivity of solution changed from 0.011 S to 0.0005 S.

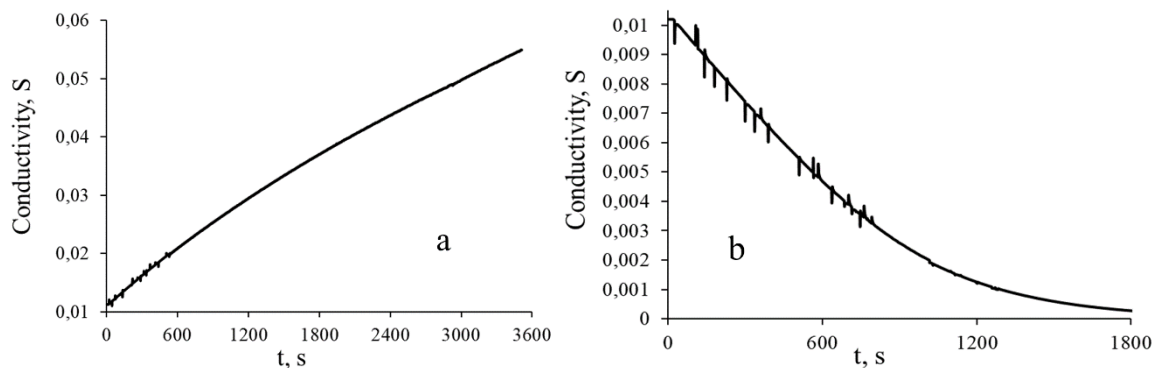


Figure 3. Time dependence of conductivity at concentration (a) and at desalination (b) process.

Acknowledgement. The study is realized with the financial support of the Russian Science Foundation, project № 22-79-10177.

References

1. Veerman J., Post J. W., Saakes M., Metz S. J., Harmsen G. J. Reducing power losses caused by ionic shortcut currents in reverse electrodesialysis stacks by a validated model // J. Memb. Sci. 2008. V.310. P. 418–430.
2. Culcasi A., Gurreri L., Zaffora A., Cosenza A., Tamburini A., Cipollina A., Micale G. Ionic shortcut currents via manifolds in reverse electrodesialysis stacks // Desal. 2020. V. 485. No. 114450.
3. Qamar A., Kerdi S., Ali S.M., Shon H., Vrouwenvelder J. S., Ghaffour N. Novel hole-pillar spacer design for improved hydrodynamics and biofouling mitigation in membrane filtration // Sci. Rep. 2021. V.11. No. 6979.

THE EFFECT OF THE CONDITIONS FOR OBTAINING MEMBRANES FROM PERFLUORINATED IONOMERS ON THEIR PROTON CONDUCTIVITY, HYDROGEN PERMEABILITY AND ELECTROCHEMICAL PARAMETERS OF FUEL CELLS BASED ON THEM

¹Sofia Morozova, ¹Sergey Golubkov, ¹Tatiana Statsenko, ¹Vladimir Likhomanov, ²Grigorii Don, ³Evgenii Sanginov, ³Andrei Belmesov, ¹Aleksey Kashin, ³Aleksey Levchenko

¹Moscow Institute of Physics and Technology, National Research Institute, Institutsky Lane, d 9, Dolgoprudny, Russia, E-mail: morozova.sm@mipt.ru, golserg97@yandex.ru, tatianastatsenko@yandex.ru, vlikhomanov@gmail.com, kashin.am@mipt.ru.

²InEnergy Company Group, Moscow, 111524 Russia; E-mail: don@inenergy.ru

³Federal Research Center for Problems of Chemical Physics and Medical Chemistry of the Russian Academy of Sciences, Academician Semenov Ave., 1, Chernogolovka, Russia; E-mail: sanginov@icp.ac.ru, belmesovaa@mail.ru, a.levchenko@icp.ac.ru.

Introduction

Fuel cells (FC) based on proton exchange membranes demonstrate advanced technology and, despite existing examples of vehicles based on them, continue to actively develop towards increasing efficiency and miniaturization of devices. The present work is aimed at obtaining Aquivion-type polymer membranes by solution casting method and comparing their mechanical strength, structure, transport properties and electrochemical performance with annealing and type of liquid phase in the polymer dispersion.

Experiments

Short side chain polymer was synthesized by emulsion copolymerization of tetrafluoroethylene with 2-fluorosulphonyl perfluoroethylvinyl ether (Aquivion structure). Based on the obtained polymer, membranes were prepared using N,N-dimethylacetamide (DMAA) or a water-alcohol mixture as a liquid phase for polymer dispersion. The resulting membranes were annealed in vacuum at various temperatures. Their proton conductivity and hydrogen permeability have been studied and membrane electrode assemblies (MEA) have been tested for the best samples.

Results and Discussion

Membrane obtained from water-alcohol dispersion had higher hydrogen permeability in comparison to DMAA based films and Nafion 211, but they demonstrated higher proton conductivity (σ) slightly exceeding the data for Nafion 211 (Fig. 1a,b). MEA with the best membrane demonstrated power characteristics 400 mW/cm² which was higher than an MEA with a commercial Nafion 211 membrane.

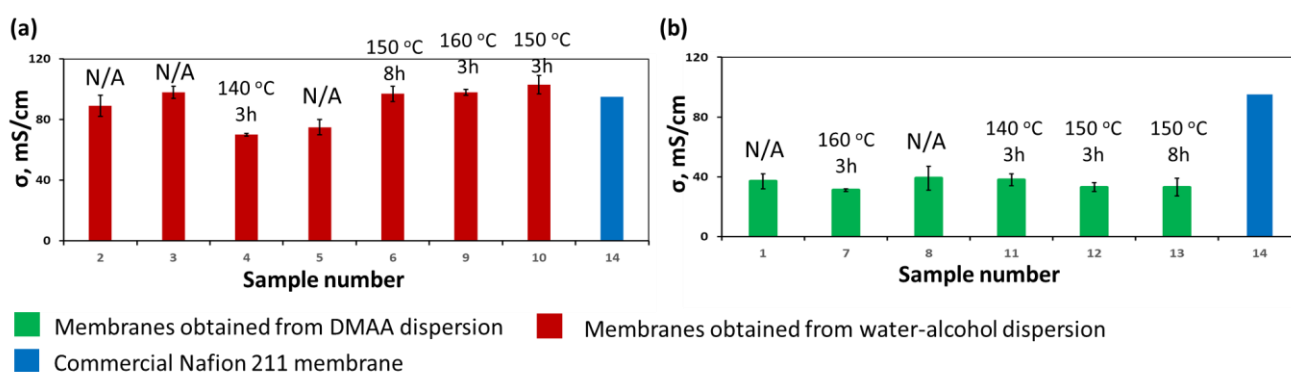


Figure 1. Proton conductivity for membranes obtained from water-alcohol based dispersions (a) and DMAA dispersions (b).

Acknowledgement. This research was financially supported by the Ministry of Science and Higher Education of the Russian Federation (State task) 075-03-2023-106, project No FSMG-2022-0012.

THEORETICAL STUDY OF THE EFFECT OF CHANGES IN THE DISSOCIATION/RECOMBINATION RATE CONSTANT IN THE DIFFUSION LAYER OF A CATION EXCHANGE MEMBRANE ON SALT ION TRANSPORT

Roman Nazarov, Anna Kovalenko, Victor Nikonenko, Makhmet Urtenov

Kuban State University, Krasnodar, Russia, E-mail: r.nazarov1998@mail.ru

Introduction

The change in the rate constant of water dissociation at interphase boundaries is important for understanding the processes occurring in transport processes using ion-exchange membranes. An increase in the rate constant of dissociation of water molecules at interphase boundaries (membrane/solution or membrane/membrane) can have several reasons, as indicated in [1].

There are three approaches to explain this increase for bipolar membranes:

1. Weakening of the H-OH bond in a water molecule under the influence of an electric field
2. Model of cooperative proton transfer through a chain of favorably oriented water molecules
3. Exponential dependence of the water dissociation rate constant on the electric field strength

This work examines the effect of the electric field on the equilibrium constant of the dissociation/recombination reaction of water molecules. It is currently accepted that the equilibrium constant in strong fields depends exponentially on the electric field strength.

Mathematical model

We propose to use a formula where, unlike others, the change in the speed of the equilibrium constant is associated with the magnitude of the space charge, and not the magnitude of the tension.

Indeed, as follows from the Poisson equation $\varepsilon_r \frac{dE}{dx} = \rho(x)$, if the intensity E is large but constant, then we find that the electrical neutrality condition $\rho(x) \equiv 0$ is satisfied. This means that there should be no increase, since, in the region of electrical neutrality, the dissociation rate constant is constant.

Thus, we find that the change in the dissociation rate should depend on the magnitude of the space charge, that is, $K_w(\rho)$. Expanding this formula into the Taylor series in ρ and limiting ourselves to the first approximation, we obtain $K_w(\rho) = K_{w0} + b\rho$, where b is a constant that must be determined, for example, from experimental data, and K_{w0} is the usual classical equilibrium constant. In this work, we conduct a study by considering b as a parameter and changing it within certain limits.

Using this formula, we propose the following mathematical model of the stationary transfer of salt ions for a 1:1 electrolyte in the diffusion layer of a cation-exchange membrane, considering the space charge and the dissociation/recombination reaction, the system of equations of which

has the form: $-\frac{dj_i}{dx} + R_i = 0$ (1), $j_i = -z_i \frac{F}{RT} D_i C_i \frac{d\varphi}{dx} - D_i \frac{dC_i}{dx}$ (2), $\frac{d^2\varphi}{dx^2} = -\frac{\rho}{\varepsilon_r}$ (3), $R_1 = R_2 = 0$

$R_3 = R_4 = k_d(\rho)C_{H_2O} - k_r C_3 C_4 = k_r (K_w(\rho) - C_3 C_4)$ (4), $z_1 = 1, z_2 = -1, z_3 = 1, z_4 = -1$

, $I = F \sum_{i=1}^4 z_i j_i$ (5)

Here (1) are the material balance equations, (2) are the Nernst-Planck equations for the flows of potassium (K^+ , $i=1$), chlorine (Cl^- , $i=2$), hydrogen (H^+ , $i=3$) and hydroxyl (OH^- , $i=4$) ions, (3) are the Poisson equation for the electric field potential, where $\rho = F(z_1 C_1 + z_2 C_2 + z_3 C_3 + z_4 C_4)$. (4) are formulas describing the reaction dissociation/recombination of water molecules, where $K_w(\rho) = K_{w0} + b\rho$, (5) is the current flow equation, which means that the current density I flowing through the cross section of the desalting

channel is determined by the flow of ions, that is, it is the Faraday current density (we neglect the charging current), ε_r is the dielectric permeability of the solution, F – Faraday number, R – universal gas constant, φ – potential, $E = -\frac{d\varphi}{dx}$ – electric field strength, C_i, j_i, D_i – concentration, flow, diffusion coefficient of the cation ($i=1$) and anion ($i=2$), $k_r = 1.1 \cdot 10^8$ ($m^3 / c \text{ mol}$) – rate constant recombination, $K_{w0} = (k_d / k_r) = 10^{-8}$ (mol^2 / m^6) – classical equilibrium constant (ionic product of water), $K_d = 2 \cdot 10^{-5} c^{-1}$ – rate constant of dissociation of water molecules.

Boundary conditions of the mathematical model: $C_1(0) = C_{10}$, $C_2(0) = C_{20}$, $C_3(0) = C_{30}$, $C_{30} \gg \sqrt{K_{w0}}$, $C_4(0) = K_{w0} / C_{30}$, $C_{10} - C_{20} + C_{30} - C_{40} = 0$, $\varphi(0) = d$, $C_1(h) = C_{1k}$, $\left(\frac{F}{RT} C_2 D_2 \frac{d\varphi}{dx} - D_2 \frac{dC_2}{dx} \right) \Big|_{x=h} = 0$, $\frac{dC_3(h)}{dx} = 0$, $\left(\frac{F}{RT} C_4 D_4 \frac{d\varphi}{dx} - D_4 \frac{dC_4}{dx} \right) \Big|_{x=h} = j_{4k}$, $\varphi(h) = 0$;

The boundary conditions assume ideal selectivity of the cation exchange membrane. The concentration of cations on the surface of the membrane is determined by its exchange capacity.

Results and Discussion

It is shown that a change in the equilibrium constant, in accordance with the proposed mathematical model, leads to an increase in the fluxes of H^+ and OH^- ions commensurate with the change in the parameter b . In this case, a local increase in the equilibrium constant occurs, for example, in the region of a quasi-equilibrium boundary layer by 50–100 times, which corresponds to order of experimental data [2].

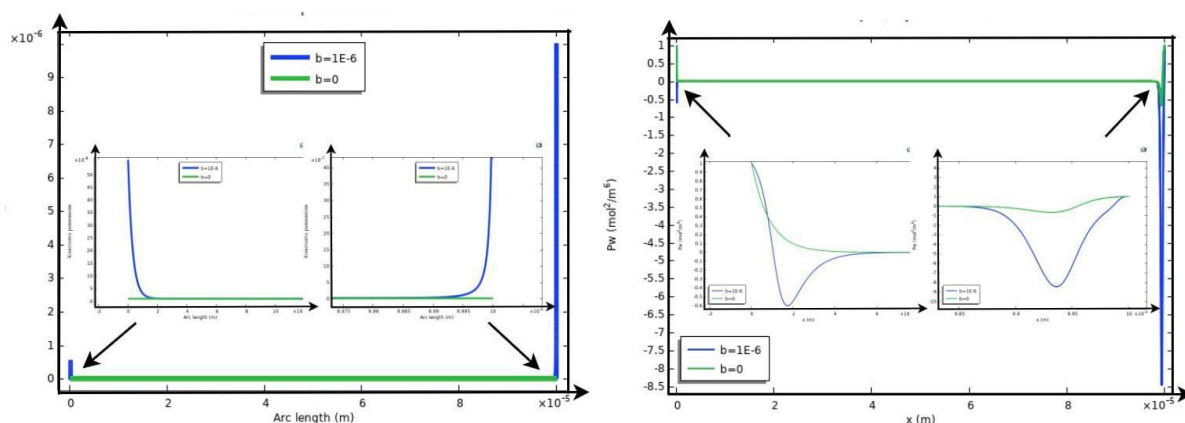


Figure 1. Equilibrium constant graph K_w , equilibrium function graph P_w

Acknowledgement. This study was supported by the Russian Science Foundation, research project no. 24-19-00648, <https://rscf.ru/project/24-19-00648>.

References

1. *Sheldeshov N.* Processes involving hydrogen and hydroxyl ions in systems with ion-exchange membranes: Dis. doc. chem. Sciences: 02.00.05. — Krasnodar. 2002. - 405 s.
2. *Nikonenko V. V., Pis'menskaya N. D., Volodina E. I.* Rate of Generation of Ions H^+ and OH^- at the Ion-Exchange Membrane/Dilute Solution Interface as a Function of the Current Density, *Russ J Electrochem*, 2005, Vol. 41, Iss. 11, P. 1205, DOI: 10.1007/s11175-005-0203-z

ALGINATE-BASED COMPOSITE MEMBRANES FOR ANTIBIOTICS REMOVAL

Alexandra Nebesskaya, Yuliia Shvorobei, Alexey Yushkin, Evgeniia Grushevenko, Tatyana Anokhina, Alexey Volkov

A.V.Topchiev Institute of Petrochemical Synthesis, RAS, Russia, *E-mail: tsanokhina@ips.ac.ru*

Introduction

As a result of the rapid development of industry, most countries face a significant threat to the safety of aquatic ecosystems. This issue became particularly actual due to the local shortage of water resources. Since industrial wastewater is the main source of pollution of drinking water, its reuse and purification are promising directions to solve the environmental problem. Among the substances polluting wastewater, antibiotics are the most dangerous, since microorganisms develop resistance to them over time [1]. Due to that, old antibiotics become ineffective for treatment, forcing the pharmaceutical industry to constantly search for new drugs. Therefore, the creation of effective methods for removal of antibiotics from wastewater are important. The use of traditional methods of wastewater treatment, such as flocculation, coagulation and flotation, leads to the effective removal of dissolved, suspended and colloidal particles. However, these methods can be ineffective for removal of some types of antibiotics. Moreover, traditional methods have a number of disadvantages associated with the complexity of the work, the duration of treatment and the high cost of reagents. Filtration processes considered as perspective alternative to these methods [2]. They do not require reagents, demand low energy costs, and are insensitive to environmental conditions. In this work, composite membranes made of polyethylene terephthalate (PET) and alginates crosslinked with cations of II and III valence metals were developed. Alginates are natural polymers that are very effective as membrane materials for filtering aqueous media due to their hydrophilic and film-forming properties, which is why they are less prone to fouling.

Experiments

Composite membranes were obtained by deposition of thin layer of alginate cross-linked with cations of II and III valence metals to the surface of PET porous support. Sodium alginate was dissolved in distilled water at a concentration of 10 wt.% until a homogeneous gel was formed. A thin layer was casted onto the surface of the PET with a doctor blade with a layer thickness of 0.2 mm and cross-linked with 0.5 mol-eq/L aqueous solutions of inorganic salts for 30 minutes. Inorganic salts were used for crosslinking metal alginates: $\text{CaCl}_2 \cdot 2\text{H}_2\text{O}$, $\text{AlCl}_3 \cdot 6\text{H}_2\text{O}$, $\text{Fe}(\text{NO}_3)_3 \cdot 9\text{H}_2\text{O}$, $\text{CuSO}_4 \cdot 5\text{H}_2\text{O}$. After crosslinking, the membranes were washed twice with distilled water. The resistance of membranes to organic solvents was determined by soaking in ethanol, N-methylpyrrolidone (NMP) and dimethylformamide (DMF). The hydrophilicity of the membrane surface was determined by measuring the wetting angle measurements using the LC-1 goniometer by the lying drop method. The membrane structure and morphology were determined by scanning electron microscopy (SEM). Dead-end filtration cells were used to study the nanofiltration properties of obtained membranes. To study the separation properties of membranes, a model dye Remazol Brilliant Blue R (626 g/mol) was used, since it has a molecular weight close to many antibiotics. The antibiotic ceftriaxone with a molecular weight of 555 g/mol was also used to validate membrane performance in antibiotics removal process. The concentrations of solutes in feed and permeate were determined using spectrophotometric analysis [3].

Results and Discussion

An analysis of the resistance of composite membranes to organic solvents showed that PET and alginates crosslinked with cations of II and III valence metals do not dissolve in pure solvents, including polar aprotic (NMP and DMF), which are characterized as aggressive solvents for many polymers (Table 1). Calcium alginate has minimal sorption characteristics. Sorption of NMP is 0.04, ethanol – 0, and DMFA – 0.02 g/g.

Table 1: Sorption of PET and metal alginates in organic solvents, g/g

	Sorption, g/g		
	NMP	DMF	Ethanol
PET	0.23	0.33	0.28
CaAlg	0.04	0.02	0
AlAlg	0.07	0.13	0
FeAlg	0.08	0.18	0
CuAlg	0.05	0.08	0

The measurement of the water contact angles showed a decrease of this parameter for composite membranes cross-linked with calcium, aluminum and copper (II) alginate from 67.6° (PET support) to 35.6-59.0°, which means an increase in the hydrophilization of the membrane surface. Hydrophilization of the surface is a factor that leads to a decrease in organic molecules fouling of membranes. To assess the fouling ability with nonpolar organic compounds, chloroform droplets were applied to the surface of composite membranes. A drop of chloroform spreads over the surface of membrane. On the surface of the PET-AlAlg and PET-FeAlg composite membranes, the droplets have a chloroform contact angle exceeding 90°.

The water permeability of the membranes decreased compared to PET support from 1.9 to 0.25-1 kg/(m²·h·bar), due to a decrease in pore size when modifying highly porous PET with aglinates of II and III valence metals. As studies of filtration characteristics show, the crosslinking metal plays an important role in the final selectivity (Table 2). Thus, in the filtration of the model solution, when the crosslinking cation changes in the Ca-Cu-Al-Fe series, the retention coefficients of the Remazol Brilliant Blue R dye increase from 21.0 to 99.3%. Thus, among the studied composite membranes, it was PET-FeAlg and PET-AlAlg that showed the best results in filtering the model solution both in terms of dye retention and in terms of permeability of the composite membrane.

Table 2: Characteristics of membranes in the process of separation of water from Remazol Brilliant Blue R (626 g/mol) at a concentration of 100 mg/L

Membran	Permeance, kg/(m ² ·h·bar)	Retention, %
PET-CaAlg	0.14	21.0
PET-CuAlg	1.01	75.2
PET-AlAlg	1.29	98.5
PET-FeAlg	1.30	99.3

A comparison of the separation properties of a composite membrane PET-FeAlg and PET during filtration of a ceftriaxone solution showed that the application of iron alginate to PET leads to an increase in the retention of the membrane by an order of magnitude: from 6.9% to 69.9% for PET and PET-FeAlg. At the same time, the permeability naturally decreases from 10.7 kg/(m²·h·bar) to 3.7 kg/(m²·h·bar) for PET and PET-FeAlg. The PET-AlAlg composite membrane, when separation the ceftriaxone solution, demonstrated permeability values higher than that of PET-FeAlg and amounted to 4.5 kg/(m²·h·bar), however, the retention of such a membrane turned out to be 16% lower compared to PET-FeAlg (Figure 1). Such characteristics of the resulting composite membranes demonstrate the high potential of its use for the removal of both dyes and antibiotics from aqueous media.

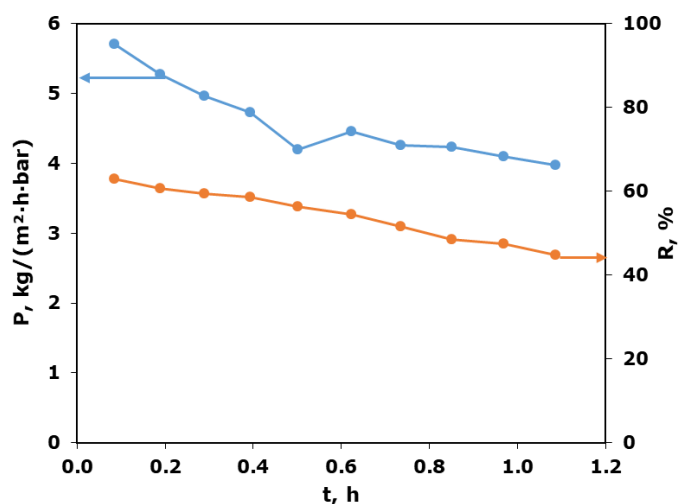


Figure 1. Retention and permeability of the PET-AlAlg composite membrane separation of an aqueous solution of sodium ceftriaxone at a concentration of 300 mg/L

Acknowledgement. The results were obtained with the financial support of the Russian Federation represented by the Ministry of Science and Higher Education of the Russian Federation. Project 13.2251.21.0166 (RF Project ID----2251.61322X0044). BRICS ISTC Agreement 075-15-2022-1218.

References

1. Ahmad F. et al. An eco-friendly hydroentangled cotton non-woven membrane with alginate hydrogel for water filtration // International Journal of Biological Macromolecules. 2024. V. 256. P. 128422.
2. Dmitrieva E.S., Nebesskaya A.P., Grushevenko E.A., Melekhina V.Ya., Vlasova A.V., Anokhina T.S., Volkov A.V. Cellulose as a modifying layer PETF-based non-woven fabric for filtration aqueous environments // Izvestiya Vysshikh Uchebnykh Zavedenii, Seriya Tekhnologiya Tekstil'noi Promyshlennosti. 2023. № 6. V.408. P. 266-278.
3. Dmitrieva E.S., Nebesskaya A.P., Grushevenko E.A., Anokhina T.S., Volkov A.V. Modified non-woven filter fabric based on PET for water purification // Izvestiya Vysshikh Uchebnykh Zavedenii, Seriya Tekhnologiya Tekstil'noi Promyshlennosti. 2023. № 6. V.408. P. 163-175.

APPLICATION OF PAN MEMBRANES FOR OIL DEASPHALTING

Alexandra Nebesskaya, Alexey Balynin, Vladimir Volkov, Alexey Yushkin

A.V.Topchiev Institute of Petrochemical Synthesis, RAS, Russia, E-mail: vvvolkov@ips.ac.ru

Introduction

Asphaltenes play a significant role in determining the properties of oil and oil products. Their content in oil can vary from 0% to 15%, and this has a direct impact on the specific gravity, viscosity, and difficulty of extraction, transportation and processing [1]. Traditionally, the deasphalting process was used to process vacuum residue associated with the production of valuable raw materials [2]. Currently, solvent deasphalting is also used in the refining of heavy oils and petroleum residues by removing undesirable components or impurities to facilitate, enable subsequent transportation, processing through thermal and catalytic cracking processes. The search for innovative technologies in the field of oil refining, which can reduce energy consumption and the cost of production processes, is a strategic priority today. One possible solution that is currently being actively investigated worldwide is the utilization of membrane separation crude oil and its products [3].

However, oil separation is the challenging tasks for membrane separation [4]. The recent active development of membranes for the separation of organic media allowed consider this process for isolation of asphaltenes from heavy oil and oil residue. Main problem in this way is membrane fouling which can be significant problem in heavy oil separation [5]. Another problem with oil fractionation connected with wide variety of oil composition. Depending on oil content, asphaltenes can form clusters and particles with size 5-300 nm [6]. As a result, membranes with different pore sizes should be applied for different oils fractionation [7-8]. Hence this work focuses on asphaltenes removal from Salyem oil using PAN membranes with different pore size.

Experiments

Porous asymmetric PAN membranes with different were prepared by non-solvent induced phase separation (NIPS). Membranes pore size varied by changing casting solution composition (polymer content, solvent type, additives). The DMSO and NMP were used for casting solution preparation. Acetone as weak solvent added to part of casting solutions to obtain membranes with the lowest pore sizes. Various carbon particles were also used as additive to casting solution. Membranes were obtained with the addition of graphene oxide (GO), particles of PAN pyrolyzed under the influence of IR radiation (IR-PAN-a) and nanodiamonds (ND).

Casting solutions were prepared by mixing PAN, solvent and additives (if added) with desired composition. Components were stirred at ambient conditions for 72 h to obtain a homogeneous solution. Then, the polymeric solution was placed in the ultrasonic bath for 30 min to ensure complete dissolution and removal of air bubbles. The polymer solution was cast on a glass plate with a doctor blade or a gap of 200 μm with a speed of 2.5 m/min. Casted film was immediately immersed in the coagulation bath (distilled water, 20°C). Obtained membranes were washed several times with distilled water and then kept in distilled water for 24 h to wash out the solvent residues. The membrane was washed with ethanol, isobutanol and, then dried at room temperature and humidity of 20%.

The dead-end cell was used for filtration measurements with 16 cm^2 effective membrane area. The concentration of asphaltenes was measured using a PE-5400UF spectrophotometer. Combined gas chromatography–mass spectrometry (GC–MS) was used for more accurate determination of the solution composition.

Results and Discussion

PAN membranes with pore sizes from 4 to 26 nm was obtained by varying solution composition. The lowest pore size 4 nm was obtained with addition of acetone as a co-solvent. Such membranes have the molecular weight cut-off value (MWCO) of 1800 g/mol. This membranes have a retention for asphaltenes of 73% at a concentration of 1 g/L and more than 95% when the oil content in the solution is 10 g/L or more (Table 1). In case crude oil filtration

membranes with lowest pore size were not permeable. Membranes with pore size from 12 to 27 demonstrated much better performance and oil permeance 0.4-2.4 L/(m²·h·bar).

Table 1: Characteristics of membranes in the process of separation of oil solutions in toluene

Membrane	Casting solution	Pore size, nm	Permeance, L/(m ² ·h·bar)				Retention, %			
			1 g/L	10 g/L	100 g/L	Crude Oil	1 g/L	10 g/L	100 g/L	Crude Oil
M-1	PAN/DMSO/acetone	4	19.5	13.2	2.6	0	73	94	99.6	-
M-2	PAN/DMSO 20/80	21	32.0	19.2	3.9	0.38	35	63	94	99.93
M-3	PAN/DMSO 15/85	27	46.0	27.0	5.4	0.84	26	58	89	99.87

Addition of carbon particles into casting solution slightly decrease pore size from 17 nm for pure PAN membrane to 15-12 nm for membranes with addition of carbon particles. This led to a decrease in the water permeance from 160 L/(m²·h·bar) to 80-120 L/(m²·h·bar). Also the addition of particles caused slight hydrophilization of the surface, as the water contact angle decreased from 65° to 48-55°. Retention of asphaltenes from crude oil was more 99.9% for all investigated membranes. At the same time according to GC-MS data membranes retain components with molecular weight higher 590 g/mol. The filtered oil became noticeably clearer (Fig. 1) with no significant changes in the concentration of compounds lower 320 g/mol. This demonstrates that porous PAN membranes can be used not only for oil deasphalting but also for oil fractionation.



Figure 1. Photographs of the initial mixture and permeate after filtration: (a) oil solutions in toluene with an oil content 100 g/l through a membrane with a pore size of 4 nm; (b) oil through a membrane with a pore size of 21 nm (b).

It was also observed, that addition of carbon particles increases oil permeance up to 2-3 times from reference PAN membrane. At the same time, addition of GO and IR-PAN-a dramatically increase irreversible fouling of membranes due to increase of surface roughness. From the other hand, addition of ND decrease fouling of obtained membranes. Such membranes demonstrated the highest oil permeance up to 2.4 L/(m²·h·bar) and recover more than 96% of initial pure toluene permeance after wash with toluene.

Acknowledgement. This work was funded by the Russian Science Foundation (Project no. 24-29-00851).

References

1. U.Farooq *et al.* Energy & Fuels. 35 (2021) 19191
2. R.N.Magomedov *et al.* Russian Journal of Applied Chemistry. 92 (2019) 1634
3. A.A.Yushkin *et al.* Membranes and Membrane Technologies. 13 (2023) 521
4. S.Chisca S. *et al.* Science. 376 (2022) 1105
5. A.A.Yushkin *et al.* Membranes and Membrane Technologies. 13 (2023) 331
6. P.Zuo *et al.* Journal of Energy Chemistry. 34 (2019) 186
7. J.Marques *et al.* Oil & Gas Science and Technology-Revue de l'IFP. 63 (2008) 139
8. M.J.T.M. Ching *et al.* Energy & Fuels. 24 (2010) 5028

MEMBRANE REGENERATION OF USED ENGINE OIL

Alexandra Nebesskaya, Alexey Yushkin, Alexander Markelov, Tatiana Anokhina, Vladimir Volkov

A.V.Topchiev Institute of Petrochemical Synthesis, RAS, Russia; E-mail: vvvolkov@ips.ac.ru

Introduction

Reducing the energy consumption of existing and new production facilities, as well as optimizing resources while minimizing the negative impact on the environment, are urgent goals in industry, including the petrochemical industry. A significant area of focus is finding energy-efficient processes for oil refining. Ultrafiltration (UF), which is a low-energy alternative to distillation for crude oil separation, is currently being explored. Another important area is the regeneration of used oils that are contaminated with toxic substances. This is particularly important for remote locations and facilities, such as the Arctic region, drilling rigs, quarries, and offshore production platforms, where the logistics costs of transporting new materials can be high.

To implement baromembrane separation, it is necessary to reduce the viscosity of the hydrocarbon medium. This can be achieved by increasing the process temperature or diluting the viscous liquid with a non-viscous, volatile solvent. Both approaches involve the creation of thermally and chemically resistant UF membranes, as well as the study of the purification process for viscous hydrocarbon media. This raises the need to solve a number of interrelated problems in the fields of both engineering and chemical science.

The main aspects of the engineering solution for the developed process of baromembrane separation include the creation of membranes with the required porosity and a narrow pore size distribution. Polyacrylonitrile (PAN) is a traditional membrane material that has been well studied both in terms of obtaining membranes with a given porous structure and in terms of ways to modify it for increased stability in organic media. Therefore, the aim of this study was to filter waste oils using membranes based on PAN.

Experiments

In this work, the ultrafiltration of used engine oil (UEO) on PAN membranes was investigated. A casting solution of 15% PAN in DMSO (dimethyl sulfoxide) was used to produce the membranes. Membranes were fabricated by the method of nonsolvent-induced phase separation (NIPS), where structures with a large number of elongated finger-shaped macro-voids are formed. The membrane structure and morphology were analyzed by scanning electron microscopy (SEM). The pore size in the membranes was determined by liquid porometry on a POROLIQ 1000 ML device. Toluene was used as a diluent to reduce the viscosity of the oil. Filtration experiments were carried out in a dead-end stirred filtration cell. The membrane rejection was estimated using solution optical density. This parameter was measured using a PE-5400UF spectrophotometer (PromEcoLab, Shanghai, China). Toluene was used as a reference solution. The optical density was determined at a wavelength of 610 nm.

Results and Discussion

The thickness of the dense layer on the surface of the resulting membrane was 0.8 nm. The membrane had an asymmetric structure with a large number of finger-shaped macro-voids and a dense layer on the surface (Figure 1).

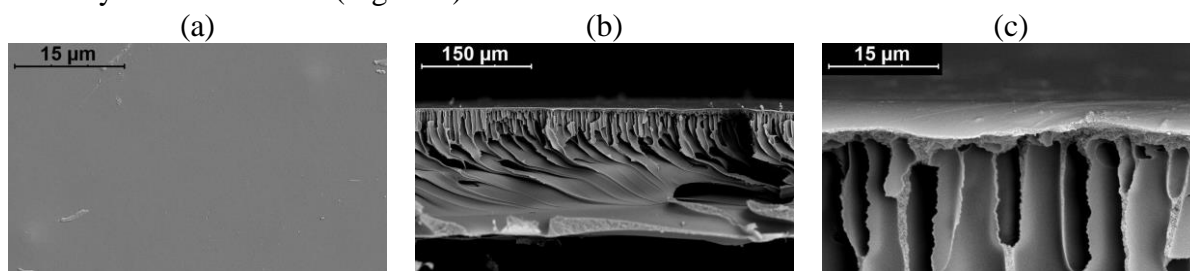


Figure 1. SEM images of the surface (a) and lateral cleavage (b, c) of PAN membranes obtained from solutions of 15% PAN in DMSO.

According to liquid porometry, the membrane pore size was 27 nm, while the largest pore size was 41 ± 3 nm. The ultrafiltration membrane was also characterized in terms of water and toluene permeability: the membrane permeability for water and toluene was 198 ± 15 and 66 ± 11 $\text{kg}/(\text{m}^2\cdot\text{h}\cdot\text{bar})$, respectively. To study the separation characteristics of the membranes, solutions with an oil content in toluene of 50 wt.% and 100 g/L were prepared. When filtering a solution of used engine oil in toluene with a mass fraction of 50 wt.% oil, the permeability of the membrane was 0.33 $\text{kg}/(\text{m}^2\cdot\text{h}\cdot\text{bar})$, while dilution to 100 g/L leads to an increase in permeability to 12.6 $\text{kg}/(\text{m}^2\cdot\text{h}\cdot\text{bar})$, which is almost 40 times higher than a less diluted solution. An increase in the oil content in the solution led to an increase in the retention capacity to 59%, which is a consequence of an increase in the size of macroparticles with an increase in their concentration in solution.

Acknowledgement. This work was funded by the Russian Science Foundation (Project no. 24-63-00026).

OXIDATIVE CONVERSION OF LIGHT ALKANES IN A CATALYTIC MEMBRANE REACTOR

Alexander Nemudry

Institute of Solid State Chemistry and Mechanochemistry SB RAS, Novosibirsk, Russia

E-mail: nemudry@solid.nsc.ru

Introduction

Environmental and climate problems, which have sharply worsened in recent years, persistently require a reduction in energy costs in industry and a transition to a circular economy. As is known, large-scale processes such as steam reforming or cracking of light hydrocarbons, which is endothermic and thermodynamically unfavorable, are among the most energy-intensive processes in petrochemistry. In this regard, the transition to exothermic processes of partial oxidation (PO)/oxidative dehydrogenation (ODH) of alkanes to obtain valuable products is a promising alternative route [1]. The main energy savings for alkane PO/ODH stem from the ability to operate under autothermal conditions, which reduces external heat requirements. Unlike current thermal or steam cracking catalysts, which require frequent extensive regeneration, carbon deposits formed over PO/ODH redox catalysts are readily removed in situ by oxygen in the reactant feed [1].

Another promising alternative for use in oxidative processes instead of cryogenic oxygen or oxygen produced by swing adsorption is the use of oxygen transport membranes (OTMs) [2]. The main advantages of dense OTMs include (i) infinite selectivity with respect to oxygen – resulting in a very pure product (>99.99% oxygen), (ii) the ability to thermally integrate oxygen separation into high temperature process - reducing the energy needed for the separation process, (iii) the modular design of OTM reactors – which makes oxygen separation more versatile and economically viable also on small and medium scale, (iv) a better process yield – as exclusively oxygen anions are allowed to diffuse through the membrane, this can cause significant effects on yield and selectivity in chemical reactions, (v) another advantage of membrane reactors is that not only air, but also water vapor and carbon dioxide can be used as a source of oxygen - which reduces the carbon footprint from large-scale processes of light hydrocarbons conversion[3].

The work presents the results of the partial oxidation of methane (POM) and oxidative dehydrogenation of ethane (ODHE) in a membrane reactor based on oxygen transport microtubular membranes (MT OTMs).

Experiments

Polycrystalline LSFM5 powder was synthesized via ceramic method from the corresponding oxides and metal carbonates. The composite SFM5-GDC was obtained by the Pechini method, materials were validated by scanning electron microscopy and X-ray diffraction techniques. Oxygen permeability measurements were performed on MT OTMs obtained from the LSFM5 powder and SFM5-GDC composite by the phase inversion method. The high-temperature experiments on the catalytic activity of the membrane in the reaction was applied in the air and CO₂-containing atmosphere.

Results and Discussion

Membrane reactor based on LSFM5 MT OTMs was tested in two modes: in the synthetic air/(20% CH₄/80% Ar) and (20% CO₂+80% N₂)/(20% CH₄/80% Ar) gradients. It has been shown that, under optimal conditions, the membrane reactor provide 100% methane conversion with H₂ and CO selectivity above 90% and a H₂/CO ratio close to 2 starting already from 900 °C (Fig.1).

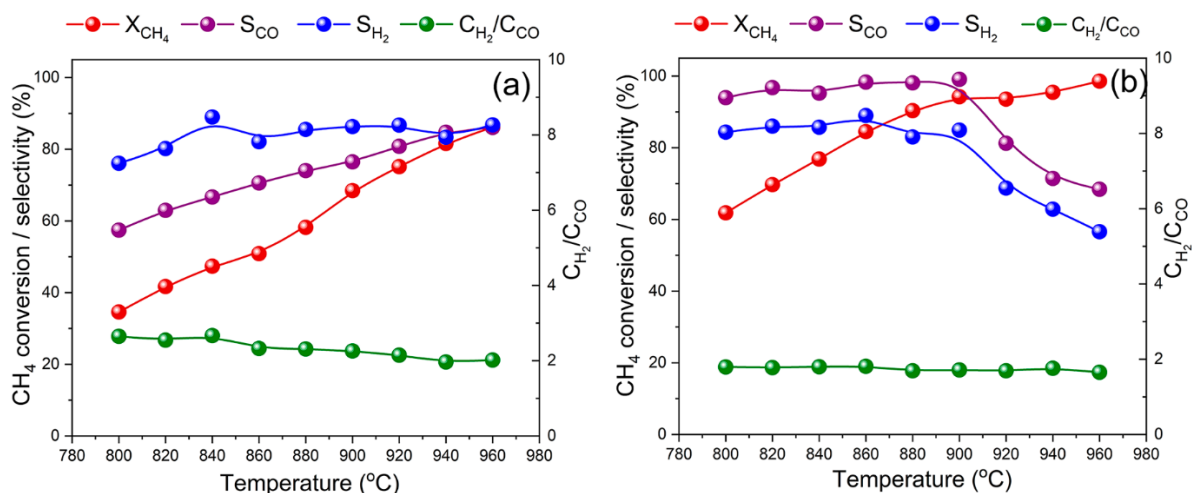


Fig. 1. Temperature dependences of methane conversion, CO/H₂ selectivity and H₂/CO ratio in air/diluted methane (a) and (CO₂+N₂)/diluted methane (b) gradients obtained on LSFM5 membranes decorated by nickel particles.

The catalytic activity of MT membranes based on SFM5-GDC in the reaction of oxidative dehydrogenation of ethane was studied as a function of temperature. It is shown that at a temperature of 900 °C in the air/Ar gradient the selectivity for ethylene reaches a value of ~ 67% with ethane conversion of ~ 95%. When CO₂ is used as an oxygen source, ethylene selectivity reaches ~ 62% and ethane conversion ~ 99% at T=900 °C.

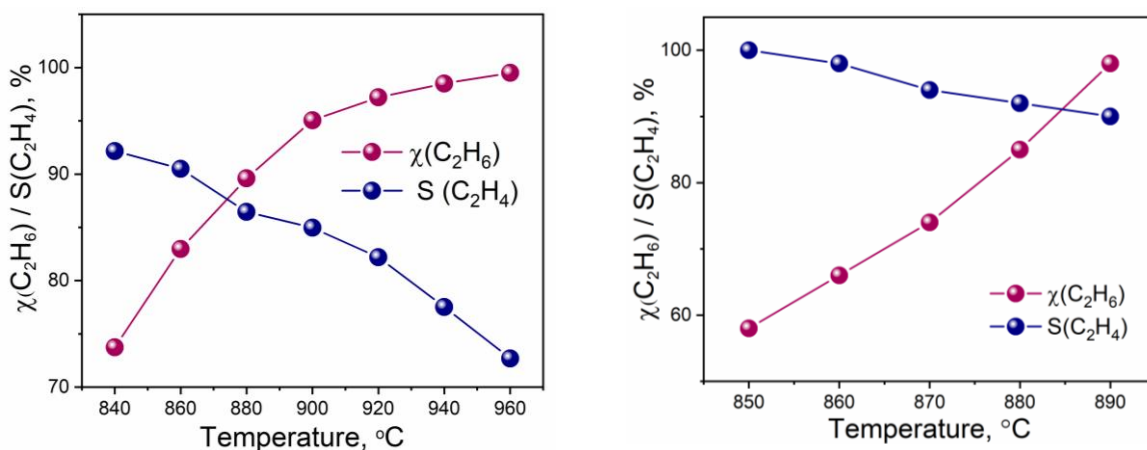


Fig.2 Ethan conversion and ethylene selectivity in SFM5-20CGO MT OTMs in CO₂/C₂H₆ gradient heated by furnace (a) and alternating current (b).

Acknowledgement. This work was financially supported by RSF grant No. 23-43-00130

References

1. Sara Najari, Samrand Saeidi, Patricia Concepcion, Dionysios D. Dionysiou, Suresh K. Bhargava, Adam F. Lee and Karen Wilson. Oxidative dehydrogenation of ethane: catalytic and mechanistic aspects and future trends, Chem. Soc. Rev., 2021, 50, 4564–4605.
2. Ragnar Kiebach, St'even Pirou, Lev Martinez Aguilera, et al. A review on dual-phase oxygen transport membranes: from fundamentals to commercial deployment. J. Mater. Chem. A, 2022, 10, 2152–2195
3. Bragina O., Nemudry A. Cobalt-free SrFe_{1-x}Mo_xO_{3-δ} perovskite hollow fiber membranes for oxygen separation // Journal of the European Ceramic Society. 2023. V. 43. P. 3421-3426.

COUPLED EFFECTS OF CONCENTRATION POLARIZATION IN SYSTEMS WITH ION-EXCHANGE MEMBRANES

Victor Nikonenko, Mikhail Sharafan, Natalia Pismenskaya

Kuban State University, Krasnodar, Russia, E-mail: v_nikonenko@mail.ru

Introduction

Concentration polarization (CP) is the phenomenon of concentration changes near membrane/solution interfaces under the influence of an external driving force [1]. These concentration changes cause other (coupled) effects, such as an increase in the system resistance and, as a consequence, in the potential drop at a given current density. In addition, due to a strong decrease of electrolyte concentration at the membrane surface, an extended space charge region (SCR) develops from initially equilibrium electrical double layer. The action of the external electric field on the SCR gives rise to electroconvection, which (1) enhances delivery of the “fresh” electrolyte solution from the bulk solution to the membrane surface and (2) promote the removal of the depleted solution from the membrane surface to the bulk solution. A small concentration of salt ions at the membrane surface encourages also generation of H^+/OH^- ions, since newly appeared water ions can compete in charge transfer with salt ions.

Discussion

The above effects are discussed in the presentation. In particular, the antagonistic nature of two coupled phenomena, electroconvection and water splitting, is analyzed. It is found that when a membrane is modified in such a way that electroconvection is enhanced, water splitting decreases; conversely, when a modification increases water splitting, it leads to a decrease in electroconvection. Special attention is paid to concentration polarization in membrane systems with ampholyte-containing solutions. Although the catalytic mechanism of water dissociation, known as “water splitting”, is rather well understood [2,3], another mechanism called “acid dissociation” mechanism has recently been discovered [4]. In the origin of this mechanism is the Donnan exclusion of H^+ cations as coions from an anion-exchange membrane. When an acid anion of an amphoteric substance, such as $H_2PO_4^-$, enters an anion-exchange membrane, it gets into an environment whose pH is higher than the pH of the external solution, since there is a tendency to medium the pH of which is higher than the pH of the external solution, because there is a trend of exclusion of H^+ ions. Therefore, a part of $H_2PO_4^-$ anions when crossing the membrane interface dissociate, and H^+ ions are released into the near-membrane diluted solution.

Fig. 1 represents different coupled effects of concentration polarization.

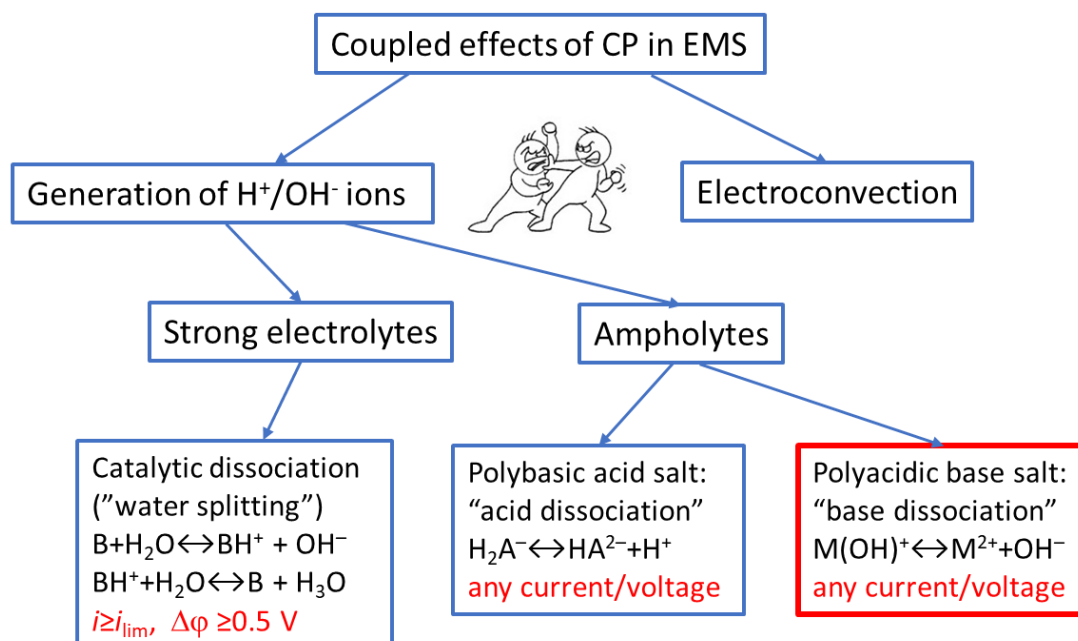


Figure 1. Coupled effects of concentration polarization in systems with ion-exchange membranes

The red box refers to the case non-studied in the literature. The scheme of the possible reactions is anticipated by similarity with the case of a polybasic acid salt.

The report discusses phenomena associated with concentration polarization, methods of modifying the membrane surface to enhance electroconvection and weaken the dissociation of water molecules, the use of separators and other techniques, including the application of a pressure field.

A better understanding of these phenomena allows one to enhance the desirable ones and eliminate the undesirable ones.

Acknowledgment. We are grateful to the Russian Science Foundation (project 24-19-00451) for financial support.

References

1. *Guiver M., et al.*, Membrane Terminology, in: *E. Hoek, V.V. Tarabara* (Eds.), Encyclopedia of Membrane Science and Technology; Wiley, Hoboken, NJ. 2013. V. 3, pp. 2219–2228.
2. *Simons R.*, Strong electric field effects on proton transfer between membrane bound amines and water // *Nature* 1979. V. 280, Issue 5725. 824-826.
3. *Zabolotskii V.I., Shel'deshov N.V., Gnusin N.P.*, Dissociation of water molecules in systems with ion-exchange membranes // *Russ. Chem. Rev.* 1988. V. 57 (8). 801.
4. *Rybalkina O.A., Sharafan M.V., Nikonenko V.V., Pismenskaya N.D.* Two mechanisms of H⁺/OH⁻ ion generation in anion-exchange membrane systems with polybasic acid salt solutions // *J. Memb. Sci.* 2022. V. 651. 120449.

ALKALI PRODUCTION BY BIPOLAR MEMBRANE ELECTRODIALYSIS FROM CARBONATE CONTAINING SALT

Elena Nosova, Stanislav Melnikov, Victor Zabolotsky

Kuban State University, Krasnodar, Russia, *E-mail: nosova.el@inbox.ru*

Introduction

The study of electromembrane processes, which involve the combination of electrochemical generation of hydrogen and hydroxyl ions through bipolar membranes and chemical reactions in solution, is of significant interest in membrane electrochemistry. These processes are relevant for the production of lithium and sodium hydroxides through the conversion of salts using bipolar membranes in electrodialysis. Bipolar membranes are composite materials composed of two layers that accelerate the dissociation of water under an external electric field, leading to the formation of hydrogen and hydroxide ions that enter the solution on both sides of the membrane. The possibility of producing hydroxides, including lithium hydroxide, in a single step using carbonates of these metals, is also of interest.

Experiments

The study of alkali production through bipolar electrodialysis was carried out using a laboratory-scale electrodialysis apparatus (LabED, Kuban State University, Russia). The BMED stack included two electrodes and 5 membrane couples within a three chambered unit with a single unit configuration CEM-BM-AEM. Each membrane unit included CEM (MK-40), AEM (MA-41) and BM (MB-3), all manufactured by «ShchekinoAzot» Russia. The effective area of the membranes was 1 dm². Solutions of sodium carbonate and lithium were used as the initial solutions, with additional solutions of sodium sulfate and lithium studied for comparison. The initial concentrations of the salt solutions were 0.5 mol-eq/dm³ and 0.3 mol-eq/dm³ (for Li₂CO₃ due to its low solubility, which is 1.33 grams per 100 grams of H₂O at 20°C). The concentration of the salts was kept constant throughout the experiment, within ±0.05 mol-eq/dm³. To maintain conductivity at the start of the process, 0.1 mol-eq/dm³ hydroxide solution was added to the alkaline chamber and 0.05 mol-eq/dm³ Na₂SO₄ to the acid chamber when converting a solution containing carbonate ions, or 0.1 mol-eq/dm³ H₂SO₄ was used for a sulfate-containing salt solution. The solution flow rate was 10 l/h. The current density studied was 2 A/dm².

The monitored parameters included: voltage across the electrodialysis module, electrical conductivity, pH in all compartments of the device, and the concentration of sodium hydroxide in the alkaline compartment, as well as the content of sulfate and carbonate ions in the sodium hydroxide solution. The concentrations of the resulting alkaline solution and the content of carbonate impurities were determined using potentiometric titration. The content of sulfate ions was measured using ion chromatography.

Results and Discussion

Figure 1 displays the relationships between the concentration of sodium and lithium hydroxides over time, the alkali current efficiency, and the specific energy consumption dependencies on the alkali concentration in the alkaline chamber.

In the process of obtaining lithium hydroxide and sodium hydroxide from carbonate and sulfate containing salts using a laboratory electrodialysis apparatus, the concentration of alkalis from carbonate containing salts in the alkali chamber increase more than that of sulfate containing salts (Fig. 1a). As a result, the integral current efficiency of alkalis from carbonate containing salts is higher (Fig. 1b).

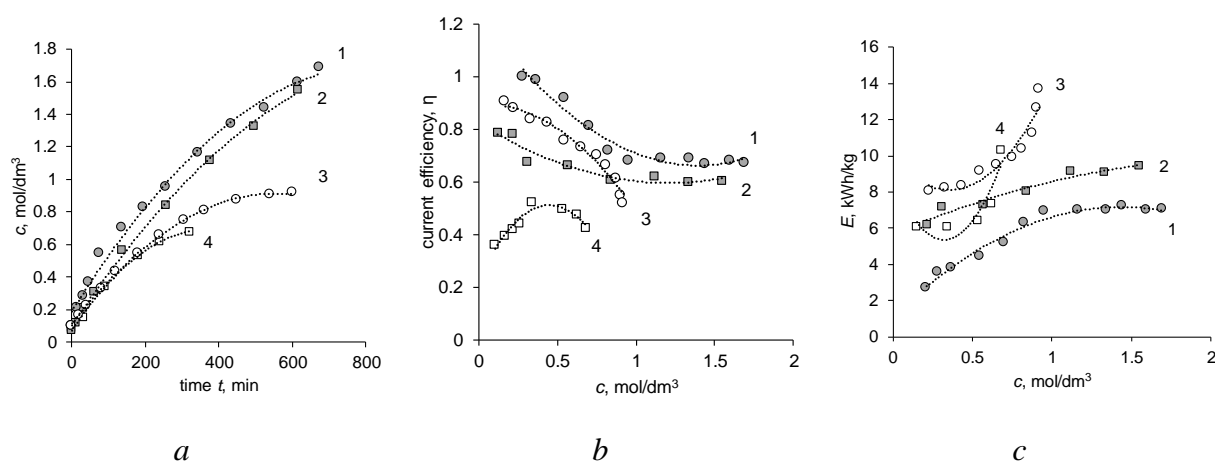
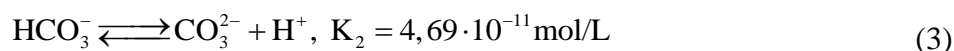
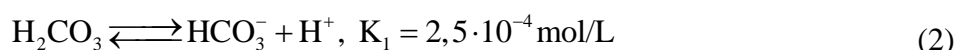
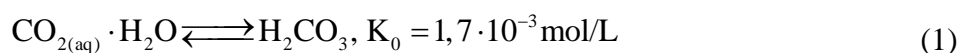


Fig. 1. The dependence of the concentration of sodium (1, 3) and lithium (2, 4) hydroxides in the alkaline chamber on the time of the process (a), the dependence of the current output (b) and specific energy consumption (c) on the concentration of alkali.

The feeding solution: 1, 2 – carbonate containing salt; 3, 4 – sulfate containing salt

The observed differences in alkali current efficiency, depending on the concentration of the final product, indicate various mechanisms that limit the achievement of maximum alkali concentration. When using sulfate salt as a starting solution, hydrogen ions accumulate in the acid chamber. An increase in the concentration of sulfuric acid leads to the protonation of ionogenic groups in the cation exchange layer, reducing its exchange capacity and increasing diffusion permeability. This diffusion flow from the acidic chamber to the alkaline one prevents further accumulation of acid and alkali, thereby limiting the maximum alkali concentration that can be achieved.

In the event that a carbonate salt is used as the starting solution, the alkaline current efficiency is maintained at a high level, even at elevated alkaline concentrations. The processes occurring in the acidic compartment of the electrolysizer are described in reference [1]. The form of carbonic acid in a solution depends on its pH value. At pH values below 4.5, carbonic acid dominates, which exists in aqueous solutions as dissolved carbon dioxide molecules. Between pH levels of 4.5 and 8.2, bicarbonate ions dominate. At pH values above 8.2, carbonate ions become the dominant form. The balance between these different forms of carbonic acid can be expressed by equations:



The reaction between carbonate ions and hydrogen ions, which occurs on the bipolar membrane, inhibits the accumulation of acid in the acidic chamber. This reaction eliminates the contribution of diffusional acid transport, and it can be inferred that the limiting factor for increasing the concentration of the product in the alkaline compartment is the osmotic transfer of water from the salt compartment through the cation exchange membrane.

Analysis of the mass composition of the solution in the alkaline chamber (Fig. 2) reveals significant contamination of the alkali with sulfate ions when using salts containing sulfates (more than 30% for Na_2SO_4 and 40% for Li_2SO_4). In contrast, there is no more than 20% contamination with sulfate and carbonate ions when salts containing carbonate are used.

Although the mass transfer properties of the process are improved when a carbonate-based salt is used, it is still not possible to completely prevent the loss of selectivity, which results in a decrease in the purity of the final alkali product. This can be attributed to the formation of bicarbonate ions in the acid chamber, which is caused by the recombination of hydrogen ions and carbonate ions. In addition, bicarbonate ions present in the cation exchange layer of the bipolar

membrane can be converted to CO₂ [2], which can facilitate the diffusion of other ions, such as sulfate ions, into the alkali solution. As a result, these contaminants can lower the purity of the product. The implementation of this operating mode, in which weak acid anions are prevented from entering the cation exchange layer, is expected to improve the performance of the process and enhance the purity of the final product.

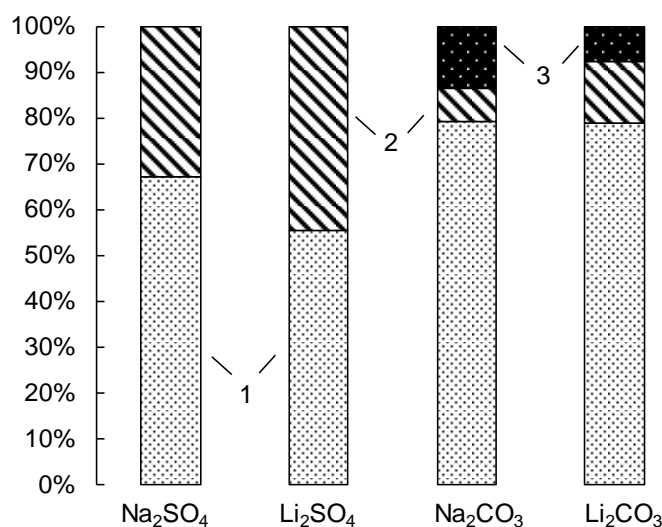


Fig. 2. The content of impurities in the sodium and lithium hydroxide solutions at different initial solutions in the salt chamber.

1 – alkali; 2 – sulfate ions; 3 – carbonate ions

In this study, the production of alkali through the process of bipolar electro dialysis, using carbonate-based salts and MB-3 bipolar membranes, was investigated. The study found that, when compared to producing alkali from solutions containing strong acid anions, such as sodium and lithium sulfates, it is possible to obtain a higher concentration of final alkali products, ranging from 0.92 M to 1.7 M for sodium hydroxide (NaOH) and from 0.68 M to 1.59 M for lithium hydroxide (LiOH), under similar operating conditions. Based on the analysis results, it can be concluded that carbonate-based salts demonstrate relatively higher efficiency in this process and produce less pollution compared to salts containing sulfates.

Acknowledgement. The research was carried out with the financial support of the Russian Science Foundation № 22-13-00439 <https://www.rscf.ru/project/22-13-00439/>

References

1. Nosova, E.N., Musatova, D.M., Melnikov, S.S., Zabolotsky V. I. Study of the Production of Sodium Hydroxide by Bipolar Electro dialysis from Sodium Carbonate Solution // Membr. Membr. Technol. 2023. V. 5. P. 303–312.
2. Melnikova E.D., Tsygurina K.A., Pismenskaya N.D., Nikonenko V.V. Influence of Protonation–Deprotonation Reactions on the Diffusion of Ammonium Chloride through Anion-Exchange Membrane // Membr. Membr. Technol. 2021. V. 3. P. 324–333.

FEATURES OF STUDYING CATALYTIC MATERIALS AND THIN FILMS USING TRANSMISSION ELECTRON MICROSCOPY

Ilya Pankov, Arshak Tsururyan

Institute of Physical and Organic Chemistry, Rostov-on-Don, Russia; E-mail: ipankov@sfedu.ru

Introduction

Transmission electron microscopy (TEM) is an analytical method used to visualize the smallest structures of matter. In contrast to optical microscopes, which use visible light, TEM can reveal detail at the atomic level, magnifying structures up to 50 million times. This can be feasible due to electrons' ability to have significantly shorter wavelength than the wavelength of visible light, when accelerated in a strong electromagnetic field, increasing the microscope's resolution by several orders of magnitude.

TEM exists in different forms, but they all share the same fundamental principles. The two main types of TEM instruments are conventional TEM and STEM (scanning transmission electron microscopy).

Zooming down to the atomic scale allows scientists to see the fundamental building blocks of different materials such as nanoparticle catalysts, batteries, semiconductor devices, and various kinds of films and membranes. Focused electron beams can also be used to manipulate materials *in situ*, allowing to study and discover "nanotechnologies" and new phenomena. The potential level of detail at this scale makes it possible to understand the relationship between structure, properties and performance, allowing scientists to design nanomaterials in a bottom-up manner.

The purpose of this work is to demonstrate the capabilities of TEM (and various related methods) in the study of a wide range of materials, such as: catalytic materials, membranes, films and nanocrystals.

Experiments

All results presented were obtained using a Multi-purpose Electron Microscope JEM-F200 (JEOL, Japan), located in the share use center "High-resolution electron microscopy" of the Southern Federal University (Rostov-on-Don, SFEDU)

Microscope is equipped cold field emission electron gun, operating at accelerating voltage of 200 kV; high-resolution CMOS AMT camera with 4096x3000 pixels resolution; EDX spectrometer Bruker Xflash 6T/60 Quantax 400-STEM with 4000 channels, including an energy-dispersive Peltier-cooled XFlash detector, 0.45 mm detector thickness and -25°C working temperature and secondary electrons detector (SEI) which allows you to obtain three-dimensional images in the HAADF mode.

Results and Discussion

Figure 1 shows the study of NiAl-layered double hydroxide (LDH) nanosheets with embedded Pd, synthesized using co-precipitation method. The presence of dispersed palladium improved the catalytic performance of this material for oxygen evolution reaction (OER) and hydrogen evolution reaction (HER) using as-prepared Pd-NiAl-LDH nanosheets in 1.0 M KOH solution. Pd-NiAl-LDH materials showed significantly improved activity, stability and overpotential. The Pd-NiAl-LDH electrocatalyst remained stable for 48h with minimal potential deviations observed in both OER and HER. Moreover, Pd-NiAl-LDH materials showed better activity than NiAl-LDH. It was possible to confirm the presence of trace amounts of palladium and its dispersed presence between the sheets using TEM and EDX methods.

Figure 2 shows a study of the phase composition of periodic Mo/Si multilayers with different thicknesses of silicon and molybdenum layers. A cross section of the sample was obtained using a JEOL EM-09100IS ion slicer. To study the phases and microstructure of a periodic multilayer, high-resolution TEM was used. In particular, the nanobeam diffraction (NBD) method was used, which allows one to obtain a diffraction pattern from a very small surface area (in this case, approximately 5x5 nm).

Although the intermetallic silicide phases (Mo_5Si_3 , Mo_3Si and MoSi_2) developed similarly in multilayer and bilayer systems, differences in specific phases were observed compared to bilayer systems in the Mo-on-Si and Si-on-Mo sequences. The amorphous silicon layer in periodic multilayers is highly disordered compared to the amorphous silicon layer in bilayer films. This is due to the formation of specific silicide phases in periodic multilayer and bilayer systems.

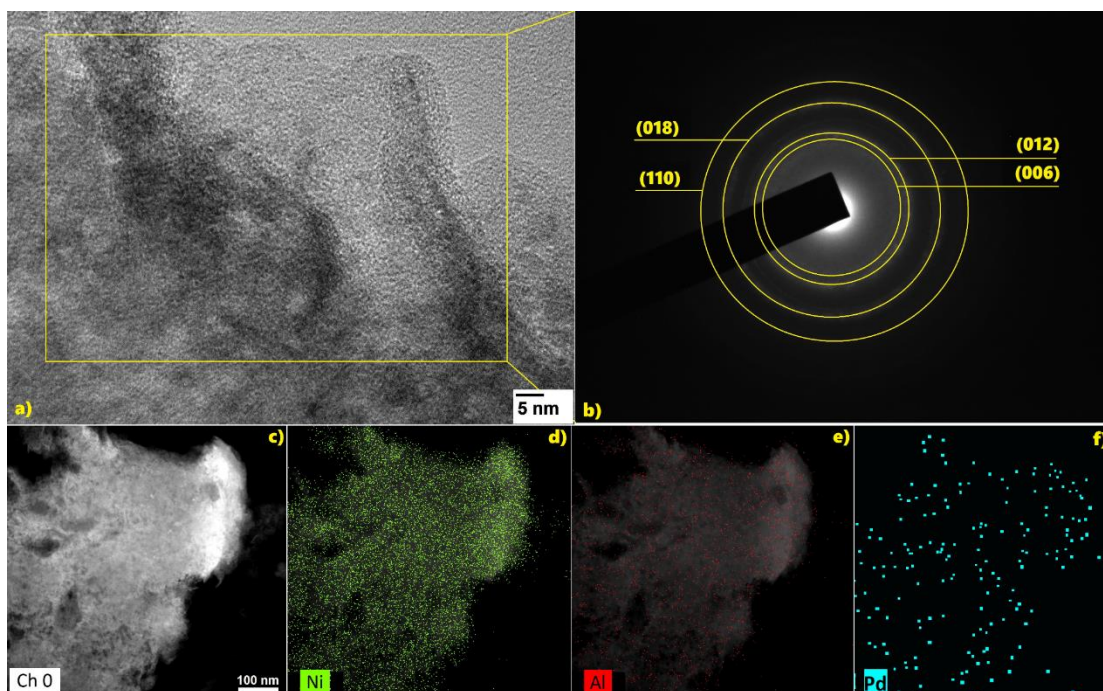


Figure 1. Study of Pd-NiAl-LDH nanosheets: a) highlighted area for SAED (yellow rectangle); b) SAED with highlighted patterns for NiAl-LDH; c-f) EDX elemental mapping including Ch0 base image

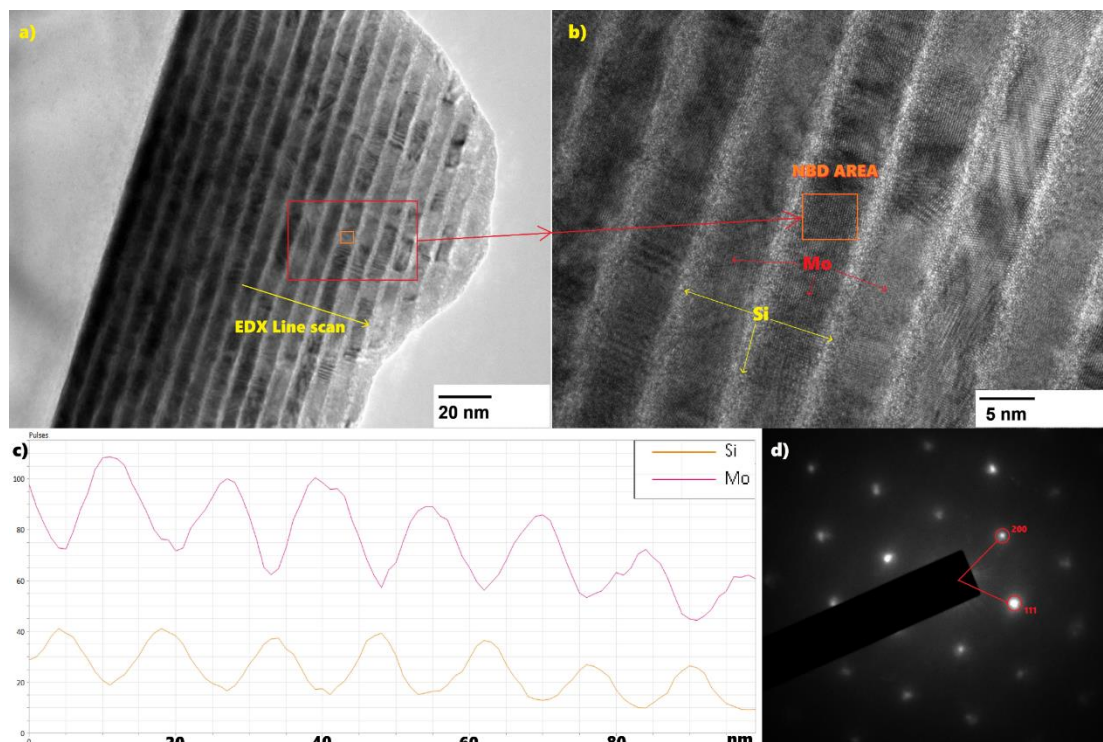


Figure 2. Mo/Si multilayers: a) selected study area: image area b is highlighted with a red rectangle, the EDX line scanning area is highlighted with a yellow line, nanobeam diffraction area with orange rectangle; b) High-resolution image with highlighted area for nanobeam diffraction (NBD); c) EDX line-scan with scale in nm; d) NBD diffraction image for a single Mo layer

TEM study of Al-doped (1–10 at.% Al) thin nanocrystalline transparent ZnO films, which were synthesized by solid-phase pyrolysis at 700 °C, is shown in Figure 3.

TEM showed that the films were continuous and had a uniform distribution of nanoparticles with an average size of 15–20 nm. TEM and EDX confirmed the production of Al-doped ZnO films. The transmittance of Al-doped ZnO films in the range of 400–1000 nm is more than 94%. The introduction of 1% Al into ZnO leads to a narrowing of the band gap compared to ZnO to a minimum value of 3.26 eV and a sharp decrease in the response time to radiation with a wavelength of 400 nm. An increase in aluminum concentration leads to a slight increase in the band gap, which is associated with the Burstein–Moss effect.

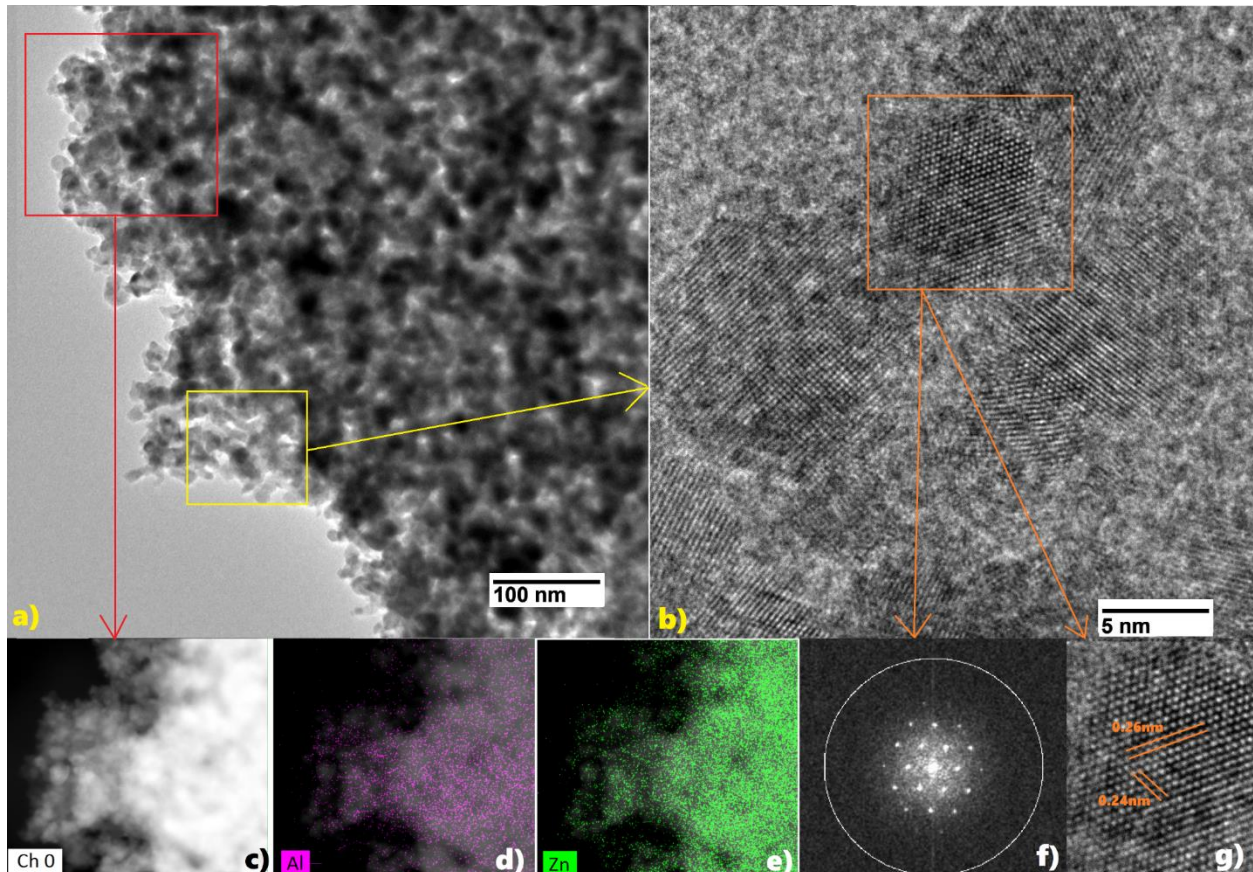


Figure 3. Al-doped nanocrystalline transparent ZnO thin film: a) area of study with highlighted areas for EDX mapping (red) and HRTEM (yellow); b) HRTEM image of single ZnO nanoparticle; c-e) elemental mapping of thin film; f) FFT pattern of single nanoparticle from image b; g) selected interlayer distances in the nanoparticle from figure b

References

1. Kalusulingam R. *et al* Highly Efficient Water Splitting with Pd-Integrated NiAl-LDH Nanosheets as Bifunctional Electrocatalysts // ACS Energy & Fuels. 2023. V. 37(17). P. 13319–13330.
2. Alexey T. Kozakov *et al* Investigation of nanostructural and electronic properties of silicides intermetallic in Mo/Si interfaces of periodic multilayers and bilayer structures // Bull Mater Sci. 2023. V. 46. P. 21.
3. Victor V. Petrov *et al* Polycrystalline Transparent Al-Doped ZnO Thin Films for Photosensitivity and Optoelectronic Applications // Nanomaterials. 2023. V. 13. P. 2348.

OPTIMIZATION OF METHODS FOR SYNTHESIS OF Pt-BASED ELECTROCATALYSTS TO INCREASE THEIR FUNCTIONAL CHARACTERISTICS

Kirill Paperzh, Julia Pankova, Anastasia Alekseenko, Vladimir Guterman
Southern federal university, Rostov-on-Don, Russia, E-mail: kpaperzh@yandex.ru

Introduction

Proton exchange membrane fuel cells (PEMFC) with zero emissions of harmful substances into the atmosphere are one of the key components of the rapidly developing hydrogen energy industry. An integral part necessary for the operation of PEMFC is an electrocatalyst that accelerates the occurrence of current-generating reactions: at the cathode - the electroreduction of oxygen, and at the anode - the electrooxidation of hydrogen. The oxygen electroreduction reaction (ORR) at the cathode occurs at a low rate, which leads to a high overvoltage and, as a consequence, a decrease in the power characteristics of PEMFC. Commercially produced PEMFCs use composites based on platinum nanoparticles (NPs) (less commonly, its alloys) and an electrically conductive carbon support as catalysts. The distribution of platinum nanoparticles in the catalytic layer must be uniform over the entire surface of the carbon support, which is necessary for access of reagents to the electrochemically active surface of platinum and elimination of diffusion problems. A commercially in demand electrocatalyst must be characterized by high values of active surface area (ESA) and activity in the ORR, as well as be resistant to degradation during the operation of the device and maintain high residual activity. To improve the functional parameters of a catalyst, it is necessary to learn how to control its morphology (the size and shape of metal nanoparticles, their composition and spatial distribution over the surface of the support), because it determines the characteristics of the final product [1]. In this regard, it is necessary to develop and optimize methods for the synthesis of highly efficient Pt-based electrocatalysts that combine scalability, speed and reproducibility of the characteristics of the final product.

Experiments

To develop and optimize methods for producing Pt/C with the ability to control the morphology of catalysts, the influence of temperature conditions, the presence and absence of a carbon carrier before nucleation during the synthesis process on the final parameters of the materials were studied [1, 2]. The structural and morphological characteristics of the obtained Pt/C materials were studied using the methods of X-ray diffractometry, thermogravimetry, and transmission electron microscopy. The electrochemical parameters of the obtained catalysts (ESA, ORR activity, stability) were studied using cyclic and linear voltammetry. The commercial analogue JM20 was used as a comparison catalyst.

A study of the influence of temperature conditions on the average size of platinum particles and ESA values showed that with an increase in the temperature of the reaction system from 60 to 90°C during the synthesis process, the average crystallite size and the average size of platinum nanoparticles decrease slightly, by approximately 0.1-0.2 nm, and ESA values increase by 10–12 m² g⁻¹Pt (Fig. 1).

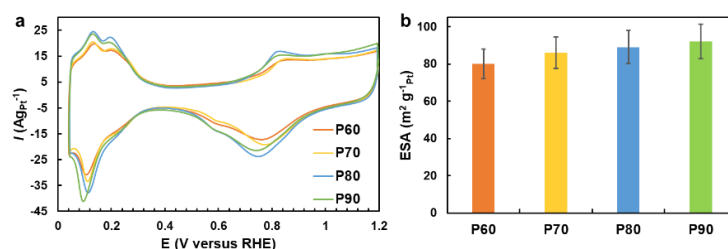


Figure 1. (a) Cyclic voltammograms of the synthesized Pt/C samples. The potential sweep rate is 20 mV s⁻¹. The electrolyte is the 0.1 M HClO₄ solution saturated with Ar. (b) Histograms of the ESA values calculated from cyclic voltammograms. Pt/C materials are hereinafter referred to as P60, P70, P80 and P90, where the specified number corresponds to the synthesis temperature in degrees Celsius.

The discovered effect of temperature in liquid-phase synthesis during homogeneous nucleation makes it possible to select the optimal temperature, which is in the range of 80–90°C, to obtain electrocatalysts with high ESA values.

A comparative study of the structure of the P80, PA80 and P80C, PA80C Pt/C samples obtained by introducing the carbon suspension into the system after and before the synthesis, respectively, has been carried out. For the materials obtained under conditions of the formic acid synthesis (PA80 and PA80C), the most intense reflection peak of the 111 platinum facet is slightly narrower (Fig. 2a) than for the P80 and P80C materials obtained by the formaldehyde method, which indicates a larger particle size.

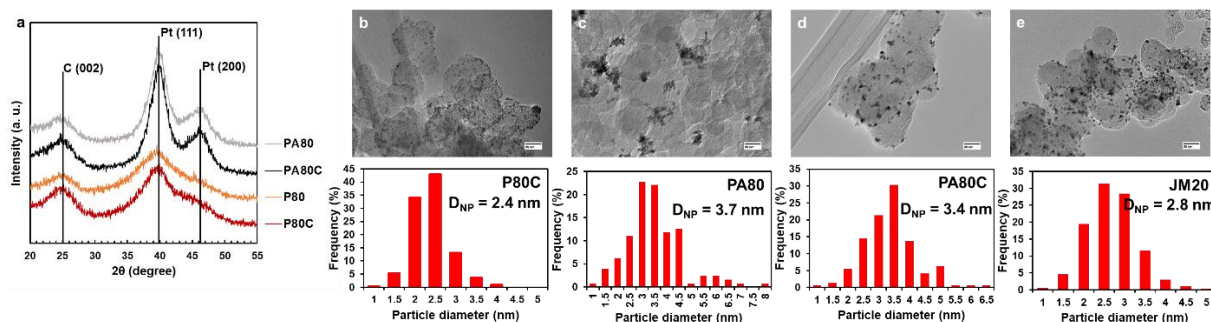


Figure 2. (a) X-ray diffraction patterns of the Pt/C materials. TEM micrographs of the obtained samples and histograms of the NPs' size distribution in the corresponding materials P80C (a), PA80 (b), PA80C (c) and JM20 (d).

The larger particle size in the PA80 and PA80C samples obtained under conditions of the formic acid synthesis compared to P80 and P80C is also confirmed by the TEM method. The size dispersion is almost 1.5 times wider and the average particle size is 1–1.4 nm larger than those of the formaldehyde-synthesized materials (Fig. 2). The materials obtained by the formaldehyde synthesis method are only characterized by a smaller average size of platinum NPs compared to the commercial analog JM20 (Fig. 2). It is worth noting that the aggregation degree of particles calculated from the ratio of the values of the determined ESA and the geometric surface area of Pt decreases with the synthesis being carried out in the carbon suspension (Table 1). The absence of any changes in the size of the formed NPs indicates that there is no significant contribution of the heterogeneous nucleation in the systems containing formaldehyde. The presence of the carbon support in the initial reaction medium contributes to the rapid sorption of the formed platinum NPs, which prevents the aggregation of the particles formed. In the PA80C sample obtained under conditions of the formic acid synthesis in the carbon suspension, the size of Pt NPs is smaller than that of PA80 (Table 1). This may be a reflection of the contribution of the heterogeneous nucleation to the process of the phase formation of Pt NPs. Under conditions of the heterogeneous nucleation, the activation energy for the nucleation of a new phase is known to decrease. This effect is due to a decrease in the energy required for the formation of new interphase surfaces during the nucleation at the already existing interphase boundary.

Table 1: Structural-morphological and electrochemical characteristics of the Pt/C

Sample	D_{XRD} (nm)	ESA ($m^2 g^{-1}_{Pt}$)	S_{geom} ($m^2 g^{-1}_{Pt}$)	Aggregation degree (%)
P80	1.4	89	122	30
P80C	1.4	106	117	10
PA80	3.1	27	76	64
PA80C	2.7	59	82	30

Thus, carrying out the synthesis in the carbon suspension leads to an increase in the ESA of the Pt/C materials. In the event of the formaldehyde synthesis, this is due to the rapid sorption of Pt NPs, which prevents their aggregation in the solution, and in the case of the formic acid synthesis, this may also be due to the contribution of the heterogeneous nucleation to the Pt phase formation process. It is noteworthy that the formaldehyde and formic acid methods for synthesizing the electrocatalysts have a number of differences, e. g., the acidity of the medium at which the reduction process proceeds.

Taking into account the above requirements for the formaldehyde synthesis, we have obtained the Pt/C home-made catalyst in the amount of 1 g at a temperature of 80 °C in the reaction system, with the introduction of the carbon support before the phase formation. The platinum mass fraction in the resulting Pt/C home-made is 20%. The ESA values of the commercial catalyst JM20 are by 23 m² g⁻¹_{Pt} less than those of the Pt/C home-made material (Fig. 3a).

According to the potentiodynamic curves of the ORR at different rotation speeds, the Koutetsky–Levich dependence has been plotted (Fig. 3b, c), using which the electrokinetic parameters of the reaction have been estimated. The mass activity in the ORR of the Pt/C home-made material has proved to be by 13 A g⁻¹_{Pt} higher than that of the commercial analog.

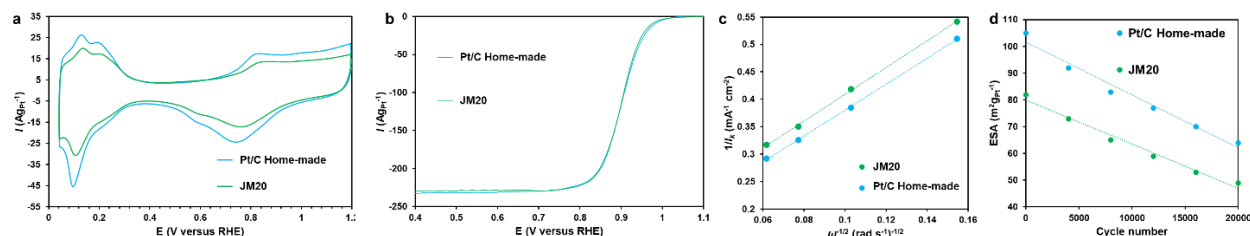


Figure 3. (a) Cyclic voltammograms of the Pt/C samples. (b) Potentiodynamic polarization curves of the ORR. The RDE rotation speed is 1600 rpm. O₂ atmosphere. (c) Dependence of the current strength on the rotation speed of the RDE in the Koutecky–Levich coordinates. (d) Change in the ESA during the stress-test in the mode.

According to the results of the stress-testing, we may point out the ongoing degradation of both the home-made material and its commercial analog. The decrease in the ESA values occurs almost linearly for both the samples (Fig. 3d). The stability of the studied catalysts has turned out to be close, however, the Pt/C home-made sample exhibits the higher initial and residual values of the ESA at the end of stress testing compared to the JM20.

To obtain the materials by the formaldehyde synthesis method with a platinum crystallite size of less than 1.5 nm, an average NPs' size of less than 2.5 nm, their narrow size dispersion (from 1 to 4 nm) and low aggregation, as well as the ESA values of more than 85 m² g⁻¹_{Pt}, it is necessary to use a temperature mode of at least 80°C and the carbon support introduced into the reaction medium before the phase formation and the heating.

Acknowledgement. This research was financially supported by the Ministry of Science and Higher Education of the Russian Federation (State Assignment in the Field of Scientific Activity No. FENW-2023-0016).

References

1. Nefedkin S.I., Ivanenko A.V., Klimova M.A., Pavlov V.I., Panov S.V., Shubenkov S.V., Guterman V.E., Alekseenko A.A., Belenov S.V., Paperzh K.O. Russian technologies and nanostructural materials in high specific power systems based on hydrogen–air fuel cells with an open cathode // Nanotechnologies in Russia. 2020. V. 15. P. 370–378.
2. Danilenko M.V., Guterman V.E., Vetrova E.V., Metelitsa A.V., Paperzh K.O., Pankov I.V., Safronenko O.I. Nucleation/growth of the platinum nanoparticles under the liquid phase synthesis // Colloids and Surfaces A: Physicochemical and Engineering Aspects. 2021. V. 630. No 127125.
3. Bayan Yu., Paperzh K., Danilenko M., Alekseenko D., Pankova Yu., Pankov I., Alekseenko A. Control Over Morphological Characteristics of the Pt/C Catalysts Obtained by the Liquid-Phase Synthesis // Physics and Mechanics of New Materials and Their Applications. PHENMA 2023. Springer Proceedings in Materials. 2024. V. 41. P. 3–15.

DECIPHERING NANOSTRUCTURAL EVOLUTION OF Pt-BASED ELECTROCATALYST VIA IDENTICAL LOCATION TRANSMISSION ELECTRON MICROSCOPY

¹Angelina Pavlets, ¹Yana Astravukh, ¹Anastasia Alekseenko, ¹Ilya Pankov, ²Eugeny Gerasimov, ¹Vladimir Guterman

¹Southern Federal University, Rostov-on-Don, Russia; *E-mail: angelina.pavlez@mail.ru*

²Boreskov Institute of Catalysis, Novosibirsk, Russia

Introduction

Electrocatalysts play a pivotal role in advancing proton-exchange membrane fuel cell (PEMFC) technology for hydrogen energy applications [1]. Electrocatalysts for the PEMFC cathode, which are nanoparticles of platinum or its alloys deposited on a carbon support, must exhibit high activity in the oxygen reduction reaction (ORR), maintain their characteristics during operation, and contain less expensive platinum than their analogues, available today [1].

The need to produce these materials encourages the search for new approaches to controlling their microstructure, which, in turn, requires an assessment of structural characteristics for real-world catalysts at the nanoscale. The complexity of this assessment is largely due to the fact that the composition and condition of the catalyst surface as a whole and the platinum-containing nanoparticles (NPs) in particular may differ significantly under real operating conditions and in the “as-prepared” state [2].

To study the processes of the electrocatalysts surface and NPs structure rearrangement, the method of identical location transmission electron microscopy (IL-TEM) imaging is used, which allows for the evaluation of morphological changes occurring at the same surface section of nano-objects [2].

In our previous work [3] we have shown that the conditions of electrochemical activation, in particular the value of the upper limiting potential (UPL), affects the activity of PtCu/C electrodes in the oxygen reduction reaction (ORR). It has been found that the bimetallic catalysts activated in the potential range up to 1.0 V exhibit 1.5–2 times higher specific and mass activity in the ORR compared to the equivalent samples activated with a higher UPL.

The object of this research is the PtCu/C_N catalyst synthesized using a carbon support doped with nitrogen. To obtain the catalyst, the gram-scale synthesis technology, which is deemed promising for commercial use, has been applied. It has been previously established that the application of bimetallic PtCu NPs to the surface of particles of an N-doped carbon support (C_N) makes it possible to produce electrocatalysts characterized by enhanced stability and ORR activity compared to the Pt/C and PtCu/C materials based on standard carbon black supports [4]. The unique method for synthesizing bimetallic NPs with a core–shell structure, which is based on the application of a gradient approach, has allowed further increasing the ORR activity of the PtCu/C_N catalyst [5].

Experiments

The multistage liquid-phase synthesis of the PtCu/C catalysts was carried out in the water–ethylene glycol solution [5]. Sodium borohydride was used as the reducing agent. At the first stage, copper NPs were formed on the surface of the support. Therefore, during the second and third synthesis stages, platinum and copper atoms were deposited on the obtained cores, and at the fourth stage, we only deposited platinum atoms, thus forming a platinum shell. The sample is labeled as G-N.

We used an N-doped support produced by PROMETHEUS R&D by special treatment of Ketjenblack EC600JD. The resulting PtCu/C_N catalyst contains a 21% Pt loading. The composition of the metal component determined by the X-ray fluorescence with total reflection (TXRF) analysis is Pt:Cu = 1:1.

The composition of the metal component was determined by TXRF. The phase composition as well as the average size of PtCu crystallites were determined by the X-ray powder diffraction (XRD) method.

The size distribution, average size and structure of NPs were assessed by transmission electron microscopy (TEM), high-angle annular dark-field scanning transmission electron microscopy (HAADF-STEM), scanning electron microscopy (SEM) and secondary electron imaging microscopy (SEI). The composition of the catalyst local sections was studied using energy-dispersive X-ray spectroscopy (EDX).

The electrochemical behavior of the catalysts was studied by cycling and linear voltammetry.

When comparing the functional characteristics of the catalysts, the commercial Pt/C catalyst (JM20) (HiSPEC3000, Johnson Matthey, 20% Pt loading) with a close platinum content was chosen as the conventional sample.

Results and Discussion

The electrochemical behavior of the G-N catalyst has been studied after its activation in two potential ranges (0.04–1.0 V and 0.04–1.2 V). The ESA values determined by the given CVs, in turn, also almost do not depend on the activation mode (Figure 1a). It is worth noting that the resulting PtCu/C_N catalyst exhibits a relatively high surface area, which is only slightly inferior to that of the commercial Pt/C analog (JM20) (Figure 1d).

Unlike the ESA, the mass activity of the catalyst in the ORR depends on the UPL during the preceding activation stage. After cycling the catalyst up to E=1.0 V, the mass and specific activity of the material has proved to be 1.7 times higher than after cycling up to E=1.2 V (Figure 1 c, e, f). This fact confirms the significant influence of the limiting activation potential on the functional characteristics of platinum–copper catalysts established by us in [3]. According to the measurement results, the mass activity of the obtained G-N catalyst after less and more hard activation modes has turned out to be, respectively, 5 and 3 times higher than that of JM20 (Figure 1e). It should be noted that the preceding activation mode has no effect on the ORR activity of the Pt/C catalyst [3].

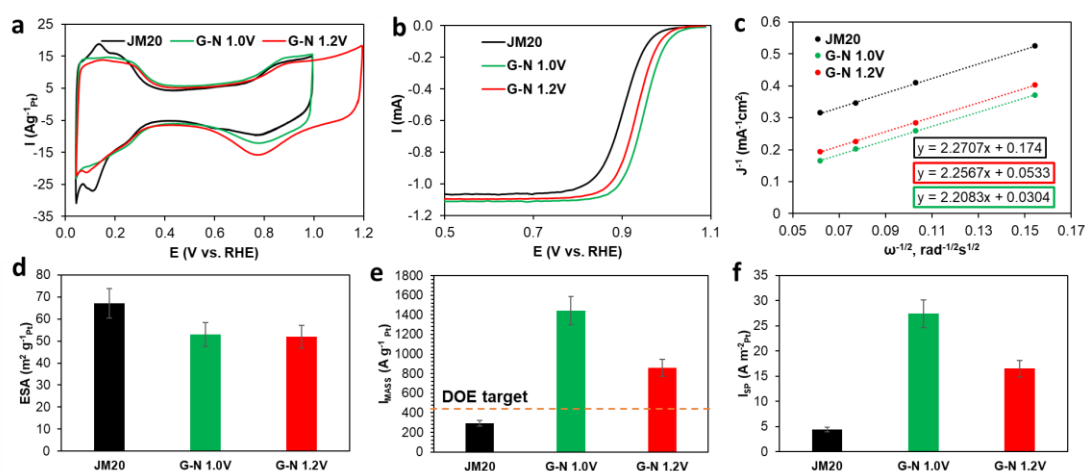


Figure 1. CVs of the catalysts after their activation up to 1.0 V (JM20 and G-N) and up to 1.2 V (G-N) (a); linear sweep voltammograms of the ORR at 1600 rpm (b) and the corresponding dependences in the Koutecky–Levich coordinates (c). Histograms of the ESA (d), mass activity (e) and specific activity (f) values for the catalysts. The orange line represents the U.S. Department of Energy's (DOE) 2020 mass activity target (e).

To identify the reasons for the significant difference in the activity of the PtCu/C_N catalyst after various activation modes, we have conducted a detailed study of the material microstructure before and after the activation by the IL-TEM method (Figure 2). It has been found that after the activation up to the UPL=1.2 V, the particle is compressed, accompanied by a decrease in its size in two directions by almost 1.4 and 0.7 nm, as well as a thickening of the section, which can be deemed a platinum shell, by 0.4 nm compared to the initial state (Figure 2 a, b). With an increase in the UPL up to 1.4 V, the particle tends to take a more regular spherical shape, and the shell thickens by another 0.3 nm, with the core–shell structure being still preserved (Figure 2c). Increasing the UPL up to 1.6 V is conducive to the complete rearrangement of the NP into a “solid-solution”

structure, as well as a further decrease in its size caused by the dissolution of platinum atoms. It is noteworthy that despite the presence of the carbon support sections subjected to degradation, there is no oxidation observed for carbon in contact with the studied NP even at the higher UPL=1.6 V (Figure 2 d). The carbon sections with an amorphous structure appear to be subjected to the oxidation to a greater extent, the presence of contact with the platinum NP not being the main cause of the support oxidation.

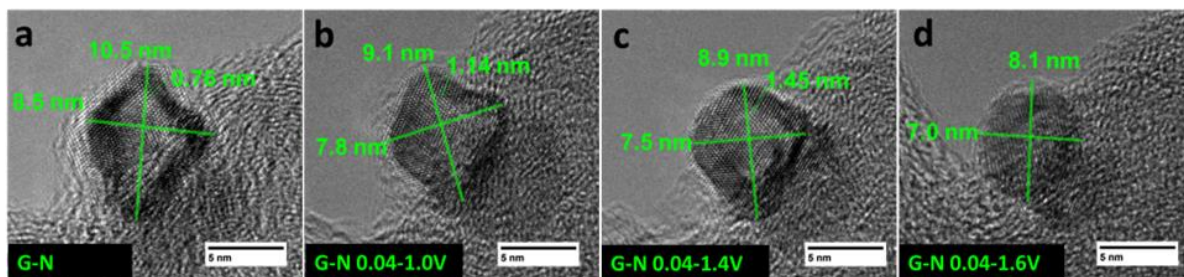


Figure 2. HR-TEM images of an individual NP for the PtCu/C_N sample at various stages of the study.

In this experiment, we have also determined the composition of the metal component for the same section of the catalyst surface, which varies as follows: Pt_{2.3}Cu (initial sample), Pt_{2.6}Cu (0.04–1.0 V activation), Pt_{3.7}Cu (0.04–1.4 V activation), Pt_{5.9}Cu (0.04–1.6 V activation). As the UPL increases, there is a significant decrease observed in the relative copper content as well as an increase in the platinum one. Thus, the particle compression shown in Figure 2 can be associated with both the active leaching of copper and the more moderate dissolution of platinum during the electrochemical treatment.

The work performed demonstrates that the PtCu/C_N catalyst studied behaves as a “living” changing object during the electrochemical activation. These alterations are caused by the spatial movement of NPs as well as the changes in their composition, size, structure and shape. In this regard, the transition from the cyclic activation mode at the UPL=1.0 V to the mode at the UPL=1.2 V does not result in a substantial change in the composition of NPs and the ESA of the catalyst, although it significantly reduces its activity in the ORR. The main reason for this effect is believed to be associated with the features of the NPs structure rearrangement, leading to an increase in the thickness of the NPs platinum shell and a decrease in the promoting effect of the “inner” copper atoms after the activation of the catalyst at the UPL=1.2 V.

Acknowledgement. This study conducted at the Southern Federal University was financially supported by the Russian Science Foundation (grant 23-79-00058)

References

1. *Filippov S.P., Yaroslavtsev A.B.* Hydrogen energy: development prospects and materials // Russ. Chem. Rev. 2021. V. 90. P. 627–643.
2. *Smykala S., Liszka B., Tomiczek A.E., Pawlyta M.* Using the IL-TEM Technique to Understand the Mechanism and Improve the Durability of Platinum Cathode Catalysts for Proton-Exchange Membrane Fuel Cells // Materials. 2024. V. 17. P. 1384.
3. *Alekseenko A.A., Pavlets A.S., Belenov S.V., Safronenko O. I., Pankov I.V., Guterman V.E.* The Electrochemical Activation Mode as a Way to Exceptional ORR Performance of Nanostructured PtCu/C Materials // Appl. Surf. Sci. 2022. V.595 P.153533.
4. *Alekseenko A., Pavlets A., Moguchikh E., Tolstunov M., Gribov E., Belenov S., Guterman V.* Platinum-Containing Nanoparticles on N-Doped Carbon Supports as an Advanced Electrocatalyst for the Oxygen Reduction Reaction // Catalysts. 2022. V.12. P. 414.
5. *Alekseenko A.A., Pavlets A.S., Mikheykin A.S., Belenov S. V., Guterman V.E.* The Integrated Approach to Studying the Microstructure of De-Alloyed PtCu/C Electrocatalysts for PEMFCs // Appl. Surf. Sci. 2023. V.631. P. 157539.

METHODS FOR THE CREATION OF MEMBRANE ALLOYS FOR THE PRODUCTION OF HIGH-PURITY HYDROGEN

Iliya Petriev, Polina Pushankina, Georgiy Andreev, Sergey Ivanin, Marina Papezhuk, Alexandr Simonov, Nikita Prokhorov

Kuban State University, Krasnodar, Russia, E-mail: petriev_iliya@mail.ru

Introduction

Palladium-based membranes are used for gas separation and production of high purity hydrogen. The main important characteristics of palladium membranes are high permeability and selectivity for hydrogen (product purity 99.999%) [1]. However, pure palladium membranes are prone to hydrogen embrittlement and have a high cost. The solution seems to be alloying them with other base metals, which will increase the strength of the membranes when working in a hydrogen atmosphere and reduce the cost of the final product. Such a most promising material for creating hydrogen permeable membranes is an alloy of palladium and copper with an optimal copper content of 40% [2].

Experiments

In the study, samples of Pd-Cu 40% alloy foils were obtained, made by three methods: melting and rolling with intermediate annealing, magnetron sputtering using a solid target and a composite target. The essence of the first method was to produce a homogeneous Pd-Cu 40% alloy by melting the components in an electric arc furnace in an argon atmosphere. To achieve uniformity, the alloy was obtained by a series of melts. Next, the resulting ingot was rolled out on a roller machine with intermediate annealing to a thickness of 20 microns. The essence of the second method was to obtain thin defect-free films of Pd-Cu 40% alloy by magnetron sputtering from a solid target. Palladium-copper foil with a copper content of 40%, obtained by the first method, was used as a target. As a result of spraying, thin films of Pd-Cu alloy 40% with a thickness of 300 nm were obtained, deposited on both sides of the niobium base. As part of the third method, the palladium-copper film was made using a composite target assembled from rolled palladium and copper foils with an area ratio of 60:40. This technique makes it possible to quickly and easily obtain alloys with different ratios and composition of components.

Results and Discussion

Samples of the obtained Pd-Cu 40% films were studied as membranes in hydrogen transport processes. Figure 1 shows data on the dependence of the density of the penetrating hydrogen flow on overpressure for Pd-Cu40% membranes manufactured by magnetron sputtering using solid (a) and composite (b) targets and by melting and rolling with intermediate annealing (c).

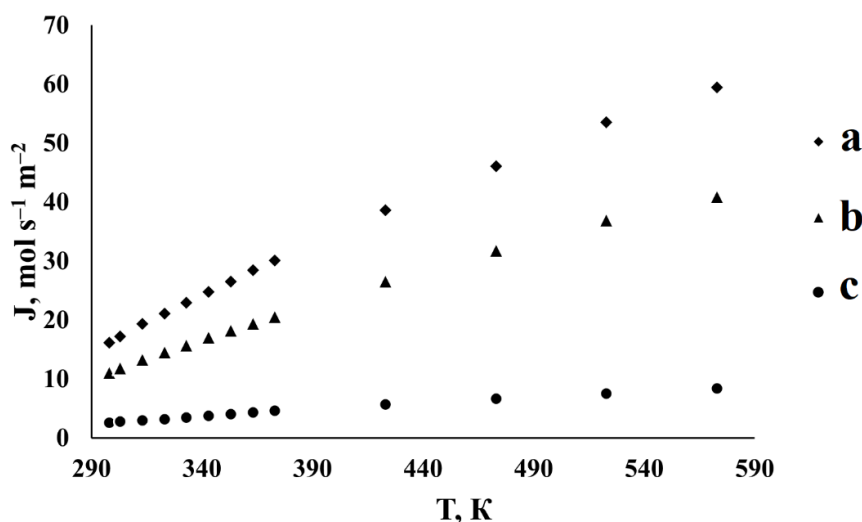


Figure 1. Temperature dependence of the density of the penetrating hydrogen flow at an overpressure of 0.1 MPa on the inlet side of the membranes of the Pd-Cu alloy is 40%.

According to the presented data, the highest flow density was demonstrated by membranes manufactured by magnetron sputtering. Both membranes obtained using solid and composite targets had sufficiently close values of the penetrating flux densities – 60 and 40 mol s⁻¹ m⁻². The obtained values turned out to be up to 7 times higher than for a membrane manufactured by melting and rolling with intermediate annealing, which demonstrated numerical values of flow density up to 7 mol s⁻¹ m⁻². The recorded significant increase in the flux density of membranes obtained by magnetron sputtering is probably due to a significant decrease in film thickness and ordering of the solid solution to form a β -phase with a less dense crystal lattice, compared with the HCC lattice of α -aphasic.

As a result of the work carried out, it can be concluded that the magnetron sputtering method is a fairly promising method for obtaining defect-free thin-film materials with high permeability. The method is also characterized by significant savings in the consumption of precious metal by reducing the thickness of the resulting films.

Acknowledgement. This research was funded by the Russian Science Foundation and the Kuban Scientific Foundation grant No. 24-19-20070, <https://rscf.ru/project/24-19-20070/>.

References

1. Filipov. S.P., Yaroslavtsev. A.B. *Hydrogen energy: development prospects and materials* // *Russian Chemical Reviews*, 2021, V. 90, P. 627–643.
2. Burkhanov G.S., Gorina N.B., Kolchugina N.B., Roshan N.R. // *Russian Chemical Journal*, 2006, V. 50, P. 36-41.

THE INFLUENCE OF PULSED ELECTRIC FIELDS ON THE TARTRATE STABILIZATION EFFICIENCY OF WINE MATERIALS BY ELECTRODIALYSIS

Natalia Pismenskaya, Evgeniia Pasechnaya, Anastasiia Klevtsova, Anastasiia Korshunova, Daria Chuprynina

Kuban State University, Krasnodar, Russia, E-mail: n_pismen@mail.ru

Introduction

Electrodialysis (ED) is increasingly used for tartrate stabilization of wine. This process preserves valuable components and has a low environmental impact. The widespread introduction of ED tartrate stabilization of wine into the winery industry is limited by fouling of ion-exchange membranes (IEMs) and a decrease in the transport characteristics of IEMs during their operation [1]. There are also difficulties with the rather limited range of IEMs currently used for tartrate stabilization of wine. However, recently many new experimental and commercial IEMs have appeared. In addition, a number of studies have been published [2,3], which show the effectiveness of replacing traditional ED current modes (direct continuous electric field, CEF) with pulsed electric field (PEF) current modes.

The purpose of this work is to evaluate the applicability of homogeneous (CJMA-3//CJMC-3 and AMX-Sb//CMX-Sb), as well as heterogeneous (MA-41//MK-40 and AMH-PES//CMH-PES) ion exchange membranes for ED tartrate stabilization of wine using CEF or PEF current modes.

Experiments

Tartrate stabilization of wine was carried out in batch mode using a six-compartment laboratory ED cell. The experiment was carried out until the electrical conductivity in the desalination stream decreased by 20%, which corresponds to the conditions of reducing the concentration of tartrates to the specified values [4]. Two current modes were used in the experiments: CEF and PEF.

Before and after ED process the quantitative content of potassium, tartrate and chloride removed from the desalination stream was determined using ion chromatography. Then, the degree of extraction of ion i was calculated as:

$$\gamma_i = \frac{(c_o^i - c_t^i)}{c_o^i} \cdot 100\% \quad (1)$$

Here c_o and c_t are the molar concentrations of the i ion at the initial moment and at the ED duration t , respectively. In addition, energy consumption in the ED process was estimated.

Results and Discussion

The results of the experiments are presented in Table 1.

Table 1: The Degree of Extraction of Potassium Cations (K^+), Tartrate ($H_{(2-x)}T^{x-}$) and Chloride (Cl^-) Anions from a Model Wine in the Desalination Stream of the ED Setup

Cation-exchange membrane	Current mode	The degree of extraction, %	Anion-exchange membrane	Current mode	The degree of extraction, %	
		K^+			$H_{(2-x)}T^{x-}$	Cl^-
CMX-Sb	CEF	19.0	AMX-Sb	CEF	19.9	32.1
	PEF	13.1		PEF	24.0	32.2
CJMC-3	CEF	5.5	CJMA-3	CEF	17.5	18.1
	PEF	15.5		PEF	19.0	20.0
MK-40	CEF	19.5	MA-41	CEF	7.5	42.2
	PEF	23.9		PEF	10.1	52.1
CMH-PES	CEF	20.1	AMH-PES	CEF	10.2	41.9
	PEF	22.3		PEF	13.1	48.0

The structural parameters of heterogeneous MK-40 and CMH-PES membranes ensure removal of K^+ cations comparable to homogeneous CJMC-3 and CMX-Sb membranes. At the same time, the transport of large, highly hydrated tartrate anions in heterogeneous MA-41 and AMH-PES

membranes is sterically hindered. The preferable transfer of chloride anions through these membranes is the result of these steric hindrances, despite the concentration of which in the model wine is an order of magnitude lower than that of tartrate anions (Table 1).

It follows from estimates of the energy consumption of the ED tartrate stabilization of model wine, that the use of PEF current mode requires less electrical energy than the use of CEF current mode (Fig. 1). Energy savings range from 10 to 33% for various membrane pairs. Energy consumption is reduced most significantly when using membrane pairs AMX-Sb//CMX-Sb (33%) and AMH-PES//CMH-PES (21%).

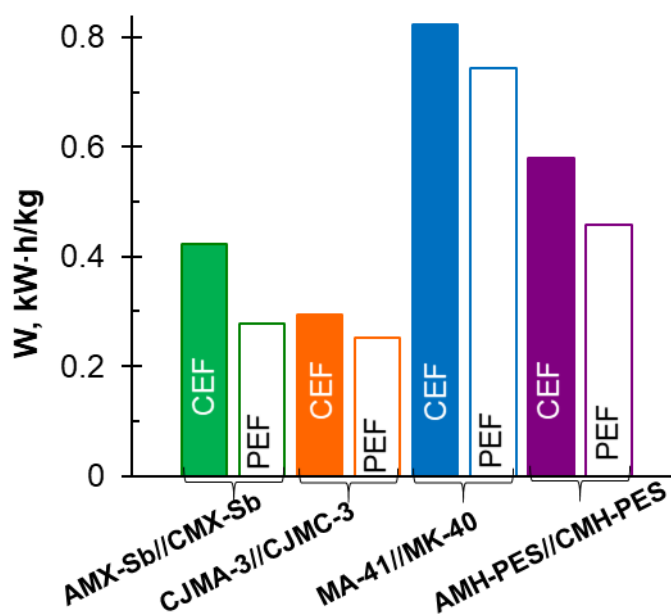


Figure 1. Energy Consumption for ED Tartrate Stabilization of Model Wine Using the Study Membrane Pairs Referred to 1 kg of Extracted Tartrates.

Acknowledgement. The Kuban Science Foundation, project No. MFI-20.1/78, funded this study.

References

1. *Bdiri M., Perreault V., Mikhaylin S., Larchet C., Hellal F., Bazinet L., Dammak L.* Identification of phenolic compounds and their fouling mechanisms in ion-exchange membranes used at an industrial scale for wine tartaric stabilization by electrodialysis // *Sep. Purif. Technol.* 2020. V. 233(115995)
2. *Cournoyer A., Bazinet L.* Electrodialysis Processes an Answer to Industrial Sustainability: Toward the Concept of Eco-Circular Economy?—A Review // *Membranes.* 2023. V. 13. (205)
3. *Nichka V. S., Nikonenko V. V., Bazinet L.* Fouling Mitigation by Optimizing Flow Rate and Pulsed Electric Field during Bipolar Membrane Electroacidification of Caseinate Solution // *Membranes.* 2021. V. 11(534)
4. *Benítez J. G.* Comparison of electrodialysis and cold treatment on an industrial scale for tartrate stabilization of sherry wines // *J. Food Eng.* 2003. V. 58 (4) P. 373-378.

MINERALIZATION OF PHOTOPOLYMER-BASED MICROPLASTICS ON A GRANULAR ANODE MADE OF SUB-STOICHIOMETRIC TITANIUM OXIDE

Victoria Plis, Andrey Kislyi, Ilya Moroz, Vera Guliaeva, Yuri Prokhorov, Anastasiia Klevtsova

Kuban State University, Krasnodar, Russia, E-mail: viikapliss@mail.ru

Introduction

Electrochemical oxidation advanced processes (EAOPs) are widely used for the treatment of wastewater and natural waters polluted with various organic compounds, as they are highly efficient, easy to optimize and quite versatile. Among EAOPs, one of the popular methods is anodic oxidation, which generates hydroxyl radicals with high oxidizing activity on the anode surface [1].

Porous materials are the most promising for anodic oxidation. Sub-stoichiometric titanium oxide (Ti_4O_7) is used, which has a large electrochemical active surface area, increasing the oxidation rate due to a rapid delivery of organic substances to the electrode surface [2]. Moreover, this material has high conductivity, chemical stability, and high oxygen evolution overpotential. Particle electrodes may be a simple alternative to porous electrodes [3].

In this study, anodic oxidation of photopolymer-based microplastics was investigated. Photopolymers are used in 3D printing and various engineering applications and are hazardous to human health and the environment if disposed of improperly.

Experiments

The experimental setup consists of an electrochemical flow cell and a hydraulic system providing a continuous supply of solution at a constant rate. The constant current is maintained by means of a current source, the potential drop between the cathode and anode is recorded by a voltmeter. The electrochemical cell is a rectangular flow electrolysis chamber with a plate stainless steel cathode and a particle anode made of porous Ti_4O_7 . The electrodes are divided by a mesh separator made of inert material (polypropylene). The sealed case of the cell is made of polytetrafluoroethylene, which ensures the tightness of the system.

The microplastic suspension was obtained by dissolving of photopolymer resin in water (0.5 g per 100 ml) followed by UV irradiation for 15 minutes. As a result, the almost transparent solution became turbid and the largest microplastic particles settled to the bottom of the container after a few hours. The suspension with the finest microplastic particles was then taken from the top of the solution container after 12 hours of settling.

Before starting the experiment, to evaluate the effect of microplastic deposition in the pores of the anode, the tested solution was pumped through the cell without current for 30 minutes. Before and after pumping, samples were taken. Then the experiment was conducted at 0.5 A current for 3 hours. The concentration of microplastic particles was evaluated by the turbidity of the solution.

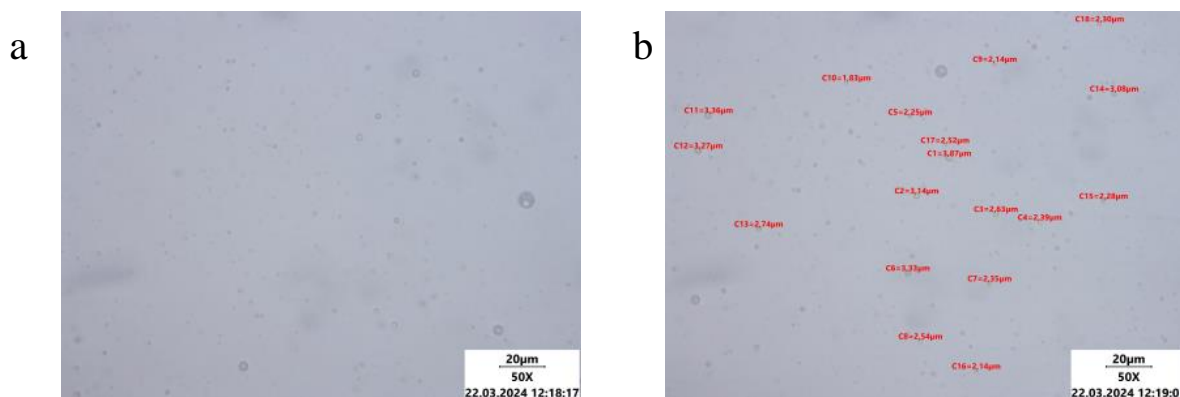


Figure 1. Optical Imaging of Microplastic Particles (a) and Particle Size Estimation (b).

Results and Discussion

The optical density values obtained during the experiment and presented in Table 1 indicate partial sorption of microplastic particles by the anode granules. It is shown that after 30 minutes the most of particles of microplastics were sorbed by anode. After that the electrical current was switched on. In the presence of the background electrolyte sodium chloride (NaCl) in the system, the concentration of particles decreases more than 20 times compared to the system with sodium sulphate (Na₂SO₄), in which the concentration of microplastic decreased 2.5 times, indicating the possible generation of chlorine radicals actively involved in the process. However, in both cases the microplastic concentration in the samples was minimal, indicating the high efficiency of the applied process: sorption and anodic oxidation.

Table 1: Optical Density of Samples

	Photopolymer + 0.1M NaCl	Photopolymer + 0.1M Na ₂ SO ₄
Before experiment	0.841	0.658
After 30 minutes of pumping without current	0.214	0.047
After 3 hours of anodic oxidation, current is 0.5 A	0.009	0.018

Acknowledgments. The study is realized with the financial support of the Russian Science Foundation, project № 22-79-10177.

References

1. *Sirés I., Brillas E., Oturan M. A., Rodrigo M. A., Panizza M.* Electrochemical advanced oxidation processes: Today and tomorrow. A review // *Environ. Sci. Pollut. Res.* 2014. V. 21. P. 8336-8367.
2. *Trellu C., Coetsier C., Rouch J. C., Esmilaire R., Rivallin M., Cretin M., Causserand C.* Mineralization of organic pollutants by anodic oxidation using reactive electrochemical membrane synthesized from carbothermal reduction of TiO₂ // *Water Res.* 2018. V. 131. P. 310-319.
3. *GracePavithra K., Senthil Kumar P., Jaikumar V., SundarRajan P. S.* A review on three-dimensional electrochemical systems: analysis of influencing parameters and cleaner approach mechanism for wastewater // *Rev. Environ. Sci. Biotechnol.* 2020. V. 19. P. 873-896.

CHARACTERIZATION OF PORE-FILLING CATION - EXCHANGE MEMBRANE IN SODIUM CHLORIDE SOLUTION

¹Maria Ponomar, ²Elizaveta Korzhova, ²Dmitry Lopatin, ¹Veronika Sarapulova, ³Lasaad Dammak, ²Igor Voroshilov

¹Kuban State University, Krasnodar, Russia, *E-mail: ponomar.marie@yandex.ru*

²Krasnodar Compressor Plant LLC, Krasnodar region, Dinskaya, Russia, *E-mail: lizelotavocal@mail.ru*

³Institute de Chimie et des Matériaux de Paris Est, UMR 7182 CNRS-Université Paris-Est, Thiais, France

Introduction

Perfluorinated polymer cation-exchange membranes (PPM) have long been successfully used as solid electrolytes in fuel cells and separating film in membrane electrolyzers, electrolysists, and sensors [1]. It is well-known that American perfluorosulfonic acid (PFSA) materials, such as Nafion® membranes (DuPont de Nemours, USA) are the most extensively applied materials for such membrane type. The incorporation of an inert polymer reinforcing cloth to the composition is one of common way to increase the mechanical strength of this membranes (Nafion N438 or Nafion 324) [2], though it leads to decrease in some important characteristics.

In this work, we have investigated some characteristics of experimental PPM designated below as M1. M1 was prepared by pore-filling method. This membrane have practical potential for import substitution. Nafion N438 membrane was examined for comparison.

Experiments

Nafion N438, which known also as Teflon Fabric Reinforced Membrane (TFRN) [5], is reinforced with plain weave fabric. This monofilament reinforcement fabric is made from polytetrafluoroethylene (PTFE). The mesh cells of the fabric have dimensions $300 \times 300 \times 0.320$ mm³. Experimental M1 cation-exchange membrane contains a non-woven fluoropolymer reinforcing filler.

Characterization included scanning electron microscopy (SEM), FTIR-spectroscopy, as well as measuring of the water uptake and ion-exchange capacity. In addition, the concentration dependences of specific electrical conductivity of the membranes were obtained using the difference method with clip-type cell, then the data were treated with microheterogeneous model [3]. The concentration dependences of integral coefficient of diffusion permeability were determined using two-chamber flow-through cell. Determined dependences were used for evaluation of counterion transport numbers by the algorithm suggested in study [4]. The experiments were conducted in NaCl solutions at 25°C.

Results and Discussion

Table 1 presents both membranes characteristics, including thickness (l_{sw}), ion exchange capacity (Q_{sw}) in the swollen state, surface contact angles (θ_{sw}) and tensile strength.

Table 1: Properties of Investigated Membranes in Na⁺ Form

Membrane	l_{sw} , μm	Q , mmol/g _{sw}	W , g _{H₂O} / g _{dry}	θ_{sw} , grad	Tensile strength, MPa
Nafion N438	340 ± 6	0.91	0.21	*SI 80 ± 4 SII 62 ± 5	27.5 [2]
M1	38 ± 3	0.48	0.28	SI 74 ± 3 SII 74 ± 3	46.7

*SI and SII are opposite membrane surfaces

The thickness of the swollen Nafion N438 membrane is several times greater than that of the swollen M1 membrane. The ion exchange capacity of this commercial membrane almost two time higher compared to M1 membrane.

The SEM images of the surface SI (Fig. 1a) and cross-section (Fig. 1b) of M1 membranes show that the fibers acting as reinforcing material are distributed chaotically within the ion exchange material.

Table 2 lists the values of volume fraction of intergel phase (f_2) and of specific conductivity of the membrane in isoelectrical conductivity point (k_{iso}) found from concentration dependences of specific electrical conductivity of the membranes (Fig. 2a). The k_{iso} parameter characterizes the conductivity of the gel phase of the membranes and gives insight on the transport characteristics of ionconductive polymer the membrane is produced from. The f_2 parameter corresponds to the fraction of the membrane volume occupied by electroneutral solution and also allows evaluating its pore size.

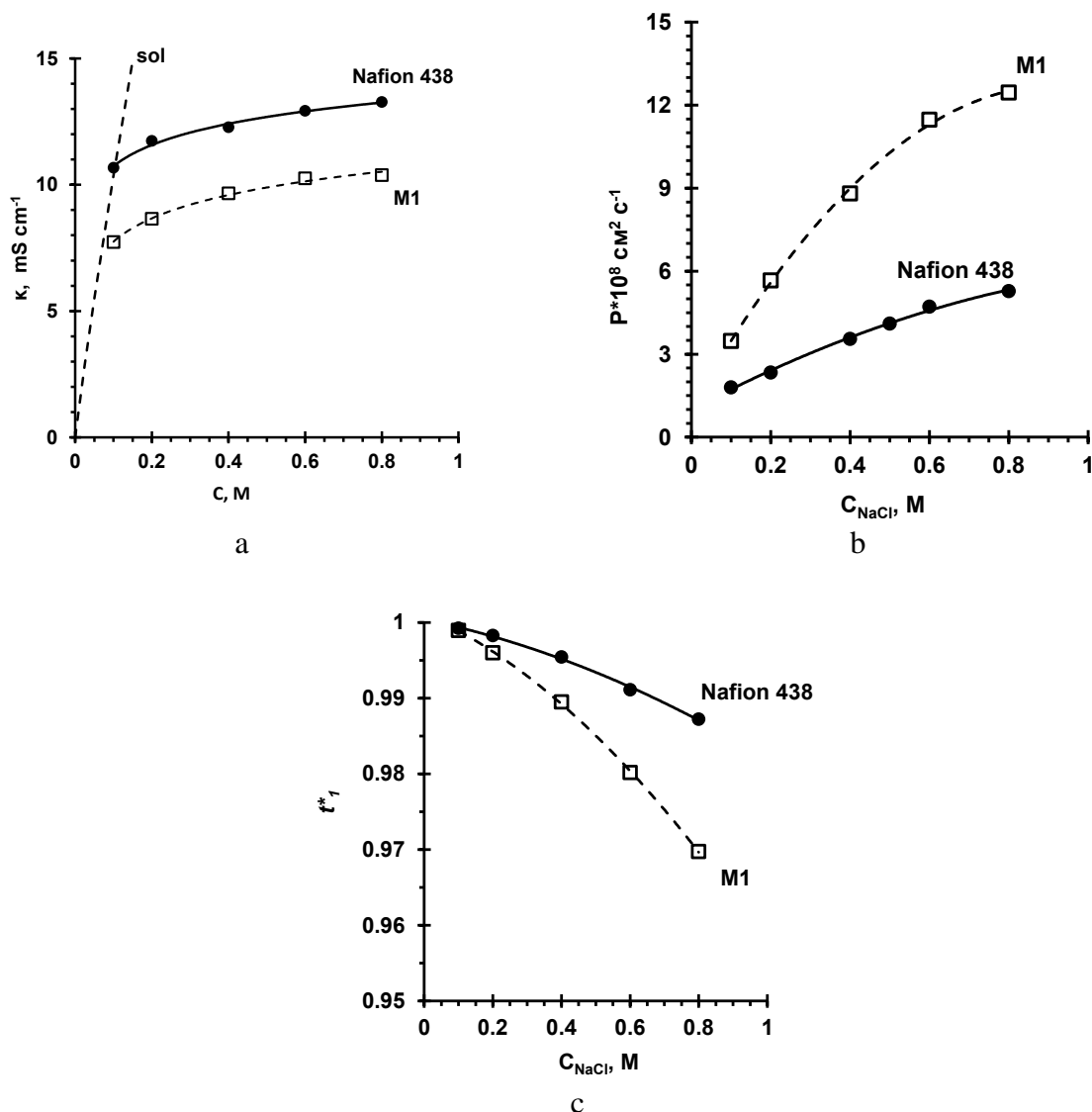


Figure 2. Concentration Dependences of Electrical Conductivity (a), Diffusion Permeability (b) and Transport Numbers of Counterions (c) Through Studied Membranes.

Table 2: Selected Characteristics of Studied Membranes in NaCl Solution

Membrane	κ , mS cm ⁻¹	R , Ohm cm ²	k_{iso} , mS cm ⁻¹	f_2
Nafion N438	12.9	2.6	10.9	0.10
M1	10.3	0.3	7.4	0.15

*in 0.6 M NaCl solution

It follows from the obtained data that the specific electrical conductivity of M1 membrane is comparable with conductivity Nafion N438. At the same time, the f_2 values of membrane M1 higher than the f_2 measured for Nafion N438, indicating the presence of large pores within the M1 membrane.

It should be noted that M1 membrane possess the integral coefficient of diffusion permeability that exceeds the values measured for commercial Nafion N438 membrane (Fig. 2b). The concentration dependences of integral coefficient of diffusion permeability of M1 membranes are

closer to the values typical for commercial heterogeneous membrane MK-40 or homogeneous membrane FujiFim CEM Type 1 [6].

In dilute ($C < 0.1$ M) NaCl solution the counterion transport numbers through all studied membranes tend to 1 (Fig. 2c). At higher NaCl concentrations the selectivity of M1 cation exchange membrane is noticeably lower, due to either the higher values of f_2 , or/and the low ion-exchange capacity.

Hence the M1 membrane possess strong mechanical properties (tensile strength of 46.7 MPa) as well as good electrochemical characteristics such as low electrical resistance (< 0.4 Ohm cm^2), high cation transport number (> 0.97). The selectivity of the M1 membrane with a high f_2 value can be improved by partially eliminating structural defects caused by the embedding of the reinforcing cloth.

Acknowledgement. This research was financially supported by the Russian Science Foundation, research project no. 23-79-01261. The authors are grateful to M.E. Sokolov (the collective center for Diagnostics of Structure and Properties of Nanomaterials at Kuban State University) for the SEM measurements.

References

1. Pourcelly G., Nikonenko V. V., Pismenskaya N. D., Yaroslavtsev A. B., Ciferri A., Perico A. Ionic interactions in natural and synthetic macromolecules, a Chapter in a Book, Appl.Charg. Membr. Sep. Fuel Cells Emerg. Process, Hoboken, 2012.
2. Yesaswi C. S., Sreekanth, P. R. Evaluation of dynamic mechanical properties of teflon fabric reinforced artificial muscle material // Materials Today: Proceedings. 2020. V. 27. P. 936-939.
3. Zabolotsky V. I., Nikonenko V. V. Effect of structural membrane inhomogeneity on transport properties // J. Memb. Sci. 1993. V. 79. P. 181-198.
4. Larchet C., Dammak L., Auclair B., Parchikov S., Nikonenko V. A simplified procedure for ion-exchange membrane characterization // New Journal of Chemistry. 2004. V. 28. №10. P. 1260-1267.
5. Yesaswi C. S., Sahu S. K., Sreekanth P. S. R. Experimental investigation of electro-mechanical behavior of silver-coated Teflon Fabric-Reinforced Nafion Ionic Polymer Metal Composite with carbon nanotubes and graphene nanoparticles // Polymers. 2022. V. 14. Art. № 5497.
6. Sarapulova V., Shkorkina I., Mareev S., Pismenskaya N., Kononenko N., Larchet C., Dammak L., Nikonenko V. Transport characteristics of Fujifilm ion-exchange membranes as compared to homogeneous membranes AMX and CMX and to heterogeneous membranes MK-40 and MA-41 // Membranes. 2019. V. 9. P. 1-23.

MODELING OF ANALYTE BEHAVIOR AND PRECONCENTRATION IN TERNARY ELECTROLYTE SYSTEMS

^{1,2}Roman Ponomarev, ^{1,3}Maxim Alekseev, ¹Georgy Ganchenko, ²Irina Morshneva, ^{1,4}Evgeny Demekhin

¹Laboratory of micro- and nanoscale electro- and hydrodynamics, Financial University, Moscow, Russia
E-mail: GSGanchenko@fa.ru

²South Federal University, Rostov-on-Don, Russia

³Kuban State University, Krasnodar, Russia

⁴Laboratory of General Aeromechanics, Institute of Mechanics, Moscow State University, Moscow, Russia

Introduction

The development of lab-on-chip technology is one of the most promising applications of microfluidic devices [1]. These devices are used for conducting various medical tests on samples at the microscale. A major challenge in the development of these devices is overcoming the issues related to low concentrations, mixing, and separation.

Recently, superconcentration techniques have become popular in this field [2, 3]. Superconcentration occurs near ion-selective membranes, leading to an increase in analyte concentrations up to millions of times in a localized area. While experiments have confirmed the existence of this phenomenon, the precise conditions for its occurrence remain unknown. This is due to the difficulty in solving this problem analytically or numerically.

The system of Nernst-Planck-Poisson-Stokes (NPPS) equations is non-linear, becoming even more complex when considering each ion type separately. Therefore, the problem cannot be solved using conventional methods. In addition to the various parameters that may be varied, the issue also encompasses thin Debye layers, which typically occur near ion-selective interfaces. These layers substantially complicate numerical computations, hence we will consider simplified models with a view to studying concentration.

Results and Discussion

In this paper, we examine the NPPS system in various configurations, starting with a fundamental formulation for a binary electrolyte in the absence of advection. As an illustration, we use the decomposition method [4] to reduce the system of partial differential equations to a single equation [5]. Next, we apply this approach analogously for a ternary electrolyte. Having solved the resulting equation via asymptotic decomposition, we analyze the outer and inner solutions.

Furthermore, we consider a more complex formulation with sliding velocities for limiting and underlimiting currents, building upon the work of Rubinstein and Zaltzman [6].

An exact analytical solution to the system has not yet been found in general. However, some approximate solutions have been derived, which provide a good understanding of the system's behavior. Equations have also been formulated to help elucidate the effects of superconcentration on the system. The analysis of external and internal solutions, obtained through asymptotic expansion, reveals a complex relationship between the solution of the system and the charge number of the third species.

The results could also be applied to improve electrobaromembrane methods for metal recovery from electrolytic solutions [7].

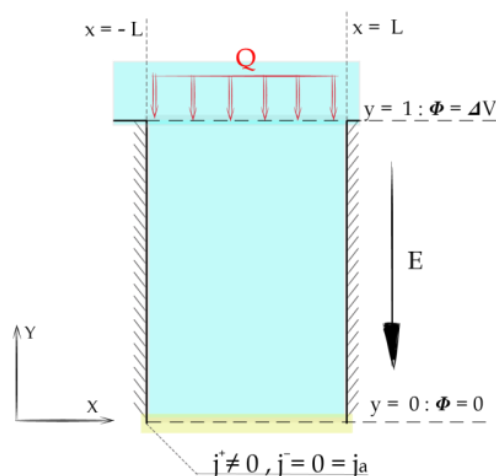


Figure 1. Geometric statement of the problem.

Acknowledgement. The work was supported by the Russian Science Foundation, project 22-79-10085.

References

1. Kumar S. *et al.* Quantifying PON1 on HDL with nanoparticle-gated electrokinetic membrane sensor for accurate cardiovascular risk assessment // *Nat Commun.* 2023. V. 14(1). P. 557.
2. Ouyang W. *et al.* Deciphering ion concentration polarization-based electrokinetic molecular concentration at the micro-nanofluidic interface: theoretical limits and scaling laws // *Nanoscale.* 2018. V. 10(32). P. 15187–15194.
3. Berzina B., Anand R. K. Tutorial review: Enrichment and separation of neutral and charged species by ion concentration polarization focusing // *Anal. Chim. Acta.* 2020. V. 1128. P. 149–173.
4. Kovalenko A. V., Khromykh A. A., Urtenov M. Kh. Decomposition of the two-dimensional Nernst-Planck-Poisson equations for a ternary electrolyte // *Dokl Math.* 2014. V. 90(2). P. 635–636.
5. Demekhin E. A., Ponomarev R. R., Alekseev M. S., Morshneva I. V., Ganchenko G. S. Electrokinetic instability of a highly charged and weakly diffusing analyte in a buffer electrolyte near an ion-selective surface // *Eur. Phys. J. Spec. Top.* 2024.
6. Rubinstein I., Zaltzman B. Electro-osmotically induced convection at a permselective membrane // *Phys Rev E.* 2000. V. 62(2). P. 2238–2251.
7. Butylskii D. *et al.* Application of Hybrid Electrobaromembrane Process for Selective Recovery of Lithium from Cobalt- and Nickel-Containing Leaching Solutions // *Membranes.* 2023. V. 13(5). P. 509.

ASYMMETRY IN DIFFUSION PERMEABILITY OF COMMERCIAL ION-EXCHANGE MEMBRANES AS A RESULT OF DISCREPANCY IN SURFACE ROUGHNESS OF DIFFERENT SIDES

Mikhail Porozhnyy, Veronika Sarapulova, Maria Ponomar, Victor Nikonenko

Kuban State University, Krasnodar, Russia, E-mail: porozhnyj@mail.ru

Introduction

In terms of fundamental understanding of membrane structure and its main properties, the basics of membrane surface properties influence on transport characteristics is among the most topical issue, since the first electrolyte–membrane interaction occurs at the membrane surface. Many research papers emphasize the effect of surface properties on membrane performance in electrochemical processes [1,2]. Furthermore, such influence on the transport characteristics of anisotropic membranes is noted even in the absence of an electric field. For example, the studies [3,4] present the asymmetry of diffusion permeability of the surface-modified MF-4SC/PANI membrane. The results suggest that membrane sides orientation in a diffusion cell defines the concentration dependence of the diffusion permeability coefficient of the membrane. This effect is determined by the ion concentration gradient within the membrane, which complicates ion transfer in one of the directions [5].

However, asymmetry of the transport properties can also be observed for commercial samples. The study of this issue is quite important for the purposes of developing methods for membrane modification or fundamental studies of the structure-transport properties relationship. This paper presents a study of the effect of surface roughness on the asymmetry of the diffusion permeability of commercial ion-exchange membranes.

Experiments

In this work, the characteristics of the homogeneous cation-exchange membranes Neosepta CMX (Astom, Japan), CJMC-3 (Hefei Chemjoy Polymer Materials, China), SYMC-2 (Anhui Zhongke Shenyang, China), Fuji CEM Type 1 (Fujifim, The Netherlands) are studied. Diffusion permeability in sodium chloride solutions is determined using a two-compartment flow cell. Surface roughness is studied using the TR200 profilometer [6]. All membranes underwent standard salt pretreatment before measurements. The optical microscope SOPTOP CX40M (Yuyao, Zhejiang, P.R. China) with a digital USB camera was used to visualize the surface and cross section of swollen ion-exchange membranes.

Results and Discussion

Table 1 presents the membrane surface roughness parameters. The CMX membrane has identical properties of both surfaces within the measurement error. Other membranes have asymmetric properties of both surfaces (surface I for each membrane has higher values of the r , R_t и R_a).

Table 1: Roughness Characteristics of Swollen Membranes

Membrane	Surface	r	R_t , μm	R_a , μm	S_m , μm
CMX	I	1.003	31.3 ± 3.8	4.9 ± 0.5	605 ± 78
	II	1.003	30.5 ± 3.8	4.7 ± 0.6	540 ± 53
CJMC-3	I	1.006	19.2 ± 2.6	2.9 ± 0.4	280 ± 20
	II	1.002	15.4 ± 4.8	2.8 ± 0.4	285 ± 27
SYMC-2	I	1.022	62.4 ± 3.8	11.8 ± 0.5	357 ± 30
	II	1.000	11.6 ± 1.5	1.7 ± 0.3	514 ± 80
Fuji CEM Type 1	I	1.003	40.5 ± 8.3	7.6 ± 1.1	952 ± 138
	II	1.001	38.5 ± 3.4	6.8 ± 0.9	707 ± 140

r is the roughness factor; R_t is the height distance between the deepest valley and the highest hill; R_a is the arithmetic mean roughness; S_m is the mean width of the profile elements.

In order to illustrate the differences in surface properties of different sides of commercial membranes, Figure 1 presents optical images of the surfaces and cross-section of the SYMC-2 membrane, as well as profilograms of the surfaces.

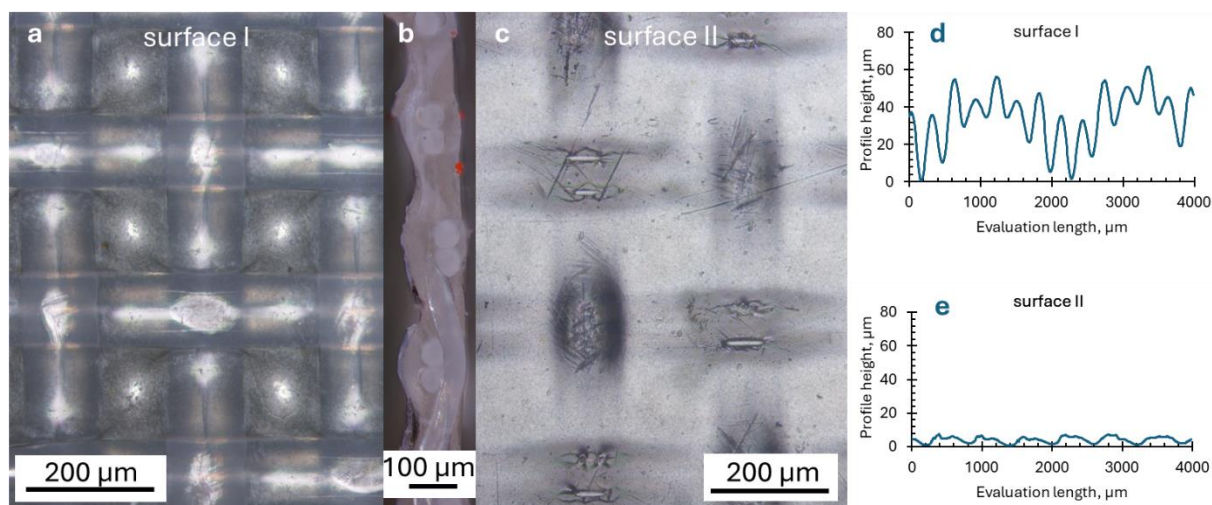


Figure 1. Optical Images of the Surfaces I (a), II (c) and Cross-Section (b) of the SYMC-2; and Profilograms of the Relevant Surfaces I (d) and II (e).

The concentration dependences of membranes diffusion permeability obtained with the surface I or II facing the electrolyte solution are shown in Figure 2.

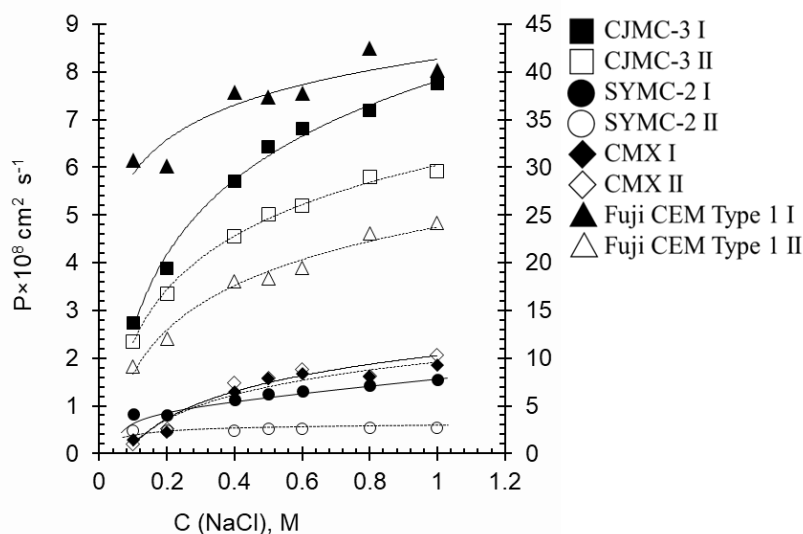


Figure 2. Concentration Dependences of the Integral Coefficient of Diffusion Permeability of the Studied IEM. The Solid Lines are Guides for the Eye.

As Figure 2 shows, that the membranes characterized by asymmetric surface properties demonstrate asymmetry in diffusion permeability as well. There is also a notable correlation between surface roughness of the membrane side facing electrolyte solution and membrane transport properties: the more prominent roughness of the surface, the higher the diffusion permeability coefficients. In [7], authors observed similar effects in gas separation membranes. The demonstrated phenomenon of an increase in membrane permeability due to rougher surface facing gases is explained by the growth in active surface area and changes in surface free energy. Such an explanation might be also applied in our case. Another contributing factor is probably hydrodynamics of the electrolyte solution flow near the membrane surface of a particular roughness when determining diffusion permeability in the two-compartment cell. The rougher surface causes more turbulence and better stirring of the electrolyte solution in its compartment, which provides faster delivery of ions from the bulk solution to the membrane surface and intensifies transport across the membrane.

Acknowledgement. This research was financially supported by the Ministry of Science and Higher Education of the Russian Federation, project number FZEN-2024-0002.

References

1. *Nebavskaya K. A., Sarapulova V. V., Sabbatovskiy K. G., Sobolev V. D., Pismenskaya N. D., Sistat P., Cretin M., Nikonenko V. V.* Impact of ion exchange membrane surface charge and hydrophobicity on electroconvection at underlimiting and overlimiting currents // *J. Membr. Sci.* 2017. V. 523. P. 36-44.
2. *Pismenskaya N. D., Nikonenko V. V., Melnik N. A., Shevtsova K. A., Belova E. I., Pourcelly G., Cot D., Dammak L., Larchet C.* Evolution with Time of Hydrophobicity and Microrelief of a Cation-Exchange Membrane Surface and Its Impact on Overlimiting Mass Transfer // *J. Phys. Chem. B.* 2012. V.116(7). P. 2145-2161.
3. *Falina I. V., Demina O. A., Kononenko N. A., Myakinchenko I. A.* A Model Description of Diffusion Permeability of Bilayer Ion-Exchange Membranes // *Coll. J.* 2020. V. 82(2). P. 244-251.
4. *Lysova, A. A., Stenina, I. A., Gorbunova, Y. G., Yaroslavtsev, A. B.* Preparation of MF-4SC composite membranes with the anisotropic distribution of polyaniline and ion-transport asymmetry *Polym. Sci. Ser. B.* 2011. V. 53(1-2). P. 35-41.
5. *Osipov A. K., Volkov A. O., Safronova E. Y., Yaroslavtsev A. B.* Ion transfer asymmetry in Nafion membranes with gradient distribution of acid salts of heteropoly acids // *Russ. J. Inorg. Chem.* 2017. V. 62. P. 723-728
6. *Ponomar M., Krasnyuk E., Butylskii D., Nikonenko V., Wang Y., Jiang C., Xu T., Pismenskaya N.* Sessile Drop Method: Critical Analysis and Optimization for Measuring the Contact Angle of an Ion-Exchange Membrane Surface // *Membranes.* 2022. V. 12 (765).
7. *Sazanova T. S., Otvagina K. V., Kryuchkov S. S., Zarubin D. M., Fukina D. G., Vorotyntsev A. V., Vorotyntsev I. V.* Revealing the Surface Effect on Gas Transport and Mechanical Properties in Nonporous Polymeric Membranes in Terms of Surface Free Energy // *Langmuir.* 2020. V. 36(43). P.12911-12921.

THEORETICAL AND EXPERIMENTAL STUDY OF ANODIC OXIDATION OF ORGANIC POLLUTANTS ON PARTICLE SUB-STOICHIOMETRIC TITANIUM OXIDE ANODE IN A FLAT ELECTROLYSIS CHAMBER

Yuri Prokhorov, Andrey Kislyi, Ilya Moroz, Vera Guliaeva, Victoria Plis, Anastasiia Klevtsova, Semyon Mareev

Kuban State University, Krasnodar, Russia, E-mail: yuriprohor@gmail.com

Introduction

In recent years, electrochemical advanced oxidation processes (EAOPs) became a widely used for the treatment of wastewater and natural waters contaminated with various organic compounds due to the high oxidation efficiency, simplicity of design and versatility. Anodic oxidation (AO) is the most common among EAOPs. This method allows the oxidation of organic compounds without the use of chemical reagents through the generation of highly active hydroxyl radicals or by direct electron transfer from the compound to the electrode surface [1].

Porous materials, such as sub-stoichiometric titanium oxide (Ti_4O_7), are the most promising ones for AO [2]. It has a large electrochemical active surface area, and the porous structure allows to intensify the process rate due to the rapid delivery of organic compounds to the electrode surface, which increases the total oxidation process rate. Besides, Ti_4O_7 has chemical stability, high electrical conductivity and a high oxygen evolution overpotential. As a simple alternative for porous electrodes, particle electrodes may be more readily available [3].

In this study, a two-dimensional model of the AO of oxalic acid on a particle electrode was developed. Quantitative agreement between experiment and theoretical data was obtained.

Model formulation

The system under study consists of a cathode made of stainless steel, a particle anode made of porous Ti_4O_7 , as well as two layers of separators between the electrodes. The upper layer of separators is macroporous and has special grid to effectively mix the solution near the cathode surface. The lower layer has relatively small pores (approximately 1 mm) and is designed to fix the anode particles. For the simplification of simulation, the system is represented as two-dimensional instead of 3D. The schematic representation of the system under study is presented in Figure 1.

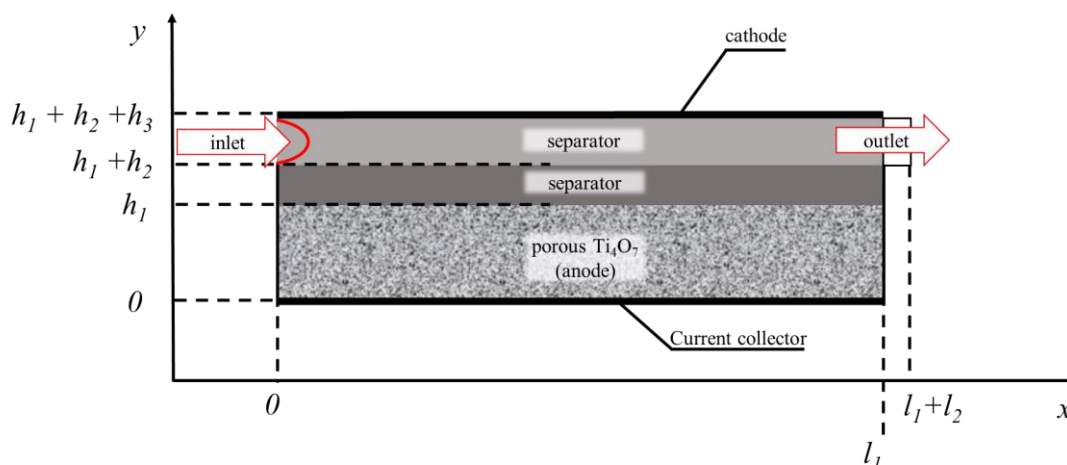


Figure 1. Schematic Representation of the System Under Study.

Based on previous studies related to the porous electrodes [4,5], a reactive transport model was developed to study the processes of AO in the reactive electrochemical membrane (REM) reactor made of electrode particles. The transport of dissolved species in solution is described by the equation system, consisting of Fick's law with the convective term, the material balance equation, Ohm's differential law for each of the phase, the charge conservation law and Darcy's law. The equation system includes two parallel reactions: direct oxidation of organic compounds and

oxygen evolution on a porous electrode, while the interaction of OH-radicals with organic molecules is not taken into account.

Results and Discussion

The kinetics of oxalic acid oxidation at different current densities was investigated. The dependences of AO concentration on time of experiment and mineralization current efficiency (MCE) on concentration at different current densities are presented in Figure 2a and b respectively. The concentration dependence at low currents has a pronounced linear character, while at high currents the dependence differs from linear in the region of small concentrations. At low currents, MCE does not depend on concentration, while at high currents it decreases with concentration. This behavior can be easily explained by reaching the limit state associated with insufficient diffusion flow of oxalic acid to the electrode surface. However, according to our calculations, the current density in the system in a wide range of concentrations does not reach the limiting state. The limiting state is the kinetics of oxidation on the electrode surface, which is associated with the proximity of formal potentials for oxidation of oxalic acid and oxygen evolution on the surface of Ti_4O_7 electrode.

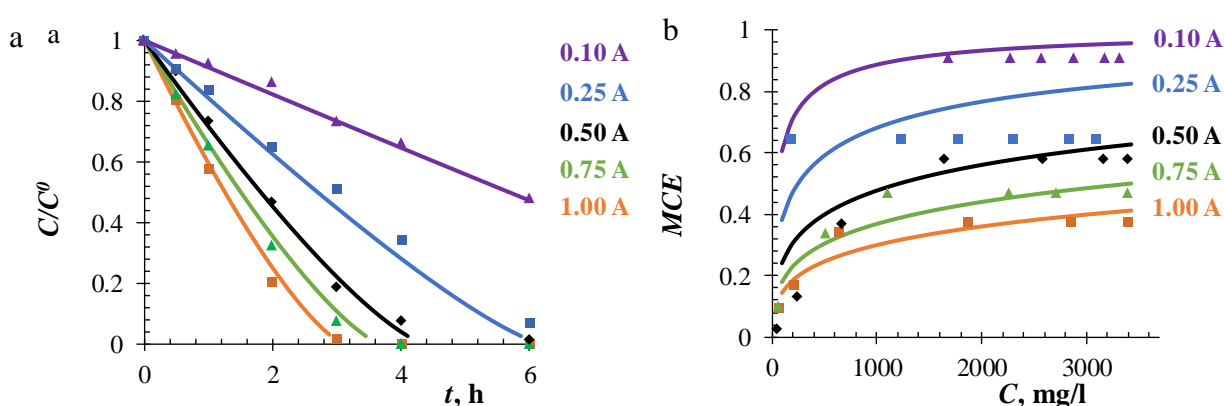


Figure 2. Dependence of C/C^0 on the Time of Experiment (a) and Mineralization Current Efficiency (MCE) on the Concentration of AO (b) at Different Current Densities.

Acknowledgments. The study is realized with the financial support of the Russian Science Foundation, project № 22-79-10177.

References

1. Panizza M., Cerisola G. Direct and mediated anodic oxidation of organic pollutants // Chem. Rev. 2009. V.109. I. 12. P. 6541-6569.
2. Trellu C., Chaplin B.P., Coetsier C., Esmilaire R., Cerneaux S., Causserand C., Cretin M. Electro-oxidation of organic pollutants by reactive electrochemical membranes // Chemosphere. 2018. V. 208. P. 159-175.
3. GracePavithra K., Senthil Kumar P., Jaikumar V., SundarRajan P. S. A review on three-dimensional electrochemical systems: analysis of influencing parameters and cleaner approach mechanism for wastewater // Rev. Environ. Sci. Biotechnol. 2020. V. 19. P. 873-896.
4. Trainham J. A., Newman J. A flow-through porous electrode model: application to metal-ion removal from dilute streams // J. Electrochem. Soc. 1977. V. 124. P. 1528-1540.
5. Doherty T., Sunderland J. G., Roberts E. P. L., Pickett D. J. An improved model of potential and current distribution within a flow-through porous electrode // Electrochim. Acta. 1996. V. 41. P. 519-526.

SYNTHESIS AND INVESTIGATION OF NANOPARTICLES WITH NON-CLASSICAL HABIT AS A HIGHLY ACTIVE CATALYST FOR HYDROGEN PROCESSES

Polina Pushankina, Georgiy Andreev, Sergey Ivanin, Marina Papezhuk, Aleksandr Simonov, Nikita Prokhorov, Stepan Dzhimak, Iliya Petriev.

Kuban State University, Krasnodar, Russia, E-mail: petriev_iliya@mail.ru

Introduction

Palladium-based membranes are a promising material for the production and purification of hydrogen in laboratory and industrial conditions [1]. However, at low temperatures (< 200 °C) they are practically impermeable. This condition can be overcome by modifying the membrane surface with nanoparticle-based catalyst coatings [2]. Palladium-based catalytic systems are sufficiently resistant to poisons such as carbon monoxide (CO), which makes them promising materials for use in hydrogen diffusion purification devices by steam reforming. The application of such coatings will allow to intensify the transport of hydrogen at low temperatures, where the surface stages have an overwhelming effect on the process of hydrogen penetration. Therefore, the aim of the study was to develop highly active catalytic systems based on Pd-Pt nanoparticles capable of intensifying hydrogen transport through palladium-based membranes at low temperatures.

Experiments

During the study, two types of coatings on the surface of palladium-silver films were synthesized using the method of electrolytic deposition according to classical and author's methods. The classical method of synthesis of palladium bilge provides for the production of particles of only spherical shape. However, variations in experimental conditions, such as current and deposition time, and the composition of the working solution, made it possible to obtain coatings of special geometry, such as nanostars. The necessary conditions for obtaining particles of such morphology are a clear ratio of components in the working solution with the addition of a surfactant, as well as a decrease in the deposition current density, compared with classical methods.

Results and Discussion

The study of the obtained nanoparticles showed that the coatings of the film samples modified with classical palladium black consisted of spherical nanoparticles with a diameter of about 90-100 nm. The modifiers synthesized by the nanostar technique consisted of pentagonally structured nanoparticles with a diameter of about 90-110 nm. Micrographs of the surface of modified films are shown in Figure 1.

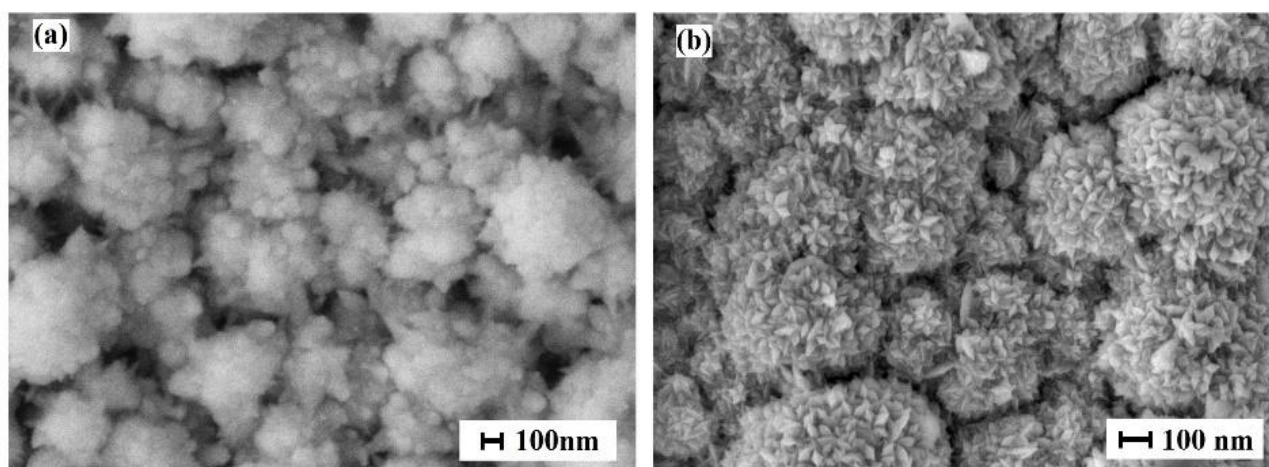


Figure 1. Micrographs of the surface of Pd-Ag films modified with classical palladium black (a) and pento-twinned Pd-Pt particles (b)

During the research, it was found that the pentagonal particles in the modifier are hollow. During etching with hydrochloric acid, the shell of the particle thinned and multiple explosive-like ruptures were formed, which is confirmed by the SEM images shown in Figure 2. The centers of destruction of pentagonal particles were the points of intersection of the boundaries of twins and disclinations on the surface of the particles, i.e. the points of maximum concentration of internal elastic stresses. Thus, it can be assumed that the content of disclinations in electrolytically synthesized particles can lead to the formation of an internal void in them. Such a particle structure certainly affects the economic benefits, expressed in reducing the consumption of precious metal.

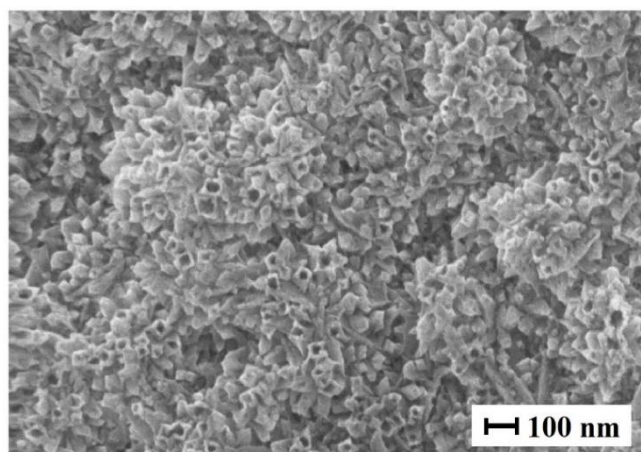


Figure 2. SEM images of Hollow Pd-Pt nanoparticles.

Thin films modified by catalytic coatings were studied in the processes of alkaline oxidation of methanol (Figure 3a). According to the results obtained, the electrode films modified with nanostars demonstrated uniquely high values of peak current density up to 60.72 mA cm^{-2} . Electrodes with classical nanoparticles had an activity 3.14 times less than the order of 19.28 mA cm^{-2} . It should be noted that all synthesized catalytic coatings demonstrated high resistance to CO poisoning and long-term stability in the reaction of alkaline oxidation of methanol. Films modified by three types of coatings were studied in the processes of low-temperature ($25\text{-}100 \text{ }^\circ\text{C}$) hydrogen transport as membranes. As can be seen from Figure 3b, the density of the penetrating hydrogen flux through nanostar-modified membranes is up to 2.1 times higher than through membranes with classical black, and an order of magnitude higher than for uncoated membranes.

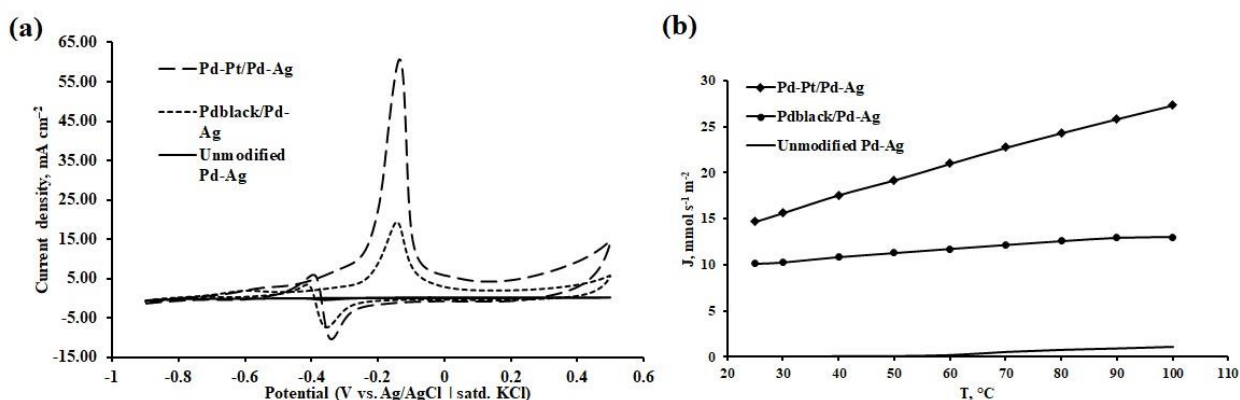


Figure 3. Catalytic and membrane studies of modified films: cyclic voltammograms of modified electrodes and uncoated in the reaction of alkaline oxidation of methanol (a), temperature dependence of the hydrogen flux density on the input side of modified membranes and uncoated (b).

The result obtained by membranes with a fundamentally new structural organization of the catalytic coating can be explained by an increase in the adsorption activity of the surface due to an increase in the number of active centers. This, in turn, affects the increase in the catalytic activity

of the material in relation to reactions involving hydrogen. Presumably, this is also the reason for a decrease in the energy barrier of dissociation and/or recombination of hydrogen molecules on the membrane surface, which leads to an increase in the rate of hydrogen penetration.

The use of nanostructured membrane materials under development will significantly intensify hydrogen transport and reduce operating temperatures, which will have a positive effect on reducing energy costs in the process of producing high-purity hydrogen. The developed membrane materials will be able to become the basis for both low-temperature hydrogen diffusion purification devices and membrane modules of steam-gas reforming reactors.

Acknowledgement. This research was funded by the Russian Science Foundation and the Kuban Scientific Foundation grant No. 22-19-20068, <https://rscf.ru/project/22-19-20068/>.

References

1. *Filipov. S.P., Yaroslavtsev. A.B.* Hydrogen energy: development prospects and materials // Russian Chemical Reviews, 2021, V. 90, P. 627–643.
2. *Petriev I., Pushankina P., Bolotin S., Lutsenko I., Kukueva E., Baryshev M.* The influence of modifying nanoflower and nanostar type Pd coatings on low temperature hydrogen permeability through Pd-containing membranes // J. Membrane Science. 2021. V. 620. № 118894.

PVDF-BASED MEMBRANES AS ELECTROLYTES FOR SOLID-STATE LITHIUM METAL BATTERIES

Anastasia Pyrkova, Irina Stenina, Andrey Yaroslavtsev

Kurnakov Institute of General and Inorganic Chemistry of the Russian Academy of Sciences, Moscow, Russia; E-mail: ab.bocharova@mail.ru

Introduction

Technology of solid-state lithium batteries attracts increasing attention in the energy sector due to their high energy density, safety, and stable operation. The key component of such batteries is electrolyte, which plays an important role in ion transport and electrochemical processes. Polyvinylidene fluoride (PVDF)-based membranes are a promising solution for use as a solid electrolyte due to their mechanical strength, wide electrochemical stability window, thermal stability, non-flammability, and lack of negative reactions with other materials. Compared to inorganic electrolytes, polymer electrolytes exhibit properties such as elasticity and plasticity, which provide a good electrode/electrolyte contact.

Experiments

Membranes were prepared by casting of dispersed or ultrasonically treated solutions of PVDF with different molecular weights (Sigma-Aldrich, $M_w = 534,000$ g/mol and Gelon, $M_w = 1,110,000$ g/mol) in two solvents (N-methylpyrrolidone (NMP) and N,N-dimethylformamide (DMF)). The morphology of the prepared membranes was analyzed using scanning electron microscopy. Mechanical properties were investigated by stress-strain curve measurements. Young's moduli were calculated. The samples were studied by X-ray diffraction, and impedance spectroscopy. To investigate the lithium conductivity, the samples were kept in 1 M LiPF₆ solution in ethylene carbonate (EC)/diethyl carbonate (DEC)/dimethyl carbonate (DMC) solvent mixture (1:1:1 by volume) for 0, 1, 24, 168 and 240 h.

Results and Discussion

All the PVDF-based membranes have porous structures regardless the molecular weight of PVDF and solvent used (Figure 1). However, the grain and pore sizes in membranes casted from PVDF with $M_w = 534,000$ g/mol is lower.

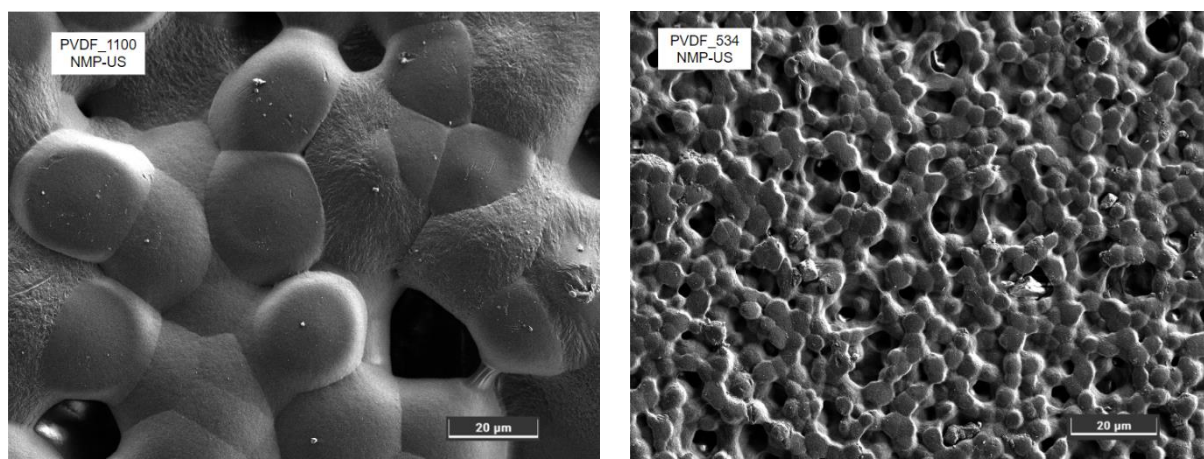


Figure 1. Surfaces of membranes casted from solutions of PVDF with different molecular weights (solvent: N-methylpyrrolidone, ultrasonic treatment).

The conductivity of membranes is influenced by molecular weight of PVDF, the solvent used, and the method of the polymer solution treatment. A comparison of the methods for the PVDF solution treatment showed that ultrasonication results in a higher conductivity than dispersion, regardless of the molecular weight of PVDF and the solvent used. The samples obtained from PVDF with $M_w = 1,110,000$ g/mol in NMP by ultrasonic treatment have higher conductivity (9.9×10^{-5} S/cm at 20 °C) than the samples prepared from solutions in DMF (2.2×10^{-5} S/cm at 20 °C). At the same time, the conductivities of membranes casted from solutions of PVDF with

$M_w = 1,110,000$ g/mol and $M_w = 534,000$ g/mol in NMP with ultrasonic treatment are 9.9×10^{-5} and 7.1×10^{-5} S/cm at 20 °C, respectively. It can be concluded that the type of solvent and the method of polymer treatment have the most significant influence on the membrane conductivity than molecular weight of PVDF. The highest conductivity was observed for samples prepared PVDF solutions in N-methylpyrrolidone with ultrasonic treatment.

Acknowledgement. This work was financially supported by Russian Science Foundation, grant No 23-19-00642, <https://rscf.ru/en/project/23-19-00642/>.

HIGHLY PERMEABLE MEMBRANES BASED ON NEW POLYPHENYLENE SULFONE AND ITS COPOLYMERS FOR ULTRAFILTRATION OF AQUEOUS MEDIA

¹Alisa Raeva, ¹Dmitry Matveev, ²Tatyana Anokhina, ¹Azamat Zhansitov, ¹Svetlana Khashirova, ¹Ilya Borisov

¹Kabardino-Balkarian State University Named after H.M. Berbekov, Nalchik, Russia

E-mail: raevaau@jps.ac.ru

²A.V. Topchiev Institute of Petrochemical Synthesis Russian Academy of Sciences, Moscow, Russia

E-mail: tsanokhina@jps.ac.ru

Introduction

The issue of drinking water treatment is becoming more and more urgent due to the pollution of fresh water sources by technogenic discharges and wastes of biogenic origin. Traditional methods of water disinfection – chlorine treatment, pasteurization, UV irradiation, ozonation, etc. – have a number of disadvantages, including the formation of harmful by-products and high energy costs. For this reason, membrane filtration, as a low-energy technology, is becoming one of the most popular alternatives for water treatment. However, when filtering microorganism-contaminated aqueous media, membranes are subject to a number of requirements, which include the ability to regenerate and sterilize. Polyphenylene sulfone (PPSU) is a promising polymer for casting filtration membranes because it has the best thermal stability, strength and resistance to hydrolysis among polysulfone-based membrane materials. However, obtaining membranes by phase-inversion method on its basis is hampered by the limited solubility of the polymer in aprotic solvents, its hydrophobicity, as well as the low molecular weight (MW) of commercial grades (48-65 kg/mol). Therefore, this work was aimed at the synthesis of modified PPSU with optimized MW and different concentration of phenolphthalein (PP) cardo fragments, creation of ultrafiltration (UF) membranes based on them and investigation of the influence of the chemical structure of polymers and copolymers on the structure and properties of the obtained material.

Experiments

In this study, two series of samples were synthesized: PPSU of different MW = 13-100 kg/mol and PPSU copolymers with different concentrations of cardo fragments from 10 to 90 mol.%. The molecular weight characteristics and chemical structure of the polymers were studied by gel permeation chromatography and nuclear magnetic resonance spectroscopy. The mechanical, rheological, surface properties of the polymers, as well as the kinetics of solution coagulation on their basis were studied. The influence of cardo fragments on the solubility of PPSU copolymers has been considered. Asymmetric membranes of different configurations were obtained. The transport and separation characteristics of the membranes were investigated using distilled water and Blue Dextran model dye solution (MW = 70 kg/mol), respectively.

Results and Discussion

Tests of the mechanical properties of the PPSU copolymers demonstrated an increase in strength from 73 to 97.9 MPa with an increase in the PP concentration from 30 to 90 mol.%. At the same time, by introducing cardo fragments into the polymer chain, we achieved a mechanical strength 1.3 times higher than the strength of commercial PPSU. The study of the rheological properties of casting solutions of PPSU copolymers showed that the introduction of the cardo monomer significantly increases the solubility of the polymer in aprotic solvents. Moreover, the highest solubility is observed at the concentration of PP 50 mol.%. It is shown that with the increasing concentration of PP monomer, the dynamic viscosity of two- and three-component polymer solutions in NMP decreases more than five times when the PP concentration in the polymer is 90 mol.%. At the same time, the introduction of the hydrophilizing additive PEG increases the solution viscosity by 4.4–6.0 times, which is a positive effect from the point of view of membrane forming.

It is found that as the concentration of the cardo monomer increases from 0 to 90 mol.%, the solution coagulation rate increases in the case of PPSU-PP/NMP solutions from 3.61 to 4.67 $\mu\text{m/s}$ and, for PPSU-PP/NMP/PEG solutions, from 3.12 to 4.42 $\mu\text{m/s}$. Reduced viscosity of cardo polymer solutions leads to an increase in the non-solvent diffusion coefficients and, as a consequence, an increase in the coagulation rate.

At the next stage of work, flat-sheet asymmetric membranes based on cardo PPSU copolymers were obtained. The results of filtration experiments are presented in Figure 1. The permeance of membranes increased with increasing concentration of PP from 17.5 $\text{L}/(\text{m}^2\cdot\text{h}\cdot\text{bar})$ (10 mol.% PP) to 85.2 $\text{L}/(\text{m}^2\cdot\text{h}\cdot\text{bar})$ (90 mol.% PP). These data are in agreement with the results of a study of the coagulation rate of polymer solutions. It was found that there is a clear correlation between the coagulation rate and the permeance of the liquid through the membrane.

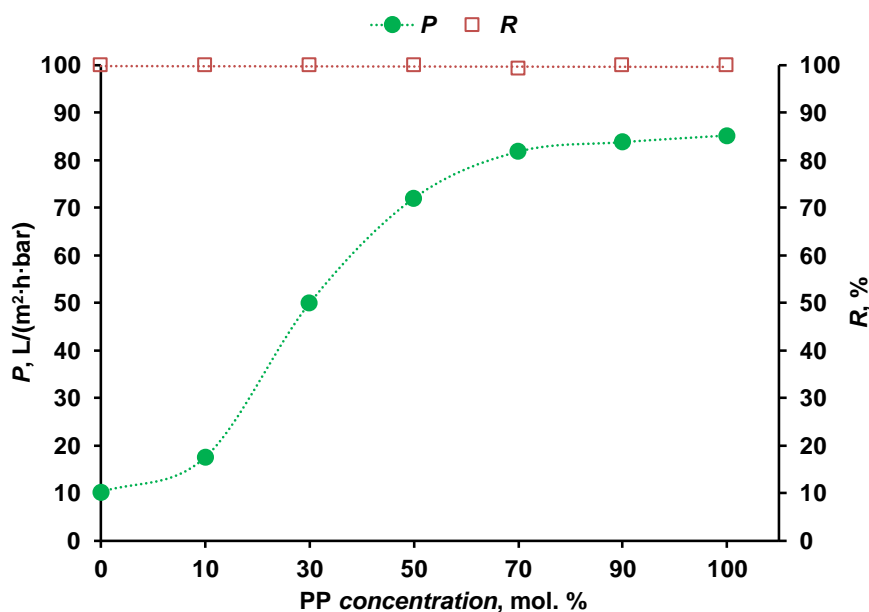
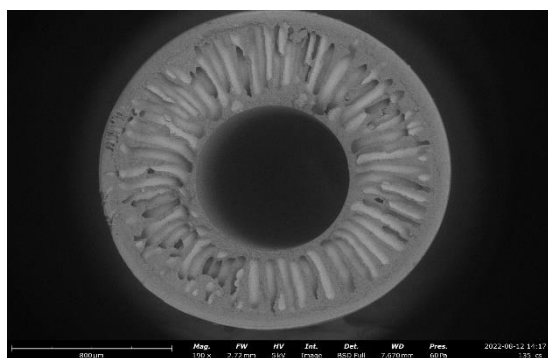


Figure 1. Dependence of Transport and Separation Properties of Flat-Sheet Asymmetric Membranes on the Concentration of Cardo Monomer.

The MW of synthesized PPSUs was controlled by varying the molar ratio of 4,4'-dihydroxybiphenyl and 4,4'-dichlorodiphenylsulfone monomers within 1:1–1.15 under the same synthesis conditions. Based on the study of rheological properties of PPSU with different molecular weights, high molecular weight PPSU with MW = 100 kg/mol was selected for the preparation of hollow fiber membranes. In order to form membranes with higher porosity and a hydrophilized surface, the pore-forming agent PEG400 was added to the spinning solution. The addition of PEG to the spinning solution led to an increase in viscosity, which makes it possible to form membranes in the region of lower PPSU concentrations of 18–20 wt. %. Such membranes had a looser structure with higher porosity.

Hollow fiber membranes with outer and inner selective layers were obtained by wet spinning method. SEM photographs of the obtained membranes are shown in Figure 2. The results of ultrafiltration experiments are presented in Table 1. It is shown that the introduction of PEG additive leads to a sharp increase in permeance by more than two orders of magnitude. For membranes with an outer selective layer the maximum value of water permeance was achieved at the composition of the spinning solution PPSU/NMP/PEG = 20/50/30 wt.%. It amounted to 96 $\text{L}/(\text{m}^2\cdot\text{h}\cdot\text{bar})$. At the same time, the membranes had high rejection (99.9%) of the model dye Blue Dextran. In the case of membranes with an inner selective layer, the water permeance was 1.2–1.5 times higher while rejection of the model dye at a high level of 99.9%. The maximum water permeance was 130.5 $\text{L}/(\text{m}^2\cdot\text{h}\cdot\text{bar})$ for PPSU/NMP/PEG = 20/50/30 wt.%.



a)



b)

Figure 2. SEM Photographs of Hollow Fiber Membranes: a) Outer Selective Layer, b) Inner Selective Layer.

Table 1: Ultrafiltration Properties of Hollow Fiber PPSU Membranes

C _P , wt.%	C _{PEG} , wt.%	Outer selective layer		Inner selective layer	
		P, L/m ² ·h·bar	R _{Blue Dextran} , %	P, L/m ² ·h·bar	R _{Blue Dextran} , %
18	0	0.7	99.9	-	-
18	20	15.7	78.6	63.6	87.5
18	25	103.6	87.8	164.7	76.9
20	0	0.2	99.9	-	-
20	20	36.6	99.9	57.4	99.9
20	25	59.9	99.9	74.5	99.9
20	30	95.7	99.9	130.5	99.0

Thus, for the first time flat-sheet UF membranes based on PPSU copolymers with permeance 1.5-8 times higher than flat-sheet PPSU membranes due to the introduction of cardo fragments, with high rejection of model dye Blue Dextran more than 99.2%, as well as high strength characteristics were obtained. Also in this work, for the first time PPSUs of different MW were synthesized and hollow fiber PPSU membranes with high filtration characteristics were obtained.

Acknowledgement. This work was funded by the Russian Science Foundation, Russia (Project no. 22-19-00711) <https://rscf.ru/en/project/22-19-00711/>.

TRANSPORT PROPERTIES OF MEMBRANES BASED ON COPOLYURETHANIMIDES IN THE PROCESS OF ORGANIC SOLVENT NANOFILTRATION

¹Alisa Raeva, ¹Ilya Borisov, ^{1,2}Andrey Didenko, ¹Tatyana Anokhina, ¹Alexander Malakhov

¹ A.V. Topchiev Institute of Petrochemical Synthesis Russian Academy of Sciences, Moscow, Russia, *E-mail: raevaau@ips.ac.ru*

²Institute of macromolecular compounds, Saint-Petersburg, Russia, *E-mail: vanilin72@yandex.ru*

Introduction

Rapid population growth and increased mobility have made modern society vulnerable to the rapid spread of new diseases across borders (such as COVID-19, SARS, and H5N1). The synthesis of antiviral drugs requires the use of various catalysts and organic solvents. This process involves a number of reactions, each of which requires the isolation of the catalyst, removal and replacement of the solvent, concentration, and isolation of the target and byproducts. Many stages of the synthesis process are carried out at temperatures between 80 and 250 °C. These separation problems in organic synthesis can be effectively solved using baromembrane processes, such as ultra- and nanofiltration. Since membrane filtration is a thermally stable process without any phase transitions, it not only reduces energy use compared to traditional separation methods such as distillation, but it also allows the separation of thermolabile substances without their degradation.

Polyimides are widely considered to be the most promising class of heat-resistant polymeric materials for addressing this challenge. Existing industrial asymmetric polyimide nanofiltration membranes from the DuraMem series (produced by Evonik using solution technology via phase inversion from aprotic solvents and subsequent membrane cross-linking to enhance stability in organic solvents) are limited in their number of polymers utilized in industry and scientific research to Lenzing P84, Matrimid, and PMDA/ODA. This paper proposes a radically different approach to membrane formation utilizing insoluble polyimides. In order to address this challenging scientific objective, new multi-block (segmented) copolymers (urethane imides), soluble in aprotic solvents, with varying lengths and chemical compositions of polyimide and polyurethane segments, will be utilized for the first time in this study.

Experiments

Synthesis of copolymers with preferred extent and ratio between aromatic and aliphatic blocks. The synthesis of copolymers is a chemical modification of the Kapton polyimide family. 0.005 mol of polycaprolactanediol (10 grams) and 0.01 mol (1.74 grams) of toluylene-2,4-diisocyanate were loaded into a three-necked flask equipped with an upper-drive agitator and a tube for supplying and withdrawing argon. The mixture was heated to 80 °C in an oil bath and kept for 1 hour. Then 0.01 (2.18 grams) moles of pyromellite dianhydride were added in the form of finely ground powder. The mixture was heated to 180 °C and stirred for two hours until the resulting melt was homogenized and the release of bubbles of carbon dioxide formed during the reaction stopped. The reaction mass was cooled to 160 °C and 47 ml of N,N-dimethylacetamide (DMAc) was poured into it to dissolve the resulting product. The concentration of the solution according to the resulting macromonomer was 23 wt. %. The macromonomer was not isolated from the reaction solution. Next, a proportional number of moles for 0.05 mol (10.9 g) dianhydride was loaded into a flask containing a prepared macromonomer solution, and for diamine it was 0.055 mol (11 g), and after that the concentration of the reaction mixture solution was adjusted to 25% by infusion of the required amount of DMAc. After the dissolution of the monomers, the reaction mixture was intensively stirred for 4 hours under argon current at room temperature to complete the diamine polyacylation reaction. A prepolymer (copolymer (urethane-amidonic acid) was obtained in a solution in DMAc. Then an imidizing mixture based on propionic anhydride, triethylamine and tetrahydrofuran was added to it. The resulting casting mixture was used for electric spinning of a non-woven coating. DMF and DMAc, which are the most commonly used amide solvents, were studied as a filtration media. Phthalocyanine with an effective particle diameter of 240 nm was chosen as the detained substance.

Results and Discussion

The developed technique for producing nonwoven material includes the introduction of a benzene diluent and an imidizing mixture consisting of propionic anhydride and triethylamine into a copolymer (urethane-imide) prepolymer solution formed as a result of the polycondensation process. Figure 1 shows a micrograph of the SEM of nanofibers forming a nonwoven coPUI material (mat).

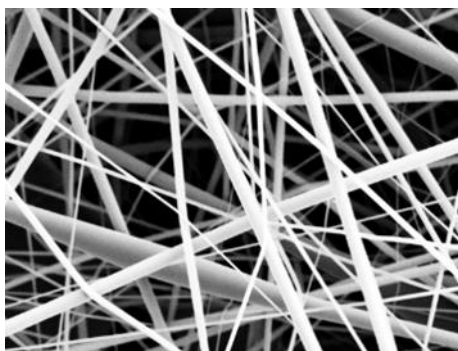


Figure 1. Micrograph of SEM Nanofibers Forming Non-Woven coPUI Material.

The fibers have a distinct cylindrical morphology. The resulting mats were heated for 30 minutes at 360 °C, respectively. The mechanical properties of the heated mats are shown in Table 1. Nonwoven coPUI mat has high strength and elasticity, as well as resistance to solvents (Table 2), acceptable for technological use as filtration membranes.

Table 1: Deformation and strength characteristics of non-woven coPUI mat

Non-woven mat	Tensile modulus, MPa	Tensile strength, MPa	Elongation at break, %
coPUI	386.54 ± 42.14	23.21 ± 3.51	26.16 ± 3.44

Table 2: The stability of non-woven adhesive in aprotic solvents at 100 ° C. "S" – the material is stable

Non-woven mat	NMP	DMAc	DMF	DMSO	toluene
coPUI	S	S	S	S	S

The results of filtration experiments are presented in Table 3.

Table 3: Filtration characteristics of non-woven coPUI

Non-woven mat	η , mPa·s	P , kg / (m ² h bar)	R phthalocyanine, %
DMAc	0.919	103	81.7
DMF	0.920	67	70.0

As you can see, the membranes retain the dissolved substance quite effectively. Moreover, the rejection and permeance in the DMAc media is higher compared to DMF. The difference in filtration properties of solvents similar in nature and viscosity seems to be an unusual fact that requires further study. The results obtained are new, since there is no data in the literature on filtration of aprotic solvents on nonwoven membranes.

Thus, we have proposed a new, technologically simpler method for producing non-woven polyimide material, compared with the known multi-stage method for producing non-woven polyimide with the need for the preparation of spinning solutions to isolate an intermediate in solid form in the form of triethylammonium salts of polyamide acid (polyimide prepolymer).

Acknowledgement. This work was funded by the Russian Science Foundation, Russia (Project no. 22-19-00831) <https://rscf.ru/en/project/22-19-00831/>.

DEPENDENCE OF STRUCTURE AND GAS TRANSPORT PROPERTIES OF POLYDECYLMETHYLSILOXANE ON THE TYPE OF CROSSLINKING AGENT

Tatyana Rokhmanka, Evgenia Grushevenko, Stepan Sokolov, Julia Matveeva, Ilya Borisov

A.V. Topchiev Institute of Petrochemical Synthesis, Russian Academy of Sciences, Moscow, Russia
E-mail: rokhmankatn@ips.ac.ru

Introduction

Separation of C₃₊ hydrocarbons from natural gas is an essential step in preparing gas streams for transportation. Traditionally, when preparing gas for transportation, oily components are removed using low-temperature separation (LTS). The efficiency of this process directly depends on the reservoir pressure. One way to improve the separation of C₃₊ hydrocarbons under lower formation pressure is through a combination of LTS and membrane gas separation. The mass-exchange parameters of the membrane gas separation process are determined by the properties of the membrane. Two important membrane parameters are the high permeability and the selectivity of the target components. Polysiloxane membranes are widely used in the membrane industry to separate C₁-C₄ hydrocarbons. These materials have high permeability and stable transport characteristics over time, due to their cross-linked polymer structure [1]. Polydecylmethylsiloxane (C10), which has record selectivity values for polysiloxanes when separating hydrocarbons, also maintains high permeability values for the target component. However, there is a significant decrease in selectivity when moving from individual gases to gas mixtures due to swelling of the polymer in the hydrocarbons. In this work, we first studied the influence of the nature and length of the crosslinking agent on the structure and transport properties of the membrane material in order to reduce swelling of this polymer in hydrocarbon mixtures.

Experiments

Cross-linked polydecylmethylsiloxane (C10) was prepared according to the procedure described in [3]. The PMHS was mixed with a 15 wt % solution of 1-decene in isooctane in the presence of Carstead catalyst (1,3-divinyl-1,1,3,3-tetramethyl disiloxane platinum (0) complex), the solution in xylene was stirred for 2 h at 60°C. Then solution of crosslinking agent (mole ratio of 1-decene/crosslinking agent = 15-20) in isooctane was added to the reaction mixture. Types and concentrations of crosslinking agent (CA) are represented in Table 1. Stirring of the reaction mixture was continued for one hour. After that, 3 wt % PMHS solution in isooctane was added to the reaction mixture to the stoichiometric ratio. Membranes were obtained by casting polymer solution on a Teflon surface with subsequent drying at 60°C until it reaches constant weight. The membrane thickness was 100±10 µm.

Table 1: Membrane abbreviations

Membrane abbreviation	Crosslinking agent	Ratio 1-decene/CA, mol/mol
C10-OD	1,7-octadiene	20
C10-DD	1,9-decadiene	20
C10-DdD	1,11-dodecadiene	20
C10-Sil500	PDMS (M _n = 500 g/mol)	15
C10-Sil25-OD	PDMS (M _n = 25000 g/mol) + 1,7-octadiene	15

In order to study the physicochemical properties of the samples, their IR and WAXS spectra and DSC curves were obtained. The sorption of toluene was determined to determine the apparent crosslinking density [4]. The study of gas transport properties for individual gases (N₂, CH₄, C₂H₆, C₄H₁₀) was performed according to the method described in [5].

Results and Discussion

In this work, the complex influence of the type (hydrocarbon or polysiloxane) and length of the cross-linking agent on the structure and transport properties of C10 was studied for the first time. It has been shown that the use of hydrocarbon or siloxane cross-linking agent has a different effect on the apparent cross-link density and the ordering of side decyl substituents in the polymer. In

particular, the apparent crosslink density in the case of diene crosslinking is significantly higher than in the case of polysiloxane crosslinking: with a comparable length of the crosslinking agent for the C10-DdD sample, the apparent crosslinking density was $2.35 \cdot 10^{-4}$ mol/g, and for C10-Sil500 $1.49 \cdot 10^{-4}$ mol/g. It can be noted that increase of crosslink length favors ordering of the side groups of C10, which is observed in low-temperature X-ray diffraction. Short hydrocarbon diene cross-linking sterically hinders the mobility of side groups due to the rigidity of the cross-linking agent chain and leads to low values of crystallinity degree. Moreover, as the length of the diene cross-link increases, the ordering of the side substituents becomes more uniform, as evidenced by X-ray diffraction data. As a result, the observed diffusion transfer of nitrogen through membranes decreases. On the contrary, the solubility coefficients in the case of increasing the length of the diene cross-link increase, which is consistent with the assumption of better ordering of the side decyl groups in the polymer.

The value of the permeability coefficient is of practical importance, since it is directly related to mass transfer through the membrane and is a superposition of diffusion and dissolution of gas in the polymer material. C10 hydrocarbon crosslinking leads to lower gas permeability coefficients for gases for which transfer occurs mainly due to the diffusion component (nitrogen, methane) compared to polysiloxane crosslinking. For ethane and n-butane there is no such clear dependence, since the sorption component makes a decisive contribution to their transfer through membranes. It is worth noting that the highest sorption selectivity is achieved for the C10-Sil25-OD sample with combined cross-linking. Apparently, such a combination of cross-linking agents (short hydrocarbon and long polysiloxane) ensures not only high availability of the dynamic free volume of the polymer for sorption, but also makes it possible to realize the properties of a side substituent.

It has been shown that using short hydrocarbon crosslinks allows obtaining samples with swelling values that are about 2 times lower than those obtained with more flexible siloxane crosslinks. The combined crosslinking variant with 1,7-octadiene and PDMS25 provides an average swelling value that lies between those of siloxane- and diene-crosslinked samples. Moreover, it was found that the C_4H_{10} permeability of the C10-Sil25-OD sample is 1.5 times higher than that of the C10-OD sample and 1.7 times higher than the C10-Sil500 sample. This effect can be attributed to the high molecular weight of the PDMS crosslink, which is known to have high gas permeability, especially for hydrocarbons. Based on the data collected for individual gases, the C10-Sil25-OD sample has been selected for use in separating a C_4H_{10}/CH_4 gas mixture (35/65 volume percent). It has been shown that at temperatures close to the low-temperature separation process ($0^\circ C$), the permeability coefficient of methane in a C_4H_{10}/CH_4 mixture is about 1.7 times higher than the corresponding permeability coefficient for individual methane. The permeability of n-butane does not change significantly during this process, while the selectivity for C_4H_{10} is significantly higher than for PDMS, with a value of about 60. This is almost twice as high as that of PDMS [6].

It has been shown that by using combined crosslinking (diene-siloxane) with a slight increase in swelling compared to diene crosslinking, it is possible to achieve a record high permeability for n-butane and a selectivity of 60 for C_4H_{10} over CH_4 in the separation of a model gas mixture. This work thus demonstrates the fundamental impact of the type of crosslinking agent on transport and separation properties for C10, within the context of solving the challenge of efficiently separating C_1 - C_4 hydrocarbons

Acknowledgement. This research was funded by the Russian Science Foundation, grant number 23-79-10265, <https://rscf.ru/project/23-79-10265/>. The work was carried out using the equipment of the Shared Research Center «Analytical center of deep oil processing and petrochemistry of TIPS RAS».

References

1. *Grushevenko E.A., et al.* Silicone rubbers with alkyl side groups for C_3+ hydrocarbon separation // *React. Funct. Polym.* 2019. V. 134. P. 156-165.

2. *Grushevenko E.A., et al.* Polyalkylmethylsiloxanes composite membranes for hydrocarbon/methane separation: Eight component mixed-gas permeation properties // *Sep. Purif. Technol.* 2020. V. 241. P. 116696.
3. *Grushevenko E. et al.* Influence of Type of Cross-Linking Agent on Structure and Transport Properties of Polydecylmethylsiloxane // *Polymers.* – 2023. – T. 15. – №. 22. – C. 4436
4. *Tan Z., Jaeger R., Vancso G.J.* Crosslinking Studies of Poly(Dimethylsiloxane) Networks: A Comparison of Inverse Gas Chromatography, Swelling Experiments and Mechanical Analysis // *Polymer.* 1994. V. 35. P. 3230–3236.
5. *Grushevenko E.A., Borisov I.L., Knyazeva A.A., Volkov V.V., Volkov A.V.* Polyalkylmethylsiloxanes Composite Membranes for Hydrocarbon/Methane Separation: Eight Component Mixed-Gas Permeation Properties // *Sep. Purif. Technol.* 2020. V. 241. P. 116696.
6. *Markova S.Y., Pelzer M., Shalygin M.G.* Peculiarities of butane transfer in poly (4-methyl-1-pentene) // *Membr. Membr. Technol.* 2021. V. 3. P. 426-433.

TRANSFER OF A MIXED SOLUTION OF STRONG AND WEAK ELECTROLYTES THROUGH ION EXCHANGE MEMBRANES

Nazar Romanyuk, Nikita Kovalchuk, Sergey Loza, Victor Zabolotsky

Kuban State University, Krasnodar, Russia, E-mail: romanyuknazar@mail.ru

Introduction

Currently, the task of recycling spent technological solutions with a complex composition is particularly acute. Such solutions include mix of strong and weak electrolyte (sodium nitrate and boric acid), which are formed as a result of the operation of nuclear power plants. Traditional methods that are used to treatment these solutions have a number of disadvantages, the main of which is the loss of valuable components. To reuse valuable components in the technological process, it is necessary to separate them. It can be carried out by electro dialysis. However, electro dialysis separation of weak and strong electrolytes solutions is complicated by a shift in the equilibrium of the dissociation reaction of a weak electrolyte in the diffusion layer of the solution, as well as inside the membrane, with the formation of an ionic form capable of being transported through ion-exchange membranes [1, 2]. This effect negatively affects the efficiency of the electromembrane separation process. The study of the mechanism of transfer of a weak electrolyte through ion-exchange membranes at different pH values, including the reaction of its dissociation in the diffusion layer of the solution, will allow controlling the process of electro dialysis separation of mixed solutions.

Experiments

In the course of the work, the study of the general and partial current-voltage characteristics (CVCs) of the anion- and cation-exchange membranes Ralex AMH PES and Ralex CMH PES in a solution of 0.01 M NaNO_3 with different boric acid content (0-0.05 M) at $\text{pH} = 5.5$ was performed. CVCs and effective numbers of ion transport through membranes were studied by the method of a rotating membrane disk (RMD) with a surface equally accessible in diffusion and electrical terms [3]. Electro dialysis separation of a model nuclear industry waste solution (0.15 M NaNO_3 and 0.75 M H_3BO_3) was also investigated on an electro dialyzer containing 5 paired chambers formed by 5 Ralex CMH PES membranes and 6 Ralex AMH PES membranes. The working area of one membrane is 0.01 m^2 .

Boric acid is a weak electrolyte and can be in various forms depending on the pH in the solution (Fig. 1).

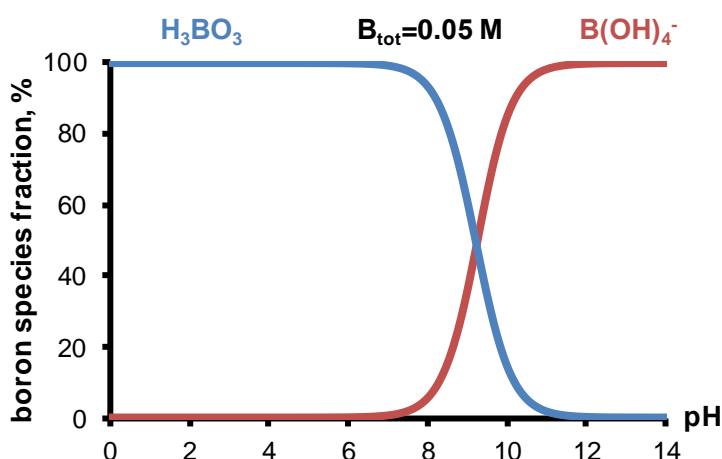
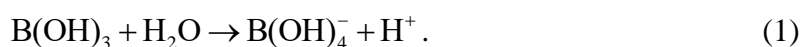


Figure 1. The distribution of boric acid forms at different pH values. The total concentration of all forms of boric acid $\sum C(\text{H}_3\text{BO}_3) = 0,05 \text{ M}$ [4]

At low pH values, boric acid is in molecular form, at high pH values, boric acid is mainly represented by the tetrahydroxyborate anion B(OH)_4^- .

Results and Discussion

In Fig. 2 a the current-voltage characteristics (CVCs) of a cation exchange membrane in a solution of 0.01 M NaNO₃ with a different content of boric acid, at pH = 5.5 are presented. The same figure shows the partial VAC for borate anions (Figure 5), calculated from the values of the effective transfer numbers at a maximum concentration of boric acid 0.05 M. The density of the limiting current of the cation exchange membrane does not depend on the content of boric acid in solution, and the transfer of borates over the entire range of current densities, due to the manifestation of the Donnan exclusion effect of coions, is absent (Fig. 2a, cur. 5). The shape of the Ralex CMH PES membrane depends on the content of boric acid. With an increase in the content of H₃BO₃ in the solution, the angle of inclination of the limiting current plateau increases. As shown by measurements of partial VAC for hydrogen cations (Fig. 2b), an increase in the angle of inclination occurs due to an increase in the intensity of hydrogen cation transfer through the cation exchange membrane with an increase in $\sum C(H_3BO_3)$. This effect is explained by the fact that when the limiting state in the electromembrane system occurs at the surface of the cation exchange membrane in the depleted layer of the solution, the equilibrium of the boric acid dissociation reaction shifts towards the formation of an ionic form:



As a result, the hydrogen cations are formed near the membrane surface and participate in mass transfer through the ion-exchange membrane.

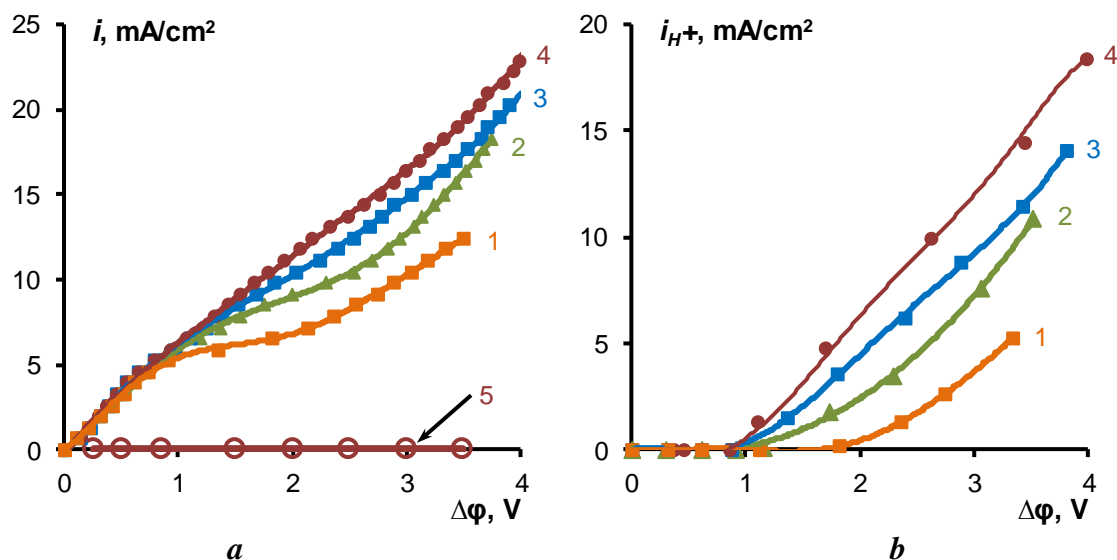


Figure 2. General and partial CVCs of the cation exchange membrane Ralex CMH PES: a-general CVCs; b – partial CVCs by the hydrogen cations. CVCs in the solutions:

1 – 0.01 M NaNO₃; 2 – 0.01 M NaNO₃+0.01 M H₃BO₃; 3 – 0.01 M NaNO₃+0.02 M H₃BO₃; 4 – 0.01 M NaNO₃+0.05 M H₃BO₃; 5 – partial CVC by the boric acid in the solution of 0.01 M NaNO₃+0.05 M H₃BO₃. Angular velocity of rotation of RMD $\omega=100$ rpm

There is almost no transport of the borate anions through the anion exchange membrane in the prelimit current mode (Fig. 3, cur. 5) because of the boric acid exists in molecular form at 5.5 pH and do not participate in electric mass transfer.

However, when the limiting state occurs, borate transfer through the anion exchange membrane begins. After reaching the limit current on the anion exchange membrane, the pH inside the membrane shifts into alkaline values. The molecular H₃BO₃ sorbed by the anion exchange membrane is transformed into borate anions and their electrodiffusion transfer through the anion exchange membrane begins. Thus, the transfer of boric acid through the anion exchange membrane at a 5.5 pH in extreme current conditions consists of a stage of diffusion of molecular boric acid into the phase of the anion exchange membrane, dissociation of H₃BO₃ with the formation of tetrahydroxyborate anion and transfer in the membrane phase by a migration mechanism.

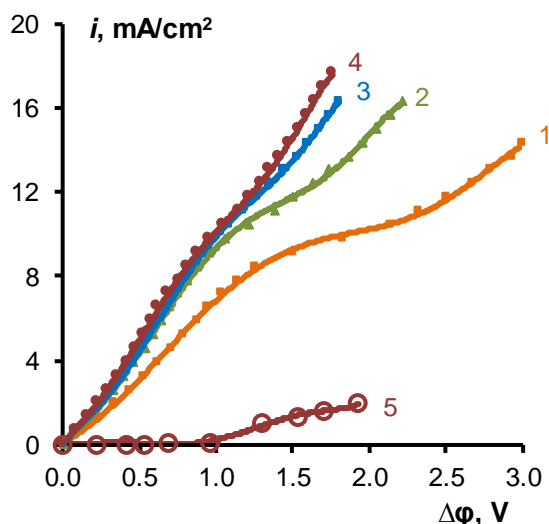


Figure 3. CVCs of anion exchange membrane Ralex AMH PES by 5.5 pH in solutions with the different concentration of boric acid:

1 – 0.01 M NaNO₃; 2 – 0.01 M NaNO₃+0.01 M H₃BO₃; 3 – 0.01 M NaNO₃+0.02 M H₃BO₃; 4 – 0.01 M NaNO₃+0.05 M H₃BO₃. 5 - partial CVC by tetrahydroxyborate anion in 0,01 M NaNO₃ + 0,05 M H₃BO₃ solution. Angular velocity of rotation of RMD $\omega=100$ rpm

The obtained data about the mechanism of boric acid transfer through individual membranes were used in the electro dialysis processing of model waste solutions from the nuclear industry. The main characteristic of electro dialysis separation – the coefficient of permselectivity ($P(\text{NaNO}_3/\text{H}_3\text{BO}_3)$) was calculated:

$$P(\text{NaNO}_3 / \text{H}_3\text{BO}_3) = \frac{J(\text{NaNO}_3)C(\text{H}_3\text{BO}_3)}{J(\text{H}_3\text{BO}_3)C(\text{NaNO}_3)}, \quad (2)$$

where $J(\text{NaNO}_3)$ is the flow of sodium nitrate, mol(m²h⁻¹); $J(\text{H}_3\text{BO}_3)$ is the flow of boric acid, mol(m²h⁻¹); $C(\text{H}_3\text{BO}_3)$ and $C(\text{NaNO}_3)$ – the concentrations of boric acid and sodium nitrate at the entrance to the desalination chambers of the electro dialyzer, M.

Data analysis shows that the electro dialysis separation of boric acid and sodium nitrate is most effective at low voltage in the pair chamber of the electro dialysis apparatus in the pre-limit current mode since this mode corresponds to the highest values of the coefficient of permselectivity ($P(\text{NaNO}_3/\text{H}_3\text{BO}_3) = 80$) and, accordingly, the lowest boron losses (less 5 %). When the limiting current on the anion exchange membrane is reached, boric acid losses increase sharply, due to an increase of the borate mass transfer through anion exchange membranes and the chemical reaction of boric acid dissociation, which mechanism is investigated by RMD.

Acknowledgement. The study was supported by a grant from the Russian Science Foundation No. 22-13-00439, <https://rscf.ru/project/22-13-00439/>

References

1. Shaposhnik V.A., Eliseeva T.V. // J. Memb. Sci. – 1999. – Vol. 161, № 1–2. – P. 223–228.
2. Belashova E.D., Pismenskaya N.D., Nikonenko V.V. [et al.] // J. Memb. Sci. – 2017. – Vol. 542. – P. 177–185.
3. Zabolotskii V.I., Sharafan M.V., Shel'deshov N.V., Lovtsov E.G. // Russ. J. Electrochem. 2008. V. 44. P. 141.
4. Sarri S., Misaelides P., Zamboulis D., Warchol J. // J. Serb. Chem. Soc. 2008. Vol. 83(2). p. 251–264.

TRANSPORT AND STRUCTURAL CHARACTERISTICS OF ION EXCHANGE MEMBRANES IN SODIUM CHLORIDE SOLUTION

Nazar Romanyuk, Aslan Achoh, Denis Bondarev, Anatoliy Minenko, Alexander Korzhov, Mikhail Sharafan

Kuban State University, Krasnodar, Russia, E-mail: romanyuknazar@mail.ru

Introduction

Ion exchange membranes are used in various fields: water treatment, food industry, wastewater treatment, recycling of industrial solutions, synthesis of various substances, electrochemical sensors, and even as an independent branch in alternative energy [1]. The effectiveness particular membrane process depends on a number of factors, the most significant of which are the properties of the membrane used. Commercially available ion exchange membranes do not always meet the requirements, therefore, the creation of new membrane materials and the improvement of existing ones is an urgent issue. The aim of our research was to investigate and compare the main transport and structural properties of various anion exchange membranes in sodium chloride solutions.

Experiments

The objects of the study were the following anion exchange membranes: the heterogeneous anion exchange membrane MA-41 (Shchekinoazot LLC, Russia), the heterogeneous anion exchange membrane Ralex AMH PES (MEGA a.s., Czech Republic), the homogeneous anion exchange membrane MA-D, developed by Department of Physical Chemistry of Kuban State University [2], and the anion exchange membrane AHT (LANRAN, People's Republic of China). Experiments were conducted to investigate the diffusion permeability of these anion exchange membranes and the electrical conductivity in sodium chloride solutions according to standard methods [3].

Results and Discussion

The concentration dependences of the integral coefficient of diffusion permeability and specific conductivity in NaCl solutions are presented in Fig. 1.

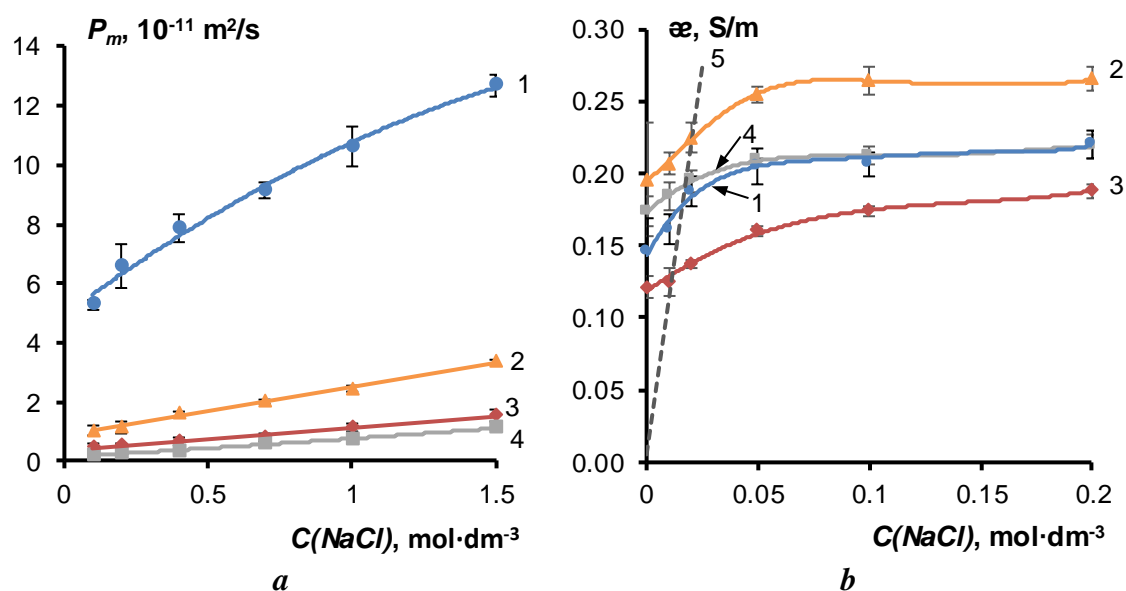


Figure 1. Concentration dependences of the integral coefficients of diffusion permeability (a) and specific conductivity (b) of anion-exchange membranes in sodium chloride solutions: 1 – MA-D; 2 – Ralex AMH PES; 3 – MA-41; 4 – AHT; 5 – data for solution NaCl

The analysis of Fig. 1 a shows that the MA-D membrane has the highest diffusion permeability (Fig. 1 a, curve 1), the value of the integral coefficient of diffusion permeability is in the range of 5×10^{-11} - 12×10^{-11} m²/s. The high diffusion permeability of the membrane reduces its selectivity in the processes of electrodialysis separation and concentration. At the same time, for the dialysis

separation process, diffusion transfer is the main one, and the separation of substances is achieved due to the high diffusion rate of one of the components of the processed solution. Therefore, the MA-D membrane is promising for use in the processes of dialysis separation of substances. The value of the diffusion permeability coefficient for electro dialysis membranes does not exceed $3 \times 10^{-11} \text{ m}^2/\text{s}$ (Fig. 1a, curves 2-4). The AHT membrane has the lowest diffusion permeability, the P_m value for this membrane is on average 4 times lower than the corresponding values for the Ralex AMH PES membrane, Fig. 1a (curves 2 and 4).

Data on the electrical conductivity and diffusion permeability of anion exchange membranes were processed within the framework of a microheterogenic model. According to this model, the ion-exchange membrane is represented as two pseudophases with different types of conductivity: the gel phase (inert polymer, polymer chains, hydrated fixed groups) and the phase of the intergel (an equilibrium solution filling the pores of the membrane).

Data analysis shows that the value of the parameter α , responsible for the mutual arrangement of conductive phases, for AHT and MA-D membranes is close to the values for electro dialysis membranes, Table 1. At the same time, the value of the electrical conductivity of these membranes in sodium chloride solutions occupies an intermediate value between the electrical conductivity of Ralex AMH PES and MA-41 membranes, Fig. 1 b.

Table 1: Transport-structural parameters of microheterogeneous model

membrane	$\alpha_{iso}, \text{ S/m}$	f_2	α	$G, 10^{-15} \text{ m}^5\text{mol}^{-1}\text{s}^{-1}$
MA-D	0.17	0.16	0.41	56,39
Ralex AMH PES	0.22	0.12	0.39	7.86
MA-41	0.13	0.15	0.28	1.37
AHT	0.19	0.06	0.38	4.55

The value of parameter f_2 (the proportion of the equilibrium solution in the membrane phase) for the AHT membrane is 2 times lower than that of other membranes. The G parameter characterizing the diffusion permeability of the gel phase of the membrane was also evaluated. The G parameter for the MA-D membrane highly differs from the rest of the membranes. This is due to the high mobility of cations in the gel phase of a homogeneous membrane MA-D.

The authors of the research [4] showed that the optimal values for transport and structural parameters in electro dialysis membranes are within the following ranges: $\alpha_{iso}=0.1-1.0 \text{ S/m}$; $G=10^{-17}-10^{-14} \text{ m}^5\text{mol}^{-1}\text{s}^{-1}$; $f_2 = 0.01-0.25$; $\alpha = 0.01-0.55$. Data analysis Table 2 shows that the parameters of the new MA-D and AHT membranes are within the these ranges, and their use in the process of electro dialysis demineralization and concentration is promising.

Acknowledgement. This work was funded by the State Assignment Project FZEN-2023-0006.

References

1. Nagarale R.K., Gohil G.S., Shahi V.K. // Advances in Colloid and Interface Science. – 2006. – Vol. 119. – P. 97-130.
2. Bondarev D.A., Achoh A.R., Bepalov A.V., Zabolotsky V.I. Pat. RU № 2 807 369 C1 20.09.2023.
3. Kononenko N.A., Demina O.A., Loza N.V., Falina I.V., Shkirskaya S.A. Membrane electrochemistry: laboratory practicum. Krasnodar: Kuban State University, 2019. – 290 p.
4. Gnusin N.P., Berezina N.P., Kononenko N.A., Demina O.A. // J. Membr. Sci. 2004. V. 243. P. 301–310.

ELECTROCONVECTION IN ELECTRODEPOSITION: ELECTROKINETIC MECHANISMS OF WAVE-LENGTH SELECTION AND PREVENTION OF THE SHORT-WAVE CATASTROPHE

Isaak Rubinstein, Boris Zaltzman

Ben-Gurion University of the Negev, Israel

Cathodic electrodeposition is the background in which two instabilities unfold: Morphological Instability and Nonequilibrium Electroosmotic Instability. Without a suitable regularization, both these instabilities are singular for shortwave perturbations in the following sense. For Morphological Instability, the plane-parallel propagation of the electrodeposition front is unstable with respect to perturbances of all wave lengths, wherein the growth rate increases indefinitely with the increase of the wave number. For Nonequilibrium Electroosmotic Instability, in terms of quasi-electroneutrality the voltage threshold is the lowest for infinitesimal wavelength perturbations of quiescence. Thus, a self-consistent theory of both instabilities must account for some regularizing mechanisms removing the ‘Shortwave Catastrophe’.

A commonly assumed regularizing mechanism for Morphological Instability is surface tension. This is not an easily measurable parameter for a solid/liquid interface. In addition, the surface tension as a regularizing mechanism yields a colloidal length scale for the fastest growing perturbation mode. This is shorter than the typically observed length scale for dendrites emerging in electrodeposition (tens of nanometers versus micrometers). As for Nonequilibrium Electroosmotic Instability, it has been known for some time that the regularizing mechanism for it is considering the finite width of the Electric Double Layer (EDL) and its adjacent Extended Space Charge (ESC). In our two recent studies, we reported that for Morphological Instability, too, considering the finite width of the EDL, combined with the finite electrode reaction rate provides a regularizing mechanism alternative to surface tension and possibly yielding a longer length scale (of the order of microns). This latter (electrokinetic/reactive scale) is the geometric average of the Debye length and the reaction/diffusion length (the ratio of the cation diffusivity to the cathodic reaction rate). This length scale has been inferred for current densities below the limiting value. In the limiting current regime, the formation of the ESC and the onset of Nonequilibrium Electroosmotic Instability yields a major further increase of the characteristic length scale towards that typical of Nonequilibrium Electroosmotic Instability (tens of microns). This is accompanied by a drastic increase of the growth rate in Morphological Instability.

In my talk I focus on the physical understanding of the mechanisms behind the short-wave catastrophe and its electrokinetic regularization. This pertains to the physical mechanism of the short-wave catastrophe in Nonequilibrium Electroosmotic Instability and its electrokinetic regularization, and the emergence of the electrokinetic/reactive length scale in Electrodeposition.

Specifically, I address the following issues:

1. The physical source of the short-wave catastrophe in Nonequilibrium Electroosmotic Instability and its electrokinetic regularization that results from considering the effect of the EDL and the ESC.
2. The physical origin of the electrokinetic/reactive length scale, in particular, (a) the role of the finite width of the EDL in regularization and (b) the reason why a finite reaction rate is necessary for regularization.
3. The physics of the Nonequilibrium Electroosmotic Instability effect on Morphological Instability.

SIMPLIFIED CHARACTERIZATION OF ION-EXCHANGE MEMBRANES FOR MODELING THE EFFICIENCY OF ELECTRODIALYSIS OF MODERATELY CONCENTRATED SOLUTIONS

Valentina Ruleva, Andrey Gorobchenko, Maria Ponomar, Victor Nikonenko

Kuban State University, Krasnodar, Russia, *E-mail: valentina.titorova@mail.ru*

Introduction

The efficiency of the electrodialysis (ED) process is determined by the characteristics of the ion-exchange membranes (IEMs) used. To control the processes of increasing the concentration of moderately concentrated electrolyte solutions in electromembrane systems, such characteristics of ion-exchange membranes as their selectivity, surface resistance and water transport numbers should be considered. Based on the mathematical modeling results, it is possible to successfully predict the efficiency of using certain membranes in the process of ED concentration with flow-through ED cells.

Experiments

Commercial heterogeneous MK-40 and MA-41 membranes (manufacturer Shchekinoazot, Russia) were applied in the experiments. According to [1], a simplified characterization of IEMs consists of measuring static properties (ion-exchange capacity, water content, membrane thickness, membrane potential) and some transport properties (electrical conductivity and diffusion permeability). Concentration dependences (where necessary) of these characteristics were obtained during the experiment.

The electrodialysis concentration process was carried out using a laboratory electrodialyzer consisting of three cell pairs formed with MK-40/MA-41 membranes with a desalination/concentration path length of 10.1 cm, which allows the results to be scaled to industrial devices [2]. The process of concentrating 2.0 M NaCl solution was carried out for 3 hours. The performance of the ED process was characterized in terms of current efficiency (η):

$$\eta = \frac{(n^{CS}(t) - n^{CS}(0))F}{NI\Delta t} \quad (1)$$

where $n^{CS}(0)$ and $n^{CS}(t)$ are the number of moles of NaCl in the concentrate stream (CS) at the initial time and at time t , respectively; N is the number of cell pairs. The values of $n^{CS}(0)$ and $n^{CS}(t)$ are found as the products of the corresponding NaCl concentrations and volumes; the number of moles of NaCl removed from the CS at each sampling is taken into account. The concentrations are determined through the measurements of the solution conductivity.

Results and Discussion

A new mathematical model of ED concentration is developed. This model, as well as the model of Sun et al. [3], is a time-dependent quasi-stationary model, however, unlike [2], it takes into account concentration changes at the membrane surface, like the model of Zabolotskii et al. [4]. The model takes into account the time-dependent ion and water fluxes through the ion-exchange membranes forming a dilute compartment and concentrate compartments. The contributions of diffusion, electromigration, osmosis and electroosmosis are described.

Concentration dependences of electrical conductivity, κ^* , integral diffusion permeability coefficient, P , true counterion transport numbers, t_l^* , and water transport numbers, t_w , of studied membranes in NaCl solution are presented in Figure 1. The trend line equations for membranes (Figure 1) are derived from the experimental data. These equations are used in the developed model to describe the concentration dependences of the corresponding transport characteristics of ion-exchange membranes.

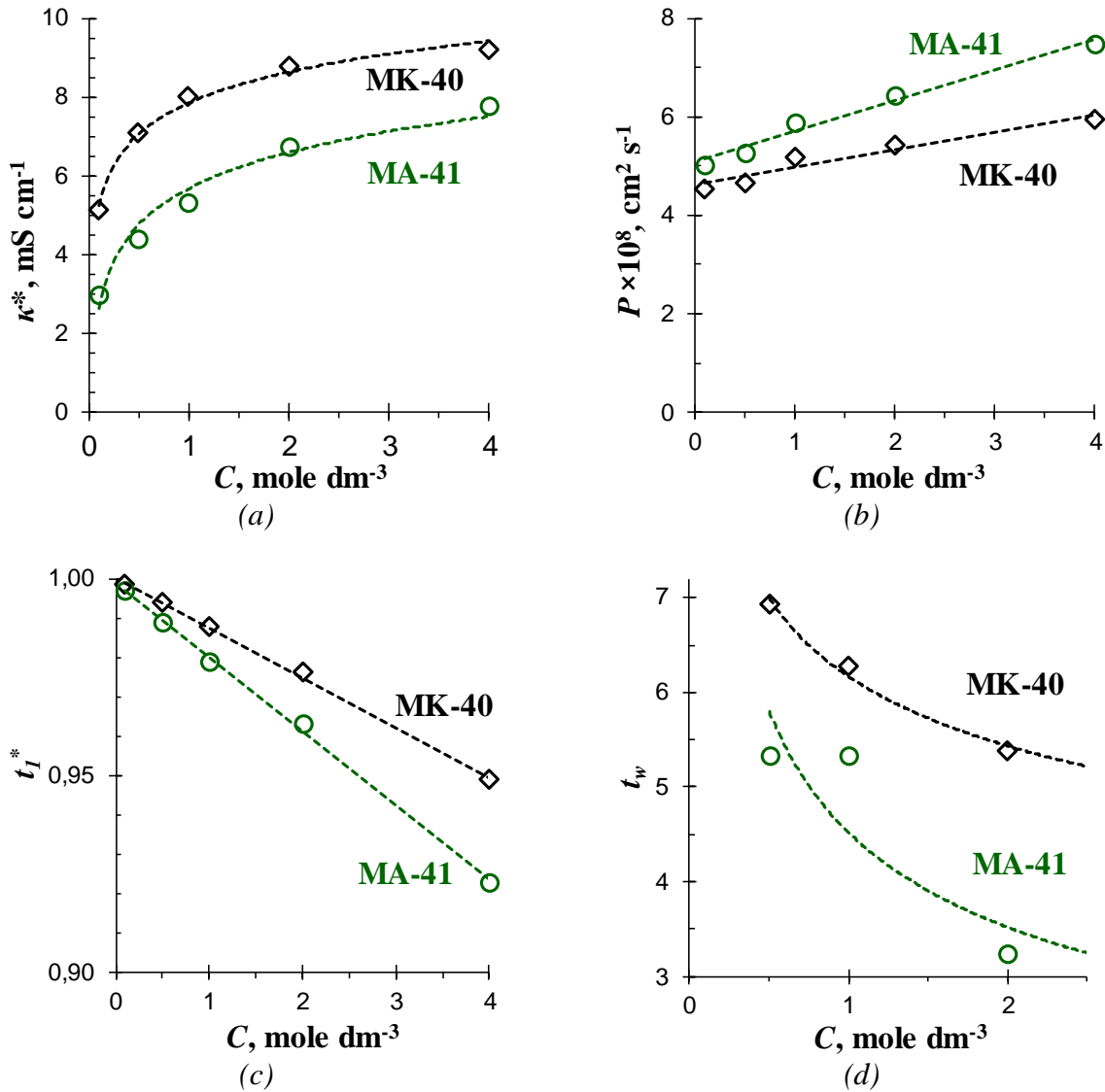


Figure 1. Concentration Dependences of Electrical Conductivity (a), Diffusion Permeability (b), True Counterion Transport Numbers (c) and Water Transport Numbers (d) of MK-40 and MA-41 Membranes in NaCl Solution. Markers are Experimental Data; Dashed Lines are Trend Lines.

Figure 2 shows the dependences of current efficiency on time for the ED concentration of NaCl solution calculated by Eq. (1) from the experimental data (the markers) and found using the developed model (the line). The discrepancy between the modeling and experimental results is 3-5 %, which is comparable to the deviation of the experimental results from each other in different experimental runs. The experimental current efficiency is slightly higher than the theoretical estimate. This is due to the local value of the coion transport number at the right membrane boundary, $t_A^*(x = d)$, is used in numerical simulation instead of the average integral value, \widehat{t}_A^* , which is present in exact. Replacing average integral value with a local value significantly simplified the model used, since the calculation of t_A^* requires the development of a more complex mathematical model based on differential equations. A rather low deviation of the simulated current efficiencies from the experimental ones (no more than 5 %) indicates the adequacy of the developed model.

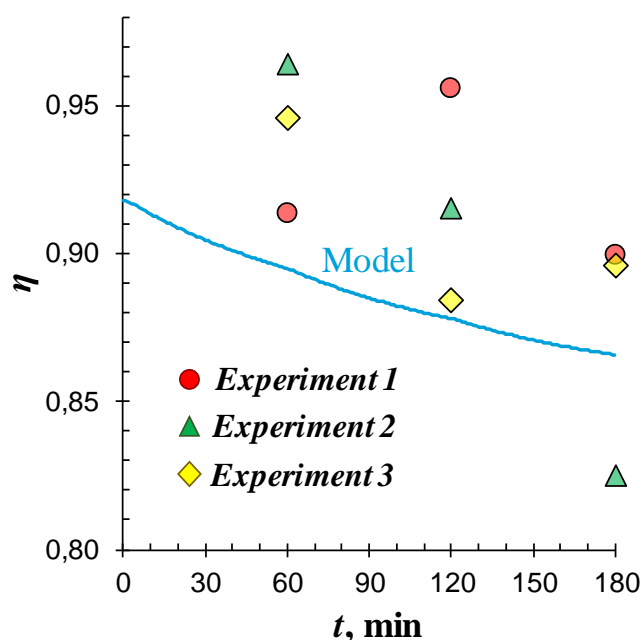


Figure 2. The Time Dependences of Current Efficiency of the Process of ED Concentration of a NaCl Solution Calculated by Eq. (1) for Three Experiments (Markers) and Found Using the Model (Blue Line).

A simple method to calculate the current efficiency, η , based on the results of measurements of membrane conductivity, κ^* , and diffusion permeability, P , is proposed. It is shown that η can be approximately evaluated through the ion transport numbers in the anion- and cation-exchange membrane, t_i^* , found from κ^* and P . The value of t_i^* should be taken in the corresponding membrane at its boundary with the concentrated solution when accounting for the current-induced concentration polarization. The deviation of the calculated value of η from its experimental value does not exceed the experimental error of the measurement of η during an ED process.

Acknowledgement. This research was financially supported by the Ministry of Science and Higher Education of the Russian Federation, project number FZEN-2024-0002.

References

1. Larchet C., Dammak L., Auclair B., Parchikov S., Nikonenko V. A simplified procedure for ion-exchange membrane characterization // *New J. Chem.* 2004. V. 28. P. 1260-1267.
2. Nikonenko V. V., Pismenskaya N. D., Istoshin A. G., Zabolotsky V. I., Shudrenko A. A., Description of mass transfer characteristics of ED and EDI apparatuses by using the similarity theory and compartmentation method // *Chem. Eng. Process. Process Intensif.* 2008. V. 946. P. 1118-1127.
3. Sun B., Zhang M., Huang S., Wang J., Zhang X. Limiting concentration during batch electro dialysis process for concentrating high salinity solutions: A theoretical and experimental study // *Desalination.* 2021. V. 498. Art № 114793.
4. Zabolotskii V. I., Shudrenko A. A., Gnusin N. P. Transport characteristics of ion-exchange membranes during electro dialytic concentration of electrolytes // *Sov. Electrochem. (English Transl. Elektro-Khimiia).* 1988. V. 24. P. 689-696.

IONIC CONDUCTIVITY ENHANCEMENT IN NANOPOROUS MEMBRANES WITH ELECTRICALLY CONDUCTIVE SURFACE

^{1,2}Ilya Ryzhkov, ^{1,2}Ivan Kharchenko, ^{1,2}Mikhail Simunin, ^{2,3}Ivan Nemtsev, ^{4,5,6}Denis Lebedev, ^{4,6}Nikita Vaulin

¹Institute of Computational Modeling, Federal Research Center KSC SB RAS, Krasnoyarsk, Russia

²Siberian Federal University, Krasnoyarsk, Russia

³Federal Research Center KSC SB RAS, Krasnoyarsk, Russia

⁴Saint Petersburg Academic University, St. Petersburg, Russia

⁵Saint Petersburg State University, St. Petersburg, Russia

⁶Institute of Analytical Instrumentation RAS, St. Petersburg, Russia

E-mail: rii@icm.krasn.ru

Introduction

The ion transport in nanoporous media plays a fundamental role in many technological processes such as water desalination, separation and purification, osmotic energy conversion, and electrochemical sensing. The ability of nanopores to transport ions under the applied electric field is characterized by the ionic conductivity, which is the ratio of ionic current to the voltage difference. Highly conductive membranes are advantageous in such processes as (reverse) electrodialysis, capacitive deionization, and hydrogen energy conversion.

In recent decades, the attention of researchers has been focused on the development of electrically conductive membranes, which surface charge can be altered by applying a prescribed potential to the membrane. It provides a powerful tool for changing and adjusting ionic selectivity, ionic conductivity, and ion rejection [1]. In a recent work [2], the ionic conductivity of nanopores with electrically conductive surface was investigated on the basis of 1D / 2D models, which were verified against experimental data. The possibility of regulating the ionic conductivity by changing the surface potential of nanopore was demonstrated.

This work deals with theoretical and experimental study of ion transport in porous anodic alumina membranes with carbon nanotubes. It is found that they demonstrate non-linear current–voltage curves due to polarization of conductive nanopore surface by the applied electric field.

Theoretical

We consider a binary aqueous 1:1 electrolyte. The membrane is modelled as an array of straight cylindrical nanopores, so it is sufficient to calculate the ion transport inside a single pore. The model is based on the 2D Nernst-Planck and Poisson equations combining convection, diffusion, and electromigration as driving forces for the fluxes of ions. The equations are solved in the nanopore, which connects two reservoirs with equal salt concentrations C_0 and different electrical potentials. At the membrane/solution interface, the Donnan equilibrium conditions are imposed. The part of electric double layer in aqueous electrolyte inside the nanopore is divided into the Stern layer, which contains water molecules, and the diffuse layer, which contains both ions and water molecules. The surface charge density σ is related to the surface potential Φ_w by

$$\sigma = C_S(\Phi_w - \Phi), \quad (1)$$

where C_S is the Stern layer capacitance and Φ is the diffuse layer potential, which can vary along the nanopore. We assume that the nanopore is initially uncharged, and the induced charge can appear only due to polarization in electric field [3]. In this case, the total charge is conserved and remains equal to zero, which determines the surface potential of the nanopore via Eq. (1).

Experimental

The porous anodic alumina membranes were prepared by the conventional method, which includes the following steps [4]: 1) electrochemical polishing of 500 μm aluminium foil 2) anodization in 0.3 M sulfuric acid electrolyte at 25 V and 5 $^\circ\text{C}$ during 8 h 3) removal of anodized

layer 4) second anodization at the same conditions during 15 h 5) selective etching of aluminum foil 6) removal of barrier layer with electrochemical detection of pore opening. As a result, free standing nanoporous membranes of 10 mm in diameter and thickness of 70 μm were obtained. The carbon nanotubes were grown inside the nanopores by catalyst-free chemical vapor deposition using ethanol vapor as a precursor and argon as a carrier gas. The synthesis conditions were as follows: temperature 750 $^{\circ}\text{C}$, pressure 0.5 bar, argon flow rate 200 ml/min, and ethanol flow rate 0.083 ml/min (in liquid phase). The SEM image of obtained membrane surface is shown in Fig. 1. The carbon nanotubes inside the pores with the inner diameter of ~ 16 nm are clearly seen.

The ionic conductivity was measured in KCl aqueous solution in a specially designed cell, where membrane was placed between two compartments with equal salt concentrations. The wire Ag/AgCl electrodes were used to apply voltage between the compartments (from -0.5 to 0.5 V) and to measure the resulting ionic current.

Results and discussion

Figure 2 shows the modelling results for a nanopore with the diameter of 16 nm and length of 70 μm . The bulk KCl concentration is 10 mM and the applied voltage difference is 100 mV. It can be seen that the applied electric field (Fig. 2a) induces the electronic surface charge density on the conductive surface (Fig. 2b) while keeping the total surface charge zero. It leads to the increase of anion (cation) concentration in the left (right) part of the nanopore (Fig. 2c), where the surface charge is positive (negative). As a result, the concentration of ions (charge carriers) inside the nanopore increases in comparison with that in the reservoirs. It leads to the enhancement of nanopore ionic conductivity in comparison with conductivity of bulk solution. If we increase the applied voltage difference, the magnitude of induced charge becomes larger, and the conductivity is enhanced further due to the increase of

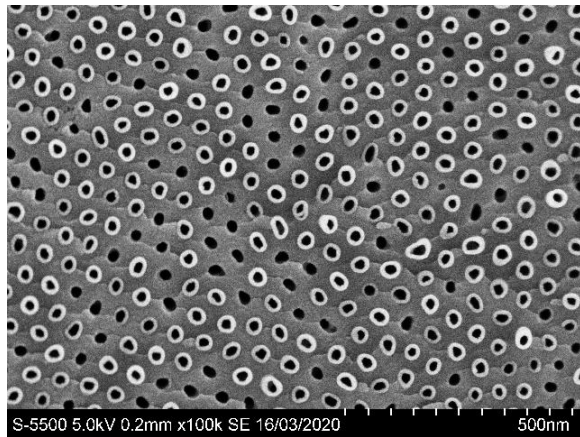


Figure 1. SEM image of porous anodic alumina membrane with carbon nanotubes.

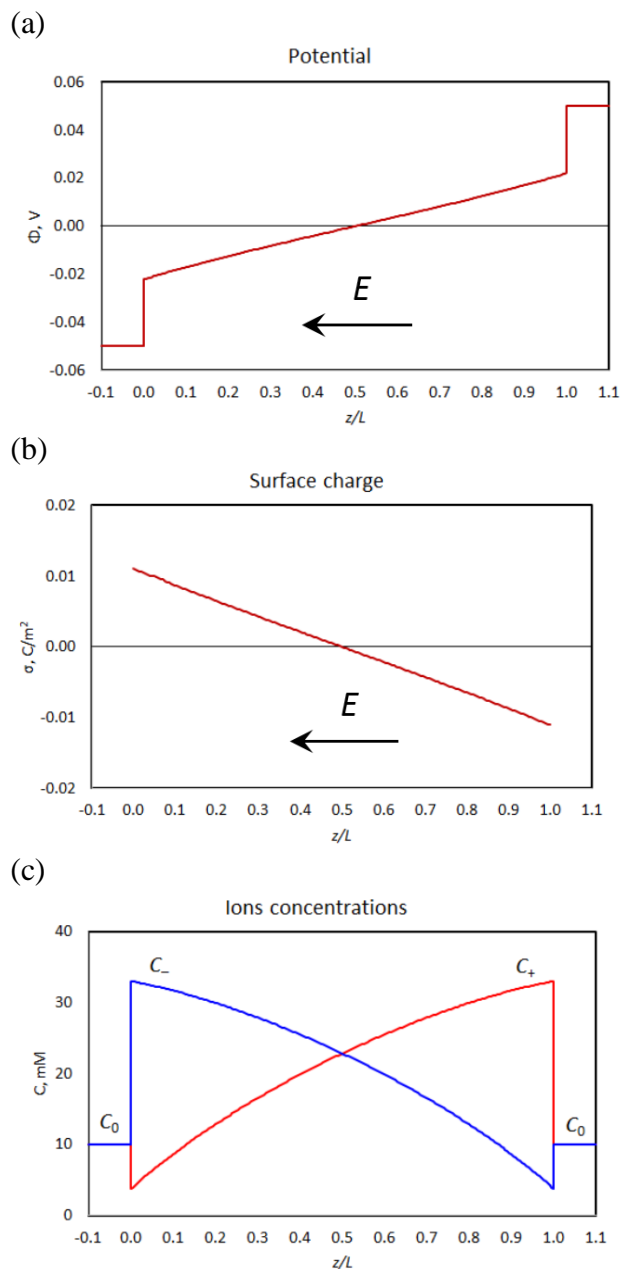


Figure 2. The cross-sectionally averaged profiles of potential (a), surface charge density (b), and ion concentrations (c) along the nanopore.

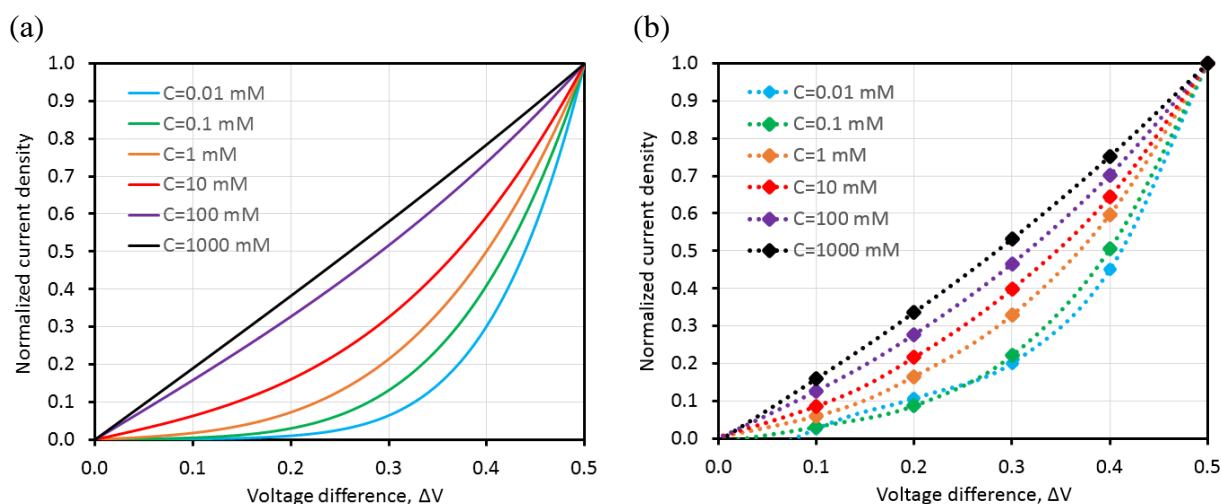


Figure 3. The dependence of normalized current density on the applied voltage difference for different salt concentrations. Model calculations (a) and experiment (b).

charge carries concentration inside the nanopore. Thus, the ionic conductivity of electrically conductive nanopores grows with the applied voltage difference, so the corresponding current-voltage curve is expected to be non-linear. However, this effect is realized when the nanopore diameter is comparable or smaller than the Debye length, which decreases with salt concentration. In this case, there is an overlap of electric double layers resulting in the increase of counter-ion concentration in positively and negatively charged parts of the nanopore.

The calculated current-voltage curves obtained for different salt concentrations confirm the above reasoning, see Fig. 3a. The current is normalized by the maximum current, which corresponds to the voltage difference of 0.5 V. At high concentrations, the curves are linear, but with decreasing concentration, the polarization of electrically conductive surface starts to affect the counter-ion concentrations inside the nanopore, so the curves become non-linear due to the enhancement of ionic conductivity with increasing the applied voltage.

The experimentally obtained current-voltage curves for porous anodic alumina membrane with carbon nanotubes are shown in Fig. 3b. They fully confirm the theoretical predictions on the non-linear behaviour of CV curves and the corresponding dependence of ionic conductivity on the applied voltage. The effect becomes stronger with decreasing salt concentration. Note that there is some quantitative difference between model calculations and experiment.

In conclusion, we have theoretically predicted and experimental confirmed the effect of ionic conductivity enhancement in electrically conductive nanoporous membranes. It occurs due to polarization of conductive surface by the electric field, which leads to the increase of charge carries concentration inside the nanopore and results in non-linear current-voltage curves.

Acknowledgments. The work is supported by the Russian Science Foundation, project 23-19-00269.

References

1. Z. Zhang, G. Huang, Y. Li, X. Che, Y. Yao, S. Ren, M. Li, Y. Wu, C. An. Electrically conductive inorganic membranes: A review on principles, characteristics and applications. *Chem. Eng. J.*, 2022, V. 427, 131987.
2. A.I. Krom, I.I. Ryzhkov. Ionic conductivity of nanopores with electrically conductive surface: comparison between 1D and 2D models. *Adv. Theory and Sim.* 2021, 2100174.
3. I.I. Ryzhkov, D.V. Lebedev, V.S. Solodovnichenko, A.V. Shiverskiy, M.M. Simunin. Induced-charge enhancement of diffusion potential in membranes with polarizable nanopores. *Phys. Rev. Letters*, 2017. V. 119, 226001.
4. I.I. Ryzhkov, I.A. Kharchenko, E.V. Mikhlina, et al. Growth of carbon nanotubes inside porous anodic alumina membranes: Simulation and experiment. *Int. J. of Heat and Mass Transfer*, 2021. V. 176, 121414.

DISPERSION-CAST PERFLUOROSULFONIC ACID MEMBRANES OF VARIOUS CHEMICAL STRUCTURE

Ekaterina Safronova, Andrey Yaroslavtsev

Kurnakov Institute of General and Inorganic Chemistry RAS, Moscow, Russia

E-mail: safronova@igic.ras.ru

Introduction

One of the most widely known polymeric ion-exchange membranes is perfluorosulfonic acid (PFSA) polymer membranes due to their unique transport properties and stability. PFSA membranes have a set of characteristics necessary for their practical application: good transport properties, strength, elasticity and chemical stability. Nafion[®] is the most well-known material. Over the years, PFSA materials with different structures, equivalent weight (EW), thicknesses have been developed and are now commercially available, making them suitable for a variety of applications. The aim of this work was comparison of the properties of PFSA membranes with different length of side chains and EW were recast from dispersions.

PFSA polymers of various structure were used to prepare dispersions in *N*-methyl-2-pyrrolidone (NMP) and isopropyl alcohol – water mixture (IPA-H₂O, v/v=80/20). Chemical structure of backbone is given on Figure 1, structure of R_F is given in Table 1. Polymers with EW ranged from 790 to 1130 mg-eqv/g were used. To form the membranes by casting procedure, the obtained dispersions were poured onto the surface of a glass Petri dish and heated to remove the solvent.

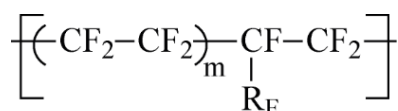


Figure 1. Chemical structure of backbone of PFSA polymers, R_F is side chain.

Table 1: Structure of side chain of PFSA polymers and trademark of analogues

R _F	Name of PFSA polymer
$-\text{O}-\text{CF}_2-\underset{\text{CF}_3}{\text{CF}}-\text{O}-\text{CF}_2-\text{CF}_2-\text{SO}_3\text{H}$	Nafion [®] / MF-4SC
$-\text{O}-\text{CF}_2-\text{CF}_2-\text{CF}_2-\text{CF}_2-\text{SO}_3\text{H}$	3M [®]
$-\text{O}-\text{CF}_2-\text{CF}_2-\text{SO}_3\text{H}$	Aquivion [®]

Viscosity of PFSA polymers increases with decrease in IEC and with shortening of side chain. For example, viscosities of 2.5 wt.% dispersions in IPA-H₂O were (η, 25°C): 9.1 mPa·s for Nafion (EW=1100 g/mol), 25.1 mPa·s for Aquivion (EW=980g/mol) and 37.7 mPa·s for Aquivion (EW=980 g/mol) polymers. The formation of dispersions is prevented by electrostatic interaction between functional sulfo groups, therefore, increasing their number (decreasing EW) makes it difficult to disperse PFSA polymers.

The water uptake and transport properties of the obtained membranes were studied. The water uptake of the membranes ranged from n(H₂O/-SO₃H)=16.8 to 44.1 in contact with water (Figure 2). Water uptake of membrane with short-side chain (Aquivion 87) both in contact with water and at low humidity is higher than that of long-side chain (Nafion 212) due to lower specific polymer chains limiting the ability to membrane deformation upon swelling. Membranes obtained by casting from dispersions in NMP are characterized by higher water uptake than from IPA- H₂O mixture due to a lower degree of agglomeration of polymer macromolecules in the dispersion.

The proton conductivity of the membranes obtained under laboratory conditions is higher than the commercial ones due to the pore and channel system optimization (Figure 3). In contact with water, the highest conductivity and lowest activation energy were obtained for membranes cast from dispersions in NMP. At both high and low humidity, higher conductivity was obtained for samples cast from dispersions based on PFSA powders due to the low viscosity of dispersions and the higher mobility of polymer moieties, which provides good conditions for pore formation.

The gas permeability of PFSA based membranes with a short-side chain is lower than that of membranes with a long-side chain and decreases with decreasing EW. For PFSA-based membranes of the same chemical composition, obtained by casting from dispersions in a water-alcohol mixture, the gas permeability is 20% higher than that from dispersions in NMP. A possible reason for the increase of non-selective transport rate is the formation of pores or caverns of large size when casting membranes from polymer dispersions with high degree of macromolecule agglomeration.

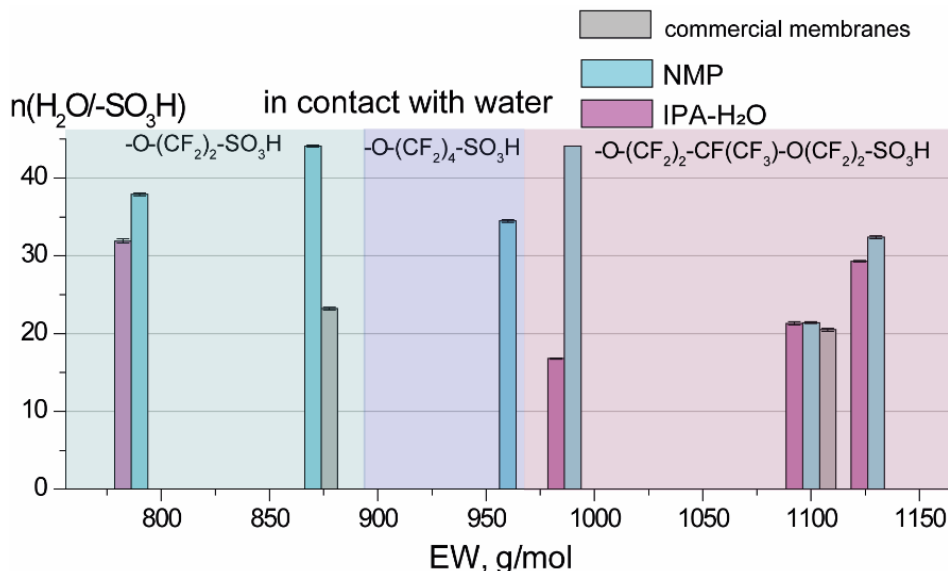


Figure 2. Water uptake in contact with water of PFSA membranes with different EW and side chain.

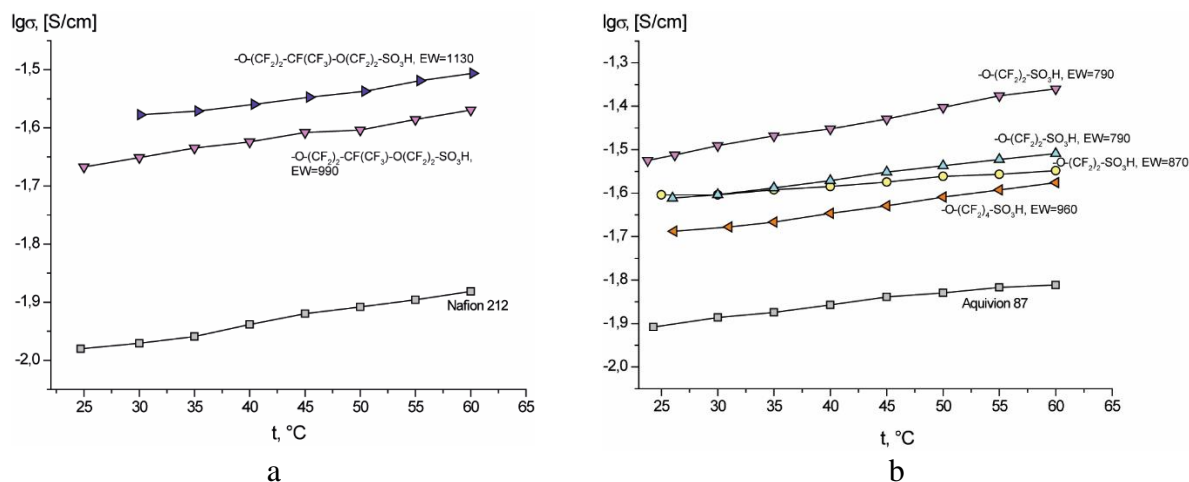


Figure 3. Proton conductivity in contact with water of PFSA membranes with long (a) and short (b) side chain. EW of commercial samples is 1100 g/mol for Nafion 212 and 870 g/mol for Aquivion 87.

Figure 4 compares the voltammetry curves and power density dependence for membrane electrode assemblies (MEAs) with Nafion® 212 and PFSA membrane with long side chain (LSC) with EW=1130. This membrane was obtained from PFSA polymer synthesized in Russia. The maximum power density of the MEA with the membrane with EW=1130 has a comparable value with Nafion 212.

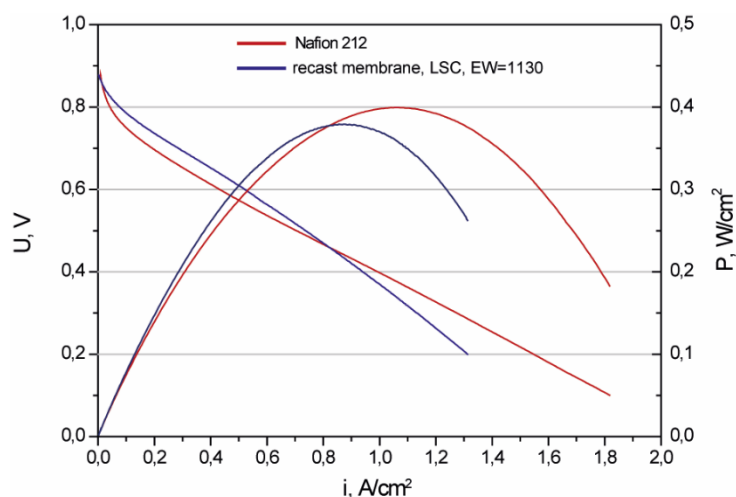


Figure 4. Voltammetry curves and power density dependence on current density for MEAs based on commercial Nafion 212 membrane (EW=1100) and analogues recast membrane with LSC with EW=1130 (RH = 100%, $t = 65^{\circ}\text{C}$).

Thus, the influence of EW, side chain length of PFSA and nature of dispersing liquid on properties of dispersions and characteristics of recast membranes was shown. To obtain films with good strength, transport, and selective properties it is advisable to use aprotic polar solvents such as 1-methyl-2-pyrrolidone, providing optimal PFSA morphology.

Acknowledgement. This study was supported by a grant from the Russian Science Foundation № 21-73-10149, <https://rscf.ru/project/21-73-10149>.

RATE CONSTANTS OF WATER DISSOCIATION IN HETEROGENEOUS MEMBRANE CONTAINING CATALYTIC ADDITIVE PARTICLES

Nikolay Sheldeshov, Nikita Kovalev, Ilya Averianov, Tatyana Karpenko, Victor Zabolotsky

Kuban State University, Krasnodar, Russia, E-mail: sheld_nv@mail.ru

Introduction

One of the main characteristics on which the possibility of practical application of a bipolar membrane (BM) depends is the current-overvoltage characteristic (CVC) of its bipolar region. The current-voltage characteristic of the bipolar region depends on many factors. Thus, the influence of the catalytic activity of ionogenic groups of ion exchangers and electric field strength at water molecule dissociation reaction rate in bipolar region of a homogeneous BM was taken into account in [1] when deriving the CVC. The structure of the bipolar region of a heterogeneous BM that does not contain a catalytic additive, taking into account the generating contacts and CVC equation of bipolar region was proposed in [2]. It is shown in [3] that addition of a catalytic additive particles into the bipolar region of a heterogeneous BM complicates its structure and leads to the appearance of new type generating contacts. In [3] the influence of the mass of particles of the catalytic additive on the electrical conductivity of the bipolar region was established. However, the method for calculating water dissociation reaction constants in both types generating contacts in such membranes still remains unknown.

The purpose of this work is to develop the method for calculating the constants of the limiting stages of water dissociation reaction in generating contacts of heterogeneous BM containing catalytic additive particles in the bipolar region.

Theory

Derivation of the current-voltage characteristic equation for the bipolar region of heterogeneous BM containing generating contacts of two types in the bipolar region leads to a rather complex equation (1) [3, equation (18)], containing five $k_{\Sigma cat|a}$, $\beta_{cat|a}$, $k_{\Sigma c|a}$, $\beta_{c|a}$, and a constants:

$$i_{het} = \left(k_{\Sigma,cat|a} \frac{\varepsilon_{cat|a} \varepsilon_0}{\beta_{cat|a}} \left[\exp(\beta_{cat|a} E_{m,cat|a}(U_b)) - \exp(\beta_{cat|a} E_{m,cat|a}(0)) \right] - \right. \\ \left. - k_{\Sigma,c|a} \frac{\varepsilon_{c|a} \varepsilon_0}{\beta_{c|a}} \left[\exp(\beta_{c|a} E_{m,c|a}(U_b)) - \exp(\beta_{c|a} E_{m,c|a}(0)) \right] \right) \alpha_c \alpha_a (1 - e^{-am_{ex}}) + \\ + k_{\Sigma,c|a} \frac{\varepsilon_{c|a} \varepsilon_0}{\beta_{c|a}} \left[\exp(\beta_{c|a} E_{m,c|a}(U_b)) - \exp(\beta_{c|a} E_{m,c|a}(0)) \right] \alpha_c \alpha_a . \quad (1)$$

Using the CVC equation (1), it is impossible to calculate all reaction constants for the dissociation of water molecules in two types of generating contacts: $k_{\Sigma cat|a}$, $\beta_{cat|a}$, $k_{\Sigma c|a}$, $\beta_{c|a}$ and constant a only from the experimentally found CVC of the BM containing catalyst particles.

The method for calculating all constants becomes possible if, at the *first stage*, using the CVC of the bipolar region, calculate the constants $k_{\Sigma c|a}$ and $\beta_{c|a}$ for generating contacts of the first type in BM without a catalyst particles according to equation (2) [3, equation (19)]:

$$i_{het} = k_{\Sigma,c|a} \frac{\varepsilon_{c|a} \varepsilon_0}{\beta_{c|a}} \left[\exp(\beta_{c|a} E_{m,c|a}(U_b)) - \exp(\beta_{c|a} E_{m,c|a}(0)) \right] \alpha_c \alpha_a . \quad (2)$$

At the *second stage* of calculating the reaction constants for the dissociation of water molecules using equation (3) [3, equation (28)] for a series of BMs with different masses of added catalyst, the parameter a is determined:

$$\kappa_{het} = (\kappa_{het}^{**} - \kappa_{het}^*) (1 - e^{-am_{ex}}) + \kappa_{het}^* . \quad (3)$$

At the *third stage*, using equation (1), the constants $k_{\Sigma_{\text{cat}|a}}$ и $\beta_{\text{cat}|a}$ are calculated for generating contacts of the second type in the BM with a catalyst, taking into account the constants $k_{\Sigma_{\text{c}|a}}$ and $\beta_{\text{c}|a}$ found at the first stage of calculation and parameter a found using equation (3).

Experiments

To calculate the reaction constants for the dissociation of water molecules in bipolar membranes, the bipolar regions CVCs of industrial bipolar membranes MB-1, MB-2 and MB-3 (Shchekinoazot), as well as the modified heterogeneous bipolar membrane MBm and aMB-2 prepared by the authors, were used. MBm was prepared by hot pressing of Ralex CMH cation exchange and Ralex AMH anion exchange heterogeneous membranes (MEGA, Czech Republic). Before pressing the layer of powder of the KF-1 cation exchanger containing phosphoric groups was applied at cation-exchange membrane surface. aMB-2 was prepared by hot pressing of Ralex CMH cation exchange and Ralex AMH anion exchange heterogeneous membranes without catalytic additive.

The electrochemical characteristics of BM were investigated in a system containing 0.1 M HNO_3 and 0.1 M NaOH by the electrochemical impedance technique in a four-electrode electrochemical cell. The measurements were carried out in the stationary state both in the absence of a superimposed direct electric current and during its flow through the BM in the mode of generation of hydrogen and hydroxyl ions. The frequency spectra of electrochemical impedance were measured in the frequency range of alternating current from 0.1 Hz to 1 MHz, evenly distributed on a logarithmic scale using an AUTOLAB 100N potentiostat-galvanostat with an FRA32M impedance measurement module.

The CVCs of the membranes bipolar regions were calculated from the dependence of the resistance of the bipolar region on the current [3]. The reaction constants of water dissociation and the parameter a were calculated from experimental data using equations (1)-(3) by nonlinear least squares method.

Results and Discussion

The rate constants for the water dissociation reaction in the bipolar regions of the MB-1, MB-2, and MB-3 membranes are significantly higher compared to the constants calculated in [1], where the heterogeneity of the BM was not taken into account (table).

The product of parameters $\alpha_c\alpha_a$ included in equations (1) and (3) was calculated using the method proposed in [2]. It is equal to 0.083 and is close to the area fraction of 0.078, which was calculated from the values for Ralex membranes $\alpha_c = 0.273$ and $\alpha_a = 0.289$, determined using scanning electron microscopy in [4].

The difference between the constants in this work and in [1] is due to the fact that in a heterogeneous BM, the dissociation reaction of water molecules occurs only in generating contacts in which the local current density is greater than the current density calculated for the visible surface of the membrane. The second reason for the larger values of the rate constant for the water dissociation reaction can be the heating in the region of the generating contacts, which should be greater than that calculated in [5] without taking into account the heterogeneity of the BM.

The rate constant for the water dissociation reaction in the bipolar region of the MBm membrane ($11.7 \cdot 10^3$ 1/s) is greater than for the MB-3 membrane with phosphoric acid groups ($3.39 \cdot 10^3$ 1/s, equation (7)). This may be due to an increase in area fraction of generating contacts of two types in the bipolar region of the MBm membrane as a result of the transfer of polyethylene from the surface layers of the original cation- and anion-exchange membranes into the layer of the catalytic additive during the production of the modified BM.

Table: Effective constants of the limiting stages of water dissociation reaction in the space charge region k_{Σ} and parameter β of heterogeneous BMs in 0.1 M NaOH – 0.1 M HNO₃ at 25°C temperature

Type BM	Types of generating contacts	Calculation using equations (9)-(11), (17), taking into account the heterogeneity of the bipolar region		Data obtained in [1] without taking into account the heterogeneity of the bipolar region		$\alpha_c \alpha_a$	$\alpha_c \alpha_a \alpha_{cat}$
		$k_s, 1/c$	$b \cdot 10^9, m/B$	$k_s, 1/c$	$b \cdot 10^9, m/B$		
MB-1	1	323±20	3.05±0.06	8.95	3.65	0.08 3	–
MB-3*	1	(3.39±0.11) 10 ³	4.59±0.07	248	6.41		–
MB-2	1	72±12**	4.54±0.22**	1.13	6.67		–
aMB-2	1	141±4	3.32±0.03	–	–		–
MBm***	1	141±4	3.32±0.03	–	–		–
	2	(11.7±0.5) 10 ³	3.67±0.10	–	–	–	0,051

* – the membrane was studied in “0.01 mol-eq./l NaOH – 0.01 mol-eq./l H₂SO₄” system at the 4°C temperature [6].

** – the calculation was carried out according to the data obtained in [7] in “0.01 M NaOH – 0.01 M HCl” system.

*** – the mass of the added catalyst is 11 g/m².

Acknowledgement. This study was supported by the Russian Science Foundation, research project no. 22-13-00439, <https://rscf.ru/project/22-13-00439>.

References

1. *Umnov V.V., Shel'deshov N.V., Zabolotskii V.I.* Current-voltage curve for the space charge region of a bipolar membrane // *Rus. J. Electrochem.* – 1999. – V. 35. – P. 871-878.
2. *Pivovarov N.Ya., Golikov A.P., Greben' V.P.* The influence of heterogeneity of bipolar membranes on their current-voltage curves // *Rus. J. Electrochem.* – 1997. – V. 33. – P. 536-543.
3. *Kovalev N.V., Karpenko T.V., Sheldeshov N.V., Zabolotsky V.I.* Preparation and electrochemical properties of heterogeneous bipolar membranes with a catalyst for the water dissociation reaction // *Membr. and Membr. Techn.* – 2021. – V. 3. – P. 231-244.
4. *Vasil'eva V.I., Zhiltsova A.V., Akberova E.M., Fataeva A.I.* Influence of surface inhomogeneity on current-voltage characteristics of heterogeneous ion exchange membranes // *Condensed Matter and Interphases.* – 2014. – V. 16. – P. 257-261.
5. *Greben' V.P., Kovarskij N.Ya.* Vliyanie vnutrennego teplovy`deleniya na vol't-ampernuyu xarakteristiku bipolyarnoj membrany` // *Zhurnal fizicheskoy ximii.* 1978. T. 52, № 9. S. 2304-2307. (in Russian)
6. *Shel'deshov N.V., Zabolotskii V.I., Pis'menskaia N.D., Gnusin N.P.* Catalysis of the water dissociation reaction by phosphoric acid group of bipolar membrane MB-3 // *Elektrokimiia.* – 1986. – V. 22. – P. 791-795.
7. *Zabolotskii V.I., Gnusin N.P., Shel'deshov N.V., Pis'menskaya N.D.* Investigation of the catalytic activity of secondary and tertiary amino groups in the dissociation of water on a bipolar MB-2 membrane // *Soviet Electrochemistry.* – 1985. – V. 21. – P. 993-996.

DIGITAL TECHNOLOGY APPLICATIONS FOR THE MEMBRANE PROCESSES DESIGN

Konstantin Shestakov, Dmitry Lazarev, Sergey Lazarev, Maxim Gessen

Tambov State Technical University, Tambov, Russia, E-mail: shestakov.kv@mail.tstu.ru

Introduction

Designing of wastewater treatment equipment is a complex task involving a number of technical and environmental aspects [1, 2]. One of the main problems in this area is the wastewater treatment efficiency. Wastewater can contain various components, including toxic substances, heavy metals, organic and other pollutants. Therefore, the equipment being developed must ensure the effective removal of all these pollutants to levels that meet safety and environmental standards.

Another problem is related to the scalability and adaptation of the treatment system to specific wastewater flows and characteristics. Different types of wastewater (industrial, domestic, agricultural) require different treatment approaches, and the equipment must be able to quickly adapt to a variety of conditions. In addition, it is important to ensure effective management of the cleaning process in order to minimize energy consumption and reduce operating costs. All these aspects should be carefully considered and integrated into the design of wastewater treatment equipment in order to ensure a safe and efficient treatment process.

An important role in the design of treatment equipment is currently occupied by digital technologies, which includes the use of specialized software for modeling, calculations and optimization of treatment systems and, in particular, membrane systems [3, 4]. This allows engineers and designers to perform more accurate and efficient process calculations, taking into account various parameters such as pressure, temperature, physico-chemical properties of substances and membrane structure.

This work is devoted to the description of the developed software package, which made it possible to automate and simplify the predicting the technological parameters of the electromembrane purification processes well as to improve the process of membrane purification system developing of the required capacity.

Experiments

The development of a software package for predicting the technological parameters of the electrochemical separation process was carried out in the Python. It is based on a mathematical description of the substance transfer through the membrane according to the improved friction theory of mass transfer and a series of experimental studies aimed at verifying the technological parameter forecasting adequacy of the separation process [5, 6].

The algorithm for predicting technological parameters can be presented as follows (Figure 1):

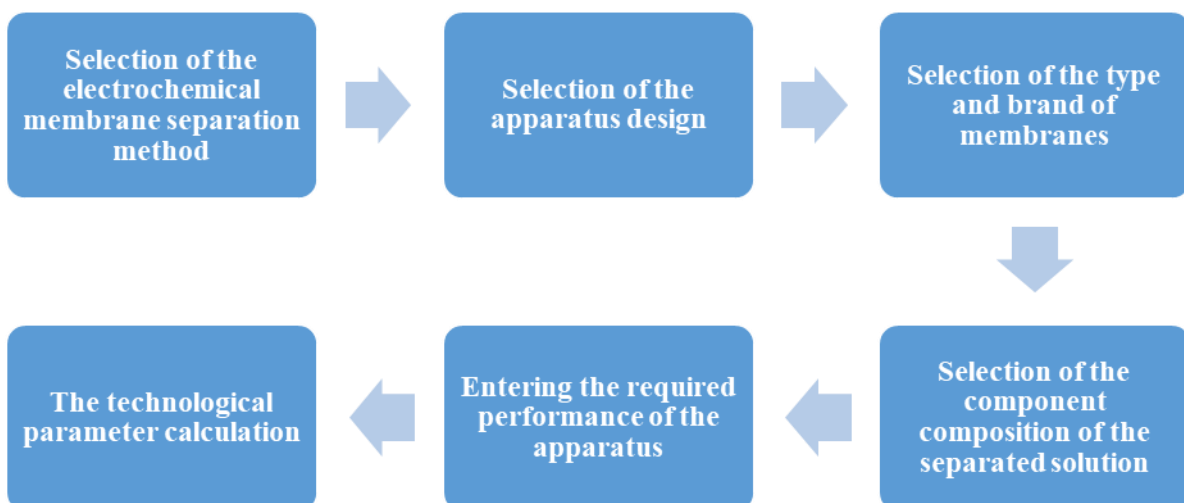


Figure 1. The general scheme of the software package.

Results and Discussion

At the first stage of the calculation, it is necessary to determine the method of electrochemical membrane separation, on which the apparatus design type will depend. At the moment, the software package provides the possibility of calculating and predicting the parameters of four types of devices – an electro dialyzer and electrobaromembrane devices of flat-chamber, tubular and roll types (Figure 2).

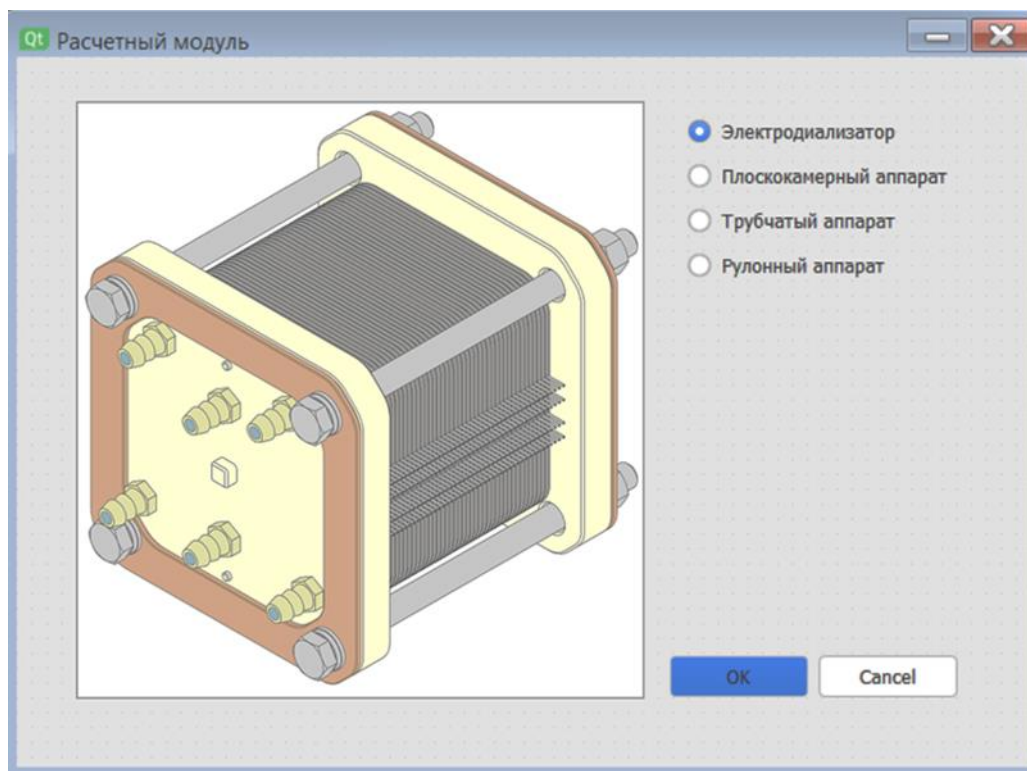


Figure 2. Apparatus type selection menu.

After confirming the apparatus type, the membrane used selection takes place. At this stage, there are restrictions on the choice of the membrane type, which are due to the previously selected design of the apparatus. For example, for electrobaromembrane apparatuses, only reverse osmosis, nanofiltration and ultrafiltration types of membranes can be selected, and for an electro dialyzer are only ion-exchange ones. This allows you to optimize the choice of membranes in accordance with the selected design of the apparatus and ensures the correct operation of the cleaning system, avoiding software errors in the calculation process.

At the next intermediate stage, you can adjust the component composition of the separated solutions, enter the values of electrical conductivity, total salinity and pH of the solution (Figure 3). The menu of this section of the software package provides the ability for all entered data resetting, saving data and loading previously saved data from a file in order to simplify the calculation process. In addition, reference information is integrated into the developed software package, which explains the procedure for filling in, saving and uploading data, as well as a number of other frequently occurring issues. This function is called by pressing the "?" button.

Before the final stage of calculating the technological parameters, the user can enter the required values for productivity and purification degree, after which he can already click on the calculation button. Next, the software package will calculate the dimensions and a number of technological parameters, which include the membrane number, the total and working areas of the membranes, current density, electricity and cooling water costs. The "Re-enter" button resets the entered data, and the "Save" button allows you to save the calculation results in text format.

The main result of the work is the developed software package that automates and simplifies the process of predicting the technological parameters of electrochemical membrane separation, as well as facilitates the development of purification systems of the required capacity. The use of

this software package allows you to predict the technological parameters of an electromembrane apparatus taking into account such input data as ion concentration, electrical voltage, electrical potential and others.

Figure 3. The menu for selecting the solution component composition.

Acknowledgement. This work was supported by the Presidential grant of the Russian Federation for young scientists and candidates of sciences MK-4774.2022.4.

References

1. Abubakar A., Abubakar M., Arowo M., Simon P., Umdagas L., Saka T., & Nasar M., Askira B., Kafle S. Aspen Plus Conceptual Design of Basic Raw Hard Water Treatment and Softening Operation // Engineering Heritage Journal. No. 4. P 141-153.
2. Gül E., Erdek M. Model-Based Optimization of a Wastewater Treatment Plant: Hakkari Case Study // Dicle Üniversitesi Fen Bilimleri Enstitüsü Dergisi. No 11(1) P. 157-172.
3. Li M. Modeling, Simulation, and Optimization of Membrane Processes // Separations. 2023. No 10(5). P. 303-305
4. Younes K., Mouhtady O., Chaouk H. The application of unsupervised machine learning to optimize water treatment membrane selection // Ann Robot Automation. 2023. No 5(1). P. 30-33.
5. Shestakov K.V. Calculation and Prediction of Kinetic Parameters of Mass Transfer through Ion-Exchange Membranes on the Basis of Friction Theory // Transactions TSTU. 2022. Vol. 28. No 4. P. 628-636.
6. Shestakov K., Lazarev S., Lazarev D., Krylov A. The solution multicomponent effect on the heavy metal ion transfer during electrodialysis // Ion Transport in Organic and Inorganic Membranes: I.T.I.M. 2023 International Conference Conference Proceedings. 2023. P. 273-275.

WATER TRANSPORT IN MODIFIED PERFLUORINATED MEMBRANES

Svetlana Shkirskaia, Natalia Kononenko, Diana Zotova

Kuban State University, Krasnodar, Russia, E-mail: shkirskaia@mail.ru

Introduction

Perfluorinated membranes are used in membrane electrolyzers and redox batteries as separating diaphragms, as well as in fuel cells as solid polyelectrolytes due to their unique properties. A promising way to improving the performance characteristics of polymer membranes and increasing their ionic conductivity under low humidity conditions is their modification with components of different natures. The incorporation of inert polymers into perfluorinated membranes makes it possible to increase their mechanical strength and reduce the crossover of uncharged particles, with these improvements being necessary for the use of the membranes in fuel cells and redox flow batteries. One of the aims of production of modified membranes is stabilization of water content and improvement of their water transport characteristics. The goal of this work was to determine the relationship between the content of an inert polymer in perfluorinated sulfonic cation-exchange membranes and their equilibrium and dynamic hydration characteristics.

Experiments

The objects of the study were perfluorinated membranes MF-4SK with varying content of inert component F-26 from 0 to 40 wt.% and F-42 from 10 to 25 wt.% on a dry membrane. The samples were obtained by casting from polymer solutions in dimethylformamide with the addition of F-26 (vinylidene fluoride copolymer with hexafluoropropylene) and F-42 (tetrafluoroethylene and vinylidene fluoride copolymer) [1]. The water transport numbers t_w (mole H₂O/F) were measured in NaCl solutions by the volumetric method in a two-chamber cell with reversible silver chloride electrodes. Experimental data [2] on measuring ion-exchange capacity (Q) and water content (W) were used to estimate equilibrium hydration characteristics – specific water content of membranes n_m (mol H₂O/mol SO₃⁻). The water distribution on the water binding energy and the effective pore radii were studied by the method of standard contact porosimetry [3].

Results and Discussion

The main physicochemical characteristics were obtained and it can be shown that, as the fraction of the inert component increases, the exchange capacity and moisture content of the samples regularly decrease. The integral coefficient of diffusion permeability and specific electrical conductivity of MF-4SC membranes in 0.1 M NaCl solution dependences on the mass fraction of inert polymers were investigated. The difference in the characters of the influence of F-26 and F-42 fluoropolymers on the transport properties of the MF-4SC membrane is because the F-26 contains free –CF₃ groups, which may hinder the denser packing of the final material, thus providing it with a higher elasticity. Porosimetric curves were used to calculate the structural characteristics of the perfluorinated membranes: the maximum porosity as the total volume of water in a sample, the specific area of the internal surface, the distance between functional groups.

The concentration dependences of water transport numbers of the studied samples in sodium chloride solutions were obtained. For all samples an increase in the concentration of the electrolyte solution regularly leads to a decrease of water transport numbers due to a reduction in the hydration number of ions in the solution. The concentration dependences of the electroosmotic permeability have been used to calculate the water transport numbers for a series of perfluorinated sulfonic cation-exchange membranes with different F-26 and F-42 contents and to reveal the relationship between the equilibrium (n_m) and dynamic (t_w) hydration characteristics of the samples. The Spiegler coefficient was calculated from data on the total water content and water transport numbers. This coefficient characterizes the fraction of water that is transported in the electric field relative to total water content in the membrane. The dependence of the Spiegler coefficient on the content of the inert component is shown in Fig. 1.

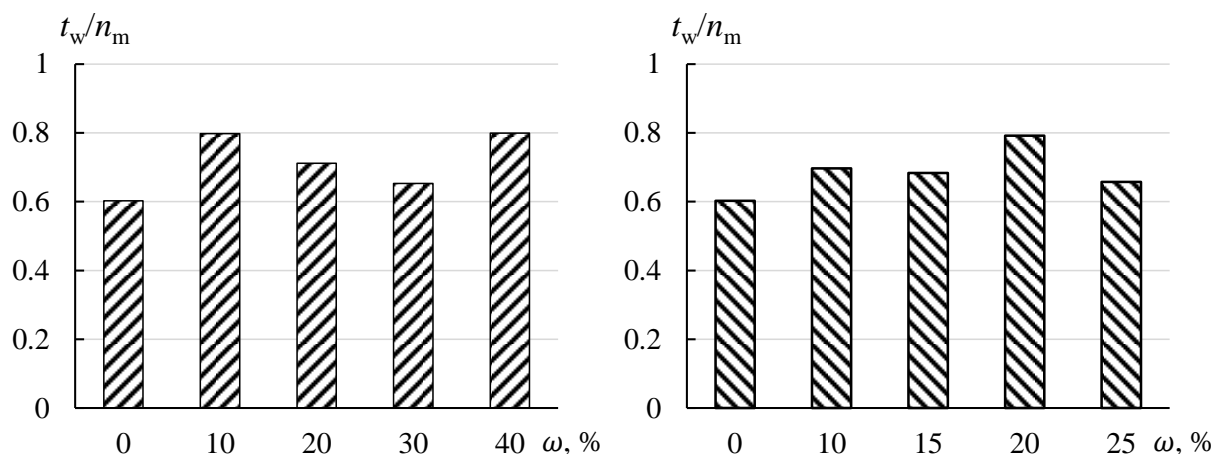


Figure 1. The relation of t_w/n_m as dependencies on F-26 (a) and F-42 (b) content in perfluorinated membranes in NaCl solutions.

As can be seen in Fig. 1, the incorporation of different amounts of the inert fluoropolymer into the structure of the MF-4SK membranes leads to a change in the t_w/n_m ratio from 0.6 to 0.8. Moreover, for all samples containing of inert fluoropolymer, the coefficient t_w/n_m is higher than that for the initial MF-4SC membrane. This means that the presence of the inert fluoropolymer enhances the hydrophobicity of the perfluorinated cation exchange membrane, thus facilitating the involvement of water in its transport with counterions in an electric field. This may be due to the effect of water slip along the inert fluoropolymer.

Conclusions

The analysis of equilibrium and dynamic hydration characteristics has shown that the nature and content of an inert component in a perfluorinated membrane has a greater effect on the state of water under equilibrium conditions than on the electroosmotic transport of water in an external electric field.

Acknowledgement. This research was financially supported by the Russian Science Foundation and Kuban Science Foundation (project No 22-19-20101), <https://rscf.ru/project/22-19-20101/>.

References

1. Falina I., Kononenko N., Timofeev S., Rybalko M., Demidenko K. Nanocomposite membranes based on fluoropolymers for electrochemical energy sources // *Membranes*. 2022. V.12. P.935.
2. Kononenko N.A., Shkirskaya S.A., Rybalko M.V., Zotova D.A. The influence of inert fluoropolymer on equilibrium and dynamic hydration characteristics of MF-4SC membrane // *Colloid Journal*. 2023. V. 85, No. 6, P. 908-916.
3. Kononenko N., Nikonenko V., Grande D., Larchet C., Dammak L., Fomenko M., Volkovich Yu. Porous structure of ion exchange membranes investigated by various techniques // *Adv. Colloid Interface Sci*. 2017. V. 246, P. 196.

FEATURES OF STRUCTURE AND IONIC CONDUCTIVITY OF Li⁺-MEMBRANES WITH NAFION STRUCTURE PLASTICIZED WITH CARBONATES

¹Lyubov Shmygleva, ¹Ruslan Kayumov, ^{1,2} Anna Lochina, ¹Alexander Lapshin

¹Federal Research Center of Problems of Chemical Physics and Medicinal Chemistry, Russian Academy of Sciences, Chernogolovka, Russia; *E-mail: shmygleval@icp.ac.ru, kayumov@icp.ac.ru*

²Moscow Institute of Physics and Technology, Dolgoprudny, Russia

Introduction

In many portable electronic devices (mobile phones, watches, toys, flashlight, etc.) batteries are power sources. Today lithium-ion batteries (LIA) are the most common. Like any electrochemical device, LIA consist of two electrodes divided by electrolyte. Despite the widespread usage of liquid electrolytes, the fire and explosion safety of the batteries based on them remains a serious problem, the solution to which can be the usage of solid polymer electrolytes [1, 2]. These electrolytes have also unipolar ion conductivity instead of bipolar in the liquid ones. Against the background of the requirements for electrolytes in LIBs, polymer membranes with the structure of commercial membrane Nafion, are very promising. Unfortunately, today Nafion membranes are not available for purchase all over the world. So, it is necessary to search for alternative polymers that would not be inferior in their properties to Nafion.

Therefore, the aim of this work was to study several commercially available Chinese membranes, plasticized with ethylene carbonate and propylene carbonate from the point of view their ion conductivity, molecular and supramolecular structure and thermal stability.

Experiments

Four types of commercial polymer cation-exchange membranes manufactured in China (Zhongding New Energy and Cantian) were carried out in this work: GP-IEM-102, GP-IEM-105, CTPEM1 and CTPEM3. These polymers have the same equivalent weight (1000 g/eq) and different thicknesses (15–125 μm). The studied polymers were purified, converted to the lithium form and dried from the water according to a standard method for Nafion membranes [6, 7]. To obtain plasticized samples, the salt forms of the polymers were kept in anhydrous EC and PC in the presence of activated molecular sieves. All manipulations with the membranes and solvents were carried out in a glove box. The properties of the membranes in lithium form were studied by the methods of simultaneous thermal analysis, IR spectroscopy, small-angle X-ray scattering and impedance spectroscopy.

Results and Discussion

The report will present the results of the methods listed above and show that the commercial analogues of Nafion studied in this work demonstrate their similarity with it in terms of chemical structure and thermal stability (up to 450 °C); and ion conductivity of these membranes is not inferior in magnitude to the conductivity of Nafion.

Acknowledgements. The reported study was supported by a grant of Russian Science Foundation No. 24-29-00484, <https://rscf.ru/en/project/24-29-00484/>.

References

1. Voropaeva D.Y., Novikova S.A., Yaroslavtsev A.B. Polymer electrolytes for metal-ion batteries // *Russ. Chem. Rev.* 2020. V. 89. P. 1132.
2. Bushkova O. V., Sanginov E.A., Chernyuk S.D., Kayumov R.R. Polymer electrolytes based on the lithium form of Nafion sulfonic cation-exchange membranes : current state of research and prospects for use in chemical power sources // *Membr. Membr. Technol.* 2022. V. 4. P. 433–454.

POSSIBILITY OF INION POLYMER MEMBRANE USING IN METAL-ION BATTERIES

¹Lyubov Shmygleva, ¹Ruslan Kayumov, ^{1,2}Anna Lochina, ¹Alexander Lapshin

¹Federal Research Center of Problems of Chemical Physics and Medicinal Chemistry, Russian Academy of Sciences, Chernogolovka, Russia; *E-mail: shmygleval@icp.ac.ru*

²Moscow Institute of Physics and Technology, Dolgoprudny, Russia

Introduction

The rapidly developing field of portable energy sources requires the search and development of effective materials for such devices. To improve the safety of the most common metal-ion batteries (MIA) (lithium- and sodium-ion), instead of a liquid electrolyte, it is proposed to use a polymer electrolyte with unipolar conductivity based on a Nafion-like electrolyte (Inion), plasticized with aprotic solvents.

In addition to the main advantages (wide window of electrochemical stability, high thermal and chemical stability, high unipolar ionic conductivity over a wide temperature range), the acidic form of the membranes with Nafion structure is easily converted into any cationic form [1, 2]. However, to achieve sufficient values of ionic conductivity, any cationic form of such a polymer must be swollen with a solvent (for usage in hydrogen-air fuel cells, the acidic form is saturated with water, and for MIA it is plasticized with aprotic solvents). By selecting the optimal aprotic solvent among carbonates, amide solvents, dimethyl sulfoxide, sulfolane, ethers, etc., or the composition of their mixture, one can achieve an expansion of the operating temperature range and window of electrochemical stability, an increase in specific ionic conductivity, as well as fire and explosion safety [2]. Plasticizers from the carbonate class, in particular cyclic ethylene carbonate (EC) and propylene carbonate (PC), are most often used for electrolyte materials MIA [3], including polymer Nafion-like ones [4, 5].

Therefore, the aim of this work was to study the effect of plasticization of the Inion membrane in lithium and sodium forms with cyclic carbonates on thermal stability, molecular and supramolecular packing, as well as ionic conductivity.

Experiments

Inion polymer membrane (InEnergy Group, Russia; Figure 1) in the acidic form with a thickness of 15 μm was purified and converted into Li^+ and Na^+ forms according to a standard method for Nafion membranes [6, 7]. To remove water, the membrane was first dried at 130 $^{\circ}\text{C}$ in a vacuum oven for 3 hours. All further manipulations with the membranes were carried out in a glove box. To obtain plasticized samples, Inion in the salt form were kept for 2 days at room temperature in anhydrous EC and PC in the presence of activated molecular sieves. The thermal stability, molecular and supramolecular packing, as well as ionic conductivity of the plasticized Inion membranes in lithium and sodium forms were studied by the methods of simultaneous thermal analysis, IR spectroscopy, small-angle X-ray scattering and impedance spectroscopy.



Figure 1. Photo of the initial Inion membrane.

Results and Discussion

The usage of EC as a plasticizer led to the fact that Inion membranes, due to an extremely high degree of saturation, ceased to be solid polymers (turned into a gel-like state), which made their further studies impossible. The swelling degree for the Inion membranes is significantly larger (4–5 times) than for Nafion. For all studied systems, the stage of thermal decomposition of the polymer matrix is observed above 450 °C. According to IR spectroscopy data, the molecular structure of Inion also completely coincides with the structure of Nafion. While differences are observed in the supramolecular packing: smaller interplanar distances for hydrophilic and hydrophobic domains of the Inion polymer matrix, especially pronounced for its lithium form. This difference appears to result in an abnormally high swelling degree of the lithium form of Inion and an abnormal swelling of the sodium form in cyclic carbonates. Despite the fact that the ionic conductivity of the Na-form of Inion, plasticized with PC, studied in this work is inferior in conductivity to Nafion, the membrane showed its promise for use in MIA after refinement of the methodology for obtaining the polymer matrix itself, as well as selection of the optimal plasticizer based on double or triple mixtures of aprotic solvents, including the usage of cyclic carbonates.

Acknowledgments. This work was performed in accordance with the state task, state registration No. 124013000692-4 and 122112100037-4.

References

1. Voropaeva D.Y., Novikova S.A., Yaroslavtsev A.B. Polymer electrolytes for metal-ion batteries // Russ. Chem. Rev. 2020. V. 89. P. 1132.
2. Bushkova O. V., Sanginov E.A., Chernyuk S.D., Kayumov R.R. Polymer electrolytes based on the lithium form of Nafion sulfonic cation-exchange membranes : current state of research and prospects for use in chemical power sources // Membr. Membr. Technol. 2022. V. 4. P. 433–454.
3. Noerochim L., Prabowo R.S., Widyastuti W., Susanti D., Subhan A., Idris N.H. Enhanced high-rate capability of iodide-doped $\text{Li}_4\text{Ti}_5\text{O}_{12}$ as an anode for lithium-ion batteries // Batteries. 2023. V. 9. P. 38.
4. Simari C., Tuccillo M., Brutti S., Nicotera I. Sodiated Nafion membranes for sodium metal aprotic batteries // Electrochim. Acta. 2022. V. 410. P. 139936.
5. Voropaeva D., Novikova S., Stenina I., Yaroslavtsev A. Nafion-212 membrane solvated by ethylene and propylene carbonates as electrolyte for lithium metal batteries // Polymers. 2023. V. 15. P. 4340.
6. Kayumov R.R., Radaeva A.P., Nechaev G. V., Lochina A.A., Lapshin A.N., Bakirov A. V., Glukhov A.A., Shmygleva L. V. Polymer electrolyte based on Nafion plasticized with carbonates and their ternary mixtures for sodium-ion batteries // Solid State Ionics. 2023. V. 399. P. 116294.
7. Krupina A.A., Kayumov R.R., Nechaev G. V., Lapshin A.N., Shmygleva L. V. Polymer electrolytes based on Na-Nafion plasticized by binary mixture of ethylene carbonate and sulfolane // Membranes. 2022. V. 12. P. 840.

DIFFUSION CHARACTERISTICS OF ION-EXCHANGE MEMBRANES IN ORGANIC ACIDS SALTS SOLUTIONS

Vladislava Shramenko, Tatyana Karpenko, Nikolay Sheldeshov

Kuban State University, Krasnodar, Russia, E-mail: vladislava.19991211@gmail.com

Introduction

Currently, bipolar electro dialysis has become widespread in order to produce acids and bases from the corresponding salts. It is becoming increasingly important to study the separation processes of complex fermentation broths in order to produce high purity individual organic acids [1]. It is necessary to study the characteristics of ion exchange membranes that are part of an electro dialysis stack to understand the processes occurring in an electro dialyzer.

One of the side processes that reduce the selectivity of ion-exchange membranes is the diffusion of electrolytes through them. This, in turn, negatively affects the efficiency of electro dialysis processes. The purpose of this work is to study the diffusion transport of organic acids salts through ion-exchange membranes.

Experiments

Heterogeneous Ralex AMH (Mega, Czech Republic) and homogeneous Lancytom® AHT (LANRAN, China) membranes were used as the anion exchange membranes under study. Neutral sodium salts of organic acids were selected as electrolytes: sodium acetate, sodium malonate, sodium citrate.

The simplest and most accessible method for studying diffusion permeability is the diffusion of electrolyte through an ion-exchange membrane into deionized water in a non-flowing two-chamber cell (Fig. 1).

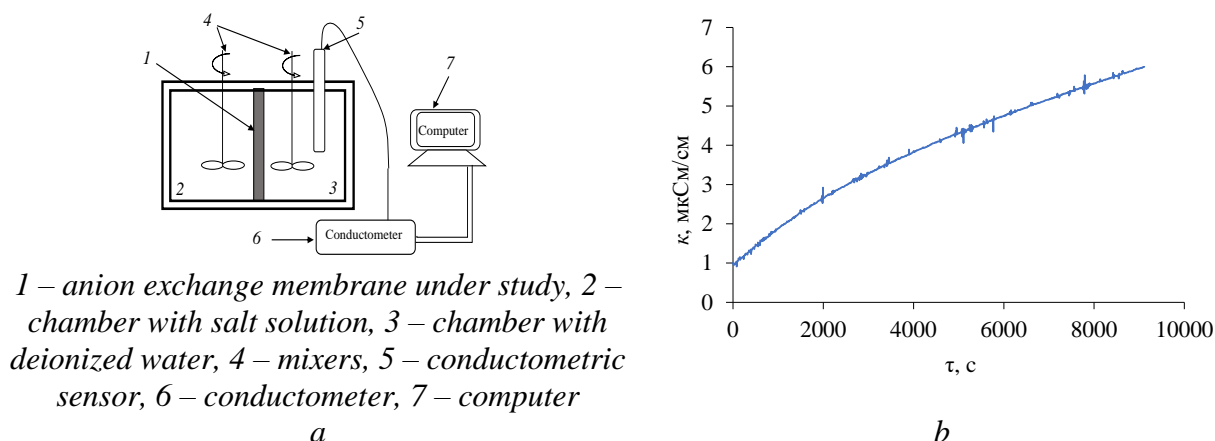


Figure 1. The scheme of a cell for measuring the membrane diffusion permeability (a) and typical dependence of the electrical conductivity of electrolyte on time.

According to the measured dependences of the electrical conductivity of solutions in chamber 3 (Fig. 1) on time, the characteristics of the diffusion transport of salts through membranes were calculated [2]: the diffusion flux of salt, its integral permeability coefficient, parameter β , differential permeability coefficient (equations (1)-(4), respectively):

$$j_m = \frac{V}{S} \frac{dc}{d\tau} \quad (1) \quad P_m = \frac{j_m d}{c} \quad (2) \quad \beta = \frac{dlgj}{dlgc} \quad (3) \quad P_m^* = \beta P_m \quad (4)$$

Results and Discussion

It is shown that the diffusion permeability of the heterogeneous anion exchange membrane Ralex AMH-PES (Fig. 2) by salts more than the homogeneous anion exchange membrane AHT (Fig. 3). When the Ralex AMH membrane swells, the rigid polyester reinforcement prevents the elongation of the membrane, which leads to an increase in its thickness. This, in turn, causes

deformation, leads to an increase in the fraction of macropores in the membrane and an increase in the diffusion permeability coefficient of the membrane.

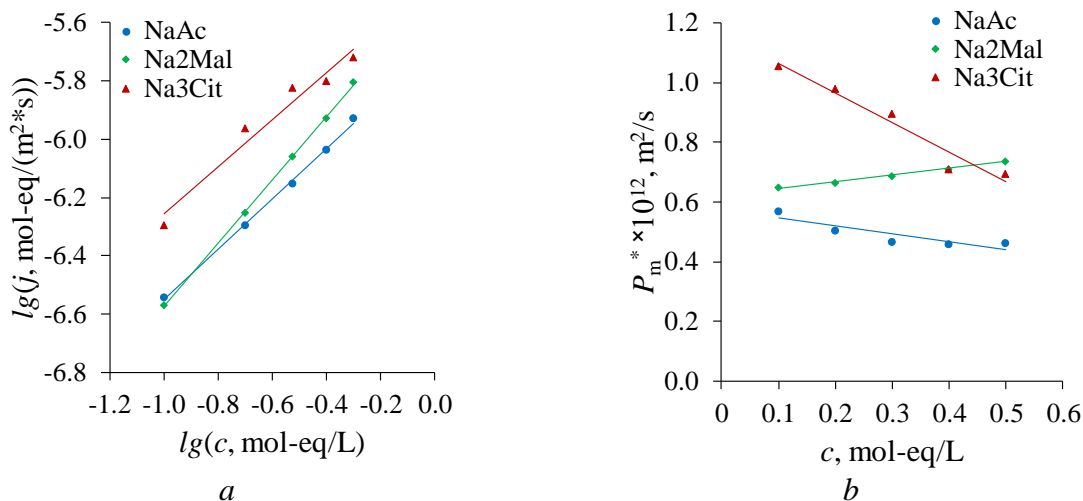


Figure 2. Concentration dependences of the fluxes (a) and the differential coefficients of diffusion permeability (b) of organic acids salts through the anion exchange membrane AHT.

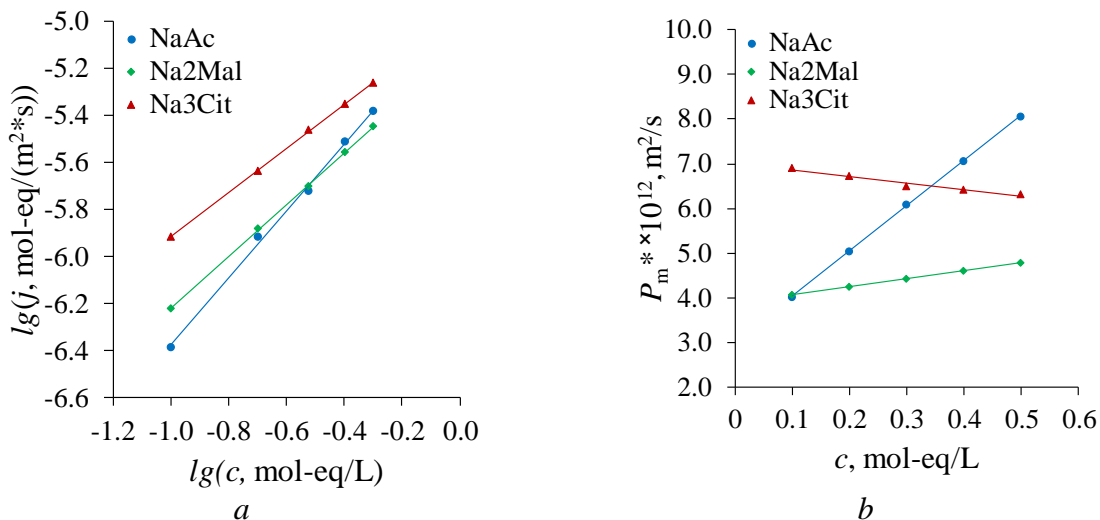


Figure 3. Concentration dependences of the fluxes in bilogarithmic coordinates (a) and the differential coefficients of diffusion permeability (b) of organic acids salts through the anion exchange membrane Ralex AMH-PES.

The differential coefficients of the diffusion permeability of sodium citrate increase with a decrease in its concentration both through homogeneous (Fig. 2b) and through heterogeneous (Fig. 3b) membrane. This is due to the appearance of sodium hydroxide in the membrane system, formed as a result of hydrolysis of citrate anions, whose diffusion permeability coefficient is higher.

As in the case of diffusion transport of organic acid salts through a heterogeneous Ralex CMH cation exchange membrane (Fig. 4), as in the case of amine salts through the heterogeneous anion exchange membrane Ralex AMH (Fig. 5), diffusion occurs mainly through the membrane pores. This is due to the fact that anions of organic acids, being co-ions in the cation exchange membrane, are excluded by the Donnan effect, the stronger than greater the electric charge, and their concentration in the membrane pores is significantly higher than in the gel phase of the cation exchanger.

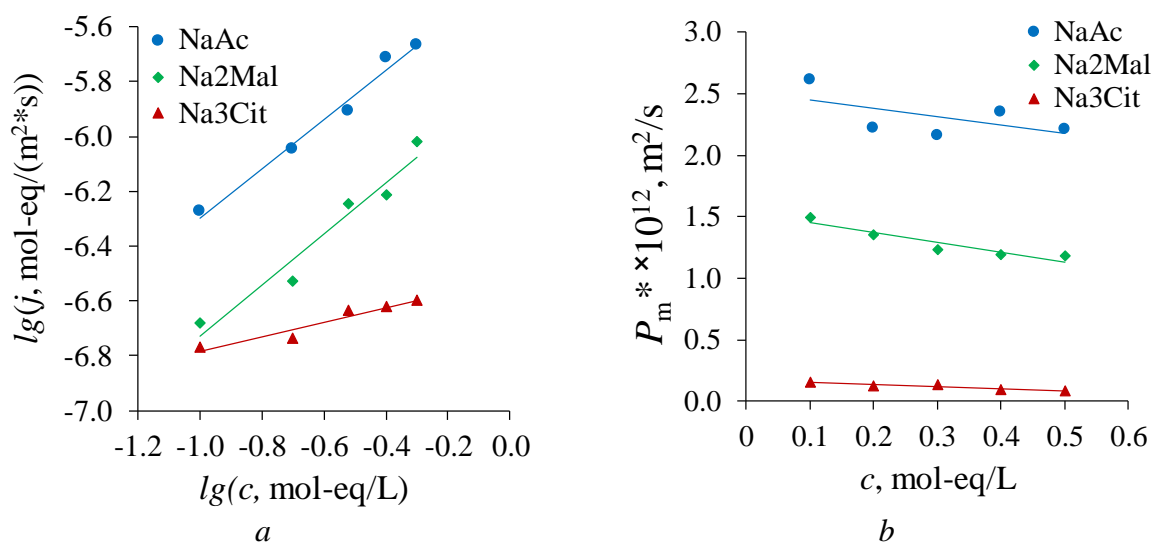


Figure 4. Concentration dependences of the fluxes in bilogarithmic coordinates (a) and the differential coefficient of diffusion permeability (b) of organic acids salts through the cation exchange membrane Ralex CMH-PES.

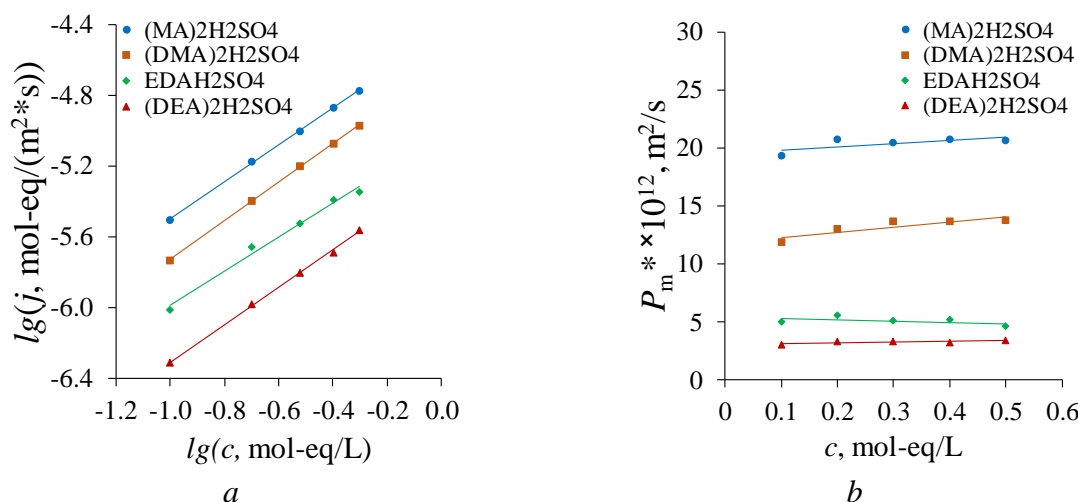


Figure 5. Concentration dependences of the fluxes in bilogarithmic coordinates (a) and the differential coefficient of diffusion permeability (b) of amine salts through the anion exchange membrane Ralex AMH-PES.

The coefficients of diffusion permeability of amine salts through a heterogeneous anion exchange membrane Ralex AMH (Fig. 5) unlike the coefficients of diffusion permeability of organic acid salts through a heterogeneous cation exchange membrane Ralex CMH (Fig. 4) do not increase with decreasing concentration of amine salts, since the dissociation constants of amine cations are orders smaller than the constants of hydrolysis of organic acid anions.

Acknowledgement. This research was financially supported by the RSF according to the research project № 23-23-00660, <https://rscf.ru/en/project/23-23-00660/>.

References

1. Melnikov, S.S., Nosova E.N., Melnikova E.D., Zabolotsky V.I. Reactive separation of inorganic and organic ions in electrodialysis with bilayer membranes // Sep. Purif. Technol. – 2021. – V. 268. – 118561.
2. Berezina N.P., Kononenko N.A., Dyomina O.A., Gnusin N.P. Characterization of ion-exchange membrane materials: Properties vs structure. // Adv. Colloid Interface Sci. 2008. V. 139. P. 3-28.

HOLLOW FIBER MEMBRANES BASED ON NIOBIUM DOPED LSF FOR OXYGEN SEPARATION

Elena Shubnikova, Olga Cherendina, Maria Khohlova, Olga Bragina, Alexander Nemudry

Institute of Solid State Chemistry and Mechanochemistry, Kutateladze, 18, Novosibirsk, Russia
E-mail: shubnikova@solid.nsc.ru

Introduction

Non-stoichiometric oxides based on ferrite lanthanum strontium are promising materials for oxygen transport membranes in catalytic membrane reactors [1]. This group of compounds has a good phase and structural stability in reducing atmospheres, compared to Co-containing oxides. However, lower values of oxygen fluxes for membranes are observed. Formation of the compositional, charge disorder by partial substitution of Fe by ferroactive highly charged cations (Mo, W, Nb, Mo) leads to nanostructuring and high transport characteristics of such compounds.

In this work, the structure and oxygen permeability of $\text{La}_{0.4}\text{Sr}_{0.6}\text{Fe}_{0.95}\text{Nb}_{0.05}\text{O}_{3-\delta}$ (LSFNb5) hollow fiber membranes were studied.

Experiments

LSFNb5 sample was prepared by the ceramic method and validated X-ray diffraction techniques. The LSFNb5 hollow fiber membranes were fabricated via phase inversion and sintering technique. The oxygen permeability measurements were carried out in a self-made high-temperature test equipment connected to the quadrupole mass spectrometer QMS 200. The outer surface of the membrane was fed with a mixture of N_2/O_2 or N_2/CO_2 in various ratios at a constant flow rate of 150 mL/min. The inner side of the HF membrane was fed with Ar at flow rate of 50 mL/min. The feed and sweep flow rates were generated by the UFGS-4 gas mixing unit (SoLO).

Results and Discussion

The evolution of the structure of LSFNb5 material at elevated temperatures and different oxygen partial pressures was studied by the in situ XRD experiments. It was demonstrated LSFNb5 oxide is stable in air and vacuum ($p_{\text{O}_2} \sim 10^{-4}$ atm) at 30-900 °C. The poroelastic/ferroelastic transitions occurred at 400 °C in air and vacuum ($p_{\text{O}_2} \sim 10^{-4}$ atm).

Oxygen permeation fluxes through LSFNb5 hollow fiber membranes were studied as a function of oxygen partial pressure at different temperatures. The values of apparent activation energy for studied membranes were determined. The results obtained indicated that the oxygen permeation process is controlled by the surface exchange reactions.

LSFNb5 hollow fiber also demonstrate high stability of oxygen fluxes in long-term oxygen permeation test.

Acknowledgement. The work was supported within the framework of the state task of the youth laboratory "Materials and Technologies of Hydrogen Energy".

References

1. Sunarso J. et al. Mixed ionic-electronic conducting (MIEC) ceramic-based membranes for oxygen separation //J. Membr. Sci. 320 (2008) 13 – 41. <https://doi.org/10.1016/j.memsci.2008.03.074>.

TRANSPORT PHENOMENA AT HETEROGENOUS ION-EXCHANGE MEMBRANES

^{1,2}Zdenek Slouka, ¹Jakub Strnad, ¹Václav Lázníčka

¹University of Chemistry and Technology in Prague, Prague, Czech Republic

E-mail: sloukaz@vscht.cz

²University of West Bohemia, New Technologies - Research Centre, Pilsen

Introduction

Ion-exchange membranes are indispensable in electromembrane separation processes, such as electrodialysis. Intensifying those processes by increasing the applied electric current is alluring yet challenging to adapt to an industrial operation. One problem is excessive Joule heat evolution, potentially leading to the burning of the whole desalination unit. Another problem is associated with overlimiting phenomena occurring at ion-exchange membranes under high current densities. These phenomena possess both positive and negative effects on desalination. While current-induced convection contributes to ion transfer by mixing ion-depleted layers with bulk, a water-splitting reaction generates hydroxide and hydronium ions, changing the local pH.

Experiments

To shed light on the intensity of various overlimiting mechanisms, we developed special cells to study current-induced processes at ion-exchange membranes. These cells, both in batch and flow-through formats, allow simultaneous process characterization by electrochemical measurements and direct optical observation using particle image velocimetry (PIV). At the same time, the cells allow measuring pH changes associated with water splitting.

Results and Discussion

Our results show that two types of convection (besides pressure-driven flow) occur in the studied systems: electroconvection and natural convection. While the first occurs due to a strong electric field acting on a nonequilibrium charge, natural convection is driven by the density gradient developing in the system owing to desalination. We describe electroconvection and natural convection qualitatively and in terms of characteristic velocities, providing insight into their potential impact on ion transfer. Interestingly, although anion-exchange (AEM) and cation-exchange (CEM) membranes are considered symmetrical in their behavior in DC electric field, they are markedly different [1]. While AEMs split water and invoke rather medium electroconvection, CEMs show no susceptibility to water splitting but develop very strong electroconvection on their surface. However, water splitting at CEM is observed upon adsorption of polylysine to its surface [4]. The polarization at both membranes is directly related to the onset of strong natural convection, dominating the flow field near the membranes. The dominant role of natural convection has been observed in simple electrodialysis systems, where it dictated the distribution of concentrations [2]. The analysis of the proceeding phenomena in a single diluate channel showed that (i) overlimiting phenomena occur upon setting conditions corresponding to the complete desalination, (ii) natural convection is an underlimiting phenomenon assisting in mixing diluate in channels without spacers, and (iii) electroconvection manifests itself as intensive chaotic waves originating at CEM [3].

Acknowledgement. The authors acknowledge the financial support from the Czech Science Foundation (grant number 20-21263S)

References

- [1] Strnad J. et al. Desalination 2024, 571, 117093.
- [2] Kovář, P. et al. Desalination 2023, 548, 116302.
- [3] Strnad J. et al Desalination 2024, 580, 117538
- [4] Strnad J. et al., Desalination 2024, , 117586

PULSE ALTERNATING CURRENT ELECTROSYNTHESIS AS AN EFFECTIVE WAY TO MULTIFUNCTIONAL MATERIALS FOR HYDROGEN ENERGY

Nina Smirnova, Tatyana Molodtsova, Anna Ulyankina, Daria Chernysheva

Platov South-Russian State Polytechnic University (NPI), Novocherkassk, Russia

E-mail: smirnova_nv@mail.ru

Introduction

Transition metal oxides (TMOs) have been widely investigated for recent decades due to their huge potential in magnetic, electronic, optical as well as energy conversion and storage applications including supercapacitors (SCs), lithium-ion batteries (LIBs), electrocatalysts, which can effectively combat the existing energy and environment crisis. However, precise synthesis of photo- and electroactive TMOs – based nanostructures is one of the key challenges that hinder the practical application of many important hydrogen energy-related electrocatalytic reactions. Therefore, the multitude of studies focusing on the catalyst fabrication make the immense effort for the rational synthesis of active and stable catalysts. Compared with conventional chemical synthesis routes, electrochemical synthesis has been considered as a sustainable and economically attractive method to produce highly efficient catalysts. Furthermore, electrochemical methods can be used to synthesize TMOs-based composite structures with carbon support, which are not easily accessible, via embedding carbon additives.

Our research group is dedicated to advancing the field of electrochemistry by developing innovative techniques for synthesizing TMOs – based nanostructures using pulse alternating current (PAC) electrochemical method. Additionally, we are interested in studying the relationship between the structural properties of these materials and their photo- and electrocatalytic performance.

Experiments

High purity metal plates (Zn, Ti, Cu, Fe, Co, Ni, W or In) used as electrodes were firstly polished using sandpaper and then washed with distilled water. The electrodes were immersed in the aqueous solutions of salts, acids or alkaline used as the electrolytes and connected to a home-designed pulse alternating current source. Other synthesis conditions as well as the resulting products and their applications are presented in detail in Table 1.

Results and Discussion

The energy conversion efficiency of photocatalysis is greatly influenced by light absorption, separation and transport of the charge carrier, the number of surface-active sites, and band structures. TMOs have important applications in photocatalysis, primarily because they can act both as active phases (i.e., bulk or self-supported catalyst) and as supports. Considering the unique properties of electrochemically synthesized materials mentioned above, Zn-, Ti-, W-, and In-containing oxide materials are viewed as promising photocatalysts with good performances. In this section, the recent progress of oxide materials obtained by the PAC electrocatalysis in some important applications of photocatalysis, including photocatalytic degradation of pollutants and oxidation of biomass as well as photoelectrochemical use is reviewed.

TiO₂ and ZnO are among the most often used photoactive materials in heterogeneous catalysis, owing to their reasonably high surface area, higher electron mobility, accelerated electron transfer and higher quantum efficiency. Electrochemical synthesis using PAC has been shown to provide easy access to the nanoparticulate form of these phases [1,2,4]. These oxide nanostructures provide a large surface area with full contact between catalysts and organic molecules and thus inspires the study of its environmental applications. Moreover, electrochemically synthesized TiO₂ nanoparticles were used in the oxidation of HMF as a photocatalyst to produce valuable DFF [5].

Apart from the photodegradation of pollutants in water, metal oxide can also be used in PEC applications. For example, WO₃ and In₂O₃ nanostructures were prepared using PAC electrocatalysis and characterized by high photoelectrochemical performances caused by the optimal morphological, electronic, and charge-transfer properties [3,13].

Table 1: PAC electrosynthesis conditions and the resulting synthesis products

Metal	Synthesis conditions			Product(s)
	$ja:jk$ ($A \cdot cm^{-2}$)	Electrolyte	Others	
Zn	2.4:1.2	2M NaCl, 2M KCl, 2M LiCl and 1M Na ₂ SO ₄	stirring and cooling	ZnO
In	2.5:2.5		stirring and cooling; annealing in air for 1h at 400 °C	c- and c/rh-In ₂ O ₃
Ti	0.2:1	2M NaCl	stirring and cooling; annealing in air for 3h at 400 - 600°C	TiO ₂
Cu	0.5:0.5		stirring and cooling	CuO or Cu ₂ O-CuO
	1:1			
	1.5:1.5			
Fe	3:3	2M NaOH	stirring and cooling	γ -Fe ₂ O ₃ /Fe ₃ O ₄
	1.2:2.4			γ -Fe ₂ O ₃ / δ -FeOOH
Co	0.5:0.5		-	Co ₃ O ₄ /CoOOH
Ni	0.25:0.5		carbon powder as support material	NiO/C
	0.5:1		multilayer graphene as support material	NiO/MLG
	0.13:0.4	multi-walled carbon nanotube as support material	NiO _x /MWCNTs	
W	3:3	0.5M C ₂ H ₂ O ₄ , 0.5M H ₂ SO ₄ and 0.5M HNO ₃	stirring and cooling; annealing in air for 3h at 500 °C	WO ₃

The electrochemical activity is mainly determined by the number of active sites, the configuration states of the atoms, and the conductivity of the active materials. Excellent electrochemical performances are expected for (oxi)hydr)oxide-based materials due to their unique structural advantages, charge storage capacity with outstanding charge-discharge performance, long cycle life and higher power density. In this section, we mainly focus on the recent progress of oxide materials obtained by the PAC electrosynthesis in the different fields of electrochemistry including supercapacitors, lithium-ion batteries, alcohol electrooxidation reaction (AEOR) applications and non-enzymatic sensors.

Metal oxide nanoparticles are studied for the AEOR due to their fascinating features of high exposed surface area for abundant catalytic active sites and large contact electrolyte area for rapid electron transfer. Recently, we reported the electrochemical synthesis of a Cu₂O-CuO bilayered polyhedra and investigated its electrocatalytic performance in the methanol oxidation reaction [6]. In addition, this approach also was successful in the synthesis of Cu₂O octahedra with suitable specific capacitance for SCs.

Moreover, other TMOs-based nanostructures are obtained using PAC electrosynthesis for energy storage applications. For example, the interaction between NiO_x material and various carbon-based supports (carbon black, multi-walled carbon nanotube or multilayer graphene) improved their electrochemical properties indicating potential applications as high-performance supercapacitor electrode materials [10-12]. In addition to Ni-based oxides, electrochemically prepared Co₃O₄/CoOOH nanocomposite material also demonstrated as a promising candidate for high-performance SCs and LIBs applications [9].

On the other hand, TMOs and their composites have been used as efficient materials for non-enzymatic electrochemical sensing applications. Our group's recent works has demonstrated electrochemically synthesized Fe-based electrocatalysts for use in EC sensors. For instance, the finding γ -Fe₂O₃/ δ -FeOOH and γ -Fe₂O₃/Fe₃O₄ nanocomposites achieved an excellent analytical performance for amperometric determination of acetaminophen and hydrogen peroxide respectively [7,8]. Therefore, electrosynthesis using pulse alternating current holds great promise for the development of the single and mixed-phased oxide catalysts for multifunctional electrochemical applications.

This work provides valuable insights into the electrochemical synthesis of transition metal oxide-based materials and their potential use as highly effective catalysts for photo- and electrocatalytic reactions as well as electrochemical energy storage systems. By using pulse alternating current, it is possible to obtain nanostructures with unique phase composition and

tailored properties, which can be optimized for hydrogen energy-related electrocatalytic reactions. With further research, pulse alternating current electrochemical synthesis may enable the development of new and improved transition metal oxide-based materials with even higher electrochemical activity, making them ideal candidates for use in a wide range of industrial processes.

References

1. Ulyankina A., Leontyev I., Avramenko M., et al. Large-scale synthesis of ZnO nanostructures by pulse electrochemical method and their photocatalytic properties // *Mater Sci Semicond Process*. 2018. V. 76. P. 7–13.
2. Ulyankina A., Molodtsova T., Gorshenkov M., et al. Photocatalytic degradation of ciprofloxacin in water at nano-ZnO prepared by pulse alternating current electrochemical synthesis // *Journal of Water Process Engineering*. 2021. V. 40. P. 101809.
3. Molodtsova T., Gorshenkov M., Kolesnikov E., et al. Fabrication of nano-In₂O₃ phase junction by pulse alternating current synthesis for enhanced photoelectrochemical performance: Unravelling the role of synthetic conditions// *Ceram Int*. 2023. V. 49. P. 10986–10992.
4. Ulyankina A., Avramenko M., Kusnetsov D., et al. Electrochemical Synthesis of TiO₂ under Pulse Alternating Current: Effect of Thermal Treatment on the Photocatalytic Activity// *ChemistrySelect*. 2019. V.4. P. 2001–2007.
5. Ulyankina A., Mitchenko S., Smirnova N. Selective Photocatalytic Oxidation of 5-HMF in Water over Electrochemically Synthesized TiO₂ Nanoparticles// *Processes*. 2020. V. 8. P. 647.
6. Ulyankina A., Leontyev I., Maslova O., et al. Copper oxides for energy storage application: Novel pulse alternating current synthesis// *Mater Sci Semicond Process*. 2018. V. 73. P. 111–116.
7. Molodtsova T., Gorshenkov M., Saliev A., et al. One-step synthesis of γ -Fe₂O₃/Fe₃O₄ nanocomposite for sensitive electrochemical detection of hydrogen peroxide// *Electrochim Acta*, 2021. V. 370. P. 137723.
8. Molodtsova T., Gorshenkov M., Kubrin S., et al. One-step access to bifunctional γ -Fe₂O₃/ δ -FeOOH electrocatalyst for oxygen reduction reaction and acetaminophen sensing // *J Taiwan Inst Chem Eng*. 2022. V.140. P.104569.
9. Chernysheva D., Vlaic C., Leontyev I., et al. Synthesis of Co₃O₄/CoOOH via electrochemical dispersion using a pulse alternating current method for lithium-ion batteries and supercapacitors// *Solid State Sci*. 2018. V. 86. P. 53–59.
10. Leontyeva D. V., Leontyev I.N., Avramenko M. V., et al. Electrochemical dispergation as a simple and effective technique toward preparation of NiO based nanocomposite for supercapacitor application// *Electrochim Acta*. 2013. V. 114. P.356–362.
11. Chernysheva D. V., Leontyev I.N., Avramenko M. V., et al. One step simultaneous electrochemical synthesis of NiO/multilayer graphene nanocomposite as an electrode material for high performance supercapacitors// *Mendeleev Communications*. 2021. V. 31. P. 160–162.
12. Shmatko V., Leontyeva D., Nevzorova N., et al. Interaction between NiO_x and MWCNT in NiO_x/MWCNTs composite: XANES and XPS study// *J Electron Spectros Relat Phenomena*. 2017. V. 220. P. 76–80.
13. Tsarenko A., Gorshenkov M., Yatsenko A., et al. Electrochemical Synthesis-Dependent Photoelectrochemical Properties of Tungsten Oxide Powders// *ChemEngineering*. 2022. P. 6.

ELECTROCHEMICAL CHARACTERISTICS OF ANION-EXCHANGE MEMBRANES IN SOLUTIONS OF TARTARIC AND CITRIC ACID SALTS

Kseniia Solonchenko, Olesya Yurchenko, Natalia Pismenskaya
Kuban State University, Krasnodar, Russia, E-mail: Olesia93rus@mail.ru

Introduction

Nutrient recovery technologies are increasingly being developed as the reuse of nutrients is a promising strategy to reduce the depletion of non-renewable resources and their environmental impact [1]. Such substances include ampholytes: dihydrophosphate, hydrotartrate, sodium dihydrocitrate. Many developed countries require a significant reduction in the concentration of these substances in wastewater and released into the environment. Citric acid, tartaric acid, which is used in large quantities in the chemical and food industries. When extracting acids, it is necessary to avoid conventional methods that produce solid residues afterwards. Therefore, electro dialysis is an environmentally friendly technology and is actively used [2,3]. The aim of this work is to study the changes in electrochemical characteristics of anion-exchange membranes (AEM) in citric acid and tartaric acid solutions that engage in protonation deprotonation reactions.

Experiments

Homogeneous anion-exchange membrane AMX (Astom, Japan), which contains quaternary ammonium groups and a small amount of secondary and tertiary amines as fixed groups, was used in the experiments. Sodium dihydrocitrate (pH=4.1) and sodium tartrate (pH=3.8) were used as the test solutions, which engage in protonation deprotonation reactions with water. Electrochemical characterizations were obtained using a four-chamber flow-through electro dialysis cell.

Results and Discussion

The current-voltage characteristics (CVCs) of the AMX membrane obtained in 0.02 M solutions of the investigated electrolytes are shown in Figure 1.

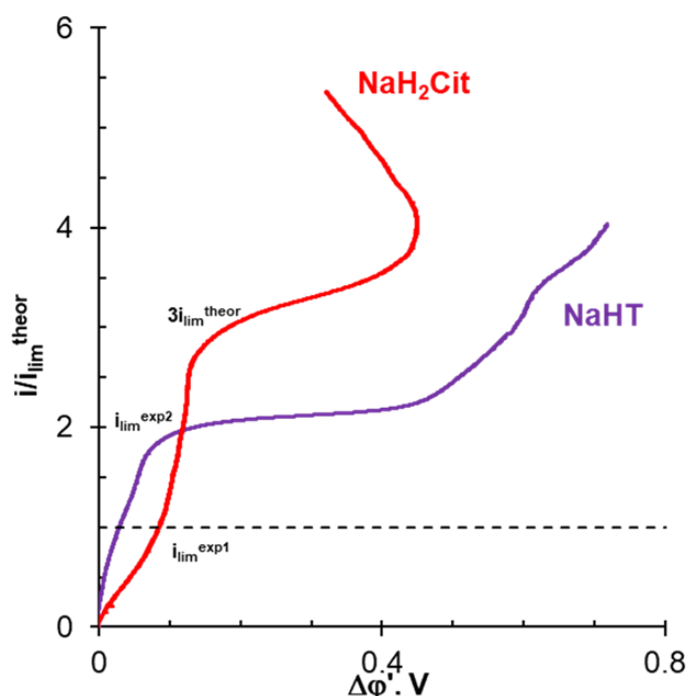


Figure 1. Current-Voltage Characteristics of the AMX Membrane Obtained in 0.02 M Solutions of the Electrolytes under Study.

The CVCs in these investigated solutions differ in their shape, which are obtained in solutions of strong electrolytes. According to these ideas, the first limiting current, i_{lim}^{exp1} , which is recorded on CVC, has the nature similar to membrane system with strong electrolyte, NaCl. It is caused by

the reduction to minimum values of the electrolyte concentration in the depleted solution near the membrane surface, as well as by the achievement of the maximum diffusion flux of weak acid anions. The more protons are released into the depleted solution, the more blurred is the sloping plateau of CVC that corresponds to this current (Figure 1). A further increase in current takes place due to the conversion of single-charged acid anions into doubly charged ones, as well as the transfer of electric charge at the AEM/depleted solution interface by protons coming from the membrane. A second limiting current, i_{lim}^{exp2} , with a well identifiable sloping plateau is recorded in the cases of NaHT. It corresponds to the state in which the AEM is almost completely saturated with doubly charged anions. In the case of the membrane system with NaH_2Cit , the reason for the higher resistance (more significant jumps of the reduced potential) compared to other studied systems at $i < i_{lim}^{theor}$, is apparently a more intensive accumulation of the molecular form of citric acid in diffuse double layer due to the reaction: $H_2Cit^- + H^+ \rightarrow H_3Cit$. This accumulation is caused by the simultaneous presence of both single- and double-charged anions in the membrane. Therefore, in the case of NaH_2Cit solution, a sloping plateau on the CVC is observed only in the vicinity of $3i_{lim}^{theor}$, when the maximum flux of H^+ ions generated due to the reaction $HCit^{2-} \rightarrow Cit^{3-} + H^+$ appears to be reached.

Obtaining these data will make it possible to study the behavior of AEM in the studied electrolytes under conditions of electric current flow and to clarify the mechanisms of mass transfer of various forms of citric and tartaric acid.

Acknowledgement. The research was supported by the grant of the Russian Science Foundation and the Kuban Science Foundation № 24-29-20097.

References

1. Robles Á. New frontiers from removal to recycling of nitrogen and phosphorus from wastewater in the circular economy // *Bioresource technology*. 2020. V. 300. - Art. 122673.
2. Novalic S., Jagschits F., Okwor J., Kulbe K. D. Behaviour of citric acid during electrodialysis // *Journal of membrane science*. 1995. V. 108(3). P. 201-205.
3. Chandra A., Tadimetri J. G. D., Chattopadhyay S. Transport hindrances with electrodialytic recovery of citric acid from solution of strong electrolytes // *Chinese journal of chemical engineering*. 2018. V. 26(2). P. 278-292.

NOVEL POLY(ESTER-BLOCK-AMIDE) MEMBRANES FOR REMOVING OF HEAVY METAL IONS BY NANOFILTRATION

Anastasia Stepanova, Anna Kuzminova, Mariia Dmitrenko, Roman Dubovenko, Anastasia Penkova

St. Petersburg State University, 7/9 Universitetskaya nab., 199034 St. Petersburg, Russia
E-mail: st113221@student.spbu.ru

Introduction

Nanofiltration is a promising method for the separation of liquids in the bioprocessing, petrochemical and pharmaceutical industries. Nanofiltration is an environmentally-friendly method of separation, for its implementation does not require expensive equipment and high energy consumption. The rapid development of nanofiltration requires the search for novel high-performance membrane materials with desired properties. Currently, the improvement of the transport properties of polymer nanofiltration membranes occurs due to the creation of mixed matrix membranes (MMMs), by modifying the polymer matrix with an inorganic and/or organic filler.

Experiments

In the present work, the novel membranes based on poly(ester-block-amide) (PEBA, Pebax® 2533, Figure 1) were prepared by introducing three zirconium-based metal-organic frameworks (Zr-MOFs) - MIL-140A, MIL-140A-AcOH-EDTA and MIL-140A-AcOH into the PEBA matrix. The specific surface area of Zr-MOFs was equal to 493.4 ± 0.2 m²/g for MIL-140A, 568.0 ± 0.1 m²/g for MIL-140A-AcOH, and 529.3 ± 0.2 m²/g for MIL-140A-AcOH-EDTA. The resulting pore diameter of Zr-MOFs are 3.1, 4.4, and 3.5 Å for MIL-140A, MIL-140A-AcOH, and MIL-140A-AcOH-EDTA, respectively. The characterization of membranes was carried out by Fourier-transform infrared spectroscopy (FTIR), scanning electron microscopy (SEM), atomic force microscopy (AFM), and thermogravimetric analysis (TGA). Transport properties of the developed membranes were investigated in nanofiltration of water with Cu²⁺, Cd²⁺, Pb²⁺ ions.

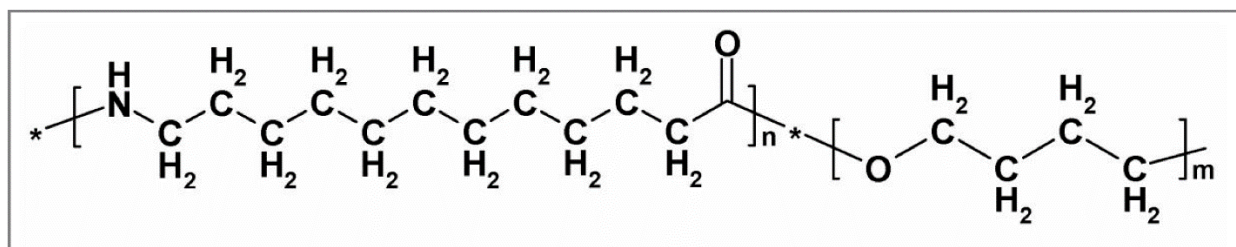


Figure 1. Pebax® 2533 structure

Results and Discussion

The applied Zr-MOFs had different structure and size (Figure 2), and therefore, affected the properties of developed PEBA-based membranes in different ways. The introduction of MIL-140A, MIL-140A-AcOH-EDTA and MIL-140A-AcOH into the PEBA matrix led to changes in the physicochemical, structural and transport properties of membranes due to the porous structure, hydrophilic/hydrophobic properties, excellent chemical and thermal stability of the Zr-MOFs.

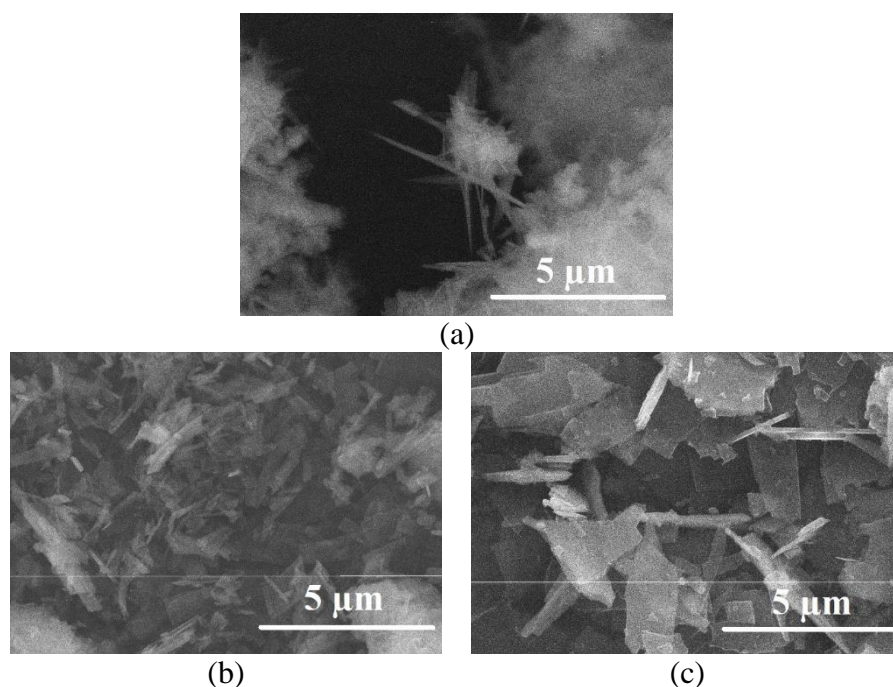


Figure 2. SEM Micrographs of the (a) MIL-140A, (b) MIL-140A-AcOH, and (c) MIL-140A-AcOH-EDTA

Acknowledgements. This research was funded by the Russian Science Foundation, grant №23-29-00473, <https://rscf.ru/project/23-29-00473/>. The experimental work of this study was facilitated by the equipment from the Resource Centre of Geomodel, Chemical Analysis and Materials Research Centre, Centre for X-ray Diffraction Methods, Magnetic Resonance Research Centre, Centre for Innovative Technologies of Composite Nanomaterials, Nanophotonics Centre, Cryogenic department, Computing Centre, Thermogravimetric and Calorimetric Research Centre and the Interdisciplinary Resource Centre for Nanotechnology at the St. Petersburg State University.

HYBRID RECAST MEMBRANES BASED ON AQUIVION® POLYMER AND INORGANIC NANOPARTICLES

^{1,2}Nastasia Stretton, ^{1,2}Ekaterina Safronova, ^{1,2}Andery Yaroslavtsev

¹Kurnakov Institute of General and Inorganic Chemistry, Russian Academy of Sciences, Moscow, Russia, *E-mail: stretton.nastasia@gmail.com*

²HSE University, Moscow, Russia

Introduction

In the 21st century, the issue of finding new environmentally friendly energy sources is quite acute. One of its solutions is the creation of fuel cells (FC). In FC, membranes based on perfluorosulfonic acid polymers of the Aquivion type are mainly used as an electrolyte [1]. Unfortunately, the available membranes do not fully satisfy the requirements for solid polymer electrolytes. The main problem is a decrease in their conductivity at low humidity. A solution to this problem may be to create hybrid materials containing inorganic dopants that help maintain moisture content and increase the proton conductivity of membranes [2]. Of interest is the study of the effect of dopants on the properties of polymers with different side chain lengths. As a result, the aim of this work was to obtain hybrid materials based on perfluorosulfonic acid polymers with a short side chain (Aquivion®), doped with hydrated silica (SiO₂) and titania (TiO₂), as well as an acidic caesium salt of phospho-tungsten heteropolyacid (Cs_xH_{3-x}PW₁₂O₄₀).

Experiments

Hybrid membranes containing 3% by weight of dopants were prepared by casting Aquivion (equivalent weight 790) dispersions in N-methyl pyrrolidone. The water uptake, proton conductivity and the mechanical properties of the obtained membranes were studied.

Results and Discussion

Membrane fouling increased significantly as operating flux increased. Figure 1 suggests that enhanced hydraulic resistance of the fouling layer induced by filtrate flow also contributed to increased fouling observed at high operating flux.

In Table 1 the water uptake of the obtained samples is shown. In contact with water, there is a significant difference in the water uptake of the tested membranes. The incorporation of dopants leads to an increase in the water uptake of the membranes by 4.3-13% by weight in the case of Aquivion-based membranes. The most significant hybrid effect is observed with the introduction of hydrated oxides.

Table 1. Water uptake (W,%) of membranes in contact with water

Membrane	Aquivion	Aquivion + Cs _x H _{3-x} PW ₁₂ O ₄₀	Aquivion + SiO ₂	Aquivion + TiO ₂
W, %	45.4	49.7	58.4	61.3

When dopants are incorporated into the pores of membranes, the proton conductivity of hybrid membranes, at RH = 100%, increases compared to the conductivity of the initial Aquivion membrane. The highest values of proton conductivity are obtained for Aquivion + Cs_xH_{3-x}PW₁₂O₄₀ (Fig. 1). This can be attributed to the increase in the concentration of protons in the membrane, which participate in the ion transport process [3].

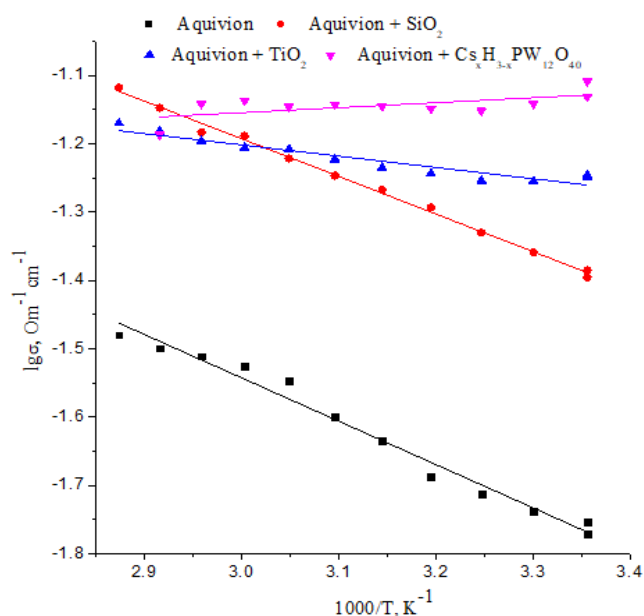


Figure 1. Proton conductivity of studied membranes measured in contact with water

The mechanical properties of the membranes based on Aquivion were also measured (Table 2). As a result of the modification of the membranes with dopants, the Young's Modulus and break strain increases compared to unmodified Aquivion.

Table 2. Mechanical properties of studied membranes at RH=32%

Membrane	Young's Modulus, MPa	Break Strain, %
Aquivion	283±3	18±2
Aquivion + Cs _x H _{3-x} PW ₁₂ O ₄₀	331±4	35±18
Aquivion + TiO ₂	337±28	35±6

In general, it should be noted that modification of Aquivion membranes with nanoparticles of hydrated SiO₂ and TiO₂ and Cs_xH_{3-x}PW₁₂O₄₀ leads to an increase in their proton conductivity at high humidity and increases water uptake.

Acknowledgement. This research was financially supported by a grant from the Russian Science Foundation № 21-73-10149.

References

1. *Filippov S.P., Yaroslavtsev A.B.* Hydrogen energy: development prospects and materials // Russ. Chem. Rev. 2021. V. 90. P. 627 - 643
2. *Wong C.Y., Wong W.Y., Ramya K., Khalid M., Kadhum A.A.H.* Additives in proton exchange membranes for low- and high-temperature fuel cell applications: A review // Int. J. Hydr. Energy. 2019. V.44. P. 6116.
3. *Osipov A. K., Safronova E. Yu., Baranchikov A.E., Yaroslavtsev A. B.* Proton Conductivity of M_xH_{3-x}PX₁₂O₄₀ and M_xH_{4-x}SiX₁₂O₄₀ (M = Rb, Cs; X = W, Mo) Acid Salts of Heteropolyacids // Neorganicheskie Materialy. 2015. V. 51. P. 1249–1254.

ANALYSIS OF PHYSICO-CHEMICAL METHODS USED IN THE DEVELOPMENT OF NOVEL TYPES OF MEMBRANES

Andrey Terentyev, Daria Afanaseva, Kseniia Plinier, Aleksandr Dyachkov

Mendeleev University of Chemical Technology of Russia, Moscow, Russia

E-mail: terentev.a.g@muctr.ru

Introduction

Ion exchange and gas separation membranes are finding wider and wider practical application. A large number of studies have been devoted to the development of new types of membranes, as well as their modification with various additives. However, in order to confirm the obtained structure, control the inclusion of introduced components or various functional groups in the membrane material, as well as to determine the obtained physico-chemical characteristics of samples, the use of various physico-chemical analytical methods (PCAM) is required.

Results and Discussion

Analysis of literature data (covering more than 100 scientific articles by Russian and foreign authors in this field of research) allows us to identify two main areas of application of PCAM: determination of the chemical composition of the obtained membranes (elemental composition, presence of definite chemical bonds and functional groups, etc.), and their physical characteristics and properties (film thickness, pore dimensions, rheological characteristics, etc.). To establish the chemical composition of membranes, the most commonly used are the various types of electron microscopy and X-ray phase (X-ray structural) analysis, covering more than 35% of all studies. Much less commonly used methods are NMR, Raman, UV and IR spectroscopy. The studies of the physical characteristics and properties of the obtained samples are often carried out using thermogravimetric analysis, microscopy, electrochemical methods (conductometry, potentiometry, voltammetry), spanning about 20% of the publications. The results of differential scanning calorimetry, data obtained on tensile testing machines, flotation method, gel chromatography, etc. are also presented.

Based on the results of the literature analysis one can conclude that the arsenal of analytical methods used is quite wide. At the same time, it should be noted that no references to any supporting analytical methods were found in almost 10% of the papers. In our opinion, the specified arsenal of analytical methods can and should be expanded, for example, by wider use of elemental analysis, mass spectrometric methods, in particular MALDI.

LOW-TEMPERATURE ION-PLASMA PRE-TREATMENT OF FIBER SYSTEMS AND ITS EFFECT ON THE STRUCTURE AND PROPERTIES OF MOSAIC COMPOSITE HETEROGENEOUS MEMBRANES POLYKON

^{1,2}Denis Terin, ¹Marina Kardash, ¹Timur Turaev, ¹Ivan Turin, ²Ilya Sinev

¹Yuri Gagarin State Technical University of Saratov, Russia, E-mail: m_kardash@mail.ru

²Saratov State University, Saratov, Russia, E-mail: terinden@mail.ru

Introduction

The need for safe drinking water, purification of wastewater from small molecular contaminants and recovery of valuable products makes membrane separation processes one of the fastest growing technologies.

Today, it is undeniable that the creation of synthetic ion-exchange membrane is possible only at the junction of macromolecular chemistry, quantum chemical calculations, electrochemistry, thermodynamics, ion exchange, colloid chemistry, modern research methods [1].



Figure 1. Trend in investments in membrane technologies (based on analysis of ~1630 patents over the last 20 years) for plasma processing of fibers or the surface of finished membranes.

These membranes are used in many electromembrane technologies: production of deionized water, food conditioning, and fabrication of water circulation systems in the chemical industry.

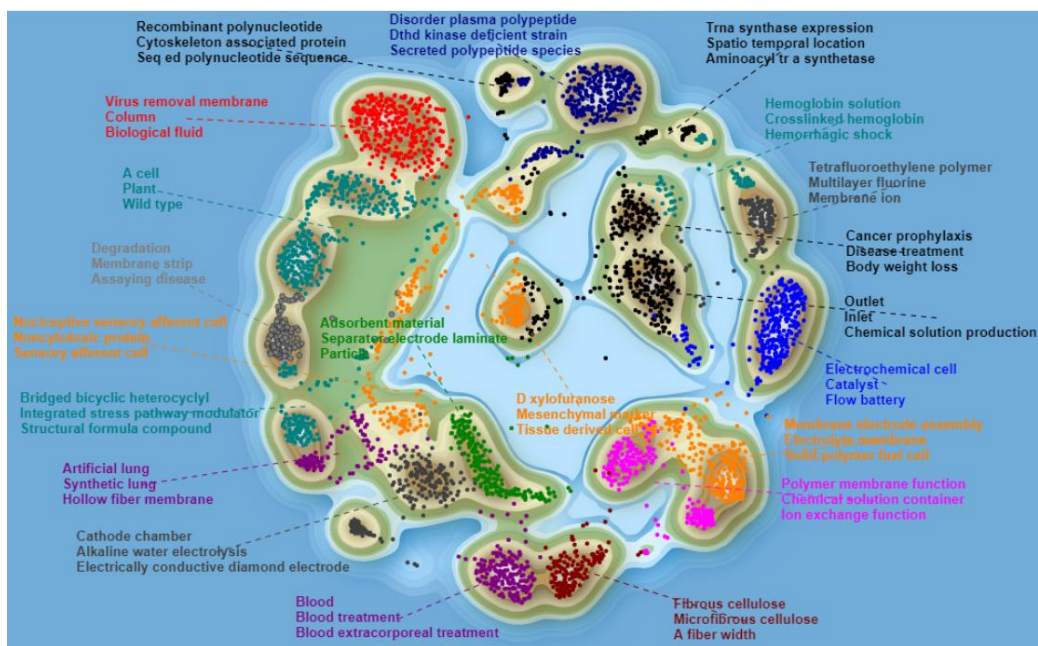


Figure 2. Relationship between fabrication technologies and areas of application of plasma-modified ion exchange materials.

A feature of such membrane systems is the ability to regulate the ratio of the functions of transport of salt ions and the generation of dissociation products by changing the thickness of one of the layers that make up the bipolar membrane (Fig. 1). One of the technologically advanced, environmentally friendly and economical ways to produce membranes is polycondensation filling. By nature, polycondensation filling consists of covalent grafting of hydrophilic anion and cation exchange components onto a matrix-fibrous base in order to expand the range of new types of membrane systems. The developed membrane systems must have a large surface area, mechanical strength, thermal stability and a low coefficient of thermal expansion. The intensive development of membrane science and technology, the continuously expanding scope of membrane applications, as well as the synthesis of new polymer structures give impetus to the development of various methods of physicochemical modification. One of the approaches to significantly improve the parameters of membranes is processes based on the treatment of membrane components with low-temperature plasma [2-3] (Fig. 2). In this work, we investigated the stages of pre-treatment of fabric made from novolac phenol-formaldehyde fibers, one of the stages is its processing in low-temperature plasma, and we also studied the effect of the post-relaxation period on the structure and properties of fabricated membranes.

Experiments

Experimental samples of heterogeneous cation-exchange materials were obtained by polycondensation filling of a fibrous system (Kynol fabric). The samples contain a cation-exchange matrix formed in the volume and surface of the fibrous system. Our cation-exchange matrix has the character of a strongly acidic cation exchanger with the $-\text{SO}_3\text{H}$ group. We have carried out a preliminary basic modification of the fibrous system under low-temperature ion-plasma conditions. The treatment was carried out with low-temperature high-frequency argon plasma at a power of 400 W for 10 minutes at a pressure of $3.7 \cdot 10^{-5}$ Torr (MTI VTC-600-PVD, South Korea). At the stage of membrane fabrication, oxidized spherical (~ 30 nm) silicon nanoparticles (no more than 1.5 wt.%) (specific surface area $112.7 \text{ m}^2/\text{g}$) were added to the monomerization composition. The transmission IR spectra of the studied fibre systems before and after plasma treatment and of heterogeneous cation exchange materials Polykon were recorded on a FTIR-840051 high-speed Fourier spectrophotometer (Shimadzu).

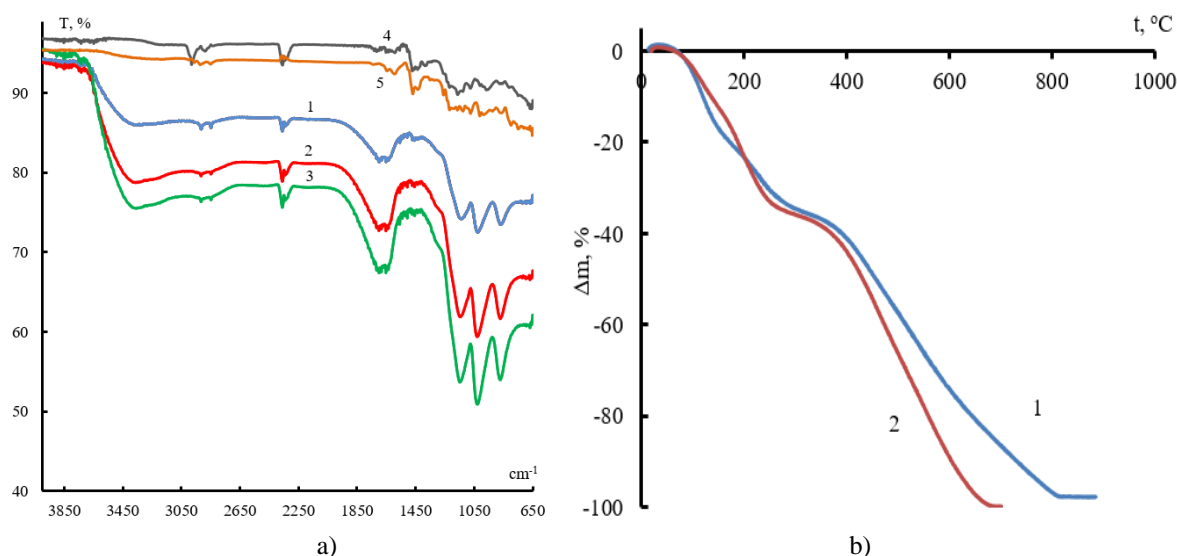


Figure 3. a) IR spectroscopy of “Polykon K+Si” samples: 1- without plasma treatment of the fiber; treated fiber in plasma at relaxation time, h: 2 – 2; 3 – 24; 4 and 5, untreated and plasma-treated (relaxation time 24 hours) fabric made of novolac phenol-formaldehyde fiber.

b). The results of a thermogravimetric study of the Polykon cation-exchange material obtained on a plasma-treated fiber system after treatment for 2 (1) and 24 (2) hours with the addition of 1.5 mass% silicon nanoparticles.

The heterogeneous cation exchange materials Polykon obtained on fiber systems (plasma treated and untreated) were studied by thermogravimetry on a Q-1500D MOM derivatograph (Hungary). The fabrication processes of developed membranes were studied using the differential scanning calorimetry method (Table 1).

Table 1. Differential scanning calorimetry of Polykon K samples on fabric made of novolac phenol-formaldehyde fiber without and treated in plasma at different relaxation times with the addition of nanodispersed silicon particles

additives	Relaxation time after plasma treatment of fiber, hour	Region of intense heat release $\frac{T_{start}-T_{end}}{T_{max}}, ^\circ C$	Heat effect $\Delta H, J/g$
without silicon nanoparticles	1	$\frac{70-110}{91}$	49,63
	2	$\frac{71-110}{90}$	47,82
	24	$\frac{72-108}{89}$	46,96
with silicon nanoparticles	1	$\frac{74-110}{93}$	83,16
	2	$\frac{69-110}{91}$	78,11
	24	$\frac{73-103}{91}$	80,10

Data from differential scanning calorimetry indicate that membranes with silicon nanoadditives have a more pronounced thermal effect, and the effect of the post-relaxation period is leveled out. The return of low-temperature plasma to the fibrous system from which the membranes were obtained allows for an improvement in physical and mechanical characteristics of at least 40-60%. At the same time, the post-relaxation period does not reduce the positive dynamics of the influence of plasma, which is especially valuable for future technology.

Conclusion

Data from differential scanning calorimetry indicate that membranes with silicon nanoadditives have a more pronounced thermal effect, and the effect of the post-relaxation period is leveled out. Low-temperature plasma treatment of the fibrous system from which the membranes are obtained allows for an improvement in physical and mechanical characteristics of at least 40-60%. At the same time, the post-relaxation period does not reduce the positive dynamics of the influence of plasma, which is especially valuable for future technology.

Acknowledgements. This work has been supported by the grants the Russian Science Foundation, RSF (project No. 23-29-00346).

References

1. Terin, D.; Kardash, M.; Ainetdinov, D.; Turaev, T.; Sinev, I. Anion-Exchange Membrane “Polikon A” Based on Polyester Fiber Fabric (Functionalized by Low-Temperature High-Frequency Plasma) with Oxidized Metal Nanoparticles. *Membranes* 2023, 13, 742. <https://doi.org/10.3390/membranes13080742>
2. Terin, D.V., Kardash, M.M., Turaev, T.A. et al. Low-Temperature Ion-Plasma Pretreatment of Fibrous Systems during Preparation of Composite Heterogeneous Membranes. *Membr. Membr. Technol.* 5, 257–265 (2023). <https://doi.org/10.1134/S2517751623040066>
3. Terin D, Kardash M, et al. Features of Thermomechanical Stability of Anionic–Cation Exchange Matrix “Polikon AC” on Viscose Non-Woven Materials. *Membranes*. 2021; 11(10):734. <https://doi.org/10.3390/membranes11100734>

POROUS STRUCTURE OF ANION EXCHANGE FIBROUS POLYKON MEMBRANES ON LAVSANE TEXTILE BASE

¹Ekaterina Tikhonova, ¹Natalia Kononenko, ¹Svetlana Shkirsraya, ²Ilya Strilets, ²Marina Kardash

¹Kuban State University, Krasnodar, Russia, E-mail: kononenk@chem.kubsu.ru

²Yuri Gagarin State Technical University of Saratov, Saratov, Russia

Introduction

Composite membranes Polykon are promising generation of polymer ion-exchange materials. They are produced by the polycondensation filling, when the synthesis of the ion exchange matrix occurs on the surface and in the structure of the fibrous base. The combination of various types of fibrous fillers and ion-exchange matrices makes it possible to obtain both cation exchange and anion exchange materials with a wide range of properties that have a number of advantages compared to ion-exchange resins or heterogeneous membranes. However, if the properties of cation exchange membranes "Polykon K" have been sufficiently well studied and described in the literature by now, then further research is needed for anion exchange membranes.

The purpose of this paper is an investigation of the water distribution on the water binding energy and the effective pore radii in "Polykon A" membranes.

Experiments and Results

A series of samples of composite ion exchange fibrous materials "Polykon A" was prepared on the base of the polymer matrix like EDE-10P resin and polyethylene terephthalate fiber ("Lavsan"). The low-temperature plasma treatment of the fibrous system (LTP) was used in combination with the introduction of the ultradispersed additives (UA) of Si (~1.5 wt.%) into the monomer composition at the stage synthesis [1]. UA of Si were obtained in different ways. Objects of study are presented in the Table 1.

Table 1: Porous structure characteristics of "Polykon A" membranes

Membrane	LTP	UA	$V_0, \text{cm}^3/\text{g}_{\text{dry}}$	$S, \text{m}^2/\text{g}$	L, nm	V_{gel}/V_0
1	-	-	1.06	714	0.57	0,64
2	+	+	1.23	714	0.57	0,68
3	+	+	1.00	523	0.48	0,73
4	+	+	1.07	892	0.63	0,52
MA-40	-	-	0.67	575	-	0.85

The method of standard contact porosimetry was applied to investigate the water volume distribution in the membrane on the water binding energy or the effective pore radii (r) [2]. The total volume of water (V_0), the area of specific internal surface (S), the average distance (L) between the neighboring fixed groups at the internal interface and the volume fraction of pores in the range of 10-100 nm (V_{gel}/V_0) were calculated from porosimetric curves [3].

Results and Discussion

The results presented in Fig.1 and Table 1. As can be seen from the integral porosimetric curves (Fig.1a), the value of total water volume is the same as in "Polykon K" membranes [4] and more than in heterogeneous commercial membrane MA-40 which is made of EDE-10P resin and polyethylene. All samples have two peaks on the differential curves (Fig.1b). The peak in the mesopore region (100 nm) corresponds to water in the ion-exchange matrix while the peak in the macropore region (3000-4000 nm) is due to the fibrous base of "Polykon A" membranes. Calculated characteristics of the porous structure of samples are presented in Table 1. As can be seen from the Table the low-temperature plasma treatment of the fibrous system and the introduction of the UA of Si into the monomer composition at the stage synthesis affect the structure and, as a consequence, properties of "Polykon A" membranes.

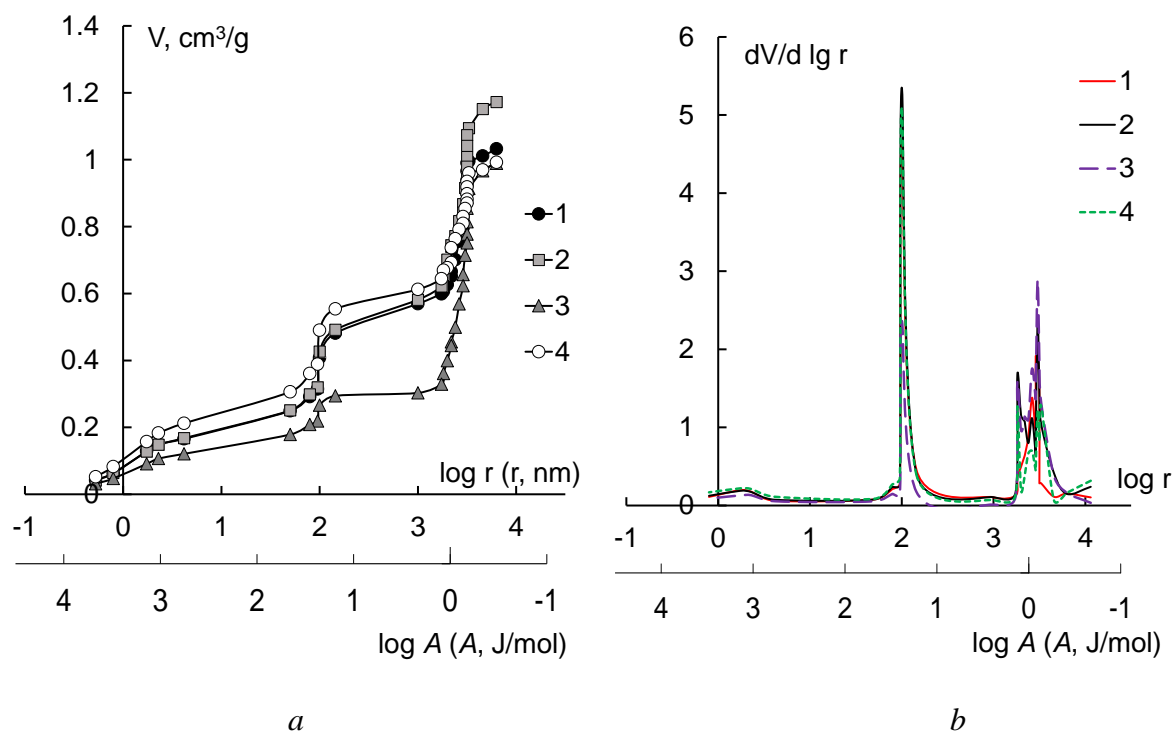


Figure 1. Integral (a) and differential (b) functions of water distribution on the water binding energy and the effective pore radii for the membranes. Curve numbers correspond to sample numbers in Table 1.

Conclusions

The value of total porosity and other characteristics of the porous structure of "Polykon A" membranes are comparable to these characteristics for "Polykon K" membranes and are significantly higher than for heterogeneous ion exchange membrane MA-40. Pre-treatment with low-temperature plasma and the introduction of ultrafine particles of Si at the stage of synthesis of the ion-exchange matrix leads to a change of the structure both "Polykon A" and "Polykon K" membranes.

Acknowledgments. This work has been supported by the Russian Science Foundation, RSF (project No. 23-29-00346)

References

1. Strilets I., Kardash M.M., Terin D.V., etc. Features of Synthesis of Anion Exchange Matrix "Polikon A" with Oxidated Ultrafine Additives on Lavsan Textile Bases // Membranes and Membrane Technologies, 2020, No. 5. P. 325-331.
2. Volkovich Yu.M., Filippov A.N., Bagotsky V.S. Structural properties of porous materials and powders used in different fields of science and technology. Springer-Verlag; 2014.
3. Kononenko N., Nikonenko V., Grande D., etc. Porous structure of ion exchange membranes investigated by various techniques // Advances in Colloid and Interface Science. 2017. Vol. 246. P. 196-216.
4. Kardash M.M., Kononenko N.A., Fomenko M.A. etc. Influence of the nature of the fibrous base of composite membranes on their structure, conductive properties and selectivity // Membranes and membrane technologies. 2016, No. 1. P. 41-47.

RECYCLING LITHIUM FROM SPENT LITHIUM-ION BATTERIES LEACHING SOLUTION USING ELECTROBAROMEMBRANE METHOD

^{1,2}Vasily Troitskiy, ¹Alexey Budnikov, ¹Dmitrii Butylskii

¹Kuban State University, Krasnodar, Russia, E-mail: d_butylskii@bk.ru

²Platov South-Russian State Polytechnic University (NPI), Novocherkassk, Russia

Introduction

Recovery of valuable components from secondary resources is an important task for waste-free production. Currently, one of the valuable components are lithium salts. These salts are used to produce batteries, ceramics, glass, lubricants, foundry powders, etc. However, only lithium-ion batteries (LIBs) are of interest for lithium recycling.

Lithium is mainly extracted using the hydrometallurgical methods according to the diagram presented in Figure 1. After leaching with sulfonic acid, a large concentration of lithium, cobalt, nickel and manganese ions remains in the filtrate. Membrane technologies can be suitable for ions separation at this stage instead of traditional reagent-based methods.

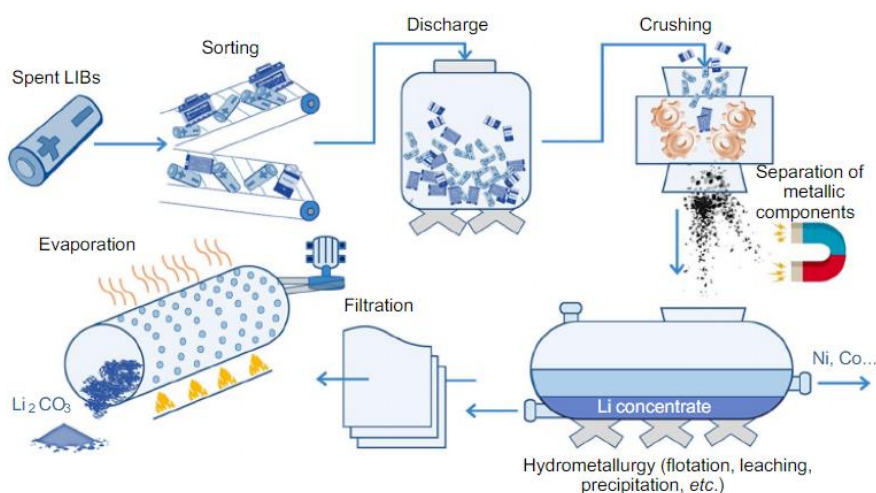


Figure 1. Scheme for processing lithium-ion batteries using the hydrometallurgical method.

Nanofiltration (NF) and selective electro dialysis (S-ED) seem to be the most suitable membrane-based technologies for this process. However, due to the trade-off effect, these methods have limitations [1, 2]. Researchers are faced with a choice between achieving high productivity or separation selectivity.

One of the few membrane technologies for which the trade-off effect is weakly expressed or does not manifest itself is the hybrid electrobaromembrane (EBM) method [3]. We investigated the possibility of a reagent-free hybrid electrobaromembrane (EBM) method for extracting valuable spent LIBs components from filtrates.

Experiments

A mixture of 0.05 M Li₂SO₄, 0.025 M CoSO₄, 0.025 M NiSO₄ and MnSO₄ (pH = 4.8) was used to determine the optimal separation parameters. In this work, a TEM #811 track-etched membrane with diameter of pores of 35 nm was used. It was produced from a polyethylene terephthalate (PET) film at the Joint Institute for Nuclear Research (Dubna, Russia). On the left- and right-hand sides, auxiliary anion-exchange MA-41 heterogeneous membranes (JCC Shchekinoazot, Pervomayskiy, Russia) were used to form flow chambers surrounded the TEM. Feed solutions of the same composition and volume (0.45 L) were pumped through chambers adjacent to the left and right of the TEM. A 0.2 M Na₂SO₄ solution was pumped through the electrode chambers (4 L). The separation experiment lasted 50 h. In the membrane system, the current density was set to 125 A/m², so that cations moved towards the cathode. At the same time, in the direction opposite to their movement in the electric field, the pressure drop (0.3 bar) set the convective flow. The

concentration of separated ions was determined using inductively coupled plasma atomic emission spectrometry.

Results and Discussion

According to Figure 2a, it is established that the amounts of substance (mol) of the coexisting ions (Co^{2+} , Ni^{2+} , Mn^{2+}) increase in the chamber through which the solution circulates without excess pressure, while the lithium amount of substance decreases. As you can see at a current density of 125 A/m^2 the fluxes of lithium and doubly charged ions is directed in different ways (Fig. 2b). It means that the average flux of Li^+ is positive (directed to cathode), but the fluxes of Co^{2+} , Ni^{2+} , Mn^{2+} ions were negatives and directed towards the anode. Their absolute values were as follows 0.2 , -0.012 , -0.03 and $-0.08 \text{ mol}/(\text{m}^2 \times \text{h})$, respectively for Li^+ , Co^{2+} , Ni^{2+} and Mn^{2+} (Fig. 2b). This allowed lithium to be fractionated from the mixed solution. Since at a given current only lithium passes into the chamber under pressure, then formally, the value $S_{\text{Li}^+/\text{M}^{2+}}$ can not be evaluated or can be equated to infinity.

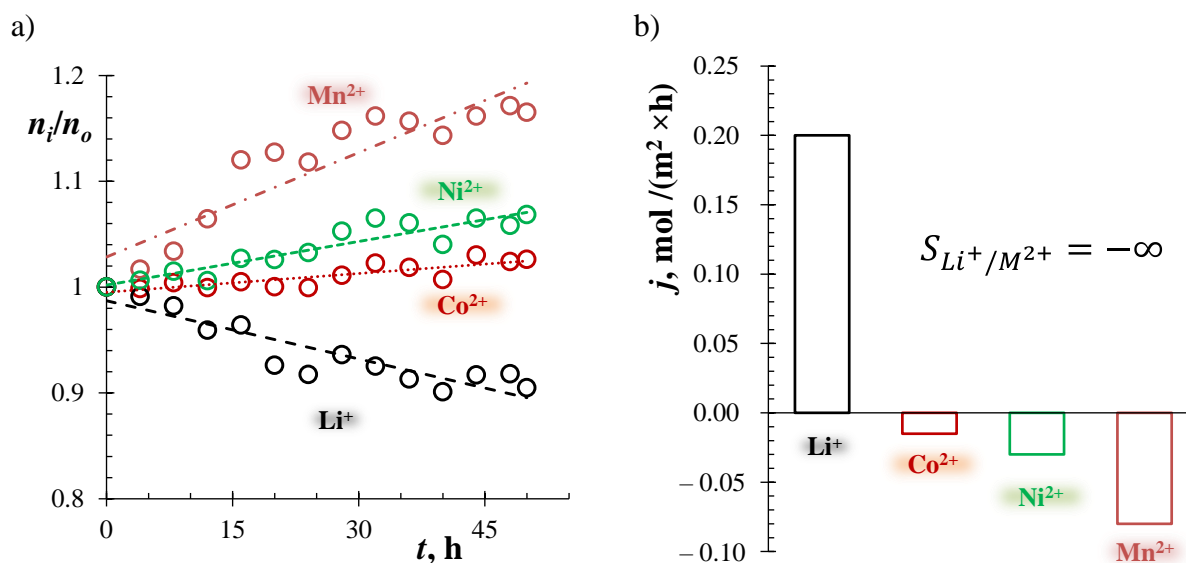


Figure 2. Changes in the lithium, cobalt, nickel and manganese amounts of substance in the chamber without pressure (a), as well as the average fluxes of separated ions through the TEM #811 track-etched membrane (b).

Acknowledgement. We are grateful to the Russian Science Foundation, project № 22-79-00178, <https://rscf.ru/en/project/22-79-00178/>

References

1. Butylskii D., Dammak L., Larchet C., Pismenskaya N. D., Nikonenko V. V. Selective recovery and re-utilization of lithium: prospects for the use of membrane methods // Russ. Chem. Rev. 2023. P. 92
2. Park, H. B., Kamcev, J., Robeson, L. M., Elimelech, M., Freeman, B. D. Maximizing the right stuff: The trade-off between membrane permeability and selectivity // Sci. 2017. V. 356. №. 6343. P. eaab0530.
3. Tang C., Yaroshchuk A., Bruening M. L. Flow through negatively charged, nanoporous membranes separates Li^+ and K^+ due to induced electromigration // ChemComm. 2020. V. 56. №. 74. P. 10954-10957.

MODELING OF STATIONARY THERMOPERVAPORATION OF A TWO-COMPONENT MIXTURE

¹Alexander Troshkin, ¹Daria Khanukaeva, ²Petr Aleksandrov, ¹Anatoly Filippov

¹Gubkin University, Moscow, Russia, E-mail: sasha.troshkin.02@mail.ru

²"Kurs-Simbirsk" JSC, Ulyanovsk, Russia, E-mail: darkpriest@mail.ru

Introduction

Mixture separation is highly requested technology in modern life. This predefines the intensive development of membrane technologies and, in particular, pervaporation [1]. Despite the existence of significant amount of experimental data in vacuum pervaporation, in sweeping gas pervaporation and in thermopervaporation the lack of proper mathematical models for these processes is observed. The present work is devoted to the development of a mathematical model for stationary thermopervaporation.

Statement of the problem

A pervaporation cell is presented in Fig. 1. A water-methanol solution with a given methanol mass fraction ω_{s_0} circulates to the left of the membrane, and to the right, vapors of the target component are accumulated. The temperatures of the feed solution (T_f) and permeate (T_p) are given, as well as the thermal conductivity coefficients λ, λ_m of water-methanol solution and a saturated membrane, respectively. The origin of the x axis oriented in the direction of the process, is posed at the membrane working side. The problem is solved in the following areas: $-\delta < x < 0$ – the diffusion layer (1), $0 < x < h$ – the membrane area (2), where h is the membrane thickness, $h < x < B$ – the vapor part of the permeate area (3).

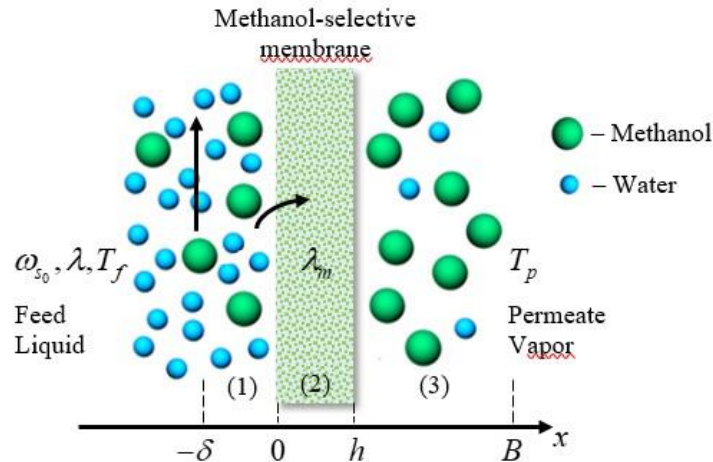


Figure 1. The scheme of the pervaporation membrane cell

The model of stationary thermopervaporation under development includes equations for the temperature distribution in the liquid-membrane-vapor system, thermal diffusion equations, as well as boundary conditions on all interphase surfaces, representing continuity of temperature and diffusion fluxes, jumps in concentration and heat fluxes.

The thermodiffusion mechanism that describes thermopervaporation includes diffusion through thermal activation of the system and concentration diffusion of molecules. It is worth noting that it is enough to consider one of the components of the mixture (for example, methanol), since the value of the mass fraction of the other can be found from the relation $\omega_s + \omega_w = 1$, where ω_s, ω_w – mass fractions of methanol (s) and water (w), respectively. Since a stationary process is considered, the thermodiffusion equations turn into the condition of conservation of thermodiffusion flux $S_i, i = 1, 2, 3$ in each of the aforementioned areas:

$$S_i = -\rho_i D_i \frac{d\omega_{s_i}}{dx} - \frac{k_{T_s}^i \omega_{s_i} (1 - \omega_{s_i}) D_i}{T_i} \rho_i \frac{dT_i}{dx},$$

where ω_{s_i} are the unknown mass fractions of methanol, D_i are the diffusion coefficients, ρ_i are the densities of the mixtures allowing for their aggregate condition, k_{Ts}^i are the thermal diffusion constants, T_i are the temperature distribution functions in each of the areas, respectively. We demonstrated that the temperature distribution can be described by linear functions in each of the areas, because the liquid-vapor phase transition occurring inside the membrane can be described as taking place on the working side of the membrane.

The boundary conditions are

- the continuity of thermodiffusion flux: $S_1|_{x=0} = S_2|_{x=0}$, $S_2|_{x=h} = S_3|_{x=h}$;
- the given value of the methanol mass fraction at the boundary $x = -\delta$: $\omega_{s_1}|_{x=-\delta} = \omega_{s_0}$;
- jumps in the mass fraction of methanol on both membrane surfaces:

$$x=0: \frac{1}{\frac{1}{\rho_s} + \frac{1}{\rho_w \omega_{s_1}} - \frac{1}{\rho_w}} = \frac{\gamma_s^v}{\frac{1}{\rho_s^v} + \frac{1}{\rho_w^v \omega_{s_2}} - \frac{1}{\rho_w^v}}; \quad x=h: \frac{\gamma_s}{\frac{1}{\rho_s^v} + \frac{1}{\rho_w^v \omega_{s_2}} - \frac{1}{\rho_w^v}} = \frac{1}{\frac{1}{\rho_s^v} + \frac{1}{\rho_w^v \omega_{s_3}} - \frac{1}{\rho_w^v}},$$

where ρ_s, ρ_w are the densities of components in the liquid phase, ρ_s^v, ρ_w^v are the densities of components in the vapor mixture, γ_s, γ_s^v are the distribution coefficients showing the affinity of the membrane to methanol, besides, γ_s^v takes into account the process of evaporation on the membrane working side, i.e. $\gamma_s^v \gg \gamma_s$;

- the given value of the methanol mass fraction at the boundary $x = B$: $\omega_{s_3}|_{x=B} = \omega_B$.

Solution and discussion

The boundary value problem was solved numerically. The distributions of mass fractions in each of the studied areas were obtained. It is worth noting that in the limiting case, when full saturation is established, the component fluxes in each of the areas are equal to zero and the solution can be obtained analytically.

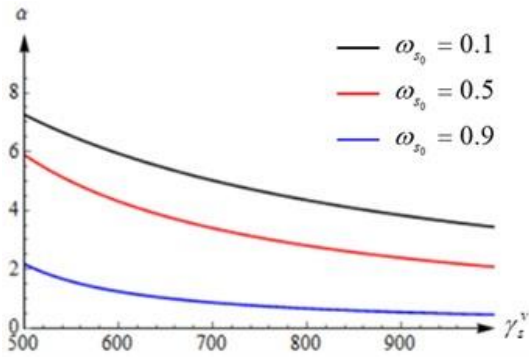


Figure 2. Dependence of separation factor α on γ_s^v

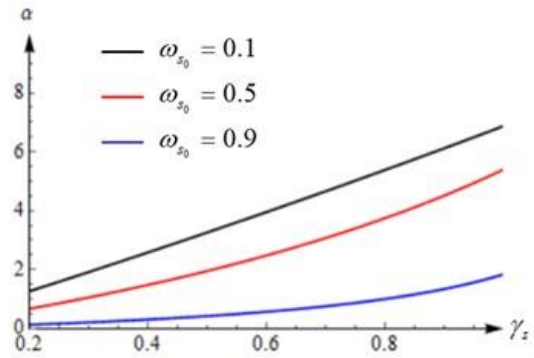


Figure 3. Dependence of separation factor α on γ_s

The efficiency of the thermopervaporation process is determined by the separation factor α , as well as the pervaporation separation index $PSI = J_{total}(\alpha - 1)$, where J_{total} is the total flux through the membrane. Analysis of the dependences of the separation factor on all parameters of the problem showed that the most significantly it is affected by the methanol content in the initial mixture ω_{s_0} , as well as coefficients γ_s and γ_s^v , representing the characteristics of the membrane. Fig.2 shows the dependence of the separation factor on γ_s and γ_s^v with methanol mass fraction ω_{s_0} in the feed solution equal to 0.1; 0.5; 0.9. The curves were plotted for the following values of

the problem parameters: $k_{T_s}^1 = 0.25$; $k_{T_s}^2 = 0.2$; $\rho_s = 750 \text{ kg/m}^3$; $\rho_w = 990 \text{ kg/m}^3$; $\rho_s^v = 1.41 \text{ kg/m}^3$; $\rho_w^v = 0.2 \text{ kg/m}^3$; $h = 40 \cdot 10^{-6} \text{ m}$; $\delta = 100 \cdot 10^{-6} \text{ m}$; $T_p = 343 \text{ K}$; $T_f = 353 \text{ K}$; $\lambda = 0.37 \text{ J/(m}\cdot\text{s}\cdot\text{K)}$; $\lambda_m = 0.27 \text{ J/(m}\cdot\text{s}\cdot\text{K)}$; and also $\gamma_s = 0.75$ for Fig.2; $\gamma_s^v = 700$ for Fig.3.

It can be seen in Fig.2 and Fig.3 that the lower the mass fraction of the target component in the initial mixture, the higher the separation factor. Therefore, pervaporation is effective for ultra-high separation of diluted mixtures.

Comparison with the experiments

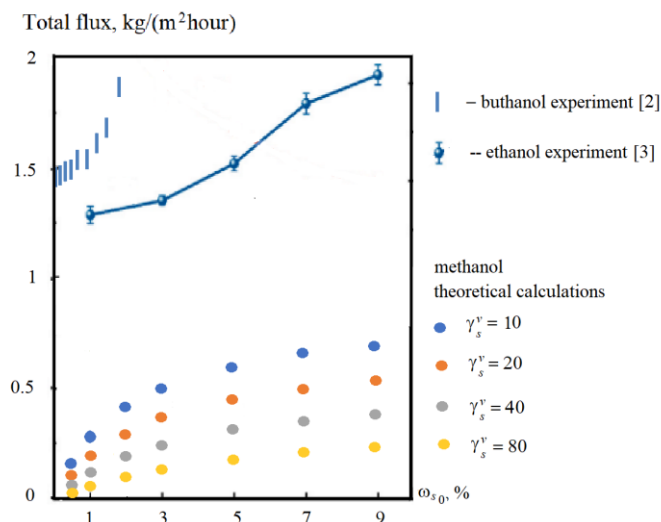


Figure 4. Total flux as a function of the target component fraction in the feed solution measured in experiments [2] (bars), [3] (line) and calculated in the present work (points).

The theoretically obtained solution was compared with the experimental data of works [2, 3]. The dependences of the total diffusion flux on the mass fraction of butanol [2], ethanol [3] and methanol in the feed solution are shown in Fig.4. The direct coincidence of the presented dependences should not be expected, as they are obtained for different substances. Nevertheless, parameter γ_s^v allows to fit experimental data in the framework of the developed model.

Thus, the developed model represents the quantitative instrument for the analysis of the quality and efficiency of the mixture separation process. Within the framework of a computational experiment, it allows to study the dependence of thermopervaporation on all the process parameters.

Acknowledgments. The work is supported by RSF (grant No. 23-19-00520, <https://rscf.ru/project/23-19-00520/>).

References

1. A.M. Polyakov Some aspects of the pervaporative separation of liquid mixtures. Part 1 // Critical technologies. Membranes. 2004. № 4 (24). P. 29-44.
2. I.L. Borisov, G.S. Golubev, V.P. Vasilevsky, A.V. Volkov, V.V. Volkov Novel hybrid process for bio-butanol recovery: Thermopervaporation with porous condenser assisted by phase separation // J.Membr. Sci., V. 523, 2017, P. 291-300.
3. Sinan Cheng, Zhiyuan Liu, Xingda Yang, Chunxi Li, Hongwei Fan, Hong Meng Graphdiyne-based integrated membrane for enhanced alcohol-permselective pervaporation // J. Membr. Sci., V. 693, 2024, 122397.

STRUCTURE AND PROPERTIES OF THE MODIFIED “POLYKON” MOSAIC MEMBRANES

¹Timur Turaev, ¹Marina Kardash, ^{1,2}Denis Terin

¹Yuri Gagarin State Technical University of Saratov, Saratov, Russia, E-mail: tim.tur.al@gmail.com,

²Saratov State University, Saratov, Russia, E-mail: terinden@mail.ru

Introduction

Mosaic "Polykon" - heterogeneous ion-exchange materials. The prospects of this type of membrane were previously discussed in works [1-3]. Our membranes are fabricated using polycondensation filling method. Due to the peculiarity of polycondensation filling, the preliminary choice of the fibrous matrix was based on their compliance with a number of criteria: not to swell and not to degrade in the synthesis and curing environment, not to lose physico-mechanical properties with technological parameters of the process. Based on the requirements put forward and the selected ionite matrix systems, we settled on the following fibrous systems: Fabric based on NPF fibers (fabric based on phenol-formaldehyde fiber), and Lavsan fabric FL-4 (polyethylene terephthalate fiber). To work out the technical techniques and technological parameters of all processes, a further step in this direction was to study the influence of the chemical nature and textile structure of fibers and fabrics on the wettability of the components of anionite and cationite matrices.

Experiments

Samples with a length of 30 cm were prepared for testing and fixed in the device, after which they were immersed in a cuvette with prepared monomerization solutions before the first contact by 1-3 mm. Measurements were carried out by recording the rise of the wetting boundary with a certain time interval (60 s), until a complete equilibrium state was established. Kinetic curves of wettability were constructed based on the obtained data. The coordinates were the lifting height and the impregnation time.

Results and Discussion

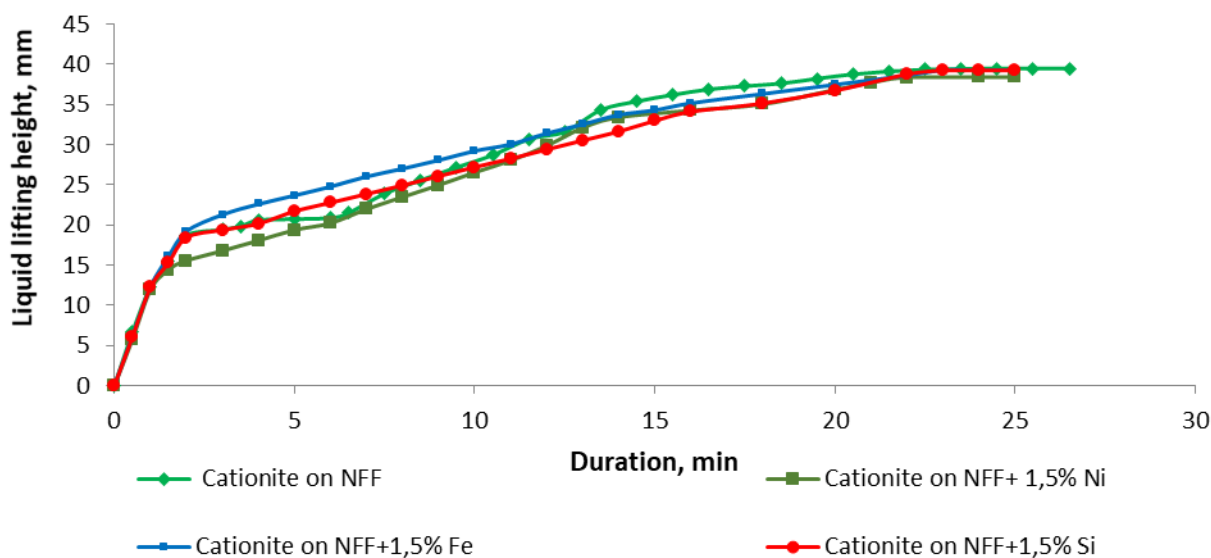


Figure 1. The effect of the introduction of ultradisperse additives into the monomerase composition of the cationic component of the mosaic membrane on the wetting process of the NPF fiber fabric

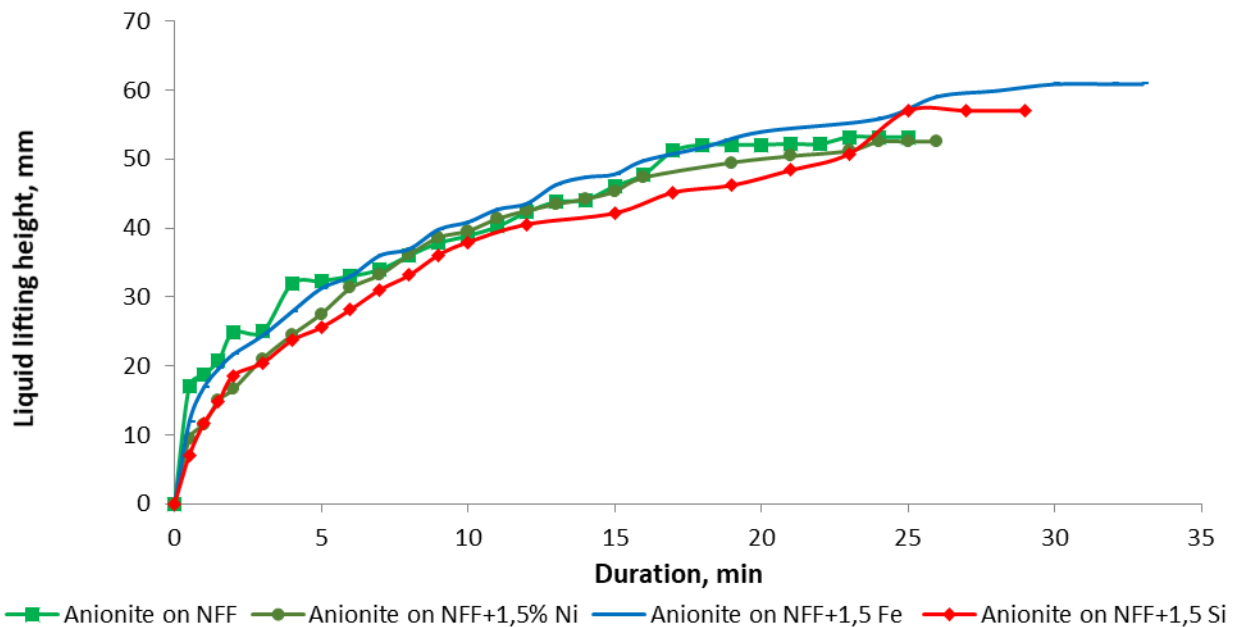


Figure 2. The effect of the introduction of ultradisperse additives into the monomerase composition of the anionite component of the mosaic membrane on the wetting process of the NPF fiber fabric

The effect of the introduction of ultrafine additives into the monomerization compositions of both cationite (Figure 1) and anionite (Figure 2) composite mosaic membranes on the course of the wetting process of the fibrous base of which was a fabric made of NFF fibers was noted.

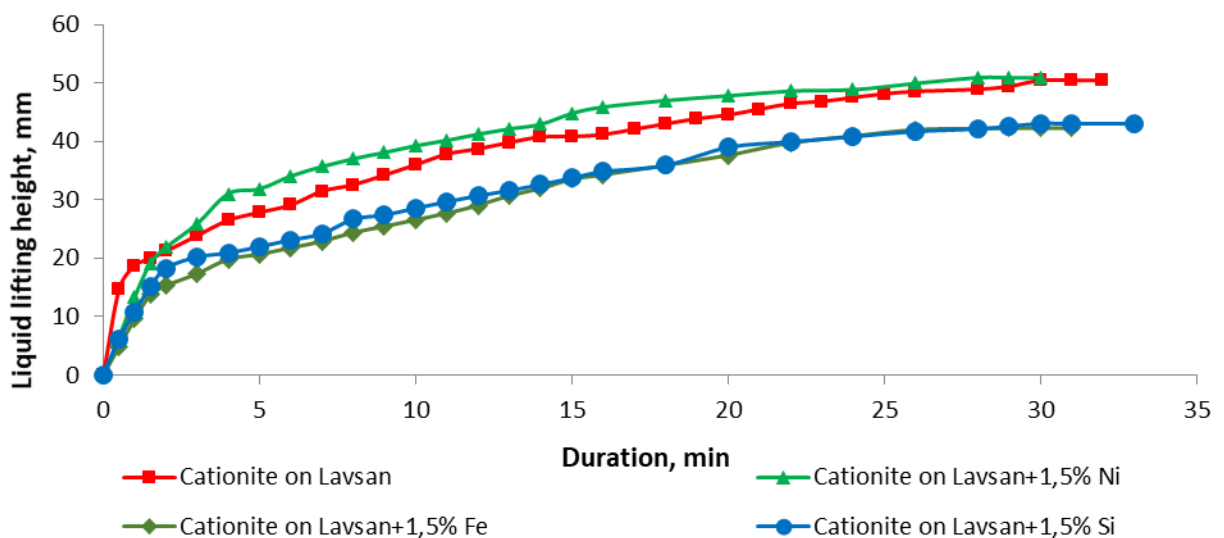


Figure 3. The effect of the introduction of ultradisperse additives into the monomerase composition of the cationic component of the mosaic membrane on the wetting process of Lavsan fabric FL-4

As the conducted studies have shown, the chemical nature of the fibrous base plays a significant role, so on a fibrous basis of dacron fabric it can be noted that the introduction of Fe and Si oxides reduces both the initial velocity and the max lifting height (10-12%), while there are no noticeable changes with the introduction of Ni oxides (Figure 3).

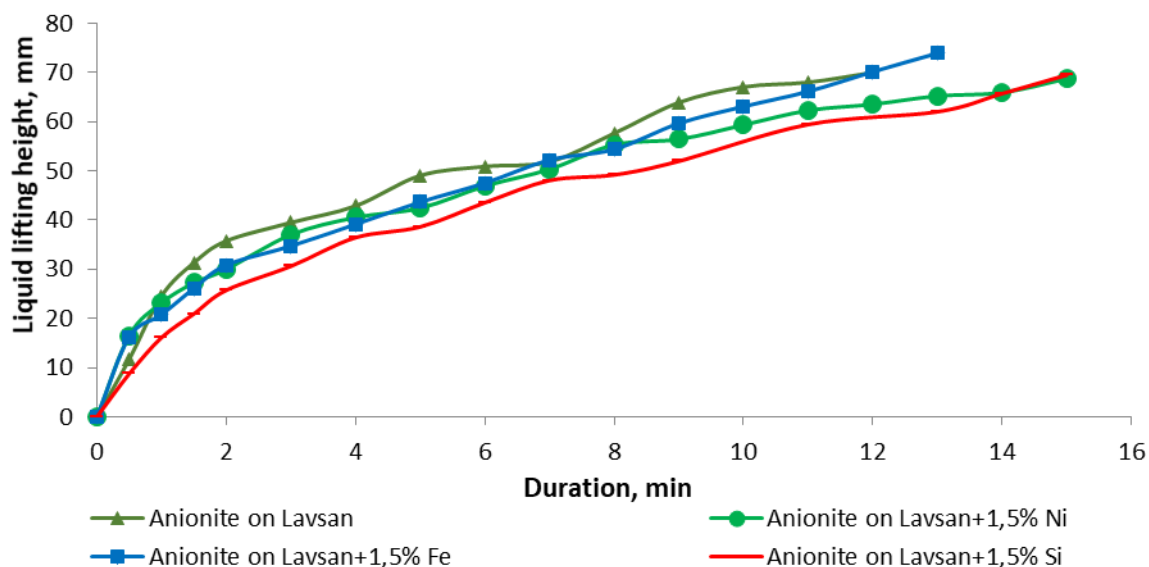


Figure 4. The effect of the introduction of ultradisperse additives into the monomerase composition of the anionite component of the mosaic membrane on the wetting process of Lavsan fabric FL-4

A similar effect is noted on the anionite components, so the introduction of ultrafine additives into the monomerization composition of the anionite (Figure 4) composite mosaic membranes on the course of the wetting process of the fibrous base, which was dacron fabric, slightly affects the course of the wetting process.

Conclusions

Based on the conducted studies, it can be concluded that the introduction of ultrafine additives into the monomerization composition of both anionite and cationite components of the mosaic membrane does not require changes in the technological parameters of the wetting process.

Acknowledgement. This work has been supported by the Russian Science Foundation, RSF (project No. 23-29-00346)

References

1. Terin, D.; Kardash, M.; Ainetdinov, D.; Turaev, T.; Sinev, I. Anion-Exchange Membrane “Polikon A” Based on Polyester Fiber Fabric (Functionalized by Low-Temperature High-Frequency Plasma) with Oxidized Metal Nanoparticles. // *Membranes* 2023, 13, 742. <https://doi.org/10.3390/membranes13080742>
2. Terin D., Kardash M., Tsyplyayev S., Korchagin S., Cherkasov V., Druzhinina T. Features of thermomechanical stability of anionic–cation exchange matrix “Polykon AC” on viscose non-woven materials. // *Membranes*. 2021. V. 11. № 10. P.734
3. Terin D.V., Kardash M.M., Turaev T.A., Ainetdinov D.V. Low-temperature ion-plasma pretreatment of fibrous systems during preparation of composite heterogeneous membranes // *Membranes and Membrane Technologies*. 2023. V. 5. № 4. P. 257-265.

MATHEMATICAL MODELING OF OVERLIMITING MASS TRANSFER IN A THREE-LAYER ELECTROMEMBRANE SYSTEM IN GALVANODYNAMIC MODE

Aminat Uzdenova

Umar Aliev Karachai-Cherkess State University, Karachaevsk, Russia, E-mail: uzd_am@mail.ru

Introduction

Mathematical modeling of mass transport in a three-layer system containing an ion-exchange membrane and two electrolyte layers makes it possible to describe the selective properties of the membrane by determining its fixed charge density. This paper developed a two-dimensional mathematical model of ion transfer in a three-layer system for the galvanodynamic mode, when the current density in the system is set. The model is formulated as a boundary value problem for the system of Nernst–Planck–Poisson and Navier–Stokes equations. The electric field mode is determined using a galvanodynamic boundary condition that relates the normal component of the potential gradient and the current density.

Mathematical model

The considered area of the electro dialysis membrane system includes half of the desalting channel (1), the cation-exchange membrane (2) and half of the concentration channel (3), Figure 1. The transport of ions in all three layers is described using the Nernst–Planck–Poisson equations. Poisson's equation describes the electric field, accounting the fixed charge of the membrane in layer (2) and the extended space charge region formed in the desalting channel during the flow the overlimiting current. The solution flow in layers (1) and (3) governed by the Navier–Stokes equation, considering the effect of the electric field on the space charge region. The electric mode is modeled using the galvanodynamic boundary condition [1].

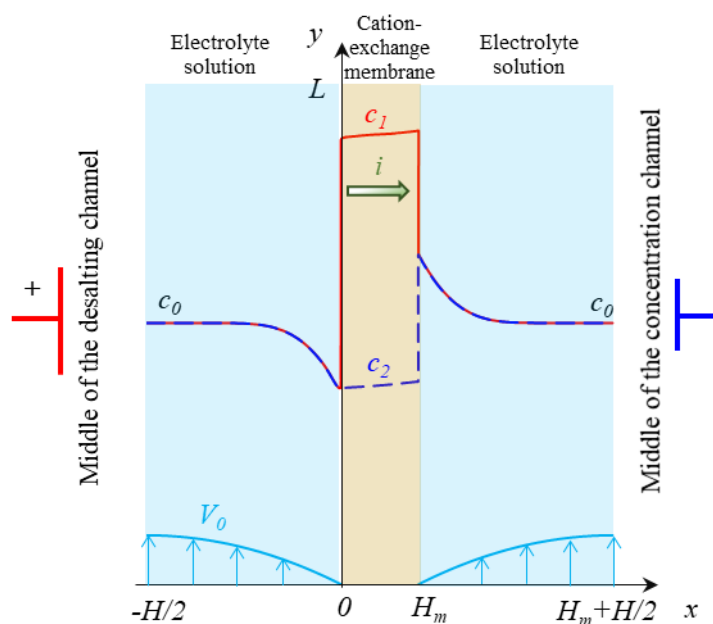
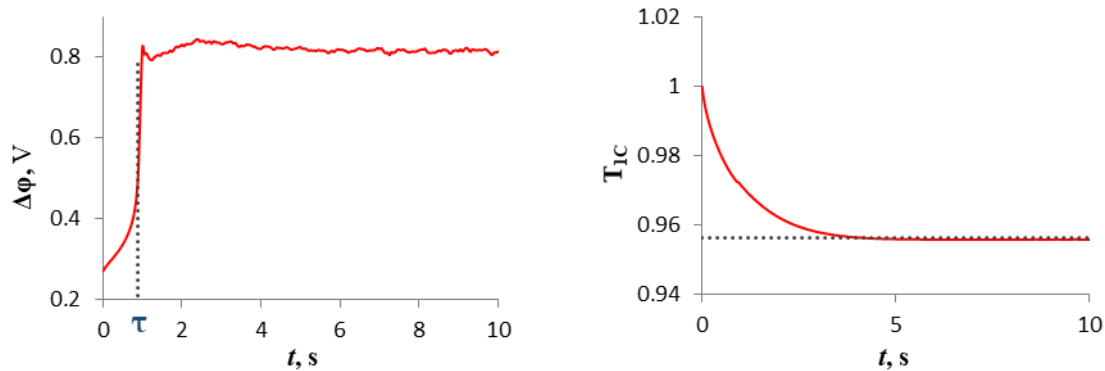


Figure 1. Scheme of a three-layer membrane system with forced flow with an average speed V_0 and profiles of concentrations of cations (c_1 , red line) and anions (c_2 , blue line) at current flow density i

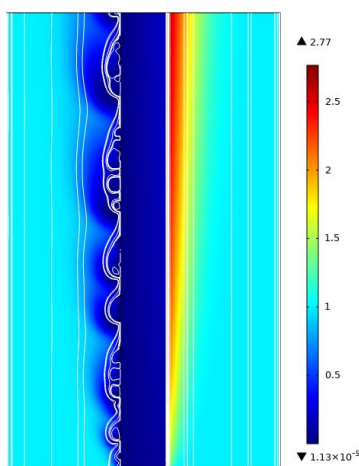
Results and Discussion

Figure 2a shows the chronopotentiogram (ChP) calculated using the proposed model. The transition time of the calculation shown in Figure 2 differs from Sand's analytical estimate by less than 1%. The cation transport number in the membrane decreases over time and is stable at a value of 0.956 (Fig. 2b). The electroconvection developing in the desalting channel is shown in Figure 2c.



(a)

(b)



(c)

Figure 2. ChP (a), cation transfer number in the cation-exchange membrane (b), anion concentration (shown in color) and streamlines (white lines) at $t=10$ s (c), calculated for a solution of 0.1 mol/m^3 NaCl and the fixed membrane charge of 4 mol/m^3 at $i = 1.5i_{\text{lim}}$

Thus, the proposed model makes it possible to numerically calculate ion concentrations, electric potential, space charge, solution flow and ChP of the ion-exchange membrane and two adjacent layers of binary electrolyte in galvanodynamic mode. The model takes into account the formation of the extended space charge region and the development of electroconvection near the membrane under the overlimiting DC current. The model calculation results are in good agreement with Sand's analytical assessment of the transition time.

Acknowledgment. The reported study was funded by the Russian Science Foundation grant No. 23-29-00534, <https://rscf.ru/en/project/23-29-00534/>.

References

1. Uzdenova, A. 2D Mathematical Modelling of Overlimiting Transfer Enhanced by Electroconvection in Flow-Through Electrodialysis Membrane Cells in Galvanodynamic Mode // Membranes 2019. V. 9, 39.

ANTIBATE INFLUENCE OF THE FRACTION AND SIZES OF ION EXCHANGE RESIN PARTICLES ON THE PROPERTIES OF THE HETEROGENEOUS MEMBRANE MK-40

Vera Vasil'eva, Elmara Akberova, Svetlana Dobryden, Yana Bespalova
Voronezh State University, Voronezh, Russia, E-mail: viv155@mail.ru

Introduction

By varying the ratio of the conductive and inert phases or the particle size of the ion exchange resin, it is possible not only to achieve a compromise between the electrochemical and mechanical properties of the obtained samples of heterogeneous ion exchange membranes, but also to enhance the overlimiting mass transfer in the electromembrane system due to changes in the geometric and electrical heterogeneity of the membrane surface. The purpose of the work was to study the effect of changes in the content and size of the cation exchange resin particle in experimental membranes on their transport, structural and physicochemical properties.

Experiments

The objects of study were two series of experimental samples of heterogeneous cation exchange membranes MK-40. They were manufactured at LLC IE Shchekinoazot (Russia). The first batch of membranes differed in the mass fraction of ion exchange resin. It varied in the range from 55 to 69 wt %. In the samples of the second batch of membranes, the particle size of the ion-exchanger varied from <20 to 56-71 μm . In this case, the resin content was standard and amounted to 65 wt %.

The physicochemical properties of the membranes were determined using conventional methods. The specific electrical conductivity of the membranes κ_m was determined from data on their resistance measured by the mercury-contact method. The diffusion properties (integral coefficient of diffusion permeability P_m) of the membranes were determined by estimating the amount of electrolyte transferred from a salt solution of a set concentration through the test membrane into clean water. The transport properties of membranes were determined at the Department of Physical Chemistry, Faculty of Chemistry and High Technologies of KubSU. Before the study, all membranes were subjected to chemical conditioning according to the generally accepted method. The studies of the surface and cross-section morphology of the membranes in swollen state were carried out by scanning electron microscopy (SEM) using a JSM-6510 LV microscope (Japan). The quantitative estimation of fraction and size of ion-exchangers (S) and macropores (P) was carried out with the help of the authors' software by using the digital processing of SEM images [1].

Results and Discussion

Effect of mass fraction of ion exchange resin

Comparison of the properties of experimental membranes with different mass fractions of ion exchange resin revealed the influence of the ion-exchanger content on their structural characteristics (Fig. 1).

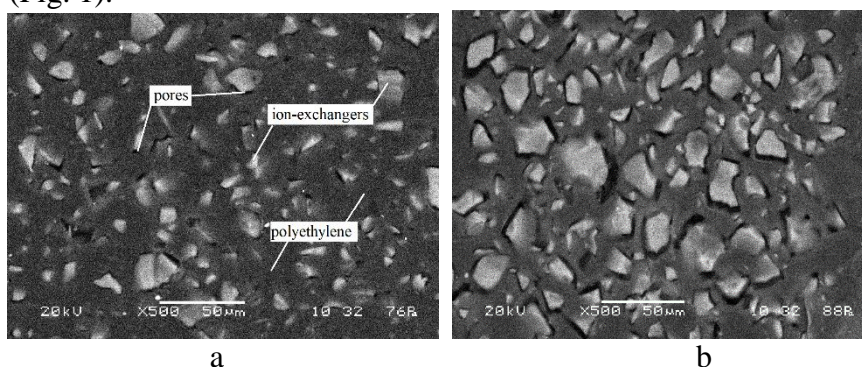


Figure 1. Micrographs of the surface of swollen MK-40 membranes with cation-exchange resin content of 55 (a) and 69 (b) wt %.

With a higher mass fraction of ion exchange resin in the MK-40 membrane, larger particles are visualized on the surface. It is obvious that when producing membranes with a low resin content, large particles are predominantly found in the bulk of the samples. With an increase in the content of the ion exchange resin, the SEM method established an increase in the proportion of ion exchanger particles on the surface by almost 2 times. This is accompanied by a 4-fold increase in the proportion of macropores. The sizes of ion-exchangers and macropores increase by 1.5 times and 2 times, respectively.

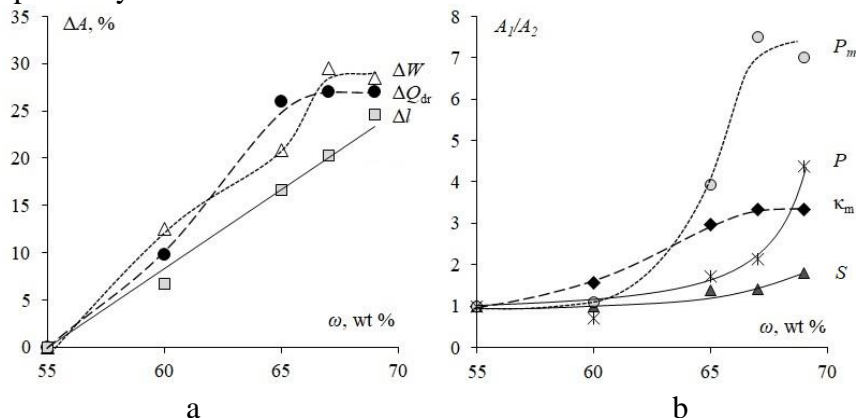


Figure 2. Dependences of relative changes in physicochemical (a), transport and structural (b) properties of the MK-40 membrane on the mass fraction of ion exchange resin (ω , wt %).

$$\Delta A, \% = 100 \cdot (A_x - A_{55\%}) / A_{55\%}, A_1/A_2 = A_x/A_{55\%}.$$

Data on changes in the structure of the membrane surface obtained from SEM are consistent with changes in physicochemical and transport properties (Fig. 2). For membranes, with an increase in the mass fraction of ion exchange resin, there is a natural increase in the exchange capacity (Q_{dr}), moisture content (W), thickness (l) and specific electrical conductivity κ_m . The increase in diffusion permeability (P_m) is due to an increase in macroporosity and moisture content of membrane samples.

Effect of ion exchange resin particle size

Micrographs of the surface of swollen samples of MK-40 membranes with different sizes of resin particles are presented in Fig. 3a and 3b.

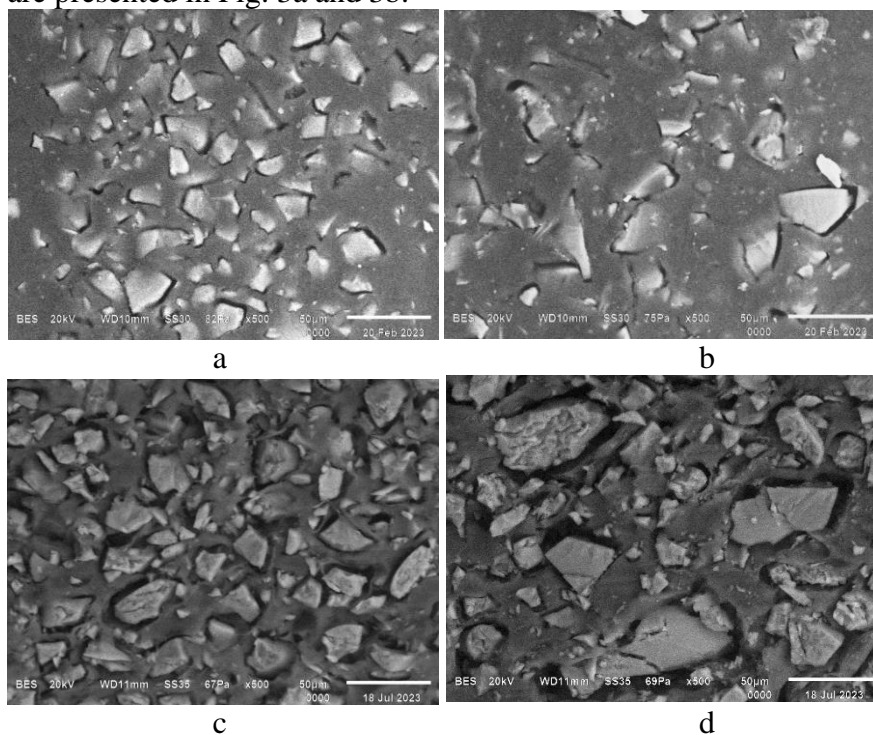


Figure 3. SEM images of the surface (a and b) and the cross-section (c and d) of swollen MK-40 membranes with sizes of cation exchange resin: $<20 \mu\text{m}$ (a and c), $56-71 \mu\text{m}$ (b and d).

Visualization of the membrane surface has showed that a number of established features of surface morphology require explanation. Firstly, a decrease in the proportion and weighted average radius of ion exchange resin areas on the membrane surface was revealed with an increase in the size of the ion-exchanger particles set during production. Secondly, the presence of small and the absence of large ion-exchangers was established for membranes with resin particle sizes in the range of 56-71 μm . Third, a decrease in surface macroporosity was found, but an increase in macropore size by more than 20% with increasing resin particle size. Clarifications were obtained by studying the membrane internal structure (Fig. 3c and 3d).

Comparison of SEM images of the surface and cross section of swollen samples of MK-40 membranes with different resin particle sizes revealed differences in their structural characteristics. For a membrane with a maximum resin particle size, a 2-fold increase in the proportion of the conductive phase on the section compared to the membrane surface was established. This fact is associated with the extrusion of plastic polyethylene from the bulk onto the surface during the production of membranes, leading to encapsulation of resin particles. It has been established that particles with a radius from 16 to 31 μm are absent on the surface, but their share is 40% of the total area of the ion-exchanger phase in the cross-section of the membrane. A greater macroporosity of the section compared to the membrane surface was revealed; macropores in the range of 10-12 μm are absent on the surface but make up 35% in the section.

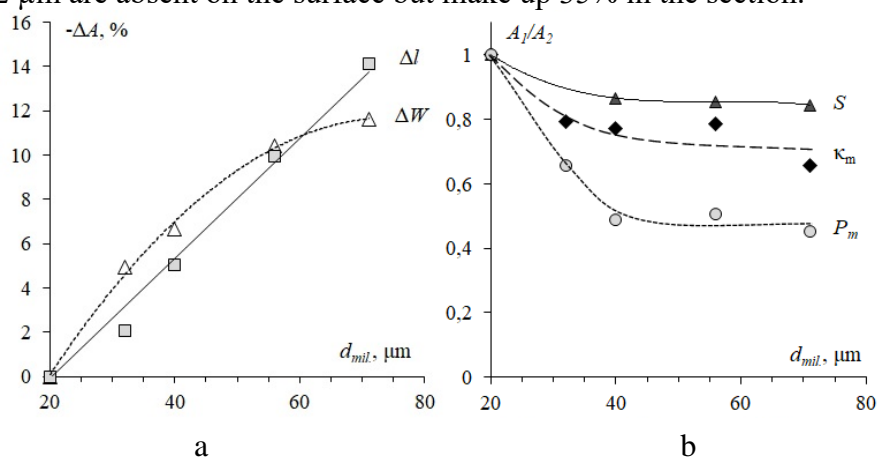


Figure 4. Dependences of relative changes in physicochemical (a), transport and structural (b) properties of the MK-40 membrane on the particle size of the ion exchange resin ($d_{mil}, \mu\text{m}$). $\Delta A, \% = 100 \cdot (A_x - A_{<20}) / A_{<20}$, $A_1/A_2 = A_x/A_{<20}$.

The exchange capacity of the membranes remains almost constant as the particle size of the ion-exchanger decreases, which corresponds to its equal content in the samples. It is 2.50 ± 0.02 mmol/g_{dry}. For experimental membranes, as the size of the ion-exchanger particles increases, the moisture content decreases by 12%, the electrical conductivity and diffusion permeability of the membranes decrease by 35 and 55%, respectively (Fig. 4).

Thus, the effect of the antibate influence of the fraction and size of resin particles on the characteristics of heterogeneous ion exchange membranes has been established. An increase in the fraction of ion exchange resin in membranes causes an increase in the values of physicochemical, transport and structural characteristics, and an increase in the size of resin particles causes their decrease.

Acknowledgements. The study was supported by a grant from the Russian Science Foundation No. 21-19-00397, <https://rscf.ru/en/project/21-19-00397/>

References

1. Akberova E. M., Vasil'eva V. I. // Electrochemistry Communications. 2020. 111. Art. No 106659.

PRODUCTION OF GAS DIFFUSION LAYERS USING FLUOROPLASTICS

Yulia Vilacheva, Alexander Lysenko

St. Petersburg State University of Industrial Technologies and design 191186, St. Petersburg

E-mail: vilachevay@bk.ru

Introduction

Hydrogen energy, in the context of the search for alternative energy sources and the partial abandonment of traditional fuel, is a promising direction for the development of global industry. The conversion of hydrogen's chemical energy directly into electrical energy occurs as a result of an electrochemical reaction occurring in a fuel cell (FC). The scheme and operating principle of the fuel cell are shown in Fig. 1.

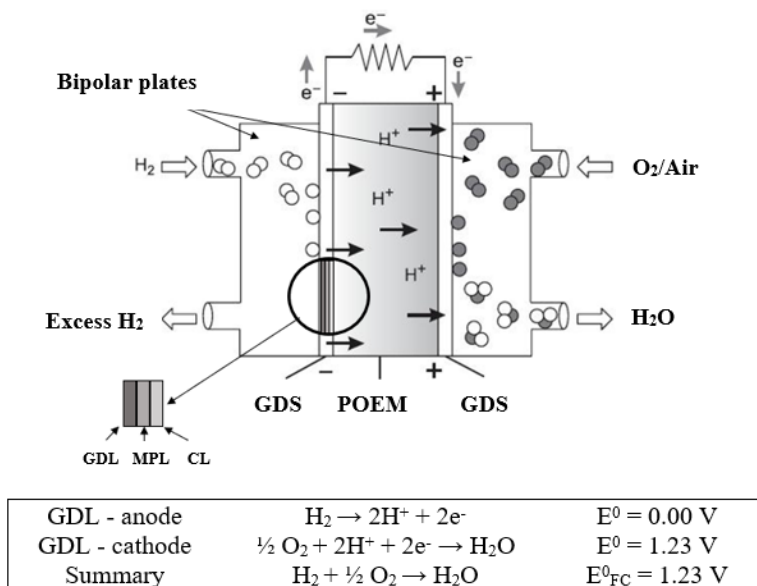


Figure 1 – Scheme and operating principle of FC [1]

Conventional symbols in Fig. 1: gas diffusion substrate (GDS), consisting of: gas diffusion layer (GDL), microporous layer (MPL), catalytically active layer (CL); proton exchange polymer membrane (POEM) One of the structural units of fuel cells is the gas diffusion layer (GDL), which is responsible for the uniform distribution of reagents near the catalyst layer, ensuring electronic conductivity and the effective removal of water as a by-product of the reaction. GDS must have high electrical conductivity (electrical resistivity less than 80 mOhm/cm²), certain values of surface density (100 - 120 g/m²), porosity (porosity in the range of 50-90%) and hydrophobicity (contact angle of at least 110°) [2].

Experiments

In this research, GDLs were obtained in the form of composites based on carbon graphitized fabrics from a polyoxadiazole precursor (possessing low electrical resistance and high porosity) and a hydrophobizing fluoroplastic binder. Since fluoroplastic is a dielectric, electrically conductive fillers were introduced into its solution: carbon black (CB) in an amount of 5; 10; 15 wt. % relative to the polymer; carbon nanotubes (CNTs) and highly dispersed conductive graphenes in the amount of 1; 2.5; 5 wt. % relative to the polymer. The content of fluoroplastic matrices in the composites was 5 - 15 wt. %.

Results and Discussion

Graphs of the dependence of electrical resistance on matrix content at the same filler content are presented in Figure 2.

The specific electrical resistance of GDLs without dispersed electrically conductive fillers increases from 15 to 80 mOhm/cm² with an increase in the fluoroplastic matrix content from 5 to 15 wt. %. According to the data obtained during the study, with an increase in the content of all

types of dispersed fillers, the electrical resistance of the composites decreases at the selected matrix content. When introducing 5, 10, 15 wt. % specifications relative to the fluoroplastic matrix, the resistance of the composites decreases from 15 mOhm/cm² to 8.0; 7.0 and 6.5 mOhm/cm², respectively, with a matrix content of 5 wt. %. With a fluoroplastic matrix content of 15 wt. % resistance of composites with the same amounts of carbon black (5, 10, 15 wt. %) decreases from 80 mOhm/cm² to 75, 70 and 69 mOhm/cm².

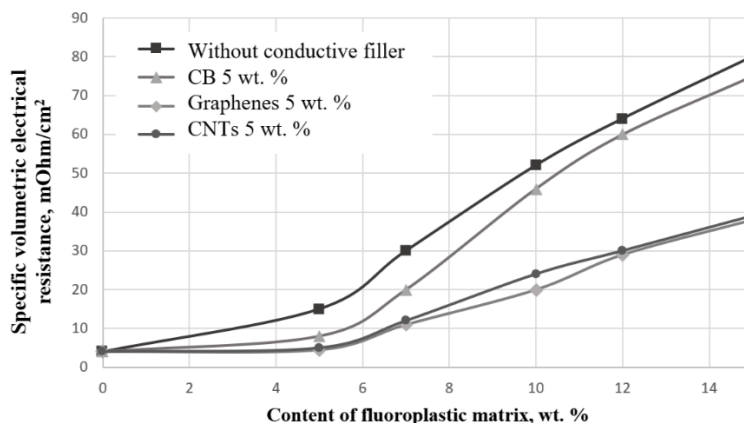


Figure 2 – Dependence of the electrical resistivity of the GDLs on the content of the fluoroplastic matrices

In the same range of matrices contents (from 5 to 15 wt.%), the resistance of composites with CNTs in an amount of 1.0; 2.5; 5.0% increases accordingly from 6.0; 5.0 and 4.5 mOhm/cm² to 50, 41 and 38 mOhm/cm². Similar values were obtained when graphenes were introduced into the composition of the compounds, which makes them, along with CNTs, effective fillers that reduce the electrical resistance of composites.

With an increase in the amount of fluoroplastic in the studied range, the total porosity of the composites decreases from 60% to 50%, and the surface density increases from 95 to 120 g/m², regardless of the content and type of dispersed electrically conductive fillers. The contact angle for all types of HDS is 130 ± 5°.

The experiments showed that CNTs and dispersed conductive graphenes are more effective as electrically conductive additives than carbon black. The introduction of 1% CNTs/graphenes reduces the electrical resistance by 60% relative to the original composites, while the introduction of 5% CB reduces it by 40%. At the same time, in the aggregate of other indicators, the optimal matrix content is 7-12 wt. % [3].

Based on the data obtained, HDS was selected with a fluoroplastic matrices content of 10 wt. %, modified with dispersed electrically conductive graphenes in an amount of 5 wt. % for studies of output power and current density arising during the operation of fuel cells. Tests in a fuel cell showed that the resulting GDS have an output voltage of 1000 mV, and the maximum current density reaches -1980 mA, which corresponds to these indicators of imported industrial analogues chosen as objects of comparison.

Composites containing an effective electrically conductive filler are promising for the development of GDS low-temperature fuel cells.

References

1. Vilacheva Yu. Yu.. Carbon for hydrogen energy Yu. Yu. Vilacheva, A. A. Lysenko // Composite world. – 2023. -No. 4 (105). – P. 26 – 27.
2. Bagotsky V. S. Fuel Cells: Problems and Solutions. Wiley, Hoboken, Nj, 2009. 320 p.
3. Vilacheva, Yu.Yu. Preparation of carbon papers with fluoroplastic binders / Yu.Yu. Vilacheva, V.V. Martsenyuk // Nanostructured, fibrous and composite materials: materials of the All-Russian scientific conference and youth competition of scientific reports / St. Petersburg State University of Industrial Technologies and Design. – St. Petersburg: FSBEI HE “SPbGUPTD”, 2022. – P. 18-19

ALUMINUM-ION BATTERIES

Yury Volkovich

A.N. Frumkin Institute of Physical chemistry & Electrochemistry of RAS, Moscow, Russia

E-mail: yuvolf40@mail.ru

Introduction

Currently, lithium-ion batteries (LIB) are the most common in the world. They are used in electronics (phones, laptops, tablets, etc.), as well as electric vehicles. LIBs are produced in the billions per year. However, they have the following serious disadvantages. They are explosive and fire hazardous. Another disadvantage is that there are limited quantities of lithium in the world, and therefore it is expensive and its price is rising, especially in connection with such mass production of LIBs. In recent years, aluminum-ion batteries (AIB) have begun to be intensively developed in the most developed countries. This is due to the fact that, unlike lithium, the world's reserves of aluminum are practically unlimited.

Main part

An aluminum ion battery (AIB) is a rechargeable electrochemical device that uses aluminum as the negative electrode. The charging/discharging processes in AIA occur according to a principle similar to LIB. AIB have the following advantages over LIB: 1) Aluminum reserves are unlimited, since it is the third most abundant chemical element and the first most abundant metal in the earth's crust. 2) Aluminum is three times more energy-intensive than lithium, since its charge/discharge involves three electrons per aluminum atom, while the charge/discharge of a lithium atom involves only one electron. 3) Aluminum batteries are fire and explosion proof. The theoretical volumetric capacity of AIB is 8040 mAh/cm³ compared to 2046 mAh/cm³ for LIB. Due to the low cost and abundance of raw materials (aluminum ~ 1520 \$/t, graphite ~ 654 \$/t, NaCl ~ 152 \$/t and AlCl₃ ~ 1521 \$/t), AIB shows very good prospects for commercial application. For comparison, we note that the cost of lithium is \$80,000/t, and this cost is constantly growing.

To date, AIAs are already being produced in the USA, Australia, Germany and China. Thus, we can say that the era of aluminum energy is coming. The role of the negative electrode in AIB is most often performed by aluminum foil, and the role of the positive electrode. often performs a carbon (graphite or graphene) electrode in which the process of intercalation/deintercalation of Al⁺³ cations occurs. In this case, the structure of the carbon electrode in the AIA should ensure the occurrence of this process, taking into account the fact that the size of Al⁺³ is larger than the size of Li⁺. To date, AIAs are already being produced in the USA, Australia, China and Germany.

In [1], spinel cathode material Al_{2/3}Li_{1/3}Mn₂O₄ was synthesized using an electrochemical transformation reaction using LiMn₂O₄ as a precursor. The cathode provided a discharge capacity of 151.8 mAh/g at a current density of 100 mA/g, maintaining 64.1% capacity over 1000 cycles. The full cell showed a high energy density of 183 Wh/kg. In [2], defective cobalt-manganese oxide nanosheets were studied as a cathode material for aqueous AIBs. A very high energy density of 685 Wh/kg (based on cathode and anode mass) and a reversible capacity of 585 mAh/g at 100 mA/g were achieved with 78% retention after 300 cycles. These characteristics are higher than those of commercial LIBs.

[3] constructed a porous Al foil anode for high-speed AIB. Porous Al foil coated with a uniform layer of carbon (pAl/C) was prepared by etching, deposition and curing of polyacrylonitrile and subsequent carbonization. The AIB cell with pAl/C anode and natural graphite cathode demonstrated a reversible capacity of 104 mAh/g at 2C. It also showed a high power density of 3701 W/kg. Compared with Al foil, the discharge rate and power density were significantly improved due to the increase in specific surface area.

Conclusion. Thus, aluminum-ion batteries are extremely promising for commercial use.

References

1. R. Li, C. Xu, X. Wu, J. Zhang, X. Yuan, F. Wang, *Energy Storage Materials*, **53** . 514 (2022)
2. J. Yang, W. Gong, F. Geng, *Advanced Functional Materials*, **33**, 2301202 (2023)
3. X. Tong, F. Zhang, B. Ji, M. Sheng, Y. Tang, *Adv. Mater.* , **28** , 9979 (2016)

CUPPER (II) ION EXCHANGE MECHANISM IN AMINO PHOSPHONIC POLYAMPHOLITES STUDIED BY EPR.

Vitaly Volkov, Irina Avilova

Federal Research Center of Problems of Chemical Physics and Medicinal Chemistry RAS, Chernogolovka, Russia, E-mail: vitwolf@mail.ru, i.avilova@icp.ac.ru

Introduction

Aminophosphonic polyampholytes are widely used for selective sorption of polyvalent ions as well as in catalytic processes. The structure of metal ion complexes and kinetics of ligand exchange are fundamental problems. In the case of paramagnetic transition metal ions electron paramagnetic resonance (EPR) technique is a strong tool of this information obtaining. We have investigated structure and sorption-desorption kinetics of copper (II) complexes in polyampholytes containing phosphonic groups only (CMF); phosphonic groups and dimethylamine (PA-1), trimethylamine (PA-2), diethylamine (PA-3), pyridine (PA-4), ethylenediamine (PA-5) groups.

Experiments

The list of polyampholytes and some physical chemistry properties are given in Table 1.

Table 1: Some physical-chemistry characteristics of polyampholytes

Brand of ampholyte	Ion-exchange groups	DVB content, %	Ion-exchange capacity, mg-eq/g	
			NaOH	HCL
PA-1	-CH ₂ PO(OH) ₂ -CH ₂ N(CH ₃) ₂	10	3.08	1.71
PA-2	-CH ₂ PO(OH) ₂ -CH ₂ N(CH ₃) ₃	10	1.33	1.56
PA-3	-CH ₂ PO(OH) ₂ -CH ₂ N(C ₂ H ₅) ₂	10	2.84	1.13
PA-4	-CH ₂ PO(OH) ₂ -CH ₂ NC ₆ H ₅	10	1.65	1.70
PA-5	-CH ₂ PO(OH) ₂ -CH ₂ NH(CH ₂) ₂ NH ₂	10	2.81	2.35
CMF	-CH ₂ PO(OH) ₂ -CH ₂ Cl	10	3.2	-

Note: PA and KMF ampholytes are macro porous ionites.

EPR spectra of Cu²⁺ polymeric complexes were recorded on Bruker spectrometer ER-420 Endor. For kinetic investigations the spectra recorded in 10 sec. Sorption copper (II) was carried out from CuCl₂ or CuSO₄ aqueous solutions. The following desorption was realized by HCl aqueous solution.

Results and Discussion

The example of Cu²⁺ EPR spectra shows in Figure 1. At low copper (II) contents spectra are asymmetric lines which are typical for immobile complexes described by the next spin Hamiltonian of axial symmetry (1).

$$\hat{H} = \beta [g_{\parallel} H_{\parallel} S_z + g_{\perp} (H_x S_x + H_y S_y)] + A_{\parallel} S_z I_z + A_{\perp} (S_x I_x + S_y I_y) \quad (1)$$

where g_{\parallel} , g_{\perp} components of g -factor; A_{\parallel} , A_{\perp} - constants of ultrafine structure in parallel and perpendicular orientations relatively to external magnetic field; S_x , S_y , S_z ; I_x , I_y , I_z - projections of electron and nuclear spins. Constants of ultrafine structure and g -factors obtained from EPR spectra enable to identify copper (II) complexes structure. It was concluded that in CMF tetragonal Cu²⁺ complex forms by two phosphonic groups and four water molecules Cu(R-HPO₃)₂(H₂O)₄. The same complexes are formed in ampholytes PA-1, PA-2, PA-3, and PA-4. In PA-5 copper (II) forms Cu(R-HPO₃)₂(H₂O)₄, Cu(R-N)₄(H₂O)₂²⁺ and Cu(R-N)₂(H₂O)₄²⁺ complexes where four and two nitrogen atoms coordinate Cu²⁺ ion. Evolution of copper (II) spectra during copper sorption from 0.001 N aqueous CuSO₄ solutions is shown in Figure 1.

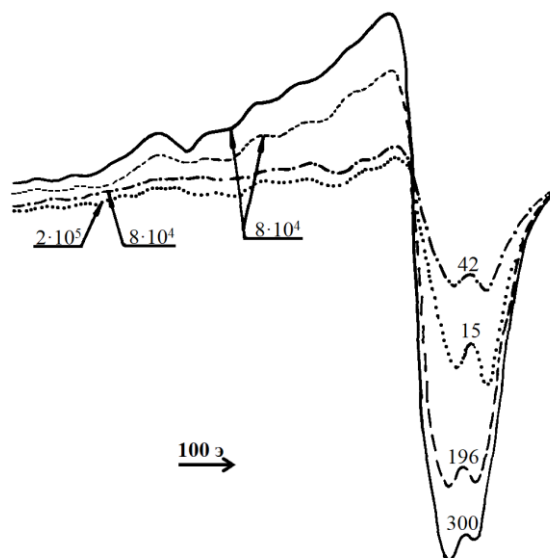


Figure 1. EPR spectra copper (II) in PA-5 recorded at different sorption time (in minutes) during copper sorption from 0.001 N aqueous solutions CuSO₄. Figures on the arrow are gains.

On the basis of these data partial kinetics curves for different copper (II) complexes are obtained. In Figure 2 an example of Cu²⁺ EPR spectra evolution during desorption by hydrochloric acid aqueous solution is shown. This process is rather complicated: Amino complexes of copper (II) Cu(R-N)₄(H₂O)₂²⁺ transfer in aqua complexes Cu(H₂O)₆²⁺, complexes Cu(R-N)₂(H₂O)₄²⁺ in Cu(H₂O)₆²⁺ and Cu(R-HPO₃)₂(H₂O)₄ (2).

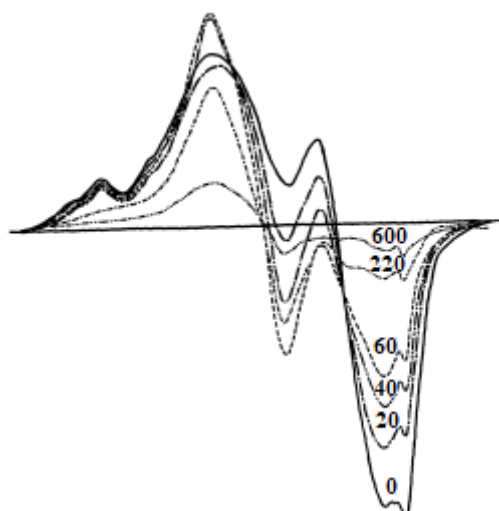
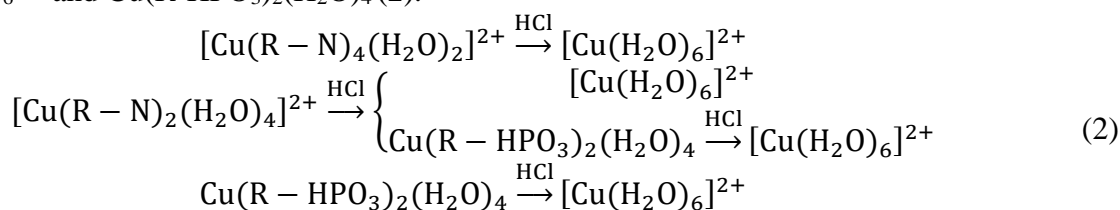


Figure 2. EPR spectra of copper (II) in PA-5 at different desorption time (in seconds) by 0.1 N HCL aqueous solution.

The concentrations of Cu(H₂O)₆²⁺ and Cu(R-HPO₃)₂(H₂O)₄ in amphotite grain increase initially as it is shown in Figure 3.

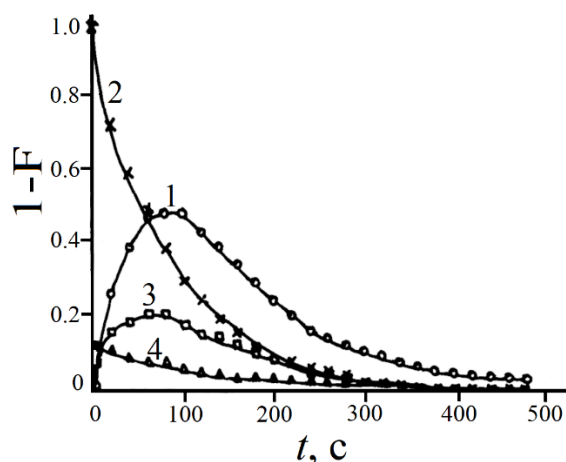


Figure 3. Kinetic curves of copper (II) desorption in PA-5 by 0.1 N aqueous HCl solutions. 1 - $\text{Cu}(\text{H}_2\text{O})_6^{2+}$; 2 - $\text{Cu}(\text{R-N})_2(\text{H}_2\text{O})_4^{2+}$; 3 - $\text{Cu}(\text{R-HPO}_3)_2(\text{H}_2\text{O})_4$; 4 - $\text{Cu}(\text{R-N})_4(\text{H}_2\text{O})_2^{2+}$ complexes.

In Figure 4 the example of complexes the example of $\text{Cu}(\text{R-N})_2(\text{H}_2\text{O})_4^{2+}$ destruction and $\text{Cu}(\text{H}_2\text{O})_6^{2+}$ desorption by 0.1 HCl aqueous solution in PA-5 with different grain diameters are shown. The kinetic of copper (II) concentration decreasing is approximated by external diffusion kinetics.

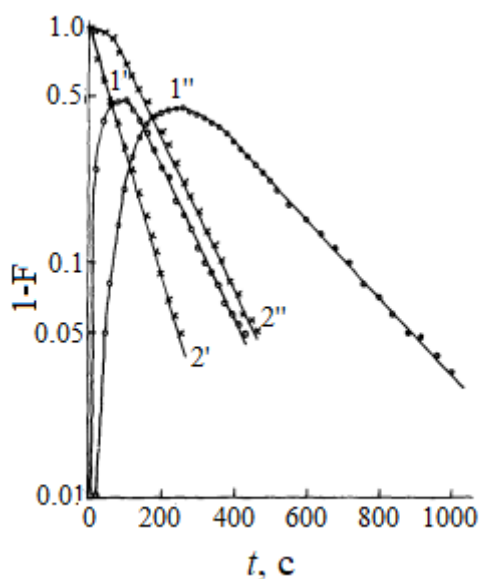


Figure 4. Kinetic curves copper (II) desorption from PA-5 by 0.1 N HCl aqueous solution. Ampholit grain diameters d are 0.33 mm (1, 1') and 0.73 mm (2, 2'). Curves 1, 1' - aqua complexes, 2, 2' - $\text{Cu}(\text{R-N})_2(\text{H}_2\text{O})_4^{2+}$ complexes.

Summary

Dynamic EPR spectra registration gave opportunity to obtain kinetic curves of partial copper (II) complexes sorption and desorption. These partial kinetic was approximated by simple models of ion exchange processes.

Acknowledgments. Measurements were performed using equipment of the Multi-User Analytical Center of the Federal Research Center of Problems of Chemical Physics and Medicinal Chemistry RAS with the support of State Assignment of the Federal Research Center of Problems of Chemical Physics and Medicinal Chemistry RAS (state registration No FFSG-2024-0008/124013000743-3).

PERFLUOROSULFONIC ACID MEMBRANES AQUIVION® AS GEL-POLYMER ELECTROLYTES FOR LITHIUM METAL BATTERIES

Daria Voropaeva, Ekaterina Safronova, Svetlana Novikova, Andrey Yaroslavtsev

Kurnakov Institute of General and Inorganic Chemistry, Russian Academy of Sciences, Moscow, Russia

E-mail: voropaeva@igic.ras.ru

Introduction

Lithium metal batteries, where lithium metal is utilized as the anode, may allow for twice the energy density of traditional lithium-ion batteries, which currently reaches ~250 Wh/kg. The most important challenge that limits its large-scale application is dendrite growth through the electrolyte, leading to deterioration of the electrochemical performance of the battery and eventually short circuits [1]. According to the space-charge theory, low lithium transference numbers in the electrolyte lead to dendrite formation. Thus, using single-ion conducting electrolytes, in which anions are bound to the polymer matrix, is one way to prevent the formation of dendrites. Gel-polymer electrolytes based on perfluorinated cation-exchange membranes are promising electrolytes for lithium metal batteries due to the strength and chemical stability of the fluorinated matrix, high values of ionic conductivity and cation transference numbers, which contribute to the suppression of dendrite formation. The purpose of this work was to compare main characteristics of polymer electrolytes based on Aquivion® perfluorinated sulfocationic membranes and polar aprotic solvents, including their lithium conductivity, transference numbers, and stability against lithium metal, to evaluate their suitability in lithium metal batteries.

Experiments

The membranes Aquivion-87 and Aquivion-98 were conditioned by a standard procedure, then soaked in 0.1M LiOH solution for 48 h under constant stirring to obtain membranes in Li⁺ form. The ion-exchange capacity (IEC, mg-equiv/g) of the Aquivion-87 and Aquivion-98 membranes was measured by acid-base titration. To obtain the polymer electrolytes, dry Aquivion-87 and Aquivion-98 membranes in Li⁺ form were placed in a dry argon-filled glove box with a moisture and oxygen content <5 ppm (SPECS, Russia) and placed in a solution containing equal volumes of ethylene carbonate – propylene carbonate (EC-PC) or EC – *N,N*-dimethylacetamide (EC-DMA). The membranes were soaked in this solvent over activated molecular sieves (3 Å) for one day. The ionic conductivity of the obtained samples of polymer electrolytes in Li⁺ form plasticized by EC-PC and EC-DMA was studied by impedance spectroscopy in the temperature range of –20...+50°C in an argon atmosphere. Li⁺ transference numbers (T_{Li^+}) were estimated using the Bruce-Vincent method [2] in Li|Aquivion|Li coin-type cells. The cells were polarized by a potential difference $\Delta V=5$ or 10 mV. The interfacial resistance was measured before and after polarization by alternating current impedance. To assess the stability of the obtained polymer electrolytes against lithium metal, galvanostatic cycling was performed: current density of ± 0.1 mA/cm² with a cut-off capacity ± 0.05 mAh/cm² in symmetrical Li|membrane|Li coin-type cell CR2032. To evaluate the possibility of using the investigated polymer electrolytes in real lithium metal batteries, we checked coin-type cells with a lithium metal anode and LiFePO₄ (LFP) cathode. The required current was calculated based on the mass of active cathode material for each electrochemical cell.

Results and Discussion

Based on acid-base titration data, the IEC values for Aquivion-87 and Aquivion-98 membranes are 1.13 and 0.96 mg-eq/g, respectively. The solvation process increases the thickness of the membranes from 50 to 63-78 μm . The number of solvent molecules per functional sulfonic group increases with the increment of membrane IEC while moving from Aquivion-98 to Aquivion-87. The increase is by a factor of 1.4 for the EC-PC mixture and by a factor of 2 for the EC-DMA mixture. Ionic conductivity of the membranes, regardless of the solvent nature, increases with increasing degree of solvation. The ionic conductivity of the Aquivion-87 membrane exceeds Aquivion-98 when solvated with a similar solvent mixture due to the higher concentration of

charge carriers and the degree of solvation. The ionic conductivity of membranes solvated by EC-PC mixture does not exceed $9 \cdot 10^{-5}$ S/cm. Obtained values are comparable to the literature data for Nafion membranes. The use of the EC-DMA mixture leads to an order of magnitude increase in the ionic conductivity of the membranes compared to EC-PC. Obtained values of ionic conductivity of membranes solvated by EC-DMA mixture ($\sim 10^{-3}$ S/cm) meet the requirements for electrolytes for lithium metal batteries. Obtained T_{Li^+} values were 0.88 and 0.93 for Aquivion-87 and Aquivion-98 membranes solvated by EC-PC and 0.69 for samples solvated by EC-DMA.

The difference between the average charge and discharge plateau potentials for the LFP|Li cell with polymer electrolyte, containing EC-DMA, and the same cell with liquid electrolyte is comparable at 0.1C (Figure 1), which indicates that the membrane electrolyte with conductivity of the order of 10^{-3} S/cm does not contribute significantly to the battery resistance, and this parameter is determined by ohmic losses during lithium transfer through the carbon coating and the charged (discharged) layer of cathode material formed on the sample surface.

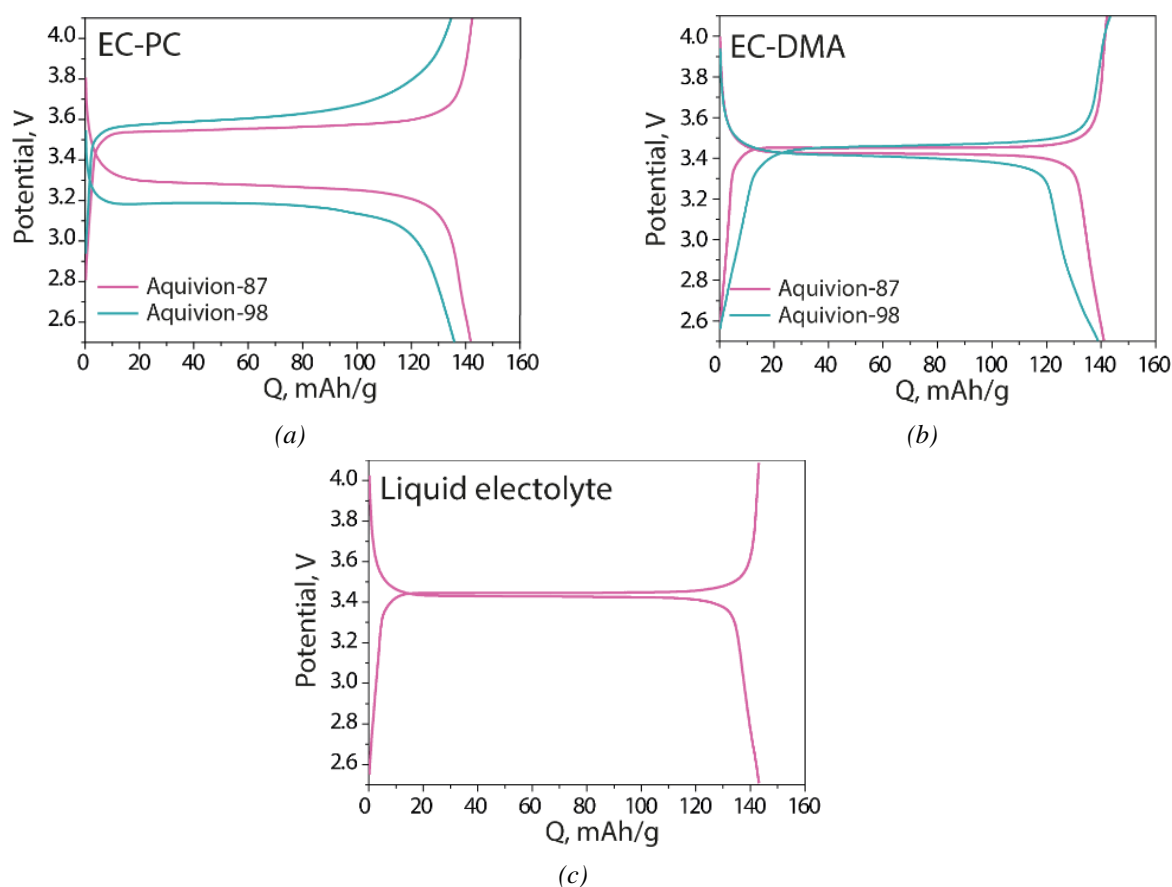


Figure 1. Typical charge-discharge curves of LFP|Li batteries with (a) Aquivion-EC-PC, (b) Aquivion-EC-DMA and (c) liquid electrolyte at 0.1C and room temperature (20th cycle).

Initial discharge capacity of LFP|Li batteries with Aquivion-87-EC-DMA and Aquivion-98-EC-DMA electrolytes was 142 and 136 mA/h/g at a cycling rate of 0.1C (Figures 1 and 2), respectively, and is practically the same as the capacity of a similar cell with liquid electrolyte ($Q_{\text{discharge}}=143$ mA/h/g). Indicated values correspond to 84% and 80% of the theoretical specific capacity of the LFP electrode. Initial discharge capacity of LFP|Li batteries with Aquivion-87-EC-PC and Aquivion-98-EC-PC and electrolytes was 141 mA/h/g and 132 mA/h/g at a cycling rate of 0.1C (Figures 1 and 2), respectively, which correspond to 83% and 78% of the theoretical specific capacity of the LFP electrode. The obtained capacity values for the investigated cells are quite close and vary within limits close to the experimental error. But this difference becomes more noticeable with increasing C-rate. Thus, when increasing the rate from 0.1C to 0.5C and 1C, the discharge capacity of the membrane Aquivion-87-EC-PC decreases by 75% and 90%, while Aquivion-87-EC-DMA decreases only by 3% and 7% due to the higher ionic conductivity of the membranes solvated by the EC-DMA mixture (Figure 2). Battery cell with membrane electrolyte

Aquivion-87-EC-DMA have shown a discharge capacity of 136 mAh/g at 1C that is comparable with or exceed the best results obtained for LFP|Li batteries with liquid electrolyte. After cycling for 70 cycles at 0.1C, capacity retention was 98.8%, 99.9%, 96.3% and 94.4% for cells with Aquivion-87-EC-DMA, Aquivion-98-EC-DMA, Aquivion-87-EC-PC, Aquivion-98-EC-PC electrolytes, respectively.

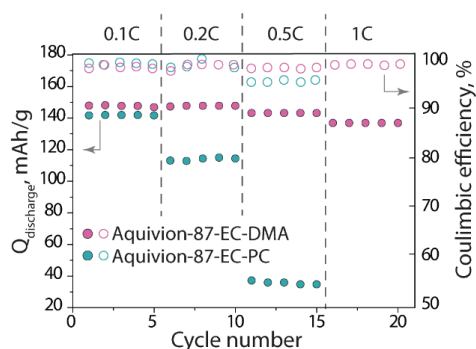


Figure 2. Values of discharge capacity and Coulombic efficiency at room temperature and different C-rates of LFP|Li batteries with Aquivion-87-EC-PC and Aquivion-87-EC-DMA electrolytes (indicated in the figure).

Acknowledgement. This work was financially supported by the Russian Science Foundation, grant No. 21-73-10149, <https://rscf.ru/project/21-73-10149>.

References

1. Qi M.; Xie L.; Han Q.; Zhu L.; Chen L.; Cao X. An Overview of the Key Challenges and Strategies for Lithium Metal Anodes // *J. Energy Storage* 2022. V. 47. Art. No 103641.
2. Evans J.; Vincent C. A.; Bruce P. G. Electrochemical Measurement of Transference Numbers in Polymer Electrolytes // *Polymer (Guildf)*. 1987. V. 28 (13). P. 2324–2328.

NEXT GENERATION ION EXCHANGE MEMBRANES

Tongwen Xu

Key Laboratory of Precision and Intelligent Chemistry, Department of Applied Chemistry, School of Chemistry and Materials Science, University of Science and Technology of China, Hefei, 230026, P. R. China, *E-mail: twxu@ustc.edu.cn*

Environmental and energy-related technologies, such as redox flow batteries, fuel cells, water electrolysis, and electro dialysis-based ion separation, are crucial to realizing peak carbon emissions and carbon neutrality. All these mentioned technologies are based on electromembrane processes and require ion exchange membranes (IEMs) to fulfill selective ion transport and the separation of anode reactions from the cathode reaction.[1] The traditional IEMs, represented by the perfluorocarbon Nafion, feature microphase-separated structure, and are well developed but suffer from the notorious conductivity/selectivity tradeoff.[2] To break this tradeoff, our group has developed the microporous paradigm with confined micropores as ion channels and demonstrated this concept with membranes made from charged polymers of intrinsic microporosity [3, 4] and ultramicroporous polymer framework membranes[5, 6]. The rigidly confined micropores within these membranes can endow both ultrahigh size-exclusion-imposed ion selectivity and ultraefficient free volume-induced permeability.[2] Notably, with the combination of rigid pore confinement and multi-interaction between ion and membrane, ultramicroporous triazine framework membranes could achieve near-frictionless ion flow.[5] The new micropore-confined IEMs have demonstrated great effectiveness in flow batteries [4, 5] and water electrolysis [6], and we believe they will also contribute to the big development of other electromembrane processes.

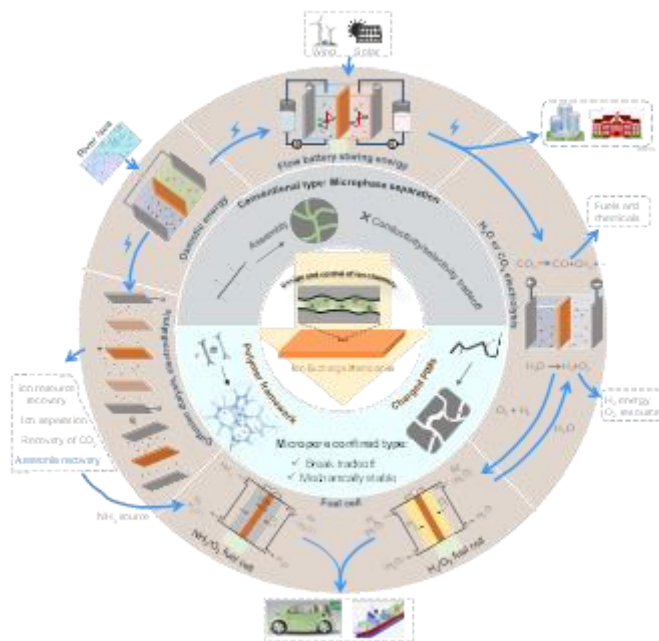


Figure 1. The conventional IEMs and Our proposed IEMs with micropore confined channels, and their potential applications.

References

1. Zuo, P. P.; Xu, Z. A.; Zhu, Q.; Ran, J.; Ge, L.; Ge, X. L.; Wu, L.; Yang, Z. J.; Xu, T. W. Ion Exchange Membranes: Constructing and Tuning Ion Transport Channels. *Adv. Funct. Mater.* 2022, 32, 2207366.
2. Zuo, P. P.; Ran, J.; Ye, C. C.; Li, X. Y.; Xu, T. W.; Yang, Z. J. Advancing Ion Selective Membranes with Micropore Ion Channels in the Interaction Confinement Regime. *ACS Nano* 2024, 18, 6016–6027.
3. Yang, Z. J.; Guo, R.; Malpass-Evans, R.; Carta, M.; McKeown, N. B.; Guiver, M. D.; Wu, L.; Xu, T. W. Highly Conductive Anion-Exchange Membranes from Microporous Troger's Base Polymers. *Angew. Chem., Int. Ed.* 2016, 55, 11499–11502.

4. Zuo, P. P.; Li, Y.; Wang, A.; Tan, R.; Liu, Y.; Liang, X.; Sheng, F.; Tang, G.; Ge, L.; Wu, L.; Song, Q.; McKeown, N. B.; Yang, Z. J.; Xu, T. W. Sulfonated Microporous Polymer Membranes with Fast and Selective Ion Transport for Electrochemical Energy Conversion and Storage. *Angew. Chem., Int. Ed.* 2020, 59, 9564–9573.
5. Zuo, P. P.; Ye, C. C.; Jiao, Z. R.; Luo, J.; Fang, J. K.; Schubert, U. S.; McKeown, N. B.; Liu, T. L.; Yang, Z. J.; Xu, T. W. Near-frictionless ion transport within triazine framework membranes. *Nature* 2023, 617, 299–305
6. Song, W. J.; Kang, P.; Xu, W.; Liu, X.; Zhang, H. Q.; Liang, X.; Ye, B. J.; Zhang, H. J.; Yang, Z. J.; Wu, L.; Ge, X. L.; Xu, T. W. Upscaled production of an ultramicroporous anion-exchange membrane enables long-term operation in electrochemical energy devices. *Nat. Commun.* 2023, 14, 2732.

PROSPECTS AND CHALLENGES OF HYDROGEN ENERGY

Andrey Yaroslavtsev

¹Kurnakov Institute of General and Inorganic Chemistry of the Russian Academy of Sciences (IGIC RAS), Moscow, Russia, *E-mail: yaroslav@igic.ras.ru*

²AO TVEL, 115409, Moscow, Kashirskoe highway, 49

Energy is still the most in-demand product. However, humanity has changed its main energy sources every century for the last three centuries due to economic expediency. The next change will be driven by humanity's concern about the deterioration of the environmental situation, a significant contribution to which is due precisely to the development of traditional energy. In this regard, it is believed that the 21st century will be marked by a transition to renewable energy sources (energy from the sun, wind, water...). A constant energy supply based on these sources is impossible without the development of energy storage devices, the main of which will be metal-ion batteries and the hydrogen cycle. The purpose of this report is to analyze current trends in the development of hydrogen energy in the world and in Russia. Moreover, fuel cells can be used to provide backup power and power equipment in the field.

One of the main problems standing on this path is the need to obtain elemental hydrogen. The hydrogen energy development program adopted in Russia was initially mainly focused on the production of hydrogen. However, the main methods for its production are associated with the conversion of natural gas and carbon, which currently occupy more than 98% of the world market [1]. At the same time, in accordance with the Paris Convention, only so-called "green" hydrogen produced from renewable sources will be sold on the international market. First of all, this includes hydrogen produced from biomass and electrolysis of water, and in the latter case, only hydrogen produced using the same renewable energy sources will be in demand. In this regard, in addition to the obvious need for fuel cells, significant attention will be paid to electrolyzers designed to produce hydrogen [2]. In addition, as part of the development of hydrogen energy, it is necessary to solve three more important problems related to the purification, storage and transportation of hydrogen. The main method of hydrogen purification at the moment is short-cycle adsorption, but membrane hydrogen purification is becoming increasingly popular. And if actively developed polymer and carbon membranes can only provide primary purification of hydrogen, membranes based on palladium alloys make it possible to provide deep hydrogen purification.

Among the methods of hydrogen storage, the most common currently is its compression, which is energy-intensive and requires the manufacture of new high-pressure cylinders. In addition, hydrogen storage seems very promising in the form of hydrides, primarily alloys, capable of absorbing quantities of hydrogen that exceed liquid hydrogen in terms of storage density.

With regard to the transportation of hydrogen, the most discussed are its transportation in cylinders, in a liquid state and using gas pipelines as an additive to natural gas. Their obvious disadvantages are energy consumption, which will significantly increase the cost of hydrogen, and the use of pipelines is complicated by significant risks associated with possible detonation and hydrogen embrittlement. In this regard, the idea of the liquid carriers (primarily cyclic hydrocarbons and ammonia, capable of participating in the processes of dehydrogenation and hydrogenation under relatively mild conditions) use is currently very popular. Lower alcohols can be added to this list, which can give quite large quantities hydrogen during steam reforming processes. The use of membrane catalysis in these processes makes it possible to obtain high-purity hydrogen in one stage.

In modern literature there are different types of fuel cells, which were initially divided according to operating temperature into low-temperature (up to 130°C), high-temperature (above 600°C) and medium-temperature. A more common classification is based on the type of membrane (electrolyte) used. From this point of view, solid polymer, alkaline, phosphoric acid, molten carbonate and solid oxide fuel cells were usually distinguished. Recently, in the world literature, the first of them, not very successfully, began to be called fuel cells based on proton exchange membranes. Alkaline fuel cells have been transformed into fuel cells based on ion exchange membranes, but this concept is not very suitable for installations that use porous membranes

impregnated with an alkali solution. Phosphoric acid fuel cells are currently almost completely reduced to units based on polybenzimidazole doped with phosphoric acid (which are often called high-temperature polymer fuel cells). Finally, two more types of devices based on medium-temperature membranes based on anhydrous acid phosphates and/or sulfates and the increasingly popular high-temperature fuel cells based on oxides with protic (or mixed proton and oxygen) conductivity have separated from solid oxide fuel cells. At the same time, there are other classifications based on the type of fuel used, the principle of heat removal, the fuel cell fragment on which the design of solid oxide fuel cells is based, etc. In this regard, we divided fuel cells according to the type of membrane used [2].

Electrolyzers can be formally thought of as fuel cells operating in reverse, generating hydrogen and oxygen from water. However, radicals are generated as intermediate products, which typically results in high overvoltage in electrolyzers. To reduce it, catalysts other than fuel cells are used [3].

The most popular type of membranes used to design fuel cells are perfluorinated sulfonic cation exchange membranes of the Nafion or Aquivion type with a short side chain. At the same time, intensive searches are being conducted for their cheaper analogues with high ionic conductivity and low gas permeability. The advantage of fuel cells based on anion-exchange membranes was mainly considered to be the novelty of this approach, although it is worth noting that the first fuel cells and electrolyzers that operated on Soviet spacecraft were, in fact, largely their prototypes. The advantage of such fuel cells is the lower corrosive activity of the environment. This allows us to count on the possibility of using non-perfluorinated membranes and catalysts based on transition metals in them. This will lead to a reduction in the cost of both fuel cells themselves and the electricity generated using them. The main problems of fuel cells on anion-exchange membranes are the low rate of hydrogen oxidation and a sharp drop in membrane conductivity due to the sorption of carbon dioxide; therefore, only gases deeply purified from CO₂, usually oxygen and hydrogen, can be used to feed them [4]. As for electrolyzers, another interesting solution was found for them - using polymer membranes with a structure close to asbestos, coated with oxides of refrigerated metals.

Acknowledgement. The work was carried out with the financial support of the Russian Science Foundation, project No. 21-73-20229.

References

1. *Stenina I., Yaroslavtsev A. Modern Technologies of Hydrogen Production.// Processes 2023, V. 11, N56.*
2. *Stenina I.A., Yaroslavtsev A.B. Prospects for the Development of Hydrogen Energy. Polymer Membranes for Fuel Cells and Electrolyzers.// Membranes Membrane Technol., 2024, V. 6, P. 15–26.*
3. *Liu L., Wang Y., Zhao Y., Wang Y., Zhang Z., Wu T., Qin W., Liu S., Jia B., Wu H., Zhang D., Qu X., Chhowalla M., Qin M. Ultrahigh Pt-Mass-Activity Hydrogen Evolution Catalyst Electrodeposited from Bulk Pt.// Adv. Funct. Mater. 2022. V. 32. N. 2112207.*
4. *Bellini M., Pagliaro M.V., Lenarda A., Fornasiero P., Marelli M., Evangelisti C., Innocenti M., Jia Q., Mukerjee S., Jankovic J., Wang L., Varcoe J.R., Krishnamurthy C.B., Grinberg I., Davydova E., Dekel D.R., Miller H.A., Vizza F. Palladium–Ceria Catalysts with Enhanced Alkaline Hydrogen Oxidation Activity for Anion Exchange Membrane Fuel Cells // ACS Appl. Energy Mater. 2019. V. 2. P. 4999-5008.*

REMOVAL OF SULFONAMIDE ANTIBIOTICS FROM WATER WITH USING OF BIOCHARS AND NANOFILTRATION

Ala Yaskevich, Tatiana Plisko, Victor Kasperchik, Katsiaryna Burts, Maryia Makarava, Maria Krasnova, Alexandr Bilydukevich

Institute of physical organic chemistry NASB, Minsk, Belarus, *E-mail: yaskevich1909@gmail.com*

Introduction

Last time contamination of environment by antibiotics and other pharmaceuticals becomes the serious ecological problem. For removal of these ones chemical, sorption, oxidative, membrane, biological methods and special constructed wetlands are used [1]. Developing of water purification technology with using of biochar (activated carbon obtained from biomass of plant or animal origin) is one of the promising solution of this problem. For example adding 0.5 g/l of biochar may increase recovery of sulfonamide antibiotics (SAA) from swine breeding wastewater by more than 30 % and reduce membrane fouling [2]. From the other hand nanofiltration (NF) can effectively remove from the water multivalent ions and organic substances with molecular mass more than 200 including antibiotics (up to 99 %) [3]. In this paper methods of fine water purification from sulfonamide antibiotics were investigated with using of adsorption on a specially obtained biochars, nanofiltration membranes and in combination of these ones.

Experiments

Compositional NF membranes were obtained by interfacial polycondensation (IPC) on the surface of ultrafiltration (UF) membranes made of polysulfone (PS). Formation of initial PS membranes was carried out from 2 types of casting solution:

- 1 – PS–polyvinyl pyrrolidone (PVP)–N,N–dimethyl acetamide (DMAA);
- 2 – PS–polyethylene glycol (PEG)–PVP–DMAA.

Water solution of piperazine (PIP) and solution of trimesoyl chloride (TMC) in Nefras C2 were used for the interfacial polycondensation. Determination of the transport characteristics of obtained NF membranes were conducted in the stirred filtration cell (200 min^{-1}) at transmembrane pressure 0.5 MPa. Concentrations of calibrant ($0.2\% \text{ MgSO}_4$) in filtrate and in a bulk solution were determined by interferometer LIR–2.

Sulfadimethoxine («BLDpharm», China) as a model SAA was used in experiments for water purification. Concentration of sulfadimethoxine was controlled by spectrophotometer Metertech SP8001 (wavelength 267 nm). Mini column with biochar (thickness of layer 3 cm) was made for conducting of experiments for water purification from SAA. Biochar with particle size in a range 380–830 μm was obtained by combination of pyrolysis and hydrothermal carbonization. Samples of the biochar were supplied by Xenan Normal University (China). Circulation of water with dissolved antibiotic through the column with biochar was provided by peristaltic pump at 90 ml/min. Pressure drop in these conditions was negligible. For intensification of sorption processes 0.0125 mmol/l potassium peroxomonosulfate (PMS) was added to sulfadimethoxine solution. When PMS interacting with a stable radicals of biochar generated active oxygen leads to the degradation of dissolved antibiotics.

Results and Discussion

Two different types of NF membranes were obtained by reaction of the interfacial polycondensation on the initial UF membranes (table). Formation composition 1 (PS–PVP–DMAA) was allowed to obtain structures with a middle selectivity ($R_{\text{MgSO}_4} = 91\text{-}95\%$). The most selective NF membranes were obtained from formation composition 2 (PS–PEG–DMAA). In this case rejection of MgSO_4 was 99 % and higher.

Table. Transport characteristics of NF membranes. Calibrant – 0.2% MgSO₄

Nanofiltration membrane	Composition of ultrafiltration membrane	J, l m ⁻² h ⁻¹	R, %
NF-1	PS-PVP-DMAA	11-38	91-95
NF-2	PS-PEG-PVP-DMAA	19-27	≥99

Investigation of influence of the concentration and circulation time of antibiotic solution through column with biochar is presented on figure 1. Efficiency of SAA removal from solutions by a combination of biochar adsorption and nanofiltration is presented on figure 2. As it can be seen from experimental data degree of the antibiotic removal from the water solution with concentration 5 mg/l increases in time and after 30 minutes carrying out of sorption process becomes 71%. Then a slight decreasing of amount of the adsorbed antibiotic is observed. After increasing of antibiotic concentration up to 21 mg/l degree of antibiotic removal was 69 % after 10 minutes of carrying out of sorption process. Then degree of removal was increasing up to 88 %.

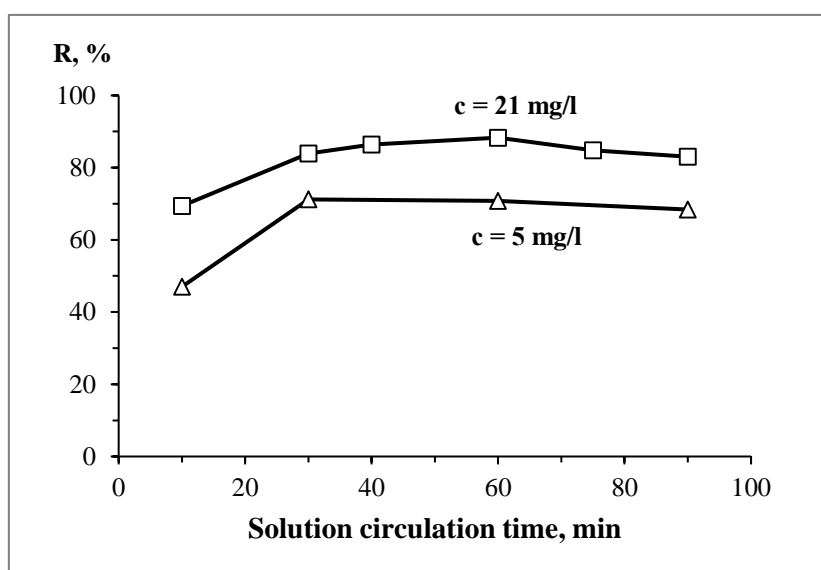


Figure 1. SAA removal rate vs. solution circulation time through a biochar column.

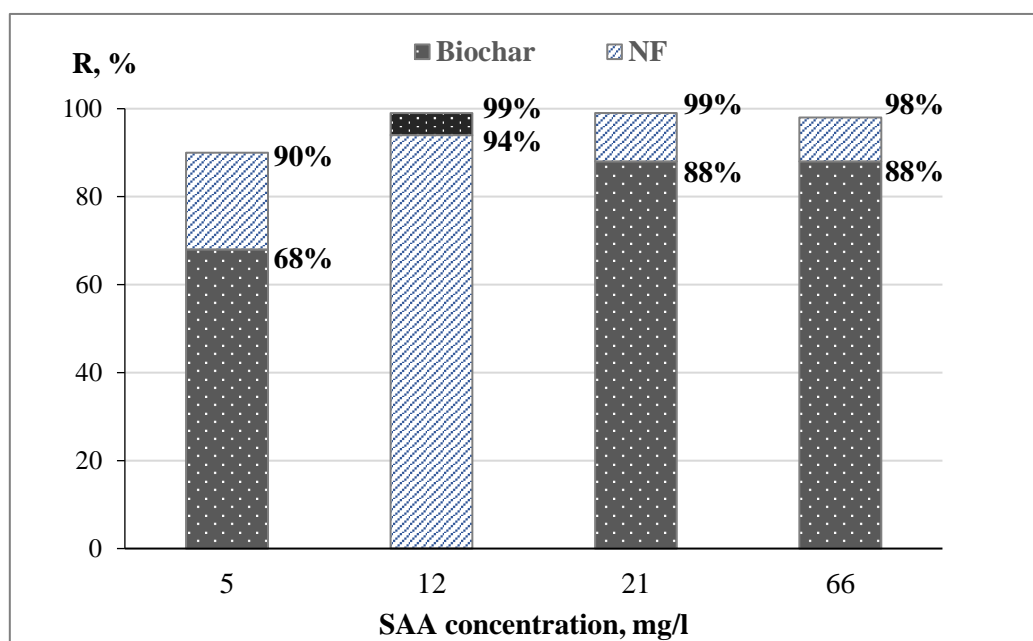


Figure 2. Efficiency of SAA removal from solutions by a combination of biochar adsorption and nanofiltration.

Finish purification of water from antibiotics and products of its degradation was carried out on nanofiltration membranes with the highest selectivity (NF-2). Degree of antibiotic removal from solution with initial concentration 5 mg/l after sorption on biochar and filtration on NF membrane was increased up to 90 % (figure 2). For solution with initial concentration 21 mg/l finish purification with using of NF membrane was removed SAA up to 99 %. For solution with highest concentration SAA (66 mg/l) after 95 minutes of sorption on biochar degree of removal was 88 % and after nanofiltration stage – 98 %. Investigation of the one step of nanofiltration of SAA solution with 12 mg/l was showed that degree of antibiotic removal was reached 94 %. Finish purification of obtained filtrate on column with biochar during 40 minutes was allowed degree of SAA removal up to 99% and higher.

Thus it was established that combination of adsorption on biochar with additional radical degradation and nanofiltration with using of compositional membranes obtained by interfacial polycondensation on the surface of ultrafiltration membranes made of polysulfone was allowed SAA removal from water solutions on 90–99% in dependence on conditions of process conducting.

Acknowledgements. Work is supported by the Belorussian Foundation for Basic Research, projectX23KI-024.

References

1. *De Ilurdoz M.S., Sadhwani J.J., Reboso J.V.* Antibiotic removal processes from water & wastewater for the protection of the aquatic environment-a review // *J. Water Proc. Eng.* 2022. V. 45. P. 102–474.
2. *Cheng D. [et al.]* Improving sulfonamide antibiotics removal from swine wastewater by supplying a new pomelo peel derived biochar in an anaerobic membrane bioreactor // *Biores. Tech.* 2021. V. 319. P. 124–160.
3. *Zhao S. [et al.]* Removal of antibiotics using polyethylenimine cross-linked nanofiltration membranes: Relating membrane performance to surface charge characteristics// *Chem. Eng. J.* 2018. V. 335. P. 101–109.

GRAFTED MEMBRANES BASED ON FLUORINATED FILMS AND POLYANILINE FOR ION SEPARATION

Polina Yurova, Irina Stenina, Andrey Yaroslavtsev

Kurnakov Institute of General and Inorganic Chemistry RAS, Moscow, Russia

E-mail: polina31415@mail.ru

Introduction

The rapid development of society and population growth lead to the need for the most efficient use of the resources available to humanity. In particular, one of the most important resources is fresh water. Electrodialysis (ED) is an effective method of water purifying. In addition, ED allows separating ions of the same signs, but of different valences [1]. ED uses cation- and anion-exchange membranes [2]. It is promising to develop new ion selective materials to increase the efficiency of electrodialysis. Graft polymerization is one of useful methods for the production of ion-exchange membranes. Moreover, certain properties can be imparted to ion-exchange membranes by additional modification with conducting polymers. Polyaniline is a conducting polymer that is easy to synthesize, stable, and has anion-exchange properties. An anion-exchange layer on a cation-exchange membrane can reduce the amount of doubly charged cations in membrane, which can lead to increased selectivity to singly charged cations.

Experiments

Cation-exchange membranes based on PVDF or ETFE films and polystyrene were obtained by the emulsion method with further sulfonation of the grafted polystyrene using chlorosulfuric acid and hydrolysis of functional groups. Then, membranes were conditioned by heating in a sodium chloride solution and water. Only one side of the membrane was modified by polyaniline. To do this, membrane was fixed in a two-section cell. A solution of aniline hydrochloride was in one of the sections, and water in another. The membrane was kept in the cell for 10 minutes, after that the aniline hydrochloride solution was replaced with an oxidizing agent ($(\text{NH}_4)_2\text{S}_2\text{O}_8$). Before studying of the obtained samples, membranes were washed by a sodium chloride solution and water.

Ion exchange capacity, conductivity in contact with water, transport numbers and selectivity were determined for the prepared samples.

Results and Discussion

The conductivity and transport numbers of the grafted membranes based on both PVDF and ETFE films strongly depend on the grafting degree. Membranes for modification were selected based on the combination of these parameters. Modification with polyaniline leads to an increase in the cation transport number from 0.7 to 0.9 and higher for membranes based on PVDF films. The obtained samples demonstrate a significant increase in selectivity to sodium and lithium cations: $P(\text{Na}/\text{Ca})$ increase from 0.7 to 1.9 and $P(\text{Li}/\text{Mg})$ from 0.5 to 2.8. The introduction of polyaniline into as-prepared membranes leads to a decrease in conductivity in the sodium form, but for ion separation tasks this deterioration in properties is insignificant.

Thus, in this study, a method for manufacturing of materials with high selectivity towards singly charged ions and high cation transport numbers was developed.

Acknowledgement. This work was financially supported by Russian Science Foundation, grant No 23-43-00138, <https://rscf.ru/en/project/23-43-00138/>.

References

1. Tekinalp Ö., Zimmermann P., Holdcroft S., Burheim O.S., Deng L. Cation Exchange Membranes and Process Optimizations in Electrodialysis for Selective Metal Separation: A Review // *Membranes* 2023, 13, 566
2. Sedighi M., Mahdi Behvand Usefi M., Fauzi Ismail A., Ghasemi M. Environmental sustainability and ions removal through electrodialysis desalination: Operating conditions and process parameters // *Desalination*, 2023, 549, 116319

MULTILAYER ION EXCHANGE MEMBRANES AND ELECTROMEMBRANE PROCESSES FOR ENVIRONMENTALLY FRIENDLY CLOSED CYCLE TECHNOLOGIES

Victor Zabolotsky, Stanislav Melnikov, Sergey Loza, Nikolay Sheldeshov, Aslan Achoh, Nikita Kovalev, Denis Bondarev

Kuban State University, Krasnodar, Russia, *E-mail: vizab@chem.kubsu.ru*

This paper presents the results of research aimed at addressing two significant challenges in membrane electrochemistry. The first objective concerns membrane materials and involves the development of bilayer membranes with high charge selectivity. The second objective pertains to the electrodialysis technique and focuses on enhancing the mass transfer properties of the electrodialysis process using bipolar membranes.

To tackle the first issue, various approaches have been devised to create bilayer ion-exchange membranes, both heterogeneous and homogeneous, with exceptional selectivity towards singly charged metal cations. An anion exchange layer composed of a copolymer of N,N-dimethyl-N,N-diallylammonium chloride and ethyl methacrylate was selected. Notably, homogeneous bilayer membranes were successfully fabricated by combining the MF-4SK cation exchange membrane with the developed copolymer. Through scanning electron microscopy and IR spectroscopy, the presence of a modifying anion-exchange layer on both types of bilayer membranes was confirmed.

In all instances of the developed bilayer membranes, the limiting electrodiffusion current value was found to be dependent on the thickness of the modifying layer. The specific selective permeability of these membranes was shown to be governed by the equilibrium and transport characteristics of the modifying layer, particularly for co-ions. By utilizing the experimentally determined parameters of electromembrane systems with the bilayer membranes, a previously established four-layer model of ion transport in mixed solutions of ternary electrolytes was validated. However, a loss of selectivity was observed in all bilayer membrane samples once the limiting state was reached.

The implementation of bilayer membranes has significantly enhanced the selectivity of membranes towards singly charged ions during concentration processes. The findings regarding the impact of electrolyte nature and membrane properties on transport mechanisms can be instrumental in the design and operation of electrodialyzer concentrators.

A methodology has been devised for computing the effective constants of the limiting stages of the water dissociation reaction in heterogeneous bipolar membranes containing a catalytic additive. This method leverages the current-voltage characteristic equation, aligning with contemporary fundamental insights into the water molecule dissociation mechanism in bipolar membranes and the structure of heterogeneous bipolar membranes.

The research outcomes also encompass the production of sodium and lithium hydroxides from carbonate and sulfate solutions using asymmetric bipolar membranes. Notably, utilizing sodium carbonate as the initial solution has enabled a substantial increase in the resulting alkali concentration from 0.92 M to 1.7 M under comparable process conditions. The current efficiency for alkali exceeds 70% in all experiments when sodium carbonate is employed, whereas it drops to 40-50% when producing alkali from a sodium sulfate solution with NaOH concentrations exceeding 0.8 M. The energy consumption for transferring one kilogram of alkali ranges from 2.8 to 13.9 kWh/kg at operating current densities of 1-3 A/dm².

Acknowledgement. This study was supported by the Russian Science Foundation, research project no. 22-13-00439, <https://rscf.ru/project/22-13-00439>.

THE APPLICATION OF CAPACITIVE DEIONIZATION FOR WATER TREATMENT AND RESOURCE RECOVERY

Changyong Zhang

CAS Key Laboratory of Urban Pollutant Conversion, Department of Environmental Science and Engineering, University of Science & Technology of China, Hefei 230026, China

E-mail: changyongzhang@ustc.edu.cn

With the increasing severity of global water scarcity, a myriad of scientific activities is directed towards advancing brackish water desalination and wastewater remediation technologies. Flow-electrode capacitive deionization (FCDI), a newly developed electrochemically driven ion removal approach combining ion-exchange membranes and flowable particle electrodes, has been actively explored over the past seven years, driven by the possibility of energy-efficient, sustainable and fully continuous production of high-quality fresh water, as well as flexible management of the particle electrodes and concentrate stream.¹ Here, we provide a comprehensive overview of current advances of this interesting technology with particular attention given to FCDI principles, designs (including cell architecture and electrode and separator options), operational modes (including approaches to management of the flowable electrodes), characterizations and modelling, and environmental applications for water treatment and resource recovery. Furthermore, we introduce the definitions and performance metrics that should be used so that fair assessments and comparisons can be made between different systems and separation conditions.² We then highlight the most pressing challenges (i.e. operation and capital cost, scale-up and commercialization) in full scale application of this technology. We conclude this state-of-the-art review by considering the overall outlook of the technology and discussing areas requiring particular attention in future.

References

1. Changyong Zhang, Jinxing Ma, Lei Wu, Jingyi Sun, Li Wang, Tianyu Li, T. David Waite*. Flow electrode capacitive deionization (FCDI): recent developments, environmental applications and future perspectives. *Environmental Science & Technology*. 2021, 55, 5243-4267.
2. Changyong Zhang, Lei Wu, Jinxing Ma, An Ninh Pham, Min Wang, and T. David Waite*. Integrated flow-electrode capacitive deionization and microfiltration system for continuous and energy-efficient brackish water desalination. *Environmental Science & Technology*. 2019, 53(22), 13364-13373.
3. Changyong Zhang, Jinxing Ma, Jingke Song, Calvin He, and T. David Waite*. Continuous ammonia recovery from wastewaters using an integrated capacitive flow electrode membrane stripping system. *Environmental Science & Technology*. 2018, 52(24), 14275-14285.
4. Changyong Zhang, Xiang Cheng, Min Wang, Jinxing Ma, Richard Collins, Andrew Kinsela, Ying Zhang, T. David Waite*. Phosphate recovery as vivianite using a flow-electrode capacitive desalination (FCDI) and fluidized bed crystallization (FBC) coupled system. *Water Research*. 2021, 194, 116939.

IMPACT OF STRUCTURE OF REDOX POLYMER ON ELECTROCHEMICAL PROPERTIES OF GLUCOSE BIOSENSORS

¹Ekaterina Zolotukhina, ¹Alexei Vinyukov, ¹Andrey Starikov, ¹Ekaterina Gerasimova, ¹Sofia Kleinikova, ¹Konstantin Gor'kov, ²Vsevolod Pavlov

¹Federal Research Center of Chemical Physics and Medicinal Chemistry of Russian Academy of Sciences, Chernogolovka, 142432, Russia, *E-mail: zolek@icp.ac.ru*

²M.V. Lomonosov Moscow State University, Moscow, Russia

Introduction

Glucose biosensors applying for glucose in blood or interstitial fluid analysis functioned on the base of mediated bioelectrocatalytic reaction between enzyme glucose oxidase (mostly used) and mediator. The mediators in biosensors for continuous monitoring of glucose level in interstitial fluid (SCMG) constructed from redox polymer with functional redox centers (transition metal complexes) and chemical groups allowing to bind the enzyme with polymer structure via coordination or covalent bonds. The polymer structure and the nature of redox center are important for selective, sensitive and long-term analysis of glucose level in tissue fluid of human. In Russia the commercial or R&D technologies for fabrication of such biosensors or redox polymers are absent. So, the approaches for synthetic procedure, design of such polymers and studying of their electrochemical properties in the structure of biosensor is very important task for creation of domestic products for glycemia continuous control. This work is dealing with development of synthetic procedure of various types of redox polymers based on ferrocene derivatives or osmium (III) complexes as the redox centers and studying of their electrochemical and electroanalytical properties in glucose bio-oxidation reaction.

Experiments

Three types of redox-polymers were synthesized based on poly-4-vinylpyridine (PVP) by the use of original synthetic approaches. 6-ferrocenyl(*n*-hexyl)amine, osmium (III) N,N'-dimethyl-2,2'-biimidazolium dichloride and [Os(III)(N,N'-dimethyl-2,2'-biimidazolium)₂(N-(6-aminohexyl)-N'-methyl-2,2'-biimidazolium)](Cl₆)₃ were used for modification of PVP. As a result, two redox polymers with covalently bounded redox centers (ferrocene-containing, Fc-RP, and Os(III)-containing, Os-RP(II)) and one redox polymer with coordinately bounded redox centers, Os-RP(I), were designed. These polymers were used for sensor active layer preparation. The glucose oxidase, GOx, solution and cross-linking agent, PEGDGE, were mixed with redox-polymers solutions. In some experiments the carbon black was added to composition of active layer to increase the electron conductivity. Drop casting method was used to modify the working electrode of three-electrode screen-printed test-strips (SPE). Glucose model solutions (0, 1, 2, 5, 10, 20, 30 mM) in potassium phosphate buffer, pH 7.4, isotonized with 0.15 M sodium chloride, were used for amperometric measurements.

Results and Discussion

The work of SCMG sensors is based on conjugation of biochemical reaction between enzyme with glucose and electrochemical reaction of redox polymer transformation on electrode. The oxidation of reduced enzyme forming during biochemical reaction occurs as a result of its reaction with transition metal ions of redox centers of polymer. This interaction leads to reduction of polymer redox centers. The polarization of working electrode at potential corresponded to oxidation of mediator reduced form allows to measure the read-out current of sensor. To realize this complicated mechanism of biosensor functioning the enzymatic and redox centers should be placed close to each other with uniform distribution in the whole polymer layer. Stability of read-out signal in time is provided for cross-linking of all components participating in bioelectrochemical reaction. So, the ratio of redox polymer to GOx in active layer, the nature of redox center, the nature and concentration of cross-linking agent were the key factors for glucose sensitivity of prepared SPEs. In addition, the nature of redox centers played an important role in electroanalytical properties of modified SPEs. SPE modified with Fc-RP demonstrated reversible

redox-responses at 0.2 V in buffer solution vs silver chloride electrode. This value is too high for sufficient analytical properties of glucose biosensors due to ascorbic acid and other analytes cross sensitivity. Nevertheless, these sensors demonstrated the good calibration dependence on glucose concentration in solution. However, one week later the responses were diminished several times due to degradation processes in active layer. Similar effect was described in our previous work [1].

The low content of redox centers in Os-RP(I) leads to absence of any visible redox-responses on CVs for corresponding SPEs, while as an individual component Os(III) complex using for preparation of this redox polymer demonstrated reversible redox peaks at -0.3 V vs silver chloride electrode.

The best stability and electroanalytical properties demonstrated the SPEs modified with Os-RP(II) active layer. The redox transformation of such complex occurred at -0.23 V. Optimization of active layer composition allowed to achieve the high current responses in dependence on glucose concentration with high stability in long-term tests with permanent polarization. So, these redox-polymers could be considered in SCMG devices.

Acknowledgement. This was supported within the thematic map 124013000692-4.

References

1. *E.V. Zolotukhina, E.V. Gerasimova, V.V. Sorokin, M.G. Levchenko, A.S. Freiman, Y.E. Silina.* The impact of the functional layer composition of glucose test-strips on the stability of electrochemical response // *Chemosensors*. 2022. V. 10(8). P. 298. 10.3390/chemosensors10080298

TOWARDS REDOX MEDIATOR NATURE AND COMPOSITION OF ACTIVE LAYER IN STABILITY OF GLUCOSE TEST-STRIPS DURING STORAGE

¹Ekaterina Zolotukhina, ¹Alisa Freiman, ¹Ekaterina Gerasimova, ²Polina Afanasieva

¹Federal Research Center of Chemical Physics and Medicinal Chemistry of Russian Academy of Sciences, Chernogolovka, 142432, Russia, *E-mail: zolek@icp.ac.ru*

²M.V. Lomonosov Moscow State University, Moscow, Russia

Introduction

Glucose biosensors applying for glucose in blood functioned on the base of mediated bioelectrocatalytic reaction between enzyme glucose oxidase (mostly used) and redox mediator. Commercially used glucose test strips mostly used ferricyanide/ferrocyanide redox transformation for conjugation of biochemical reaction and electron transfer on the electrode. To achieve the long-term stability during storage of test-strips the gel polymers like carboxymethylcellulose (CMC) or other types of polymers used in composition of active layer. To prevent the degradation of enzyme activity the carbohydrates additions and cross-linking agents are using. This work is dealing with study of impact of design and composition of active layer for glucose test-strips on stability of electroanalytical response of biosensor during storage stress-test.

Experiments

Ferricyanide (FC) and ferrocene (Fc) redox mediators were used for active layer preparation. Glucose oxidase (GOx) was used as an active enzyme, CMC, sodium alginate (ALG) and Aerosil 380 (AS) were used as the gel and filler agents. PEGDGE as a cross-linking agent were used for several tests. The high temperature storage during several weeks were used as a stress-test to check the long-term stability of test-strips response. Amperometric measurements at oxidative peak potential of redox mediator were used for calibration of test strips in model glucose solutions pH 7.4.

Results and Discussion

Composition and nature of gel components of active layer strongly affected on stability of electrochemical response of test strips [1]. For the conventional test-strips without usage of any filler agents, i.e. CMC/FC/GOx, the degradation of sensitivity on 25% occurred already after 10 days of stress-test at 55 °C (corresponds to 247 days of storage at 20 °C) and reached 36% for 30th day (corresponds to 741 days of storage). The reason of such an extensive degradation is the multidirectional changes of current responses occurring in the whole range of glucose concentration: thus, at the low glucose concentration the current increases and at the high concentration it decreases. In contrast, for the ALG-based test-strips containing 24 mg/mL GOx in citrate buffer, pH 6.0, (CMC/ALG/FC/GOx) after the initial diminution of sensitivity on 20% within the consequent 28 days (corresponds to 624 days of storage at 20 °C) the sensitivity was practically the same, i.e. $3.1 \pm 0.2 \mu\text{A}/\text{mM}$ with only 7.7% of current variation. The diminution of GOx content in the layer or replacement of citrate buffer by phosphate one with pH 7.4 did not change this tendency for the ALG-based gels. The reason of deviation from linearity seen at the high glucose concentration for the ALG-containing gels is the diminution of current responses. At the same time, the degradation degree of sensitivity for the AS-containing test-strips as well as deviation from linearity were much higher and the current diminution occurs already for analytically significant level of glucose, i.e. 0 – 5 mM. Moreover, for the AS-containing gels the degradation degree strongly depended on buffer type. In citrate buffer the degradation degree of sensitivity for the gels based on AS was about 30% - 55% in dependence on GOx concentration. In phosphate buffer with pH 7.4 the diminution in sensitivity reached the level of ~ 80%.

The current degradation occurring during test-stress discussed above can be a result of two processes: (I) the mediator loss/change and/or (II) protein activity lost, i.e. due to water loss. It should be mentioned that the loss of enzyme activity in the majority leads to complete and fast signal degradation (loss of activity happens immediately after heating) in the whole concentration range or to the gradual decrease of electrochemical response.

To verify a separate role of process (I) or (II) and to show the impact of biochemical reaction caused by change in enzyme activity at the high glucose concentration level apart from a parallel mediator degradation on the electrochemical response, next, GOx was deactivated by heating of test-strips at 120 °C for 30 s. In this case the loss of sensitivity was visible in the whole tested concentration range. In other words, the degradation of enzyme (process II) was responsible for the lost in sensitivity of glucose test-strips. Hence, the reason of current degradation at high glucose concentration during heating at 55 °C (corresponds to 24 months at 20 °C) most likely was caused by instability of RedOx (process I) mediator (i.e. FC) than by degradation of bioreceptor (GOx).

The LDI-MS analysis and UV-visible spectroscopy verify the degradation of FC inside the active layer due to chemical interaction of this mediator with organic components.

The use of Fc as a mediator increased the stability of analytical response of test-strips during stress-tests. Keeping in mind the insolubility of this redox-mediator the carbon additions was used in composition of active layer. The results of safety tests are presented on Fig. 1.

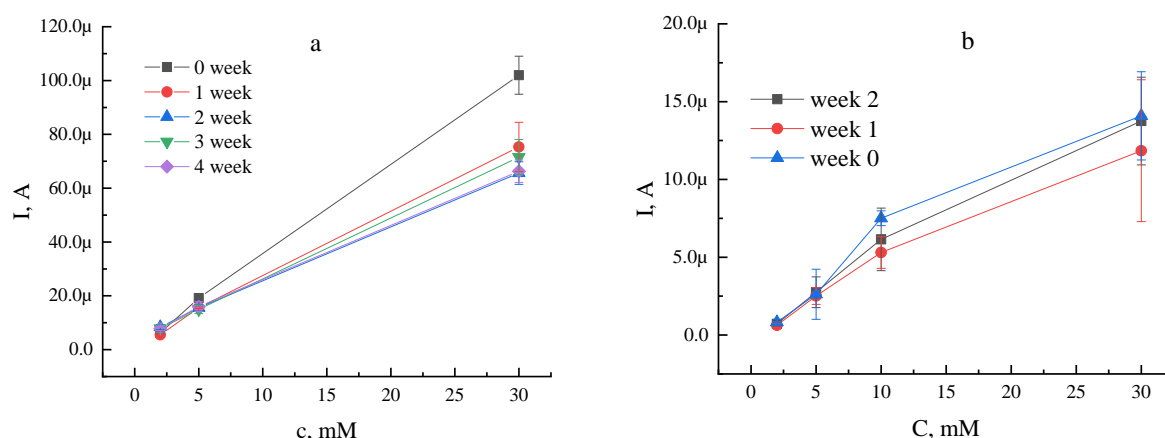


Figure 1. The results of stress-tests during storage of test-strips with FC (a) and Fc (b) at high temperature.

To sum it up, the water balance in layer supported by filler agent and the stability of using redox mediator are the key factors for stability of electrochemical properties of glucose test-strips during storage.

Acknowledgement. This was supported within the thematic map 124013000692-4.

References

1. E.V. Zolotukhina, E.V. Gerasimova, V.V. Sorokin, M.G. Levchenko, A.S. Freiman, Y.E. Silina. The impact of the functional layer composition of glucose test-strips on the stability of electrochemical response // *Chemosensors*. 2022. V. 10(8). P. 298. 10.3390/chemosensors10080298

Index of author

A

Achov A. 14, 17, 159, 265,
338
Afanaseva D. 302
Afanasieva P. 342
Ahmadova J. A. 20
Akberova E. 23, 318
Akimochkina G. 119
Aleksandrov P. 116, 310
Alekseenko A. 26, 29, 42, 203,
227, 230
Alekseenko D. 29
Alekseev M. 32, 87, 242
Alimov V. 130
Andreev G. 35, 233, 249
Andreyanov F. 173
Anisimov A. 37
Anokhina T. 37, 49, 189, 191,
210, 215, 254, 257
Arapova M. 40, 52, 54,
Astashkina O. 152
Astravukh Y. 26, 230
Averianov I. 109, 277
Avilova I. 324

B

Balynin A. 213
Baranov O. 164
Barros K. S. 41
Bayan J. 26
Bazhenov S. 49, 95, 106, 189
Belenov S. 29, 42
Belmesov A. 207
Bermeshev M. 173
Bespalova Y. 318
Biesheuvel M. 45
Bilyukevich A. 334
Bondarev D. 14, 17, 46, 265,
338
Borisov I. 49, 97, 189, 191,
254, 257, 259
Bragina O. 40, 52, 54, 59,
291
Brant J. 138
Brehant A. 78
Brovkina M. 169
Budnikov A. 55, 308
Burts K. 334
Busko V. 130

Busnyuk A. 130
Butylskii D. 55, 57, 308
Bychkov S. 40

C

Cherendina O. 59, 291
Chernysheva D. 293
Chizhik S. 145
Chubyr N. 60
Chuprynina D. 127, 235
Cihanoğlu A. 63
Cipollina A. 64, 78
Cortina J. L. 64
Culcasi A. 64

D

Dammak L. 239
Danilenko M. 104
Demekhin E. 32, 84, 87, 242
Demidenko K. 67, 71, 133
Didenko A. 49, 257
Dmitrenko M. 69, 70, 157, 201, 298
Dobryden S. 318
Don G. 207
Dubovenko R. 69, 70, 157, 201,
298
Dyachkov A. 302
Dzhimak S. 35, 249

E

Elshina M. 71
Elsuf'iev E. 119
Ermakova L. 80
Ershova T. 37
Esina A. 73
Eterevszkova S. 197
Evdochenko E. 100
Fadeeva N. 119
Falina E. 71
Falina I. 67, 75, 133, 167,
169, 174, 199
Faykov I. 76
Filingeri A. 64, 78
Filippov A. 80, 116, 310
Filloux E. 78
Fomenko E. 119
Fouad M. 83
Frants E. 84
Freiman A. 342

G

Ganchenko G. 32, 87, 242
 Gerasimov E. 230
 Gerasimova E. 340, 342
 Gessen M. 280
 Gil V. 89
 Goikhman M. 76
 Golubenko D. 179
 Golubev G. 97
 Golubkov S. 207
 Gor'kov K. 340
 Gorobchenko A. 92, 187, 268
 Grushevenko E. 95, 97, 191, 210, 259
 Guliaeva V. 100, 122, 237, 247
 Guskov R. 83, 102, 145
 Guterman V. 26, 29, 104, 227, 230

I

Ivanchenko A. 174
 Ivanin S. 35, 233, 249

K

Kalmykov D. 95, 106
 Kardash M. 303, 306, 313
 Karpenko T. 109, 277, 288
 Karyakina A. 157
 Kashin A. 207
 Kasperchik V. 334
 Kayumov R. 112, 163, 285, 286
 Kazakovtseva C. 114
 Khanukaeva D. 116, 310
 Kharchenko I. 119, 271
 Khashirova S. 49, 254
 Khohlova M. 59, 291
 Kim K. 146
 Kislyi A. 100, 122, 124, 237, 247
 Kleinikova S. 340
 Klevtsova A. 100, 127, 235, 237, 247
 Kolinko P. 130
 Kononenko N. 73, 75, 133, 169, 174, 199, 268, 283, 306
 Korshunova A. 127, 235
 Korzhov A. 135, 265
 Korzhova E. 138, 164, 239
 Kovalchuk N. 71, 140, 171, 262
 Kovalenko A. 60, 114, 142, 208
 Kovalev I. 83, 102, 145
 Kovalev N. 277, 338
 Kozaderov O. 146, 149

Kozaderova O. 146, 149
 Kozhokar E. 26
 Kozlova M. 203
 Kozmai A. 89, 124
 Krasnova M. 334
 Krylov A. 84
 Kudrinskaya O. 152
 Kulshrestha V. 154
 Kutenko N. 155
 Kuzminova A. 69, 70, 157, 201, 298

L

de Labastida M. F. 64
 Laipanova Z. 60
 Lapshin A. 112, 285, 286
 Lazarev D. 280
 Lazarev S. 280
 Láznička V. 292
 Lebedev D. 271
 Lebedev K. 159
 Levchenko A. 207
 Li X. 162
 Likhomanov V. 207
 Livshits A. 130
 Lochina A. 112, 163, 285, 286
 Lopatin D. 89, 138, 164, 239
 Lopez J. 64
 Loza J. 71, 167
 Loza N. 75, 155, 167, 169
 Loza S. 71, 135, 140, 171, 262, 338
 Lunin A. 173
 Lyapishev K. 174
 Lysenko A. 321
 Lysova A. 177, 179

M

Makarava M. 334
 Maksimova A. 181
 Malakhov A. 257
 Manin A. 179, 184
 Mareev A. 187
 Mareev S. 32, 92, 124, 187, 247
 Markelov A. 215
 Matveev D. 29, 189, 191, 254
 Matveeva J. 95, 259
 Melnikov S. 14, 17, 46, 194, 197, 221, 338
 Menshikov V. 42
 Meshcheryakova E. 133, 199
 Micale G. 64, 78
 Mikhailovskaya O. 201

Mikulan A.	70		
Minenko A.	265		
Moguchikh E.	26, 42, 203		
Molodtsova T.	293		
Moroz I.	32, 100, 122, 187, 205, 237, 247		
Morozova S.	207		
Morshneva I.	242		
Muzafarov A.	37		
Myznikov D.	70		
N			
Nazarov R.	208		
Nebesskaya A.	210, 213, 215		
Nechaev G.	163		
Nemtsev I.	271		
Nemudry A.	40, 52, 54, 59, 83, 102, 145, 217, 291		
Nevelskaya A.	42		
Niftaliev S.	146		
Nikonenko V.	57, 92, 124, 142, 187, 205, 208, 219, 244, 268		
Nosova E.	221		
Novikov A.	52		
Novikova S.	327		
P			
Pankov I.	224, 230		
Pankova J.	26, 227		
Paperzh K.	26, 104, 227		
Papezhuk M.	35, 233, 249		
Pasechnaya E.	127, 235		
Pasechnik A.	71		
Patykovskaya M.	114		
Pavlets A.	26, 42, 203, 230		
Pavlov V.	340		
Penkova A.	69, 70, 157, 201, 298		
Peredistov E.	130		
Pérez-Herranz V.	41		
Petriev I.	35, 233, 249		
Petryakov M.	187, 205		
Philibert M.	78		
Philippova T.	80		
Pismenskaya N.	127, 219, 235, 296		
Pismenskiy A.	142		
Plekunova V.	71		
Plinier K.	302		
Plis V.	100, 122, 237, 247		
Plisko T.	334		
Polotskaya G.	76		
Ponomar M.	127, 205, 239, 244, 268		
		Ponomarev R.	242
		Popov M.	83, 102, 145
		Popov V.	87
		Porozhnyy M.	89, 244
		Prokhorov N.	35, 233, 249
		Prokhorov Y.	100, 122, 237, 247
		Pulyalina A.	76
		Pushankina P.	35, 233, 249
		Pyrkova A.	252
R			
		Raeva A.	254, 257
		Rokhmanka T.	97, 259
		Romanyuk N.	140, 171, 262, 265
		Rubinstein I.	267
		Ruleva V.	205, 268
		Ryzhkov I.	45, 119, 181, 271
S			
		Safronova E.	274, 300, 327
		Salichov R.	57
		Saltykov S.	130
		Samoilenko A.	46
		Sanginov E.	207
		Sarapulova V.	239, 244
		Selyutin A.	69
		Sharafan M.	17, 135, 219, 265
		Shchegolikhina O.	37
		Sheldeshov N.	109, 277, 288, 338
		Shelistov V.	87
		Shestakov K.	280
		Shirokikh S.	106
		Shkirskaaya S.	73, 268, 283
		Shmygleva L.	112, 163, 285, 286
		Shramenko V.	109, 288
		Shubnikova E.	40, 52, 54, 59, 291
		Shvorobei Y.	210
		Simonov A.	35, 233, 249
		Simunin M.	271
		Sinev I.	303
		Slouka Z.	292
		Smirnova N.	57, 140, 293
		Sokolov S.	259
		Solonchenko K.	296
		Solovyova A.	203
		Starikov A.	340
		Statsenko T.	207
		Stenina I.	252, 337
		Stepanova A.	157, 298
		Stretton N.	300
		Strilets I.	306

Strnad J.	292	Volkov Vladimir	49, 189, 191, 213, 215
Sushkova K.	70, 201	Volkov Vitaly	324
T			
Tamburini A.	64, 78	Volkova I.	119
Terentyev A.	302	Voropaeva D.	327
Terin D.	303, 313	Voroshilov I.	89, 164, 239
Tikhonova E.	306	X	
Timofeev S.	67, 133, 169, 199	Xu T.	330
Titskaya E.	67	Y	
Troitskiy V.	55, 57, 308	Yaroslavtsev A.	177, 179, 184, 252, 274, 300, 327, 332, 337
Troshkin A.	310	Yaskevich A.	334
Tsaturyan A.	224	Yurchenko O.	296
Turaev T.	303, 313	Yurova P.	337
Turin I.	303	Yushkin A.	210, 213, 215
U			
Ulyankina A.	293	Z	
Urtenov M.	60, 114, 142, 208	Zabolotsky V.	14, 159, 171, 194, 197, 221, 262, 277, 338
Uzdenova A.	316	Zaitseva E.	104
V			
Vasilenko P.	159	Zaltzman B.	267
Vasil'eva V.	23, 159, 318	Zhang C.	339
Vasilevskii V.	49, 191	Zhansitov A.	254
Vaulin N.	271	Zolotukhina E.	340, 342
Velizarov S.	41	Zotova D.	283
Vilacheva Y.	321		
Vinyukov A.	340		
Volfkovich Y.	323		
Volkov A.	49, 210		



ISBN 978-5-6049504-4-9



9 785604 950449

ISBN 978-5-6049504-4-9

Подписано в печать 20.05.2024г. Формат А4.
Печать цифровая. Бумага 120 гр. офсетная.Заказ № 2005/2024
Тираж 200 экз.

Отпечатано с готового макета ИП Капустина И.В.
Типография " Bestprint"
350040, г. Краснодар, ул. Селезнева 4/А, оф. 49-50
www.bestprint.info e-mail:office@bestprint.info